The Sixth Infrared and Raman Users Group Conference (IRUG6)

Marcello Picollo, editor

organized by
Istituto di Fisica Applicata "Nello Carrara" IFAC – CNR

in collaboration with
Opificio delle Pietre Dure and
Ente Cassa di Risparmio di Firenze

Proceedings of the Sixth Infrared and Raman Users Group Conference (IRUG6)

Florence, Italy March 29th – April 1st 2004

organized by **Istituto di Fisica Applicata "*Nello Carrara*" IFAC – CNR**

in collaboration with

Opificio delle Pietre Dure and **Ente Cassa di Risparmio di Firenze**

Editor
Marcello Picollo (IFAC-CNR)

il prato

Mission

The international Infrared and Raman Users' Group (IRUG) is dedicated to the professional development of its members by providing a forum for the exchange of infrared (IR) and Raman spectroscopic information, reference spectra and materials. IRUG is composed primarily of individuals within the art conservation and historic preservation fields who use IR and Raman spectroscopy to study the world's cultural heritage.

At biennial meetings, the IRUG initiative is sustained by members and invited speakers who present papers on a range of topics. A primary goal of IRUG is to improve and expand the data generated and shared by its members. Toward this end, a cooperative database of IR and Raman spectra relevant to cultural materials has been undertaken.

IRUG web site: www.irug.org

North, Central, South America
Beth Price
Philadelphia Museum of Art
Tel: +1 215 684 7552
Fax: +1 215 684 7550
email: bprice@philamuseum.org

Europe
Boris Pretzel
Victoria & Albert Museum
+44 (0)20 7942 2116
+44 (0)20 7942 2092
email: boris.pretzel@vam.ac.uk

Africa, Asia, Australia
Janice Carlson
Philadelphia Museum of Art
Tel: +1 302 239 2158
Fax: +1 215 684 7550
email: jncarlson1@comcast.net

Front Cover
Benozzo Gozzoli, Cappella dei Magi (detail), Palazzo Medici Riccardi, Florence.

Dear Readers,

The 6th Infrared and Raman Users Group Conference was held from March 29th to April 1st 2004 in Florence, Italy. It was a great pleasure to see approximately 100 participants from Europe, Japan, North and South America. The speakers presented new developments and applications of the Infrared and Raman techniques used in the field of art conservation.

As local organizer of the event, I would like to thank the *Ente Cassa di Risparmio di Firenze* for giving us the Conference venue at the Palazzo Incontri, the *Opificio delle Pietre Dure* for hosting the IRUG poster session in their premises, and *Kent State University Florence Program* for having hosted IRUG6 welcome cocktail party reception and 2004 IRUG Board of Directors meeting at their beautiful new location in Florence. I am also grateful to the *Agenzia per il Turismo*, the *Comune di Firenze*, *Remspec Corporation*, and the *Ente Cassa di Risparmio di Firenze* for their generous contribution in making this Conference possible at no cost to its participants. I also wish to express my gratitude to Pier Luigi Emiliani and Giorgio Bonsanti for their precious advice and support, as well as to the *Opificio delle Pietre Dure* and the *Associazione degli Industriali della Provincia di Firenze* for their helpful collaboration in organizing the event. Furthermore, I would like to thank Bruno Radicati, Lorenzo Stefani, Laura Balcerzak and Simone Porcinai for their invaluable help in the final organization of the event. Moreover, I really appreciated contribution of my colleagues Mauro Bacci, Janice Carlson, Simone Porcinai, Boris Pretzel, Beth Price, and Scott Williams in making this Volume of Proceedings possible through their useful and constructive suggestions to the authors of the papers. And, finally, I wish to thank my wife, Sirpa, whose enthusiastic support and useful suggestions helped me during the entire process of making this event possible.

On Monday March 29th, the Conference was opened by Letizia Paradiso, Cristina Acidini Luchinat and Pier Luigi Emiliani in the magnificent Sala Verde of Palazzo Incontri, which was generously offered by the *Ente Cassa di Risparmio di Firenze*.

Letizia Paradiso, on behalf of Alberto Carmi, President of the *Ente Cassa di Risparmio di Firenze*, gave a warm welcome to all the participants, and briefly reported on the activities of sponsorship and financial support of the *Ente* in the conservation, preservation, valorization of and research on the Florentine Cultural Heritage. In particular she emphasized the fact that in the last three years the *Ente* has been more active in supporting scientific research projects than before. It was thus very active in supporting IFAC-CNR for the organization of IRUG6 Conference in Florence.

Cristina Acidini Luchinat, Head of the *Opificio delle Pietre Dure Institute*, brought her greetings to the participants by emphasizing the significance of having such a distinguished group of conservation scientists in the heart of a city imbued with a cultural heritage. She acknowledged the importance that scientific research has in the preservation of the cultural heritage and the benefit that meetings, such as IRUG, bring to art conservation by enabling interaction and exchange between various research groups.

Lastly, Pier Luigi Emiliani, Director of the *Institute for Applied Physics "Nello Carrara"* of the Italian National Research Council, welcomed all the conservators and scientists who attended this event, and stressed the work done at his Institute in the study of the Cultural Heritage and the long standing research activities in this field carried out by the Applied Spectroscopy Group of IFAC-CNR led by Mauro Bacci.

The three speakers expressed their good wishes for a successful meeting that would surely produce results that will be important not only from a scientific point of view, but that may also have direct application to supporting the sometimes difficult decisions that need to be made in art conservation.

The 40 oral presentations took place at Palazzo Incontri during the first three days. Lively discussion followed the scientific presentations and continued during the coffee and lunch breaks at Palazzo Incontri. At the end of the first day, all participants and accompanying guests were invited to a welcome cocktail party at the new location of the *Kent State University Florence Program*, in the medieval Palazzo dei Cerchi.

The last day of the Conference, dedicated to the poster session, took place at the Library of the *Opificio delle Pietre Dure*. 21 posters were presented in this session, highlighting the importance of this format for the presentation of interesting and promising Infrared or Raman spectroscopic data and methodologies.

It was gratifying to see the enthusiasm and involvement of the participants. The Conference provided a splendid opportunity to exchange ideas, scientific results and recent developments in the field of conservation science. It also offered the possibility to strengthen contacts between the attendees consisting of scientists, conservators, and scholars, underscoring the importance of the IRUG initiative for our field.

We look forward with great pleasure and anticipation to the seventh IRUG meeting, scheduled for 2006 at the Museum of Modern Art in New York.

Marcello Picollo
IFAC – CNR
IRUG 6 Local Conference Organizer

Mi è gradito in primo luogo portare il saluto di Alberto Carmi, Presidente dell'Ente Cassa di Risparmio di Firenze. Vorrei appena ricordare, per chi ci conosce un po' meno, che l'Ente Cassa di Risparmio di Firenze è un'istituzione privata senza fine di lucro che svolge funzioni di sostegno finanziario e partecipa direttamente e attivamente alla realizzazione di progetti nei settori dei beni e delle attività culturali, della ricerca scientifica, delle iniziative socio assistenziali, dell'ambiente.

Un convegno così specialistico come quello di oggi forse non genera immediatamente nell'opinione pubblica l'impatto emotivo che i contenuti meritano, ma la presenza di tanti autorevoli personalità del settore provenienti dall'Italia e dall'estero, la nostra stessa partecipazione come Ente Cassa, stanno a testimoniare l'importanza che va attribuita invece alla materia e agli argomenti che saranno affrontati nel corso della giornata.

Considerato poi che non si parla in astratto di ricerche e metodiche scientifiche ma della loro applicazione a qualcosa che ci è più intimamente famigliare, come le opere d'arte, patrimonio comune dell'umanità e delle sue tradizioni nei diversi Paesi e alle varie latitudini, direi che c'è abbastanza di che discutere e su cui confrontarsi con passione e nel modo più ampio e costruttivo possibile.

Mi pare che ci siano tutte le premesse per far ciò, a cominciare innanzitutto dal contesto ambientale: Firenze è una città nella quale si viene sempre volentieri per incontrarsi, per concretizzare opportunità di scambio e stabilire relazioni di amicizia. Firenze è inoltre sede di prestigiosi laboratori di restauro e di ricerca scientifica, oltre ad essere quell'incomparabile concentrato di bellezze artistiche che tutti conoscono.

Bene hanno fatto quindi gli organizzatori del convegno a coinvolgere la nostra Città in questa occasione di lavoro e di studio. Un pensiero grato lo rivolgiamo in particolare all'Istituto di Fisica Applicata "Nello Carrara" che si è fatto garante dell'operazione alla quale l'Ente Cassa ha partecipato con convinzione, anche perché una porzione consistente delle sue risorse finanziarie è abitualmente destinata proprio alla conservazione, restauro e valorizzazione del patrimonio artistico e culturale, e non potrebbe essere diversamente: abbiamo accennato a Firenze, ma pensiamo al territorio circostante e alla straordinaria ricchezza, in generale, delle tante testimonianze storiche, culturali ed artistiche che la Toscana può vantare.

L'idea di questo convegno è piaciuta all'Ente Cassa anche per un altro motivo molto importante: la possibilità di giungere ad una migliore e ancora più responsabile attività di conservazione attraverso una conoscenza più profonda dei materiali di cui sono composte le singole opere d'arte. Si tratta evidentemente di un passaggio decisivo, ormai imprescindibile da qualsiasi intervento di restauro si voglia attualmente mettere in cantiere e portare a felice compimento. Potete quindi comprendere come sia estremamente importante per l'Ente, che spesso partecipa ad iniziative di restauro anche di grande rilievo, avere la sicurezza di poter condividere progetti legati ad una diagnostica scientifica di base accurata e metodicamente impostata, la quale costituisca la premessa sufficiente e necessaria per poter poi operare proficuamente in tutte le fasi successive.

Non mi resta che rivolgere ai presenti l'augurio di buon lavoro e l'auspicio per la riuscita e il pieno successo di questo incontro internazionale. Grazie

Antonio Gherdovich
Vice Direttore Generale Ente Cassa di Risparmio di Firenze

I am pleased to express a warm welcome from Alberto Carmi, President of the *Ente Cassa di Risparmio di Firenze*. For those who are not familiar with the *Ente Cassa di Risparmio di Firenze*, I would like to explain that it is a private non-profit institute whose activities include financial support and direct active participation in projects in the fields of cultural heritage, scientific research, environment research, and social assistance.
A conference as specialized as today's event may not immediately generate the public recognition that it deserves, but the presence of so many professionals and specialists from Italy and abroad, as well as our own participation, confirms the importance of the subject matter and the discussions that will be addressed. Considering that these discussions do not revolve around abstract research concepts and scientific methodologies, but instead consider their practical application to something much more familiar — artwork, the shared cultural patrimony of various countries and traditions, I would say that there will be enough substance for passionate discussion and exchange in the most broad and constructive manner possible.
It seems to me that this event offers great potential, beginning with its setting. Florence is indeed a city where one always comes with pleasure to meet with others, to provide opportunities for exchange, and to establish friendly relationships. Florence also houses prestigious conservation and scientific research laboratories, as well as some of the greatest art collections known.
Therefore, the organizers of the conference have done well in choosing our city for this opportunity to work and study. We wish to express our gratitude in particular to the *Istituto di Fisica Applicata "Nello Carrara"* for organizing event in which *Ente Cassa* is participating with conviction. A consistent part of our financial resources is allocated to artistic and cultural heritage conservation, restoration, and valorization. Our support goes not only to Florence, but also to the surrounding territory, benefiting the numerous historical, cultural and artistic treasures that exist throughout Tuscany.
Ente Cassa was interested in this conference for another important reason: the possibility to achieve better and even more responsible conservation activities through more thorough understanding of the materials that compose individual works of art. Obviously, this knowledge serves an important role in any successful restoration intervention. You may therefore appreciate the importance of this opportunity for *Ente Cassa*, which often participates in significant restoration projects, to support scientific and diagnostic projects that accurately and methodically provide a necessary basis for all successive conservation and restoration phases. I wish all the participants luck in their research activities and hope that this international event will be a great success.

Antonio Gherdovich
Vice Direttore Generale Ente Cassa di Risparmio di Firenze

Con grande soddisfazione vedo aver luogo a Firenze, per iniziativa dell' Istituto di Fisica Applicata –"Nello Carrara" IFAC il sesto incontro dell'IRUG, che riunisce così numerosi e prestigiosi esperti da diversi paesi, e colgo l'opportunità per confermare l'entusiasmo con il quale ho accolto l'iniziativa fin dal suo primo annuncio, assicurando la partecipazione costruttiva dell'Opificio delle Pietre Dure e caldeggiando il non meno indispensabile sostegno dell'Ente Cassa di Risparmio di Firenze, che anche questa volta ha guardato con favore a un'iniziativa che sancisce un passo avanti nell'alleanza fra arte e scienza.
E' quest'alleanza che a Firenze si è stabilita fin dagli anni '30 del Novecento, e che ha conosciuto nel tempo un percorso esponenziale di crescita, ivi comprendendo il picco – di tragedia, ma anche di sviluppo – rappresentato dall'alluvione del 1966, con quello che ne seguì in termini di recupero del patrimonio architettonico e artistico danneggiato.
La tendenza degli ultimi lustri, della quale l'Opificio nelle sue componenti scientifiche e, non meno, nei settori di restauro si è fatto propulsivo interprete, vede in espansione e in affinamento le indagini conoscitive sulle opere d'arte, a scopo di diagnostica ma non soltanto, di tipo non invasivo. Tra queste, la IR and Raman spectroscopy appare particolarmente promettente, sia per i risultati già prodotti, sia per le prospettive che le si aprono dinanzi.
Da storico dell'arte so bene, e non esito a riaffermare, che di per sé i dati acquisiti con qualsiasi tecnologia, anche la più sofisticata, non sono portatori di informazioni certe, ma piuttosto di indicazioni che vanno interpretate: e in questo lavoro di interpretazione l'esperto scientifico è chiamato a condividere il suo sapere con almeno due altre professionalità cruciali, lo storico (dell'arte, dell'archeologia e di quant'altro) e il restauratore. Proprio l'integrazione fra i loro diversi expertis e, atteggiamenti e terminologie rappresenta la frontiera della nostra sfida quotidiana, nel capire quel che l'opera d'arte ha da dire e da chiedere nel suo muto linguaggio.
Sono certa che da questo incontro dell'IRUG, come da quelli che seguiranno, scaturiranno nuovi stimoli alla ricerca e scambi preziosi di informazioni e di vedute. E' con questa certezza che auguro a tutti gli intervenuti buon soggiorno a Firenze e buon lavoro.

Cristina Acidini Luchinat
Soprintendente, Opificio delle Pietre Dure di Firenze

The fact that the Sixth IRUG Conference, organized by the *Istituto di Fisica Applicata "Nello Carrara"* (Institute of Applied Physics), a part of the Italian National Research Council, is taking place in Florence gives me great pleasure. I am also glad to see the large number of experts from various countries who are participating here in this gathering. I would like to take this opportunity to reconfirm the enthusiasm that I felt when I first heard about the conference and then agreed to the participation of the *Opificio delle Pietre Dure*. I also warmly encouraged the support of the *Ente Cassa di Risparmio di Firenze* which has once again sustained an initiative that can be considered a further step forward in the collaboration between art and science.

This specific collaboration had already begun to take shape in the 1930's, and continued to develop considerably over time, including the focal point - in the form of a tragedy, but also of development - represented by the Flood of 1966, and by the vast campaign for the restoration of the architectural and artistic patrimony damaged by this unfortunate event.

Over the past several decades, as one of the world's leaders in conservation science and restoration activities, the *Opificio* has encouraged the expansion and improvement of non-invasive methodologies of diagnosis and analysis relative to works of art. Among these, IR and Raman spectroscopies seem particularly promising, both for the results already obtained and also for their potential as regards future applications.

As an art historian, I understand and am fully aware that data obtained with any technology, no matter how sophisticated, do not provide absolute results *per se*, but rather information that requires interpretation. The scientific expert participates in this task of interpretation, and shares his or her scientific knowledge with professionals in at least two other crucial fields: historians (of art, archeology, and so forth) and restorers. It is this sharing of different specific expertise, approaches and terminology that provides a daily challenge to understanding the message and expression of works of art.

I am certain that this IRUG conference, like those that will follow, will provide new stimuli for research and an invaluable exchange of information and viewpoints. And, armed with this certainty, I wish all of you a wonderful stay in Florence and a very successful meeting.

Cristina Acidini Luchinat
Soprintendente, Opificio delle Pietre Dure di Firenze

IRUG6 Conference - Final Program

Florence 29th March – 1st April 2004

PALAZZO INCONTRI - SALA VERDE AUDITORIUM Via de' Pucci 1

Monday 29th March

09:00-10:00 **REGISTRATION** at location **Palazzo Incontri**

10:00-10:20 *WELCOME*
Letizia Paradiso (Ente Cassa di Risparmio di Firenze)
Cristina Acidini Luchinat (Director of Opificio delle Pietre Dure, Firenze)
Pier Luigi Emiliani (Director of Istituto di Fisica Applicata "Nello Carrara")
Marcello Picollo (local organizer IRUG6 Conference)

10:20-10:50 COFFEE BREAK

ORAL presentations

Moderator: Boris Pretzel (Victoria and Albert Museum, UK)

10:50-11:10 B. Price (Philadelphia Museum of Art, USA), K. Ehrman (Digital Bridgeway Inc., USA) *Promoting Global Access to the Infrared and Raman Users Group Spectral Database* p. 17

11:10-11:30 Y. Matsuda (Tohoku University of Art & Design, Japan) presented by M. Tsukada *Development of the in-house database system for artistic materials linked with FT-IR spectral library and its application to the conservation education* p. 25

11:30-11:50 S. Pierce (Department of Chemistry, Duke University, USA) *FTIR Methodologies for the Analysis of Contaminants Removed from Polychrome Statues with an Erbium:YAG Laser at 2.94 microns* p. 26

11:50-12:10 A. Vila (Facultat de Belles Arts, Universitat de Barcelona, Spain) *A fast procedure for fake Euro notes identification based on FTIR (ATR) technique. An example of prints characterization* p. 35

12:10-12:30 Discussion

12:30-14:00 LUNCH BREAK

Moderator: Janice Carlson (Philadelphia Museum of Art, USA)

14:00-14:20 S. Lake (Hirshhorn Museum and Sculpture Garden, Smithsonian Institution, USA) *Paul Thek's Fishman: IR spectroscopy of degraded latex* p. 36

14:20-14:40 M. Favaro (ICIS – CNR, Padua, Italy) *Identification of unknown acrylic resin applied on stone sculptures of Porta della Carta, Ducal Palace, Venice* p. 41

14:40-15:00 R.E. Ploeger and H.F. Shurvell (Department of Art, Queen's University, Canada) *Infrared analysis of material leached by water from acrylic paint films* p. 46

15:00-15:20 D. Scalarone (Department of Chemistry IPM, University of Turin, Italy) *Infrared spectroscopy monitoring of surfactant phase-separation and stability in waterborne organic coatings and acrylic artists' paints* p. 52

15:20-15:50 COFFEE BREAK

Moderator: Scott Williams (Canadian Conservation Institute, Canada)

15:50-16:10 J. Jonsson (Tate Gallery, UK) *Separation of acrylic paint components and their identification with FTIR spectroscopy* p. 58

16:10-16:30 J. Boon (FOM Institute AMOLF, The Netherlands) *Imaging microspectroscopy studies of paint cross sections* p. 66

16:30-16:50 M. Cotte (Centre de Recherche et de Restauration des Musées de France, Paris, France) *Synchrotron infrared microscopy of ancient biological and cosmetics material* p. 75

16:50-17:10 K. Helwig (Canadian Conservation Institute, Canada) presented by S. Williams *Analysis of the Materials of Several Canadian Artists Using Fourier Transform Infrared Spectroscopy* p. 83

18:00-19:30 ***Welcome cocktail at Kent State University in Florence – Vicolo dei Cerchi 1***

Tuesday 30th March

Moderator: Francesca Casadio (Art Institute of Chicago, USA)

09:00-09:20 A. Schoenemann (The Getty Conservation Institute, USA) *The application of Raman and FTIR micro spectroscopy for the study of drying oils* p. 84

09:20-09:40 D. Thickett (Birkbeck College, University of London, UK) *The Analysis of Iron Corrosion Products with FTIR and Raman Spectroscopies* p. 86

09:40-10:00 K. Trentelman (Detroit Institute of Arts, Center for Conservation, USA) *Building a multi-dimensional Raman database: the effect of excitation wavelength and binding media on Raman spectra of artists' pigments.* p. 94

10:00-10:20 A. Zoppi (LENS, University of Florence, Italy) *Micro-Raman imaging of ceramics components* p.101

10:20-10:50 COFFEE BREAK

Moderator: Karen Trentelman (Detroit Institute of Arts, Center for Conservation, USA)

10:50-11:10 M. Leona (Metropolitan Museum of Art, USA) *Sub-nanogram level identification by Surface Enhanced Raman Scattering of alizarin from madder lakes found in works of art* p.105

11:10-11:30 D. de Faria (Laboratório de Espectroscopia Molecular University of São Paulo, Brazil) *Raman spectroscopy of Brazilian archaeological and ethnographic resins* p.113

11:30-11:50 H.G.M. Edwards (Dept of Chemical and Forensic Sciences, University of Bradford, UK) *Raman Spectroscopy Applied to Biomaterials in Art History and the Preservation of Cultural Heritage* p.121

11:50-12:10 P. Vandenabeele (Ghent University, Laboratory of Analytical Chemistry, Belgium) *The use of a Mobile Raman spectrometer for the in situ analysis of objects of art* p.127

12:10-12:30 Discussion

12:30-14:00 LUNCH BREAK

Moderator: Beth Price (Philadelphia Museum of Art, USA)

14:00-14:20 A. van Loon (FOM Institute AMOLF, The Netherlands) *Identification and localization of proteinaceous compounds in paint samples with infrared spectroscopic techniques - scope and limitations* p.130

14:20-14:40 R. Mazzeo (University of Bologna, Chemistry Department, Italy) *Examination of fresh and aged Chinese organic binding media using FTIR spectroscopy* p.137

14:40-15:00 M. Sato (Nara National Research Institute for Cultural Properties, Japan) *Microscopic FT-IR identification of ancient textile fibers, natural dyestuffs and Japanese lacquers* p.138

15:00-15:20 N. Vrinceanu ("Gh. Asachi" Technical Univesity, Faculty Of Chemistry, Romania) presented by M. Picollo *Stabilization and protection of cellulosic supports with a photosensitive polymeric system* p.142

15:20-16:00 COFFEE BREAK

16:00-18:00 **Business Meeting**

18:00-19:30 ***Tour Museum of San Marco – Piazza San Marco***

Wednesday 31st March

Moderator: Jaap Boon (FOM Institute AMOLF, The Netherlands)

09:00-09:20 S. de Groot (Netherlands Institute for Cultural Heritage, The Netherlands) *FTIR analysis of 4 paintings by Pierre-Auguste Renoir'* p.143

09:20-09:40 J.F. García-martínez (Facultat de Belles Arts, Universitat de Barcelona, Spain) *Discrimination of contemporary artistic prints based on the FTIR analysis* p.149

09:40-10:00 H. Khanjian (The Getty Conservation Institute, USA) *The Study of Photographic Coatings Using Angle Resolved ATR-FTIR Spectrometry* p.154

10:00-10:20 T. van Oosten (Netherlands Institute for Cultural Heritage, The Netherlands) *The use of FTIR spectroscopy for the study of the influence of Impranil DLV and Plextol B, as impregnating agents, on the ageing of polyurethane (PUR) foams* p.155

10:20-10:50 COFFEE BREAK

Moderator: Oscar Chiantore (Department of Chemistry IPM, University of Turin, Italy)

10:50-11:10 D. Stulik (The Getty Conservation Institute, USA) *Identification of Natural and Synthetic Dyes and Colorants in Tinted Photographs* p.162

11:10-11:30 L. Balcerzak (IFAC – CNR, Florence, Italy) *Non-invasive Fibers Optic Reflectance MIR spectroscopic analysis of white painted layers* p.163

11:30-11:50 C. Miliani (ISTM – CNR, Perugia, Italy) *Reflectance FTIR study of altered calcium carbonate surface* p.169

11:50-12:10 S. Williams (Canadian Conservation Institute, Canada) *In-situ, mid-IR spectroscopic analysis of objects at museums using portable IR spectrometers* p.170

12:10-12:30 Discussion

12:30-14:00 LUNCH BREAK

Moderator: Marco Leona (Metropolitan Museum of Art, USA)

14:00-14:20 F. Casadio (Art Institute of Chicago, USA) *Decoration of Meissen Porcelain: Raman microscopy as an aid for authentication and dating* p.178

14:20-14:40 A. Cavicchioli (Laboratório de Espectroscopia Molecular-Instituto de Química-University of São Paulo, Brazil) *FT-Raman studies of thin films of natural varnishes* p.158

14:40-15:00 D. Bersani (Physics Department - University of Parma, Italy) *Raman and GC/MS investigation of Parmigianino's wall paintings in Santa Maria della Steccata church in Parma (Italy)* p.191

15:00-15:20 K. Smith (McCrone Associates, USA) *Raman Analysis of Native American Dyed Artifacts* p.195

15:20-15:50 COFFEE BREAK

Moderator: Francesca Piqué (The Getty Conservation Institute, Los Angeles, USA)

15:50-16:10 P.S. Middleton (Peterborough Regional College, UK) *Painters and Decorators in Roman Britain: Raman studies of Romano-British wall painting pigments and techniques* p.198

16:10-16:30 S. Denoël (European Center of Archaeometry, University of Liége, Belgium) *Comparative study of the pigments found in illuminated manuscripts of the 16th century in Belgium: study of a particular case the Gerard van der Stappen Book's of Hours* p.205

16:30-16:50 C. Ricci (Chemistry Department, University of Perugia, Italy) *Original and fake blue pigments from the church of S. Francesco in Montefalco painted by Benozzo Gozzoli: a spectroscopic approach* p.213

16:50-17:10 S. Pagès-Camagna (Centre de Recherche et de Restauration des Musées de France, France) *Synthesis and weathering process of Egyptian green: Structural characterisation by Raman microspectromety of a synthetic copper silicate used as pigment* p.220

17:10-17:30 ***Final remarks on oral presentations***

OPIFICIO delle PIETRE DURE – Biblioteca, Via Alfani 78

Thursday 1st April

09:30-12:00 ***POSTER Session***

K. Andrikopoulos (Art Diagnosis Centre, Greece)
Vibrational Spectroscopy reveals the techniques implemented for the production of Hadra hydriai by the Rhodian laboratory (3rd –2nd century B.C. p.228

L. Appolonia (Soprintendenza Beni e Attività Culturali Val d'Aosta, Italy)
Use of Infrared Photoacustic system in Cultural Heritage Analysis p.229

E. Carretti (Consortium CSGI, Department of Chemistry, University of Florence, Italy)
FTIR spectroscopy to monitor selective cleaning on wall painting surfaces p.239

F. Casadio (Art Institute of Chicago, USA)
A novel approach to an old problem: application of TG/FTIR for evaluating materials for storage and display cases p.244

E.M.Castellucci (LENS, University of Florence, Italy)
Evaluation of the analytical potential of Raman microscopy combined with elemental techniques p.246

A. Cosentino (University of Catania, Italy)
ColoRaman project: characterization of oil, tempera and fresco colors using Raman and Fluorescence Spectroscopies p.247

N. Ferrer (Serveis Cientificotècnics.Universitat de Barcelona, Spain)
Characterization of ink components in ancient manuscripts by FTIR spectroscopy p.252

G. Giachi (Soprintendenza per i Beni Archeologici della Toscana, Florence, Italy)
Resin and pitch of Pinaceae wood in the findings of the ancient harbor of Pisa p.253

V. Hayez (Vrije Universiteit Brussel, Belgium)
Micro-Raman spectroscopy used for the study of corrosion products on copper alloys p.259

C. Herm (Dresden Academy of Fine Arts, Germany)
Infrared spectroscopic study of some more metal soaps p.267

12:00-12:30 ***Final remarks on poster presentations***

12:30 **End of IRUG6**

ORAL PRESENTATIONS

Promoting Global Access to the Infrared and Raman Users Group Spectral Database

B. Price[1], B. Pretzel[2], J. Carlson[3], K. Ehrman[4]
[1] Box 7646, Philadelphia Museum of Art, Philadelphia, PA, 19101, USA;
[2] Victoria and Albert Museum, So. Kensington, London, SW7 2RL, UK;
[3] Winterthur Museum, Garden and Library (retired), Winterthur, DE, 19735, USA;
[4] Digital Bridgeway, Inc., Philadelphia, PA, USA

Abstract

Many of the world's leading scientific institutions and organizations recognize that data from publicly funded scientific research should be openly available. Providing open access to scientific information is considered good stewardship and is a guiding principle of the Infrared and Raman Users Group (IRUG). Toward this end, in 2003 IRUG developed and placed on its website (www.irug.org) a publicly accessible version of its Spectral Database, along with a spectroscopic bibliography, threaded discussion forum, and software for submission and review of spectra.
By providing efficient, global access to infrared and Raman data, IRUG fosters international collaborations, and facilitates the intellectual and research contributions of the preservation and academic communities. The sharing of such data is a challenging undertaking in which technological, institutional, financial, and legal considerations must be balanced. This paper will discuss, in the context of the complexity and benefits of sharing resources, the next phase of the development of the IRUG Spectral Database: providing universal desktop access via the Internet to all interested parties. The IRUG website software and database construction will also be reviewed.

Introduction

The Infrared and Raman Users Group (IRUG) is an independent organization of conservation professionals who use infrared (IR) and Raman spectroscopy for the analysis of cultural materials [1]. Since its first informal meeting in 1993, IRUG has worked to facilitate the exchange of spectroscopic information and reliable spectra for the analysis of works of art, architecture and archeological materials. Throughout its history, a primary goal of IRUG has been the development and distribution of its collaborative spectral database. The database has become a valuable resource for the study and preservation of the world's cultural property.
Early database initiatives involved the collection of spectra from interested parties. These spectra were distributed from 1993 to 1995. In order to improve the quality, uniformity and reliability of spectra, guidelines for contributions were instituted in 1998/9. Under the guidelines a customized, platform-independent JCAMP-DX spectral file format with integrated descriptive text was developed [2, 3]. Spectra were also peer-reviewed by a committee of conservation scientist editors [4]. These new standards were applied to the Infrared and Raman Users Group Spectral Database, Edition 2000, which was released in 2001 [5]. Edition 2000 contained 1250 systematically named and indexed spectra, both electronic and printed, that were voluntarily contributed by fifty international institutions [6].
Edition 2000 was a substantial achievement. Nevertheless, there were some limitations in the process undertaken to compile the 1250 spectra. First, the formatting and editing was done manually, which was very time consuming. Second, Edition 2000 was only available in hard copy and as discrete electronic JCAMP text files - they were not readily searchable and needed to be distributed by regular mail. Since IRUG envisioned a growing spectral collection with periodic updates, a more efficient, cost-effective means to collect, manage, and distribute spectra was needed. Consequently, in 2001 IRUG decided to develop and place a web database on the Group's website at www.irug.org.
There were several reasons that a web database was viewed as a preferred vehicle for collecting, formatting, managing and distributing the spectra. In the new web database, spectra could be stored as tables of data rather than discrete JCAMP text files. It would no longer be necessary to format spectra manually - they could be automatically reconstructed from the data in the tables. This meant that the database would always be completely current and users would be able to perform queries against the tables, which was not previously possible. Users would also be able to view and download new IRUG spectra directly from the website. Additionally, contributions of spectra could be made via the website rather than email or regular mail. Such Internet accessibility would not only improve the exchange of spectra but would also lower the costs of maintenance and distribution.

New Resources for IRUG Website

In 2002, IRUG contracted Digital Bridgeway, Inc. of Philadelphia, to develop the web database in order to streamline the collection, storage and distribution of spectra. The web pages were constructed with Microsoft Active Server Pages and the underlying database using Microsoft SQL Server 7. The site is currently hosted on a Microsoft Windows 2000 server. In 2003, the following eight new features were made available via the IRUG website:

1. Online version of Edition 2000 Spectral Database
2. Spectroscopic and Materials Bibliography
3. Spectra and Bibliographic Citations Submission Software
4. Spectra Review Software
5. Discussion Forum
6. Participating Institutions, Technical Resources Links
7. Management Software
8. Help articles

These features are described in a later section of this paper.

Considerations Regarding IRUG Policy of Open Access to the Database

Promoting global access to the online database is consistent with the primary goal of IRUG to improve, expand and distribute the IR and Raman data shared by its members. The expected merits of unfettered access to such data are considerable: open scientific inquiry, new and improved research, studies of data collection methods and measurements, and education of students and researchers [7].

Throughout the development of the IRUG Database, a guiding principle has been that access should be restricted only by legitimate considerations. Some self-evident considerations are technological, operational and financial in nature. Furthermore, as an international organization comprising a number of diverse institutions, IRUG must strive to satisfy their legal and cultural needs as much as possible.

IRUG is obligated to operate within copyright and other complex laws involving the international use of scientific databases. The policies that govern sharing and access of data via scientific databases vary from country to country, and are often approached differently by government, not-for-profit, and commercial entities [8-9]. Moreover, many government grants, especially in the US, are contingent upon making aspects of the funded work publicly available. An in-depth discussion of these issues is beyond the scope of this paper and the reader is referred to the articles cited in the Reference section [10-16].

A second consideration for the Group is respect for the intellectual property of others. Although contributors license their spectra to IRUG for annotation and compilation, they still retain ownership and any copyright to their own spectra. When contributors submit spectra, they agree to permit use of the spectra by others. Because of this permission, use of the spectra does not violate any copyright retained by the contributor. Furthermore, all IRUG spectra used in publications and reports are to be properly attributed to both the contributor and IRUG.

The third imperative is to reward and encourage contributors. This is especially important since the database initiative is dependent upon donation of spectra. For contributions of 10 or more approved spectra or equivalent support, contributors receive the entire edited and annotated digitized database for use in their laboratories. Under this policy, submissions of spectra to the database continue to grow.

Probably the greatest challenge for IRUG is to balance open access with the incentives needed to attract contributors. Encouraging scientific contribution requires rewarding the contributor, who is typically a member of the conservation or academic fields. Creating special status for contributors helps to develop a sense of shared intellectual ownership of the database, as well as a sense of community. In order to balance these interests and obligations, the Group's current data access policy is two-tiered. In this two-tiered system, the general public can perform searches of the on-line database and bibliography, view and print spectra and citations, and access links to technical resources and institutions. In addition to the general public access, contributors are rewarded with additional capabilities; they can download high-resolution electronic spectral data for use on their own computers and participate in a threaded discussion group. This two-tiered approach balances the need to provide incentives for contributors while still making the database publicly accessible via the Internet.

Using the New Website Features - Searching Edition 2000 and the Bibliography

Online *Edition 2000* can be accessed via the IRUG *home page* navigation bar and is keyword searchable (Fig. 1). To begin a search, the user enters a keyword or term in the *Search Engine* (Fig. 2). The system displays a *Search Results* list (Fig. 3) with a quick hit count, search term reminder, and summary information about each spectrum (material common name, material class, originating institution name, and filename). The spectrum is viewable by clicking on its filename. The pop-up window displays the spectrum in 4000–400 cm^{-1} and expanded 1850-400 cm^{-1} views (Fig. 4), and can be printed on A4 and US letter paper.
The online *Spectroscopic and Materials Bibliography* is also publicly accessible via the home page navigation bar. Various subject matter categories such as material class, instrumentation, spectroscopic theory, and spectral interpretation can be searched by keyword queries. After entering a keyword or term, a *Results List* is displayed with quick hit count and complete citation information. The bibliographic citations can also be printed.

Overview of the Regime for Contributing Spectra

The overall process for contributing a spectrum involves a submission sequence, a review process and incorporation of the spectrum into the database. IRUG has three regional Chairpersons to assist contributors wishing to submit spectra [17].
The process for submitting spectra is outlined in Figure 5. The submission steps are as follows: 1) convert native spectrum to raw JCAMP-DX file with spectrometer software, 2) login to IRUG website, 3) fill out submission form, 4) attach JCAMP-DX file, and 5) submit form and file. Since the database only accepts JCAMP files, the contributor must have the spectrum file in that format. This should be accomplished with spectrometer software before logging into the IRUG system. The raw JCAMP file will later be reconstructed into an IRUG-JCAMP formatted file.
To submit spectra to the online database, a contributor must sign into www.irug.org. The contributor enters her/his user name and password on the *Login Page*, which is accessed from *Site Services* on the home page navigation bar (Fig. 6). Contributors must request a temporary password from their regional chair to initiate access and a new password must be created when they first login. Afterward, contributors can reset their passwords and manage their own user profile, such as changes in contact information, via *Manage My Information* located in *Site Services*.
Once logged in, the contributor submits a spectrum for review by clicking on *Step 1: Begin a New Submission* (Fig. 6). The system displays a *submission form* prompting the contributor to fill in various information fields such as material name, source, age, color, state, instrument, and instrument conditions (Fig. 7) [18]. To assist the contributor, each information field has a *Help* link to descriptions and examples. The information supplied by the contributor is what makes IRUG spectra so useful. It is stored in the database tables along with the numerical xy data and used to construct the final IRUG-JCAMP compliant formatted spectrum.
When the submission form is completed, the contributor attaches the corresponding raw JCAMP-DX file from her/his computer or network. The contributor then sends the submission to the Review Committee for evaluation in *Step 2: Check and Send Submissions to the Review Committee*. Once the submission is completed, the contributor can monitor its status and that of previously submitted spectra in *Step 3: Check Submission Status*.

Spectra Review – the Review Committee

After contributors submit their spectra they are automatically sent via the web software to the Review Committee. The Review Committee consists of twenty-two conservation scientists who evaluate submissions for quality and completeness [19]. IRUG protocol requires that a minimum of two reviewers evaluate each submission. The reviewers are notified if there are new submissions in the system when they log into the *Review Committee Software* in *Site Services* (Fig. 6).
After clicking on *Step 1: Review and Evaluate Submissions*, reviewers have access to several tools to evaluate a spectrum. These include a thumbnail for a quick, first look at the spectrum, a viewable/downloadable raw JCAMP-DX file, and the *Editor*. The *Editor* is a specially designed software application that allows reviewers to compare the information supplied by the contributor on the submission form with that in the raw JCAMP-DX file. It is the means by which reviewers annotate a submission with comments. The *Editor* software also aggregates all of the reviewer's comments and allows the reviewer to decide on a course of action for the spectrum (Fig. 8). There are three possible actions for a spectrum: accept as is, accept with minor revision, or return for revision-resubmission. Minor revisions typically include misspellings and misclassifications. Spectra exhibiting excessive noise; totally

absorbing bands; interference fringes; extremely sloping, elevated or negative baselines; spurious peaks or contaminants; data collected outside a detector's range; or that are misidentified require revision.
Three Senior Editors (regional Chairpersons) consider the reviewers' comments and recommendations, and act accordingly. Accepted spectra are added to the database. If needed, minor revisions are made to spectra, which are then added to the database. Spectra that are returned may be revised and re-submitted by the contributor, if so desired.

Database Updates - Dissemination of Spectra

The database is updated on a periodic basis, at least once a year, with the newly submitted spectra. Contributors can download new digital spectra in the updated database through *Site Services: Get Database Updates.*

Bibliographic Submission and Review

Online *Bibliography* submission options are also available under *Site Services.* The system accommodates literature citations from books, periodicals or electronic publications. After clicking on the appropriate source type, the system displays the corresponding submission form. The user fills in all pertinent information fields such as authors, editors, translators, publishers, volumes, pages, and URL's. The user must also assign the citation to one or more of the subject matter categories. The Review Committee reviews bibliographic submissions.

Discussion Forum

A threaded discussion group is available via *Site Services* for the discussion of technical questions among contributors.

Conclusion

With the development of the new web database and software, IRUG has made Edition 2000 and the spectroscopic bibliography widely accessible and easy to navigate for both contributors and the general public. Its two-tiered system of access creates an incentive for database contribution by allowing contributors to download spectra onto their own computers. Thus far, over fifty institutions share in the credit for the online database that continues to grow as a result of the worldwide collaboration. Open sharing of peer-reviewed scientific data gathered from such a large collaboration is unprecedented within the conservation field. The IRUG model of sharing infrared and Raman spectra balances the needs of many diverse organizations. Its success should promote unfettered access to other types of conservation research data and information.
IRUG invites visitors to its website at www.irug.org and welcomes contributions of infrared and Raman spectra and literature citations.

Acknowledgements

IRUG is grateful to the many contributors and reviewers who generously provided their spectra and expertise for this initiative. Support for the web development was provided by the National Center for Preservation Technology and Training (NCPTT), Samuel H. Kress Foundation; St. Gobain Corporation Foundation; Philadelphia Museum of Art (PMA); Victoria and Albert Museum; Winterthur Museum, Garden and Library; and Institute for Applied Physics, Nello Carrara. IRUG also acknowledges Mark Abrams; Catherine H. Gillespie [Montgomery, McCracken, Walker and Rhodes, LLP, (MMWR), Philadelphia]; Peter Konin and Andrew Lins (PMA); Robert Silverman; Joseph P. Stapleton (MMWR); Mary Striegel (NCPTT); and Mayumi Yoshizawa (PMA) for their guidance and support.

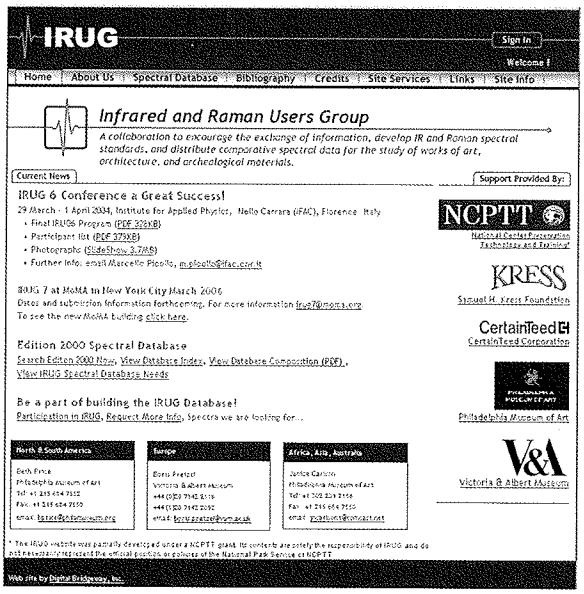

Figure 1: www.irug.org home page

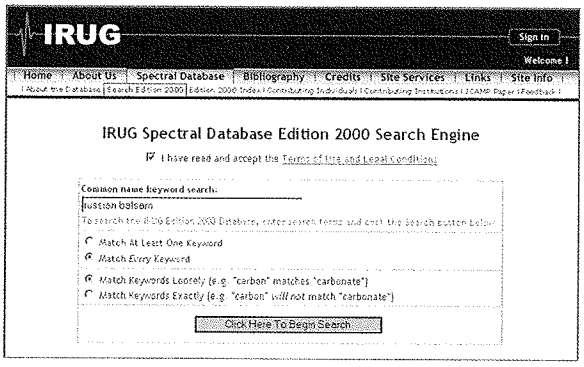

Figure 2: IRUG Edition 2000 Search Engine

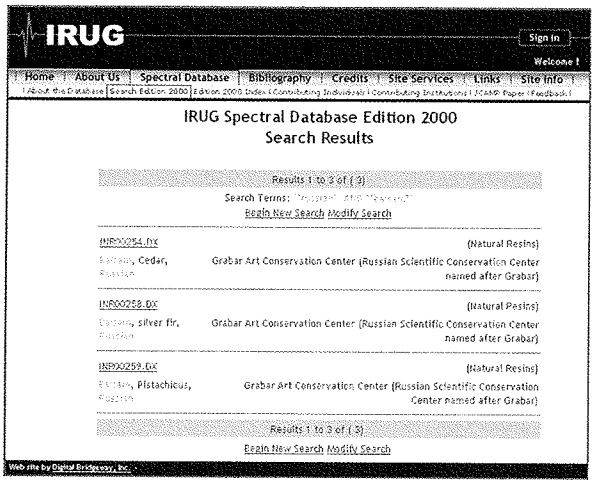

Figure 3: IRUG Edition 2000 search results list

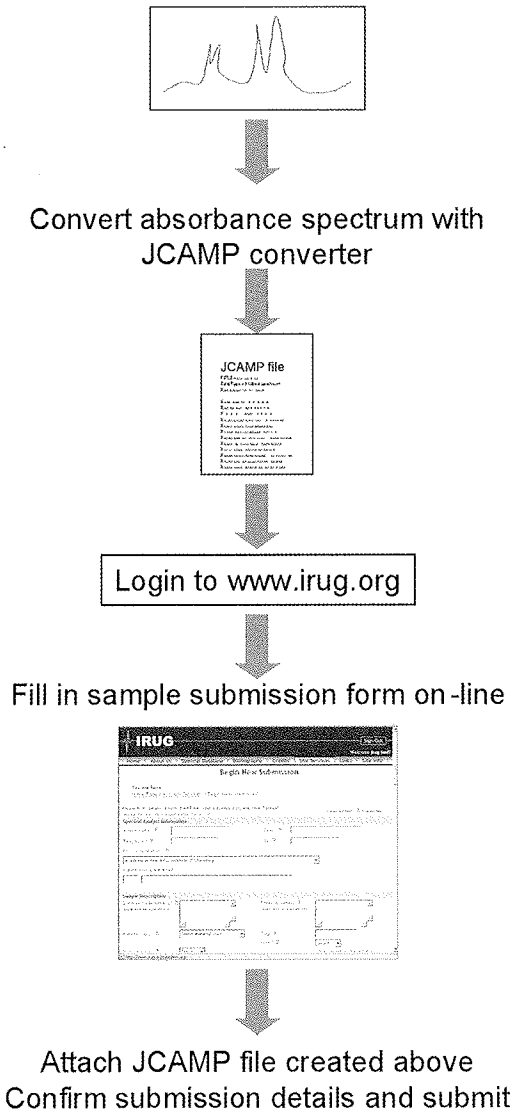

Figure 5: Online spectra submission procedure

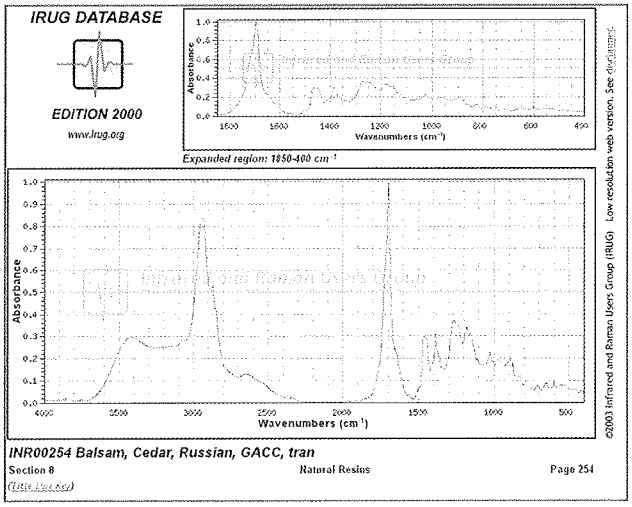

Figure 4: IRUG Edition 2000 search result - spectrum view

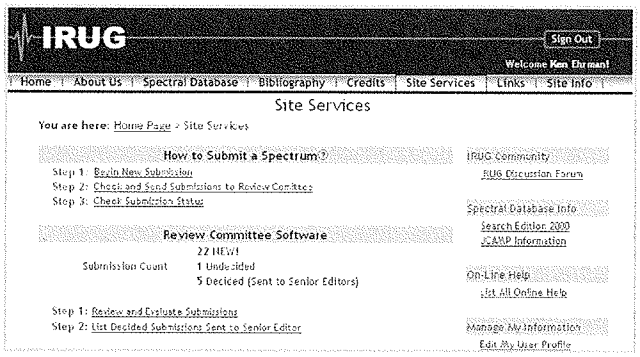

Figure 6: IRUG site services page

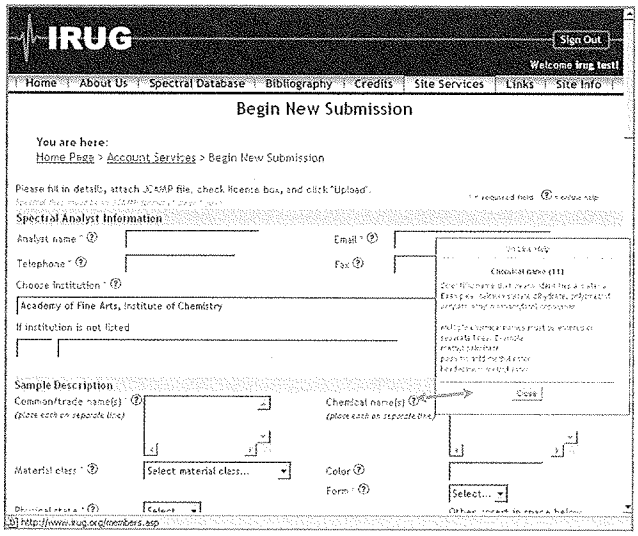

Figure 7: IRUG submission form with expanded help entry

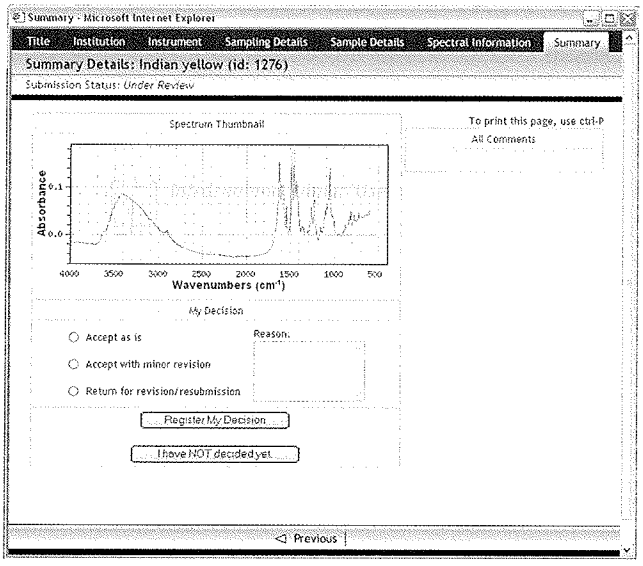

Figure 8 The 'Editor' tool - summary page

References

1. IRUG is registered as a not-for-profit corporation in the State of Pennsylvania, US.

2. For a complete format description see Pretzel, B., Price, B. and Carlson, J., *JCAMP-DX Spectral File Format for Submissions to the Infrared and Raman Users Group Database,* (1 Feb 1999, last updated 11 Mar 2003) <http://www.irug.org/ed2k/jcamp.asp> (accessed 20 Jan 2004).
3. See also McDonald, R. and Wilks, P., 'JCAMP-DX: A Standard Form for the Exchange of Infrared Spectra in Computer Readable Form' *Applied Spectroscopy* (1998) 42 (1) 151-163.
<http://www.jcamp.org/protocols.html#ir4.24> (accessed 12 July 2004).

4. For list of *Edition 2000* editors see <www.irug.org/ed2k/search.asp>.

5. IRUG, *Infrared and Raman Users Group Spectral Database, Edition 2000,* Infrared and Raman Users Group, Philadelphia, (2001).

6. See Contributing Institutions list at <http://www.irug.org/credits/institution.asp>.

7. Organization for Economic Cooperation and Development. '*OECD Promoting Access to Public Research Data for Scientific, Economic, and Social Development: Follow-up Group on Issues of Access to Publicly Funded Research Data Final Report',* (Mar 2003), <http://dataaccess.ucsd.edu/FinalReport.htm> (accessed 24 Jan. 2004).

8. Arzberger, P. et al., 'An International Framework to Promote Access to Data', *Science* (2004) 303 1777-1778.

9. Maurer, S., 'Raw Knowledge: Protecting Technical Databases for Science and Industry' *Proceedings of the Workshop on Promoting Access to Scientific and Technical Data for the Public Interest: An Assessment of Policy Options*, National Academy Press, Washington, DC (1999) 12-40.

10. National Research Council, *A Question of Balance: Private Rights and the Public Interest in Scientific and Technical Databases*, National Academy Press, Washington, DC (1999).

11. National Research Council, *Proceedings of the Workshop on Promoting Access to Scientific and Technical Data for the Public Interest: An Assessment of Policy Options*, National Academy Press, Washington, DC, 1999.

12. Committee on Issues in the Transborder Flow of Scientific Data, et al., Bits *of Power: Issues in Global Access to Scientific Data.* National Academy Press: Washington, DC, 1997.

13. David, P., *The Digital Technology Boomerang: New Intellectual Property Rights Threaten Global "Open Science"<http://dataaccess.uscd.edu/NIWInew.htm>* (accessed 15 Feb 2004).

14. Wouters, P., Schröder, P., Eds., 'Promise And Practice In Data Sharing', *The Public Domain of Digital Research Data*, NIWI-KNAW, Amsterdam (2003). <http://www.niwi.knaw.nl/en/nerdi2/publ/author/paul/toon> (accessed 12 July 2004).

15. Wouters, P., 'Policies on Digital Research Data: An International Survey', *The Public Domain of Digital Research Data,* P. Wouters and P. Schröder, Eds., NIWI-KNAW, Amsterdam (2002).

16. Wouters, P., Data *Sharing Policies*, Networked Research and Digital Information, NIWI-KNAW (2002) <http://dataaccess.ucsd.edu/NIWInew.html> (accessed 20 Jan 2004).

17. See IRUG homepage <http://www.irug.org> for chairpersons contact information.

18. The system retains repeated information such as name, institution, and spectrometer to facilitate multiple submissions.

19. See Review Committee at <http://www.irug.org/credits/review_committee.asp>.

Development of the In-house Database System for Artistic Materials Linked with FTIR Spectral Library and Its Application to the Conservation Education

Yasunori Matsuda and Ai Miyazawa
Tohoku University of Art & Design, Japan

Abstract

The in-house database system for artistic materials linked with FTIR spectral library has been developed. More than 900 kinds of artistic materials, including pigments, resins, fibers, lacquers, dyes, and oils etc., have been collected for the database system. The conception of the system has been mainly user-oriented. It is constituted three parts; 1) each material in a glass sampler labeled for order, which is collected in sample storage, 2) a digital file form of the FileMaker Pro. Software filled with several features of each material, order number, classification, nomenclature (name), form and figure, color and so on, and 3) the FTIR spectral library in the personal computer system linked with these digital data. The library is built of each spectral datum corresponding each material using the Perkin-Elmer Software. The library is also available for the material retrieval and identification. The purpose of this developing project is not only convenience for conservators but also conservation education for undergraduate students. The application of the system to a program for the conservation science education is now being in practice. The contents of the application and its estimation will be presented in the conference.

FTIR Methodologies for the Analysis of Contaminants Removed from Polychrome Statues with an Erbium:YAG Laser at 2.94 μm

Sarah E. Pierce[1], Peter Ingram[2], Myron L. Wolbarsht[3], Adele de Cruz[4], Richard A. Palmer[1]*
[1] Department of Chemistry, Duke University, Durham, NC 27708-0346, USA
[2] Department of Pathology, Duke University, Durham, NC, 27708-0319, USA
[3] Department of Biomedical Engineering, Duke University, Durham, NC 27708-0086, USA
[4] Duke University Museum of Art, Durham, NC, 27708-0732, USA

Abstract

The noninvasive removal of encrustations and contaminants from aged polychrome statues with an innovative, low-energy Erbium:YAG (Er:YAG) laser was studied using spectroscopic methods. This study answers questions concerning the safety and effectiveness of the laser on painted stone surfaces. The samples included marble, limestone, and sandstone pieces. Fourier transform infrared (FTIR) spectroscopy on BaF_2 (barium fluoride) windows and on pressed KBr (potassium bromide) disks was used to study the substances that were ablated from the surfaces. Fragments from the surfaces before and after cleaning were investigated using FTIR-attenuated total reflectance (ATR) spectroscopy to identify any molecular changes due to laser-surface interactions. No significant changes to the underlying surfaces were found. These conclusions were confirmed using microphotograph comparisons of the surfaces before and after laser cleaning. X-ray fluorescence (XRF) analysis was used to confirm the elemental composition of the paint on the statues and of the material ablated from the surfaces. Results indicate that the laser did not induce chemical change in the stone, the patinas, or the polychrome surfaces, while effectively removing contaminants.

Introduction

Lasers were first introduced in art conservation in the mid 1970s when John Asmus used a ruby laser to remove lime from an encrusted da Vinci fresco in Florence [1]. Since then, a variety of lasers have been studied to determine the best balance between effectiveness and control. At present, the neodymium:YAG (Nd:YAG) laser is the most widely used in art conservation primarily due to its relative selectivity and efficiency. Indeed, comparison studies at different wavelengths have shown that irradiation at 1.064 μm, the fundamental wavelength of the Nd:YAG laser, appears to work best on sandstone surfaces[2]. However, studies by Cooper and Klein have indicated that the Nd:YAG laser can cause discoloration in both light marble and lead white pigment [3,4].
Given these results, an investigation of other lasers is warranted. The Erbium:YAG (Er:YAG) laser emits energy at a longer wavelength, 2.94 μm, than any other laser currently in use in conservation. It has been used for a variety of medical applications, such as skin resurfacing [5], and has recently been studied as a method for cleaning oil paintings [6,7]. This study examines the use of the Er:YAG laser to clean stone sculpture.
Stone works present several unique challenges to the conservator. Cleaning with acids or solvents can be especially damaging to the porous surfaces and the delicate pigments on the stone. Even when it is feasible to use such solvents, the complex composition of the dark crusts that can form on stonework can render the solvents ineffective [8]. Another class of damage is biodeterioration caused by lichens. The results of these growths are difficult to repair, and the traditional methods of cleaning are often as harmful as the lichen themselves [9,10]. Thus, one of the most exciting uses for lasers in art conservation is the removal of crusts, lichens, and other contaminants from the surfaces of delicate stone.
The emitting wavelength of the Er:YAG laser lies within the envelope of the broad N-H and O-H stretching absorptions. As a result, surface moisture, either naturally present or deliberately applied, effectively "stains" the surface, absorbing the laser energy in explosive vaporization, and the associated contaminants are micro-steam distilled from the surface[11]. In addition to this efficient and selective physical removal mechanism, the Er:YAG is intrinsically safe in that its energy (at about 0.4 eV) is well below the threshold for photochemical damage (the breaking of bonds), and the strong OH/NH absorption assures penetration depth is limited to 1-2 microns [6].

Experimental Section

Sculptures
Four pieces were studied (Figure 1):

Figure 1. Works examined during study. Clockwise from top left: Madonna and Child, Roman Entablature, Head of Man, Head of Apostle.

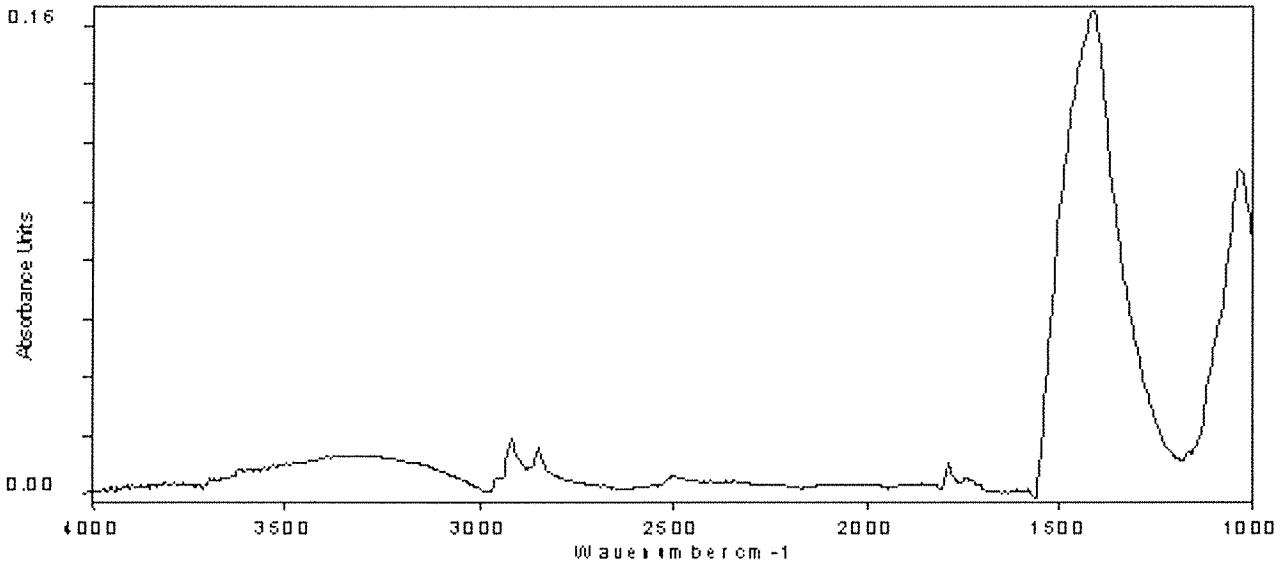

Figure 2. FTIR spectrum of material ablated from the Roman Entablature.

Roman Entablature
This is an approximately 1 m long fragment of a 2nd century AD Carrara marble entablature with some black veining. Samples of ablated material were taken on calcium fluoride (CaF_2) windows.

Madonna and Child
This is a 16th century Italian marble statue of the Madonna holding her infant. The polychrome surface has traces of white, pink, and red pigments as well as gold leaf. A grey film covers the surface. Samples of ablated material were taken on CaF_2 and barium fluoride (BaF_2) windows.

Head of Apostle
This is a 14th century French limestone piece. The polychrome surface has traces of brown, red, pink, white, and black pigments. The colors are obscured by a discolored layer of egg white. Samples of ablated material were taken on CaF_2, BaF_2, and potassium bromide (KBr) windows.

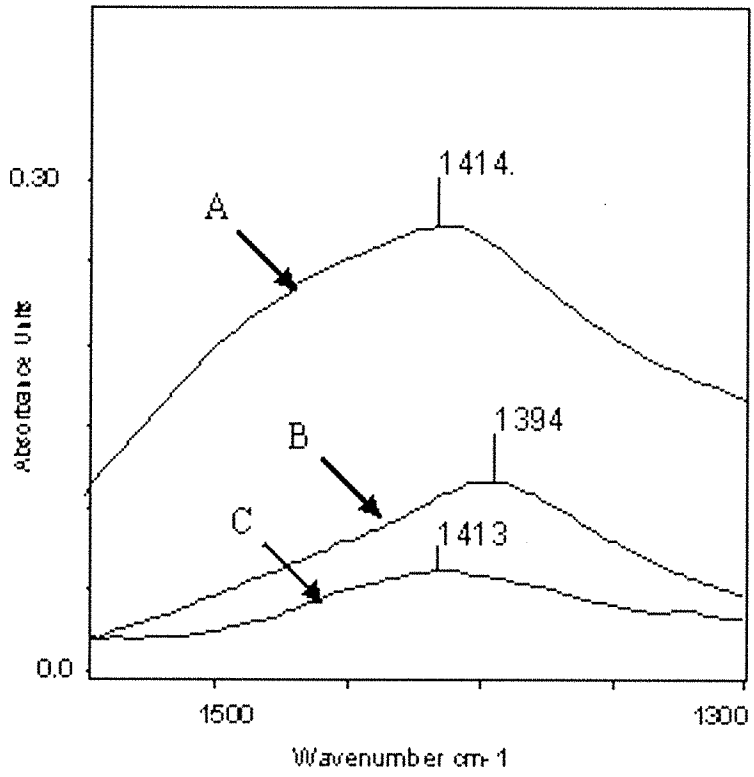

Figure 3. Comparison of spectra from the Roman Entablature. A. FTIR spectrum of material ablated from Roman Entablature. B. FTIR-ATR spectrum from small piece after ablation. C. FTIR-ATR spectrum from small piece of uncleaned calcite.

Head of Man: This is a 13th century French sandstone piece. It was found buried and has suffered from significant deterioration due to biological growths. It is encrusted with several varieties of lichen and with mud. Samples of ablated material were taken on CaF_2 and KBr windows.

Methodologies

Samples were taken during the cleaning of the sculptures with the laser. Two Er:YAG lasers, delivering energy at 2.94 μm (0.4 eV), were used in the cleaning process. These lasers and their specifications are described in greater detail by de Cruz [12]. The Mona Laser Conservator 2940 and the High Power Erbium Crystalase, both manufactured by Schwartz Electro Optics emit a 250 microsecond macropulse. This macropulse consists of 1-2 microsecond duration micropulses 12-14 microseconds apart. The only difference between the two lasers is the maximum power levels and delivery system. For the removal of mineral encrustations and lichens energies used varied from 96-126 mJ/pulse, focused at 1 mm^2 at 15 Hz. In the absence of mineral encrustations, the energy used varied from 12-15 mJ/ pulse. In some cases, the surfaces were dampened with water or dilute ammonium hydroxide, which act as thermal stains marking the materials for removal (see above). The sampling technique used in this study allows for a minimum of sample preparation for spectroscopy. To collect ablated material CaF_2, BaF_2, or KBr

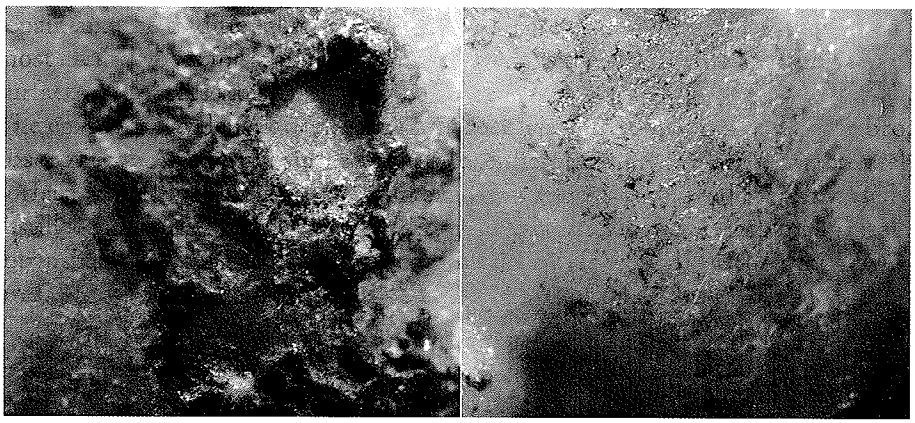

Figure 4. Microphotograph of Roman Entablature before (left) and after cleaning.

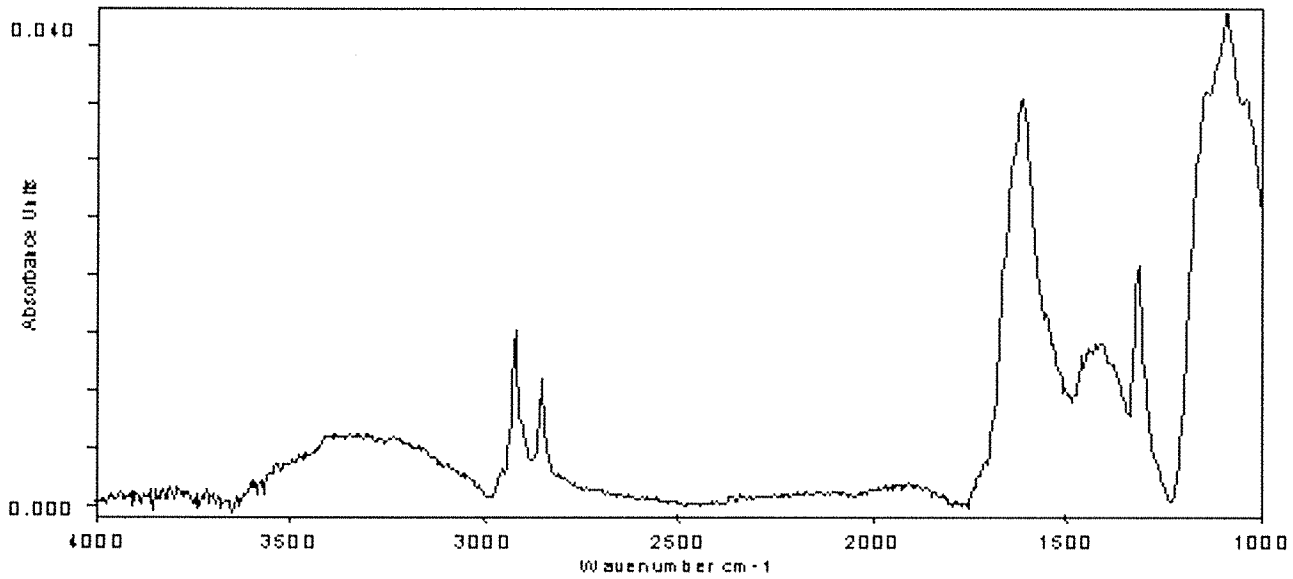

Figure 5. FTIR spectrum of material ablated from a painted section of the Madonna and Child.

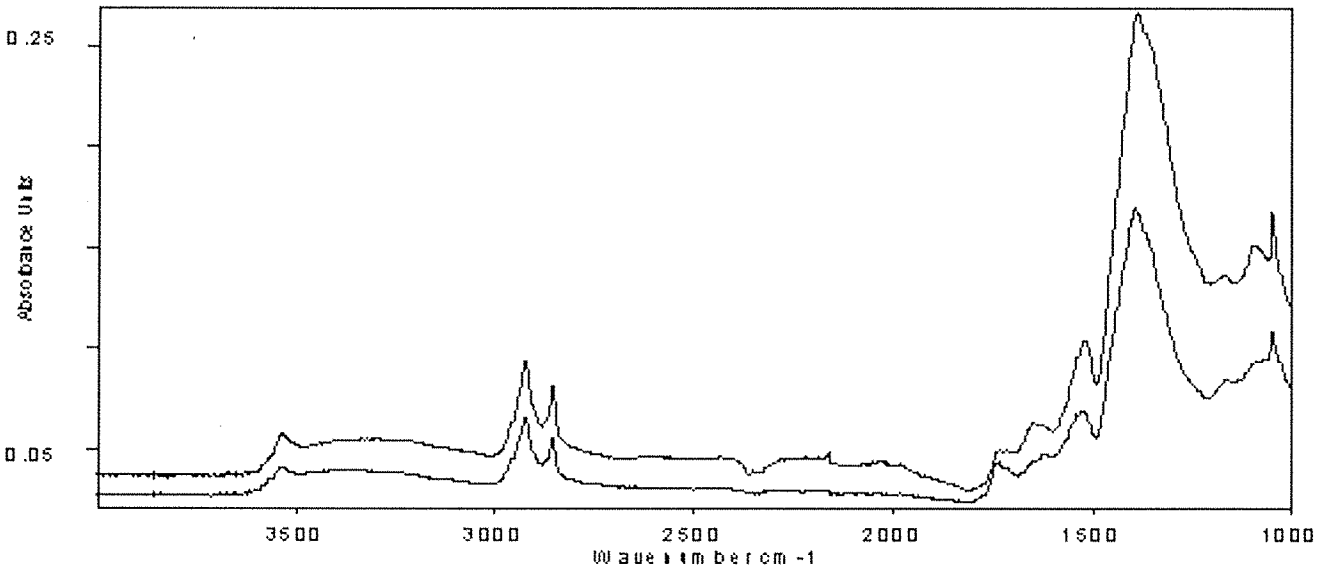

Figure 6. FTIR ATR spectra taken of a small fragment from the surface of the Madonna and Child before (top) and after laser ablation.

windows were placed between the laser and the surface during ablation with the window within 1 mm of the surface to be ablated. As the materials are ablated from the surface, they are collected on the undersurface of the window. The windows are approximately 25 mm in diameter and 3 mm thick. The window materials were chosen for their transparency in the IR region. KBr has the largest transparency window in our spectral region of interest; however, its hygroscopicity and relative fragility are drawbacks in working with rapid evaporation techniques. CaF_2 and BaF_2 were found to be much more useful in this technique despite more restrictive low-energy cutoff (1000 and 800 cm^{-1}, respectively, versus 400 cm^{-1} for KBr). Infrared transmission spectra of the ablated material were measured directly on the collection windows by use of a Bruker IFS 66 v/s Fourier transform infrared (FTIR) spectrometer with OPUS-NT 3.1 software. The instrument is equipped with a KBr beamsplitter and a DTGS detector. The aperture was set at 5 mm. The resolution was set at 4 cm^{-1}, and 32 scans were taken for each spectrum. A baseline correction was performed on each spectrum.

Samples were also taken from the surfaces before and after laser ablation. The samples were taken by the conservator with a scalpel and collected in separate glass vials. These samples were approximately 1 mm in diameter. They were analyzed

with FTIR-ATR spectroscopy by placing the samples (with the exposed surface of the sample face down) on the internal reflectance element (IRE). A Teflon tip was tightened down over the sample to ensure good contact between the samples and the IRE. The instrument used for these measurements was a Nicolet Avatar 360 E.S.P. FTIR spectrometer fitted with a Smart MIRacle ATR attachment. Omnic E.S.P. 5.1 software was used to calculate and display the spectra. The ATR attachment employs a single reflection diamond IRE with a 2 mm diameter sampling area. Spectra were taken with 32 scans at 4 cm^{-1} resolution. The spectra were later transferred to OPUS software to ensure a uniform display. No baseline correction was performed.

X-ray fluorescence (XRF) spectra of removed materials were measured to provide elemental analysis data. Material ablated from the surface of the *Roman Entablature* was analyzed directly on a calcium fluoride collection window. In order to reduce charging in the sample due to the electron beam, the window was coated with an evaporated gold layer. Samples taken directly from the surface of the *Madonna and Child* were also examined with XRF. The samples removed with the scalpel were attached to aluminum stubs with double sided carbon tape to reduce charging. Analysis was performed with a Jeol 6400 scanning electron microscope with a Gresham energy dispersive 30 mm^2 ATW x-ray detector and a pulse processor manufactured by 4pi Analysis. Interpretation was done on a Macintosh G4 computer with 4pi Analysis Revolution software. Mapping and imaging of the surface was done with ImagnSpec software.

***Results*:**

Roman Entablature.

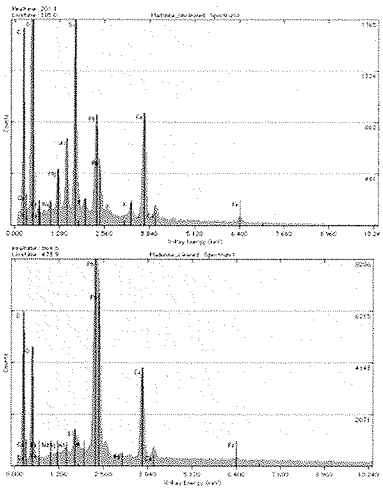

Figure 7. XRF spectra of fragment from Madonna and Child before (top) and after cleaning.

Material was ablated onto CaF_2 windows at 126 mJ/pulse. The FTIR spectrum of the ablated material (Figure 2) shows several significant peaks at 2497, 1791, and 1415 cm^{-1}. Also present is the broad O-H/N-H absorption centered at 3318 cm^{-1} and a peak at 1033 cm^{-1}, in addition to hydrocarbon peaks at 2918 and 2848 cm^{-1}.

Figure 3 shows a comparison of three spectra from material taken from the *Roman Entablature*. Spectrum A corresponds to an FTIR spectrum of material ablated from the surface. Spectrum B is the FTIR-ATR spectrum of a fragment from an area cleaned of encrustation. Spectrum C is a FTIR-ATR spectrum of a fragment from an uncleaned area of the work. In spectrum B, the most intense peak is seen at 1394 cm^{-1}, while the ablated material shows the peak shifted to 1414 cm^{-1}. The sample from the uncleaned area also shows a strong peak at 1413 cm^{-1}. The microphotographs from before and after laser cleaning (Figure 4) show the surface with and without the dark crust.

Madonna and Child

Material was ablated onto CaF_2 and BaF_2 windows at 13-15 mJ/pulse. Samples were ablated either dry or after dampening (effectively staining) the surface with dilute ammonium hydroxide.

The spectrum of material ablated from the dry painted surface (Figure 5) shows notable peaks at 1616, 1415, 1315, 1149, and 1091 cm^{-1}. Figure 6 shows the FTIR-ATR spectrum of fragments taken before and after laser ablation. Several differences between the spectra are worth noting. Specifically, the peak at 1616 cm^{-1} is significantly diminished in the spectrum of the sample taken after cleaning. Also, the peak that was seen at 1090 cm^{-1} in the spectrum of the uncleaned surface becomes a shoulder centered at 1100 cm^{-1} in the spectrum of the cleaned surface. The peak at 1540 cm^{-1} is much smaller in the spectrum of the surface after ablation. In addition, the peak at 1415 cm^{-1} is also much weaker.

XRF spectra (Figure 7) of the samples before and after cleaning show a remarkable difference in the relative amounts of contaminants. Aluminum and silicon both decreased precipitately in the spectrum of the cleaned surface.

Head of Apostle

Samples were ablated from the *Head of Apostle* onto CaF_2, BaF_2, and KBr windows at 12-15 mJ/pulse. These samples were taken from areas on the neck and the cheek.

Figure 8 shows the FTIR transmission spectrum of the ablated material from the Head of Apostle. Hydrocarbon peaks at 2915 and 2848 cm^{-1}, which were seen in many spectra of ablated material, were seen here as well; however, the relative peak heights were much higher in this case. The strongest absorbance was at 1620 cm^{-1} with other peaks at 1317, 1160, and 1091 cm^{-1}.

A comparison of the FTIR-ATR spectra from samples taken before and after ablation (Figure 9) shows several

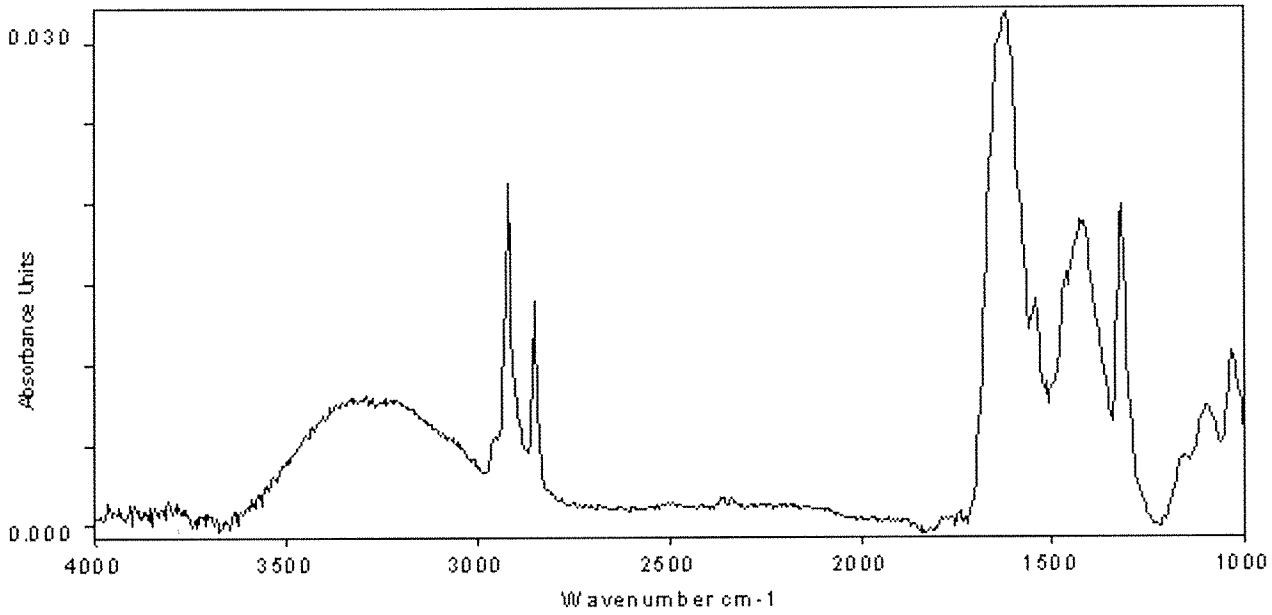

Figure 8. FTIR transmission spectrum of material ablated from Head of Apostle.

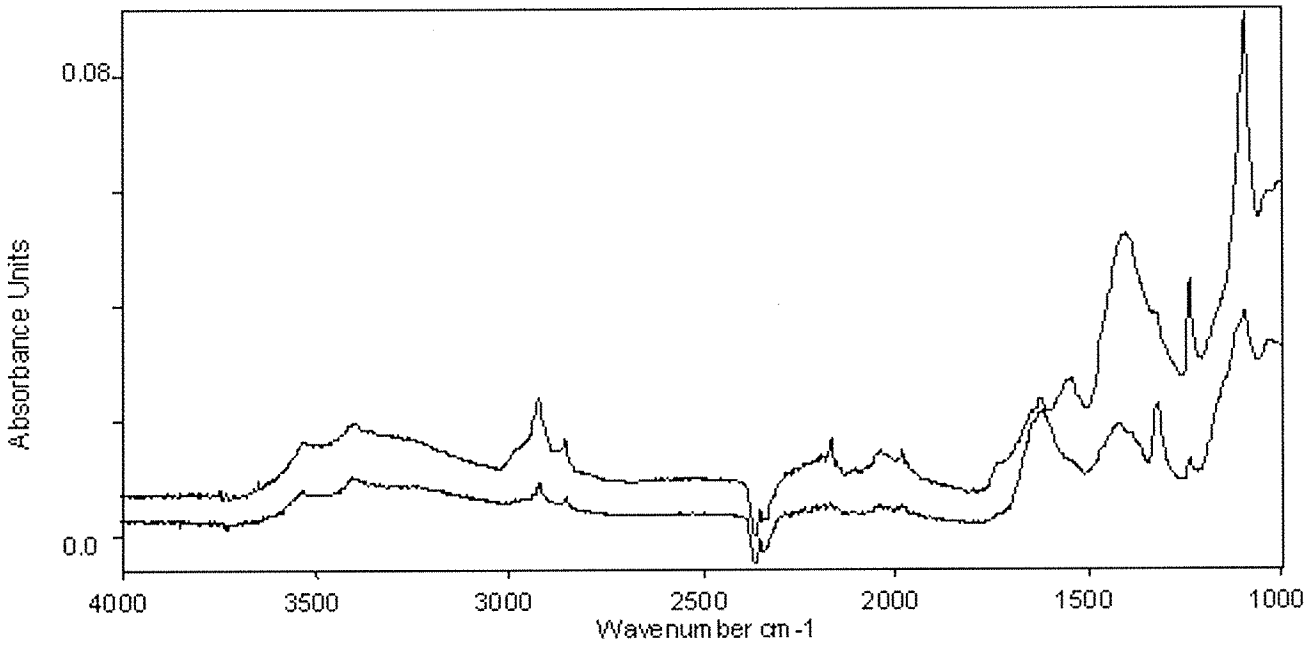

Figure 9. FTIR ATR spectra of small piece taken from Head of Apostle before (top) and after laser cleaning.

changes after laser cleaning. The peak seen at 1541 cm^{-1} in the spectrum of the material from the uncleaned surface is not seen in the spectrum of the cleaned surface. Also, the hydrocarbon peaks at 2919 and 2857 cm^{-1} are both diminished. A peak at 1236 cm^{-1} is also reduced in the spectrum from surface exposed to laser radiation. The large C-O peak at 1398 cm^{-1} has shifted to 1415 cm^{-1}. This peak also was diminished, allowing the shoulder at 1317 cm^{-1} to become a well-resolved peak.

Head of Man

Material was ablated from the surface onto CaF_2 windows at 96-115 mJ/pulse. Samples were taken from various areas of the surface where there were several different types of lichen that had attached to the stone.

The ablated material produced a complex spectrum (Figure 10). A very strong absorbance is seen at 1659 cm^{-1} with a shoulder at 1541 cm^{-1}. There is also a very strong, broad absorbance at 3288 cm^{-1}. Several peaks are also seen

between 1167 and 1030 cm^{-1}. In addition to the C-O peak seen at 1414 cm^{-1}, there is also a shoulder at 1461 cm^{-1}. Samples removed from the surface with a scalpel showed the extent of the lichen growth (Figure 11). We attempted to remove the lichen without sampling the stone. The spectrum of this sample shows peaks at 3288, 1659, 1541, 1461, 1414, 1167, 1030 cm^{-1} whereas the spectrum from the cleaned fragment has only a peak at 1410 cm^{-1}.

Discussion

The *Roman Entablature* data show the effects of the laser on a patina marble surface. The shift in the C-O peak from 1415 to 1394 cm^{-1} (Figure 3) initially indicates that the laser is causing a change in the nature of the stone; however, the spectrum of the sample from the uncleaned marble shows that to be false. Both the uncleaned marble and the material ablated from the surface of the marble gave the same peak position for carbonate (the peak at 1415 cm^{-1}). Since both the ablate and the uncleaned marble have the same peak position while the spectrum of the cleaned

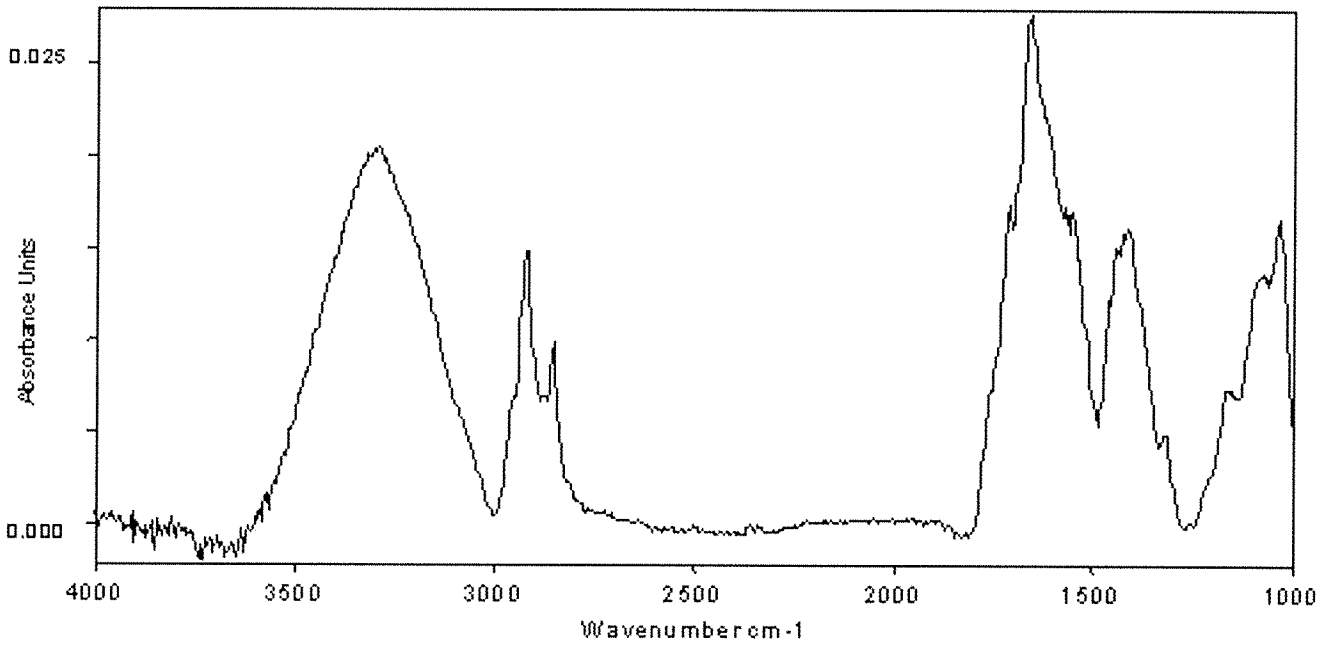

Figure 10. FTIR spectrum of material ablated from lichen encrusted area on Head of Man.

marble gives a peak at 1394 cm^{-1}, it is clear that the shift is due to the removal of the calcite extrusion. Removing this material leaves the original marble underneath (Figure 4).

Other materials that were contained in the encrustation were removed as well. Specifically, the broad absorption seen at 3318 and the peak at 1033 cm^{-1} in the ablated material are associated with components of the soil embedded in the calcite encrustation that was removed from the piece during cleaning. The spectrum of aluminosilicates, such as kaolin, the major component of soil, shows both the broad absorbance due to hydration and the 1033 cm^{-1} peak due to Si-O stretching [13]. Finally, the hydrocarbon peaks may be due to either soot or to organic material in the soil.

The spectrum of the ablated material from the *Madonna and Child* (Figure 5) indicates that the laser has removed several contaminates. The 1616 and 1149 cm^{-1} peaks correspond to calcium sulfate dihydrate, gypsum. Gypsum forms on calcareous stone when that stone is in the presence of sulfur and nitrogen oxides and moisture. Also, the 1315 cm^{-1} peak is characteristic of whewellite. Whewellite, calcium oxalate monohydrate, forms as the result of biodeterioration of stone or from the degradation of pigments. A comparison of the spectra of the surfaces before and after ablation further indicates that the substrate was not damaged during cleaning (Figure 6). The absorbances corresponding to the polychrome do not change significantly in the cleaned spectrum as seen in the hydrocarbon peaks, hydroxyl band, and peaks related to carbonyl stretching at 1730, 1648, and 1101 cm^{-1}. However, the XRF data (Figure 7) clearly reveal the difference between the uncleaned and cleaned surfaces. In the spectrum from the uncleaned sample, aluminum and silicon are the most abundant elements besides calcium, oxygen, and carbon. This is due to the presence of aluminosilicates. The XRF spectrum of the cleaned surface shows a dominant lead peak while the levels of aluminum and silicon are now relatively insignificant. Contaminants such as gypsum and whewellite have similar elemental composition to the marble itself and cannot be identified through XRF. However, XRF is a good complement to FTIR spectroscopy in this case. Together, the two methods provide a more complete

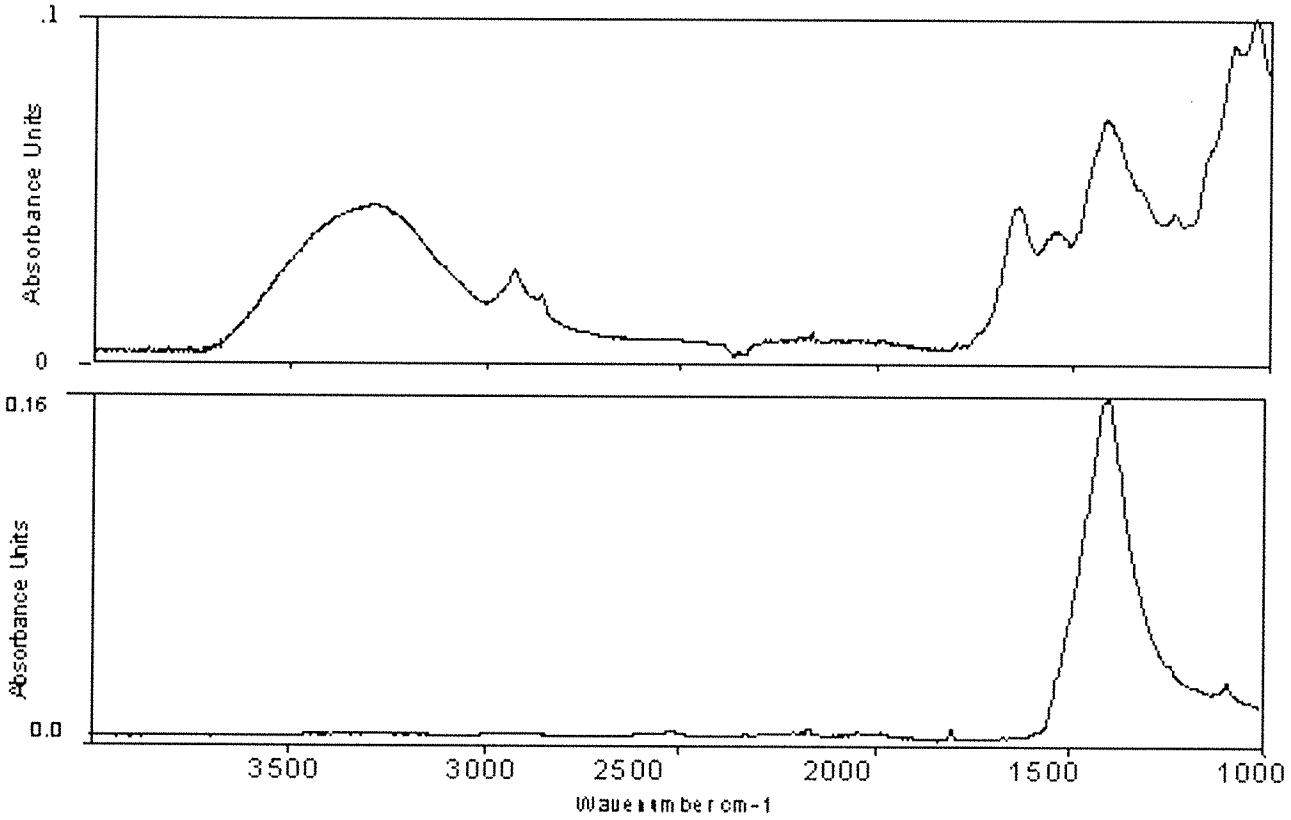

Figure 11. FTIR ATR spectra of small pieces taken from Head of Man before (a) and after (b) laser cleaning.

picture of the contaminants on the surface of the statue.

The data from the *Head of Apostle* demonstrate the Er:YAG laser's ability to selectively remove certain layers. When a trained conservator controls the laser, the contaminants can be removed one layer at a time leaving the original color surface unaltered. The strong hydrocarbon peaks in the spectrum of the ablated material (Figure 8) indicate that the discolored layer was removed from the surface. These bands, in addition to those at 1651, 1541, 1419, and 1236 cm^{-1} are consistent with a layer of egg emulsion applied over the color surface. The discoloration of this layer accounts for the degradation of the appearance of the piece. Such layers, embedded in the paint matrix are impossible to remove with solvents. In addition, the peaks at 1620, 1160 and 1091 cm^{-1} indicate that gypsum was also removed, and the peak at 1317 cm^{-1} is consistent with whewellite, which can form as the result of pigment degradation. The FTIR-ATR spectra also are consistant with the removal of gypsum and egg, as seen in the reduction of peaks at 1620 and 1160 cm^{-1} and 2916, 2849, 1541 and 1236 cm^{-1}. The characteristic whewellite peak at 1317 cm^{-1} is not reduced, however. This may be explained by reasoning that the whewellite is related to the pigment and would not be totally removed without removing pigment as well.

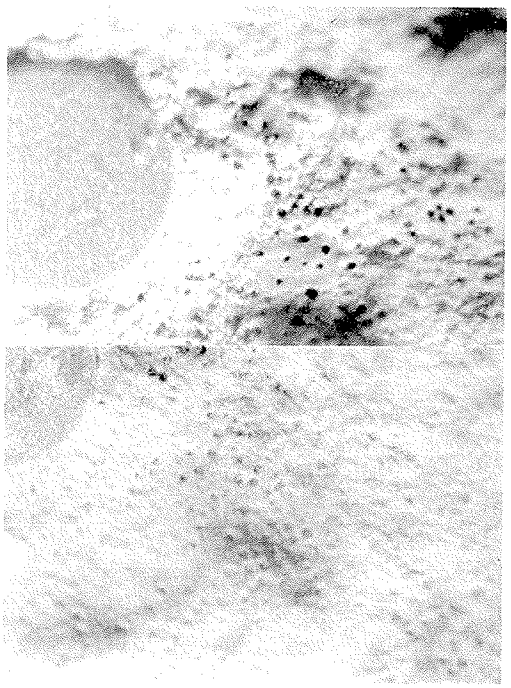

Figure 12. Microphotograph of Head of Man before (top) and after laser cleaning.

The stone of the *Head of Man* piece is weakened by the lichen growths. Burial has caused the lichens to grow extensively on the damp, calcareous surface (Figure 1). The spectrum of the ablated material clearly indicates that biological material was removed from the surface of the stone. For instance, amide bands at 1659 and 1541 cm^{-1} can be seen in the spectrum for the material ablated from a spot of grey lichen on the surface and indicate the presence of proteins and/or peptides (Figure 10). The peak for the NH stretching vibration is seen at 3288 cm^{-1}, and polysaccharide linkages are

seen in the three peaks from 1167 to 1030 cm^{-1}. In addition to the C-O peak seen at 1414 cm^{-1}, there are hydrocarbon peaks at 2917, 2850, and 1461 cm^{-1}. The ATR spectrum of material from the cleaned surface shows that the laser has removed all the lichen and other organic material (Figure 11b). Microphotographs of the surface before and after cleaning (Figure 12) also indicate that the surface has been completely cleaned of lichen.

Conclusion

The Er:YAG laser removed organic and inorganic materials from the sculpture safely and effectively. There was no discoloration or visible damage to either the stone or polychrome as a result of the ablation process. The stone surfaces appeared visibly smoother and cleaner after laser treatment. However, the pieces were not overcleaned, and retained the desired patina. In addition to the removal of inorganic films, we found the laser efficient at removing lichen growths. The results from this study show that the Er:YAG is a promising treatment for lichen damage. The FTIR spectra of ablated materials and spectra of samples before and after laser ablation combined with XRF spectroscopy provide convincing evidence of the nature of the ablated materials and of the mechanism of interaction between the laser and contaminants.

References

1. Asmus, J.F., 'Laser Technique for the divestment of a lost da Vinci mural', *Journal of Vacuum Science and Technology*, **12**(6), (1975) 1352-1355.

2. Klein, S., Stratoudaki, T., Marakis, Y., Zafiropulos, V., and Dickmann, K., 'Comparative Study of different wavelengths from IR to UV applied to clean sandstone', *Applied Surface Science*, **157** (2000), 1-6.

3. Cooper, M.I., Fowles, P.S., and Tang, T.T., 'Analysis of the laser-induced discoloration of lead white pigment', *Applied Surface Science*, **201** (2002), 75-84.

4. Klein, S., Fekrsanati, S., Hildenhagen, J., Dickmann, K., Uphoff, H., Marakis, Y., and Zafiropulos, V., 'Discoloration of marble during laser cleaning by Nd:YAG laser wavelengths', *Applied Surface Science*, **171** (2001), 242-251.

5. Alster, T.S., and Bettencourt, M.S., 'Review of cutaneous lasers and their applications', *Southern Medical Journal*, **91**(9), (1998), 806-814.

6. Colombini, M.P., Andreotti, A., Lanterna, G., and Rizzi, M., 'A novel approach for high selective micro-sampling of organic painting materials by Er:YAG laser ablation', *Journal of Cultural Heritage*, **4**, (2003), 355-361.

7. de Cruz, A., Hauger, S.A., and Wolbarsht, M.L., 'The role of lasers in fine arts conservation and restoration', Optics and Photonics News **10** (7), (1999) 36-40.

8. Nord, A.G., and Ericsson, T., 'Chemical analysis of thin black layers on building stone', *Studies in Conservation*, **38** (1993), 25-35.

9. Seaward, M.R.D., 'Lichens, agents of monumental destruction', *Microbiology Today*, **30** (2003), 110-112.

10. Warscheid, Th., Braams, J., 'Biodeterioration of stone: a review', *International Biodeterioration and Biodegradation*, **46** (2000), 343-368.

11. de Cruz, A., Hauger, S.A., and Wolbarsht, M.L., 'The role of lasers in fine arts conservation and restoration', Optics and Photonics News **10** (7), (1999) 36-40.

12. de Cruz, A., Wolbarsht, M.L., Palmer, R.A., Gillikin, A.M., Pierce, S.E., Hauger, S., Adamkiewicz, E., 'Er:YAG laser applications on marble and limestone sculptures with polychrome and patina surfaces', *Lacona V, Osnabrueck, Germany, Sep. 2003*.

13. Pouchert, C. J., *Aldrich Library of FT-IR Spectra*, Aldrich Chemical Co., Milwaukee (1985).

A Fast Procedure for Fake Euro Notes Identification Based on FTIR (ATR) Technique. An Example of Prints Characterization.

A. Vila[1], N. Ferrer[2], J. Mantecón[3] and J.F. García[1]
[1] Departament de Pintura, Conservació-restauració. Facultat de Belles Arts, Universitat de Barcelona.
[2] Unitat d'espectroscòpia molecular. Serveis Científico-Tècnics. Universitat de Barcelona.
[3] Brigada de Policía Científica. Cuerpo nacional de policia.

Abstract

January 1st of 2002, the Euro was introduced as common money in many countries of the European Union. These "popular prints", composed by color inks and paper and printed as a litography, are produced by the central banks of Austria, Belgium, Finland, France, Greece, Italy, Netherlands, Portugal, Spain, Sweden and Germany. Euro notes include many security measurements but reports of the European Central Bank inform that quantity and quality of the fakes notes increase and improve each semester. Among the different values, the most widely reproduced is the 50 Euros note.

A fast and non-destructive procedure for fake notes identification by using the FTIR (ATR) microscopy that can be applied "in situ" is presented. The reproducibility of 50 Euro notes production is studied and the infrared spectra of seven locations on the note have been established. Results obtained with original notes have been compared with those of fake notes, clear differences have been found among them. Notes of 100 Euros have also been studied.

The Application of Infrared Spectroscopy to the Analysis of a Degraded Rubber Sculpture

Susan Lake[1] and Walter Hopwood[2]

[1]Hirshhorn Museum and Sculpture Garden, Smithsonian Institution, Washington, D.C.
[2]Smithsonian Center for Materials Research and Education (SCMRE), Suitland, Maryland

Abstract

Infrared spectroscopy (FTIR), in conjunction with Py-GC-MS and SEM-EDS, of samples from Paul Thek's *Fishman*, a degraded latex sculpture, was used to identify the rubber and its additives. FTIR spectra of solvent extracted samples taken from the exposed exterior and protected interior portions of the rubber gave insight into the process of oxidative degradation.

Introduction

Fishman, a hollow cast rubber sculpture made in 1968 by American artist Paul Thek, was already in poor condition when it was acquired by the Hirshhorn Museum in 1990. Recently, the deterioration has accelerated and the sculpture has become so brittle and disfigured by structural cracks and losses that it no longer can be exhibited suspended, as intended by the artist (fig 1). The dramatic change in condition of the sculpture over a relatively short period of time prompted this analytical study, with the goal of eventually assessing a course of treatment and a preservation strategy. As infrared spectroscopy is the form of instrumentation most readily available to the Hirshhorn Museum and as the museum has recently acquired several other rubber objects, the study also was undertaken to determine whether or not infrared analysis can be employed to answer a series of basic questions. Is the rubber material natural or synthetic? Because synthetic rubbers do not always react in the same way as natural rubbers, a preservation strategy for one may be inappropriate for the other. What is the likely aging mechanism of the rubber? Are additives included in the rubber? Additives will affect the rubber properties, including aging mechanisms.

Figure 1. Paul Thek, *Fishman*, 1968. Hirshhorn Museum and Sculpture Garden, Smithsonian Institution (Photograph taken in 1990)

The Hirshhorn's *Fishman* is one of four nearly identical casts made by Thek. Each is a cast of the artist's almost nude figure with attached fish forms. Each is a surviving element from large-scale temporary installations that Thek created while working in Europe, where he lived for nearly a decade [1]. Two of the sculptures are located in the Diözesanmuseum, Cologne, Germany and the other is in the Kunstmuseum, Lucerne, Switzerland. The Lucerne sculpture was damaged by smoke from a fire and was extensively restored in 1996 [2]. The Cologne versions, one that is painted and the other that is similar to the Hirshhorn version, are in relatively good condition.

Construction and Condition of *Fishman*

Examination of the Hirshhorn *Fishman* indicates that it was cast in pieces, each part made from plaster molds taken from various parts of the artist's figure into which liquid latex was poured and allowed to set. The thickness of the latex film ranges from 1.5 to 4.0 mm. Pieces of woven fabric visible in places along the edges of the rubber indicate that the rubber may have been reinforced with an embedded gauze-like material. Once cast, the latex elements were

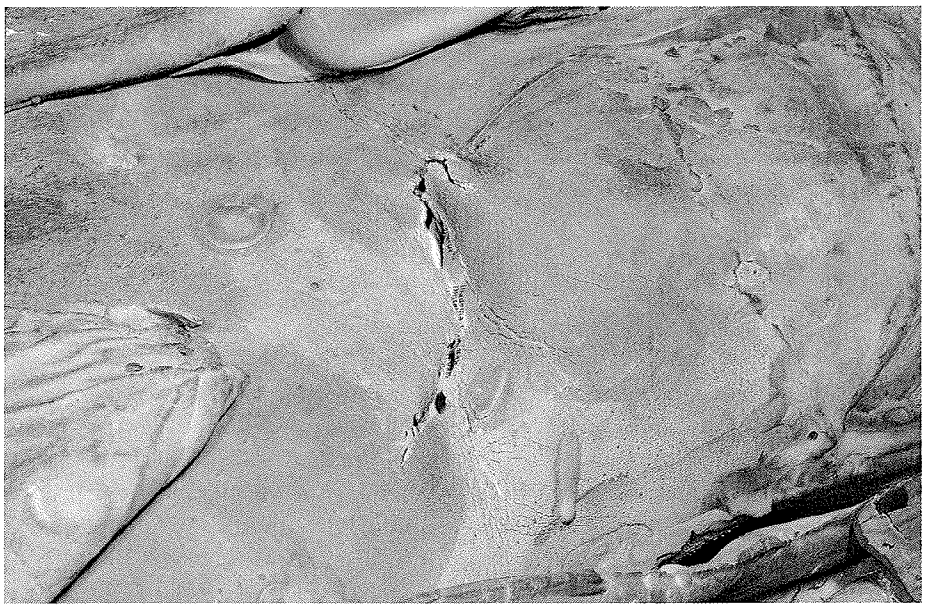

Figure 2. *Fishman*, detail of torso showing breaks in the rubber

assembled to form the figure and the abutted or overlapping seams were attached using liquid latex. The fish were apparently made by the same process and attached in the same way. The flexible latex shell has been stuffed with pieces of wadded newspaper to lend it form. Narrower parts of the interior, most notably, the fingers and toes, were stuffed with cotton batting. Most of the fish do not appear to have an interior stuffing. The figure also has a metal armature inserted down its length.

The exhibition history and old condition reports of Fishman are not available. Scant existing records indicate that the sculpture was originally flexible and probably light beige in color. It is now unevenly discolored, ranging from an ochre-like yellow to dark reddish brown. The rubber itself is hard to the touch and so brittle that exposed, thinner pieces easily snap off. Two fingers on the figure's right hand are missing, portions of most of the toes are broken, and stress cracks are visible throughout the figure. Damage is most apparent along the figure's neck and waist, both regions that would have been flexed during repeated installation. In these areas, wide splits in the rubber that extend through the film depth expose the interior newspaper and cotton batting (fig 2). Many of the once rounded fish forms are now flattened where the unsupported rubber had collapsed and is now permanently deformed.

Natural Rubber and Its Degradation

Natural Rubber, polyisoprene, is a gum resin exudation of a variety of trees and plants with unique properties, after processing, of deformation (elongation) and elastic recovery. It is a long chain, high molecular weight hydrocarbon formed by the regular end-to-end linking of the isoprene monomer (2-methyl 1,3 butadiene). The polymer chains in the raw material, or crude stage, are not significantly cross-linked and, as a result, the elastomer is thermoplastic – soft and sticky when warm and firm when cold – with little resiliency and practically no strength. When heated with sulfur, a process known as vulcanization, the chains are cross-linked by the formation of covalently bonded sulfur bridges, using the double bond available in the isoprene unit. The result is a more rigid, insoluble material with properties less affected by temperature changes. The degree of cross-linking that occurs between the sulfur and the carbon atoms determines many of the elastomer's properties. Ordinary soft, flexible rubber contains only 3-6% sulfur. When as much as 40% sulfur is added, the material is a hard, rigid product. Additionally, rubber may contain plasticizers/oils, antioxidants or antiozonants, pigments, and fillers such as chalk, clay, and barites [3].

Rubber, even when vulcanized, contains a high proportion of double bonds in the polymer backbone that are the preferred sites for degradation mechanisms involving oxidation reactions and the action of ozone. Exposure to light (ultraviolet and high energy radiation), in particular, tends to accelerate the deterioration. Humidity, heat, stress, and certain metals also have catalytic effects [4]. Most often the rubber object is subjected to several types of exposure simultaneously, which causes a rapid deterioration of its film properties.

Although the exact mechanisms of rubber degradation are complex, and still unclear, certain generalizations can be made. Oxidation and ozonation are initiated by free radicals that react with the carbon-carbon bonds of the natural rubber. Degradation may involve reduction in the length of the elastomer chains to give lower molecular weight products. Oxidation may also bring about increased cross-linking similar to the vulcanization of rubber, resulting in a three-dimensionsl structure and/or higher molecular weight. This process introduces C-O-C and C-O-O-C cross-links between and within the polymer chains, while another set of reactions between the sulfur atoms of the vulcanized rubber and oxygen breaks the cross-links [5]. Chain scission causes the tensile strength of the rubber to drop rapidly and its surface to become soft and sticky. Increased cross-linking causes the rubber to become hard and

brittle and loose its elastic properties. As a result, the rubber begins to crack at the surface. In general, the two reactions occur simultaneously. The nature of the polymer, the influences of temperature, light, and metal catalysts will determine whether chain scission or cross-linking predominates. Additionally, rubber is susceptible to stress cracking, especially in the presence of oxygen. Strain applied to an oxidized rubber object stretches the polymer chains causing some of them to break. This creates a flaw in the surface and also produces a site at the ends of the broken chains that contribute to future oxidative degradation [6].

Experimental

This study began with an in-depth technical examination of *Fishman* using a stereomicroscope for high-magnification study of the surface to gain useful information concerning the construction and condition of the sculpture. Due to the brittle condition of *Fishman*, many broken and flaking pieces of rubber were available for examination and analysis. The stereomicroscope was also used to examine pieces of rubber spall in cross-section. For infrared spectroscopic analysis, microsamples of rubber were placed onto a diamond anvil cell and compressed separately to form thin films. Additionally, samples from different depths of rubber spall were immersed for three days in 1,2-dichloroethane at room temperature. The supernatant liquids were applied drop wise to a diamond window. Upon evaporation, thin films suitable for infrared spectroscopy formed. The instrument used was a Mattson 4326 Upgrade Fourier-Transform Infrared Spectrophotometer/Spectra Tech IR Plan Microscope. Data were collected at 8 wavenumbers resolution for three minutes. Five samples from various parts of *Fishman* were analyzed using pyrolysis gas chromatography-mass spectrometry to confirm the infrared analysis. The instrument used was a CDS Analytical Pyroprobe 2000 coupled to a Varian Saturn 2000 GC/MS consisting of a capillary GC and an ion trap mass spectrometer. Samples were placed in a quartz boat, inserted into the platinum coil filament of the probe that in turn was inserted into the helium purged probe oven held at 310°C interfaced to the GC. No derivatizing reagent was used. The samples were pyrolyzed at 600°C for 10 seconds and transferred to the capillary column (VA-5; 30 m x 0.25 mm i.d.; 0.25 micron film thickness; He flow of 1.2 ml/min; splitless). The temperature program of the GC was 5 minutes at 40°C followed by a ramp at 10°C/min to 300°C and 10 minutes at 300°C. Operating conditions for the ion trap were: trap 220°C, manifold 80°C; electron multiplier 1780 V; scan range 45-600 amu; scan time 1 second; data analysis Saturn GC/MS Workstation 5.51.
Several of the rubber spalls were also analyzed using scanning electron microscopy/energy-dispersive spectroscopy (EDS) to confirm the inorganic elements present in the rubber. The instrument used was a JEOL JXA-840A scanning electron microscope (SEM) with a Thermo NORAD TN-5502 energy-dispersive x-ray analytical attachment and NORAD Vantage spectrum processing software. The system is fitted with a low atomic number detector (Pioneer Premium detector with a Norvar window). Spectra were obtained at 20 kV for a 60-s live-time acquisition. Elemental spectra were acquired for four areas of each sample.

Results of Analysis

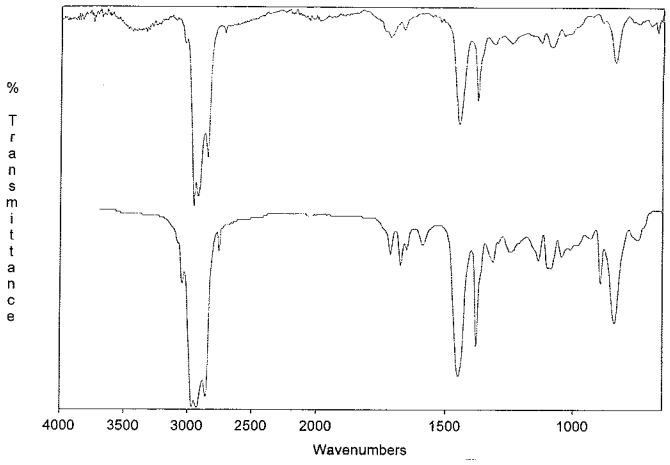

Figure 3. Top: isoprene standard: poly (1-methyl-l-cis-butylene)
Bottom: sample from *Fishman*, solvent extraction

FTIR analysis of all of the samples pressed neat onto the diamond cell gave spectra that indicate only the presence of an inorganic additive to the rubber, specifically calcium carbonate. Scrapings of the white "bloom" on the surface of the sculpture matched spectra for calcium sulfate, probably a residue of the casting process. Centrifuged solvent extracts of the rubber samples, which successfully removed the inorganic components, gave characteristic spectra for isoprene (fig. 3). As the infrared spectra of many rubbers, natural and synthetic, are similar, PY-GC-MS was used to confirm the identity. The samples produced peaks for terpenes and limonene, components of natural rubber. The pyrograms were not helpful in identifying the natural rubber oxidative products. EDS spectra collected from the different sites of the

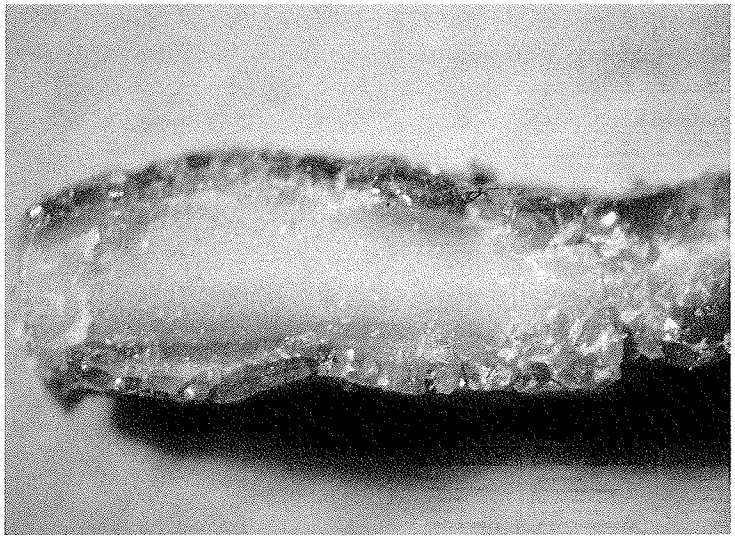

Figure 4. Unmounted cross-section from rubber spall, 2 mm thick

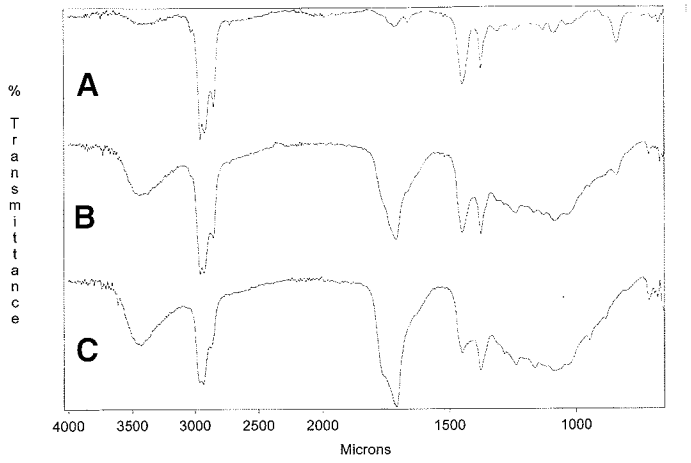

Figure 5. Solvent extracts of samples taken from the cross-section shown in figure 4: a) still-rubbery interior; b) discolored exterior crust; c) brittle surface scraping

three samples were all similar, showing a relatively even distribution throughout the rubber matix of significant amounts of calcium and smaller amounts of sulfur, aluminum and silicon. The characteristic peaks of calcium confirm the FTIR analysis and suggest that calcium carbonate was added as filler, probably by the manufacturer. The identity of this filler is significant because light-colored rubber articles are particularly susceptible to light-catalyzed oxidation [6]. The presence of aluminum and silicon indicate clay. None of the samples show the presence of copper, cobalt, manganese, or iron, metals that are known to accelerate the oxidative degradation of rubber.

Unmounted cross-sections of *Fishman's* rubber "skin" examined under the stereomicroscope all show that the exposed surfaces of the latex are significantly darker and harder than the interior regions of the same sample. Fig. 4 shows a 2 mm thick sample that has upper and lower edges that are so brittle that they shatter when cut with a scalpel. These exposed areas of the latex are discolored, progressing from dark brown on the outer surfaces to golden yellow about 0.5 mm into the sample. By contrast, the inner portion of the sample is light beige and elastic, still deforming with pressure and recovering when it is released.

Fig. 5 shows the FTIR spectra of three solvent extracts taken from the cross-section in fig. 4, each showing significantly different oxidative levels of a single sample. Spectrum (a) of the still-soft interior portion of the sample shows the olefin peaks of the rubber backbone ($R_2C=CHR$) at 3035 cm^{-1}, 1660 cm^{-1}, and 835 cm^{-1}. The intensity of these peaks has diminished in spectrum (b) of the hard, discolored crust. In spectrum (c), a surface scraping of the very brittle surface, these peaks have disappeared altogether. This suggests a reduction of double bonds along the isoprene backbone. Instead, oxidation products have appeared. A broad hydroxyl band occurs at 3035 cm^{-1}. Broad absorption bands in the fingerprint region between 1000-1300 cm^{-1} are presumably due to stretching C-O bonds in the C-O-C fragment and to the skeletal vibration of C-CO-O in esters. The small carbonyl band at 1720 cm^{-1} in spectrum (a) broadens and shifts to 1710 cm^{-1} in the two more oxidized samples, becoming the predominant functional group. This indicates that significant ether, aldehyde, ketone, and/or unsaturated ester groups and carboxylic acids are produced by the oxidative process. Also of interest is the shift in intensity of peaks at 1450cm^{-1} and 1377cm^{-1}. In the sample of the rubbery interior, the peak at 1450 cm^{-1} is larger than that at 1377 cm^{-1}. In the spectrum of the oxidized exterior "crust" these two peaks are nearly the same size. In that of the brittle surface scrapping, the peak strengths are reversed, with the one at 1377 cm^{-1} becoming larger than that at 1450 cm^{-1}. The shift in the relative sizes of these peaks may be due to the saturation of the double bonds along the polymer backbone [7]. It also is caused by the greater bending deformation of the C-H bands at 1377cm^{-1} when the olefin bonds are converted to carbonyl containing structures in the more highly oxidized samples [8].

Conclusion

Infrared spectroscopic analysis of solvent extracts from *Fishman* was used to identify the base polymer of the sculpture as isoprene. Gas chromatography was necessary to determine that it was natural rubber. The samples taken

from different depths of the rubber and dissolved in a solvent successfully traced the oxidative degradation of the rubber. While the exposed surfaces are the most oxidized, the interior regions of the rubber that are still structurally sound are somewhat protected from light and deterioration. The film or crust that is formed on the exposed surfaces of the rubber appears to protect the interior from air, serving to slow the rate of oxidation inside the material, even though the diffusion into the interior areas is not stopped completely. In the degradation process, the carbon-carbon double bonds in the isoprene backbone are oxidized to form ethers and carbonyl containing compounds (aldyhydes, ketones, acids, and esters). The infrared analysis is qualitative, giving the functional groups present in the reaction products. While no quantitative relationship is shown regarding the amounts of groups formed, it appears that certain of these groups are present in greater quantities than others. The exact process of oxidative degradation might possibly be followed more completely with Raman spectroscopy. Because the history of Fishman is largely unknown, it can only be surmised that the deteriorated state of the rubber in *Fishman* is the result of excessive exposure to light and mechanical tension during past exhibition.

Acknowledgements

Conservator Gwynne Barney has worked with rubber sculptures by Eva Hesse and shared the results of her research; Bernhard Matthäi, Conservator at the Diözesanmuseum, Cologne, provided a viewing of the unpainted *Fishman* in that collection; Chris Maines, National Gallery of Art, Washington, D.C., performed the Py-GC-MS analysis; Ron Cunningham (SCMRE) did the SEM-EDS analysis; Lee Aks, Hirshhorn Museum, took the digital photographs; Christopher Smith, Hirshhorn Museum, prepared the Photo Shop presentation and assisted in the layout of this manuscript; Irmelle Small and Katharina Greier assisted in translations.

References

1. *Paul Thek/Processions*, Institute of Contemporary Art, University of Pennsylvania. Exh. cat.: Philadelphia, Pennsylvania, 1977.

2. Scheidemann, Christian M., "Paul Thek, *Fishman*, 1968," *Zeitschrift für Kunsttechnologie und Konservierung* 10 (1996) 286-293.

3. Blank, Sharon D., "Rubber in Museums: a Conservation Problem," *AICCM Bulletin* 14 (1988) 53-87.

4. Augustana Research Foundation, *Study of Reaction of Ozone with Polybutadiene Rubbers, Report No. 5*, Rock Island, Illinois, 1954.

5. Loadman, M. J. R., "Rubber: Its History, Composition, and Prospects for Conservation," in David W. Grattan (ed), *Saving the Twentieth Century: The Conservation of Modern Materials, Ottawa, Canada, September 1991*, Canadian Conservation Institute (1993) 59-80.

6. Wake, W. C., Tidd, B. K., and Loadman, M. J. R., *Analysis of Rubber and Rubber-like Polymers*, Applied Science Publishers, London, 1983.

7. Salomon, G. and Van der Schee, "Infrared Analysis of Isomerized, Vulcanized and Oxidized Natural Rubber," *Journal of Polymer Science* 14 (1954) 181-192.

8. Pouchert, Charles J., *Aldrich Library of Infrared Spectra*, Aldrich Chemical Co., Inc., 1970.

Identification of a Water Repellent Coating Applied on Stone Sculptures of Monumental of the Ducal Palace, Venice

Monica Favaro[1], Stefan Simon[2], Pietro A. Vigato[1]
[1] CNR-ICIS, Corso Stati Uniti 4, 35127 Padova, Italy.
[2] Getty Conservation Institute 1200 Getty Center Drive, Los Angeles, CA 90049-1684.

Abstract

The aim of the present work is to investigate by μ-FT-IR the treatments performed in the recent past in order to characterize the polymers applied and their possible deterioration products on deteriorated stone surfaces.
A selection of commercially available acrylic polymers have been studied by μ-FT-IR to create a reference database. Samples collected from treated marble sculptures on the monumental entrance of the Ducal Palace in Venice have been analysed and the polymers applied have been identified by comparison of their IR spectra with those of commercial products. The solubility tests, performed on collected samples, and the infrared analyses on soluble and insoluble fractions gave useful information about the polymer degradation processes and relevant data for the development of a future conservation strategy of the sculptures.

Introduction

Synthetic polymers have been widely employed both as consolidants and water repellents for the treatment of stone materials to preserve the artifacts from further deterioration [1]. Their chemical and physical properties have been considered to determine their suitability for stone treatment, major issues being the chemical stability and the solubility in solvents commonly in use in the restoration field. These two properties are determinant factors for the reversibility of the treatment [2,3]. The synthetic polymers should ensure that treated stone does not change in the time or, at least, it should be possible completely to remove the applied products whenever problems arise. To evaluate the performance of stone treatments and/or to carry out an efficient retreatment, it is of paramount relevance to identify and characterize the polymers applied during past treatments and the related by-products, in order to plan a new methodology and for the new products to be applied.
Indeed, even for fairly recent restorations, it often proves difficult to find trustworthy information about the products and technological details. This is better in the case of the restoration of the Porta della Carta, completed in

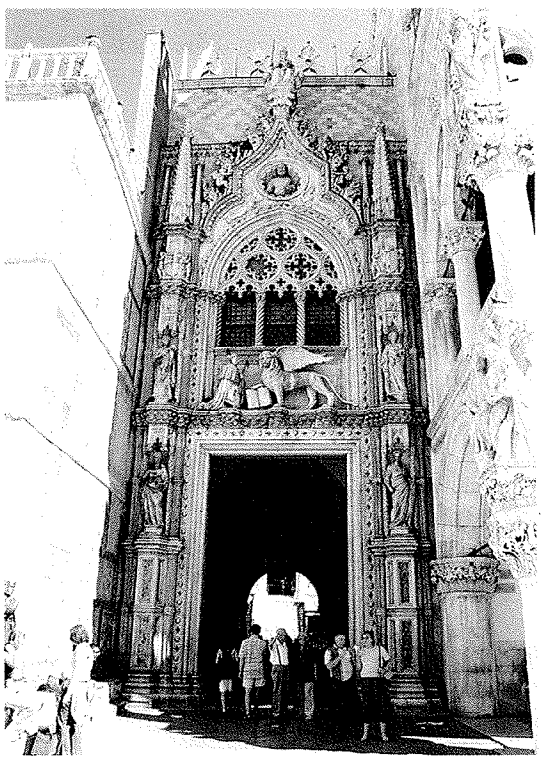

A

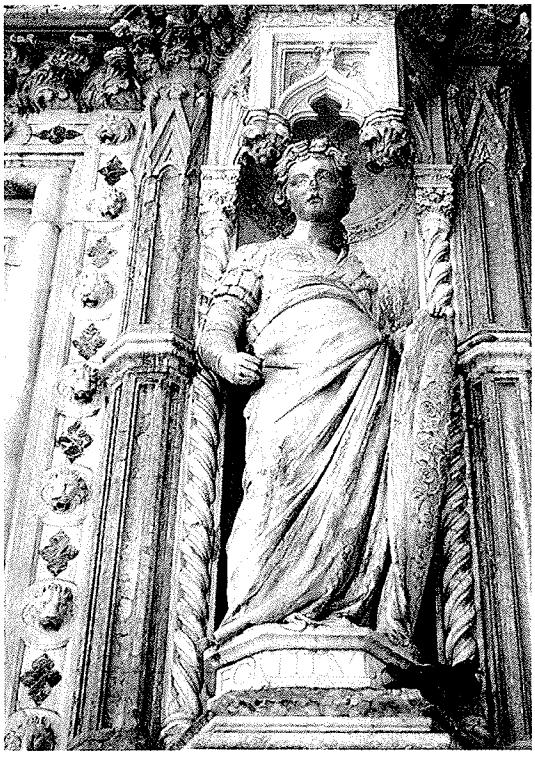

B

Figure 1: Monumental entrance, Doge Palace, Venice: a) actual view; b) sculture Fortitudo

1979 (fig. 1), for which there is at least detailed documentation [4,5]. Unfortunately, the documentation does not include details about the products applied as water repellent, thought, the present, to be the cause of the strong chromatic alteration of the marble surface.

Previous restorations on the Monumental entrance of Ducal Palace, Venice

The Monumental entrance to the Doge's Palace in San Mark's square in Venice is one of the most beautiful facades of Venetian art in the XV century [6,7].
The comprehensive restoration of the monument was performed between 1976 and 1979.
A variety of materials were used in the building of the Porta della Carta: the more abundant are strian stone, which was used for the structural parts, and Carrara marble, which was used for the sculptures.
The whole surface, including the four sculptures, was cleaned and then consolidated and protected. Two silicon based products were used as consolidant for the surfaces and finally, a thin waterproofing coating layer (E 0023, Ditta Racanello) was applied to the statues by brush [4,5].
Documentation consists of detailed written sheets, produced by the restorers. As consolidant, methyltrimethoxysilane was applied either by brush or under vacuum, while the composition of the protective layer is described as a mixture of indefinite acrylic resin and crystalline wax, without any clear reference to the chemical composition of the products.
Twenty five years after restoration, the whole structure shows a withish and slightly powdering aspect on areas affected by rain washing while the sheltered areas are mostly affected by a strong chromatic variation ranging from pale yellow to dark brown stains.
To verify whether the strong change in color could be due to the ageing of the protective coating, the first step was to clearly identify the applied product and secondly to verify the possible chemical modifications of the polymer.

Experimental section

Acrylic resins have been widely used as water repellents on outdoor artefacts. According to the wide literature, we have selected the most popular commercial acrylic polymers. Selected products have been characterized by μ-FT-IR in order to obtain a database of reference compounds necessary for the evaluation and comparison of samples collected from treated stones.
Scrapings and flakes of treated stone were collected from several areas of the sculptures, showing different degrees of decay.
Compositions of selected commercial products are reported in table 1, while sampling details are reported in table 2.
To identify the chemical structure of the applied polymer and to study the degree of reversibility and possible alteration processes, selected samples of superficial coating and treated stones have been dissolved with dichloromethane and μ-FT-IR analyses have been performed on both the soluble fraction and the insoluble residue.
The samples were placed in a microtest tube and few drops of solvent were added to cover the samples. Two hours

Table 1. Reference materials descriptions

Sample	Composition
Paraloid B72	Copolymer methylacrylate ethylmethacrylate
Paraloid B67	Homopolymer i-butylmethacrylate
Paraloid B66	Copolymer methylmethacrylate / n-butylmethacrylate

Table 2. Sampling details of samples collected from the sculptures.

Sample	Sculpture	Sampling area	Observed alterations
1	Charity	scraping from the head, sheltered area	brownish superficial patina
2	Prudence	scraping from drapery, sheltered area	chromatic alteration to dark yellow
3	Fortitudo	scraping from drapery, sheltered area	chromatic alteration to dark yellow

later, a few drops of the supernatant solution have were on a gold plate. Following gentle solvent evaporation, the residue was studied by μ FT-IR. The insoluble fraction of the samples was washed twice with dichloromethane and gently dried in air and then investigated by total reflection μ-FT-IR.

Analytical techniques

A Nicolet microscope connected to a Nicolet 560 FT-IR system, equipped with a MCT (Mercury Chromium Telluride) detector and OMNIC 32 software, was used to generate spectra. Sampling areas investigated were about

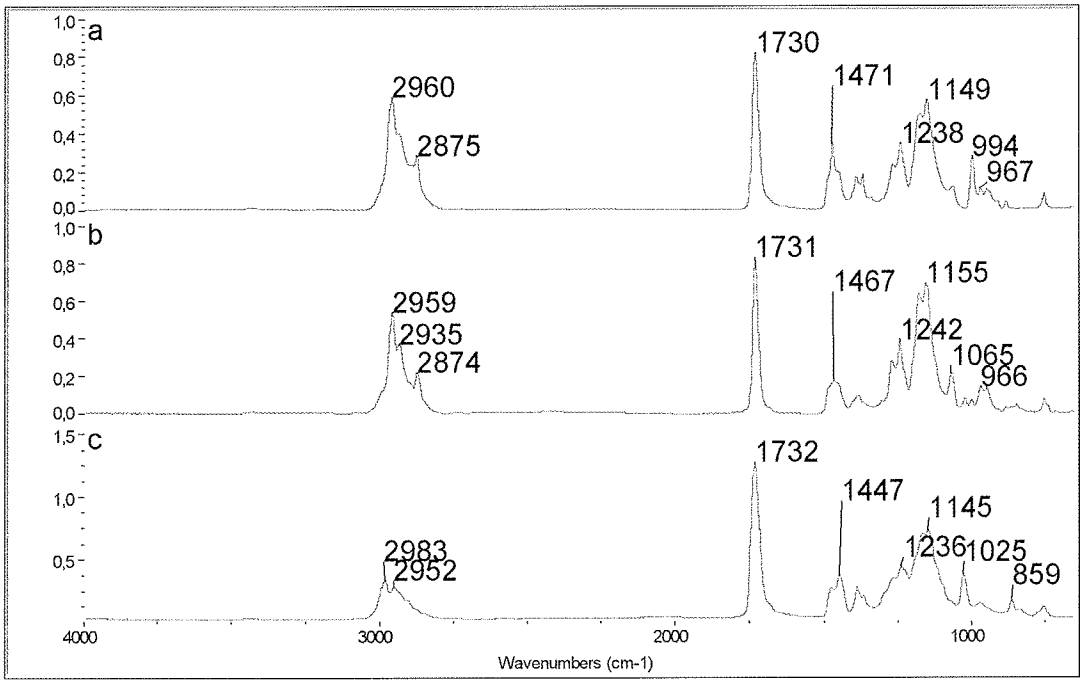

Figure 2. Absorbance spectra of reference commercial polymers: a) Paraloid B67, iso-butyl methacrylate; b) Paraloid B66, copolymer methylmethacrylate-normal butylmethacrylate; c) Paraloid B72, methylacrylate-ethylmethacrylate copolymer.

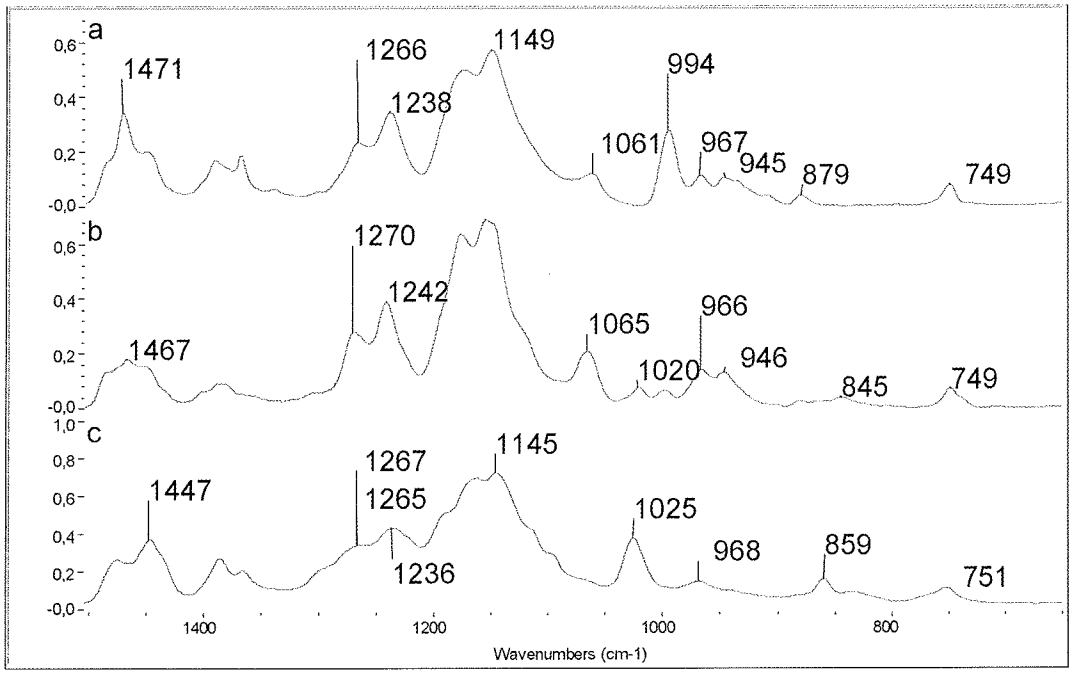

Figure 3. Absorbance spectra of reference commercial polymers in the range 1500-650 cm^{-1}: a) Paraloid B67, iso-butyl methacrylate; b) Paraloid B66, copolymer methylmethacrylate-normal; c) Paraloid B72, methylacrylate-ethylmethacrylate copolymer.

50 μm² in size. IR spectra were recorded in reflectance mode in the 4000-650 cm^{-1} range, with a resolution of 4 cm^{-1}. Collected spectra have been expressed in absorbance units and baseline corrected. Commercial polymers and soluble and insoluble fractions of collected samples were flattened on a gold plate and studied by total reflection μ-FT-IR.

Results and discussion

The μ-FT-IR spectra of commercial products are similar to those reported in the literature [8,9]. Methacrylate polymers show a sharp carbonyl absorption in the 1740-1720 cm^{-1} range, a strong band in the 1475-1450 cm^{-1} region and two weaker characteristic bands at 1269 and 1241 cm^{-1} (fig. 2). Furthermore the spectral features in the 1000 to 900 cm^{-1} range are decisive in order for distinguishing the different methacrylates. In this range, in fact, they show a characteristic absorbance pattern, depending on their side chain composition. Paraloid B72 shows a very weak absorption at 969 cm^{-1} while Paraloid B67 shows three absorptions: a sharp one at 994-996 cm^{-1} and the weak ones at 968 and 946 cm^{-1} (fig. 3).
The IR spectra, of the soluble and insoluble fractions in dichloromethane show a strong absorption at 1731-32 cm^{-1} related to the carbonylic stretching and two characteristic absorptions at 1268-62 and 1240 cm^{-1}. Moreover, weak absorptions at 1070-63, 994, 967 and 945 cm^{-1} occur and the band at 994 $cm^{-1}$is much stronger with respect to those at 967 and 945 cm^{-1} (fig. 4). Both soluble and insoluble fractions in dichloromethane show this characteristic pattern in the range 1080-900 cm^{-1}, this confirms unambiguously the presence of isobutylmethacrylate, corresponding to the commercial product Paraloid B67. The evidence of isobutylmethacrylate in the insoluble residue could be related to a cross-linking process that strongly reduces the solubility of the polymer. As already reported [10,11,12], cross-linking is strongly influenced by light; the results obtained may suggest that the same phenomena has reduced the solubility of the water repellent applied on the sculptures.
Furthermore, either soluble or insoluble fractions of the collected samples show intense absorptions detected at 3300-01, 1635-37 and around 1555 cm^{-1}. These bands, related respectively to the N-H stretching, the C=O stretching (Amide I) and N-H bending (Amide II) vibrations, have been tentatively attributed to the presence of a polyamide product, i.e. Nylon [13], possibly used as additive to stiffen polymers and increase their flexibility [14].

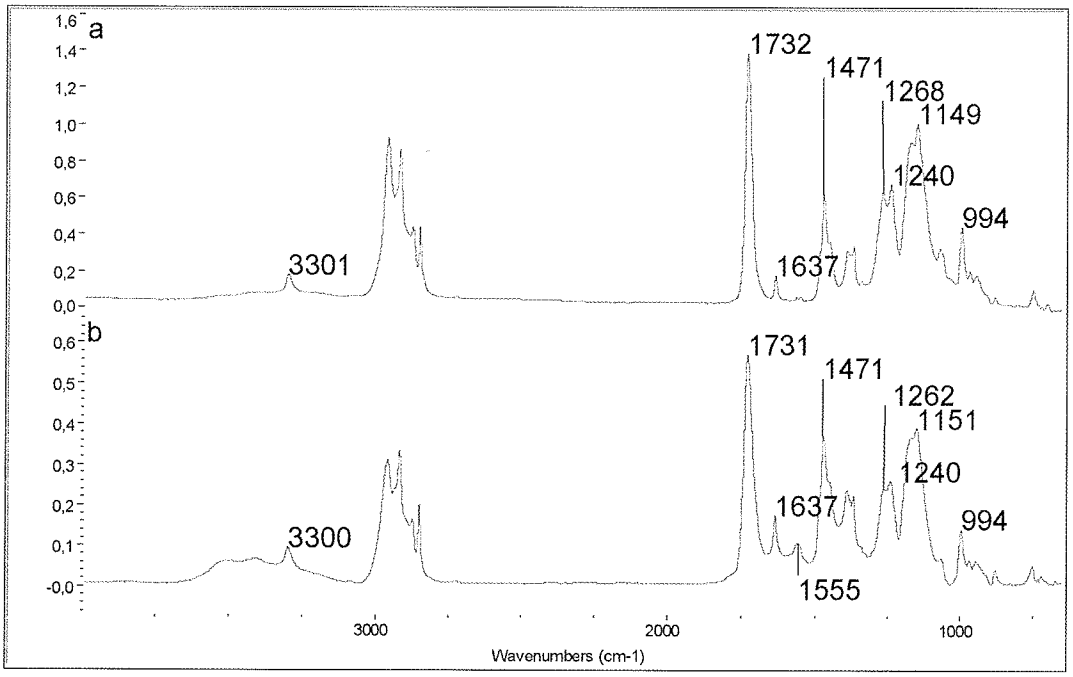

Figure 4. Sample 1: scale from the head collected from a sheltered area of the sculpture Charity. The stone surface shows a chromatic alteration to brownish tones.
IR spectra of dichloromethane soluble (a) and insoluble (b) fractions collected from the scrapped material.

Conclusion

The surface of the marble sculptures of the monumental entrance of the Ducal Palace in Venice show a strong brownish to yellowish colour that has tentatively been assigned to the ageing of the water repellent applied during

the restoration work performed during the 1970's.
To validate the hypothesis, available commercial polymers and samples collected from the sculptures have been analysed by m-FT-IR technique in order to characterize their chemical structure and to evaluate the deterioration processes possibly affecting the applied polymers. Furthermore, selected samples of superficial coating and treated stones have been treated with dichloromethane to study the solubility degree of the polymers and μ-FT-IR analyses have been performed on both soluble fraction and insoluble residue.
The results show that an isobutylmethacrylate polymer, corresponding to the commercial product Paraloid B67, has been applied as water repellent. The presence of an insoluble fraction of the acrylate polymer may be related to crosslinking processes, induced by light exposure, occurring on stone surface over the years. Moreover, an additive, that may corespond to a polyamide, has been identified as a component of the applied water repellent mixture, with the aim to increase the flexibility of the acrylate polymer.

Acknowledgements

We wish to thank arch. C. Menichelli and arch. Ettore Vio for the permission to collect samples from the main entrance of Ducal Palace in Venice.

References

1. Amoroso G.G., *Trattato di Scienza della Conservazione dei Monumenti,* Alinea Editrice s.r.l. Firenze (2002).

2. AIC. 2000. *Code of Ethics and Guidelines for Practice*. American Institute for Conservation.23–28.and commentaries.

3. Various Authors, NORMAL document 20/85 *Conservazione dei materiali lapidei: manutenzione ordinaria e straordinaria.*

4. Hempel K. and G., 'A Technical Report on the Condition of the Porta della Carta and its Restoration', in Clarke A., Rylands P. (eds), *The Restoration of the The Porta della Carta, Venice in Peril Fund, Venice 12.5.-31.7.1979*, Armenian Printing Press (1980) 37-73.

5. Antonelli V. (1979). 'Il Restauro della Porta della Carta in Venezia', in *3° Congresso Internazionale sul Deterioramento e la Conservazione della Pietra, Venezia 24-27/10/1979*,Litografia La Photograph, Padova (1979) 629-644.

6. Romano S., 'The Porta della Carta: History and Critical Analysis' in Clarke A., Rylands P. (eds) *The Restoration of the The Porta della Carta, Venice in Peril Fund, Venice 12.5.-31.7.1979*, Armenian Printing Press (1980) 15-27.

7. Franzoi, U., *The Doge's Palace in Venice*, Storti, Venice (1973)

8. Quillen Lomax S., Fisher S. L., 'An investigation of the removability of naturally aged synthetic picture varnishes' in *Journal of American Institute for Conservation*, Vol. 29, n. 2, (1990) 181-191.

9. Derrick M. R., Stulik D., Landry J. M., *Infrared Spectroscopy in Conservation science, scientific tools for conservation*, The Getty Conservation institute, Los Angeles (1999).

10. Horie C.V., *Materials for Conservation*, Butterworth-Heinemann Ltd (1987), 103-112.

11. Feller R.L., 'Resins and the properties of varnishes'in Feller R.L. et al. (eds.) *On picture varnishes and their solvents*, London: Press of Case Western Reserve University (1971) 117-168.

12. Feller R.L. 'Early studies in the cross-linking of polymers'in Feller R.L. et al. (eds.) *On picture varnishes and their solvents*, London: Press of Case Western Reserve University (1971) 195-201.

13. Silverstein R. M., Webster F. X., *Spectroscopic Identification of Organic Compounds, Sixth Edition*, John Wiley & Sons Inc. (1998) 99-102.

14. Chiantore O., Università degli studi di Torino, personal communication (27 January 2003)

Infrared Analysis of Material Leached by Water From Acrylic Paint Films

R.E. Ploeger, H.F. Shurvell, E.W. Hagan and A. Murray
Art Conservation Program, Department of Art,
Queen's University, Kingston, Ontario, K7L 3N6 Canada.

Abstract

Infrared (IR) spectra have been recorded from leachate residues produced from evaporation of water in which aged acrylic paint films have been immersed. The spectra reveal that a significant amount of material is leached from the paint films. The main components of the leachates are surfactants. IR spectra and chemical analysis show that pigments and other materials are sometimes also leached from the paint films. IR spectra have been recorded of exuded material that is observed on aged paint films. This material also appears to be surfactant and is even observed after immersion and drying of the films. Mechanical testing of strips of acrylic paint films indicate a significant stiffening accompanied by an increased embrittlement of the film after immersion in water. Real-time monitoring of changes in pH and surface tension of the water in which the paint film is immersed show that the pH increases, while the surface tension decreases with time.

Introduction

As acrylic emulsion (more accurately dispersion) paint is a relatively new artistic medium, much about its properties and conservation remains unknown. The low glass transition temperature of dried acrylic paint causes the paint surface to be soft at room temperature, so that dirt can be easily embedded. The cleaning of acrylic paintings continues to be a subject on which there is little consensus, with conservators using a variety of dry and wet techniques [1,2,3]. This study is part of an ongoing project, focused on the effects of water on acrylic paint films.
Acrylic paint is soluble in many of the usual cleaning solvents, but some paintings can be cleaned by careful swabbing with distilled water. Unfortunately, water may leach important ingredients from the paint films [4,5,6]. The resulting changes to the chemical and mechanical properties of the films may in turn lead to deterioration of the artistic works. It is therefore important to be able to identify the materials leached by water from acrylic paints. This knowledge may help with conservation procedures and the design of new acrylic paints for artists.
Infrared spectroscopy offers a method for the analysis of materials leached or exuded from acrylic paint films. In the present study, aged acrylic paint films were immersed for 24 hours in distilled water. The aqueous leachates were evaporated to dryness and the resulting residues examined using the ATR- FTIR (attenuated total reflectance-Fourier-transform infrared) spectroscopic technique. Chemical analysis was also used as an aid in the identification of the components of the material leached from the paint films. Changes in the pH and surface tension of the water in which the paint films were immersed gave an indication of the rate of leaching and the nature of the leachate material.

Experimental procedures

Paint samples
Acrylic paint films were cast on Mylar sheets and aged naturally at the Smithsonian Institution (SI) in Washington, DC, USA, or at Queen's University in Kingston, Ontario, Canada. Golden Artist Color® Titanium White (cast at Queen's: June 1999), Bone Black (cast at Queen's: February 2001), Burnt Umber (cast at SI: February 1999) and Dick Blick® Cobalt Blue (cast at SI: February 1999) were studied. These paints were based on a copolymer of *n*-butyl acrylate and methyl methacrylate. In 2003, Golden Artist Color® supplied two custom blended paints (bone black and naphthol red) of known composition. These two paints are not proprietary formulations, but were made for specific testing in art conservation research. They were both based on the Rhoplex AC-234 acrylic polymer emulsion, which is a copolymer of ethyl acrylate and methyl methacrylate.
At Queen's University, the paint films were allowed to dry and then exposed to air by attaching the Mylar sheets to a wall in the laboratory. After several months (or years) the aged paint films were removed from the Mylar support and cut into appropriate sample strips.

Sample treatment
Paint strips were immersed in distilled water for 24 hours at room temperature (22°C). Strips 12 cm x 1 cm were suspended in test tubes. Strips 6 cm x 3 cm were suspended in 50 mL beakers.
During the leaching process, the water was continuously stirred by a magnetic stirrer using a Teflon coated stirbar.

After the immersion period, the strips were removed and the water was evaporated on a hotplate. The solid leachate residues were collected and subjected to infrared spectroscopic and other chemical analysis.
By weighing the beakers before and after the treatment, the amount of material leached from a paint film was determined to be typically 7% of the film weight. This was confirmed by measuring the loss of weight of the film after immersion.

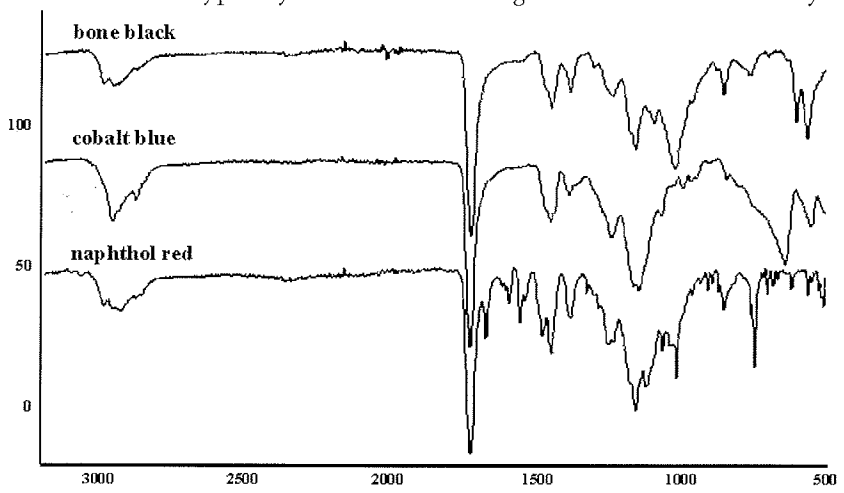

Figure 1 IR spectra of three acrylic paint films.

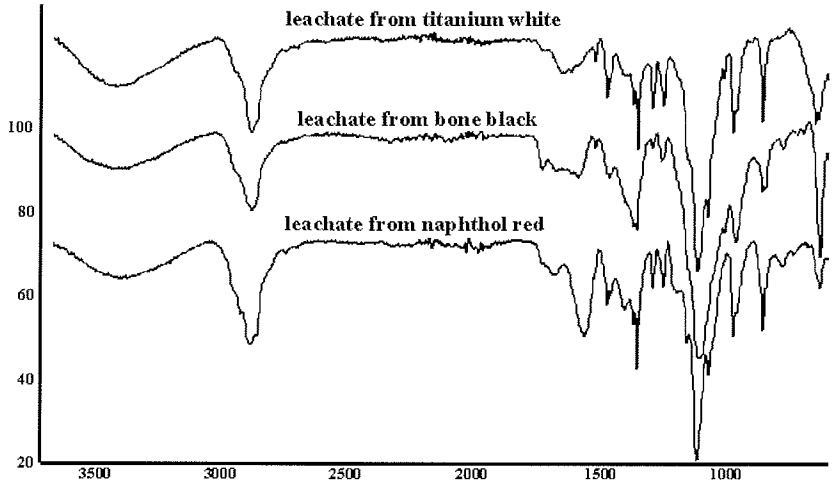

Figure 2 IR spectra of leachates from three acrylic paint films.

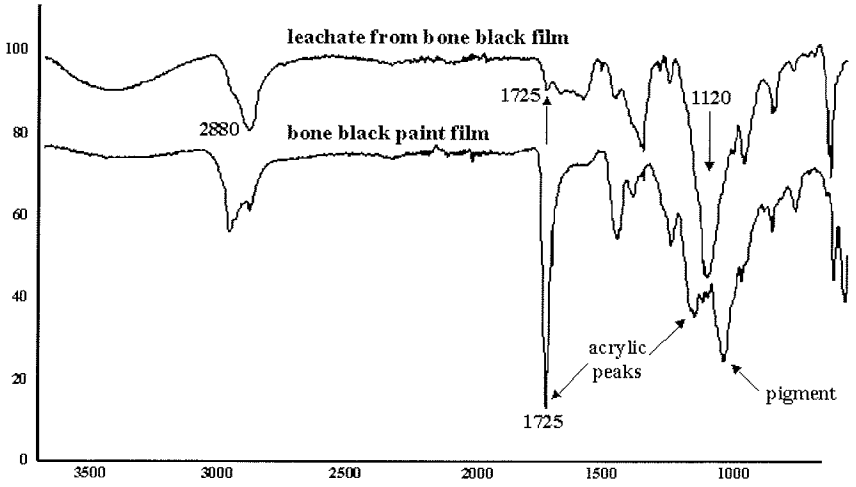

Figure 3 IR spectra of Golden bone black paint and a dried leachate.

Infrared spectroscopy
The instrument used was a Nicolet Avatar 320 FTIR (Fourier transform infrared) spectrometer. IR spectra were obtained using a "Golden Gate" single pass diamond ATR accessory. With this accessory, no sample preparation was needed. The instrument operating conditions were 32 scans at a resolution of 4 cm^{-1}.

Mechanical properties
Mechanical properties for the acrylic paint films were determined using a data acquisition system fitted to a manually operated tensiometer. The modified device consisted of a stepper motor, microcontroller, and software to facilitate precise control of strain rate and data collection. Sample dimensions and rate of testing were carried out using ASTM standard D2370-92 as a guideline. Gage length, width, and thickness were selected as 38mm, 13mm and 0.2mm respectively. The samples were stretched at a rate of 17% per minute in an environment of 50 +/- 1% RH and 21.0 +/- 0.2°C. The data is presented in the form of stress-strain curves in Figures 9 and 10.

pH and surface tension measurements
Real-time pH measurements were recorded over 24 hours using a probe placed in the water in which the paint films were immersed. The water was continuously stirred during the leaching process. A Vernier Software pH probe was used. Real-time surface tension changes were measured using the capillary rise method. A sample of paint film was immersed in distilled water in a container into which a glass capillary was suspended. The water was

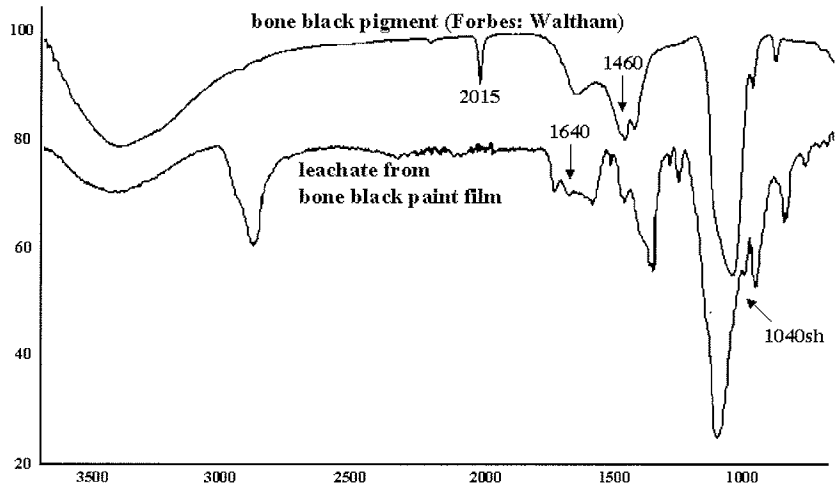

Figure 4 IR spectra of a bone black pigment (IRUG database) and the dried leachate from a bone black paint film.

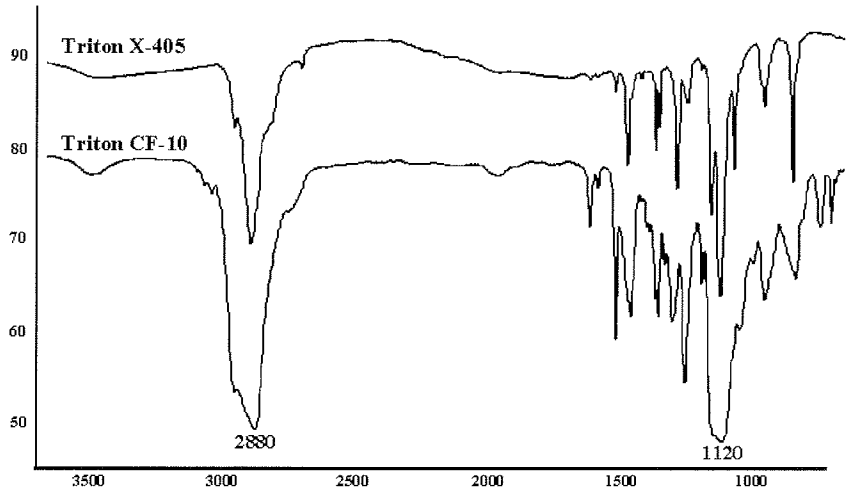

Figure 5 IR spectra of two surfactants (National Gallery, database).

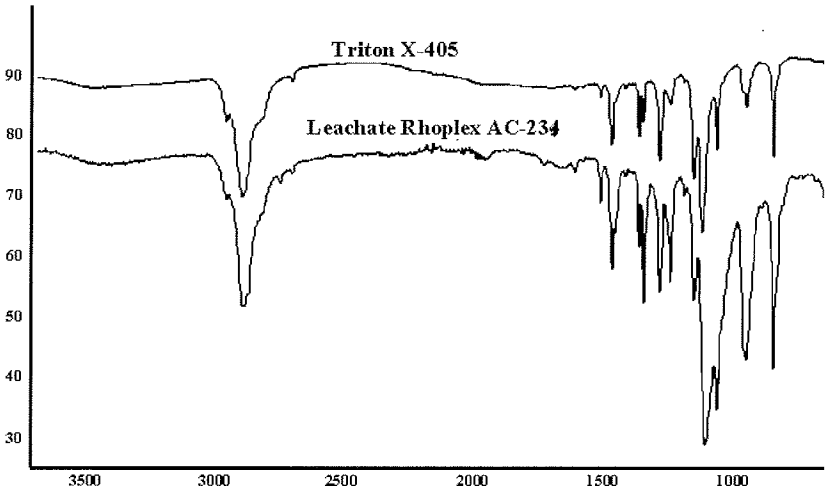

Figure 6 IR spectra of a solid surfactant (Triton X-405) and the leachate from a Rhoplex AC-234 base film.

continuously stirred and the capillary rise noted every minute over an hour.

Results

Infrared spectra of paint films and leachates

Figure 1 shows the IR spectra of films of naphthol red, cobalt blue and bone black acrylic paint. The spectra are similar, but differences that can be attributed to the different pigments are noted. Characteristic pigment bands are observed at 1040 cm^{-1} for bone black (phosphate) and 640 cm^{-1} for cobalt blue. Naphthol red has several absorptions due to aromatic rings.

The spectra of Figure 2 show that similar material has leached from the three different paint films. Some differences are noted in the 1800 – 1400 cm^{-1} region.

The spectra of Figure 3 have little in common. The weak absorption at 1725 cm^{-1} indicates that a small amount of acrylic polymer (or residual monomer) is present in the leachate.

In Figure 4, bands at 1640 and 1460 cm^{-1} are assigned to carbon (graphite). The shoulder at 1040 cm^{-1} is due to phosphate. Spectra of two bone black pigments in the IRUG database (IMP00020: Kremer-Pigmente and IMP00297: Forbes:Waltham) show the peak at 2015 cm^{-1}.

Figure 5 shows the IR spectra (supplied by Greg Smith of the National Gallery, Washington, D.C.) of two surfactants Triton X-405 and Triton CF-10. Both of these surfactants are water-soluble nonionic alkylphenol (poly)ethoxylates. Major absorption bands are noted near 2880 and 1120 cm^{-1}

It is clear from Figure 6 that a nonionic alkylphenol (poly)ethoxylates surfactant, likely Triton X-405, is the main component of the leachate from the Rhoplex AC-234 base emulsion.

Figure 7 shows that the spectrum of the leachate from the Naphthol Red paint film contains many similar

features to that of the Rhoplex AC-234 base emulsion. In addition to the surfactant absorptions, there are peaks arising from Naphthol Red pigment.

IR spectra of exudate spots on paint films

Infrared spectra were recorded from visible exudate spots and mottled areas observed on the surface of aged paint films. The spectra were compared with spectra obtained from clear areas of the paint films. It was assumed that these spots were due to material that had exuded from the paint film during the curing process. Figure 8 shows parts of the IR spectrum (between 3500 – 2700 and 1500 - 800 cm^{-1}) of an exudate spot on a titanium white paint film (lower trace). The spectrum shows several additional absorption features compared to a spectrum recorded from a clear spot on the film (middle trace).

The wavenumbers of certain of the additional features correspond with those of bands in the spectrum of the surfactant Triton X-405 (upper trace). This is especially true for the strong surfactant bands at 2884 and 1116 cm^{-1}, which are clearly seen in the spectrum of the exudate spot, but are absent from the spectrum of the clear area. The sharp peak at 1343 in the spectrum of the exudate spot is also absent from the spectrum of the clear area.

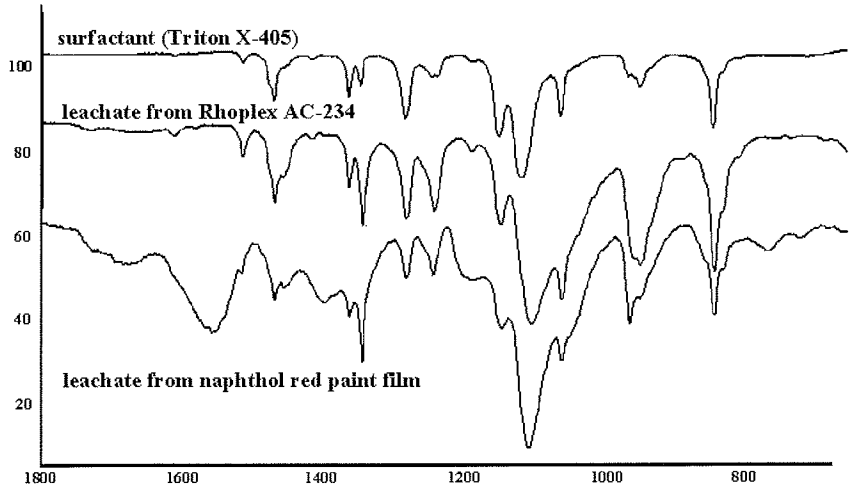

Figure 7 Part of the IR spectra of a solid surfactant, with dried leachates from films of Rhoplex AC-234 and Naphthol Red paint.

Physical and mechanical properties

It was noted that after immersion for 24 hours, the samples decreased in mass and volume. Length, width and thickness all decreased. It was observed that the paint films were very ductile and could be stretched to two or more times their initial length without breaking. Figure 9 shows how the stress-strain curve for an acrylic paint film changes with ageing. The curves of Figure 9 indicate that the film becomes stiffer (tougher), but more brittle (fractures more easily) with ageing. Figure 10 shows the stress-strain curves of a paint film after immersion for 1 minute and 24 hours compared to that of a non-immersed (control) film. Brief immersion does

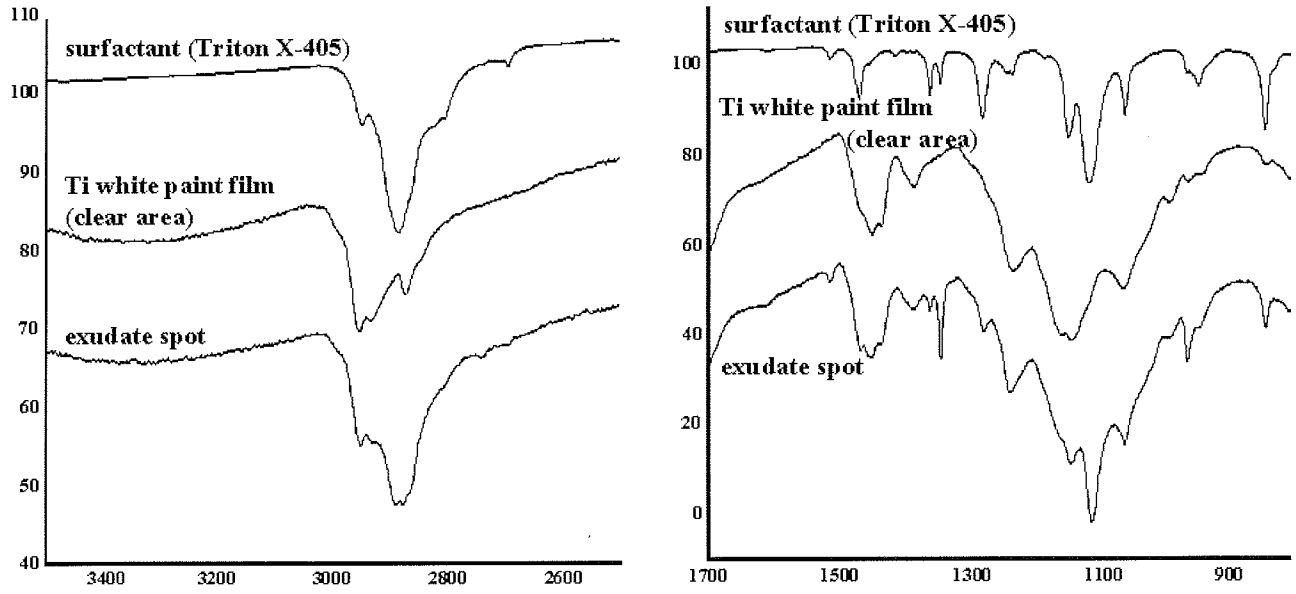

Figure 8 IR spectra between 3500 – 2700 and 1500 - 800 cm^{-1} of an exudate spot on a titanium white paint film.

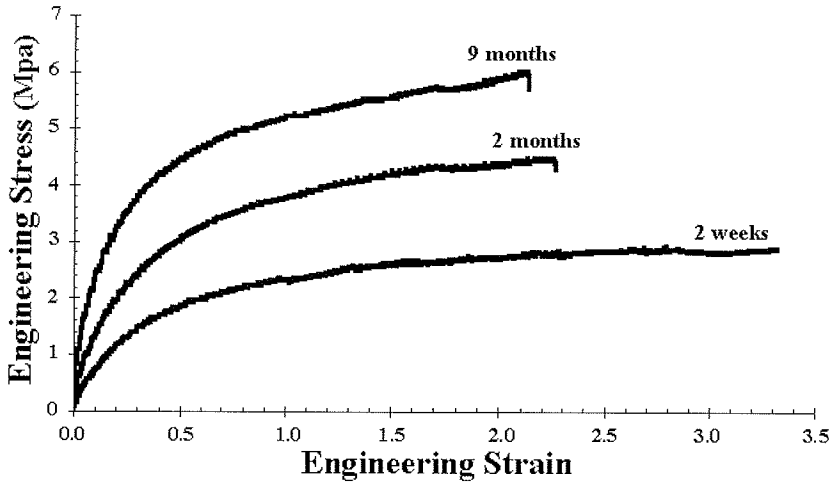

Figure 9 Stress-strain curves for AC-234 based bone black films at different ages.

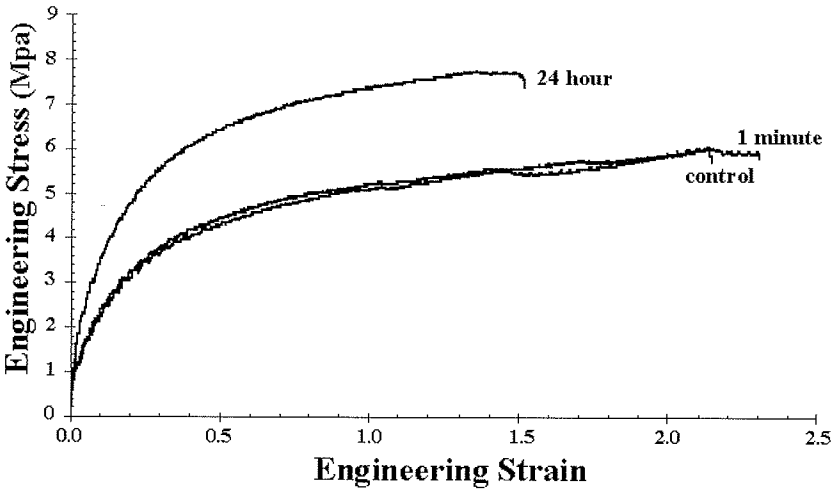

Figure 10 Stress-strain curves for AC-234 based bone black films after immersion in water.

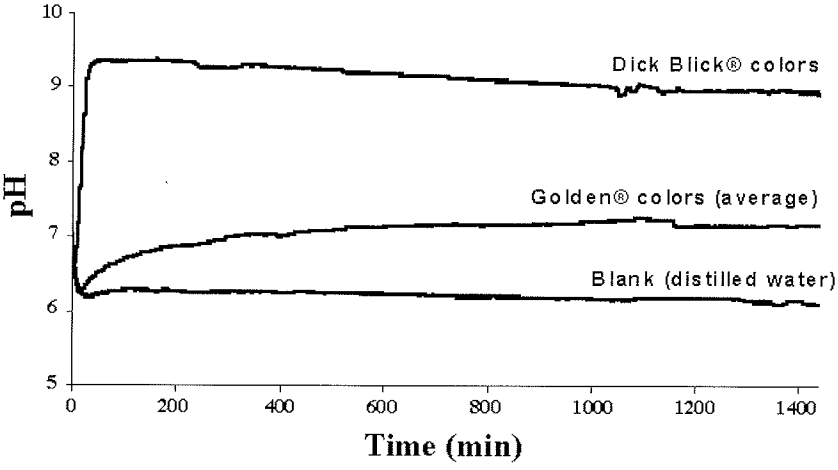

Figure 11 Average pH changes of Golden Artist Colors® acrylic paints and Dick Blick® acrylic paints.

not affect the mechanical properties of the paint film, but immersion for 24 hours causes the film to become stiffer and more brittle.

Chemical properties

Changes in pH

Figure 11 shows typical changes in pH observed during the leaching process. In all cases, there was a brief decrease in pH at the start of the immersion. This was followed by a relatively rapid increase before an equilibrium value is reached after several hours. Significant differences were observed in the results obtained between paints from different manufactures. This is most likely due to the different emulsion polymer formulations and additives used by the various manufacturers, each of which has their own unique paint formulations.

These pH variations could signify a number of different reactions, or the presence of water-soluble compounds in the paint films. Often, pH modifiers or stabilizers are added to formulations along with other types of stabilizers. Most of them have the capability of increasing the basicity of the solution. A number of different ions have been identified in the leachates from other analytical methods. Foaming of the solution was observed during the immersion, which indicates that surfactant has been leached out. Capillary rise experiments were performed on Golden Artist Color® Naphthol Red (cast: May 2003). Figure 12 shows that the surface tension of the immersion water dropped rapidly during the initial 8 to 10 minutes and then levelled off. This supports the earlier conclusion that surfactant is leached from acrylic paint films by water.

Mass spectrometry

MALDI-MS (matrix assisted laser desorption ionization mass spectrometry) was performed on the leachate residue from a Golden Artist Color® Bone Black paint film. The average molecular weight of the residue was approximately 1800 and there was

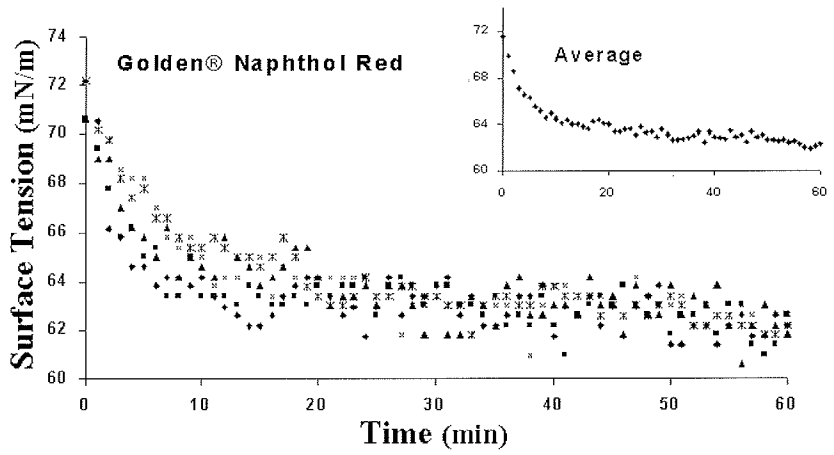

Figure 12 Surface tension changes during a one-hour immersion period.

an equal spacing of 44 mass units. This is consistent with a polyether type chain typical of Triton surfactants.

Conclusions

Infrared spectroscopic studies have shown that when acrylic paint films are immersed in water, several component s of the paint are leached out. The main component of the leachates is surfactant. For the paint samples examined in this study the surfactant appears to be a nonionic alkylphenol (poly)ethoxylate surfactant, likely Triton X-405. The exuded material found on the surface of naturally aged paint films was found to also be a nonionic alkylphenol (poly)ethoxylate surfactant. Real-time surface tension measurements indicate that the majority of the leaching occurs in the first few minutes after immersion. This is confirmed by real-time pH measurements, which also indicate that a basic (alkaline) material is leached into the water.

It has been found from measurements of mechanical properties of the paint films that the films become tougher, but more brittle (fracture more easily) after long (24 hours) immersion. It was also noted that a very short (1 minute) immersion had no noticeable effect on the mechanical properties of the paint films.

Acknowledgements

Mark Golden, (Golden Artist Colors) for supplying specially formulated acrylic paints and funding.
Marion Mecklenburg, Smithsonian Center for Materials Research and Education, for supplying testing equipment and acrylic paint samples.
Greg Smith, National Gallery of Art, Washington, D.C., for giving us access to his collection of spectra of acrylic paint additives.
The Natural Sciences and Engineering Research Council of Canada, the Canadian Foundation for Innovation, and the Ontario (Canada) Research and Development Challenge Fund, for financial support.

References

1. Jablonski, E., Learner, T., Hays, J., Golden, M., 'Conservation concerns for acrylic emulsion paints', *Reviews in Conservation,* IIC (2003) Number 4, 3-12.

2. Murray, A., Contreras de Berenfeld, C, Chang, S.Y.S., Jablonski, E., Klein, T., Riggs, M.C., Robertson, E.C., and Tse, W.M.A. 2002. "The Condition and Cleaning of Acrylic Emulsion Paint," in: Postprints, VIth Conference, Materials Research Society Fall Meeting 2001, edited by P. Vandiver, M. Goodway, and J. Mass (Boston: Materials Research Society, 2002).

3. Gavett, B., 'Techniques for cleaning acrylic paintings', *Just Paint* Golden Artist Colors, Inc. (1997) Issue 5, 1-5.
Whitmore, P., Colaluca, V. and Farrell, E., "A note on the origin of turbidity in films of an artists' acrylic paint medium," *Studies in Conservation* 41, 1996, 250-255.

Learner, T., Chiantore, O., and Scalarone, D., "Ageing studies of acrylic emulsion paints," *Preprints of the 13th Triennial meeting of the ICOM Committee for Conservation, Rio de Janeiro* (2002) vol.2 911-919).

Learner, T., "A Review of Synthetic Binding Media in Twentieth-Century Paints," *Conservator*, vol. 24, 2000, pp. 96-103.

Bondy, C., "Binder Design and Performance in Emulsion Paints," *Journal of Oil and Color Chemists' Association*, vol. 51, 1968, pp. 409-27.

FTIR Monitoring of Surfactant Phase-Separation and Stability in Waterborne Organic Coatings and Artists' Acrylic Paints

Dominique Scalarone and Oscar Chiantore
Department of IPM Chemistry, and NIS Centre of Excellence, University of Torino, via P. Giuria 7, 10125 Torino, Italy.

Abstract

This contribution reports several applications of infrared spectroscopic analysis of waterborne coatings and paints used as artists' materials and in the conservation field. By coupling size exclusion chromatography (SEC) and Fourier transform infrared spectroscopy (FTIR), simultaneous identification of polymer binders and low molecular weight polymer additives such as surfactants and organic pigments has been carried out on both unpigmented coatings and coloured artists' paints.
To monitor the migration of surfactants to the polymer/air interface, their stability and the effect of water treatments, the surface morphology of films cast from acrylic latexes has been investigated by atomic force microscopy (AFM) and surface maps have been collected by mATR-FTIR.

Introduction

In the past few decades, because of safety and environmental reasons, the coating industry has made a great effort to reduce the use of organic solvents in organic coating formulations. Hence the development of waterborne polymer dispersions.
In 1953 Primal AC 33 (Rohm & Haas) was the first acrylic dispersion to reach the market. It was recommended for painting walls, as a liquid adhesive and to consolidate porous materials, especially stone. In the following years, other acrylic products by Rohm and Haas and by other manufacturers were commercialised as heat-set adhesives and as consolidants for particular substrates such as paper and textiles.

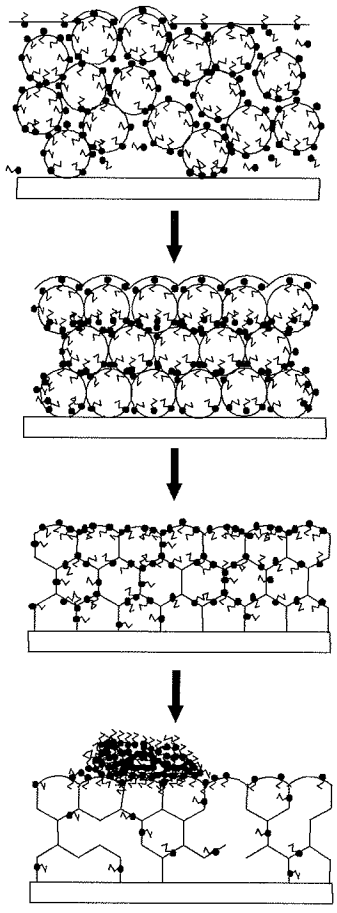

Figure 1. Schematic representation of the film formation process and of surfactant phase separation in an acrylic latex [6].

Acrylic dispersions are highly stable to light sources, humidity and temperature, show good mechanical properties and are easy to handle, as they maintain low viscosity even in presence of high molecular weight polymers. As a result of these properties, as well as their fast drying qualities and flexibility, waterborne acrylic coatings have been developed and widely used as artists' media for painting and for the conservation of art objects [1, 2]. In 1956 Liquitex became the first brand of acrylic emulsion paints specifically intended for artists.
The next step in the formulation of protective coatings for conservation was the introduction of fluorine atoms by the copolymerisation of acrylic monomers with fluorinated co-monomers. Coatings from fluorinated acrylic latexes show high UV resistance, are thermally and chemically stable and show excellent surface properties, especially in terms of high water repellency [3, 4].
The most recent generation of acrylic latexes are organic-inorganic hybrids based on reactive poly(acrylate)particles with an alkylalkoxysilane network as the outer shell [5]. Such materials are potentially interesting both as consolidants and as protectives (surface coatings) because of the possibility of modulating the relative proportions of organic and inorganic components as well as the particle size, thus affecting penetration efficacy, cohesion, adhesion, water repellency and mechanical properties.
To ensure polymerisation and the proper performances of the final product, waterborne acrylic coatings and paints require a lot of additives: surfactants, protective colloids, anti-foam agents, stabilisers, and biocides. Surfactants in particular display an important role both during the polymerisation process and in the lifetime of the coating. Surfactants are used as emulsifiers for the polymerisation process, as dispersants to stabilize the polymer particles and to provide a homogenous distribution of pigments in the polymer matrix, and as thickeners to adjust the viscosity of the paint/latex.
The types and quantities of surfactants affect the latex stability, the size of the

polymer particles and their distribution, the film formation process, and the morphology and surface properties of the final coating. Moreover it is known that, over time, surfactants migrate to the surface of the polymer film. Figure 1 shows a schematic representation of the film formation process and of surfactant phase separation.
Film formation from a polymer latex is generally described as a multistage phenomenon. In the first stage, called the wet stage, spherical polymer particles are dispersed in water and surfactants are homogeneously distributed in the bulk to stabilize the polymer particles.
In the second stage particles form a close packed array. Water is still present in the inter-particle spaces and, as the polymer particles come into contact, surfactant desorption begins. Then particle deformation and compaction follows, though individual polymer particles retain their identity. Finally, coalescence occurs: inter-particle diffusion of polymer molecules yields an isotropic coating. Coalescence promotes surfactant migration to the film surface, which means loss of adhesion, decreased water repellency, enhanced photo-degradation and reduced optical properties.
Ethoxylated non-ionic surfactants with a considerable number of ethylene oxide units (>20) are highly incompatible with the polymer; as film formation proceeds, they tend to aggregate and exude at the surface where they then degrade by oxidative chain scission.
Another important aspect, especially when dealing with artists' waterborne paints, is their cleaning that, at present, is generally performed with water or aqueous solutions. Besides the problems related to the temporary swelling of surfaces, water treatments can also significantly affect the overall composition of the dried emulsion paint as they can dangerously enhance the migration process of water soluble components, leading to the removal of surfactants and of other hydrophilic additives.
This paper describes some applications of infrared spectroscopic techniques, such as SEC-FTIR, Attenuated Total Reflectance (ATR)-FTIR and μATR-FTIR, to compositional characterisation and ageing studies of acrylic waterborne coatings and paints, focusing especially on surfactants phase separation and stability.

Experimental

Materials
A selection of acrylic emulsion paints from four different producers (*Lukascryl*, Lukas, Germany; *Rembrandt*, Royal Talens, Netherlands; *Spectracryl*, Spectrum, U.K.; *Cryla*, Daler Rowney, U.K.) and two non commercial latexes, a poly(methyl methacrylate-co-butylacrylate) (*BMM-SS4*) and a fluorinated core-shell nanostructured acrylic latex (*LF3*), have been investigated by SEC-FTIR, ATR-FTIR, μATR-FTIR mapping and AFM.
Both paints and acrylic latexes were spread as thin films on glass slides and aged under different conditions: natural ageing, thermal ageing at 60°C and 120°C and light ageing reproducing both outdoor solar exposure (xenon lamp and UV filter that absorbs wavelengths lower than 295 nm) and indoor exposure (fluorescent tubes and an ultraviolet filter to cut off radiation below 400 nm).

Size Exclusion Chromatography-Fourier Transform Infrared Spectroscopy (SEC-FTIR)
For SEC-FTIR analysis, a LC-Transform interface Series 100 (Lab Connections Inc., Marlborough, MA, USA) was used. The instrument consists of a sample deposition module for deposition of the components separated by chromatography and an optics module for infrared analysis. The chromatographic eluent is forced by a pneumatic nebulizer into a spray that impacts a rotating collection disc. The mobile phase flow diverted to the LC-FTIR interface was 50 μL/min, the collection disc moving rate 10°/min and the gas sheet temperature 50°C.
FTIR spectra of the fractionated samples were subsequently collected in reflection-absorption mode with a Thermo-Nicolet FT-IR Nexus instrument with a DTGS detector and a 4 cm^{-1} resolution.
Size-exclusion chromatography was performed with a modular SEC system composed of a Waters (USA) 515 HPLC pump, a Rheodyne (USA) 7010 injection valve, a differential refractometer ERC 7510 (Erma, Japan) and three PLgel 10μm MIXED-B (300x7.5 mm) columns (Polymer Laboratories, UK). Tetrahydrofuran was used as eluent at a total flow-rate of 1 ml/min and THF solutions were separated from solid impurities by filtration through 0.45 mm PTFE membrane filters.

Attenuated Total Reflectance - Fourier Transform Infrared Spectroscopy (ATR-FTIR)
Infrared spectroscopy was performed with the same instrument described in the previous paragraph. ATR spectra were collected with a Thermo Nicolet Smart Endurance device.

MicroATR mapping
To collect micro-ATR maps, a Thermo-Nicolet Continmum infrared microscope was used. The instrument is

equipped with a silicon crystal ATR objective, that allows non- destructive microscopic surface analysis, and with a motorized stage to provide fully automated mapping.
Maps of 700x700 µm were analysed, with a space resolution of 70 µm.

Atomic Force Microscopy
AFM analyses were performed with a Park Scientific Instruments AutoProbe LS and silicon cantilevers equipped with conical silicon tips.
All the AFM data presented here were recorded in Contact Mode, but images in Non Contact Mode were also collected to verify the absence of tip artefacts.

Results and discussion

Compositional characterisation of acrylic artists' emulsion paints
Attenuated total reflectance is a very suitable technique for the analysis of art objects as it does not require any sample preparation. It is a non-destructive technique and because of the low penetration depth of the infrared beam it allows the identification of very thin layers. However, because the ATR spectra of paints are strongly affected by the absorptions from extenders and pigments, the recognition of other components is often very difficult.
In Figure 2 the ATR spectrum of a yellow acrylic paint (*Lukascryl*, Lukas) is reported. The intense and large absorptions between 1060 and 1200 cm^{-1} are mainly due to barium sulfate, one of the extenders commonly used in modern paints. The presence of barium sulfate is also confirmed by the diagnostic peak at 983 cm^{-1}. The acrylic binder can be seen in the carbonyl peak at 1727 cm^{-1}, the C-H stretching at 2982 and 2952 cm^{-1} and the C-H bending at 1446 and 1381 cm^{-1}

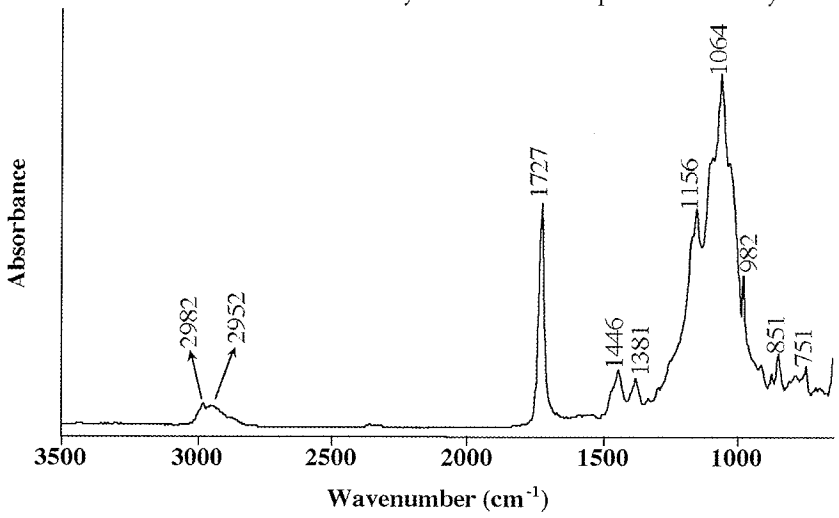

Figure 2. ATR-FTIR spectrum of a dried yellow emulsion paint.

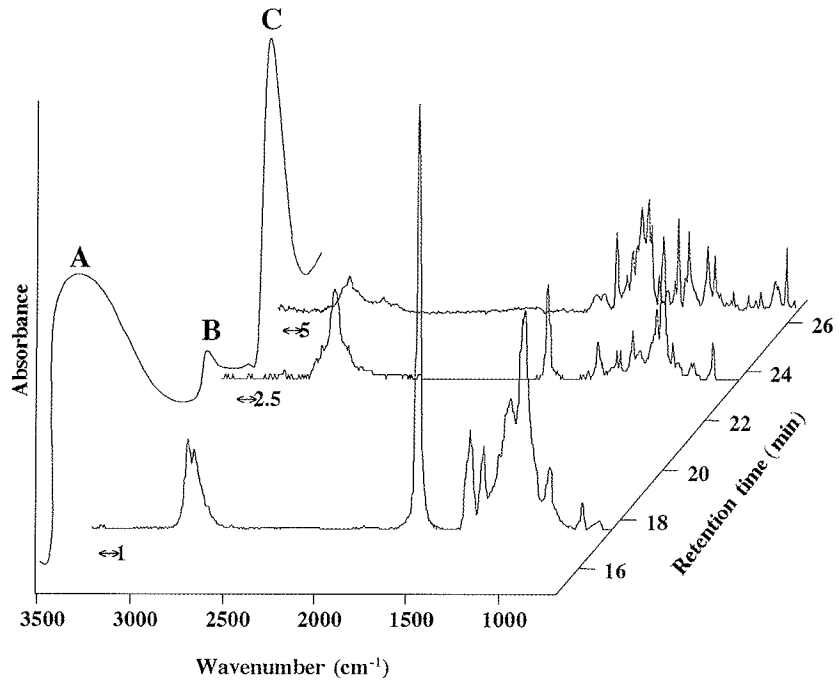

Figure 3. 3D plot obtained by SEC-FTIR of an acrylic emulsion paint. Peak A has been identified as a poly(EA-co-MMA) medium, peak B as an ethoxylated fatty alcohol surfactant and peak C as Pigment Yellow 3.

Figure 4. Phase separation and crystallisation of surfactants in an acrylic waterborne coating. Magnification x45.

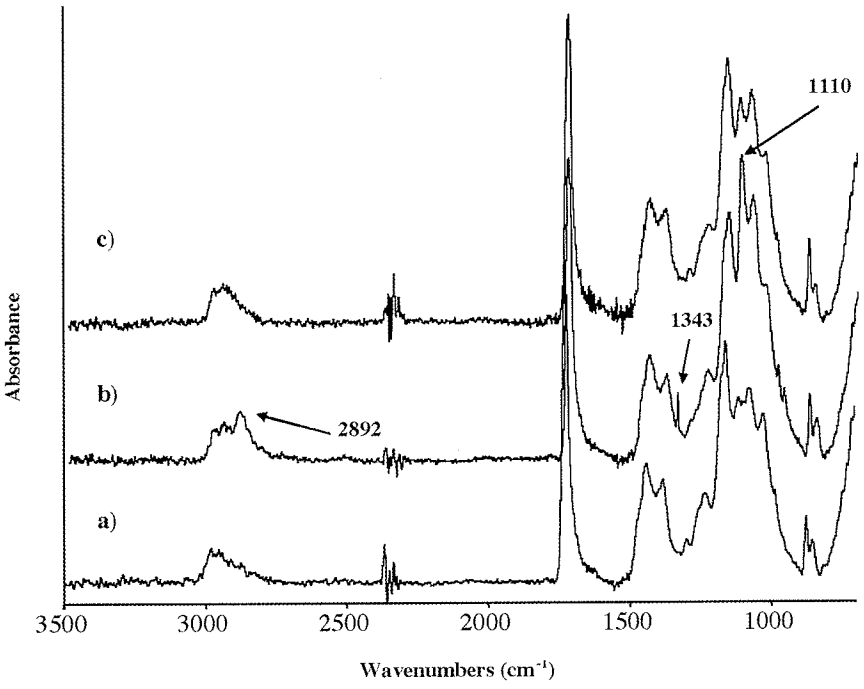

Figure 5. ATR-FTIR spectra of Rembrandt titanium white emulsion paints: a) unged; b) naturally aged for six years; c) artificially light aged for 32 weeks

[1]. Smaller absorptions between 1600 and 700 cm^{-1} indicate the presence of minor components which cannot be identified due to the strong interferences of the other constituents of the paint. Additional information on soluble organic components can be obtained by SEC-FTIR coupling. Figure 3 shows the 3D plot obtained by combination of the SEC chromatogram of the Lukas yellow emulsion paint with infrared spectra collected at retention times corresponding to the maximum intensity of each chromatographic peak. Peak A is due to the poly(EA-co-MMA) medium. Peak B has been identified as an ethoxylated fatty alcohol surfactant. The third chromatographic peak, C, eluted at longer retention times has been identified as Pigment Yellow 3.

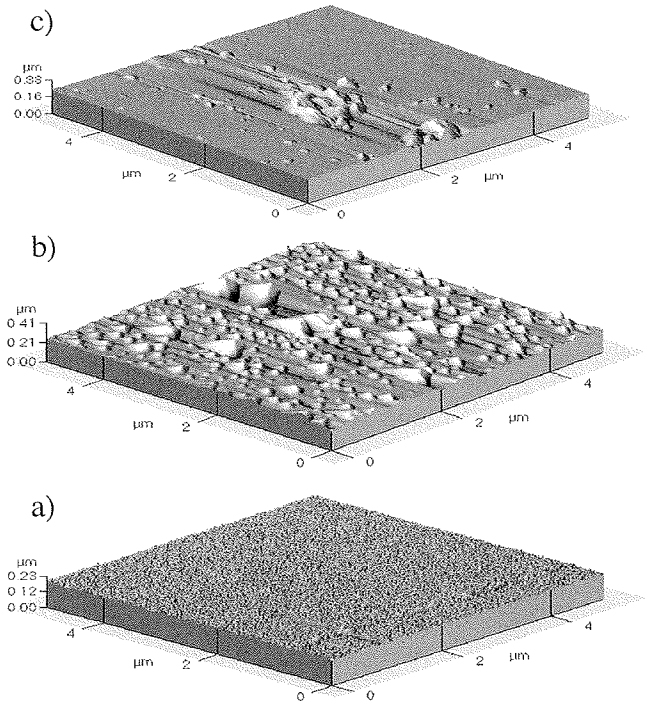

Figure 6. 3D AFM topographic images (5x5 mm) of the acrylic latex BMM-SS4 after casting at room temperature (a) and after annealing at 120°C for 170 hours (b) and 500 hours (c).

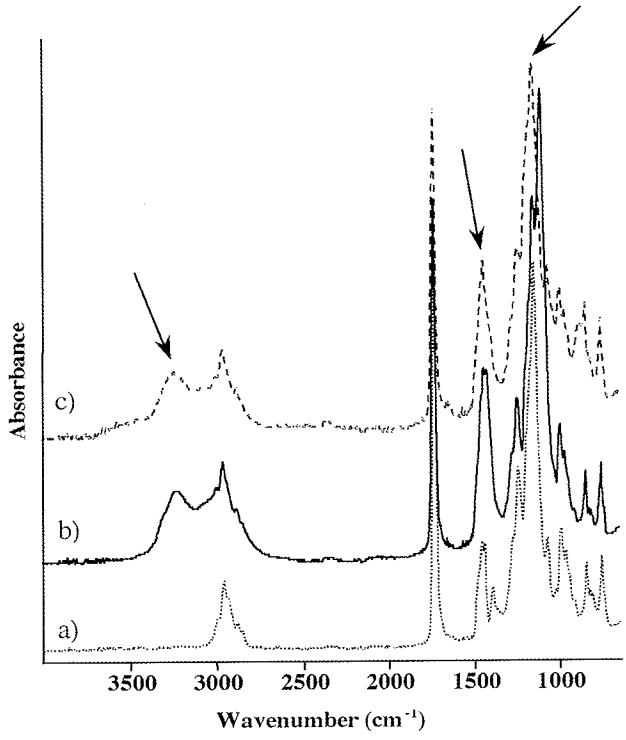

Figure 7. ATR-FTIR spectra of the acrylic latex BMM-SS4: unged (a); thermally aged at 120°C for 170 hours (b); thermally aged at 120°C for 500 hours (c).

The same conditions of analysis described in the experimental section were applied to coloured paint samples by four different producers, and two types of non-ionic surfactants (ethoxylated fatty alcohols and alkylaryl polyethoxylates) and a number of organic pigments were identified [7].

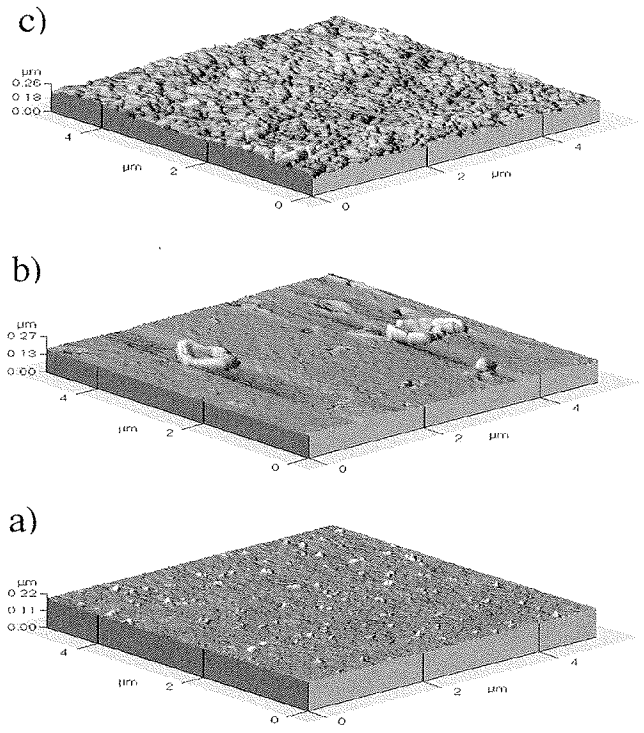

Figure 8. 3D AFM topographic images (5x5 mm) of the acrylic latex BMM-SS4 artificially light aged under a xenon lamp after 500 hours (a); after 1000 hours (b) and after rinsing with water (c).

Surface chemical and morphological characterisation

The most relevant surface morphological and chemical changes occurring over time, both under natural and accelerated ageing conditions, are primarily related to the exudation of surfactants.

On unpigmented media, phase separation of surfactants can be seen even with the naked eye. After a certain period of time, varying from latex to latex, films become translucent. At the beginning of the phenomenon, using an optical microscope, spherulitic crystals can be distinguished [8]. Then they merge and form larger translucent zones (Figure 4). Migration of surfactants obviously depends on the interactions with the polymer binder and the support. In the case of paints applied as films on glass slides, the surfactants were observed to preferentially exude at the paint/air interface.

Under extended periods of natural ageing, the total amount of surfactants decreases because of photooxidative degradation; after accelerated ageing treatments, surfactants were no longer detected by either spectroscopic or chromatographic techniques. The ATR-FTIR spectrum of a titanium white paint film prepared six years ago shows the typical absorptions of polyethoxylated type surfactants at 2892, 1343 and 1110 cm^{-1}. In the sample artificially aged under fluorescent tubes there is no spectral evidence of surfactants, which have probably degraded by photooxidation (Figure 5). The gradual disappearance of surfactants under extended ageing treatments has also been confirmed by SEC and GC-MS [7].

Migration phenomena in laboratory prepared acrylic latexes has been monitored as well and the surface morphology of the dried films has been investigated by atomic force microscopy.

On p(nBA-co-MMA) latexes dried at room temperature, discrete polymer particles were observed (Figure 6a). After heating at 120°C for two hours, complete coalescence occurs and surfactant aggregates are formed at the film surface (Figure 6b). At first the amount of exuded material increases with time and 'bumps', much larger in size than the original individual particles, appear at the polymer/air interface. After 500 hours of thermal ageing the amount of surfactant has decreased as it is partially degraded (Figure 6c). ATR-FTIR spectra show the same trend (Figure 7).

Under photooxidative ageing at outdoor exposure conditions, the migration of surfactants to the coating surface proceeds more slowly than under thermal ageing, but the features of the process are nearly the same. Figure 8 shows the AFM images of the acrylic latex BMM-SS4 aged under a xenon lamp simulating accelerated outdoor exposure. The upper AFM image shows the effect of rinsing with distilled water. As expected, 'bumps', being water-soluble,

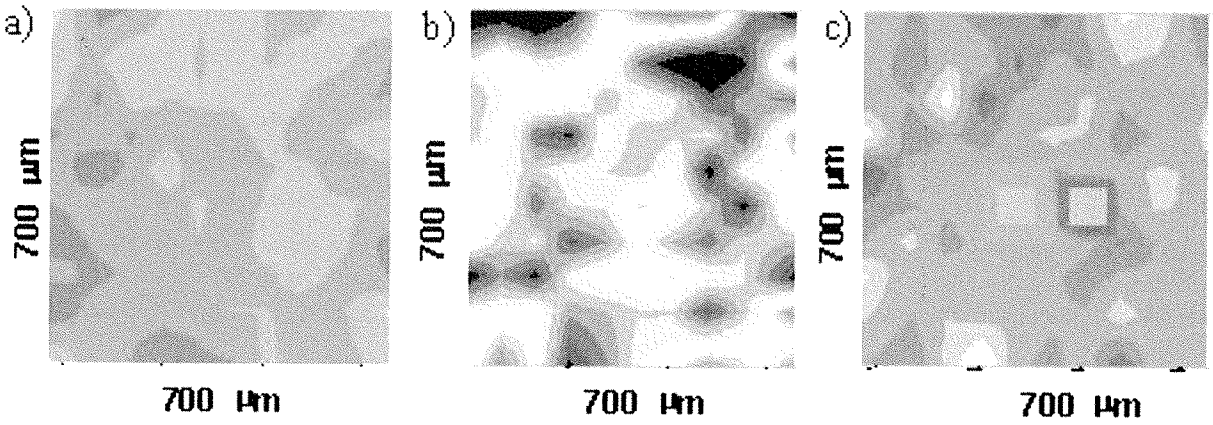

Figure 9. µATR-FTIR maps of the acrylic latex BMM-SS4 after casting at room temperature for a few days (a), after thermal ageing at 120°C for two hours, (c) after thermal ageing and rinsing with water (c).

have disappeared, while the surface below appears rougher than the original one.
Surfactant distribution of waterborne acrylic coatings has also been studied by μATR-FTIR mapping. Areas of 700x700 μm have been analysed. Maps of the height ratio of two peaks, one characteristic of the acrylic medium (1238 cm^{-1}) and the other diagnostic of polyethoxylated surfactants (1108 cm^{-1}), are reported in Figure 9.
While the map of the dried sample is homogeneous as shown by its uniform color, the map obtained after heating the film at 120°C for two hours shows an increased intensity of the IR absorption due to the surfactant, which is indicated by dark grey. Rinsing with distilled water causes the removal of the surfactant from the coating surface and the resulting map has the same colours and colour distribution as the original coating.
The same study has been carried out on a fluorinated acrylic latex. In this case AFM images show that even under thermal ageing at 120°C, complete coalescence does not happen, as the boundaries of the latex particles are still visible. It is interesting to note that surfactant migration to the polymer/air interface occurs to a smaller extent as demonstrated by the small differences in the colour maps obtained by μATR-FTIR mapping.

Conclusions

Several applications of infrared spectroscopic techniques have been applied to the characterisation of waterborne coatings and paints.
By coupling the separating power of size-exclusion chromatography with infrared spectroscopy, the organic components of acrylic emulsion paints and coatings have been resolved and good quality infrared spectra of polymer binders, surfactants and pigments have been obtained. Transmission infrared analysis of the polymer films could not detect any difference between unaged and aged samples, especially those containing inorganic components such as pigments and extenders, but ATR surface analysis highlighted important chemical and morphological changes occurring with ageing. In time, surfactants exude to the polymer/air interface where they gradually degrade by photooxidation. Phase separation of surfactants, their distribution on the coatings/paints surface and the effect of water treatments have been monitored by μATR-FTIR and AFM.

Acknowledgements

The authors wish to thank Tom Learner, Tate Gallery Conservation Department, for providing paint samples and for his invaluable co-operation, and Valter Castelvetro, Department of Chemistry and Industrial Chemistry, University of Pisa, for supplying the acrylic and fluorinated latexes.

References

1. J. Crook, T.J.S. Learner. *The Impact of Modern Paints*. London: TGPL (2000).

2. C.V. Horie. Materials for Conservation. Butterworth-Heinemann, Oxford (1987).

3. O. Chiantore, M. Lazzari, M. Aglietto, V. Castelvetro, F. Ciardelli, 'Photochemical stability of partially fluorinated acrylic protective coatings. I. Poly(2,2,2-trifluoroethyl methacrylate) and poly(1H,1H,2H,2H-perfluorodecyl methacrylate-co-2-ethylhexyl methacrylate)s, *Polymer Degradation and Stability*, 67 (2000) 461-467.

4. L. Toniolo, T. Poli, V. Castelvetro, A. Manariti, O. Chiantore, M. Lazzari, 'Tailoring new fluorinated acrylic copolymers as protective coatings for marble', *Journal of Cultural Heritage*, 3 (2002) 309-316.

5. V. Castelvetro, O. Chiantore, F. Ciardelli, G. Costa, C. De Vita, E. Taburoni, 'Water-borne silane-acrylic hybrid polymer particles for the consolidation and protection of porous stone surfaces', in: *Art & Chemie: les polymers.* Actes du Congrès, CNRS Editions, Paris (2003) 45-50.

6. A. Tzitzinou, P.M. Jenneson, A.S. Clough, J.L. Keddie, J.R. Lu, P. Zhdan, K.E. Treacher, R. Satguru, 'Surfactant concentration and morphology at the surfaces of acrylic latex films', *Progress in Organic Coating*, 35 (1999) 89-99.

7. D. Scalarone, O. Chiantore, 'Separation techniques for the analysis of artists' acrylic emulsion paints', *Journal of Separation Science*, 27(4) (2004) 263-274.

8. P.M. Whitmore, V.G. Colaluca, E. Farrell, 'A note on the origin of turbidity in films of an artists' acrylic paint medium', *Studies in Conservation*, 41 (1996) 250-255.

Separation of Acrylic Paint Components and their Identification with FTIR Spectroscopy

Dr. Julia Jönsson, Dr. Tom Learner
Tate, Millbank, London SW1P 4RG

Abstract

Although Fourier transform infrared (FTIR) spectroscopy is recognised as a useful tool for characterising acrylic emulsion paints, identification of individual paint components is often limited due to coincidental or overlapping peaks in FTIR spectra. This paper discusses improvements in FTIR analysis, made by immersing paint samples in organic solvents and hydrochloric acid to separate components prior to analysis. FTIR spectra collected for the resulting extracts and residues give a clearer indication of the components' identities while a more detailed analysis can produce spectra of isolated media, pigments and extenders. The agreement of spectra for these isolated components with those of standards is greatly improved compared to agreement between the untreated paint samples and the same standards.

Introduction

The use of FTIR to identify modern paint binders has been reported earlier, showing that it is often possible to distinguish between e.g. oil, alkyd, polyvinyl acetate (PVA), acrylic and cellulose nitrate media [1]. Many of the other major components that are typically found in modern paint formulations - pigments and extenders - also display characteristic FTIR spectra. The spectra for most paint samples are therefore often complex, with overlapping peaks from each of the main components. One particular problem is the difficulty in observing diagnostic peaks from the spectra of organic pigments, either because they are only present in relatively low concentrations, and/or because they are masked by the broad absorptions from extenders, such as calcium carbonate (chalk), calcium sulphate (gypsum), or barium sulphate (blanc fixe), which are often present in large quantities in modern paint formulations. Although less abundant additives e.g. surfactants also display characteristic FTIR spectra, they are usually present in too low concentrations to be identified in a spectrum collected in standard transmission mode.

The analysis/identification of organic pigments in paints is therefore an area which needs some attention. Although several techniques, e.g. pyrolysis - gas chromatography (PyGC) and pyrolysis - gas chromatography - mass spectrometry (PyGCMS) [2, 3], direct temperature resolved mass spectrometry (DTMS) [4], laser desorption mass spectrometry (LDMS) [4, 5] and microchemical spot tests [6, 7] have proven successful in detecting a selection of organic pigments in paint formulations, not all pigment classes are identifiable by all these methods. Even when pigments are identified by these techniques, complementary information via another technique is always of benefit, especially with FTIR instruments, which are becoming increasingly accessible and affordable to conservation scientists.

Analysis of organic pigments in modern paints leads to a more detailed understanding of the techniques used by artists in the 20th and 21st century. Knowledge of the materials used in a particular work also has a bearing on treatments used in conservation. Materials used in cleaning may, for instance, affect organic pigments differently depending on their chemical structure. By characterising paint composition prior to treatment, cleaning materials and procedures can be carefully chosen to minimise both short-term and long-term damage. The impact of ageing may also depend on the chemical nature of organic pigments. Rates of paint degradation can, under certain circumstances, be enhanced or attenuated, depending on the pigments present. Pigment analyses then play an important role in deciding the conditions under which works of art should be displayed and stored.

Synthetic organic pigments can be arranged into several chemical classes. The largest class of synthetic organic pigments, the azo pigments, is further divided into several groups, of which most relevant to artists' colours are monoazo (arylide), disazo (diarylide) and naphthol (mainly red/yellow). Non-azo pigments (polycyclic compounds) make up the remaining classes of synthetic organic pigments. Phthalocyanine pigments (blue/green) are the most frequently used polycylics in artists' colours. Less common, but nevertheless still often encountered in works of art, are the quinacridone (red/violet), perinone (red/orange), perylene (red), anthraquinone (yellow/red/blue), dioxazine (violet) and diketo-pyrrolo-pyrrole (orange/red) pigments.

Organic pigments are characterised by several sharp, intense bands in the fingerprint region of FTIR spectra (1500-500 cm^{-1}) and the potential of identifying organic pigments via these characteristic peaks has been recognised [8]. A

common approach for identifying paint components is to match FTIR spectra of unknowns with FTIR spectra of standards compiled in spectral libraries [9], however the relatively broader bands of extenders such as chalk can overlap with, and possibly even obscure, the peaks of interest, leading to poorer than necessary agreement between standards and unknowns. This paper presents measures taken to enhance spectral contributions from organic pigments and, where extender peaks significantly interfere with peaks from organic pigments, individual components have been successfully identified using a combination of organic solvent extraction, treatment with dilute hydrochloric acid and a spectral subtraction tool within OMNIC™ FTIR software.

Experimental Section

A series of twelve acrylic emulsion paints of known composition (listed in Table 1) were immersed in the organic solvents acetone, methanol and dichloromethane to investigate whether the components of organic pigment-containing modern paints could be separated to aid FTIR spectral interpretations. An additional three samples from works of art, where the identity of the pigments was uncertain (Table 1) were also analysed. Small paint fragments were placed in the tips of 1 ml vials, several drops of solvent were added to immerse the sample and the vials were ultrasonicated for at least 30 minutes. The solvents, containing extractable components of the paint, were transferred to microscope slides and allowed to evaporate to dryness. FTIR transmission spectra were collected for untreated paint samples, the dried extracts and the remaining residues. Each sample was applied to a horizontal diamond cell and pressed to a thin film with a stainless steel roller. A sample area of ~100 x 100 µm was selected with the aid of a Spectra-Tech IR plan microscope and spectra were collected with a Nicolet Avatar 360 spectrometer. 128 scans were collected at a resolution of 4 cm^{-1}. For samples where chalk was an obvious component of the paint, a paint fragment was immersed in dilute hydrochloric acid (~pH 1). After 30 minutes, the acid was removed and the sample allowed to dry. FTIR transmission spectra of the acid-treated, dried residues were collected as described above. All spectra were processed and analysed using OMNIC™ software.

Table 1

SAMPLE	PAINT	MANUFACTURER	PIGMENT CLASS
1	naphthol red light	Royal Talens Rembrandt (2003)	monoazo/perinone
2	naphthol crimson	Liquitex (1994)	monoazo
3	perylene red	Grumbacher (1994)	perylene
4	azo yellow lemon	Royal Talens Rembrandt (2003)	monoazo
5	yellow light hansa	Golden (2003)	monoazo
6	yellow light hansa	Liquitex (2003)	monoazo
7	azo yellow medium	Liquitex (1994)	monoazo
8	phthalo green	Royal Talens Rembrandt (2003)	phthalocyanine
9	phthalo green	Winsor & Newton Finity (2003)	phthalocyanine
10	phthalo blue	Liquitex (1994)	phthalocyanine
11	quinacridone red	Golden (1994)	quinacridone
12	acra violet	Liquitex (1994)	dioxazine/phthalocyanine

SAMPLE	WORK	SAMPLE DESCRIPTION
13	**G. Ayres**: *Sundark Blues*, 1994	orange paint: drying oil, azo yellow pigment, blanc fixe, alumina
14	**F. Stella**: *Hyena Stomp*, 1962	red paint: alkyd resin, azo red, chalk, silica
15	**P. Caulfield**: *Hemingway Never Ate Here*, 1999	green paint: acrylic emulsion, chalk, possible phthalocyanine green

Table 1. samples 1-12) films of tube/pot acrylic emulsion paints; samples 13-15) works from Tate's collection previously analysed with PyGCMS, FTIR and EDX.

Results & Discussion

The solvents chosen were found, in general, to separate paint components and benefit FTIR spectral interpretations. The impact of the solvents on the paints did however vary depending on the composition of the paint and the solvent in question. In most cases (samples 1, 4-9, 13-15), individual components were isolated to the extent that medium, extender (if present) and organic pigment could all be identified. For an additional three samples (2, 10, 11), the extraction process served to slightly enhance the spectral contribution from the organic pigments. Only samples 3 and 12 seemed to be unaffected and these samples contained perylene and dioxazine, so-called "high performance pigments", pigments developed with extreme resistance to e.g. light, heat, humidity, organic solvents and water. Of the three solvents investigated, dichloromethane was the most consistent in extracting media while extenders and

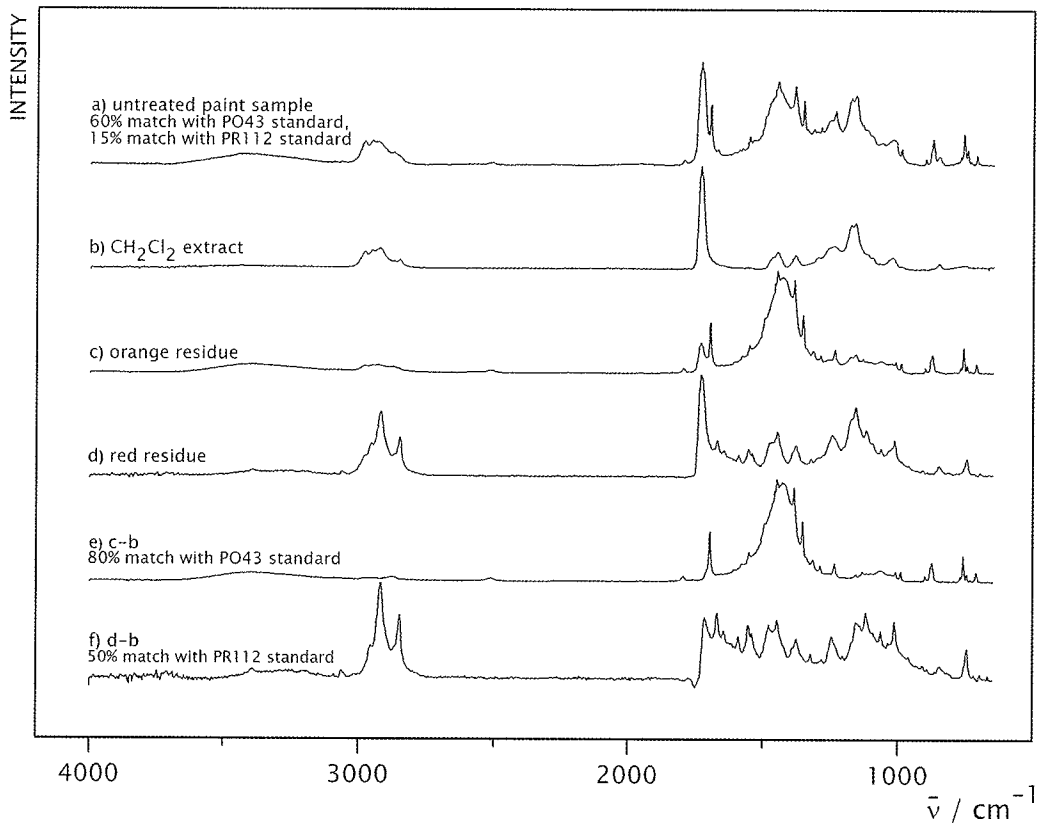

Figure 1. FTIR spectra of Naphthol Red light paint (Royal Talens). a) untreated paint sample; b-d) extract and residues following immersion in dichloromethane; e-f) separated paint components after subtraction of spectrum b (medium) using OMNIC™ software.

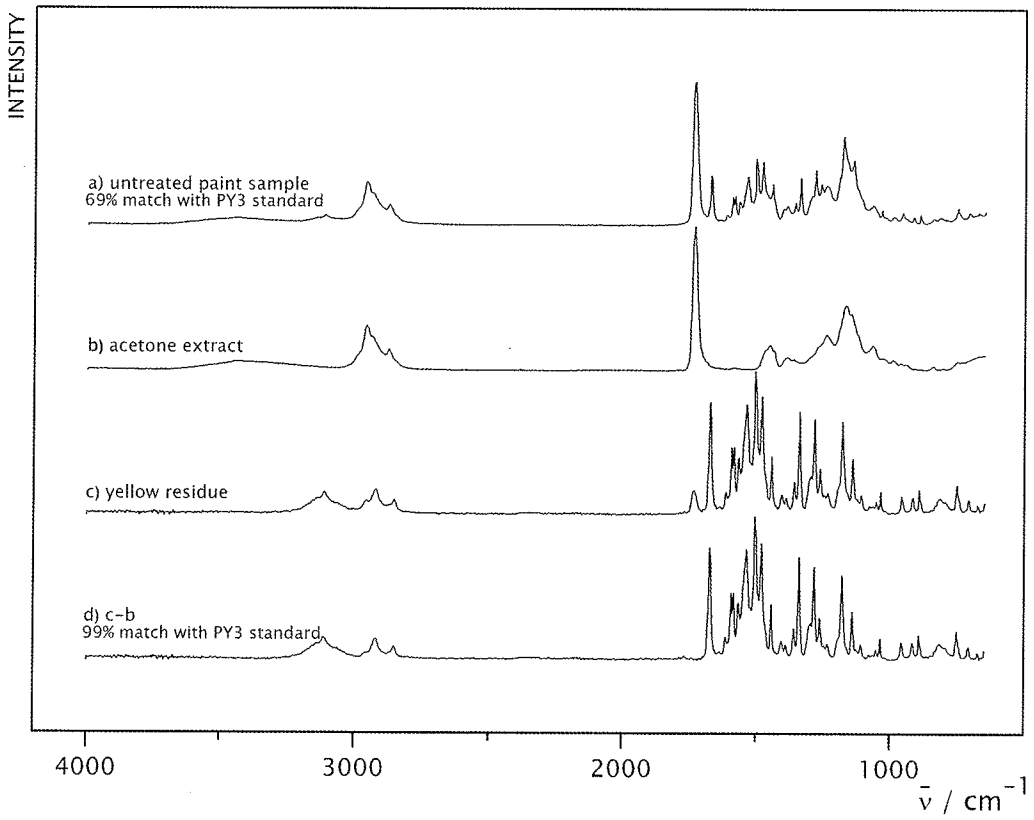

Figure 2. FTIR spectra of Yellow light hansa paint (Golden). a) untreated paint sample; b-c) extract and residue following immersion in acetone; d) isolated pigment after subtraction of spectrum b (medium) using OMNIC™ software.(medium) using OMNIC™ software.

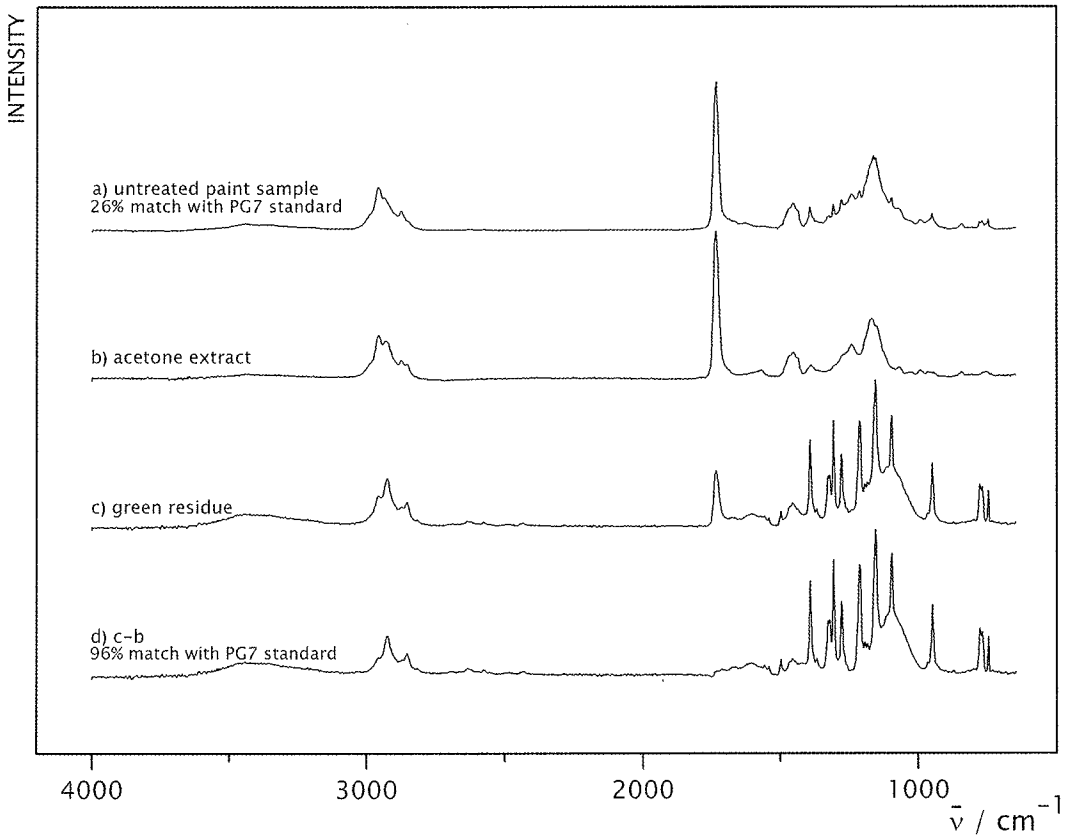

Figure 3. FTIR spectra of Finity phthalo green (Winsor & Newton). a) untreated paint sample; b-c) extract and residue after immersion in acetone; d) isolated pigment after subtraction of spectrum b (medium) using OMNIC™ software.

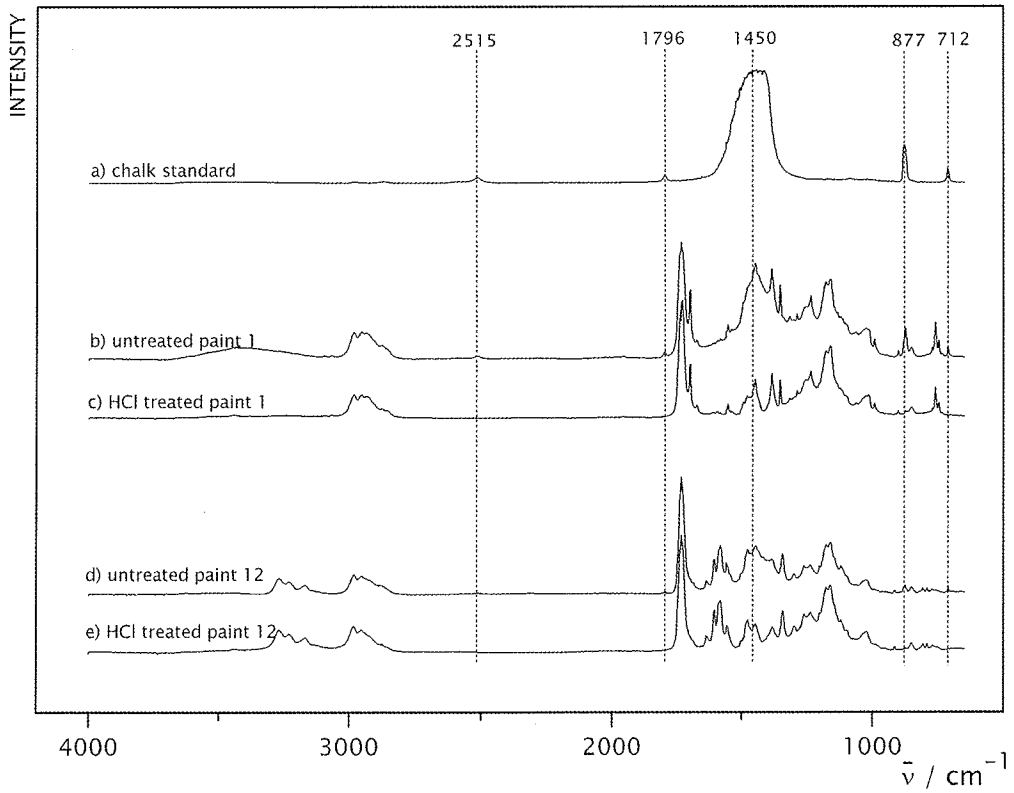

Figure 4. FTIR spectra showing the effect of dilute HCl. a) chalk standard b-c) naphthol red light paint (Talens) before and after treatment with HCl d-e) acra violet paint (Liquitex) before and after treatment with HCl. Dotted lines mark the characteristic peaks of chalk (cm^{-1}).

pigments were identified and isolated to varying degrees by each of the three solvents. The appearance of a band at about 1600 cm^{-1} in several spectra collected for methanol treated extracts, suggested some modification/degradation of the paint on immersion. Samples immersed in methanol were therefore excluded from spectral interpretations. The immersion of chalk-containing paint fragments in dilute hydrochloric acid provided a simple and effective means of dissolving chalk to eliminate interfering peaks from the IR spectra. The organic pigments appeared to be unaffected by the dilute acid and could be identified from the sharp features in the fingerprint region of the IR spectrum.

Figure 1a shows a FTIR spectrum collected for a sample of naphthol red acrylic paint (Royal Talens). The spectrum is characteristic of an acrylic emulsion paint with a predominant carbonyl stretching frequency at ~1732 cm^{-1} with peaks in the C-H stretching region at 2981 and 2854 cm^{-1} together with a doublet at 1177/1060 cm^{-1} signifying the presence of poly(ethyl acrylate/methyl methacrylate) copolymer, often abbreviated to p(EA/MMA) [1]. Peaks at 2515, 1796, ~1450, 877 and 713 cm^{-1} are all due to the use of chalk as an extender in the paint. The sharp features throughout the fingerprint region are indicative of an organic pigment.

Figure 1 shows how extracting components of the paint into dichloromethane has led to confirmation of the paint components and also the identification of two different organic pigments in the paint; PO43 and PR112. Figures 1b-d show spectra collected for the treated sample. Spectrum 1b is of the dried extract from the microscope slide and shows peaks characteristic of acrylic medium only. Spectrum 1c is of the remaining paint (an orange residue) and spectrum 1d is of a visible red/pink particulate matter that had separated from the clear medium in the dried extract. Although the paint medium was already discernable from the FTIR spectrum of the untreated paint (Figure 1a), isolation of the medium in this manner not only confirms the identification, but using FTIR software, the medium spectrum may be subtracted from other spectra collected for the same paint sample to give a clearer indication of the extender and pigments. Figure 1e for instance, shows the result when the medium spectrum (1b) is subtracted from that of the orange paint residue (1c). Peaks for chalk extender are much clearer than they appeared in the spectrum for the untreated sample and the remaining sharp peaks are in good agreement with a standard spectrum of the organic pigment PO43, also much clearer than in the untreated paint spectrum. The spectrum collected for the red/pink residue dispersed in the extract (1d) provides evidence for the presence of a second pigment, which is not noticeable in the spectrum of the untreated paint. Subtraction of the medium spectrum from spectrum 1d produces

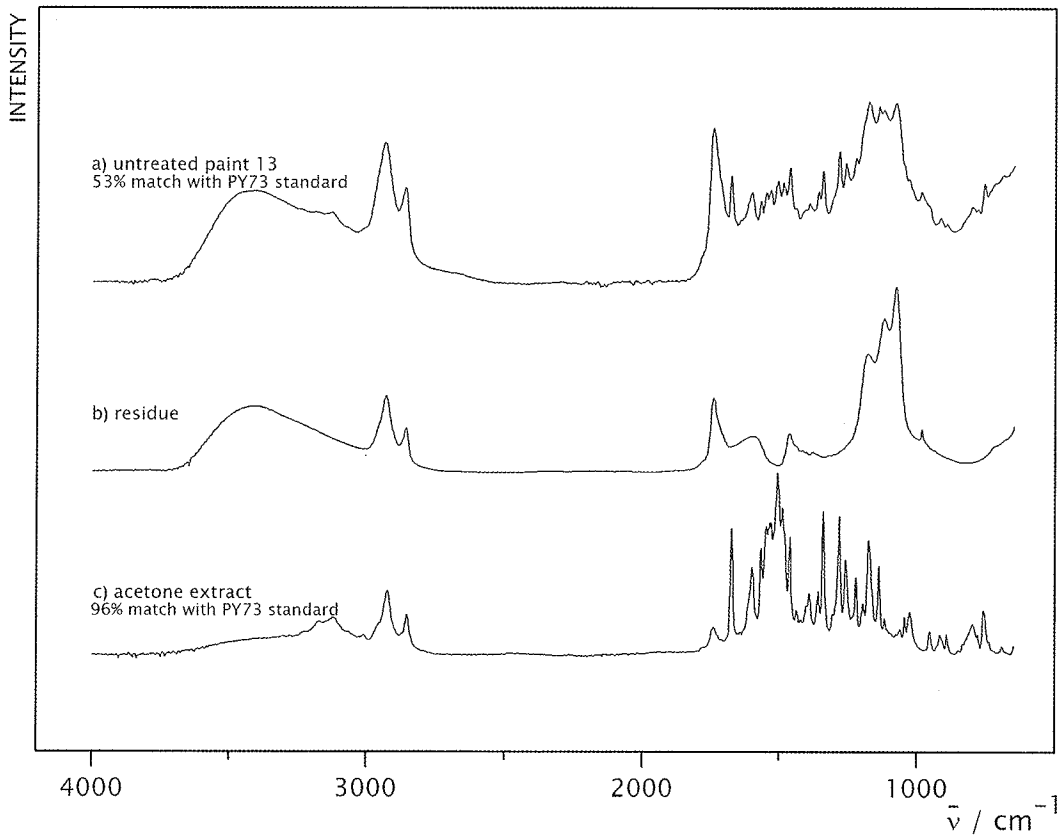

Figure 5. FTIR spectra of an orange paint fragment taken from *Sundark Blues* by Gillian Ayres. a) untreated paint sample b-c) residue and extract after immersion in acetone.

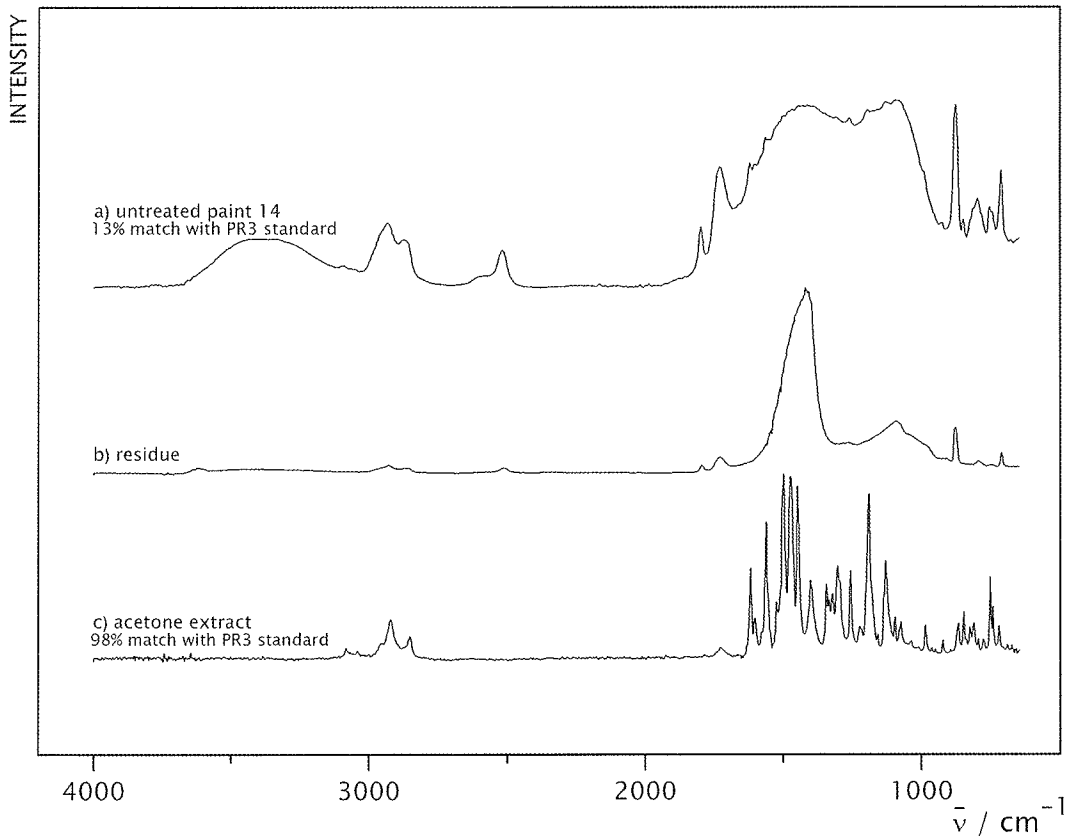

Figure 6. FTIR spectra of a red paint fragment taken from *Hyena Stomp* by Frank Stella. a) untreated paint sample b-c) residue and extract after immersion in acetone.

spectrum 1f, and despite their minor contribution to the overall spectrum, these sharp peaks are in good agreement with a standard spectrum of the organic pigment PR112.

Figure 2 shows the effects of extraction with acetone on a fragment of Yellow light Hansa paint (Golden). It was again possible to observe and resolve two components in the dried extract; clear medium and particles of organic pigment. The medium spectrum (Figure 2b) is characteristic of a poly (*n*-butyl acrylate - methyl methacrylate) copolymer and by subtracting this spectrum from the spectrum of areas of extracted yellow pigment (Figure 2c), a spectrum for the pure pigment is obtained (Figure 2d) which is in ~99% agreement with a spectrum collected for a standard specimen of PY3 pigment. The untreated paint sample provided only a 69% match with the same standard. Separating the paint into components gives a clear indication whether extenders are included, where the near perfect agreement with standard spectra of medium and organic pigment in this case strongly supports the absence of extenders.

Phthalocyanines, like perylene and dioxazine, are examples of high performance pigments designed to be, amongst having other properties, solvent resistant. As illustrated in Figure 3, immersion of the phthalocyanine containing paint Finity Phthalo Green (Winsor & Newton) in acetone led to successful separation of the components p(EA/MMA) copolymer and organic pigment PG7.

Fragments of samples 1, 4, 8 and 12 were immersed in dilute hydrochloric acid to dissolve chalk extender in these paints. Figure 4 illustrates the spectra collected for samples 1 and 12 compared with a standard spectrum of chalk. The peaks characteristic of chalk (bands at 2515, 1796, ~1450, 877 and 713 cm^{-1}) are absent for the treated paints, while the organic pigment peaks remain and are more easily identified than in the corresponding untreated samples.

Several paint fragments from works in Tate's collection were analysed with procedures similar to those described above. Three works were chosen where uncertainties remain concerning the identity of organic pigments despite previous analyses with other techniques. A brief description of results from PyGCMS, FTIR and EDX (energy dispersive X-ray) analyses is given in Table 1.

Sample 13 was a fragment of orange paint taken from *Sundark Blues* (1994) by Gillian Ayres (Tate Gallery T07003). Figure 5 shows the spectrum of the untreated paint fragment alongside spectra collected after immersion in acetone. Spectrum 5b, from the residue remaining after extraction, displays peaks characteristic of barium sulphate (blanc fixe) extender (peaks at 1177, 1116, 1070, 982 cm^{-1}) and a drying oil (C-H stretching peaks at 2934 and 2859 cm^{-1}; C=O at 1742 cm^{-1}). Spectrum 5c shows organic pigment peaks which are greatly enhanced compared to spectrum 5a,

resulting in a match with a previously collected standard of PY73 of 96% as opposed to the 53% match of the untreated sample. The analysis confirmed the identity of extender and medium and successfully isolated the organic pigment.
Extraction into acetone performed on sample 14, a sample of red paint from *Hyena Stomp* (1962) by Frank Stella (Tate Gallery T00730), produced the results presented in Figure 6. As can be seen (Figure 6a), strong absorption by extenders in the region 1700-900 cm^{-1}, obscures most features in the fingerprint region of the spectrum. A spectrum collected from a dried extract following extraction into acetone permits a more convincing identification of organic pigment PR3; a 90% match compared with 13% for the untreated sample. The identity of the extenders chalk (peaks at 2512, 1795, 1450, 878, 712 cm^{-1}) and silica (peaks at 1092 and 794 cm^{-1}) also becomes more obvious (Figure 6b).
Identification of the organic pigment PR3 in sample 14 was also made possible by the action of dilute hydrochloric acid (Figure 7). Although peaks of the silica extender persisted (Figure 7c), the characteristic peaks of calcium carbonate were eliminated and pigment PR3 was identified (85% match with standard).
Removal of chalk with dilute HCl also aided the analysis of sample 15, a sample taken from *Hemingway Never Ate Here* (1999) by Patrick Caulfield (Tate Gallery T07509) (Figure 7d-e). Revealing the organic pigment peaks by eliminating chalk allowed the identification of pigment PG7, but this was achieved only by limiting the match with standards to the fingerprint region of the spectrum. Searching in the same region of the untreated sample spectrum resulted in only a 9% match for PG7 and misleading matches with 15 other organic pigments were more significant.

Conclusions

The work presented demonstrates that by immersing acrylic emulsion paints in organic solvents and hydrochloric acid and employing spectral subtraction procedures, improvements can be made in the analysis of organic pigments with FTIR spectroscopy. Separating the major constituents of acrylic emulsion paint prior to analysis, eases the interpretation of spectra and in addition to improving the analysis of organic pigments, the presence and identity of media and extenders are confirmed.
In several cases where components of the paint are not entirely separable by these means, there is at least an enhancement in the contribution of organic pigments to the spectrum on immersion in organic solvents, which

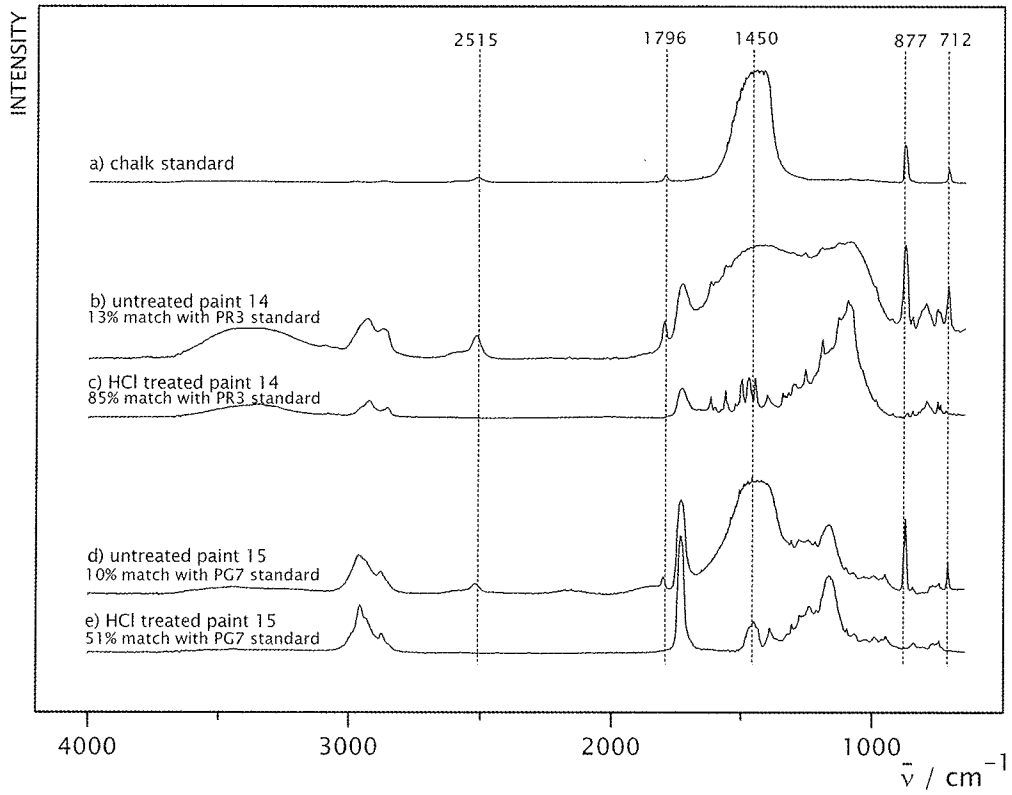

Figure 7. FTIR spectra showing the effect of dilute HCl. a) chalk standard b-c) red paint fragment from *Hyena Stomp* by Frank Stella before and after treatment with HCl d-e) green paint fragment from *Hemmingway Never Ate Here* by Patrick Caulfield before and after treatment with HCl. Dotted lines mark the characteristic peaks of chalk (cm^{-1}).

increases the chances of detecting and identifying the pigment on comparison with standards.
Treatment of chalk-containing acrylic emulsion paints with dilute hydrochloric acid appears to provide a simple and effective way of eliminating chalk extender while organic pigments seem to remain intact. Organic pigment peaks obscured by the presence of chalk in FTIR spectra become accessible resulting in greatly improved agreement with standards compiled in spectral libraries.
The techniques tested are applicable to works of art, where organic pigments have been identified, even for works in media other than acrylic emulsion; organic solvents assisted in identifying pigments in oil and alkyd media while HCl successfully eliminated chalk interferences in both alkyd and acrylic emulsion media.

Acknowledgement

The Deborah Loeb Brice Foundation is gratefully acknowledged for the financial support of a postdoctoral fellowship at Tate. Avecia, Clariant, BASF and Heubach are acknowledged for providing pigments for spectral standards.

References

1. Learner, T., 'The use of a diamond cell for the FTIR characterisation of paints and varnishes available to twentieth century artists' in B. Pretzel (ed.), *Postprints: IRUG 2 at the V&A, London, September 1995*, Victoria and Albert Museum, London (1998) 7-20.

2. Sonoda, N., 'Characterization of organic azo-pigments by pyrolysis-gas chromatography', *Studies in Conservation* (1999) **44** 195-208.

3. Scalarone, D., and Chiantore, O., 'Separation techniques for the analysis of artists' acrylic emulsion paints', *J. Sep. Science* (2004) **27** 263-274.

4. Boon, J. J., and Learner, T., 'Analytical mass spectrometry of artists' acrylic emulsion paints by direct temperature resolved mass spectrometry and laser desorption ionisation mass spectrometry', *J. Anal. Appl. Pyrolysis* (2002) **64** 327-344.

5. Wyplosz, N., 'Laser desorption mass spectrometric studies of artists' organic pigments, PhD thesis, FOM Institute for Atomic and Nuclear Physics (2003).

6. Crown, D. A., *The Forensic Examination of Paints and Pigments*, Charles C Thomas, Illinois (1968).

7. Keijzer, M., 'Microchemical analysis on synthetic organic artists' pigments discovered in the twentieth century' *ICOM committee for conservation* (1990) **1** 220-225.

8. Learner, T., 'The characterisation of acrylic painting materials and implications for their use, conservation and stability' unpublished PhD thesis, University of London (1997).

9.Price, B., and Pretzel, B., IRUG Edition 2000 spectral database, www.irug.org (accessed 2004).

Image Analytical Studies of Lead Soap Aggregates and their Relationship to Lead and Tin in 15th C Lead Tin Yellow Paints From the Sherborne Triptych.

Jaap J. Boon[1], Emily Gore[1-2], Katrien Keune[1] and Aviva Burnstock[2]
[1] Molecular Paintings Research Group, FOM Institute AMOLF, Kruislaan 407, 1098 SJ Amsterdam, NL.
[2] Courtauld Institute of Art, London, UK.

Abstract

Lead soaps and lead soap aggregates were demonstrated by imaging FTIR analysis in lead tin yellow paint samples from the wings of the 15th century Northern European Sherborne Triptych. The metal carboxylate FTIR distribution maps were compared with light microscopic, SIMS and SEM-EDX maps. Lead palmitate and stearate positive ion SIMS maps coincide spatially with the distribution of the metal carboxylates in the paint cross-sections. The maps of lead and tin originating from lead stannate in the lead tin yellow type I pigment overlay outside the metal soap aggregates and are distributed as if the lead stannates are pushed aside by the growing soap mass. Lead is also abundantly present inside the aggregates. The hypothesis put forward is that the lead tin yellow pigment originally consisted not only of lead stannate, but contained another lead containing mineral phase that reacted quantitatively with fatty acids released by ageing from the oil binding medium.

Introduction

Imaging FTIR is playing an important role in the detection of lead soap aggregates in oil paint layers. Boon and Heeren [1] reported the combined analysis of a lead soap protrusion by imaging FTIR and secondary ion mass spectrometry SIMS in the lead white underpaint layer of a double ground in Rembrandt van Rijn's *The Anatomy Lesson of Dr. Nicolaas Tulp* (MH461). SIMS information [2] on lead derivatives of palmitic and stearic acid were shown in the same area in the cross-section where high intensities of lead, palmitic and stearic fatty acid moieties coincided with FTIR information on aliphatic moiety stretch vibrations and asymmetric carboxylate stretch vibrations of metal soaps. The papers by Van der Weerd et al. [3] focussing on the FTIR and by Noble et al. [4] focussing on the painting context reported a larger number of lead soap occurrences in 17th C paintings. The scientific department of the National Gallery demonstrated lead soap aggregates in red lead and lead tin yellow-pigmented paint layers in a large number of oil paintings [5]. They propose that only the monocarboxylic fatty acids aggregate to lead soap accretions thus enriching the surrounding paint with diacids. Evidence for this comes from studies by GCMS of aggregates selected from paint layers demonstrating a remarkable absence of diacids [6] which may be caused by a difference in mobility between diacids and monocarboxylic acids. It is unclear at this stage whether the fatty acids migrate in the aged paint as free fatty acids or as lead derivatives to form the semicrystalline aggregates. It is also unclear how the properties of a paint film enriched in diacid soaps changes after aggregation of the monocarboxylic acids into separate entities.
At the Rio ICOM-CC triennial meeting Boon *et al* [7] proposed a scheme on the basis of comparative studies of the MH461 painting that lead soaps develop from a dispersed distribution during initial reaction of fatty acids with lead containing mineral matter through a stage where aggregation growth - perhaps in liquid crystalline form - takes place to later stages with swelling and protrusion through other paint layers. Keune et al. [8] indeed demonstrated the high concentrations of lead soaps by imaging FTIR, SIMS and SEMEDX in a cross-section from MH461, where aggregate formation had not yet taken place. The precise driving force of the process is presently unknown. The MH461 has been lined at least five times, which implies the mobilisation, aggregation and fusion into larger aggregates could have been accelerated since lead soaps of palmitic and stearic acid have melting points near 115 degree Celsius. On the other hand, lead soap aggregates are also observed in panel paintings. It is clear that leadhydroxycarbonates, lead oxide, lead acetate and leadplumbate (minium) can readily react with fatty acids to form soaps. Van der Weerd [9] reacted lead white under anhydrous conditions in refluxing xylene with stearic acid showing the complete conversion to stearic acid soap. Most soap formation occurs of course under conditions where environmental moisture is present. Deesterification of the oil paint medium shown by J. van den Berg et al. [10, 11] leads to an almost complete hydrolysis of the chemically dried oil paint. The wet chemical data and FTIR data suggest that mature aged oil paints are kept together by metal coordination of the acid and diacids group forming a metal soap network. This process in itself will not lead to metal soap mobilisation as we observed in some paints, unless there is a marked surplus of fatty acids due to a stoichiometric mismatch of oil, pigment and drying catalysts in the paint. Soap formation was already well known in the 19th century where it was found important to avoid soap

formation known as leathering by removal of free acids in the drying oil [12]. Little quantitative information is available on oil derived components in aged paint from paintings and their relationship to pigments and driers, so it is difficult to say or predict when paints are supersaturated with fatty substances that separate as aggregates, inclusions, protrusions, extruded masses or as blooms and efflorescent crusts. In the case of the MH461 painting, the imaging analytical studies of the early stage by Keune [7] suggest that the lead soaps are already there and aggregate by phase separation. The process of phase separation and segregation of monocarboxylic and dicarboxylic acid containing paint films is certainly worth more detailed study. New studies have recently been published on the crystal structure of lead soaps to help understanding the formation process in paintings [6, 13] and to determine the role of lead speciation [14].

The study by the National Gallery group also debunked an old adagium that believed that the well-known characteristic inclusions in lead tin yellow I (LTY-I) paints were proteinaceous. These inclusions were shown to be lead soap aggregates by GCMS and FTIR studies [5]. For a long time, painting researchers were comfortable with the explanation that LTY-I paints were emulsion paints, in which pigment and curdled protein had separated [15]. A large survey of many occurrences of LTY-I in paintings by the NG group found no evidence for proteinaceous matter. FTIR absorptions in the past had been misinterpreted as evidence for amide bonds, where metal carboxylates were present. This is understandable because the FTIR data of traditional paints in the range from 1600 – 1300 cm^{-1} is often rather complex and poorly resolved. The mechanism of formation of the inclusions in LTY paints is however still unresolved. The NG group suggests that lead stannate is the reactant with fatty acids from an oil binding medium leaving the question open on how to charge compensate the freed stannate. It is also not so clear how fatty acids can destroy the relatively stable metal salt of lead stannate (Pb_2SnO_4). The PhD thesis work by Eastaugh [16] suggests the possible existence of non-stoichiometric lead stannate phases with excess lead (as lead oxide) or tin oxide depending on the oven and cooling conditions of a lead stannate melt.

LTY-I paints in cross-section have very special characteristics. The lead soaps cause distortions of the paint layers and the pigment particle distributions that are used as a feature to identify lead tin yellow I paints [15]. Searching for an explanation, it inspired us to investigate the spatial relationship of pigments particles and organic phases using the imaging analytical tools of SIMS, FTIR, SEM-BS and SEM-EDX mapping. LTY-I paints from the 15th to 18th century are under investigation [17,18] to find out whether the distribution of the lead soaps, the tin containing mineral phases and the other pigment particles give away enough evidence to propose a mechanism that can be tested in model experiments. This paper is a first report on some cross-sections containing LTY-I taken from a 15th century triptych (*The Sherborne Triptych*) painted by an unknown northern painter. The triptych that is displayed in a chapel in Sherborne (Dorset) was studied and treated earlier by the Courtauld team. Existing samples embedded as cross-sections are reexamined in the present study.

Experimental

Painting samples

Samples containing lead tin yellow paint originate from left and right wings of the *Sherborne Triptych* (Courtauld Conservation report CIA1577) and are coded LS02, RS04, RS06 and RS21. The three panels depict the five miracles of Christ including subsidiary miracles in the upper corners. The iconography, technique and materials used are all consistent with Netherlandish painting of the latter half of the 15th century. The oak panels have chalk and animal glue grounds and then a very thin lead white and charcoal black oil priming (the media are not confirmed analytically)). Many of the pigments used are of high quality. GCMS analysis carried out at the National Gallery by Raymond White suggests the use of heat-bodied linseed oil. In 1923 when included in an exhibition of British primitives, it was attributed to the Master of Alkmaar [19]. Since then suggested attributions include Nicholas Froment, Master of Coetivy (Netherlandish working in French court), Albert Ouwater (Dutch) and Vrancke van der Stockt (Brussels city painter)[20]. The triptych is displayed in Sherborne Chapel (Dorset, UK) and is presently owned by the National Trust. No early documentation of the triptych exists, but it is believed to have either been commissioned especially for the Almshouse of St. John (built in 1442, Sherborne), or acquired soon after its completion.

Methods

FTIR

The samples were carefully re-polished dry on Micromesh© polishing cloths up to the finest mesh of 12000 to get the best surface possible. This was particularly necessary for the FTIR analysis since best reflection from surfaces is crucial for the reflective infrared analysis mode.

The FTIR imaging measurements were performed using the Bio-Rad FTS-6000 Stingray FTIR-imaging system, which combines a step-scan Michelson interferometer (Bio-Rad FTS-6000), an IR microscope (Bio-Rad UMA-500) and a 64 x 64 pixel Mercury-Cadmium-Telluride (MCT) focal plane array (IR camera) [9]. An area of 400μm x 400μm is imaged onto the 64 x 64 pixel focal plane array, giving a resolution of 6.25μm. The range of wavelengths chosen was 3800 -1000 cm^{-1}. The lower wavenumber limit was set by sensitivity of the focal plane array. The upper wavenumber limit was set by the theoretical shortest wavelength measurable according to Nyquist theorem, with an under sampling ratio of 4 [9]. The interferometer step frequency can be selected to optimise speed of measurement or signal to noise ratio. A frequency of 1Hz was chosen which allowed the frame-grabber board in the camera to average 200 images during each step to improve the signal to noise ratio [9]. The choice of spectral resolution determines the number of steps that the interferometer takes between 3800-1000 cm^{-1}. A resolution of 16 cm^{-1} was chosen, therefore the interferometer took 512 steps during the measurement procedure. Bio-Rad Win-IR Pro 2.5 software was used to control the interferometer and the ImagIR 2.1 image acquisition software.
After the calibration procedure, a background measurement was taken using a ZnSe disc and stored. Then an IR imaging measurement was taken of each sample. The resulting data was a complete interferogram for every pixel in the focal plane array. Data processing had four stages using the Win-IR Pro software, firstly the Fourier transform of both the ZnSe and sample interferograms are computed using the 'NB weak' function. Then the sample data is background corrected to reflectance units using the ZnSe measurement. Thirdly the resulting data set is truncated to the range of interest, namely 3800-1000 cm^{-1} and finally the Kramers-Kronig transformation of the data set is computed. The last computation was performed to transform the specular reflectance data to absorbance-like spectra. (Note that the majority of the detected light is specular reflected light. The quantity of specular reflected light is not only dependent on the absorption of light but also on the refractive index of the sample. Fortunately there is a fundamental relation between absorption and refraction that exists, which was first described by Kramers and Kronig. Therefore by application of the Kramers-Kronig transformation algorithm the data becomes comparable to the transmission spectra we are used to interpreting [reviewed in 9]). The resulting data set for each sample is an image taken at every interferometer step, where every pixel in the 64 x 64 array contains a complete infrared spectrum. False colour intensity maps can be generated at a particular absorption band of interest, giving an idea of the distribution of a particular functional group over the sample. The spectrum at an individual pixel was used to identify a material at a specific position in the sample.

SIMS
The static SIMS experiments were performed on a Physical Electronics (Eden Prairie, MN) TRIFT-II time-of-flight SIMS (TOF-SIMS). The surface of the sample was scanned with a 15 KeV primary ion beam from an $^{115}In^{+}$ liquid metal ion gun. The pulsed beam was non-bunched with a pulse width of 20ns, a current of 600 pA and the spot size approximately 120 nm. The primary beam was rastered over a 200 x 200 μm sample area, divided into 256 x 256 pixels. The measurements were made in both positive and negative mode were made. The surface of the sample was charge compensated with electrons pulsed in between the primary ion beam. To prevent large variations in the extraction field over the large insulation surface area of the paint cross-section a non-magnetic stainless steel plate with slits (1 mm) was placed in top of the sample. The paint cross-section (150 x 50 x 3 mm) was rinsed in hexane to reduce contamination of silicones.

SEM-EDX
Scanning Electron Microscopy studies in combination with Energy Dispersive X-ray analysis (SEM-EDX) were performed on a XL30 SFEG high vacuum electron microscope (FEI, Eindhoven, The Netherlands) with EDX system (spot analysis and elemental mapping facilities) from EDAX (Tilburg, The Netherlands). Backscatter electron images of the cross-sections were taken at 20 kV acceleration voltage at a 5 mm eucentric working distance and a spot size of 3 that corresponds to a beam diameter of 2.2 nanometer with current density of approximately 130 pA. EDX analysis was performed at a spot size setting of 4 (beam diameter 2.5 nm and current density 550 pA) to obtain a higher count rate and at an acceleration voltage of 22 kV. EDX Mapping parameters were: 512 x 400 matrix, 512 frames, 70 μs dwell time and 35 μs amplitude time. Samples were carbon coated to improve surface conduction in a CC7650 Polaron Carbon Coater with carbon fibre (Quorum Technologies, East Sussex, UK)

Results and discussion.

The cross-section from the paint of the green drapery from the robe of third figure from the left on the right wing has a lead tin yellow containing layer below a copper green glaze. The lead tin yellow paint shows two rather large

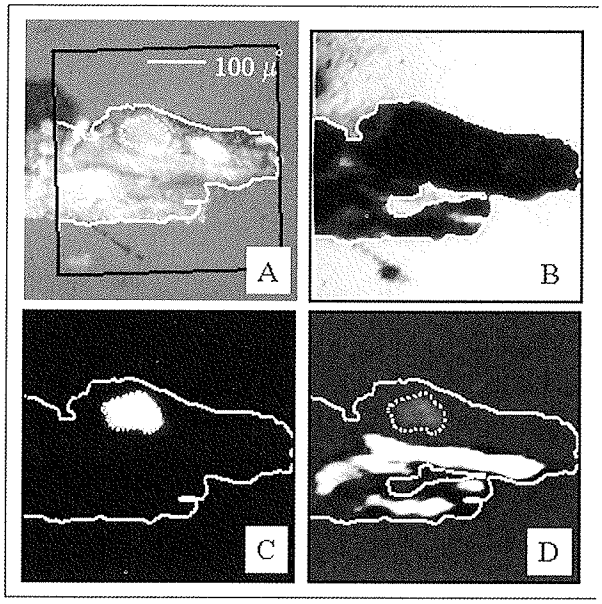

Fig.1 Light microscopic and FTIR maps of sample CIA 1577 RS06

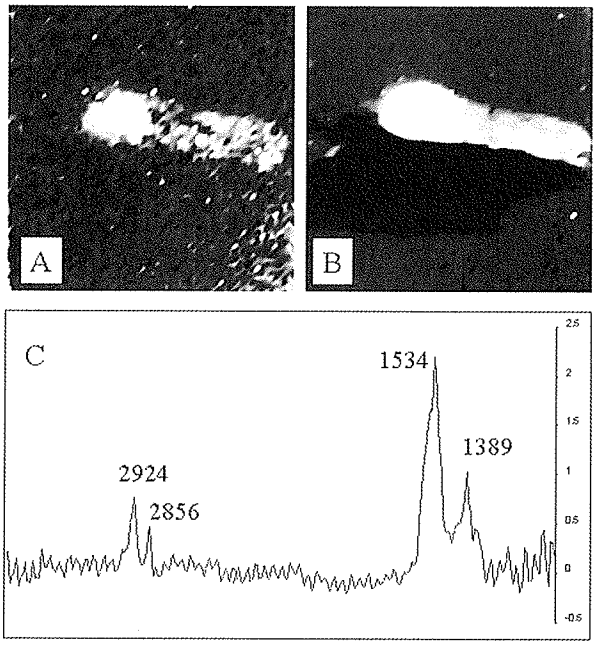

Fig 2 (below). FTIR spectrum and selected FTIR maps of lead soaps in sample CIA 1577 RS06

particles. The left one is UV-fluorescent and somewhat translucent, while the particle on the right is yellow and opaque. The right particle is presumably a lead-tin yellow pigment concretion, while the left particle is presumably a lead soap inclusion. The LTY paint layer is placed on a thin lead white and charcoal black priming on a thick chalk ground. A light microscopic micrograph is shown together with several FTIR images in Fig. 1A.

FTIR maps of the embedding medium (1724 cm^{-1}), the asymmetric stretch vibration of lead carboxylate (1534 cm^{-1}), and the CO stretch vibration of calcium carbonate (1405 cm^{-1}) are displayed in Fig. 1B, C and D. No image data were obtained on the lead stannate (LTY-I) because this pigment is mid IR-transparent. The colour coding from red (high) via yellow to green and blue (low) corresponds to the relative intensity of the FTIR data. A slight inhomogeneity of the mapped areas is often encountered and is thought to be due to surface corrugation on the microlevel. The contours of the cross-section are drawn along the boundary of the embedding medium in Fig. 1B and overlain on the other FTIR maps in order to position the maps of the lead soap and chalk within the cross-section. It is our laboratory practice to correlate light microscopic data and FTIR data in this way. The contour map of the lead soap inclusion is also plotted in Fig 1C and D. The box in 1A outlines the area investigated with the imaging FTIR. An overlay of the selected FTIR data were fitted on the light microscopic data to demonstrate the correlation of the lead soap FTIR map and the transparent inclusion on the left side.

Fig 2 shows the distribution maps of the asymmetric stretching vibrations of the CH (A) and carboxylate group (B) respectively and the FTIR spectrum from within the identified metal soap aggregate. Fig 2C demonstrates the aliphatic asymmetric and symmetric C-H stretch vibrations of the fatty acid moieties at 2924 and 2856 cm^{-1} and the asymmetric and symmetric stretch vibrations of the metal carboxylate group at 1534 cm^{-1} and 1389 cm^{-1}, which correspond with data of pure standards [5, 6, 9, 13]. The cross-section was subsequently analysed by static imaging SIMS. Selected positive ion maps corresponding to copper (m/z 63), lead (m/z 208), calcium (m/z 40), tin (m/z 120), the deprotonated negative ion of palmitic acid and the positive ions from lead soap of palmitic acid (m/z 461-463) are plotted in Fig 3.

Copper is confined to the copper glaze top layer visible in the LM picture (see Fig 1A). The copper map is slightly pushed upwards by the left inclusion suggesting a small amount of expansion of the lead soap mass. The SIMS map of calcium closely fits the FTIR map of carbonate (Fig. 1D), while the FTIR lead soap contour map (Fig 1C) overlays with the lead palmitate map (m/z 461-463) and palmitic acid map (m/z 255; negative ions) obtained by SIMS. The lead soaps of stearic acid (not shown) are also present in this area. Note that the open space somewhat in middle of both the calcium and carbonate map is due to an open space in the cross-section filled with embedding medium (Fig 1B). Lead is remarkably high in the lead soap inclusion but also spreads out below the LTY layer. Lead and tin both have relatively high intensities in the right hand yellow concretion of the lead tin yellow pigment. Smaller tin containing particles are present on the outside of the lead soap mass and elsewhere in the LTY paint layer. The tin contour of the right hand particle also corresponds with a second lead soap concentration visible in the m/z 416-463 image. There is also a slightly higher density of palmitic and stearic acid at this position. The SIMS positive

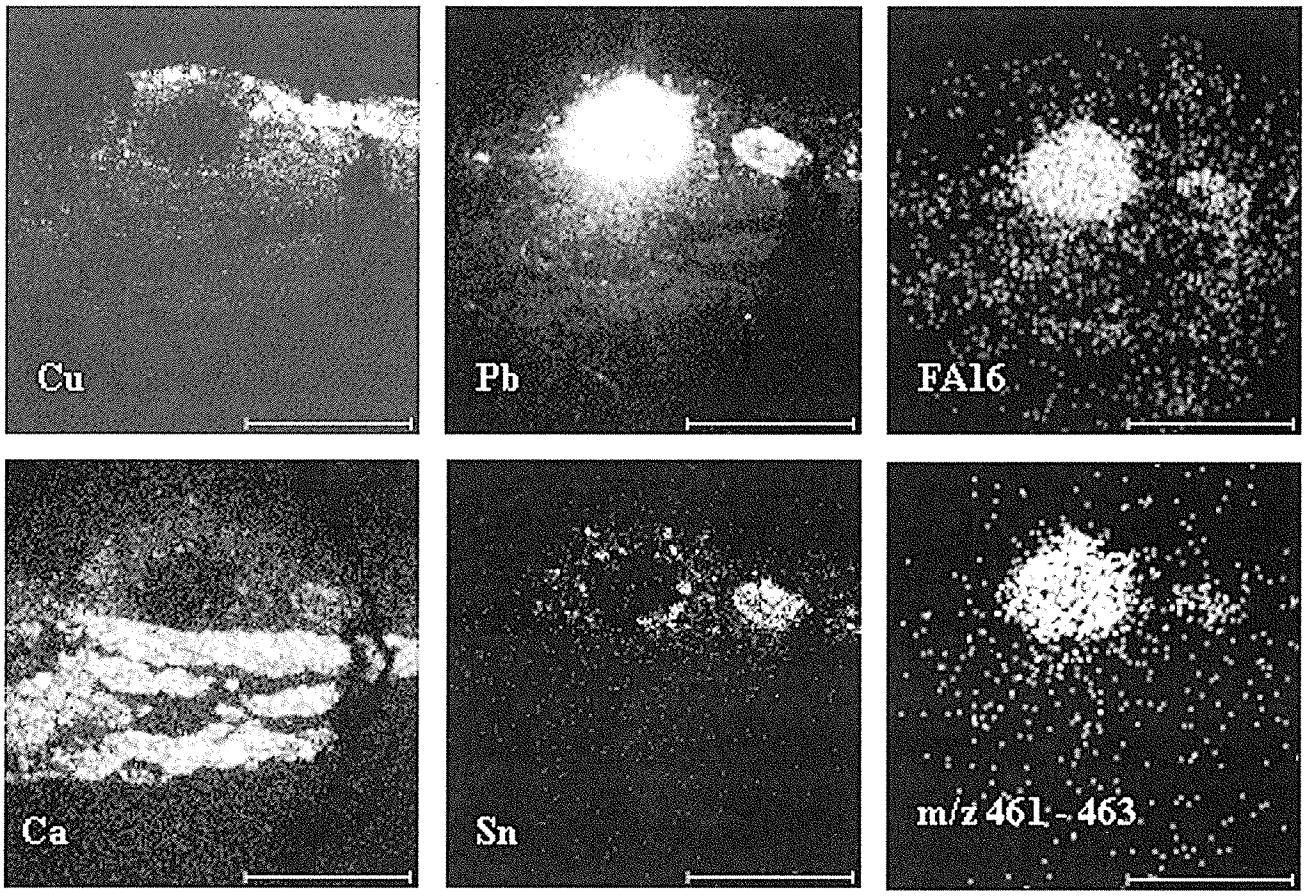

Fig 3. Imaging SIMS maps of cross-section CIA1577 RS06 depicting the maps of Ca, Cu, Pb, and Sn, palmitic acid and lead palmitate.

ion spectrum of the left inclusion is portrayed in Fig 4. The mass peaks of the lead palmitate and stearate at m/z 461-463 and 489-491 support the identification of the inclusion as an aggregate of these lead metal carboxylates. Cross-section RS04 shows several very large metal soap aggregates in a LTY layer underneath the azurite and red lake paint from the dark purple mantle of the Christ figure on the left in the right hand wing. The paint buildup in the BSE picture in Fig. 5 shows two circular mainly organic masses surrounded by particles with a very high electron reflectivity (further illustrated by the elemental maps of the right hand aggregate in Fig 6). The highly reflective layer below the inclusions is from lead white of the priming, while the lower grey layer represents the calcium carbonate ground. Above the lead tin yellow paint, angular azurite particles in grey and dark grey flakes of the red lakes are visible. The FTIR spectrum of the organic region in the right hand aggregate confirms its metal soap composition by the asymmetric stretch vibration of –CO2-Pb at 1519 cm^{-1} and the 2928 cm^{-1} of the CH stretch vibration of aliphatic fatty acid moieties. Further FTIR imaging demonstrates that metal carboxylates are present throughout the LTY layer. The map of the tin distribution in Fig 6 (Sn) clearly shows that all tin containing particles are present outside the lead soap mass. Lead is present at the same position as the tin particles but is also abundant inside the lead soap mass. Lead concentrations inside the lead soap mass that have a higher reflectivity in the BSE picture suggest that lead minerals are remineralising the soap aggregate. This phenomenon is indeed common and also observed in the cross-sections of LS02 and RS21 (not discussed further in this paper). The distribution of the azurite

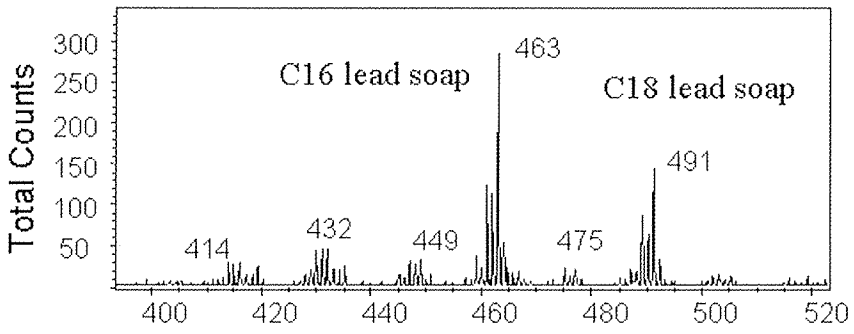

Fig 4. SIMS summation spectrum of the left inclusion area indicative of lead palmitate and stearate.

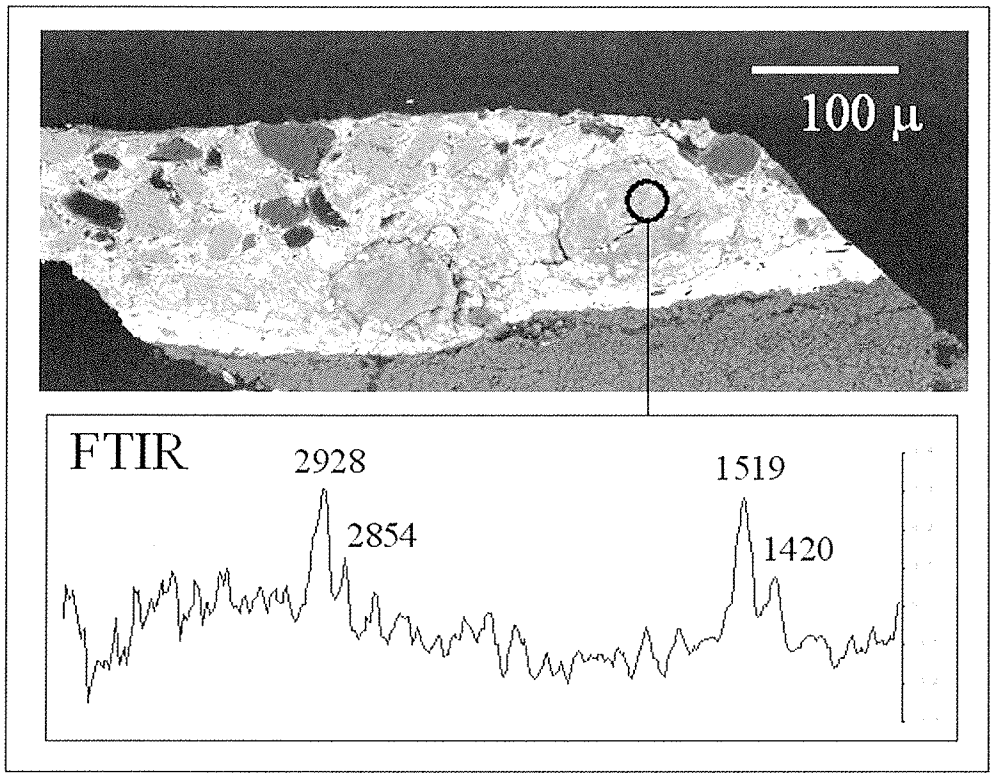

Fig. 5. SEM back scattering image of the cross-section CIA 1577 RS04 (Sherborne triptych)and a region specific FTIR spectrum the large circular lead soap aggregates on the right hand side.

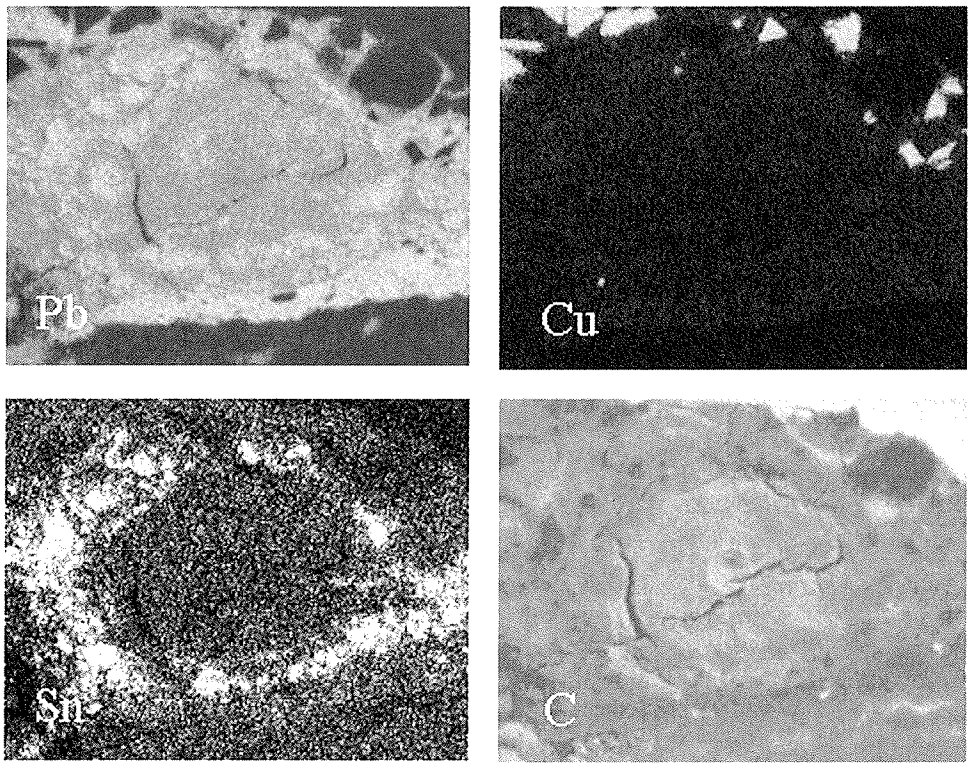

Fig 6. SEM-EDX maps of
Pb, Cu, Sn and C in CIA1577 RS04 (aggregate on the right in Fig. 5).

(see Cu map in Fig 6) suggests that the right hand inclusion has also pushed the upper paint layer upwards. Examination of these two and other cross-sections raise some questions with respect to the formation mechanism of the lead soap in relation the distribution of the tin containing phases. An explanation that lead stannate is the only source of lead in the LTY paint layer seems very unlikely. The lead stannates appear to be intact and act as particles that are moved away by the invisible force of the growing lead soap aggregate. The suggestion that stannates reduce to tinoxides [5] seems untenable and would not explain the copositioning of lead and tin. There is every reason to propose a second lead source that readily reacts with fatty acids. Possible candidates are lead oxide and minium (lead plumbate). Lead white as an addition to the LTY paint is another possibility in view of the lead soap formation in a number of 17th century paintings, but lead white seems perfectly stable in the layer underneath the LTY paint. It is our view that the distributions observed reflect an earlier proposal by Eastaugh [16] that the lead stannate melt is non-stoichiometric from the start. This could be caused by a too low temperature of the furnace or firing process. A phase diagram drawn by Eastaugh on the basis of data by Urazov [21] points out that a temperature of 780 °C must be reached in order to convert all lead and tin oxide to lead stannate. The addition of a substantial amount of minium as step B after the

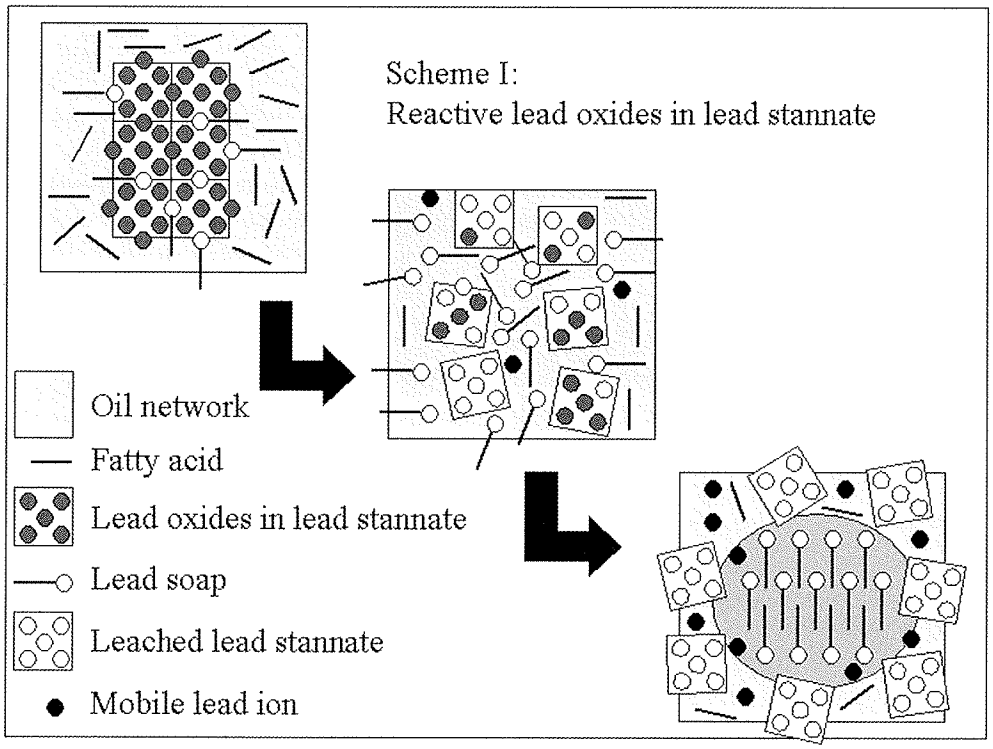

Scheme 1. (Title inside the figure)

formation of a lead stannate in the traditional Bolognese recipe [15, 16], is a potential source of additional unreacted lead oxides. If a surplus of lead oxides is present indeed, they would convert to minium upon slow cooling [16]. Interestingly, studies by Eastaugh that quantitatively determine the ratio of lead and tin in samples from LTY I paints from paintings, consistently showed a surplus of lead. This same picture is suggested by our distribution data. Scheme I summarizes our present ideas on the reactions of a hypothetical mixed phase lead tin yellow pigment in an aging oil paint. This mixed phase could be (to be specified) lead oxides inside a crystalized mass of lead stannate or may be present as mixed crystals of lead stannate and lead plumbate (Pb_2PbO_4) that have a very similar crystal structure [16]. Fatty acids released by hydrolysis of the aging oil paint will react with these lead oxides to form lead soaps outside or perhaps even inside the lead stannate matrix. The end result of this reaction is lead soaps and a leached lead stannate. Some LTY particles will fragment as a result of this process while others perhaps with less lead oxide in them and thus more solid, remain as such. The latter type of particle will have a "swiss cheese"-like porous aspect, as is obvious in RS06 (right hand particle). SEM studies point this out very clearly. Porous larger particles are in fact rather commonly encountered in LTY paint layers (also in our studies). The fine structure of these particles could be informative about their origin. The surplus of metal carboxylates – most likely monocarboxylic acid moieties because of their mobility and single point binding site – is proposed to become organised in solid semi-crystalline metal soap masses. As these masses grow till all reactants are gone, the now fragmented lead tin yellow pigment will be pushed aside and becomes contrated at the periphery of the soap mass.
This scenario suggests itself when the painting is used as the information source. The hypothesis is testable. There is still more that can be done on the residual structure of the lead stannates using nano-analytical approaches. The dynamic formation of lead soap aggregates can be modelled in the laboratory. The process of formation of non-stoichiometric lead stannates with lead oxide inclusions also requires further experimentation, especially in the light of the temperature sensitivity of the LTY I synthesis. Finally, the reactivity of lead stannate with fatty acids should be investigated with high priority.

Conclusions

There is a strong positional correlation between imaging FTIR data of metal carboxylates, lead and lead soaps of palmitic and stearic acid in lead tin yellow type I paint layers. The peripheral position of lead/tin containing mineral phases around the lead soap aggregates is demonstrated in a 500 year old paint sample. A lead stannate with microscopic lead oxide inclusions is postulated as the original lead tin yellow pigment that reacts with fatty acids from the aging oil paint binding medium. Leached lead stannate porous particle structures or completely fragmented lead stannate residues remain. As the lead soaps grow remaining lead stannates and other pigments particles are pushed aside. This process is responsible for the 'messy' aspect of lead tin yellow paint layers.

Acknowledgements

Dr. Eastaugh is thanked for making a copy of his PhD thesis on lead tin yellow pigments available. This work is supported by the FOM approved research program 49 and by the De Mayerne grant P4 on imaging analytical studies of cross-sections. The Dutch Organisation of Scientific Research (NWO), The Hague, supports both programs.

References and notes

1. R. M. A. Heeren, J. J. Boon, P. Noble, and J. Wadum. Integrating imaging FTIR and secondary ion mass spectrometry for the analysis of embedded paint cross-sections. In: J. Bridgland (Ed), *Preprints of the ICOM-CC 12th Triennial Meeting*, 29 August - 3 September, Lyon. James and James (Science Publishers) Ltd. London (1999), p.228-233

2. K. Keune and J.J. Boon. Imaging secondary ion mass spectrometry of a paint cross-section taken from an Early Netherlandish painting by Rogier van der Weyden, *Analytical Chemistry* (2004), 76(5), 1374-1385.

3. Van der Weerd J., Boon J.J., Geldof M., Heeren R.M.A., and Noble P., 'Chemical Changes in Old Master Paintings – Dissolution, metal soap formation and remineralisation processes in lead pigmented paint layers of 17th century paintings', *Zeitschrift für Kunsttechnologie und Konservierung*, (2002), 16, pp.35-52

4. Noble P., Boon, J.J. and Wadum J. Dissolution, Aggregation and Protrusion, *Art Matters* (2003), 1, p 46-61.

5. Higgit H., Spring M., and Saunders D., 'Pigment-medium interactions in oil paint films containing red lead or lead-tin yellow', *National Gallery Technical Bulletin*, 24, (2003), p.75-96

6. Plater, M.J., De Silva, B., Gelbrich, T., Hurtshouse, M.B., Higgitt, C.L. and Saunders, D.R. The characterization of lead fatty acid soaps in protrusions in aged traditional oil paint. *Polyhedron* (2003), 22, p. 3171-3179.

7. Boon J.J., van der Weerd J., Keune K., 'Mechanical and chemical changes in Old Master paintings: dissolution, metal soap formation and remineralization processes in lead pigmented ground/intermediate paint layers of 17th century paintings'. In R.Vontobel (Ed), *ICOM Committee for Conservation, 13th Triennial Meeting, Rio de Janeiro*, Vol 1, James and James (Science Publishers) Ltd. London (2002), pp.401-406

8. K. Keune, P. Noble and J. J. Boon Chemical changes in lead-pigmented oil paints: on the early stage of formation of protrusions. *Proceedings of ART 2002, the 7th International conference on Non-Destructive Testing and Microanalysis for the Diagnostics and Conservation of the Cultural and Environmental Heritage* edited by R. van Grieken, K. Janssens, L. Van't dack and G.Meersman, (2002), Antwerp, Belgium. 9 pages

9. Van der Weerd J., *Microspectroscopic analysis of traditional oil paint*, PhD thesis,University of Amsterdam; MolArt Report nr 7.

10. J. D. J. van den Berg, K. J. van den Berg, and J. J. Boon. Chemical changes in curing and ageing oil paints. In: J. Bridgland (Ed), *Preprints of the ICOM-CC 12th Triennial Meeting*, 29 August - 3 September, Lyon. James and James (Science Publishers) Ltd. London (1999), p.248-253

11. Van den Berg J., *Analytical chemical studies on traditional linseed oil paints*, PhD thesis, University of Amsterdam; MolArt Report nr 6 , (2002).

12. Carlyle, L. *The artist's Assistant.* Archetype Publications Ltd., London, (2001).

13 L. Robinet and M-C Corbeil, The characterization of metal soaps. *Studies in Conservation* 48, (2003), p. 23-40

14 Verhoeven, M., postdoc De Mayerne project on the reactivity of lead white containing paints (personal communication, 2003).

15 Kuehn, H. Lea-Tin Yellow, in: A. Roy (ed), *Artists' Pigments. A handbook of their history and characteristics*, Vol.2, Oxford University Press, (1993), pp. 83-112

16. Eastaugh, N.J. *Lead tin yellow: its history, manufacture, colour and structure.* PhD thesis University of London, Courtauld Institute of Art (1988).

17. Gore, E. *A study of the interaction between oil and pigment through the analysis of cross-sections from paintings.* Postgraduate diploma thesis in the conservation of easel paintings. Final year project, Courtauld Institute of Art, London, (2003).

18. Speleers, L. and A. van Loon working on the paintings ensemble of the Oranjezaal as part of the MOLART and De Mayerne Project (personal communication, 2003)

19. '*Exhibition of British Primitive Paintings (from the Twelfth to the Early Sixteenth Century) with some related Illuminated Manuscripts, Figure Embroidery and Alabaster Carvings*', Royal Academy of Arts, London, October-November 1923

20. Grossinger, C. 'The Raising of Lazarus: A French Primitive in Sherborne (Dorset)', *Journal of the British Archeological Association*, Vol CXXXII, (1979)

21. Urazov, G.G., E.I.Speranskaya and Z.F. Gulyanitskaya. Physico-chemical study of the reaction of lead oxide with oxides of antimony and tin. *Russ. J. Inorg. Chem. (1956) 1, p.307-311.*

Analysis of Ancient Biological and Cosmetic Material Using Synchrotron Infrared Microspectroscopy.

Marine Cotte[1], Paul Dumas[2], Philippe Walter[1]
[1] Centre de Recherche et de Restauration des Musées de France, CNRS UMR-171, Palais du Louvre, Porte des Lions, 14 quai F. Mitterrand, F75001 PARIS, France
[2] LURE and Synchrotron SOLEIL, L'Orme des Merisiers, Saint-Aubin - BP 48, 91192 GIF-sur-YVETTE CEDEX, France

Abstract

Synchrotron FT-IR microscopy was applied to the study of two archaeological-relevant samples, aimed to identify chemical composition at the highest lateral resolution possible. The high brightness of the synchrotron source enables one to achieve analysis at the theoretical diffraction limit. We have studied a twine sample, originating from a horse hair, used to stitch up skin 23 centuries ago. Comparison with modern horse hairs shows similar behaviour for relative concentrations and distribution of the lipids and proteins, as well as for the proteins secondary structure. The only marked difference is seen for the hair centre, around the medulla. The second example is a cosmetic from Ancient Egypt (13th century BC). It contains fatty soaps of which the alkyl chain and the cation can be identified. In addition to determine the chemical nature of the components, the application process for these cosmetic compounds can be envisioned thanks to the chemical image of their distribution.

Introduction

FT-IR spectroscopy has been widely used for the analysis of archaeological samples such as pigments, paints and pottery but it is seldom employed to study antique biological samples. Some articles have already pinpointed the usefulness of spectroscopic techniques to determine the state of conservation of mummified biological samples, from either Raman [1-2], or FT-IR [3] spectroscopies.
In the present study, we have use infrared microspectroscopy with a high brightness photon source: synchrotron radiation. The advantage of the microscope is the possibility of mapping the functional groups and producing corresponding chemical images of their location. The high brightness of the synchrotron source is known to produce high spectral quality (signal-to-noise) in a much shorter acquisition time and much shorter lateral resolution. We have currently probed areas of 6x6 μm^2, but, accordingly to other needs, an ultimate resolution of 3x3μm^2 might be achievable. Performances of synchrotron infrared microscopy as well as a list of operating infrared microspectroscopy beam lines can be found in [4].
We will illustrate all these advantages with two examples: the first one is a twine used to stitch up the skin of a Kazakhstan prince, 23 centuries ago. The second example is a reed, full of cosmetics, prepared in Egypt during the 13th century BC.

Methods

The experiments were performed with the MIRAGE beam-line, at Super-ACO (France) [5]. The IR microspectroscopic beam-line is equipped with a Nic-Plan IR microscope coupled to a Magna 560 FTIR spectrometer. The microscope operates in confocal mode, where the focusing Schwarzschild objective has a magnification of 32x (NA = 0.85) and the collection Schwarzschild objective a magnification of 10x (NA = 0.71). The area of illumination was determined with an adjustable aperture placed at an intermediate focal point, and re-imaged onto the sample. The upper and lower apertures are adjustable down to approximately 3x3 μm^2.
In the present study, spectra were collected in transmission mode at 8 cm^{-1} resolution using Atlms software (Thermo Nicolet Instruments). Area mapping was performed using a dual remote masking aperture to define the sample area for infrared data collection and minimize diffraction. The final format of the data was absorbance, where the background was collected through the blank substrate. For each spectrum, 100 scans at least were accumulated. An Happ-Genzel apodization function was applied for Fourier processing. Peak positions were determined using the Nicolet Omnic software (based on a polynomial least squares method). Apertures of 6x6 μm^2 were used with steps of 6 µm in both directions.

Results

Analysis of horse hair used to stitch up skin, 23 centuries ago
The sample was collected from a mummy, found during the excavations directed by HP Francfort [6] at Berel,

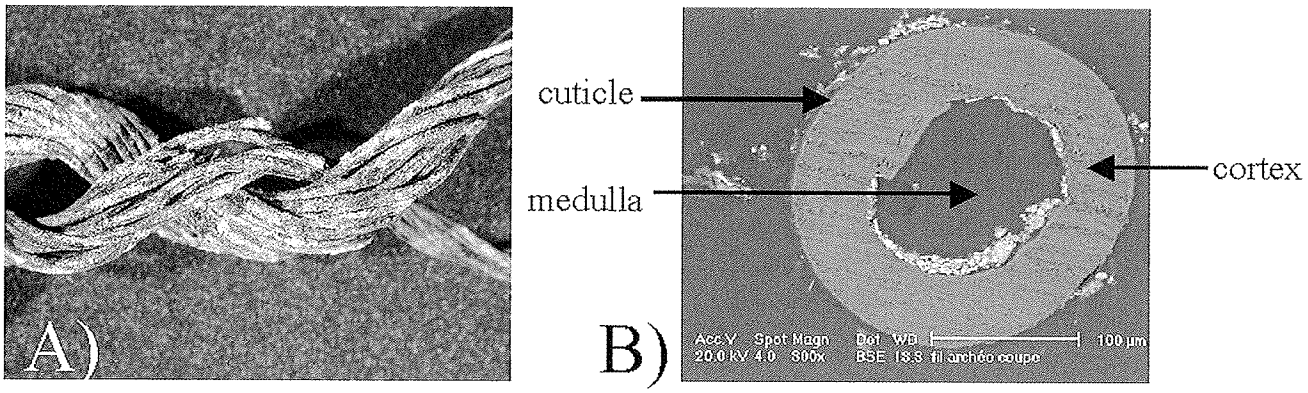

Figure1: twine used for the trepanation, observed with A) an optical microscope, B) a scanning electron microscope

in the Far East of Kazakhstan. Commonly, artificial and natural mechanisms are suggested as responsible for mummification. Additionally, beyond the cases of natural mummies, we can distinguish three different atmospheric conditions: the dry environment (like the one found in the Taklamakan desert in China, or the deserts in Egypt), the organic environment in a bog (found in England or Germany) and the permafrost conditions where the body is kept at low temperatures (like the Tyrolean Ice Man). The mummy studied here belongs to the third category and was discovered in a frozen burial, in the Altai Mountains. It seems to have been a prince or a noble of the region and dates from the 4th century BC. Anthropological observations showed that his death was due to a head wound [7]. A beginning of trepanation, perhaps with a therapeutic goal, may have contributed to his death. The subject of our study is the twine used for the trepanation (Fig. 1A). Observations with a SEM support its identification as a horse hair (Fig1B). This hypothesis is supported by two elements:

- the importance of horses for these nomadic people. A dozen of sacrificed horses were recovered in the Prince kurgan mound [8].
- the use of horse hairs in surgery described in Greek texts from the same period. For example, Hippocratis underlines the advantages of horse hair, employed with linen, to treat fistulas by ligature, because, contrary to linen, "the horse hair does not rotten" [9].

It can be noticed in Fig. 1B, that the volume of the hair, which is called cortex, seems to be perfectly preserved. On the other hand, the middle of the hair is empty, at the location of the medulla. This observation leads us to consider that either this "hole" is the result of a long alteration or it was already the case 23 centuries ago.
FT-IR analysis enabled us to check the state of conservation from a chemical point of view.

To perform transmission IR spectroscopy on the archaeological twine and on modern horse hairs, 5 µm transversal cuts were obtained with a cryomicrotom and place on a ZnS pellet.

In Fig. 2, we reported the infrared spectrum of the archaeological sample, recorded inside the cortex, and, for comparison, the equivalent spectrum recorded on a modern horse hair. Spectra exhibit similar features, which are characteristic infrared signatures for every hair: the ν(OH) at ~ 3500 cm^{-1}, the ν(NH) at ~ 3200 cm^{-1}, the ν(CH) (with the different contribution of CH_2 and CH_3 stretching bands, both with one asymmetric and one symmetric stretching band) extending from 3000 to 2800 cm^{-1}. Below 1700 cm^{-1}, the most intense bands are assigned to amide I (~ 1650 cm^{-1}) and amide II (~ 1530 cm^{-1}) [10].
The amide I band is the res ult of 80% C=O stretching, 10% C-N stretching and 10% N-H bending [11]. This signal is related with the peptide backbone of the proteins. Hence the integrated intensity of the amide I band (1711-1600 cm^{-1}) is proportional to the overall protein

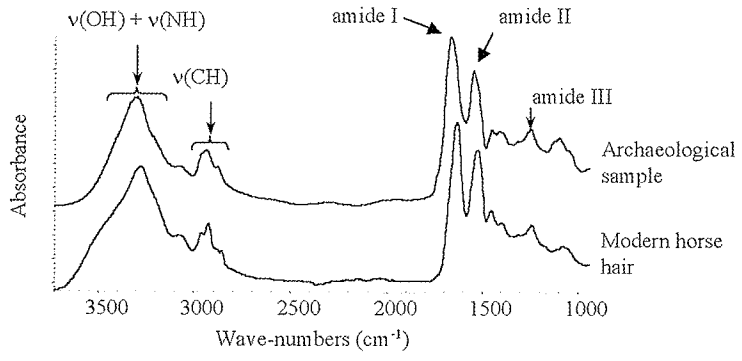

Figure 2: FT-IR spectra of the archaeological sample and a modern horse hair

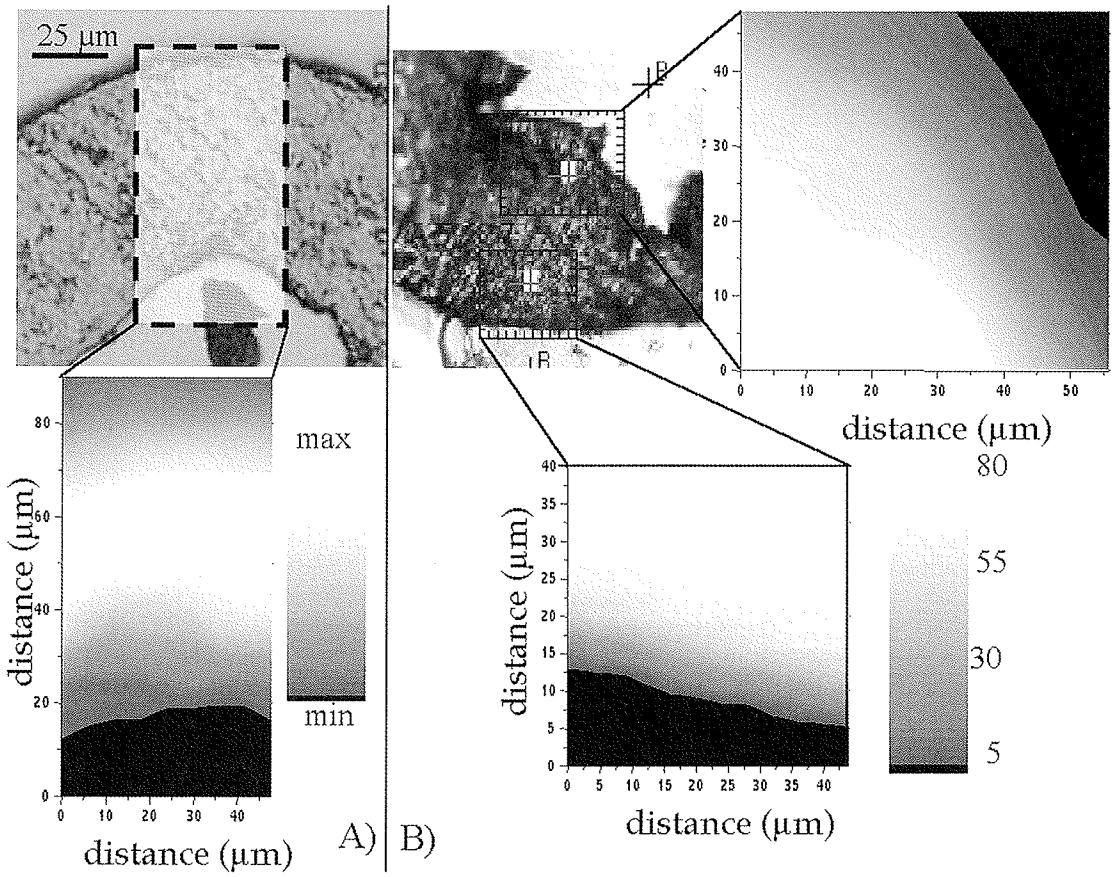

Figure 3: distribution of the proteins in the archaeological sample of Berel, calculated with the area of the amide I band (1711-1600 cm-1) A) analysis on the whole volume, B) zoom on the two surfaces

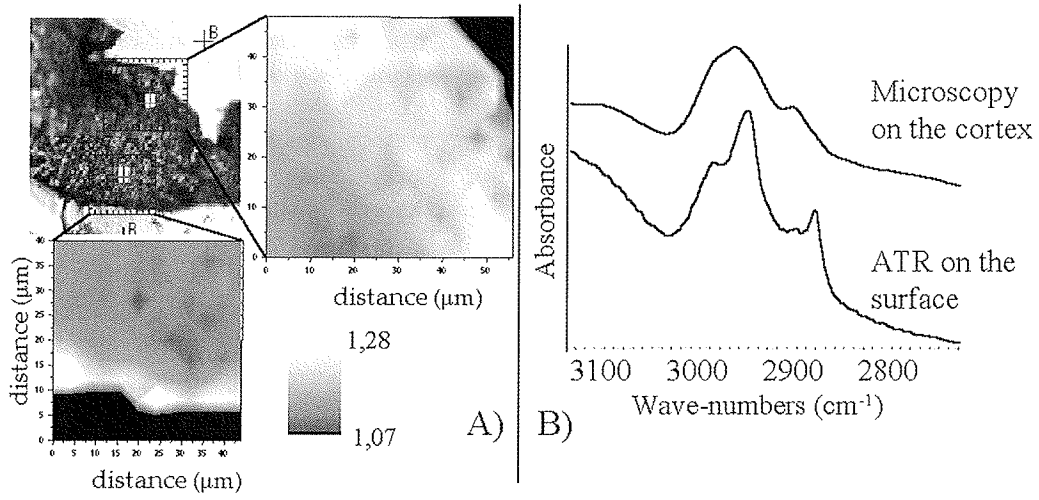

Figure 4: lipids in the archaeological sample of Berel, A) distribution calculated with the ratio of absorbance of the $\nu_{AS}(CH_2)$ (2930 cm-1) vs $\nu_{AS}(CH_3)$ (2957 cm-1), B) comparison between one spectrum acquired on the surface with Attenuated Total Reflectance and on the cortex with IR microscopy

concentration. The chemical image of the amide I band shows that intensity is higher inside the cortex (Fig.3 A). Detailed maps, recorded with a 4 µm-step, on the two inner and outer border of the cortex give a more detailed image of the gradient of proteins content on the external and internal surfaces (Fig. 3B). The scale on Fig. 3B is given for information only, because the absorption is correlated with the thickness of the sample. On a modern horse hair, the intensity of amide I band is rather constant inside the cortex, decreasing slightly inside the cuticle, and hugely inside the medulla. The comparison of the chemical maps could lead to the idea that the cuticle and the external region of the cortex are well conserved whereas the internal region of the cortex may have suffer from a beginning of degeneration of the proteins.

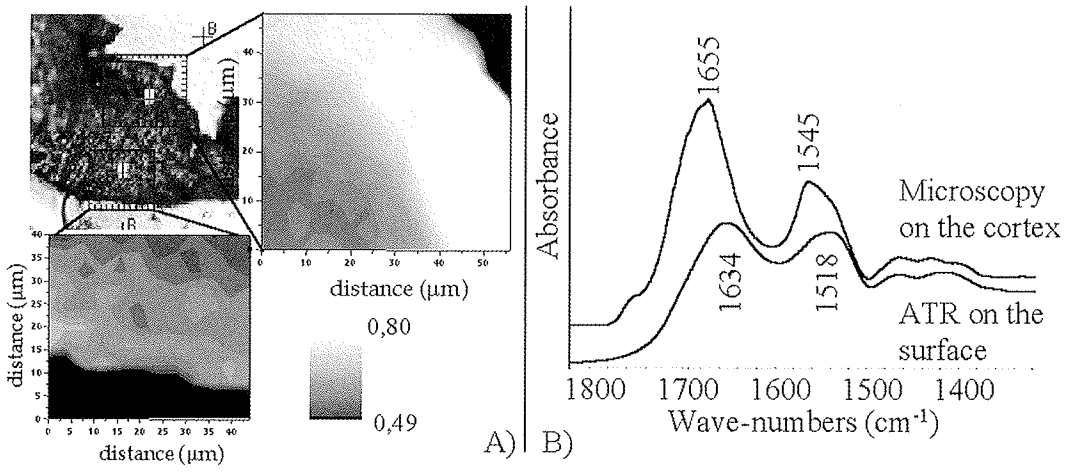

Figure 5: the proteins secondary structure in the archaeological sample of Berel, A) mapping calculated with the ratio of absorbance of the β-sheet (1630 cm-1) vs α-helix (1657 cm-1), B) comparison between one spectrum acquired on the surface with Attenuated Total Reflectance and on the cortex with IR microscopy

To estimate the lipid content, we took the ratio of the band intensity originating from the CH_2 group versus that of the CH_3 group, counting the fact that much longer alkyl chain are present in lipids than in proteins. Hence, the ratio of the absorbance of the two peaks $\nu_{AS}(CH_2)$ (2930 cm^{-1}) *vs* $\nu_{AS}(CH_3)$ (2957 cm^{-1}) is a fair estimate of the lipid content and location. This ratio is higher at the two borders (Fig. 4A). To rule out any contamination originating, from the embedding agent used for the cryo-microtomy, we also compared the signal acquired directly onto the twine surface, by Attenuated Total Reflectance, to the one from within the cortex using IR microscopy (fig. 4B). Clearly, there are more lipids on the cuticle, and more proteins in the cortex of the sample.

Modern hair [12] shows a similar distribution with a substantial concentration of lipids on the surface of the hair (the cuticle), and to a greater extent, on the middle of the hair (the medulla), which is absent in the ancient twine. The high absorption of the ν(CH) band in the internal surface of the archaeological sample may be the remains of a high lipid content 23 centuries ago.

In addition to the protein and lipid content, FT-IR spectroscopy can give information about the proteins' secondary structure, since amide I and II bands are conformation sensitive. It is commonly accepted that α-helix structures absorb at ~ 1655 cm^{-1} whereas β-sheet structures absorb at ~ 1630 cm^{-1} [11]. Hence the mapping of the ratio of the peak intensity at 1630 cm^{-1} versus the one at 1657 cm^{-1} represents the evolution of the β-sheet versus α-helix content. This amount is higher at the two borders (fig. 5A). The comparison between a spectrum acquired directly from the surface and one from within the cortex strengthens this hypothesis (fig. 5B). A similar gradient is observed on the cuticle of modern hair [13] meaning that the conditions within the kurgan (pH, temperature, moisture, light, atmosphere, etc.) have been so good that the proteinaceous structure of the cortex and the cuticle have been partly preserved. For the inner part of the cortex the comparison is more difficult since the medulla is empty. The structure may have change around the medulla, from α-helix to β-sheet. A similar degradation, marked by an enhanced amount of β-sheet, has already been noticed on the Ice-man skin and on other mummy skins [2].

Despite a possible beginning of degradation of the proteinaceous material in the core of the hair, the whole sample has suffered few variations within 23 centuries. The synchrotron beam was necessary for the acquisition of detailed mapping, particularly to observe the composition and structure variations on borders. Future analyses of other samples (hair and skin), kept in other conditions (permafrost or dry atmosphere) should enable us to better understand the evolution of biological samples and assess the effect of environment on their degradation.

In the archaeological context, this technique could find many similar applications, not only for the analysis of mummified remains but also for the study of fabrics, papers and leathers.

Analysis of a cosmetic of ancient Egypt

This example comes from Egypt and originates from the thirteenth century BC. It is a reed, full of cosmetics as can be observed by X-ray radiography (Fig. 6A). On the reed, an inscription specifying the quality of the product therein can be read, testifying to the very good conservation of the reed. The tube contains a mixture of particles of different shape, colour, and composition, with both cosmetics and bits of reed. The observation of some powder with an optical microscope revealed the presence of brighter particles, which turned out to contain important organics. The analysis was carried on 6 particles and the results obtained on one of them will be given (Fig. 6B). Some powder is directly put on a ZnS pellet and a rapid selection is made to focus on fatty rich particles. As the acquisition is made in a transmission configuration, the particles may be slightly flattened for the transmitted signal not to be completely absorbed.

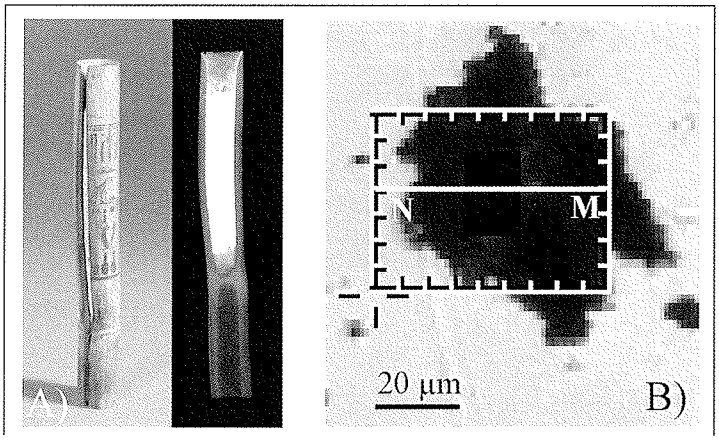

Figure 6: Analysis of an ancient cosmetic: A) the reed full of cosmetic, B) one particle analysed by synchrotron IR-microscopy

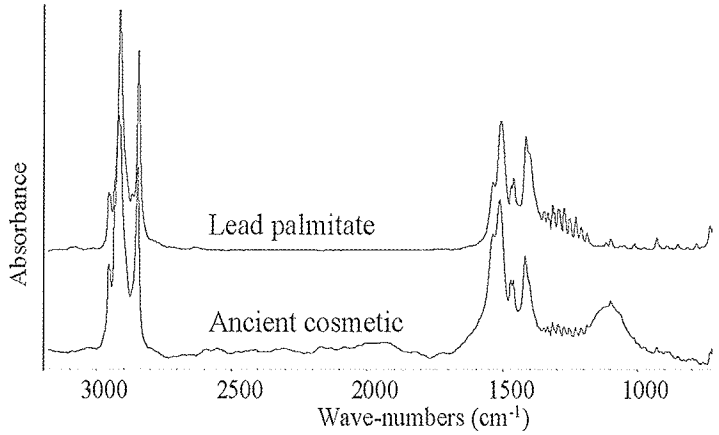

Figure 7: FT-IR spectra of the ancient cosmetic (acquisition on the right part of the particle shown in Fig.6) and lead palmitate

Fig. 7 shows a spectrum acquired on the right part of the map, compared with the modern product we propose for identification. The more intense band is at ~ 3000 cm^{-1} and reveals the presence of fatty acid chains. The mapping of this band (2977-2819 cm^{-1}) (Fig. 8A) is similar to the mapping of the carboxylate band (1566-1485 cm^{-1}) (Fig. 8B), suggesting that the two frequencies are absorbed by the same molecule: a fatty soap, whose amount is greater on the right part of the map, which corresponds to the core of the sample. On the contrary, the mapping of the mineral band (1176-972 cm^{-1}) is completely different (more important on the left part of the map) (Fig. 8C), meaning that this band is not due to the same fatty chain and the soap bands.

Focusing on the right part of the spectrum (Fig. 7), one can notice a succession of tiny peaks corresponding to CH_2 wagging and twisting vibrations. These peaks indicate that the matter is very well organised with an *all-trans* conformation of the CH_2 of the fatty chains. This observation and spectral fingerprints are very useful for the identification of the fatty soap. The analysis of the signal from 1650 and 1150 cm^{-1} enables the exact determination of the nature of both the chain and the cation.

The number and the position of the peaks from 1350 and 1150 cm^{-1} are related to the number of CH_2 group in the fatty chain [14]. More specifically, considering the myristic (C14), palmitic (C16) and stearic (C18) chain in their solid state, the number of peaks between 1320 and 1150 cm^{-1} is n/2-1 where n is the number of carbon in the C_n fatty chain. The previous chains give 6, 7 and 8 peaks respectively (fig. 9A). The 7 peaks observed in the archaeological sample prove that the fatty material is of palmitic chain composition.

To determine the nature of the cation, a set of synthesis of palmitate metallic soap was prepared, with copper, calcium, zinc, lead etc. Even though the discrimination is less obvious than for the alkyl chain, lead palmitate is the one that has the highest similarity (fig. 9B). We conclude, therefore, that the particle contains a majority of lead palmitate.

Additionally, a conformational study was conducted. The set of spectra from the point M to the point N (Fig. 6B) is plotted in fig. 10A. Different changes can be underlined:

1/ fading of the shoulder at ~ 1539 cm^{-1},

2/ melting of the doublet at 1472 cm^{-1} and 1462 cm^{-1} into a singlet at 1467 cm^{-1},

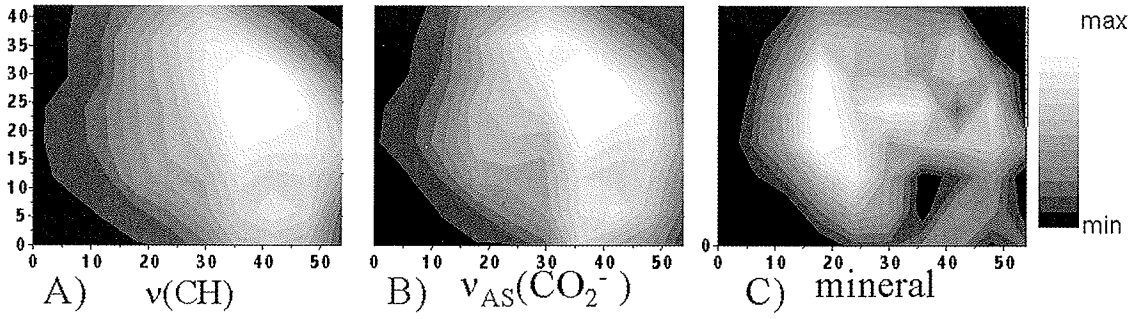

Figure 8: mapping on a particle of ancient cosmetic A) alkyl chain (2977-2819 cm-1), B) carboxylate (1566-1485 cm-1), C) mineral (1176-972 cm^{-1})

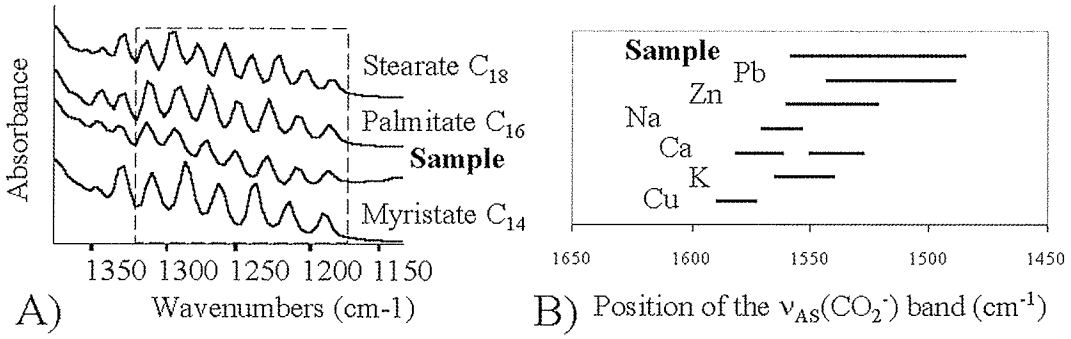

Figure 9: Identification of the fatty soap: A) the fatty chain is palmitic, B) the cation is lead

3/ broadening of the carboxylate symmetric stretching at ~ 1410 cm^{-1},
4/ disappearance of the tiny peaks of CH_2 wagging below 1350 cm^{-1}.

Fig. 10B is the spectrum change of pure lead palmitate during heating. Obviously, the same evolutions appear, which suggests that there could be an order to disorder transition from the right part to the left part of the particle. The disorder could be explained by the additional presence of fatty acid and ester, mineral and water.

Within the mineral phase, phosgenite ($Pb_2CO_3Cl_2$) could be identified. This salt has already been identified in ancient cosmetics from Egypt. Its natural presence is very low, so high amounts of phosgenite in ancient cosmetics prove that Egyptians knew how to synthesize it in aqueous solution [15]. Its spectrum is shown in Fig. 11A, and is compared with one spectrum acquired on the left part of the particle. The peak at 1530 cm^{-1} cannot be used for its location since it interferes greatly with the carboxylate asymmetric stretch. The mappings of the three other peaks are similar, and reveal

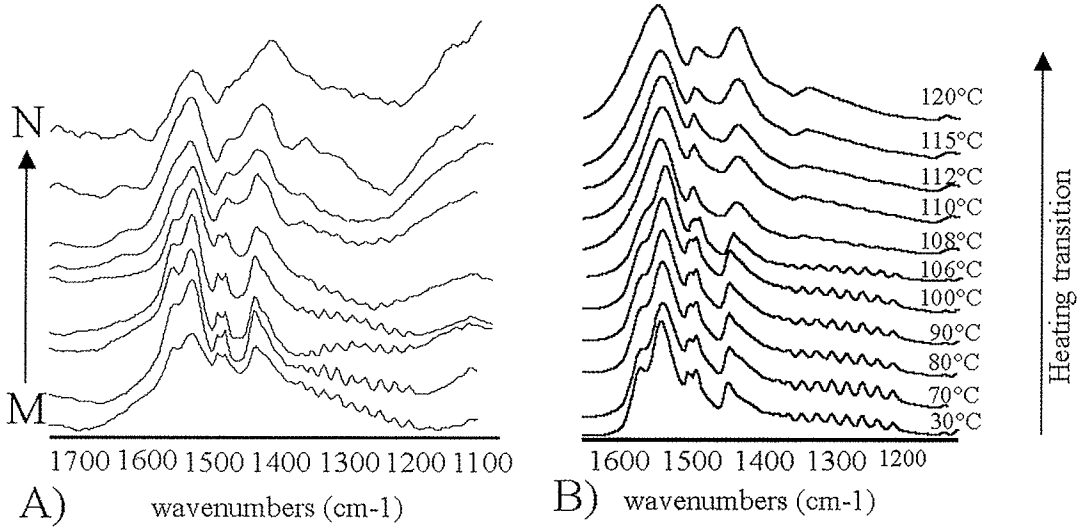

Figure 10: evolution of the IR signal between 1600 and 1200 cm-1, A) on the particle of cosmetic, from M to N (cf. Fig. 6) and B) on lead palmitate heated from 30 to 120°C

that the amount of phosgenite is more important in a rather external region, around the fatty matter (Fig. 11B). This data could shed light on the way the cosmetic was prepared. Note that phosgenite is a white salt and that ancient authors, like Pline and Dioscorides, attribute pharmaceutical qualities to it. Hence, we could imagine that the synthesis of the cosmetic followed at least two steps: first, the mixture of fat with a lead salt giving lead soap, second, the addition of phosgenite, introduced at the end, either to obtain the right colour or to limit its reaction with fat and keep it intact for a possible therapeutic use.
The superior advantage of using FT-IR spectroscopy is that it provides information about the organic and the mineral phases simultaneously. The second advantage is that it does not need any preparation or chemical degradation, it is a non-destructive method, which is always a consideration for the analysis of precious samples such as art and archaeological materials.
The infrared synchrotron source is essential in providing a very good spatial resolution which permits the analysis of very tiny quantities. It also provides the possibility of mapping to reveal the spatial distribution of the functional groups, that is an easier identification of the components.
Painting presents a lot of similarities with this analysis, according to the possible presence of fatty matter (binder) and lead salts (pigment). Moreover, the *in situ* saponification of the fatty materials by lead salts has already been observed in painting. We therefore wish to follow the studies with other cosmetics and widen it to painting materials.

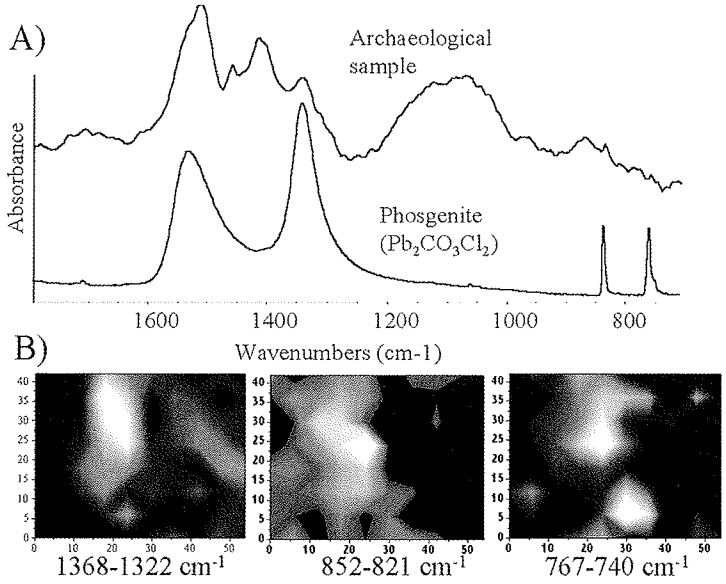

Figure 11: identification of phosgenite ($Pb_2CO_3Cl_2$) in the mineral phase of the ancient cosmetic: A) FT-IR spectrum of phosgenite compared with a spectrum acquired on the left part of the particle of a ancient cosmetic, B) the localisation of the absorption of 3 bands of the phosgenite

Conclusion

In addition to the well known advantages of FT-IR spectroscopy (identification of the component, both organic and mineral, identification of the conformation and the structure, etc.), synchrotron IR-microscopy is a powerful method for the study of archaeological samples. It enables easy and rapid acquisitions, without degradation of the sample and it requires little raw material allowing for the analysis of tiny quantities of matter. Chemical imaging is essential to complement the compound identification, more especially to separate them out in mixtures. The very good spatial resolution offered by the synchrotron beam gives very detailed mappings.
The 23 century old horse hair studied here is rather well preserved. The lipids and proteins amounts, as well as the proteins secondary structure distribution show similarity with modern samples. The only differences are observed in the core of the hair, around the medulla, which is missing. The analysis of a cosmetic from ancient Egypt has revealed important features. The presence of a particular fatty soap has been identified : lead palmitate. The location of a lead salt, phosgenite ($Pb_2CO_3Cl_2$), around the organic matter leads us to the assumption that it was added at the end of the cosmetic synthesis. Analyses of archaeological samples with synchrotron IR-microscopy are still seldom. We can hope that their number will grow soon, providing comparative data. In particular, it will be interesting to study the state of preservation of biological samples (skin, hair, etc.) depending on the atmospheric conditions of conservation as well as applying this technique to the study of paintings.

Acknowledgement

We are grateful to HP Francfort, E Crubezy and C Ziegler who provided us with the archaeological samples.

References

1. Edwards, H.G.M., Farwell, D.W., and Wynn-Williams, D.D., 'FT-Raman spectroscopy of avian mummified tissue of archaeological relevance', *Spectrochimica Acta Part A*, (1999), **55**, 2691-2703

2. Edwards, H.G.M., Gniadecka, M., Petersen, S., Hart Hansen, J.P., Faurskov Nielsen, O., Christensen, and D.H., Wulf H.C. 'NIR-FT Raman spectrosocpy as a diagnostic probe for mummified skin and nails', *Vibrational Spectroscopy,* (2002), **28**, 3-15

3. Kupper, L., Heise, H.M., Bechara, F.-G., and Stucker M., 'Micro-domain analysis of skin samples of moor-mummified corpses by evanescent wave infrared spectroscopy using silver halide fibers', *Journal of Molecular Structure*, (2001), **565-566**, 497-504

4. Dumas, P., Miller, L., 'The use of synchrotron infrared microspectroscopy in biological and biomedical investigations', *Vibrational Spectroscopy*, (2003), **32**, 3-21

5. Polack, F., Mercier, R., Nahin, L., Armellin, C., Marx, J.P., Tanguy, M., Couprie, M.E., Dumas, P., 'Optical design and performance of the IR microscope beamline at SuperACO-France', SPIE Proceedings (1999) *Denver* vol.3575*Eds G.L. Carr and P.Dumas* (1999), 13

6. Francfort, H.P., Ligabue, G., Samashev, Z., 'La fouille d'un kourgane scythe gelé du IVe siècle avant notre ère à Berel dans l'Altaï (Kazakhstan)', *Comptes rendus de l'Académie des Inscriptions et Belles-Lettres*, Editions De Boccard, Paris (2000), 775-806

7. Clisson, I., Keyser, C., Francfort, H.P., Crubézy, E., Samashev, Z., Ludes, B., 'Genetic analysis of human remains from a double inhumation in a frozen kurgan in Kazakhstan (Berel site, early 3rd Century BC)', *International Journal of Legal Medicine,* (2002), **116**, 304-308

8. Samashev, Z., and Francfort, H.P., 'Scythian Steeds, Blocks of frozen earth yield the remains of horses bearing extravagant regalia', *Archaeology*, (2002), **55**, (3), ???

9. Littré, *Hippocrate, Œuvres complètes* livre 6, p .451, JB Baillière, Paris, (1839-1861)

10. Naumann, D., 'Infrared spectroscopy in microbiology' in *Encyclopedia of Analytical Chemistry*, RA Meyers (Ed.), John Wiley & Sons Ltd, Chichester, (2000) 102-131

11. Stuart, B., *Biological applications of infrared spectroscopy*, John Wiley & Sons Ltd, Chichester, (1997)

12. Kreplak, L., Briki, F., Doucet, J., Merigoux, C., Leroy, F., Leveque, J.L., Miller, L., Carr, G.L., Williams, G.P., and Dumas, P. 'Profiling lipids across Caucasian and Afro-American hair transverse cuts, using synchrtron infrared microspectrometry', *International Journal of Cosmetic Science*, (2001), **23**, 369-74

13. Dumas, and P. Miller, L., 'Biological and biomedical applications of synchrotron infrared microspectroscopy', *Journal of biological physics*, (2003), **29**, 201-218

14. Chapman, D., *The structure of lipids by spectroscopic and X-ray techniques*, Methuen and Co LTD, London and Colchester (1965)

15. Walter, P., Martinetto, P., Tsoucaris, G., Breniaux, R., Lefebvre, M.A., Talabot, J., and Dooryhee, E., 'Making make-up in Ancient Egypt', *Nature*, (1999), **397**, 483-484

Analysis of the Materials of Several Canadian Artists using Fourier Transform Infrared Spectroscopy

Kate Helwig
Analytical Research Laboratory, Canadian Conservation Institute, Ottawa, Canada

The Analytical Research Laboratory of the Canadian Conservation Institute (CCI) has an ongoing research project aimed at developing a database of materials and techniques for a number of Canadian painters. The project is a multi disciplinary, team effort that requires the use of a range of techniques. These include Fourier transform infrared spectroscopy, x-ray diffraction, scanning electron microscopy, x-ray microanalysis, polarized light microscopy and specialized photographic techniques.

This paper will describe the application of Fourier transform infrared spectroscopy to the characterization of painting materials of three Canadian artists: Louis Dulongpré (1759-1843); Jean Dallaire (1916-1965); and Yves Gaucher (1934-2000). Interesting aspects of the pigments and media of these artists determined by infrared spectroscopy will be outlined.

Infrared spectroscopy allowed the identification of a starch-based preparatory layer in an early nineteenth-century oil painting attributed to Louis Dulongpré. Further analysis showed that the starch was not heated sufficiently to form a paste and that the lack of cohesion in the ground layer was responsible for the poor condition of the painting. Certain pigments with interesting characteristics were found in the oil paintings of Jean Dallaire. Samples containing the green pigment viridian, for example, showed the presence of several unattributed bands in the infrared spectrum. These bands were also found in some, but not all, standard samples of the pigment. Several types of acrylic media were identified in the studio materials of Yves Gaucher using infrared spectroscopy. The acrylics used correspond to information given by Gaucher's paint supplier. Also of interest in Gaucher's paints is the presence of a feldspar mineral filler, nepheline syenite. Documentary evidence suggests that Gaucher added this filler to his paint to produce a specific texture, and it appears to be an identifying characteristic of his technique.

The Application of Raman and FTIR Microspectroscopy for the Study of Drying Oils

Anna Schönemann[1], Howell G.M. Edwards[2]

[1] The Getty Conservation Institute, 1200 Getty Center Drive, Suite 700, Los Angeles, CA 90049, USA,
[2] Department of Chemical and Forensic Sciences, University of Bradford, Bradford BD7 1DP, UK,

In the field of conservation science, Raman spectroscopy has been established as a further analytical method for the investigation of materials of artifacts. It is a suitable technique for the examination of both inorganic and organic compounds. Consequently, it can be used for the identification of a wide range of components of art objects like pigments, minerals, corrosion products, and binding media. The evaluation of the spectra is mainly conducted by pattern recognition procedures on the basis of reference measurements. Raman spectroscopy also provides information on the molecular structure of compounds. In combination with results from FTIR spectroscopy, complementary structural data are obtained.

In this study, the structural examination by a combination of Raman and FTIR microspectroscopy of linseed and tung oil is presented. These oils were chosen as examples of drying oils with carbon carbon double bonds in different configurations.

Table 1 Characteristic Raman bands (cm^{-1}) of linseed and tung oil

Linseed oil	Tung oil	Attribution
2922	2921	ν (C-H)
2804	2873	ν (C-H)
1745	1749	ν (C=O)
-	1668	ν (C=C)
1656	-	ν (C=C)
-	1644	ν (C=C)
1441	1442	δ (C-H)
1300	1304	δ (C-H)
1264	1256	-
-	1166	-
1084	1084	ν (C-C)
-	1060	-
861	869	-
600	600	-

In comparison with FTIR analysis, Raman spectroscopy allows the structural examinations of nonpolar bonds with a high polarizability. In the corresponding FTIR spectrum, the absorptions tend to be weaker signals.

In examining glyceride oils with unsaturated carbon-carbon bonds, Raman spectroscopy is a suitable method because of the presence of weak polar bonds. Strong bands absorption bands were obtained by vibrations of carbon-carbon double bonds in the fatty acid chain of the glycerides. Different configurations of C=C double bonds were detected in the conjugated and non-conjugated moieties of the fatty acids in tung and linseed oil. The bands absorptions at 1668 and 1644 cm^{-1} are the most intense for tung oil and 1656 cm^{-1} for linseed oil in the Raman

spectra. Otherwise, FTIR spectroscopy is useful for bonds with a change in the dipole moment; thus, the most intense absorption was derived from the carbonyl group of the ester in oils. The carbon-carbon double bonds show weaker signals and they are suitable only for qualitative interpretation at best because of interference from the very strong carbonyl absorpition with the unsaturated C=C double bond.
Results from both methods were combined to assist in the interpretation of the molecular structures of the specimens. Preliminary data from these analyses will from the bais of detailed work in the future.

Instrumentation

Raman spectra were measured using a Renishaw inVia Raman microscope equipped with a RenCam CCD detector. The instrument has two lasers with following excitation wavelengths, a helium neon laser of 633 and a semiconductor laser of 785 nm. The laser power was kept at 1mW. A Leica microscope was selected with 3 objectives were a magnification of 5, 20, and 50 x. Wire software was used for collecting Raman spectra. The spectra were taken in a range of Raman shifts from 4000 to 500 cm^{-1}. In addition, measurements were performed using a Bruker IFS 66/FRA 106 FTRS with a Nd:YAG laser with a wavelength of 1064 nm over a similar wavenumber range.
For the FTIR measurement, a Nicolet FTIR-microscope was used. The microscope was equipped with a mercury-cadmium-telluride (MCT) detector. Spectra were taken in the range of 3200 to 500 cm^{-1} with 60 scans, a resolution of 4.0 cm^{-1} and a strong apodization.

Analysis of Iron Corrosion Products with Fourier Transform Infra-red and Raman Spectroscopies

David Thickett
English Heritage, 23 Savile Row, London, W1S 2XZ, david.

Abstract

The formation of akaganeite on archaeological iron has been studied in-situ and through experiments using infra-red and Raman spectroscopies. The mechanism appears to involve iron (II) chloride oxidising to iron (III) chloride and then hydrolysing to akaganeite. Experiments at different RHs and with a variety of contaminants confirmed that this process will not occur below 18%RH and is accelerated by the presence of copper ions and humic acid and retarded in the presence of goethite. The surface layer of the akaganeite formed has been observed to transform into either goethite or lepidocrite, releasing chloride ions. Experiments have shown that this transformation is related to adsorbed water vapour and that the transformation product depends on pH.

Introduction

Corrosion of iron occurring in a number of environments presents challenges to the cultural heritage profession. Whilst most museum situations are relatively benign with regards to atmospheric corrosion of iron, in situ social history and industrial collections can be exposed to much more aggressive environments and show significant decay. The post excavation changes undergone by archaeological iron can rapidly destroy the archaeological value of an artefact and are of serious concern. Identification and quantification of iron corrosion products is fundamental to our understanding of these processes and development of successful strategies to minimise their impact.

Material	Mineral Name	Supplier	Stated Purity	Impurity Analysis		
				SEM-EDX	XRD	FTIR
α–FeOOH	goethite	Alfa	99	99.5	goethite	
β –FeOOH	akageneite	RT Min	-		goethite	
β –FeOOH	akageneite	RT Min	-		goethite	
β –FeOOH	akageneite	Synthesised	-	[Cl]=5.7	akaganeite	
β –FeOOH	akageneite	Corrosion	-	[Cl]=9.8	akaganeite	
γ-FeOOH	lepidocrite	Alfa	99	99.6	lepidocrite	
Fe_3O_4	magnetite	Ald	99.5	99.4Si,O	magnetite	silicate
Fe_3O_4	magnetite	Alfa	99.999	100.0	magnetite	
α-Fe_2O_3	hematite	Ald	99.998	100.0	hematite	
γ-Fe_2O_3	maghemite	Alfa	99.9	99.9	maghemite	
$FeCl_2.2H_2O$	lawrencite	Alfa	99.99	100	lawrencite	
$FeCl_3$	molysite	Alfa	99.8	99.8	molysite	
$FePO_4.2H_2O$	strengite	Ald	97.17	98.9	strengite	
FeS_2	pyrite	RT Min	-	99.5	pyrite	
$Fe_{0.8-1}S$	pyrrhotite	Alfa	99.9	99.9	pyrrhotite	
$FeCO_3$	siderite	RT Min	-	99.8	siderite	
$FeCO_3$	siderite	RT Min	-	96.3Si,Al, O	siderite	silicate
$FeCO_3$	siderite	RT Min	-	98.4 Ca	siderite	calcite
$FeSO_4.4H_2O$	rozenite	Ald	99	99.3	rozenite	

Alfa ⇨ Alfa Aesar
Ald ⇨ Aldrich
RT Min ⇨ Richard Taylor Minerals Ltd
- ⇨ no purity stated, mineral samples

Table 1: Standard Materials

Table 1 shows the corrosion products reported on iron in various environments. Although infra-red and Raman spectra have been published for most of the materials reported [1,2,3], different sampling techniques are required to

accommodate the many situations faced in conservation science. Available sample sizes can be very limited and moving from potassium bromide discs to a diamond cell with beam condenser to an infra-red or Raman microscope can produce spectra from progressively smaller samples. Infra-red microscopy and confocal Raman microscopy allow *in situ* analyses. It is important to understand any differences in spectra caused by the use of different infra-red sampling methodologies and the benefits of each technique. For efficient searching, good quality libraries are required, with each library composed of spectra generated with the technique used to collect the unknown spectrum. The deterioration of vulnerable archaeological iron after excavation via akaganeite formation, is routinely controlled by storage or display in a low relative humidity environment. The critical RH for storage of such material is based on a series of experiments reported by Turgoose [4] and significant anecdotal evidence. Turgoose's experiments used relatively pure ferrous chloride mixed with iron and showed a critical RH for akaganeite formation of between 15 and 20%. This figure has been widely reported as 18%, although the justification for this is unclear. The exact role of the iron powder in the transformation is not known. Selwyn et al. Have postulated a chloride cycle as an alternative mechanism for iron corrosion, giving a different critical RH [5]. The critical RH is of obvious import to preventive conservation and since the low RHs advocated by Turgoose are difficult to attain in a practical display situation, the effects of exceeding that RH are also of interest in terms of relative risk. Experiments were undertaken to investigate the formation of akaganeite on archaeological iron, in conjunction with analyses of deteriorating iron artefacts. Combining the results of object analysis with experimental work has helped gain a better understanding of the formation mechanism. Analysis also showed transformation of thin surface layers of the akaganeite into either goethite or, in one instance, lepidocrite. Stahl et al have postulated that there is no thermal mechanism for akaganeite transformation accessible at ambient temperatures [6]. A series of experiments has been carried out to investigate whether exposure to water either as a liquid or through vapour, initiates the transformation. The role of pH on the transformation product obtained was also investigated.

Reference materials were obtained or produced for each of the corrosion products and are shown in Table 1. Materials were obtained commercially where possible and to a high purity. The identity of each material was confirmed with x-ray diffraction and the chemistry checked with scanning electron microscopy energy dispersive analysis (SEM-EDX). X-ray diffraction has a low sensitivity to some contaminants, whilst non-chemically identical contaminants should be readily detected with SEM-EDX. The materials used are also shown in Table 1.

Akaganeite, ß-FeOOH could not be obtained commercially and was synthesised by arial oxidation of iron (II) chloride at 60°C for sixteen hours [7]. The orange crystals were separated from the reaction mixture by centrifuge. The crystals were centrifuged with several washes of 18.2MΩ water until the chloride concentration in the wash water dropped below 1ppm. A relatively large sample of an akaganeite corrosion product also became available and was included.

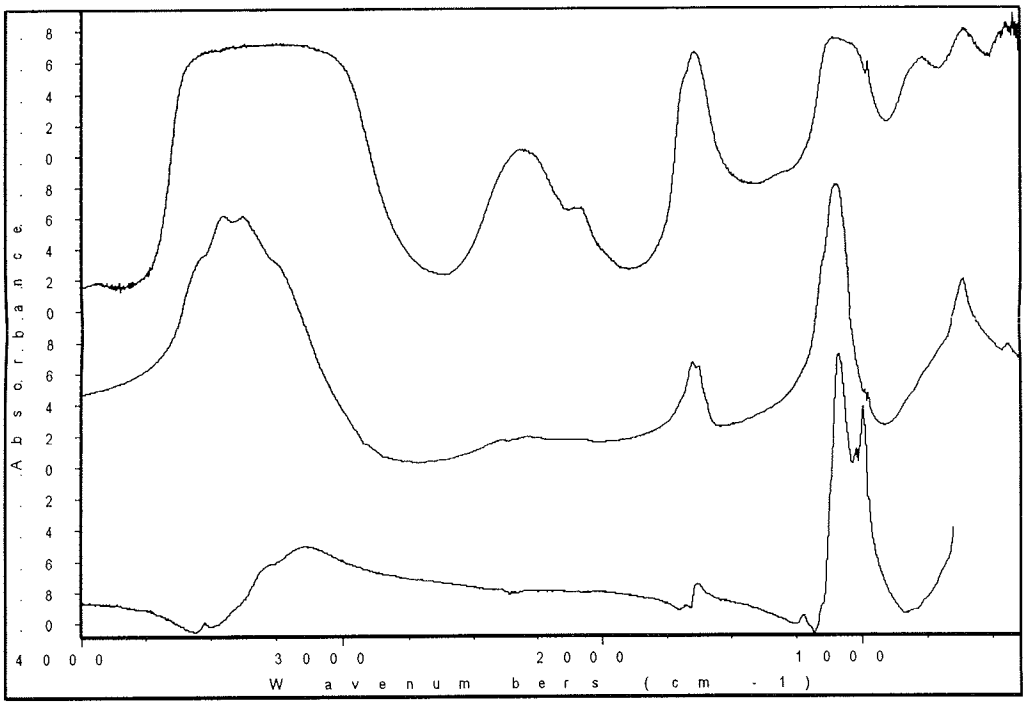

Figure 1: Iron Sulphate FTIR Spectra From Various Sampling Techniques

Each material was analysed using FTIR: quantitatively using potassium bromide discs and qualitatively with diamond cell and beam condenser; diffuse reflectance DRIFTs (all Perkin Elmer 2000); infra-red microscopy in direct reflectance mode and with attenuated total reflectance heads, Nicolet Inspect IR with silicon and zinc selenide ATR heads).
Very few differences were observed in peak position the FTIR spectra collected of the same material with different techniques. The direct reflectance FTIR microscopy showed some dispersion effects, with derivative peaks observed on goethite and magnetite. These were successfully corrected for, with the Kramers-Kronig correction. The spectra of iron sulphate showed the most differences and are included as Figure 1.

Material	Peak		Calibration		
	Position (cm^{-1})	Whh (cm^{-1}) type	Slope (Abs/mg)	Limit of linearity (mg)	Detection Limit (mg)
α – FeOOH	798	44 m	0.7713	0.884	0.050
β – FeOOH	852	53 m	0.3146	1.181	0.040
γ – FeOOH	746	32 l	0.1687	1.135	0.005
Fe_3O_4	567	41 l	0.0105	1.378	0.400
$\alpha - Fe_2O_3$	548	78 l	0.2318	0.798	0.035
$\gamma - Fe_2O_3$	638	35 l	0.1653	1.263	0.050
$FeSO_4.4H_2O$	1100	131 l	0.263	0.975	0.010
FeS_2	1130	253 m	0.0056	1.257	0.355
$FeCO_3$	1418	178 m	0.4226	0.975	0.055
$FePO_4.2H_2O$	1028	231 m	0.9788	0.674	0.015

Whh ⇨ width at half height l ⇨ Lorentzian
Type ⇨ peak type m ⇨ mixed (Lorentzian+Gaussian)

Table 2: Peak and Calibration Parameters

As can be seen, the microscope direct reflectance spectra shows better definition in the ν_1 and ν_3 region (900-1400cm^{-1}), with bands at 1240, 1088 and 996 cm-1 clearly observable [8]. The spectra do differ in the hydroxyl stretching absorptions above 3000cm^{-1}. The microscope spectra of goethite showed a shift of 10cm^{-1} in the 902cm^{-1} peak and a similar shift in the 885 cm^{-1} of lepidocrite was observed. The MCT-A detector of the microscope cuts off at 650cm^{-1}, which means it cannot detect magnetite and relies on a single peak at 694cm^{-1} for its detection of maghemite. Identification of iron chlorides requires detection below 400cm^{-1}, with only water vibrations observable in the mid infra-red. There were significant differences in the relative intensities and widths of the peaks produced by the different sampling techniques. Characteristic non overlapping peaks were selected for each material and are shown in Table 2, along with their peak shape and full width at half height.
Potassium bromide discs were produced from approximately 3mg accurately weighed sample, made up to 300mg

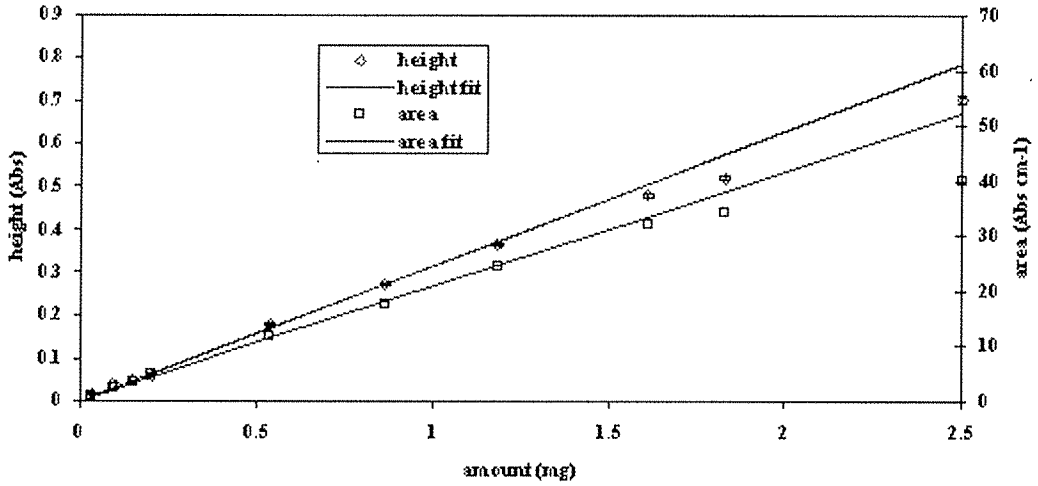

Figure 2: Akaganeite Calibrations

with ground potassium bromide. The infra-red spectrum was recorded in triplicate on a Perkin Elmer 2000 FTIR spectrometer using 32 scans. The disc was split in two portions using a scalpel, one portion was weighed and reground. The weight was made up to 300mg with freshly ground potassium bromide, the powders mixed and another disc pressed and weighed. The FTIR spectra were collected and the process repeated seven times to give a series of spectra collected with sample weights ranging from 3 to 0.001mg. This method removed replace reduced the need to weigh out very small amounts of sample accurately for the calibration and reduced the calibrations dependency on accurate weighing. The slope of the calibration line is mainly dependant on the mixing accuracy of the dilutions, and even a large error in the initial weight of sample used would have little effect on the slope. Solid state mixing of fine powders is difficult to achieve and the efficiency of this process was verified by determining the iron content in the discarded parts of the potassium bromide discs with atomic absorption spectroscopy. The calibration discs from finest and coarsest sample powder, lepidocrite and siderite were analysed. The discarded parts of the discs were dissolved in dilute hydrochloric acid and the concentration of iron determined by atomic absorption. The iron concentrations were found to match the expected values calculated from the mixing weights, within the experimental error the atomic absorption technique 0.5%.

The calibration lines were plotted using both the peak height and area for the characteristic peaks selected previously; Figure 2 shows the calibration plot for akaganeite. All of the plots showed negative deviations from straight line at higher absorbance values. The limit of linearity is important as it sets a maximum concentration, above which, the linear calibration is not valid. Limits of linearity were calculated for each calibration by comparing an independent estimate of the variance derived from the duplicate measurements (pure error mean square) with one derived from assuming a linear model (lack of fit mean square). Detection limits for the materials were determined as the lowest concentration at which a 95% confidence interval did not contain zero.

Calibrating against the peak area was found to give an extended linear range compared to calibrations against the peak heights. However, peak height is less affected by slight peak overlap, which is very likely, considering the broad nature of several of the peaks and the mixtures likely to be encountered. Hence peak height was used. The calibration information is included in Table 2. As can be seen magnetite and iron sulphides give a very weak response for infra-red spectroscopy. Both of these materials also frequently occur as hard, well adherent layers (and in the case of iron sulphides extremely thin layers) which are difficult to sample.

The reference materials were also analysed with Raman spectroscopy, Dilor Infinity confocal microscope with wavelength doubled Neodinium Yttrium Aluminium Garnet (532nm 4mW) and diode lasers (780nm 2mW). The 532nm laser was found to produce useable spectra much more quickly than the 780nm laser, although for materials such as magnetite this still required long collection times. Spectra were collected with the lasers filtered down to not more than 25% of their full power. Akaganeite and lepidocrite were observed to convert under the high fluence of the focused laser beam, initially to maghemite and then hematite. Thermo-gravimetric and differential scanning calorimetry analysis of the standard materials used, showed that the relevant transformations began at 219°C for the lepidocrite sample studied and 175°C for the akaganeite. Goethite, which could not be made to transform was found to have a transformation temperature onset above 269°C. Similarly the magnetites examined could not be made to transform to hematite, even with 100% laser power through the x100 lense, though this phenomena has been reported during Raman analysis [1]. The measured onset transformation temperatures for the magnetite materials ranged from 311°C. Whether a transformation occurs under the laser illumination used for Raman microscopy depends on the materials surface temperature exceeding the transformation temperature. The transformation temperature is affected by chemistry, crystallinity, particle size and shape. The surface temperature depends on the laser power density at the surface (the fluence), the absorptivity of the material at that wavelength (which will also depend on the surface roughness) and the transfer properties of the material for the heat absorbed.

Akaganeite Formation

Dover castle has extensive tunnels cut into a chalk cliff below it. Historically significant communications equipment from World War II is displayed in part of the tunnel complex. The underground porous chalk tunnels present an aggressive environment with high ambient RH and high concentrations of airborne salt particles from the sea. Corrosion on sheet steel casings was found to consist primarily of akaganeite, confirming the role of chlorides in the corrosion process. The very aggressive environment has necessitated the use of a commercial corrosion inhibiting film to protect the steel. This product performed extremely well in the ISO9227 salt spray corrosion tests. Despite the materials application some new small instances of rust were observed. Examination with infra-red microscopy again detected primarily akaganeite. No peaks from the corrosion inhibitor were observed in corroded areas indicating that insufficient application was at fault, due to the very large areas coated. Further trials are in progress

to determine the optimum lifetime of the inhibitor to inform the re-treatment regime.
A display at Porchester Castle incorporated archaeological iron objects originating from occupation phases from the Roman (290-430AD), Anglo Saxon (5th –11th century AD) and later periods. The relative humidity in the showcases containing iron was controlled with dried silica gel (between 40 and 110kg gel per m^3 of case volume). Despite the high specification showcases, designed to protect the iron from the high ambient RH environment and the large volumes of silica gel, over five times that normally recommended, several objects were observed to be spalling small pieces of iron corrosion product. Since the display sits on a sprung wooden floor and the objects are fixed on cantilever type mounts, then vibration was a potential alternative cause for the spalling besides ongoing corrosion. Several pieces were collected and analysed using a beam condenser and diamond cell. The spectra were consistent with akaganeite showing absorptions at 852 and 670 cm^{-1}. This indicated that active corrosion was taking place and vibration was not the primary cause of the spalling. Monitoring of the RH inside the showcases, showed that although the cases attained 10% about 30 days after the introduction of dried silica, this rose to between 30 and 42% over the next 5 months depending on the case. The current regime involved replacing the gel on a six monthly cycle, this was reduced to 4 months to ensure the RH would not exceed 20%, in any of the display cases.
The akaganeite formation reactions were studied by exposing iron (II) chloride powder to a range of relative humidities. The presence of other metal ions, iron corrosion products and humic species are all reported to affect the formation and crystallisation of iron oxyhydroxides. Copper is often used in conjunction with iron, and in chloride burial environments, cuprous chloride can form. Ishikawa et al have shown that cuprous ions do not affect the crystallisation of akaganeite from iron (III) solutions [9]. However, cuprous chloride has a low deliquescent RH and its affect on the critical RH was investigated. The presence of organic soil components such as humic and fulvic acids, has a significant effect on several of the important reactions relating to iron corrosion. It stabilises iron (II) ions, affects the rate of oxidation of those ions to iron (III) and affects the crystallisation of iron (III) compounds [10]. Many important archaeological iron objects originate from inhumations. Iron oxides and oxyhydroxides affect the mix of corrosion products formed [11] and the effect of the most common, goethite was investigated. Powdered samples of ferrous chloride (Alfa 99.5%) mixed 1:1 with iron (Fluka 99.98%); 1:1:1 with iron and cuprous chloride (Alfa 99.5%); 1:1:1 with iron and humic acid (Aldwych no purity specified) and 1:1:1 with iron and goethite (Alfa 99%). The mixtures were accurately weighed and exposed to 5, 10, 15, 16.7, 18.4, 20, 25, 30, 35, 40, 45, 50 and 70% RH atmospheres, generated above glycerol solutions at ambient temperature. The mixtures were reweighed after 4, 8, and 30 days. Each time a 1mg samples were removed and pressed as a KBr disc. The formation of akaganeite was followed using the 852 peak and the calibration developed previously. Quantification of the amount of akaganeite produced determines whether the iron powder is transformed into akaganeite. Results are shown in Figure 3.

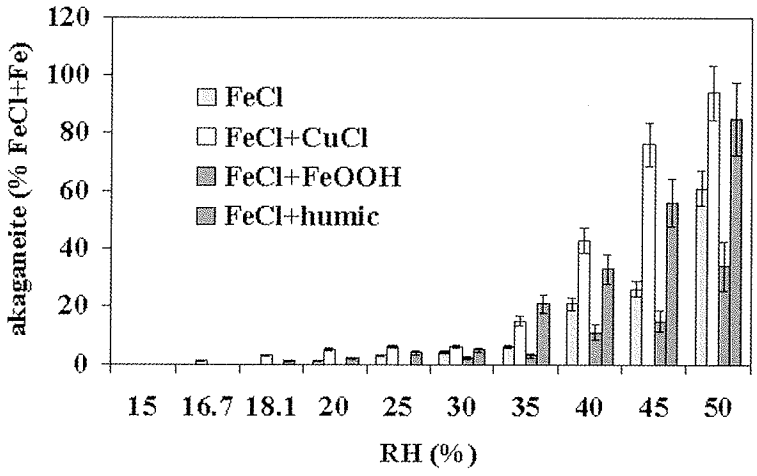

Figure 3: Akaganeite Formation Tests

As can be seen the critical RH for pure iron (II) chloride is 18% and only copper reduces this slightly to 15%. The amount of akaganeite formed increases dramatically from 30% and the additions still show this same trend. The amount of akaganeite formed is greater than that which could be generated from just the iron (II) chloride and some must be formed from the iron powder present. Copper chloride and humic acid both increase the akaganeite transformation rate, whilst goethite reduces it.

Accelerated buried corrosion tests had been undertaken to try and mimic archaeological iron.. The tests comprised burying iron discs in cristabolite sand with sodium chloride and hydrochloric acid solutions at 30, 50, 70 and 90°C. When the cristabolite sand was gently removed after 90 days at the lower temperatures, a complex pattern of pale yellow crystals with darker brown edges was observed on disc surfaces. Analysis with Raman confocal microscopy identified three phases present, iron (II) chloride, iron (III) chloride and akaganeite. The iron (II) chloride was present in the centre of the crystals, whilst iron (III) chloride was present towards the edges. The brown edges were identified as akaganeite. Analyses taken over a period of several weeks indicated that the iron (II) chloride was slowly oxidising first to iron (III) chloride, which then appeared to transform to akaganeite.

Akaganeite Transformation

When examined under magnification, a pale yellow coating was observed on the brown akaganeite samples from Porchester Castle. Analysis with both FTIR and Raman microscopy could only identify akaganeite, when the microscope was focussed on the yellow material. Cross sections were prepared in Araldite 753 epoxy resin, polished and coated with carbon for scanning electron microscopy energy dispersive analysis (SEM-EDX). This showed that the brown akaganeite contained iron, oxygen and chlorine , whilst the yellow areas contained much less chlorine, but had the same ration of iron to oxygen. Analysis of the yellow areas with FTIR microscopy (direct reflection) and Raman microscopy detected only akaganeite. The cross sections were further analysed using a Nicolet Inspect IR microscope with silicon and zinc selenide attenuated total reflection heads. The different refractive indices of the ATR crystal materials causes different information depths for the two crystals. The spectra obtained contained absorptions characteristic of akaganeite, however additional absorptions were observed at 902 and 1141cm^{-1}, indicating that the yellow material is goethite. The goethite absorptions were much stronger on the silicon ATR spectrum as would be expected from its higher refractive index and hence shallower information depth.
One object with a lepidocrite conversion layer was also analysed. This originated from an artefact treated with alkaline sulphite. Lepidocrite is reported to form from iron solutions in the higher end of neutral pHs, and it is possible that residual alkali from the conservation treatment has influenced the akaganeite transformation. SEM-EDX examination detected sodium in the sample.
The cross sections produced from the Porchester material did not allow an accurate estimate of the goethite layer thickness by microscopy. The pieces were small and the cross sections irregular. Further samples were prepared by

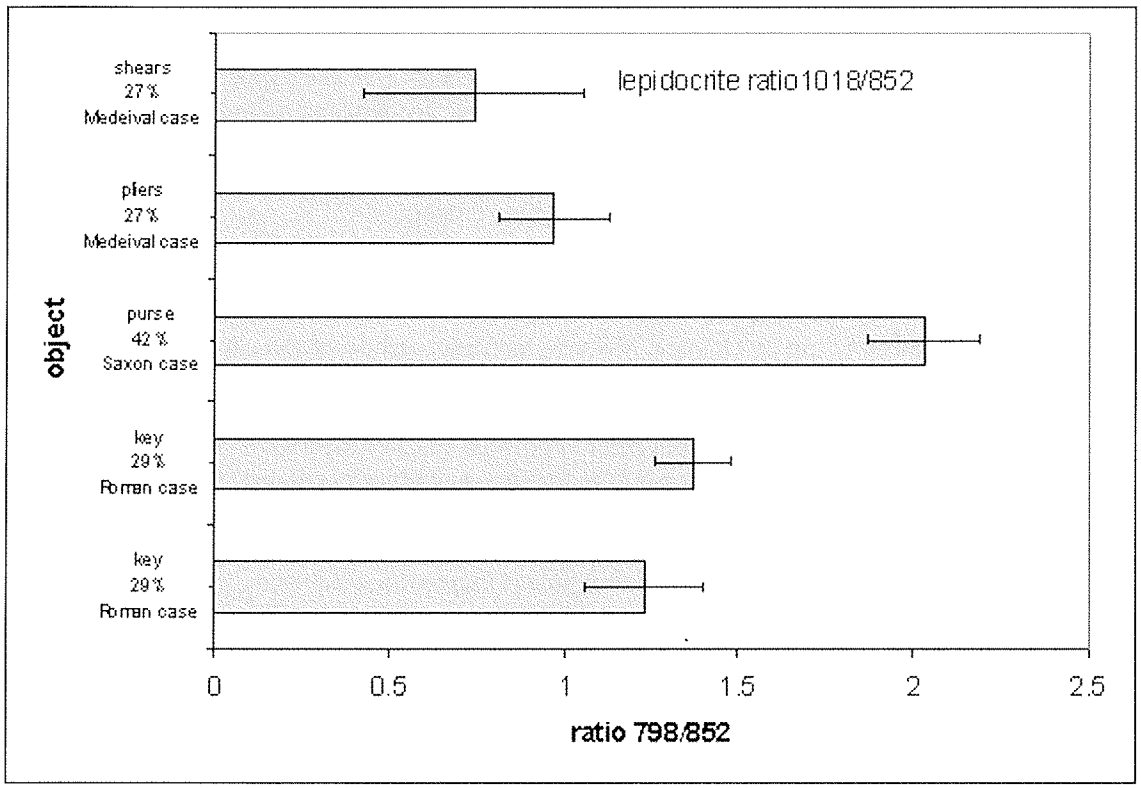

Figure 4: ATR of Akaganeite Corrosion Products

placing both spalled akaganeite pieces and samples removed from the object surfaces onto a PTFE sheet. A mould was placed around the pieces and Araldite 753 epoxy resin poured over the samples, to encapsulate them presenting one clear 'face'. The surface of the samples were then analysed with ATR FTIR microscopy as described previously. Some adjustment of the sample position was required to produce a surface analysis from the sample and avoid the epoxy resin, but this could readily be judged from the FTIR spectra. The amount of goethite present was determined from the ratio of the absorbance at 798cm^{-1} to that at 852cm^{-1}(akaganeite). Results are show in Figure 4. The samples from objects exposed to higher RHs appear to have thicker conversion layers of goethite present. This is consistent with the reported reconstructive transformation of akaganeite to goethite under the influence of water [12]. However, the exhibition has been installed for almost fifteen years and the akaganeite may have occurred earlier in the high RH cases and hence had longer to transform.

A series of experiments was undertaken to study the transformation, by exposing akaganeite samples to liquid water, and water adjusted to pH 8 with the addition of sodium hydrogen carbonate and sodium carbonate. Samples were also exposed to the different RH atmospheres described previously. Both akaganeite corrosion product and synthetic akaganeite samples were studied, as SEM-EDX of akaganeite corrosion products generally showed a higher chloride concentration in the corrosion products than in the synthesised akaganeite. The akaganeite samples were ground and pressed into 1mm thick discs, which were then broken into several pieces for the various exposure experiments. After exposure the surfaces of the disc pieces were examined with the Spectratech Golden Gate diamond ATR. After 60 days exposure goethite was detected on the samples exposed to liquid water and 70 and 50% RHs, but not the other RHs. The experiments will be continued to determine if conversion occurs at lower RHs. Lepidocrite was detected instead of goethite on the sample exposed to the pH 8 water, confirming the role of the alkali residue from treatment in the appearance of lepidocrite on one of the Porchester samples.

Conclusions

FTIR and Raman spectroscopies have proved invaluable for the study of iron corrosion reactions. They have found ready application for situations ranging from rapid identification to more in depth quantitative experimental work. In many ways the two techniques complement each other being suited for analysis of different minerals and samples in different situations. The progress in instrumentation that now allows *in-situ* analyses has been immensely beneficial. Analyses on corroding object surfaces have confirmed that the necessarily simplistic experimental and theoretical models of iron corrosion are occurring in real situations. The surface analyses have also helped to guide experimental work.

The critical RH for akaganeite formation was verified at 18% for pure samples and slightly lowered by the addition of copper ions. Significant akaganeite formation was observed above 30% RH and copper and humic acids increased the amount of akaganeite formed, whilst goethite reduced it. Evidence of further transformation of the akaganeite after formation has been found on artefacts and a mechanism based on water vapour adsorption verified experimentally. Whilst chloride is released in this process, the amount is small and the risk from this process is probably small. The transformation is retarded by a low RH environment.

References

1. de Faria, D.L.A., Venacio Silva, S. and de Oliveira, M.T., 'Raman microscopy of some iron oxides and oxyhydroxides', *Journal of Raman Spectroscopy* (1997) **28** 873-878.

2. Raman, A., Kuban, B. and Razvan, A., 'The application of infrared spectroscopy to the study of atmospheric rust systems – I standard spectra and illustrative applications to identify rust phases in natural atmospheric corrosion products', *Corrosion Science* (1991) **32**(12) 1295-1306.

3. Nyquist, R.A. and Kagel, R.O., *Infrared Spectra of Inorganic Compounds*, Academic Press, New York (1971)

4. Turgoose, S., 'Post-excavation changes in iron antiquities', *Studies in Conservation* (1982) **27** 97-101.

5. Selwyn, L.S.,Sirois, P.J. and Argyropoulus,V., 'The corrosion of archaeological iron', *Studies in Conservation*, (1999) **44** 217-232.

6. Stahl, K.,Nielson, K., Jiang, J., Lebech, B., Hanson, J.C., Norby, P. and van Lanschot, J., 'On the akaganeite

crystal structure, phase transformations and possible role in post-excavational corrosion of iron artefacts', *Corrosion Science*, (2003) **45** 2563-2575

7. Cornell, R. M. and Schwertmann, U., *The Iron Oxides* 2nd Edition, Wiley VCH, New York (2003)

8. Parfitt, R.L. and Smart, S.C.. 'Infrared spectra from binuclear bridging complexes of sulphate adsorbed on goethite (α–FeOOH)'. *Journal of the Chemical Society Faraday Transactions*, (1977) 173, 796-802.

9. Ishikawa,T.,Katoh,R.,Yasukawa,A.,Kandori,K.Nakayama,T. and Yuse,F., 'Influences of metal ions on the formation of β–FeOOH particles', *Corrosion Science* (2001) **43** 1727-1738.

10. Pullin, M.J., and Cabaniss, S.E. 'The effects of pH, ionic strength, and iron-fulvic acid interactions on the kinetics of non-photochemical iron transformations. II. The kinetics of complexation and dark reduction', *Geochimica et Cosmochimica Acta* (2003) 67(21) 4067-4077.

11. Ishikawa,T., Kondo,Y., Yasukawa,A. and Kandoori,K., 'Formation of magnetite in the presence of ferric oxyhydroxides', *Corrosion Science* (1998) 40(7) 1239-1251.

12. Turgoose, S., 'The nature of surviving iron objects', *Postprints of National Maritime Museum Monograph Number 53, Conservation of Iron*, Greenwich, London (1982) 1-7.

Building a Multi-dimensional Raman Database: the Effect of Excitation Wavelength and Binding Medium on the Raman Spectra of Artists' Pigments

Karen Trentelman[1,2] and Carole Havlik[1]

[1] The Detroit Institute of Arts, 5200 Woodward Avenue, Detroit MI 48202 USA.
[2] new address: The Getty Conservation Institute, 1200 Getty Center Drive, Suite 700, Los Angeles, CA 90049 USA

Abstract

The Raman spectra of artists' pigments were evaluated as a function of excitation wavelength and binding medium. The results demonstrated the importance of using an excitation wavelength that avoids excited electronic states of the analyte, which can lead to intense fluorescence. Resonance enhancement was found to cause significant variation in the relative intensity of Raman bands in several species, emphasizing the need for inclusion of spectra acquired at multiple excitation wavelengths in libraries or databases of Raman spectra. The presence of a binding medium contributes a variety of effects, ranging from no effect to the introduction of additional Raman bands to the production of a large fluorescence background to improvement of the signal to noise ratio. The effects of absorption, resonance enhancement, quenching, and instrument parameters are discussed.

Introduction

Raman microscopy has proved to be exceptionally effective for the identification of most artists' pigments, and libraries of Raman spectra have been generated for historic pigments [1,2], dyes [3], enamel/glaze pigments [4] and modern synthetic pigments [5]. However, the usefulness of these libraries may be limited by the fact that the Raman spectrum for some pigments may vary considerably with excitation wavelength [6]. A further limitation is that most libraries are constructed using pure pigment samples, whereas pigments in works of art typically are mixed with a binding medium that may influence the resulting Raman spectrum.

In this paper we discuss some of the results from our study of the effect of excitation wavelength and binding medium on the Raman spectrum of artists' pigments. So far, we have measured the Raman spectral response of nine pigments in each of five different binding media (plus a dry, unbound sample) at four different excitation wavelengths (785 nm, 632.8 nm, 514.5 nm and 488 nm). The pigments selected for this initial study were: red ochre ($Fe_2O_3 \cdot H_2O$ + clay impurities), Hansa yellow (acetoacetarylide azo PY1), chrome yellow (lead chromate, $PbCrO_4$), verdigris (basic copper acetate, $Cu(C_2H_3O_2)_2 \cdot 2Cu(OH)_2$), phthalocyanine green (copper-chloro phthalocyanine), indigo (indigotin, $C_{16}H_{10}N_2O_2$), artificial ultramarine (sodium aluminum silicate, $Na_{6-10}Al_6Si_6O_{24}S_{2-4}$), azurite (basic copper carbonate, $2CuCO_3 \cdot Cu(OH)_2$), and titanium white (anatase TiO_2). The five binding media were collodion, egg yolk, gum arabic, linseed oil, and polyvinyl acetate.

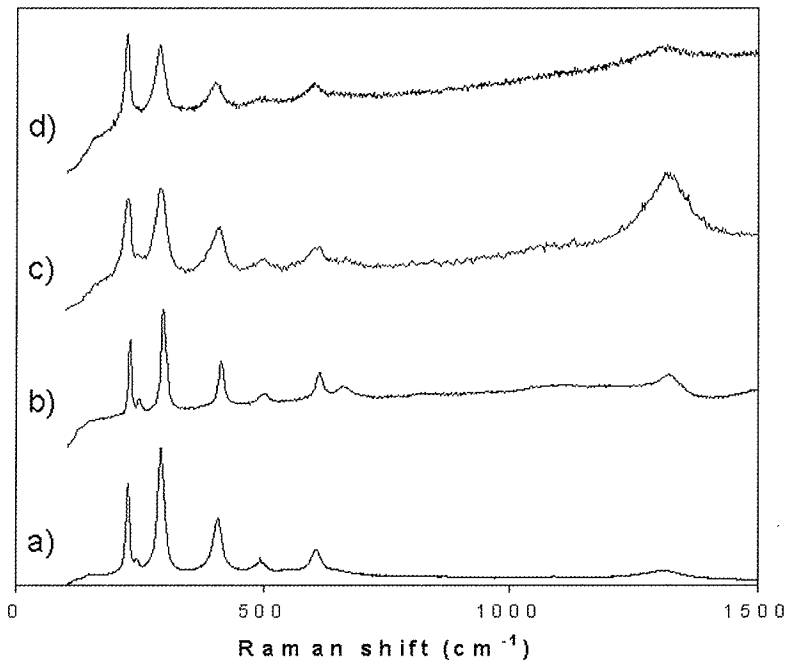

Figure 1: Raman spectra of red ochre (dry powder) acquired using a) 785 nm, b) 632.8 nm, c) 514.5 nm and d) 488 nm excitation. Intensities are not to scale.

Experimental

Samples of dry powdered pigment were ground in each of the five binding media listed above and the resulting mixture spread on a glass microscope slide and allowed to dry thoroughly. Samples of dry

pigment were also placed on a glass microscope for analysis.
All Raman spectra were recorded using a Renishaw 1000 Raman microscope equipped with one of four excitation sources: 488 nm Ar ion laser, 514.5 nm Ar ion laser, 632.8 nm He-Ne laser or 785 nm diode laser. For each sample, a series of neutral density filters was used to adjust the power level at the sample surface to achieve the maximum signal level without inducing thermal damage. The total acquisition time of each spectrum ranged between 30 and 120 seconds.

Results and Discussion

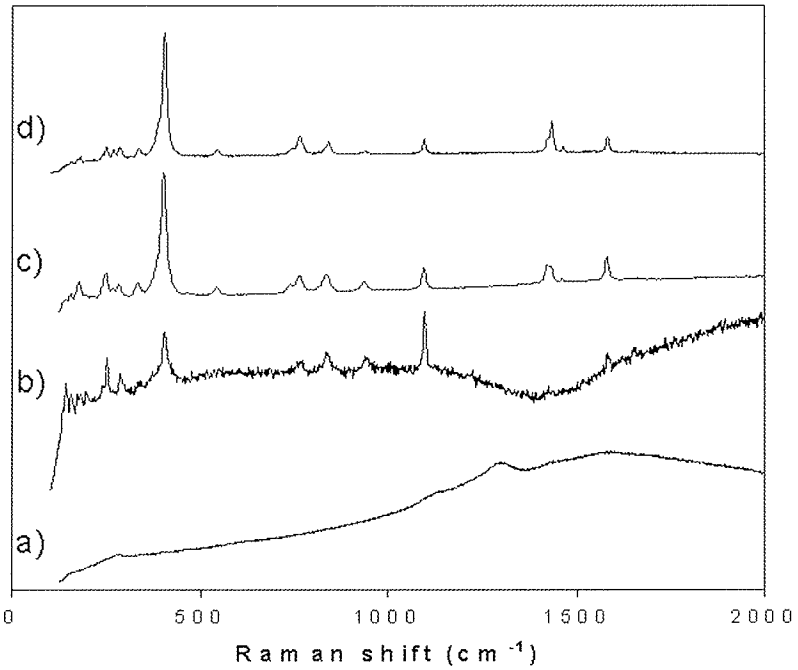

Figure 2: Raman spectra of azurite (dry powder) acquired using a) 785 nm, b) 632.8 nm, c) 514.5 nm and d) 488 nm excitation. Intensities are not to scale.

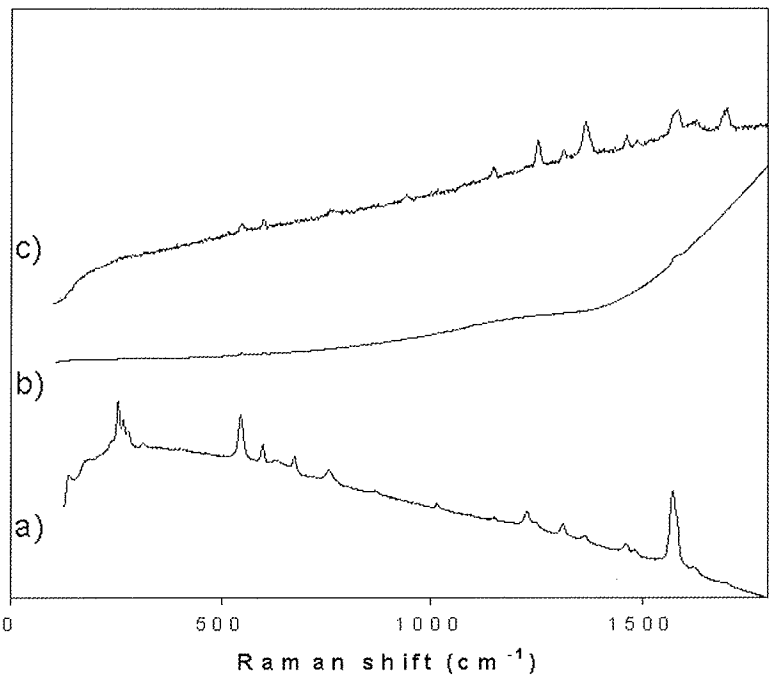

Figure 3: Raman spectra of indigo (dry powder) acquired using a) 785 nm, b) 632.8 nm and c) 488 nm excitation. Intensities are not to scale.

Effect of excitation wavelength: absorption
The Raman spectrum of each pigment, dry and in each of the five binding media, was examined as a function of excitation wavelength. In order to better illustrate the effects of each excitation wavelength, both instrumental and those inherent to the molecular systems involved, all spectra shown are raw, *i.e.* no baseline correction or other data manipulation has been performed.
The intensity of Raman scattering is proportional to $\bar{\nu}_0^4$, where $\bar{\nu}_0$ is the frequency of the excitation laser expressed in reciprocal centimeters ($\bar{\nu} = \nu/c = \lambda^{-1}$ where c is the speed of light, ν is the frequency and λ is the wavelength). Based on this principle alone Raman scattering is predicted to be significantly stronger for shorter wavelengths, but in practice, competition from fluorescence arising from the excitation of excited electronic states frequently overwhelms and negates the $\bar{\nu}_0^4$ advantage. This is particularly true for many (colorless) organic species, where the first excited electronic state lies in the ultraviolet. In such cases, longer excitation wavelengths (typically 785 nm or longer) that do not provide sufficient energy to excite electronic transitions that lead to fluorescence may successfully be employed.
Colored pigments have electronic absorption bands in some part of the visible region of the spectrum, and therefore the excitation wavelength should be selected to avoid absorption while maximizing the Raman signal. Illustrating this effect, the Raman spectra of red ochre, indigo, and azurite as a function of excitation wavelength are presented in Figures 1, 2 and 3, respectively. The Raman spectra from the sample of red ochre (specifically, the α-Fe_2O_3 component of the pigment) show a decreasing contribution from fluorescence with increasing excitation wavelength. This is

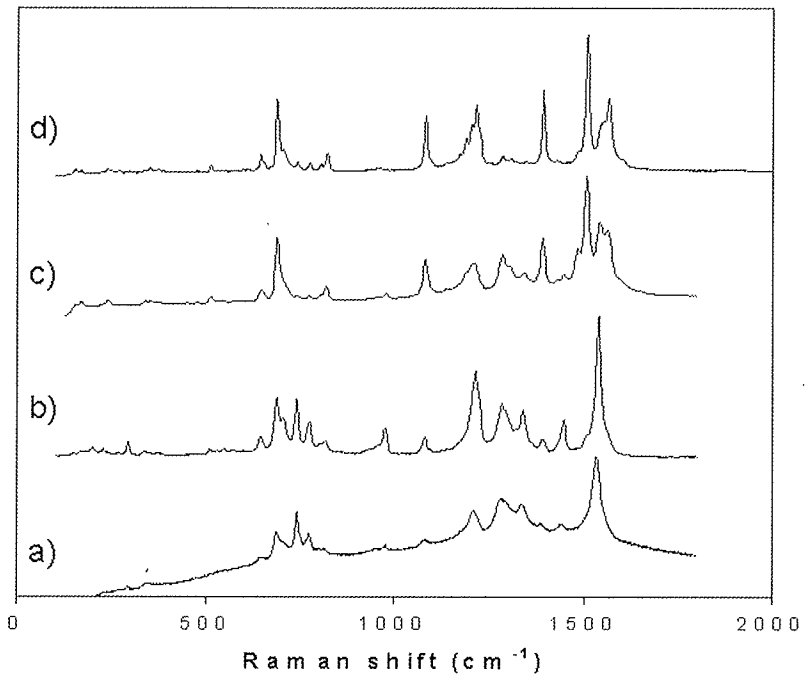

Figure 4: Raman spectra of phthalocyanine green (dry, powder) taken using a) 785 nm, b) 632.8 nm, c) 514.5 nm and d) 488 nm excitation. Intensities are not to scale.

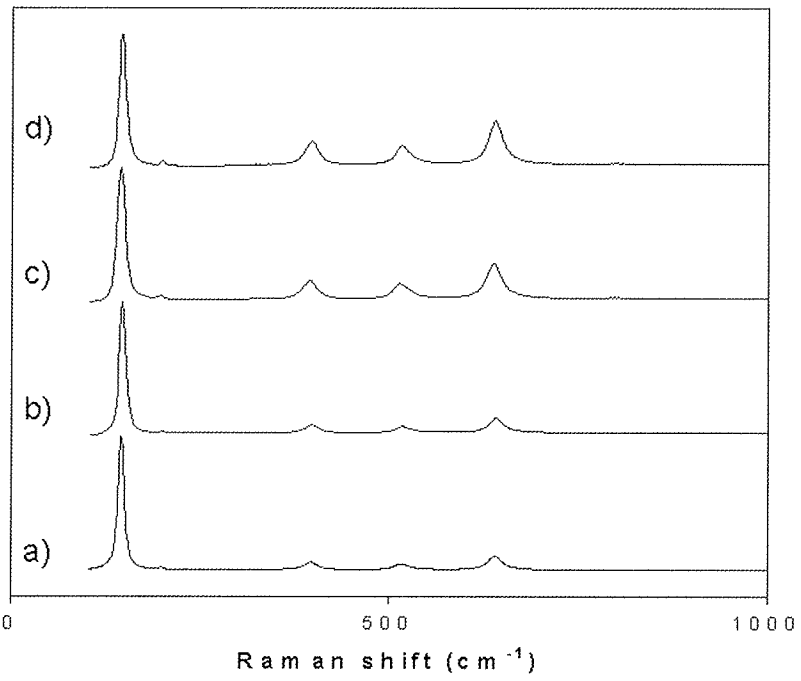

Figure 5: Raman spectra of anatase TiO_2 (dry, powder) acquired using a) 785 nm, b) 632.8 nm, c) 514.5 nm and d) 488 nm excitation. Intensities are not to scale.

consistent with a model in which the first excited electronic state lies in the blue region of the visible spectrum, excitation to which produces fluorescence. As the excitation wavelength increases, the Raman scattering virtual state shifts further in energy from the electronic excited state, resulting in decreased fluorescence.

In contrast, the blue pigment azurite absorbs in the red region of the visible spectrum [7], and indeed, the Raman spectra shown in Figure 2 demonstrate the opposite wavelength dependence to that observed for α-Fe_2O_3: the fluorescence contribution is greatest with longer wavelengths and decreases with decreasing excitation wavelength. In terms of the energy level model discussed above, the use of shorter wavelength excitation may scatter off a virtual state lying at a higher energy than the electronic absorption band, thereby avoiding fluorescence.

The Raman spectra obtained from indigo (Figure 3) illustrate the relationship between absorption and fluorescence particularly well. Indigo has an absorption maximum near 600 nm [8], and excitation with 632.8 nm radiation, near the absorption maximum, produced a strong fluorescence background. However, excitation with either 488 nm or 785 nm produced discernable Raman spectra. Although these spectra are not entirely free from fluorescence, indicating that some absorption is still occurring, it is important to note that by shifting the excitation wavelength away from the absorption maximum, either to higher or lower energies, the contribution from fluorescence could be sufficiently reduced to allow detection of the Raman signal.

Effect of excitation wavelength: resonance enhancement

Besides fluorescence, absorption can lead to the competing, and often beneficial, effect of resonance enhancement. Resonance enhancement can occur when the incident light approaches a coupled electronic-vibrational (vibronic) absorption of the sample molecule. Enhancement can also occur when the laser wavelength is near an absorption maximum, but is not yet within the absorption band: this condition is known as preresonant scattering [9]. An example of resonance enhancement can be seen in the spectra of α-Fe_2O_3 shown in Figure 1. The phonon overtone at 1320 cm^{-1} [10] is markedly stronger in the spectrum obtained using 514.5 nm excitation, suggesting the vibration is resonantly enhanced. Note that the relative intensities of the other bands do not change significantly with excitation wavelength, illustrating an

important aspect of resonance enhancement: enhancement occurs for vibrations associated with the chromophore being excited; vibrations in other parts of the molecule may not be enhanced, or may be enhanced at different wavelengths.
Resonance enhancement of multiple vibrations at different excitation wavelengths is illustrated in the Raman spectra obtained for phthalocyanine green, shown in Figure 4. In this case, some bands are enhanced with shorter excitation wavelengths (for example, the band near 1100 cm^{-1}), while others are enhanced at longer excitation wavelengths (such as the band near 1600 cm^{-1}). For the purposes of building an effective Raman library, consideration of resonance enhancement is of obvious importance: the relative band intensities in spectra acquired with different excitation wavelengths may be sufficiently different that a spectrum acquired at a single wavelength would be inadequate for identification purposes.

Effect of excitation wavelength: instrument response function
Variation in peak relative intensity as a function of excitation wavelength may also be the result of instrumental effects. For example, as shown in Figure 5, the intensity of the 144 cm^{-1} band in anatase (TiO_2) appears to decrease relative to the bands at higher shifts as the excitation wavelength decreases from 785 nm to 488 nm. Anatase has a sharp absorption edge near 400 nm [11], which is unlikely to produce preresonant enhancement even with 488 nm excitation, making it improbable that the bands at higher shifts are being resonantly enhanced. Therefore, the observed change in relative intensity must be attributable to some other factor, in this case a variation in the instrument response function.
In addition to molecule dependent parameters such as the Raman scattering cross-section, the Raman signal produced by an individual spectrometer is also dependent on instrument specific factors. The collection efficiency of a spectrometer depends on several factors including the efficiency of the detector and transmission function of the spectrometer (which includes the efficiency of the collection optics, grating, beam splitters cutoff filter and other optics)[9]. In the case of the spectra for anatase shown in Figure 5, the apparent reduction with decreasing wavelength in relative intensity of the band at 144 cm^{-1} is most likely a reflection of the reduced efficiency of the cutoff filter at shorter wavelengths, thereby resulting in an increased attenuation of the bands at very small Raman shifts.

Effect of binding medium
The effect of the binding medium on the Raman spectrum of a pigment varied considerably from pigment to pigment. In some cases, most notably Hansa Yellow, the binding medium had little or no apparent effect on the observed Raman spectrum. However, as expected, in many cases the presence of a binding medium introduced significant fluorescence that obscured the Raman signal. Nevertheless, with judicious choice of excitation wavelength, an identifiable Raman spectrum was obtained from every pigment/binding medium combination tested in this study.
The effects of absorption, resonance enhancement and instrument response discussed above are equally important in the spectra obtained with different binding media. For example, only fluorescence could be observed for red ochre mixed with linseed oil when excited with 488 nm radiation, but at 785 nm the spectrum of α-Fe_2O_3 was clearly visible together with bands attributable to linseed oil. Similarly, for ultramarine in egg yolk, shown in Figure 6, although the presence of the binding medium introduces a significant amount of fluorescence background, the major peaks associated with ultramarine are still clearly visible. Interestingly, resonance enhancement is also a factor here: egg yolk contains carotenoids, and the C-C stretching bands in the 1100-1200 cm^{-1} region and the C=C stretching bands in the 1500-1600 cm^{-1} region are strongly resonantly enhanced [12]. Moreover, the bands of ultramarine exhibited enhancement with shorter excitation wavelengths, undoubtedly contributing to the fact that both components of this mixture yielded strong, identifiable bands with 514.5 nm excitation.
Although in most cases the presence of a binding medium introduced either fluorescence or additional peaks from the medium, in the case of azurite, and to a lesser extent verdigris and indigo, the opposite was observed: the addition of a binding medium enhanced the Raman signal of the pigment. This somewhat unexpected result is illustrated in the spectra from obtained from azurite, presented in Figure 7. Note that for the dry pigment, as discussed above with respect to Figure 2, only fluorescence could be observed with 785 nm excitation whereas a strong Raman signal could be obtained using shorter excitation wavelengths. However, the opposite behavior was observed for azurite suspended in linseed oil: with 785 nm excitation the major peaks attributable to azurite are clearly visible while with 488 nm only fluorescence could be observed. This result is most likely explained by the combination of two factors: the wavelength dependence of the oil absorption bands and quenching of the azurite fluorescence.

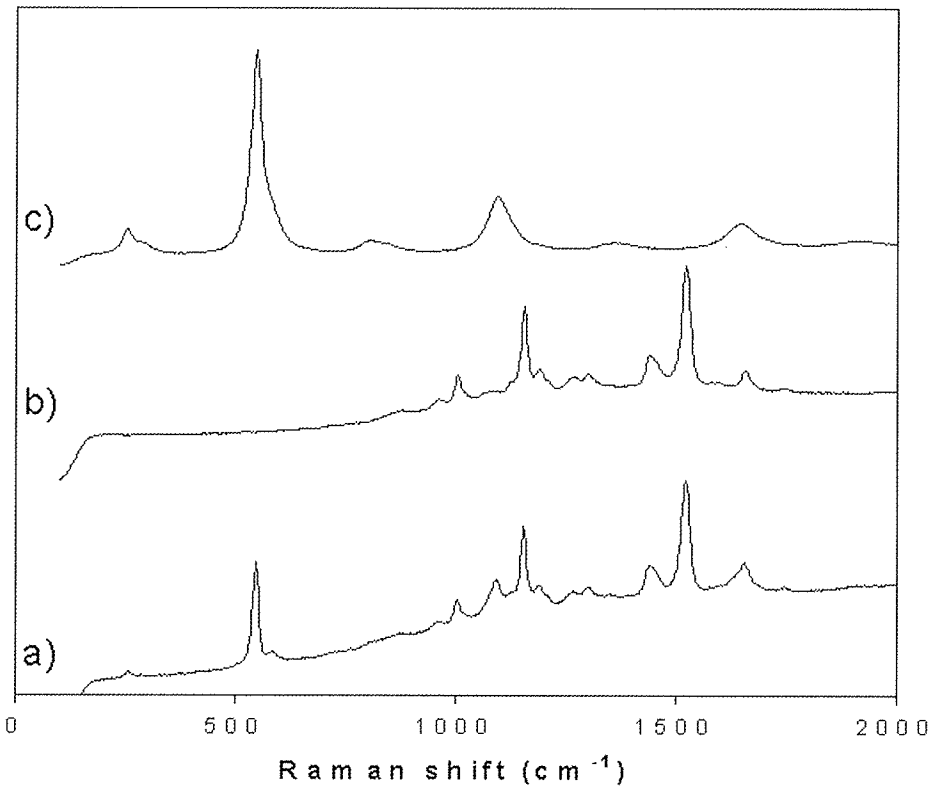

Figure 6: Raman spectra acquired using 514 nm excitation of a) ultramarine in egg yolk, b) egg yolk, and c) ultramarine (dry). Intensities are not to scale.

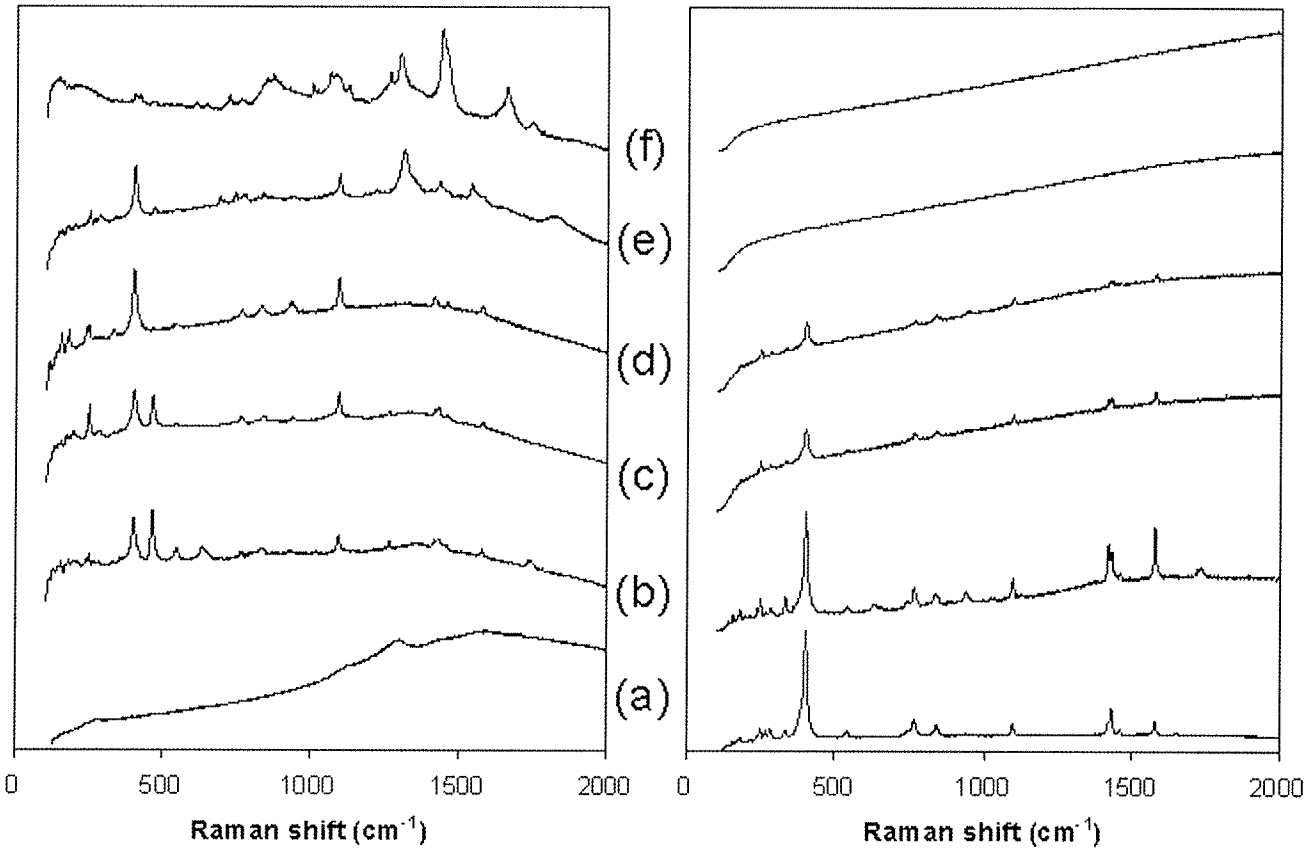

Figure 7: Raman spectra of azurite acquired using (left) 785 nm excitation and (right) 488 nm excitation in various binding media: a) dry, b) pva, c) gum arabic, d) collodion, e) linseed oil and f) egg yolk. Intensities are not to scale.

As discussed above, fluorescence may be avoided (or at least minimized) by employing an excitation wavelength as far away from the electronic absorption bands of the molecule as possible. In the case of linseed oil, excitation using 785 nm radiation was successfully used to observe bands attributable to the oil whereas shorter wavelengths produced only fluorescence. However, azurite absorbs in the red region of the visible spectrum, and consequently fluoresces strongly when excited with 785 nm radiation. Therefore, there must be a synergistic effect between the azurite and the oil medium to allow the Raman spectrum of azurite to be obtained using 785 nm excitation. The most likely explanation is that the oil serves to quench the fluorescence from the azurite through a non-radiative coupling mechanism, thereby allowing the weaker Raman scattering signal to be observed.

Summary/Conclusions

This study explored the effect of excitation wavelength on the Raman spectra of a selected group of artists' pigments. The range of pigment colors examined, including white, blue, green, yellow, orange and red, permitted the effect of absorption bands lying in the visible region of the spectrum to be evaluated. In general, longer wavelengths (632.8 nm and 785 nm) were found to be most useful for the study of red, orange and yellow pigments while shorter wavelengths (514.5 nm and 488 nm) were found to be more useful for the study of blue and green pigments. Another important factor was found to be the resonance Raman effect. Resonance enhancement can significantly increase the Raman scattering cross section, allowing the Raman signal to successfully compete with any contribution from fluorescence. Resonance enhancement of different vibrations can occur at different wavelengths, resulting in spectra that appear dissimilar when acquired with different excitation wavelengths. Therefore, it is particularly important that libraries include spectra collected at multiple excitation wavelengths for any material found to show wavelength dependent relative intensity variation.

The effect of a binding medium on the spectrum of the various pigments ranged from no effect, to the creation of fluorescence which overwhelms the signal from the pigment, to the introduction of additional peaks from the binding medium. In most cases, the binding medium/pigment mixtures showed similar wavelength dependence to the dry pigments, but in a few cases, most notably the blue pigment azurite, the presence of binding medium served to enhance the Raman signal from the pigment. We speculate that the binding medium may quench fluorescence originating from the pigment, thus allowing the Raman signal to be detected.

It is significant to note that by appropriate selection of excitation wavelength, a discernable Raman spectrum could be obtained for each pigment/binding media combination examined in this study. However, a user examining an unknown may not have access to multiple excitation wavelengths, and therefore a library of Raman spectra of pigments ideally should include spectra acquired at multiple wavelengths and in as many different media environments as possible.

Acknowledgements

The authors gratefully acknowledge Renishaw, Inc. for the loan of a Renishaw 1000 Raman microscope equipped with 514.5 and 785 nm excitation sources; Ann O'Neill, Dairene Uy and Willes H. Weber of Ford Motor Company Scientific Research Laboratories for the use of Renishaw 1000 Raman microscopes equipped with 488 and 632.8 nm excitation sources. Financial support for C.H. during her third-year internship was provided by the Andrew W. Mellon Foundation.

References

1. Burgio. L. and Clark, R.H.J., 'Library of FT-Raman spectra of pigments, minerals, pigment media and varnishes, and supplement to library of Raman spectra of pigments with visible excitation, *Spectrochimica Acta* A57 (2001) 1491-1521

2. Bell, I.M., Clark, R.J.H., and Gibbs, P.J., 'Raman spectroscopic library of natural and synthetic pigments (pre-~1850 AD).', *Spectrochimica Acta Part A* **53** (1997) 2159-2179.

3. Guineau, B., 'Non-destructive analysis of organic pigments and dyes using Raman microprobe, microfluorometer or absorption microspectrophotometer.', *Studies in Conservation* **34** (1989) 38-44.

4. Colomban, P., Sagon, G., and Faurel, X., 'Differentiation of antique ceramics from the Raman spectra of their coloured glazes and paintings', *Journal of Raman Spectroscopy* **32** (2001) 351-360.

5. Vandenabeele, P., Moens, L., Edwards, H.G.M., and Dams, R., 'Raman spectroscopic database of azo pigments and application to modern art studies.', *J. Raman Spectrosc.* (2000) 509-517.

6. Coupry, C., 'Application of Raman microspectrometry to art objects', *Analusis* **28** (2000) 39-46.

7. Gettens, R.J. and Fitzhugh, E.W., 'Azurite and Blue Verditer' in A. Roy, *Artists' Pigments: A Handbook of Their History and Characteristics,* Oxford University Press, Oxford (1993) 23-36.

8. Schweppe, H., 'Indigo and Woad' in E.W. FitzHugh, *Artists' Pigments" A Handbook of Their History and Characteristics,* Oxford University Press, Oxford (1997) 81-108.

9. McCreery, R.L., *Raman Spectroscopy for Chemical Analysis,* John Wiley & Sons, Inc., New York (2000) .

10. Massey, M.J., Baier, U., Merlin, R., and Weber, W.H., 'Effects of pressure and isotopic substitution on the Raman spectrum of α-Fe_2O_3: Identification of two-magnon scattering.', *Physical Review B* **41** (1990) 7822-7827.

11. Laver, M., 'Titanium Dioxide Whites' in E.W. FitzHugh, *Artists' Pigments: A Handbook of Their History and Characteristics,* Oxford University Press, New York (1997) 295-355.

12. Withnall, R., Chowdhry, B.Z., Silver, J., Edwards, H.G.M., and de Oliveira, L.F.C., 'Raman spectra of carotenoids in natural products', *Spectrochimica Acta Part A* **59** (2003) 2207-2212.

Global Raman Imaginig on Ceramics

Angela Zoppi, Cristiana Lofrumento, Emilio Mario Castellucci
Lens and Dipartimento di Chimica, Polo Scientifico di Sesto Fiorentino, Università di Firenze, 50019 Sesto Fiorentino, Firenze, (I)

Abstract

The application of the global Raman imaging technique for the compositional characterisation of archaeological pottery samples is presented here and discussed. Imaging measurements were performed on raw ceramic fragments as well as on polished cross-sections. While global images of quartz and rutile grains were recorded inside the ceramic body of the fragments, filtering the main Raman bands at 465 and 435 cm^{-1}, the roughness of the surface hindered good quality images of the hematite distribution in the slip layer. Due to the smoothed surface of the cross-sections, the method appeared to be more sensitive and images could be acquired even on wide areas. The flatness of sample surfaces appeared thus to be of crucial importance for good quality images and advisable for a compositional mapping measurement.

Introduction

Compared to micro-Raman spectroscopy, global Raman imaging enables measurement over a wider sample area. This is accomplished by moving a beam-expander which, acting as a glass, defocuses the laser beam onto the sample: the irradiated sample area diameter ranges from a few microns to even a few tens of microns, according to the beam expander position and to the magnification objective used to illuminate the sample. Moreover, the Raman light, instead of being dispersed by a grating, is filtered by means of optical band-pass filters. The transmitted Raman light intensity, captured by the CCD detector, is then reported as a bidimensional image over the irradiated sample area. The global image thus obtained reveals the illuminated sample area parts emanating the suitable wavenumber Raman light to be transmitted by the selected filter.
We began testing Raman imaging on pottery fragments of *Terra Sigillata* French wares. The samples had already been analysed by punctual micro-Raman spectroscopy revealing a highly compacted slip layer made mostly of hematite, while feldspars, quartz and rutile were mainly identified in the inner body [1]. Raman imaging was applied to have a better investigation of mineralogical components' relative distribution.
However, the wrinkled face of the fragments hindered a completely homogeneous illumination of the sample surface; this was particularly evident with high defocusing values. Yet this phenomenon was interfered less when keeping a low beam-expansion value, especially for small grain illumination.
In order to check the surface roughness effect, some measurements were taken on smoothed samples as well. These are polished cross-sections of Syrian pottery waster samples. The results are presented and discussed in the below section.

Experimental section

The technique
The global imaging experiments were performed using a micro-Raman Renishaw RM2000 apparatus.
The imaging optical path is defined by an angle-tuned bandpass filters motorised wheel used to filter the selected Raman band; the transmitted light is then directly sent onto the CCD detector, bypassing the lens-slit-grating optical elements used for spectrograph experiments.
The defocusing of the laser beam is accomplished by a "beam-expander", which is a glass made of a fixed 40x and a movable 4x objectives separated by a 10 microns pin-hole. The more the 4x objective is moved away from its focus, the wider the irradiated sample area. Typical laser-spot diameters, measured under the 50x microscope objective, are 20 μm (50% defocusing value) and 40 μm (100% defocusing value).
The Raman light, filtered by the Notch filter and transmitted by the band-pass filters, is sent onto the CCD target giving rise to an almost circular spot whose dimensions depend upon the defocusing value. The intensity measured by each pixel is then read individually and plotted as a bidimensional image. By selecting a proper CCD area the obtained image represents the intensity distribution along the irradiated sample area of the filtered light.
Since grating and filter lightpaths are separate, the spectral position of the band to be imaged should be verified before, and this is done recording a filter spectrum. The bandpass of each filter used in a filter spectrum is

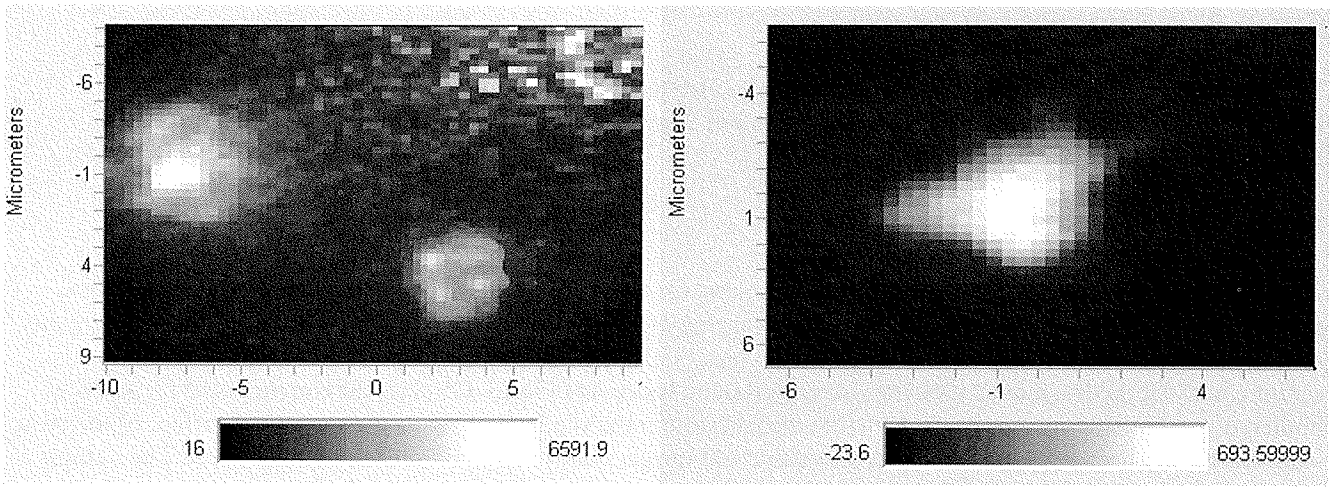

Figure 1: Global images recorded while filtering the 435 cm^{-1} Raman band of rutile (50x obj., 50% defocusing value). The profile of rutile grains is clearly reproduced.

approximately 10 to 20 cm^{-1}, leading to a resolving power much lower than the one of a grating spectrum (4-5 cm^{-1}). Imaging measurements were performed using the Argon laser source (515 nm). For sample illumination the 50x and 20x microscope objectives were used. Global images were recorded under 50% and 100% defocusing values and the CCD area was selected as a rectangle tangent to the light spot. Exposing times varied from 30 s to 300 s. To compensate for non uniformity of the defocused laser beam and pixels response, the recorded image files were divided by a proper flatfield file. The flatfield was taken on a silicium wafer sample under the same experimental conditions (microscope objective, defocusing value, CCD area) as the former ones.

Samples

Terra Sigillata raw samples analyses were accomplished on small fragments dated back to the end of the first century AD and belonging to the La Graufesenque French site. They are characterised by a very fine slip, red or brown, with a rather waxy shine, that is typical of classic fine type wares of the early Roman period. Global images of the main mineralogical phases (rutile, quartz, hematite, etc.) were taken on both the inner body and the external slip.
Due to interference from the rough surface, the method was subsequently tested on smoothed samples.
Measurements were carried out on polished cross-sections of waster samples of a Syrian production in Tell Beydar, dated back to the III millennium BC. Also these samples had already been characterised by micro Raman spectroscopy [2].

Results

Global images of rutile and quartz were recorded on the inner body of *Sigillata* raw samples.
Figure 1 reports the results obtained filtering the rutile Raman band at 435 cm^{-1} over an area of approximately 20x20 μm at two different points. The intensity distribution of the rutile band reveals the presence of high intensity spots (less than 4 μm wide), corresponding respectively to two yellowish grains (left image) and a single white rutile grain (right image) inside the examined sample areas.
Also global images of quartz were recorded filtering the 465 cm^{-1} Raman band. The presence inside the ceramic body of variously shaped and sized quartz grains was thus revealed. Once again the shape of single grains was well reproduced by the relative images files.
Afterwards, measurements were carried out on the red slip of the *Sigillata* samples to test global imaging method on a uniform compositional area. Since the slip contains mainly hematite, its distribution was checked by recording filter images of the main Raman band at 285 cm^{-1}. However in this case results disagreed with the expected ones, probably because of the sample surface roughness, since almost black images were obtained, as the reported one in figure 2.
As a final test, global imaging technique was applied on a polished cross-section of a waster Syrian ceramic. There, the effect of surface roughness was minimized and wider areas could be investigated without loosing sensitivity.
Figure 3 reports the image of the 710 cm^{-1} intensity distribution taken with the 20x objective and 100% defocusing, collecting light from a rather wide area. The shape of a chromite grain was correctly reproduced.

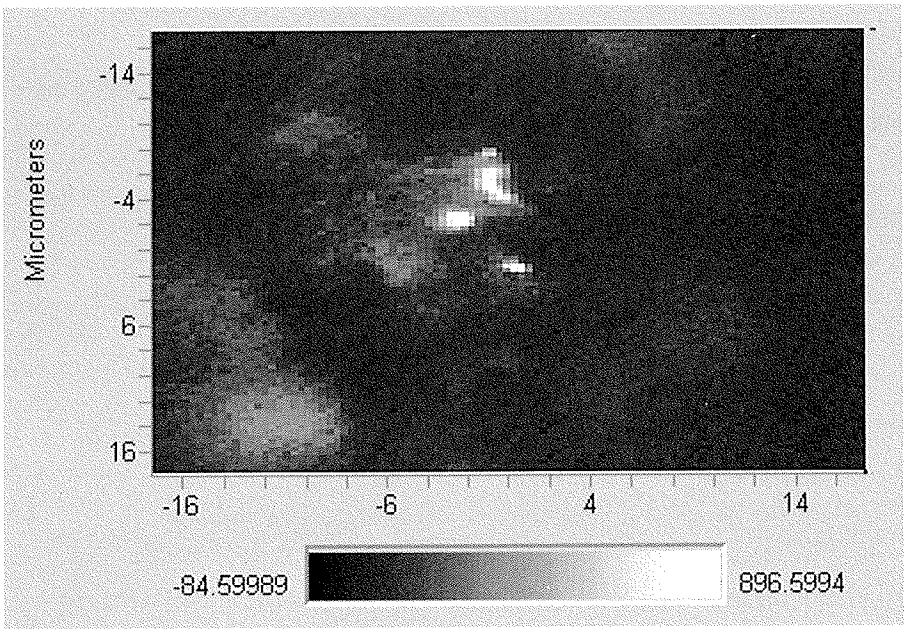

Figure 2: Global image recorded while filtering the 285 cm^{-1} Raman band of hematite (50x obj., 50% defocusing value) on the red slip of a *Terra Sigillata* fragment.

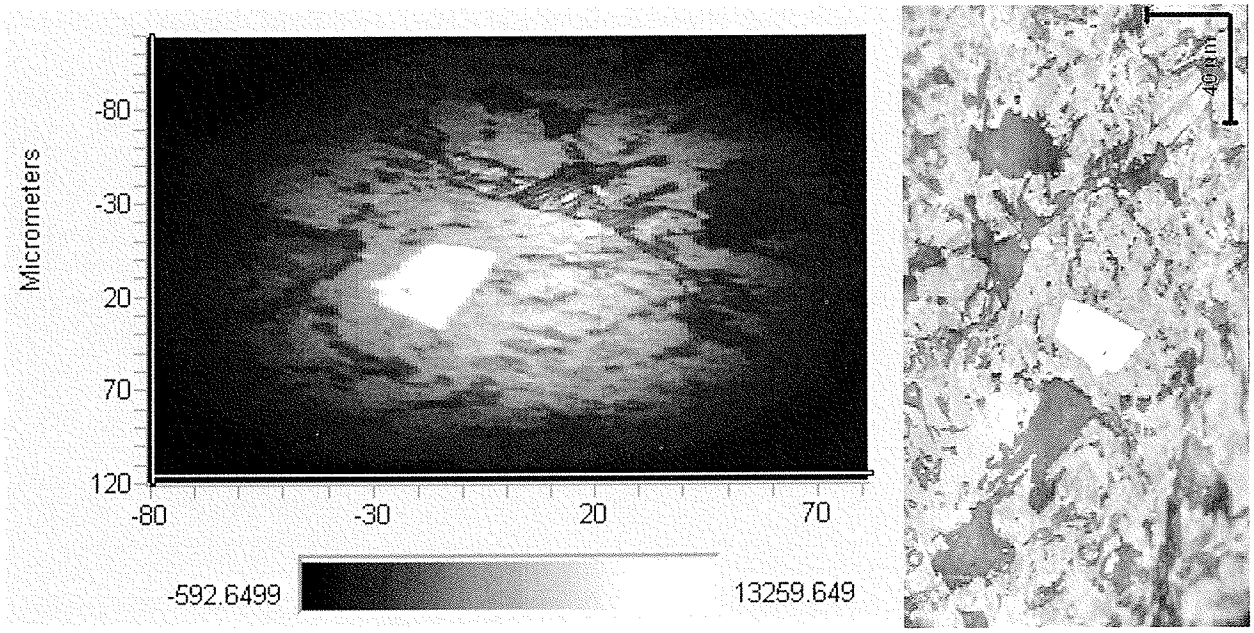

Figure 3: Global image (left) recorded while filtering the 710 cm^{-1} Raman band of chromite (20x obj., 100% defocusing value) taken on a Syrian waster cross-section (right).

Conclusion

Surface roughness of the *Sigillata* raw fragments did not hinder the acquisition of good quality global images of quartz and rutile components, detected even as very small grains inside the ceramic body.
However, the rough surface did interfere with the hematite distribution checked inside the slip layer. We think that careful attention should be paid to even weaker band images (as for feldspars) for correct interpretation, especially when wide areas are investigated, and it would be worthy to work with polished sections as smoothed surfaces.
Once the surface roughness question is solved, we think the global imaging technique could be fit for mapping the spatial distribution of mineralogical components in a ceramic material, providing a novel way for the study of the ceramic composition and hopefully for a quantitative analysis.

References

1. Lofrumento C., Zoppi A., Castellucci E. M., 'Micro-Raman spectroscopy on ancient ceramics: a study on French Sigillata wares', *Journal of Raman Spectroscopy*, **35** (2004) 650-655.

2. Zoppi A., Lofrumento C., Castellucci E. M., Migliorini M. G., 'Micro-Raman technique for phase analysis on archaeological ceramics', *Spectroscopy Europe*, (2002) **14** (5) 16-21.

Sub-nanogram Level Identification of Alizarin by Surface Enhanced Raman Scattering

Marco Leona
Department of Scientific Research, the Metropolitan Museum of Art, 1000 Fifth Avenue, New york, NY 10028

Abstract

A new method is presented to identify alizarin, the main component of madder lakes, in works of art. After a combined extraction/aggregation procedure with NaOH in a silver colloid, a microscopic sample of paint is examined by Surface Enhanced Raman Spectroscopy. Absorption of alizarin on the surface of colloidal silver particles quenches the fluorescence that hinders observation of the ordinary Raman spectrum of alizarin, and allows detection of alizarin at sub-nanogram levels. The method is effective on synthetic alizarin, on madder root extracts and on alizarin and madder lakes. The SERS spectra of alizarin show strong pH dependence, suggesting that the geometry of adsorption is different for different stages of dissociation of the alizarin molecule.

Introducition

Raman spectroscopy, initially applied to the study of materials found in works of art in the 1980s [1, 2], has now become an established technique in archaeometry, conservation science and material art history (for a complete review, see [3]). The technique lends itself both to in situ analysis and microscopic (microsampling) applications, and it is an ideal complement to techniques such as Fourier Transform Infrared Microspectroscopy (FTIR), Scanning Electron Microscopy (SEM-EDS) and X-ray Diffractometry (XRD). While the contribution of Raman spectroscopy to the study of artists' materials and techniques is undeniable, a survey of published studies ([3] and references therein) would show a definite bias towards inorganic pigments, gemstones, and minerals (and most inorganic pigments and all gemstones, at least in antiquity are of course, minerals). Organic colorants, dyes, and binding media and varnishes represent a minority among the subjects studied by Raman spectroscopy. These materials are generally poor Raman scatterers, strong fluorescers, or both. Near Infrared Fourier Transform Raman Spectroscopy (NIR-FTR) does provide an alternative to dispersive Raman [3], but with all of the problems connected to the switch to NIR excitation, such as decrease in scattered intensity due to the ν^4 dependency, pronounced heating of darkly colored samples, and limited suitability to microscopic applications.

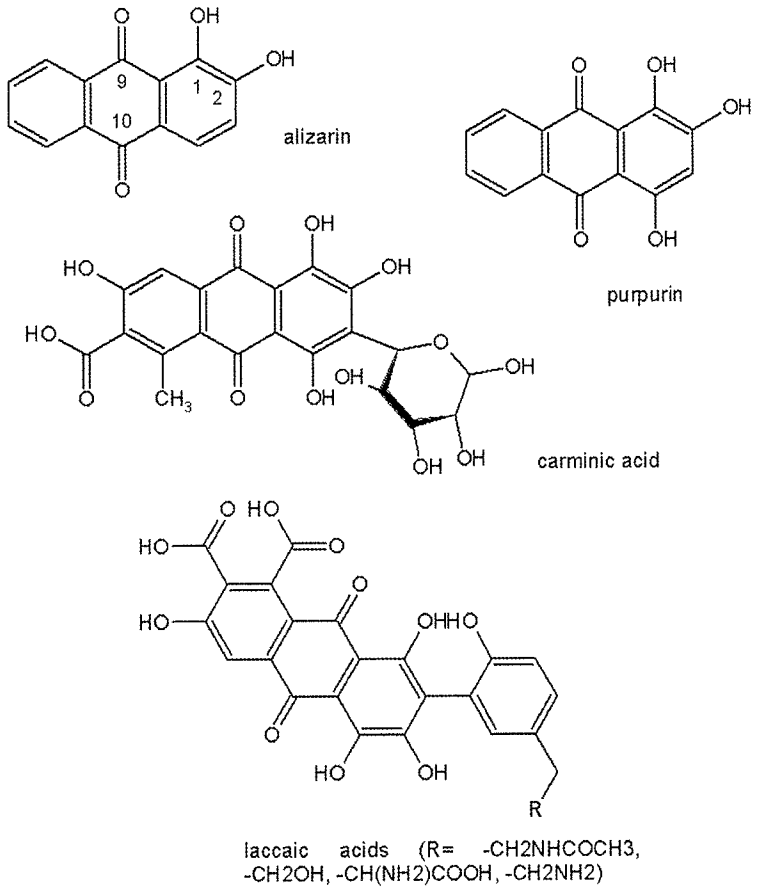

Figure 1: Natural anthraquinone dyes: alizarin; purpurin; carminic acid; laccaic acids

The case of dyes and organic pigments is particularly interesting. Organic colorants are, by definition and by economic necessity, molecules with high extinction coefficients in the visible radiation range: in other words, substances with high tinting power, or the ability to provide intense coloration even when used in small quantities.
This makes the task of identifying organic colorants extremely difficult: in some cases, UV-visible reflectance techniques can lead to positive identification (for instance in the case of indigo used as a pigment or in Maya blue [4, 5]) or at least some level of discrimination (as is the case for the natural anthraquinone

dyes [6]) without the need to take a sample. In the majority of cases though, UV-Visible reflectance spectra do not show the degree of detail necessary for fingerprinting unknown materials, and samples have to be obtained and processed for analysis by techniques with greater discriminatory power, such as High Performance Liquid Chromatography [7].
FTIR techniques suffer from interference from supports, binding media and extenders; dispersive Raman spectroscopy has been successful in only a few cases [3].
The case of the anthraquinone dyes (figure 1) is a good example of important natural products that are extremely difficult if not impossible to analyze by dispersive Raman spectroscopy.
Madder, cochineal and lac dye [8,9] are important dyestuffs either found as mordant dyes on textiles, or complexed with aluminum and calcium as lake pigments in European paintings and oriental works of art. The FT-Raman spectra of madder lake and cochineal carmine have been published [10], and while the conventional Raman spectrum of uncomplexed purpurin has been obtained with 632.8 nm excitation [11], the same publication lists alizarin amongst the pigment for which no spectrum can be obtained at either 514 or 632.8 nm. A spectrum of alizarin obtained in a dispersive Raman system at 785 nm excitation will be presented later in this study.
While ordinary Raman spectroscopy does not appear *per se* to be an ideal technique for the identification of anthraquinone dyes, and FT-Raman does not have the sensitivity or the selectivity of HPLC, the Raman effect can, in particular conditions, be used to detect anthraquinones at sub-micromolar concentrations.
The discovery of Surface Enhanced Raman Scattering (SERS) in the mid 1970s [12, 13, 14] and more important, the demonstration of single molecule Raman Spectroscopy in the late 1990s [15, 16] open the possibility for Raman spectroscopy to be used as an extremely sensitive tool for the identification of organic molecules. SERS is a complex effect observed when organic molecules are adsorbed on atomically rough metal surfaces: a complete description is beyond the scope of this article, but an excellent review is by Campion and Kambhampati [17]. In short, when studying by Raman spectroscopy organic molecules adsorbed on atomically rough metal surfaces, the incident (laser) and scattered (Raman) electromagnetic fields are intensified by resonance with the metal plasmon (the surface electrons standing wave). Additionally, interactions between the energy levels of the metal and of the molecule can lead to resonance conditions or quench any fluorescence through ultrafast electron transfer from the molecule excited states to the metal [18].
The observation of single molecule Raman spectra from species that are known to be fluorescent implies that SERS produces an enhancement of the Raman effect of up to 14 orders of magnitude. This enhancement has tremendous implications towards ultra-sensitive detection of natural dyes in works of art: the technique is extremely promising for analyzing microscopic samples of lake pigments and dyed fibers. While SERS is in theory possible with any nanosized metal support, in practice, plasmon resonance limits the metals which support SERS to those which show plasmon resonance at the wavelength commonly used for Raman excitation: these are most commonly Au, Ag and Cu. In the course of this study, after brief experimentation with Au and Cu, Ag was elected as the most effective support. The nanoscale roughness condition was satisfied by using solution-reduced colloids, a very common SERS support.
A problem to be expected in the SERS study of anthraquinone dyes on metal colloids is the difficulty of obtaining efficient adsorption of hydroxy-anthraquinones (such as alizarin, carminic acid, etc.) on the Ag surface. Colloidal particles prepared by reduction from solution, usually with sodium citrate as a reducing agent, are in fact surrounded by a layer of negatively charged citrate ions. Stable adsorption to this layer is difficult for acidic molecules like the hydroxyl-anthraquinones. Conditions in which adsorption was indeed realized and SERS spectra observed will be described herewith.
The results obtained for alizarin, the simplest natural anthraquinone dye, one of the main constituents of madder (*rubia tinctorum*), show that SERS is indeed applicable to the study of artists' materials and that it is superior in sensitivity to established techniques such as HPLC and LC-MS (a note presenting an early application of SERS to the study of alizarin was recently found [19]: the present study demonstrates a different experimental setup, with improved sample handling characteristics and sensitivity. Additionally, an article recently submitted to the spectroscopic literature, and dealing with the same topic presented here was just brought to the author's attention, in advance of print [20])

Experimental

Materials, colloid preparation and sample treatment
Synthetic alizarin was obtained from Aldrich (1,2-dihydroxyanthraquinone 122777 dye content 97%) and purified by recrystallization from absolute alcohol; madder root from Kremer Pigments; Rose Madder watercolor paint from

Grumbacher (alumina lake of synthetic alizarin in gum arabic medium). Madder root extracts were prepared from madder root pieces by simple ethanolic extraction at room temperature. Historical samples of genuine madder lake were obtained form the Forbes collection at the Los Angeles County Museum of Art (Hatfield Genuine Madder). Ag colloid was prepared following the method of Lee and Meisel [21] by reduction of silver nitrate (Aldrich 209139 Silver Nitrate 99.9%) with sodium citrate (Aldrich W302600 Sodium Citrate Dihydrate): all solutions were prepared with 18MΩ water. In some cases, poly-L-lysine (Aldrich p4707 poly-L-lysine solution 0.01%) was used to facilitate adsorption of alizarin on the Ag colloid [22]. Due to the extreme sensitivity of the method, and the possible influence of trace impurities on the synthesis of the Ag sol, all glassware was thoroughly cleaned by washing with mild detergent, immersion in aqua regia or piranha mixture (H_2SO_4/H_2O_2 3:1 v/v), and rinsing in 18MΩ water.
Lake pigments were hydrolyzed by treatment with a solution of NaOH in 18MΩ water (pH12). The method was designed for use on microscopic samples: a fragment of approximately 0.1 to 0.5 mm was deposited on a gold mirror slide, treated with 1 µl of the NaOH solution and the drop heated to dryness on a hot plate. Ag sol was then added to the dry residue and the spectra recorded immediately.

Raman Spectroscopy

Raman spectra were recorded with a Chromex Senturion Raman Microscope equipped with a 70 mW 785 nm laser diode. Spectra were recorded between 400 and 1800 cm^{-1} using a 1200 rulings/mm holographic grating. Spectral calibration was achieved using the proprietary system Sure_Cal [23]. The ordinary Raman (OR) spectrum of alizarin was recorded both conventionally and employing a new technique for the rejection of fluorescence. The technique is based on the acquisition of Raman spectra at two slightly different excitation wavelengths (wavelength difference is typically between 0.3 and 0.7 nm), their subtraction and the subsequent integration of the resulting spectra (Shifted Excitation Raman Difference Spectroscopy or SERDS). The method has been described in detail elsewhere [24]. The samples were analyzed in the instrument's large sample chamber using long-working distance infinity corrected microscope objectives (Olympus LMPlan 20x and Olympus LMPlan IR 100x). SERS spectra were obtained directly from drops of Ag sol – dye solution mixtures deposited on a gold mirror slide, by focusing on the bottom of the drop. Integration times varied between 5s and 10s, power to the sample varied between 25% and 100% of the total available power.

Results

Raman spectra of synthetic alizarin were easily obtained by re-crystallizing it from water on a gold mirror and focusing on one of the microcrystals thus obtained. Contact with the polished metal surface assists in reducing the fluorescence generally observed when examining alizarin by Raman spectroscopy (possibly by increasing the efficiency of Raman excitation by optical containment, or by providing a non-radiative pathway for excited states decay). The spectral quality was further improved by recording spectra in SERDS mode. It was also found that a Raman spectrum can be obtained from the bulk material, but the quality of the data is inferior. The spectrum obtained from a micro-crystal on a gold mirror (figure 2) is quite different in relative intensities ratios from that obtained by FT-Raman [10], but this is probably due to the intrinsic differences between the two instrumental setups, rather than to any surface enhancement. Peak positions are in good accord with FT-Raman data and with the FTIR spectrum (not shown here).

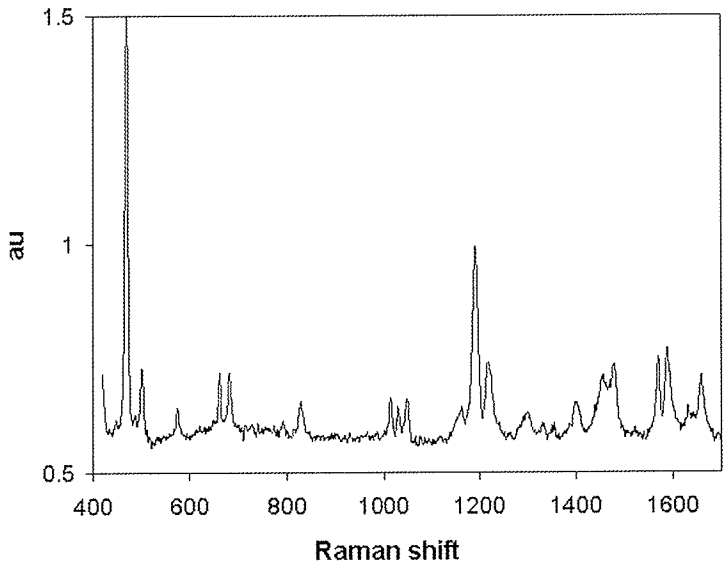

Figure 2: Ordinary Raman spectrum of alizarin

While extraction of dye from a lake sample or a textile and re-crystallization is a possible method of analysis, and sensitivity is only limited by the ability to locate a microcrystal and focus the laser beam onto it, sample size and handling issues make identification of alizarin by ordinary Raman rather impractical. Identification of the

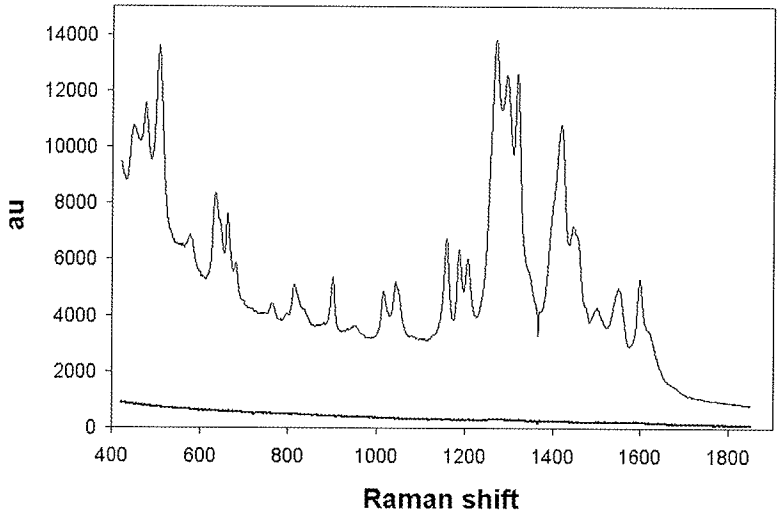

Figure 3: SERS spectrum of alizarin with poly-L-lysine (the lower line is the spectrum of an Ag and NaOH blank)

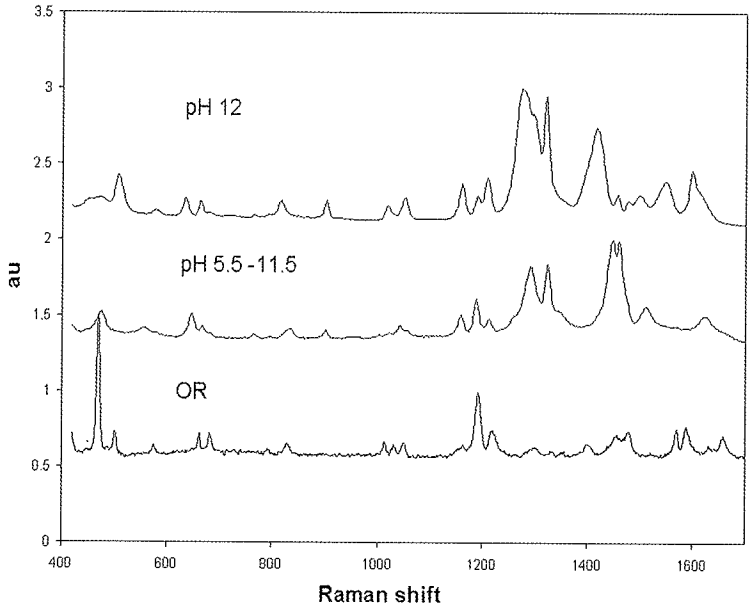

Figure 4: Ordinary Raman (OR) spectrum of alizarin and SERS spectra of mono and bi-dissociated alizarin

dye directly from a solution treated with Ag sol simplifies handling and results in higher sensitivity.

Colloid preparation according to Lee and Meisel [21] yielded a gray poly-disperse Ag sol. Mixing a saturated solution of synthetic alizarin in water at 20 °C with the Ag sol did not produce aggregation nor result in enhanced spectra, as opposed to what observed in a test performed with Rhodamine 6G, a dye known to adsorb very efficiently on Ag nanoparticles. Use of aggregants such as sodium chloride, potassium nitrate or nitric acid did not produce any enhancement.

Addition of poly-L-lysine to the alizarin-sol mixture resulted in immediate aggregation of the colloid and strong enhancement of the Raman signal. The comparison between the spectra of the Ag sol – alizarin solution mixture before and after addition of poly-L-lysine is particularly effective in demonstrating the entity of the surface enhancement (figure 3). A conservative estimate of the sensitivity of the technique would show that picogram detection limits are well within reach. The data in figure 3 (more than 10,000 counts/second) were obtained from a one microliter drop of a room temperature saturated solution of synthetic alizarin. Using published figures for the solubility of alizarin in water [25], the total quantity of alizarin present in the drop is in the order of 4-500 picogram. Given the high intensity of the spectrum and the fact that the total volume probed with the 20x microscope objective used is actually smaller than one microliter, the detection limit of the technique can safely be estimated to be in the tens of picogram range.

On raising the pH to above 12, it was noticed that SERS spectra could be obtained without the addition of poly-L-lysine: this is probably due to the fact that at these pH values alizarin can replace the citrate layer and adsorb directly to Ag.

Successive experiments at different pH ranges (addition of HNO_3 or NaOH to obtain pH < 3; pH 5.5-11.5; and pH > 12) revealed a strong dependence of the effect and of the spectral features on the dissociation state of the molecule (figure 4).

Alizarin behaves as a diprotic acid with dissociation constants pK1 and pK2 of approximately 6.6 and 12.4, respectively [26]. The first dissociation constant refers to the deprotonation of the hydroxyl in position 2 and the second to the deprotonation of the hydroxyl in position 1. No spectrum was obtained at pH values below 5.5 (undissociated alizarin). Enhanced spectra were obtained between pH 5.5 and 11.5 after adding poly-L-lysine; the spectral features did not vary on raising the pH from 5.5 to 11.5 (monodissociated alizarin). Enhanced spectra were obtained without poly-L-lysine at pH values of 12 and above (bidissociated alizarin).

Alizarin easily forms chelates with Al and Ca ions: its use as a mordant dye or as a lake pigment depend indeed on the formation of complexes with metal cations [27]. It is to be expected that the geometry of the alizarin-Ag

adsorbate be sensitive to the dissociation stage of the molecule, with the possibility of chelates through O9, O1 or O2.
The ordinary Raman spectrum of alizarin (figure 2 and table 1) can be interpreted by comparison with the vibrational spectra of 9,10-anthraquinone [28] and 1-hydroxy, 9,10-anthraquinone [29].

Alizarin OR		SERS pH 6-11		SERS pH 12		Attribution
1659	m	1666	sh	1620	sh	Stretch C10=O
1632	w	1623	m	1600	s	Stretch C9=O
1589	m	1588	sh			Ring stretch
1570	m	1568	sh	1551	s	Ring stretch
		1511	m		m	phenolate
				1501	w	unassigned
1478	m	1473	sh	1478	m	Ring stretch + OH
1455	m	1460	s	1458	m	Ring stretch
		1448	s			Ring stretch
		1416	sh	1418	vs	phenolate
1401	m			1399	sh	unassigned
1356	w	1349	sh			C1-O stretch
1330	w	1324	s	1321	s	Ring stretch
1304	w	1293	s	1296	s	Ring stretch
1261	w	1259	sh	1275	s	C2-O stretch
1217	m	1213	m	1210	s	Ring stretch (C1...C9)
1191	s	1188	s	1189	m	Ring stretch
1164	w	1160	m	1160	s	Ring stretch
1049	m	1056	w	1052	m	CH in plane bending
1031	w	1041	m			skeletal
1013	m	1021	w	1020	m	
		1001	w			
		902	w	903		
828	m	833	m	816		
		797	w			
		766	w	767	w	
		724	w			
682	m	668	m	664		
662	m	648	m	636		
575	w	578	w	581	w	
		557	w			
501	m			508		
488	w					
470	vs	476	s	476	br	
448	w			450	br	

Table 1: Raman spectrum of alizarin (OR: ordinary Raman; SERS pH 6-11: SERS spectrum of monodissociated alizarin; SERS pH12: SERS spectrum of bidissociated alizarin)

As can be expected, in absence of chemisorption and surface enhancement, C=O vibrations do not show as intense bands in the Raman spectrum. The stretching vibration of C10=O is at the same frequency as in anthraquinone, while the frequency of the C9=O stretch is lowered as a result of the partial single bond character due to resonance (which raises the bond order of C1-O and lowers that of C9=O [29]). The C1-O and C2-O stretches can be tentatively assigned to very weak bands observed at 1356 cm^{-1} (C1-O) and 1261 cm^{-1} (C2-O): this compares with the value observed in phenol (1249 cm^{-1}) if one allows for the partial lowering increase in bond order for C1-O [28]. The most intense vibrations, at 1191 cm^{-1} and at 470 cm^{-1}, are a ring stretch and a skeletal vibration, respectively.
In the case of the spectrum observed in the pH range 5.5-11.5, besides an overall increase in signal-to-noise ration, a preferential enhancement of several vibrations was noticed. The bands between 1260-1350 cm^{-1} and 1440-1520 cm^{-1} are intensely affected by poly-L-lysine mediated adsorption on Ag nanoparticles. These bands correspond to ring

stretch vibrations and ring stretches coupled with C-O stretches. Identical enhancements were noticed in a study of the adsorption of alizarin on TiO_2 colloids (where chemisorption and ultrafast electron transfer from the alizarin excited state to the TiO_2 conduction band lead to a situation similar to surface enhancement) [18]. Adsorption kynetics measurements and the analysis of the C=O stretching frequencies led the authors to propose a five-member ring chelate O1-C1-C2-O2 for the adsorption of alizarin on TiO_2. Indeed, there is relatively little enhancement of the C=O stretching vibrations, which appear as a broad band at 1623 cm^{-1} and a shoulder at 1666 cm^{-1}. The reversal of the intensity ratio between C9=O and C10=O may be an inductive effect, connected to the closer proximity of the C9=O group to the adsorption site and a possible stronger coupling of its vibration to enhanced modes. The as-yet unpublished SERS study of alizarin mentioned earlier [20] presents SERS spectra of alizarin on Ag obtained in the absence of poly-L-lysine. These spectra look slightly different than those presented and the authors reach a very different conclusion on the adsorbate geometry, postulating that the dissociation order for alizarin in Ag sol adsorption condition is inverted, with the OH in position 1 dissociating first. This would lead to alizarin adsorbing on Ag as a six-member ring O-C9-C-C1-O chelate. It is possible that the geometry of the alizarin-Ag complex is different whether poly-L-lysine is present or not.

The spectrum of bi-dissociated alizarin presented here corresponds well to the spectrum published in [20]: spectral evidence suggests that alizarin adsorbs on Ag in this case with a O-C9-C-C1-O geometry, with the hydroxyl in position 2 dissociated, as a phenolate ion. The peak at 1420 cm^{-1} can be interpreted as due to the phenolate vibration (an attribution substantiated by the spectrum of the Na salt of 1-hydroxy-anthraquinone in [29]). The positions of the C=O stretch bands further corroborates this interpretation: an intense band at 1600 cm^{-1} correspond to the downshifted and enhanced vibration of C9=O (involved in the Ag adsorbate), while C10=O remains at 1630 cm^{-1}, as observed in the monodissociated case. The proposed geometries of the adsorbates are shown in figure 5.

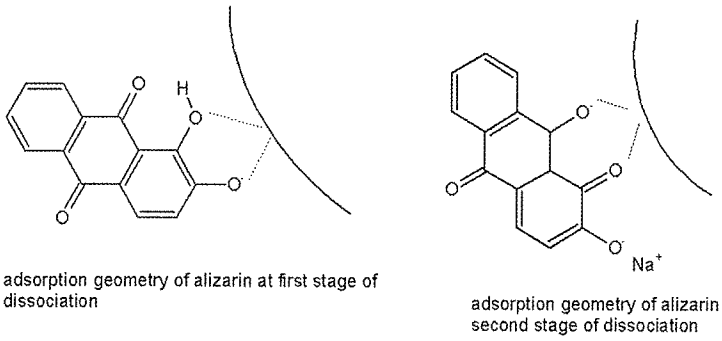

adsorption geometry of alizarin at first stage of dissociation

adsorption geometry of alizarin at second stage of dissociation

Figure 5: Adsorption geometry for mono- and bi-dissociated alizarin on Ag

In order to test the effectiveness of SERS as a method of identification of natural dyes, tests were conducted on purpurin, the other major component of lake pigments prepared from madder root. While residual fluorescence seems to be always a problem in presence of purpurin, SERS spectra of synthetic purpurin and natural madder ethanolic extracts (containing alizarin, purpurin and several other anthraquinones [7,8]) of sufficient quality were obtained. Finally, a one-step procedure to extract the anthraquinones and record SERS spectra from microscopic samples of lake pigments was developed. Extraction and adsorption-aggregation are obtained by treatment of the sample, deposited on a gold microscope slide with one drop of NaOH solution and heating to dryness followed by addition of Ag sol. No solvent extraction or separation is needed: the Raman spectrum can be measured directly from the drop. Examples of spectra obtained by this procedure on a pigment sample (Hatfield genuine madder) are compared to spectra of alizarin and purpurin in figure 6.

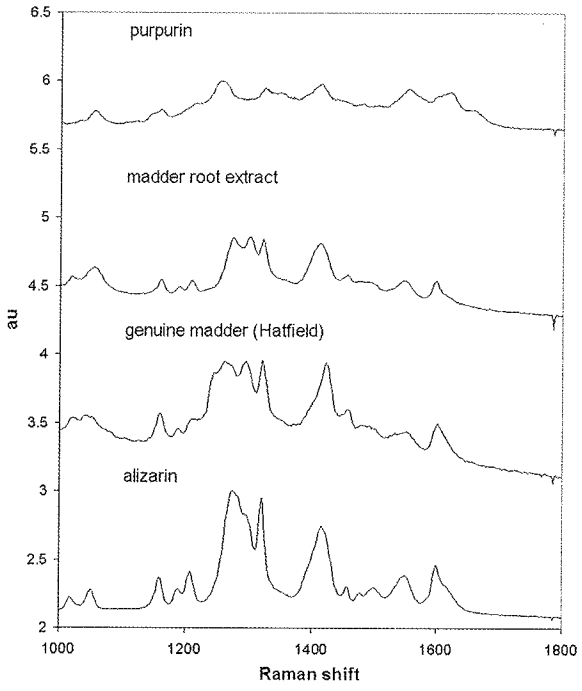

Figure 6: SERS spectra of madder and alizarin lakes compared with alizarin and purpurin

Conclusion

Raman spectroscopy can be adapted to the detection of natural dyes in works of art. Problems due to fluorescence

and low sensitivity can be solved simultaneously by exploiting the surface enhancement observed when the dye molecules are adsorbed on Ag nanoparticles. A practical method for the identification of alizarin and purpurin in samples of natural madder lakes and of alizarin alone in synthetic alizarin lakes was presented. The sensitivity of the method is estimated to be in the tens of picogram range or better.

Acknowledgements

Most of the experimental work was conducted when the author was senior conservation scientist at the Los Angeles County Museum of Art. Raman research there was supported by a generous grant from the Andrew W. Mellon Foundation. Laura Balcerzak, Camilla Chandler Frost intern in Conservation Science, provided invaluable assistance in background research on colloid preparation and aggregant agents effects. Concha Domingo at CSIC Madrid kindly provided an advance-of-print copy of her paper on SERS of alizarin, and Silvia Centeno and Nobuko Shibayama at the Metropolitan Museum of Art lent their advice and provided helpful information.

References

1. Guineau, B., 'Microanalysis of painted manuscripts and of colored archaeological materials by Raman laser microprobe', Journal of Forensic Science (1984) **29**(2) 471-485

2. Guineau, B., 'L'étude des pigments par les moyens de la microspectrométrie Raman' in F. Delamare, T. Hackens, and B. Helly, Eds. *'PACT* 17, Datation-Caractérisation des peintures pariétales et murales. 4th European postgraduate course', Oleffe, Court-Saint-Etienne, Belgium. (1987) 259-294.

3. Smith, and Clark, R.J.H. 'Raman microscopy in art history and conservation science', *Reviews in Conservation* (2001) **2** 96-110

4. Leona, M., and Winter, J., 'Fiber Optics Reflectance Spectroscopy: a unique tool for the investigation of Japanese paintings', *Studies in Conservation* (2001) **46** 153-62.

5. Leona, M., Casadio, F., Bacci, M., and Picollo, M., 'Identification of the pre-Columbian pigment Maya blue on works of art by non-invasive UV-Vis and Raman spectroscopic techniques', *Journal of the American Institute for Conservation* (2004) **43** 39-546.

6. Guineau, B. 'Experiments in the identification of colorants in situ: possibilities and limitations' in Rogers, P.W. editor *Dyes in history and archaeology 10* Annual meeting of the Association of Researchers into dyes in history and archaeology, London, 1992 55-59.

7. Wouters, J. 'High performance liquid chromatography of anthraquinones: analysis of plant and insect extracts and dyed textiles', *Studies in Conservation* (1985) **30**(3) 119-128.

8. Schweppe, H., and Winter, J., 'Madder and Alizarin' in West Fitzhugh, E. (editor) *Artists' pigments; a handbook of their history and characteristics, Volume 3*, National Gallery of Art, Washington (1997) 109-142.

9. Schweppe, H., and Roosen-Runge, H., 'Carmine - cochineal carmine and kermes carmine' in Feller, R.L. (editor) *Artists' pigments; A handbook of their history and characteristics, Volume 1*, National Gallery of Art, Washington (1986) 255-283.

10. Burgio, L. and Clark, R.J.H. 'Library of FT-Raman spectra of pigments, minerals, pigment media and varnishes, and supplement to existing library of Raman spectra of pigments with visible excitation' *Spectrochimica Acta Part A: Molecular and Biomolecular Spectroscopy* (2001) **57**(7) 1491-1521.

11. Bell, I.M., Clark, R.J.H., and Gibbs, P.J., 'Raman Spectroscopic Library of Natural and Synthetic Pigments (pre-~1850 AD)' *http://www.chem.ucl.ac.uk/resources/raman/speclib.html.*

12. Fleischmann, M., Hendra, P.J., and McQuillan, A.J.,' Raman spectra of pyridine adsorbed at a silver electrode'

Chemical Physic Letters (1974) **26**(2) 163-166.

13. Jeanmaire, D.L., and Van Duyne, R.P., 'Surface Raman spectroelectrochemistry. Part 1: heterocyclic, aromatic, and aliphatic amines adsorbed on the anodized silver electrode' *Journal of Electroanalytical Chemistry* (1977) **84**(1) 1-20.

14. Albrecht, M.G., and Creighton, J.A. 'Anomalously intense Raman spectra of pyridine at a silver electrode' *Journal of the American Chemical Society* (1977) **99** 5215-5227.

15. Nie, S., and Emory, S.E., 'Probing single molecules and single nanoparticles by surface-enahanced Raman scattering' *Science* (1997) **275** 1102-1106.

16. Kneipp, K., Wang, Y., Kneipp, H., Perelman, L.T., Itzkan, I., Dasari, R.R., and Feld, M.S., 'Single molecule detection using surface-enhanced Raman scattering (SERS)' *Physical Review Letters* (1997) **78**(9) 1667-1670.

17. Campion, A. and Kambhampati, P., 'Surface-enhanced Raman scattering' *Chemical Society Reviews* (1998) **27** 241-250.

18. Shoute, L.C., and Loppnow, G.R., 'Excited state dynamics of alizarin-sensitized TiO_2 nanoparticles from resonance Raman spectroscopy' *Journal of Chemical Physics* (2002) **117**(2) 842-850.

19. Guineau, B., and Guichard, V., 'Identification des colorants organiques naturels par microspectrometrie raman de resonance et par effet Raman exalte de surface (SERS)' in *ICOM committee for conservation: 8th triennial meeting, Sidney, Australia, 6-11 September, 1987. Preprints. Volume 2,* The Getty Conservation Institute, Marina del Rey (1987) 659-666.

20. Canamares, M.V., Garcia-Ramos, J.V., Domingo, C., and Sanchez-Cortes, S., 'Surface-enhanced Raman scattering study of the anthraquinone pigment alizarin adsorption on Ag nanoparticles' *Journal of Raman Spectroscopy* forthcoming.

21. Lee, P.C., and Meisel, D., 'Adsorption and surface-enhanced Raman of dyes on silver and gold sols' *Journal of Physical Chemistry* (1982) **86** 3391-3395.

22. Munro, C.H., Smith, W.E., and White, P.C., 'Use of poly(L-lysine) and ascorbic acid for surface enhanced resonance Raman scattering analysis of acidic monoazo dyes' *Analyst* (1993) **118** 731-733.

23. Allen, F.S., Zhao, J., and Butterfield, D.S., 'Apparatus for measuring and applying instrumentation correction to produce a standard Raman spectrum' US Patent 6,141,095. Assigned to Chromex, Inc., Albuquerque, NM. 2000.

24. Zhao, J., Carrabba, M.M., and Allen, F.S., 'Automated fluorescence rejection using shifted excitation raman difference spectroscopy' *Applied Spectroscopy* (2002) 56(7) 834-45.

25. The Merck Index, 12th Edition, CRC Press, 1996.

26. Miliani, C., Romani, A., and Favaro, G., 'Acidichromic effect in 1,2-di- and 1,2,4-tri-hydroxyanthraquinones. A spectrophotometric and fluorimetric study' *Journal of Physical Organic Chemistry* (2000) **13** 141-150.

27. Wunderlich, K.H., and Bergerhoff, G., 'Konstitution und farbe von alizarin- und purpurin-farblacken' *Chemische Berichte* (1994) **127** 1185-1190.

28. Ball, B., Zhou, X., and Liu, R., 'Density functional theory study of vibrational spectra. 8. Assignment of fundamental vibration modes of 9,10-anthraquinone and 9,10-anthraquinone-d_8' *Spectrochimica Acta Part A* (1996) **52** 1803-1814.

29. Dutta, P.K., and Hutt, J.A., 'Infrared and Resonance Raman spectroscopic studies of 1-hydroxy-9, 10-anthraquinone and its metal complexes' Journal of Raman Spectroscopy (1987) **18** 339-344.

Raman Spectroscopy of Brazilian Archaeological and Ethnographic Resins

Dalva L.A. de Faria[1], Silvia Cunha Lima[2], Marisa C. Afonso and Howell G.M. Edwards[3]

[1] Laboratório de Espectroscopia Molecular, Instituto de Química, Universidade de São Paulo, C.P. 26077, 05513-970, São Paulo, Brazil
[2] Museu de Arqueologia e Etnologia da Universidade de São Paulo Av. Prof. Almeida Prado 1466, 05508-900 São Paulo, Brazil
[3] Department of Chemical and Forensic Sciences, University of Bradford BD7 1DP Bradford, UK

Abstract

Perhaps the greatest challenge in the investigation of cultural heritage objects is the need to obtain a significant amount of information from samples that quite often cannot be destroyed or damaged by the analytical procedure employed. Raman spectroscopy fulfils such a task with some advantages over other similar techniques.
Resins are largely used by different cultures to make adornments and decorative objects, but are also used as glue, waterproofing compounds etc. and as such are commonly found in museums. Natural resins are complex chemical systems, leading to specific experimental difficulties; in the case of Raman spectroscopy, the main problem is the fluorescence generally presented by the samples, making mandatory the use of NIR excitation (FT-Raman). In this work twenty ethnographic resins were studied by FT-Raman spectroscopy and the results compared with the data obtained for an archaeological resin lip-plug (*tembetá*).
The samples were classified into five categories, depending on the characteristics of their Raman spectra, but most of them are diterpenic resins. Very dark samples only generated a thermal background due to the absorption of the laser radiation.

Introduction

Spectroscopic techniques are increasingly used in the investigation of cultural heritage objects and Raman spectroscopy has been claimed by some as one of the most powerful tools currently available, with the additional advantage that the analysis can be conducted non-destructively. Fiber optics can be used to focus the laser and collect the scattered light from specific spots on the object or, in the case of Raman microscopy, the spectra can be obtained directly from the sample placed on the microscope stage. This represents an obvious advantage over IR spectroscopy, where very rarely a sample can be studied without any type of manipulation such as solubilization in an appropriate solvent, dispersing in KBr or oils, crushing for ATR etc.
Besides such sampling characteristics, a Raman spectrum is much simpler to analyse than an IR one as overtones and combination bands are not observed except when the laser light is strongly absorbed by the sample, giving rise a resonance Raman effect which is very convenient for the investigation of coloured pigments. Additionally, spatial resolution is much better with Raman than with IR microscopy permitting the investigation of heterogeneities at the micrometric level.
All of these aspects are of remarkable importance in the investigation of resins, as problems with solubility can be anticipated, particularly in the case of degraded samples; partial solubility may give rise to selective extraction of specific fractions from the sample that are not representative of the bulk material. Even when it is possible to collect a small amount of sample from the object, the dispersion of the resin in KBr or in a mineral oil (such as Nujol or Kel-F) can be difficult, giving rise to artefacts in the IR spectrum. Finally, the better spatial resolution available in Raman techniques is crucial in differentiating deteriorated from non-deteriorated areas in the object and in performing interface studies or for the identification of inclusions.
The main drawback in Raman spectroscopy is fluorescence, which is a quite common feature in organic compounds. Among the possibilities to overcome the problem, the change of the exciting laser line is the most commonly used. When none of the visible lines available are useful, excitation in the NIR (1064 nm) is used coupled with an interferometer (FT-Raman spectroscopy). Thus FT-Raman spectroscopy is largely used in the investigation of resins [1], their ageing or degradation processes [2] and even composites [3].
In general, the study of natural resins is complicated by the fact that they present quite a complex chemical structure, very prone to degradation and eventually consist of a heterogeneous mixture of compounds. With Raman spectroscopy, the direct implications of these characteristics on the spectrum are the fluorescence background and band broadening. The problems associated with chemical complexity and heterogeneity can be

overcome by systematic investigations of resins whose chemical composition is well known but it has to be emphasized that the composition of a resin can change even when considering plants of the same species, highlighting the importance in combining chemical (composition and spectroscopy) with botanical information.
In the literature a large number of works have focused on the identification of inorganic pigments by Raman spectroscopy [4], however, biomaterials and resins are substantially less investigated, since sample complexity and degradation processes can make data acquisition and interpretation quite difficult.
Resins have been extensively used by many different cultures throughout history in the manufacture of decorative objects (such as small sculptures or jewellery) and as adhesive or waterproofing compounds. Raman spectroscopy has been very successfully applied in the investigation of archaeological resins [5], and, recently a study of an Indian lip-plug (ca. 1600 BP) found in an archaeological site in the south-east of Brazil was carried out [6]. Ethnographic resins used by different Indian groups in Brazil are also currently under investigation [7] aiming at the identification of the resin compositions and the achievement of a better understanding of their uses by comparison with data collected from Brazilian indian objects kept in museum collections. Such an aspect is particularly important in the case of indian groups that are close to extinction, with only a few hundred individuals remaining, if their culture is to be preserved.
In the present work Raman spectroscopic data from both Brazilian ethnographic and archaeological resins are discussed with the aim of identifying their chemical composition. In a more general perspective, resins from South America are not as frequently investigated as those from Europe and Asia. Thus, establishing a database is highly desirable and will permit a future comparison with the data already available in the literature.

Experimental section

1. Material

A. Samples
A *tembetá* is a lip adornment (lip-plug) used to represent the attainment of adulthood by different indian groups in Brazil. The archaeological resin *tembetá* was recovered from an excavation of a Guarani tribe habitation in an archaeological site (Pernilongo) at Iepê, south of São Paulo State, Brazil. It is about 1600 years old and in appearance it is a tapered cylinder with a cross-bar at the top. It was found split in pieces together with other smaller fragments, which probably were used as ear adornments; they were found buried inside a 50 cm sediment layer, close to a water reservoir and it is therefore believed that the fragments were covered by water and sediments (ca. 20 cm) and, in drier periods, only by sediments.

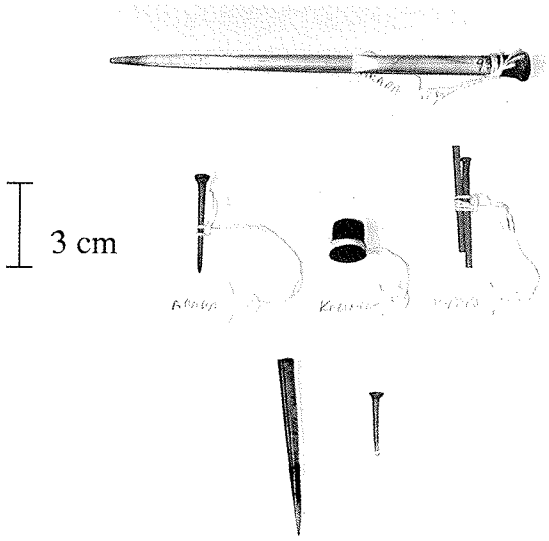

Figure 1:- Ethnographic resin tembetás (samples XVIII, XIX and XX - see Table 1)

Ethnographic resin consisted of 20 different resin samples from the Amazon and Central areas in Brazil, which

belong to the Museum of Archaeology and Ethnology of the University of São Paulo's (MAE-USP) collection. Their age ranged from about 40 to 100 years and, externally, they generally present a yellow, red, dark brown or black colour. An inspection of the internal regions of the black and dark brown samples frequently reveals bright and mostly red resins. Three samples (9034, 13606 and 9310) were ethnographic *tembetás* (50-60 years old); they are yellow coloured objects and were collected directly from the tribes. A detailed description of the samples is given in the Table below (Table 1).

B. Instrumentation

FT-Raman spectra were obtained from a Bruker RFS-100/S with Nd^{3+}/YAG laser excitation at 1064 nm (laser spot was approximately 100 μm in diameter at the sample) and fitted with a liquid N_2 cooled Ge detector. Spectra were recorded with 4 cm^{-1} spectral resolution and the number of scans accumulated to provide adequate signal-to-noise ratio was dependent on the sample. Raman spectra excited with visible radiation were also obtained (Renishaw Raman microscope, using the 632.8 and 785 nm lines); in some cases the vibrational bands were swamped by the strong fluorescent background. For the Raman analysis, no sample preparation was undertaken and the resins were studied as received, whereas for the IR measurements (400-4000 cm^{-1}) films were prepared on KRS5 windows from the resin solutions. However, solubilization was not complete for any of the studied samples. Infrared spectra were recorded in a Bomem MB100 instrument.

2. Results

The emphasis of this work is the use of Raman spectroscopy in the characterization of resins with historical and/or cultural relevance, since it is a non-destructive technique, providing structural information that can be valuable for conservation and restoration purposes. Other techniques, including FTIR, CG-MS etc, can be very useful too, but in some these cases small amounts of material must be destroyed in the course of the analysis. Nevertheless, a future step in this investigation is to complement the information provided by Raman spectroscopy e.g. by FTIR (single bounce ATR) and pyrolysis.

Excitation in the visible was also used but the data quality is much poorer than with excitation in the NIR, due to the fluorescence background and, for this reason, in this work only the FT-Raman spectra are reported.

In Fig. 2 the C-H stretching region is shown for the three *tembetás* already described; the lower spectrum was obtained from a diterpenic resin (*Hymeneaea Stig. Mart.* resin, locally known as Jatobá resin) which can be found widely spread in Brazil.

For the Jatobá resin the main peaks are at 2871 and 2925 cm^{-1} whereas for the *tembetás* the corresponding bands appears at 2878 and 2937 cm^{-1}, respectively. As noted elsewhere [6], this spectral region is not particularly useful in the characterization of resins, but the data clearly indicate that the *tembetás* are quite similar in composition but differ from the Jatobá resin.

An inspection in the fingerprinting region (Fig. 3) reveals that the differences are in fact very significant: the strongest bands in the Jatobá resin spectrum show up at 1445, 1525 and 1647 cm^{-1} whereas for the *tembetás* they appear at 1460, 1660 and 1723 cm^{-1}. The ca. 1445 cm^{-1} band (Jatobá resin) has a shoulder at higher wavenumber; in the *tembetás* spectra the relative contribution of both bands is nearly the same.

In the 1600-1750 cm^{-1} region the differences are even more striking: the ν(C=C) vibration at 1647 cm^{-1} (Jatobá) shows up at 1660 cm^{-1} and another band (medium intensity) appear at ca. 1720 cm^{-1}.

Jatobá resin is usually yellowish when fresh, changing to dark yellow on ageing, but curiously the investigated sample is deep red, which suggests that the ca. 1520 cm^{-1} band corresponds to a carotene like compound; this assignment is confirmed by the presence of a weaker feature at ca. 1150 cm^{-1}. The observation of these two bands has been used as a marker characteristic of carotene-like structures [8]. It must be emphasized that these bands are not present in the *tembetás* spectra; as shown in Fig. 1 these *tembetás* are yellow, thus reinforcing the assignment of the 1520 and 1150 cm^{-1} bands to a carotenoid compound.

In Fig. 4 the Raman spectra of resins I, II, II, V and IX are presented and it is clear that the spectra of resins III and IX are different from resins I, II and V. By comparison with the Jatobá resin which is known to be rich in diterpenoids they can be described as diterpenic resins with the most significant bands showing up at 3080, 2930, 2870, 1662 (sh), 1644, 1460, 1445, 1204, 1180 and 724 cm^{-1}.

In the case of resins I, II and V the strong peaks at ca. 1150 and 1520 cm^{-1} strongly suggest that a carotenoid-like compound is present. A completely different behaviour is observed with sample IV: the quality of the spectrum is very poor (Fig. 5) but the spectral features that can be seen are consistent with those of a gum.

Following the same rationale, the Raman spectra of the other resins presented a regular pattern and were divided into 4 categories: diterpenic probably with carotenoid structures (strongest peaks at ca. 1150 and 1520 cm^{-1}),

SAMPLE #	DESCRIPTION
I	Collection number 9524.Tukuna, Amazon (1958). "Red resin for ceramics" (externally shows a yellow colour, internally it is red -orange)
II	Collection number 5053. Javaé, Goiás (1909). No further information (externally: black, inter nally: bright red)
III	Collection number 5050. Javaé (no further information)
IV	Collection number 2816. Karajá ?
V	Collection number 6952. Kaxinawá. Curanja river at the Peruvian border (1950). Sample enclosed by leaves (externally: black, internally: red, soft and sticky)
VI	Collection number 6956. Kaxinawá. resin rod. (externally: black and rigid, internally: sticky)
VII	Collection number 12318. Urubu, Maranhão (1966). "Resin for restauration" (externally and internally : dark brown, hard)
VIII	Collection number 114. Krahô, Goiás (1947) Angico resin. Inside: glassy shine)
IX	Collection number 4125. Tukano, Amazonas (1907).
X	Collection number 12693. Xikrin, Caeteté River, Pará (1968), Bees wax.
XI	Collection number 5052. Javaé, Araguaia River, Go iás (1909). Yellow resin.
XII	Collection number 5054 Javaé, Araguaia River, Goiás (1909). Red resin.
XIII	Collection number 10499. Suyá, Alto Xingu (1960). Jatobá resin.
XIV	Collection number 6068. Tucurina, Acre (1950),
XV	Collection number 7617 Tiri yó, Venezuela border (1952). Wax.
XVI	Collection number 3475. Nambikwara, Mato Grosso (1939). Tube with wax.
XVII	Collection number 7683. Tiriyó, Venezuela border (1952). Wax.
XVIII	Collection number 9034. Kabixiana Mato Grosso (1939). Resin tembetá.
XIX	Collection number 13606. Tupari, Guaporé River, Acre (1956). Resin tembetá.
XX	Collection number 9310.Uruku, site location not given (1953). Resin tembetá

Table 1:- Description of ethnographic resins studied in this work; information includes the indian group, where the samples were collected, when they were collected and general characteristics (all the samples belong to the Museum of Archaeology and Ethnology of the University of São Paulo).

diterpenic based in the labdane structure (by comparison with the Jatobá resin spectrum), gums (bands of similar intensity at 800 and 1650 cm^{-1}) and black samples which were not possible to investigate by Raman spectroscopy as the thermal or fluorescent background swamps the vibrational bands.

The remaining resins (XI and XIV) do not fit into these categories as their Raman spectra follow a completely different pattern (Figs. 6 and 7). So far, it is not possible to make any definitive statements about their composition (diterpenic or triterpenic) but it is likely that they are diterpenic resins whose composition is not based on labdane or abietane compounds. This point is currently under investigation.

Finally, some samples were too dark to be studied in the NIR and only the thermal background was observed even using low laser power.

4. Discussions

A Previous research on the discrimination protocol for diterpenoids and triterpenoids has shown that the wavenumber region 1520-1750 cm^{-1} is crucial for the discrimination in the terpenoid classification. When the Raman spectra of the archaeological *tembetá* is compared with *Pinus halepensis*, *Cedrus libani* and *Pistacia lentiscus* resins the presence of two major Raman bands in this region, namely 1702 and 1656 cm^{-1} is indicative of a triterpenoid resin as diterpenoid ones, containing predominantly abietane compounds, have strong bands at approximately 1650 or lower and 1611 cm^{-1}, sometimes with a band near 1635 cm^{-1} whose intensity increases

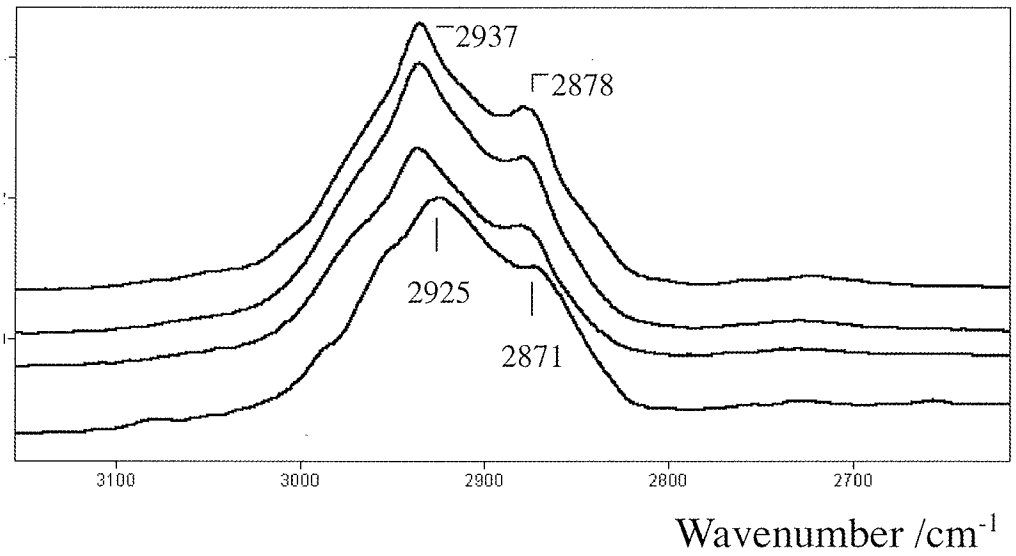

Figure 2: FT-Raman spectra of ethnographic resin tembetá in the ν(C-H) region. From the top, they correspond to samples XVIII, XIX and XX - see Table 1. The lower spectrum is from a diterpenic resin (Jatobá resin) and was included for comparison purposes.

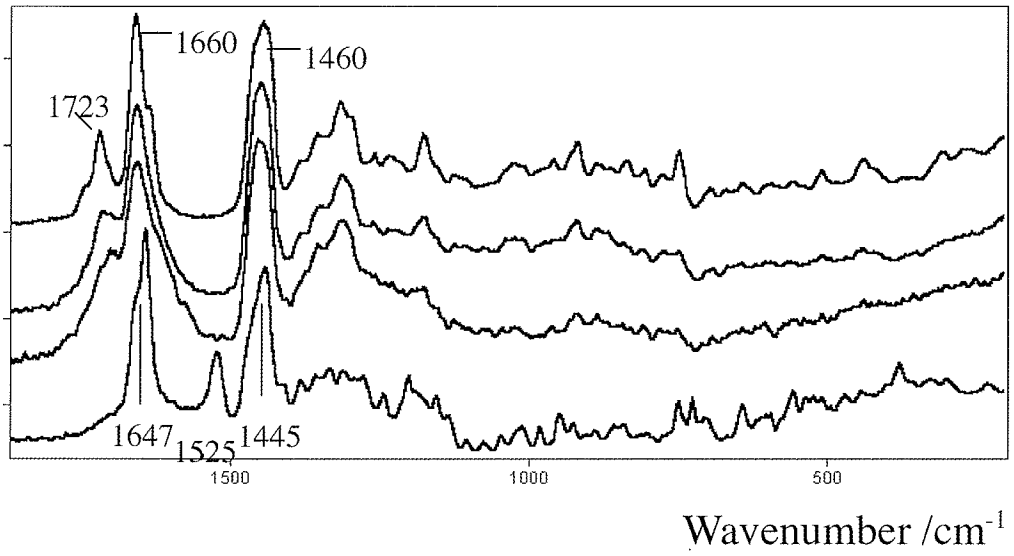

Figure 3: FT-Raman spectra of ethnographic resin tembetá. From the top, they correspond to samples XVIII, XIX and XX - see Table 1. The lower spectrum is from a diterpenic resin (Jatobá resin) and was included for comparison purposes.

with specimen degradation. On the other hand, *Pistacia* resins always have a slightly higher wavenumber feature at about 1655 cm^{-1} and a weaker band near 1705 cm^{-1}. Degradation produces a weaker shoulder around 1620 cm^{-1}. Hence, spectra indicate that the archaeological *tembetá* resin is a triterpenoid, whose composition is near that of *Pistacia* resins. A confirmation of the triterpenoid classification of the *tembetá* resin is the presence of a doublet at about 1460/1440 cm^{-1}, in which the two bands are of similar intensity. The ν(CH) stretching region (not shown) is not definitive enough for unambiguous identification or classification of the unknown resin as diterpenoid or triterpenoid.

There is a tradition that Indian tribes from the south-east of Brazil and Paraguay used a resin from *Hymenaea stigonocarpa Mart. (Jatobá)* to construct artefacts; the Raman spectrum of such resin was obtained and on the basis of the protocol used here, the *Jatobá do Cerrado* resin is unambiguously not the source for the *tembetá* artefact, since it is a diterpenoid in composition as indicated by a strong feature at 1634 cm^{-1}, with weaker shoulders at about 1650 and 1640 cm^{-1}. We are as yet unable to obtain specimens of likely contemporary

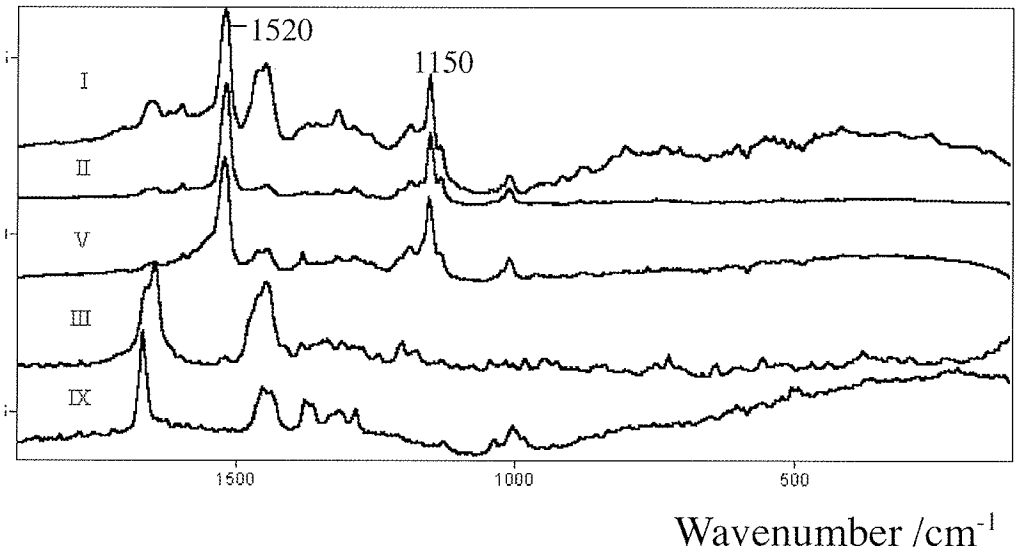

Figure 4: FT-Raman spectra of ethnographic resins.

Figure 5: FT-Raman spectrum of sample IV. Despite the poor data quality, the bands observed on the background are suggestive that sample IV is a gum.

alternatives, which could have been used in the construction of the archaeological resin *tembetá* and, indeed, it appears that geoecologists are of the opinion that changes in climate and population movement make it unlikely that the precise botanical sourcing of the *tembetá* resin will emerge.

The successful investigation of the *tembetá* inspired the investigation of ethnographic resins, aiming at the construction of a database with Raman spectra of Brazilian resins, which can be applied to museum objects. The results obtained so far have revealed some interesting features: although the resins look similar by visual inspection, their Raman spectra are significantly different allowing the samples to be classified into 5 groups: (i) diterpenoid resins in association with carotenoids (intense bands at 1517 and 1153 cm^{-1}); (ii) diterpenoid resins, probably with its structure based on the labdane skeleton (most significant bands at 3080, 2930, 2870, 1520, 1155 and 1012 cm^{-1}); (iii) gum, probably, with bands of similar intensities between 1650 and 800 cm^{-1} and (iv) resins which give rise to good quality Raman spectra but do not fit in any of the categories above and are probably diterpenic resins not based in the labdane or abietane skeleton; and (v) poor light scatterer resins (black samples) – for these cases no Raman spectra can be recorded due to the thermal background generated by sample heating. As mentioned before, such classification is based on previous studies reported in the literature involving a large number of resins and gums from different sources; unfortunately none of them included resins from the Amazon area.

FTIR spectra obtained from the samples (not shown) were not used in this work since it seems that they do not represent the sample as a whole, but only the most soluble fractions as, in any case, the complete solubilization was not achieved even using a mixture of solvents.

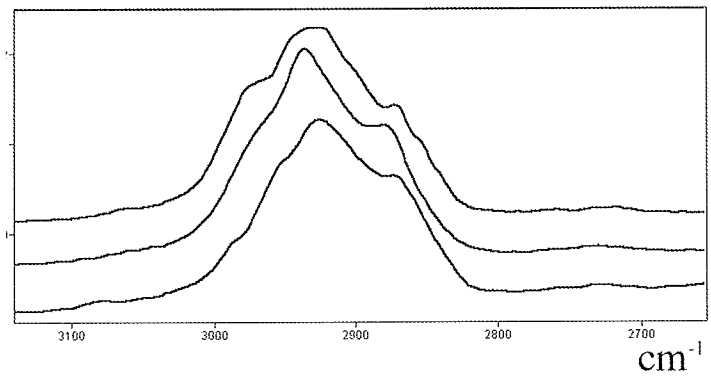

Figure 6: FT-Raman spectra of samples XI and XIV, from the top, in the ν (CH) region. The lower trace corresponds to Jatobá resin and was included for comparison purposes.

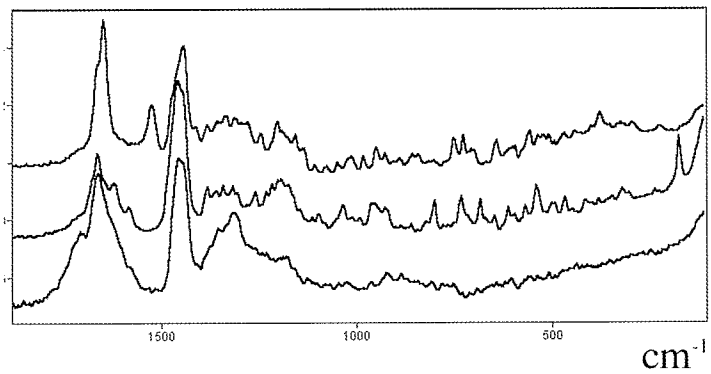

Figure 7: FT-Raman spectra of samples XI and XIV, from the bottom. The upper trace corresponds to Jatobá resin and was included for comparison purposes.

Conclusion

Raman spectroscopy shows promise in the investigation of archaeological and ethnographic resins with the aim of obtaining information on their composition in a non-destructive procedure. Excitation in the NIR was used due to the fluorescence presented by most samples and reasonable quality spectra were obtained for all the resins except the very dark ones, where heating caused by the laser line (1064 nm) absorption created a thermal background that swamped the Raman bands.

Reference

1. Vandenabeele, P., Grimaldi, D.M., Edwards, H.G.M., Moens, L., 'Raman spectroscopy of different types of Mexican copal resins', *Spectrochim. Acta, Part A - Mol. Biomol. Spectrosc.*, **59** (10), 2003, 2221-2229.

2. Chaplin, A., Hamerton, I., Herman, H., Mudhar, A.K., Shaw, S.J., 'Studying water uptake effects in resins based on cyanate ester/bismaleimide blends', *Polymer*, **41** (11), 2000, 3945-3956.

3. Puglia, D., Valentini, L., Kenny, J.M., 'Analysis of the cure reaction of carbon nanotubes/epoxy resin composites through thermal analysis and Raman spectroscopy', *J. Appl. Pol. Sci.*, 88 (2), 2003, 452-458.

4. Edwards, H.G.M., 'Raman Microscopy in Art and Archaeology', *Spectroscopy*, **17** (2), 2002, 16-40.

5. Brody, R.H., Edwards, H.G.M., and Pollard, A.M., 'Fourier-Transform Spectroscopic Study of Natural Resins of Archaeological Interest', *Biopolymer*, 67 (2), 2002, 129-141.

6. deFaria, D. L. A., Edwards, H. G.M., Afonso, M.C., Brody, R. H., Morais, J. L., 'Raman Spectroscopy analysis of a Tembetá: a Resin Archaeological Artefact in Need of Conservation", *Spectrochim. Acta, Part A - Mol. Biomol. Spectrosc.*, in press; 60, 2004, 1505-1513.

7. deFaria, D.L.A., Lima, S.C., Edwards, H.G.M., 'Raman Investigation of Brazilian Ethnographic Resins", International Conference on the Applications of Raman Spectroscopy in Art and Archaeology, Ghent (Belgium), 2003.

8. Withnall, R., Chowdhry, B.Z., Silver, J., Edwards, H.G.M., deOliveira, L.F.C., 'Raman Spectra of Carotenoids in Natural Products', *Spectrochim. Acta, Part A - Mol. Biomol. Spectrosc.*, **59** (10), 2003, 2207-2212.

Raman Spectroscopy Applied to Biomaterials in Art History and the Preservation of Cultural Heritage

H.G.M. Edwards and T. Munshi
Chemical and Forensic Sciences, School of Pharmacy, University of Bradford, Bradford BD7 1DP, UK.

Abstract

This paper reviews the contributions of Raman spectroscopy to the non-destructive characterisation of biological materials, including the sourcing of resins and the identification of biodegradation of art and archaeological artefacts. The advantages of Raman spectroscopy for non-destructive analysis are well-appreciated. However, the ability to record molecular information about organic and inorganic species present in a heterogeneous specimen at the same time, the insensitivity of the Raman scattering process to water and hydroxyl groups which removes the necessity for sample desiccation, and the ease of illumination for samples of very small and very large sizes and unusual shapes are also apparent. Several examples are used to illustrate the application of Raman spectroscopic techniques to the characterisation of biomaterials and for the preservation of cultural heritage through case studies in the following areas: wall-paintings and rock art, human and animal tissues and skeletal remains, fabrics, resins and ivories.

Introduction

The degradation of materials exposed to the environment or in a burial context can affect the observed Raman bands in predictable and recognisable ways, which can assist in the interpretation of the deteriorative processes through characteristic or key spectral biomarkers. The degradation processes by which archaeological materials undergo chemical and physical changes are diverse and include desiccation, absorption of chemical species from the soil, waterlogging of artefacts, radiation damage through excessive insolation exposure, bacterial attack and oxidative fission at unsaturated chemical sites. Raman spectra can provide a potentially unique source of data on the historical environmental conditions to which artwork or specimens have been subjected and can give archaeologists and scientific conservators a new perspective on excavated artefacts and materials. This is particularly important for archaeological biomaterials because of their relative fragility and sensitivity to chemical, biological and environmental deterioration [1]. The application of chemical analysis to archaeological specimens can be traced back to the late 18th and early 19th Century; in 1815, Sir Humphry Davy read a paper entitled "*Some Experiments and Observations on the Colours used in Painting by the Ancients*" to the Royal Society and thereby probably laid claim to the first publication [2] in this field. Davy's analytical work comprised an extensive study of the pigments on wall-paintings excavated at Pompeii and palaces in Rome using classical chemical methods. In his paper, Davy refers to previously unpublished analytical studies made by savants and communicated verbally to him, and tantalisingly refers to his minimal sampling of these precious archaeological specimens which were in the care of his friend, Canova. Hence, the recognition that destructive sampling for the provision of analytical chemical information, although undesirable, was fundamentally necessary. For example, the classic chemical analytical work of Eccles and Rackham [3] on porcelains in museums required the destruction of whole items for the gravimetric determination of ceramic body compositions.

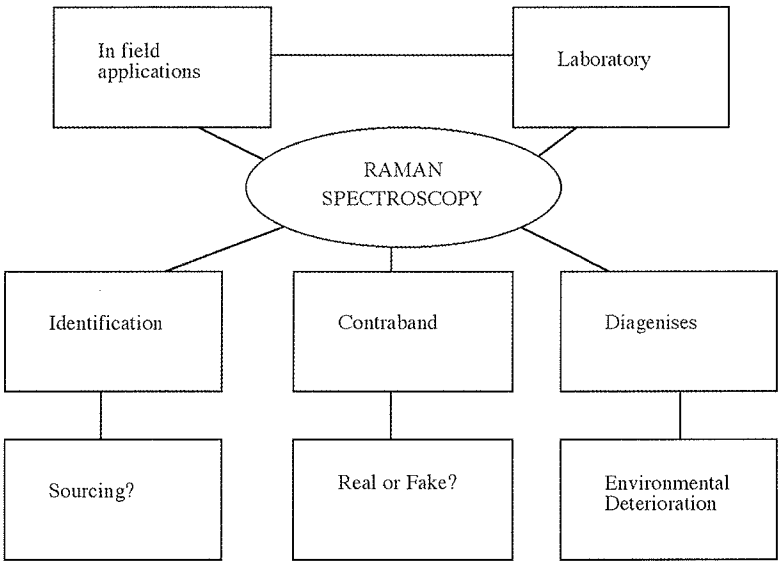

Figure 1. The close relationship between Raman spectroscopic applications in art history, archaeology and forensic science.

The renaissance in chemical analysis applied to archaeological and historical specimens in the last decade has hence focused on non-destructive microsampling spectroscopic techniques [4,5]. Combinations of several analytical techniques, which now frequently include Raman spectroscopy or microspectroscopy, are now being advocated

for the scientific provenancing of artefacts; the spectroscopic data are interpreted with reference to compositions of minerals, dyes and pigments which were known to have been used in recipes at the time of creation of the artwork. This *forensic* application for spectroscopic data analysis is now accepted as a rigorous exercise for Raman spectroscopy and art provenancing [6]. The close relationship between Raman spectroscopic applications in art history, archaeology and forensic science is illustrated in Figure 1.
The major features of Raman spectroscopy in its application to the analysis of art historical and archaeological works can be summarised as follows:
Microsampling; requiring only pg or ng of material at the focal volume of a laser beam.
In situ applications; using remote sensing probes, particularly for inaccessible or very large objects.
Organic and inorganic compositions; of qualitative and possibly quantitative nature – simultaneously acquired from the same specimens and over a much extended wavenumber range than is normally achievable using infrared instruments.
Deterioration and degradation studies; this is of importance for the preservation of art and cultural heritage.
Here, we shall provide some examples from our own studies of a range of archaeological and art historical biomaterials which illustrate the application of Raman spectroscopy to the identification, sourcing and biodeterioration of specimens in museum collections and in the environment.

Experimental

Specimens were obtained from museum collections and archaeological sites as indicated. They were analysed non-destructively and returned after the Raman spectra were recorded using two instruments:
1064 μm excitation with a Nd^{3+}/YAG laser, a Bruker IFS 66/FRA 106 instrument and Ramanscope attachment. Wavenumber range 3500-100 cm^{-1}; spectral resolution 4 cm^{-1}. Spectral footprint, 8-10 μm with 100x lens objective.
785 nm excitation with a diode laser, Renishaw *"In Via"* microscope system. Wavenumber range 3400-100 cm^{-1}; spectral resolution 2 cm^{-1}. Spectral footprint, 2 mm with 100x lens objective.
Multiple scans were collected for each system to improve signal-to-noise ratios; generally, this required some 2000-4000 scans at 1064 nm (total time ~ 30-75 minutes.) and 20 scans at 785 nm (total time ~ 10 minutes).
For the biomaterials and deteriorated specimens studied in this work, the accessibility of Raman spectra recorded at shorter wavelength was normally prevented by fluorescence emission which swamped the weaker Raman spectra.

Results and Discussion

A summary of the range of tissues and biomaterials studied recently in our laboratories is provided in Figure 2:

- Skin
- Hair
- Bone
- Teeth
- Nail

} All contain proteinaceous components with keratotic signatures. Degradation in burial environments -Diagenesis (?)

- Ivories
- Animal skins
- Furs

} Contraband material (?) Real or Fake (?)

- Textiles
- Fibres
- Resins

} Deterioration Stains Geographical Sourcing

Figure 2. Tissues and Biomaterials

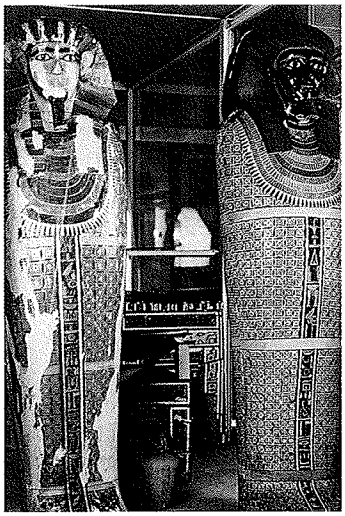

Figure 3. Sarcophagi from the tomb of the two brothers

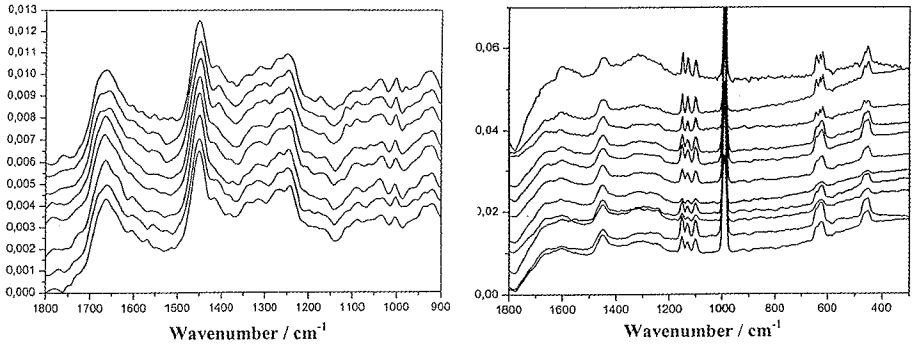

Figure 4.A: Raman spectral stack plot of well-preserved mummified skin of XIIth Dynasty Egyptian burial; 1064 nm excitation.
B: Raman spectral stack plot of degraded human skin from the same mummy, ca 4000 years old, showing evidence of chemical residues from the mummification process (from S. Petersen et al., ref [7])

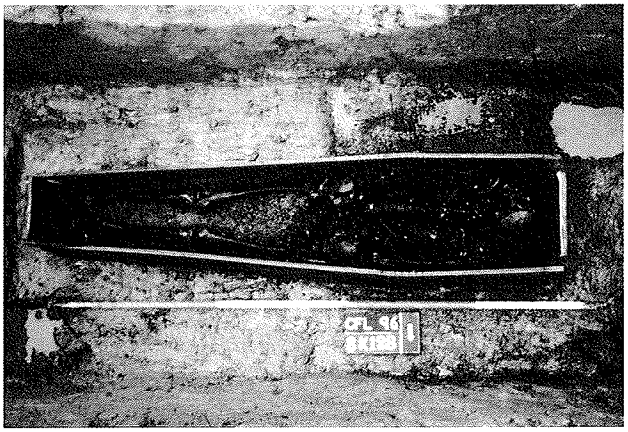

Figure 5. 18th Century burial, found in extension to Newcastle Infirmary

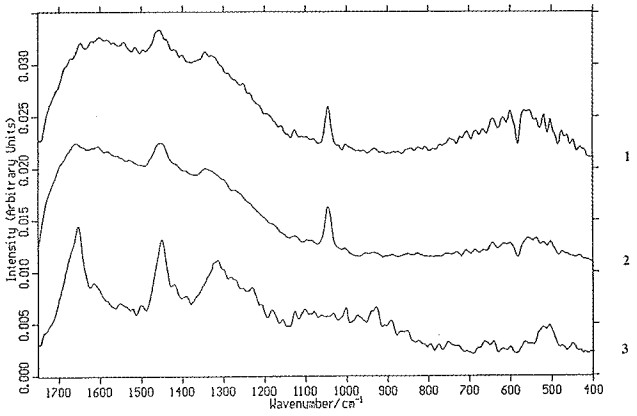

Figure 6. Raman spectra of archaeological hair specimens 1 & 2 = showing a band at ca. 1050 cm^{-1} characteristic of basic lead carbonate and 3 = modern contemporary hair specimen.

Mummified tissue: Raman spectroscopy has provided some important novel information on the characterisation of degraded biodeteriorated tissue from archaeological environments. The height of mummification in Ancient Egypt occurred in the Middle Kingdom; the mummy of Nekht-Ankh (12th Dynasty; *ca* 2000 BC) has been analysed – this mummy, from the "Tomb of the Two Brothers" excavated by Flinders Petrie in 1906, is now in the Manchester Museum (Figure 3). The mummy is of significance for analytical science as it was the first to be subjected to a scientific unwrapping, by Margaret Murray in the University of Manchester in 1906. The skin of the mummy is shown from Raman spectroscopy to be in a variable state of preservation [4] – spectral stackplots show that in some specimens the skin is well preserved as evidenced by the clearly defined amide I and associated modes of skin proteins, whereas in others the degradation of the proteins is shown by the broad, diffuse spectra. It is interesting that in the region where residual bands of the mummification chemicals still remain, viz those of sodium sulfate from the natron used, the skin protein bands indicate a very badly preserved skin structure (Figure 4). Specimens of textiles from the mummy wrappings have also been analysed and information about their deterioration obtained from the Raman spectra.

Hair provides another example of the use of Raman spectroscopy for assessment of biodeterioration; hair consists of keratinous proteins and can survive for considerable times in adverse burial conditions. In Figure 5, the hair from a waterlogged skeletal burial (Figure 5) from the late 18th Century shows evidence of broad protein bands and significant deterioration, despite its apparent survival when all other soft tissue had been degraded [6]. The presence of a spectral signature for basic lead carbonate in the hair specimen from the skeletal remains shown in Figure 5 indicate its association with a lead coffin found elsewhere on site [8]. In comparison, the hair specimen belonging to engineer Robert Stephenson, who died in 1859, shows an excellent state of preservation as it had been kept in an

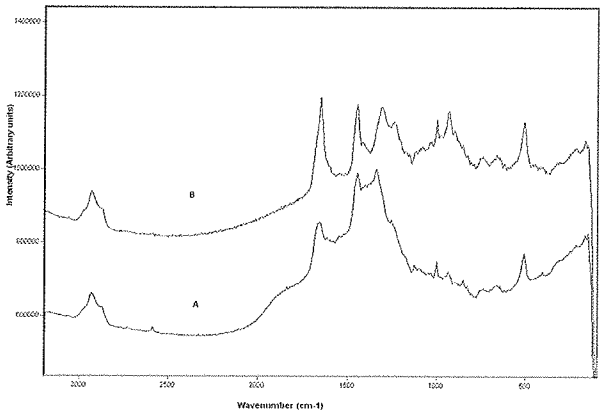

Figure 7. Robert Stephenson's Hair A: Modern grey hair, B: Robert Stephenson's grey hair

Figure 8. Eye-bead from an Egyptian 18th Dynasty cat's head

A unique specimen of an eye-bead from an Egyptian 18th Dynasty cat mummy (Figure 8) was believed to be either amber or brown glass; it was neither, as the Raman spectrum shows – the eye-bead spectrum is characteristic of keratin and is closely matched with that of a claw or horn, which suggested the possibility of a hitherto unrecognised funerary practice was perhaps being operated (Figure 9) [9].

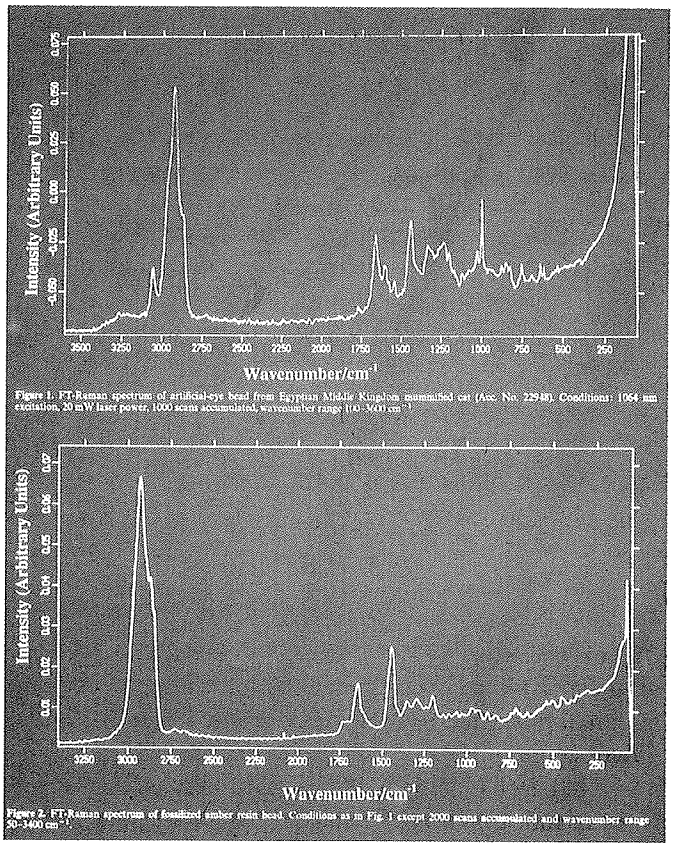

Figure 9. Top spectrum = FT-Raman spectrum of artificial-eye bead from Egyptian Middle Kingdom mummified cat. Bottom spectrum = FT-Raman spectrum of fossilised amber resin bead.

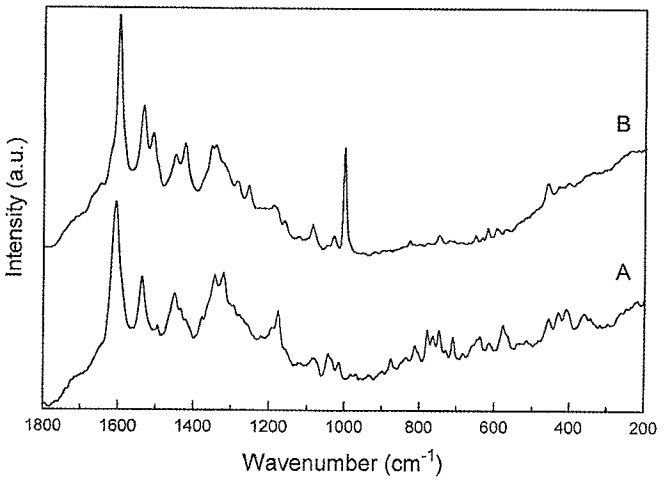

Figure 10. Raman spectra of dragons blood resins from different periods (A) i.e. *Dracaena cinnabari* resin and (B) *Daemonorops draco*

archive (Figure 7). The difference in the spectra is Significant and the presence of sharper protein features in the 19th Century specimen is striking; perhaps, the most significant spectral feature possessed by Stephenson's hair, however, is that of the ν (S-S) stretching mode near 500 cm^{-1} which has disappeared from the archaeological specimen. Other features in the Raman spectrum of Stephenson's hair are ascribed to proprietary additives and cosmetics in use at that time.

A unique specimen of an eye-bead from an Egyptian 18th Dynasty cat mummy (Figure 8) was believed to be either amber or brown glass; it was neither, as the Raman spectrum shows – the eye-bead spectrum is characteristic of keratin and is closely matched with that of a claw or horn, which suggested the possibility of a hitherto unrecognised

funerary practice was perhaps being operated (Figure 9) [9].
Other tissues investigated by Raman spectroscopy include teeth, bone and nail; for all of these, evidence of ancient practices and preservations are forthcoming. An ancient Brazilian *tembeta* or lip-plug made of organic material is believed unique and Raman spectroscopy has assisted in the identification of the resin in its construction for restoration purposes [10]. The presence of haematite on 3000 year-old skeletal remains ("ochred bone") has also indicated the adoption of ancient funerary technology from the Raman microscopic identification of key spectral biomarker features [11].

Resins and Sourcing of Materials
Dragon's blood resins have been used in decorative arts and medicine for two thousand years; initially coming from an East-African source on the island of Socotra, the *Dracaena cinnabari* resin gives a significantly different spectrum (A in Figure 10) from that of an alternative source, *Daemonorops draco* used since the Middle Ages. The use of Raman spectroscopy as a botanical discriminator aids the geographical sourcing of ancient resins on artefacts which can provide the archaeologist and art historian with novel information about ancient trade routes and cultures.
The *Mary Rose* (Figure 11) flagship of King Henry VIII's navy, was sunk in the English Church in 1545 with the loss of 345 lives in an engagement with a French naval force. Excavation of the wreck has revealed much information about Tudor life. The surgeon-barber's medicine chest contained several sealed ceramic jars and wooden containers for inorganic and organic molecules used for medicinal potions and for the treatment of wounds. Raman analysis of several of these correspond with known texts of *materia medica* of the 16th Century and can be attributed to aromatic resins such as frankincense and myrrh. Inorganic materials found include gypsum, carbon, sulfur and haematite.

Wall-paintings/frescoes.
The damage caused by lichen hyphal penetration of mediaeval and Renaissance artwork can be illustrated by the wall paintings in ancient churches in Spain – where damage to the 14th Century artwork has been attributed to lichen colonisation, despite high concentrations of lead, antimony and mercury in the mineral pigments of the wall-paintings. Lichens have successfully invaded the artwork and caused problems for archaeologists responsible for their preservation. Although the integrity of the substrate has been compromised it is clear that Raman spectroscopic analysis have identified areas most "at risk" from the biosignatures of lichen chemicals present – hence the analyses represent an *early warning* method for conservators. An interesting point relates to the hierarchical use of expensive pigments in mediaeval artwork; at Basconcillos del Tozo, *cinnabar* was used for Christ and *lapis lazuli* for the Virgin Mary whereas St. Peter was painted in *minium*.
In the Palazzo Farnese, a 16th Century palace at Caprarola some 60 miles North of Rome, the frescoes painted in 1560 by Zuccari are very significantly damaged by the invasion of aggressive lichen colonies of *Dirina massiliensis* forma *sorediata*, an organism which can produce up to 50% of its biomass as hydrated calcium oxalate. With some 80% of the paintings covered by lichen, Raman analyses have indicated that approximately 1 kg of calcite substrate per sq. metre has been converted into fragile calcium oxalate, so destroying the platform on which the artwork is based. Raman analytical studies on cored samples have also shown that lichen hyphae are present up to 10 mm inside the basal calcite – hence, mere removal of surface growths for restorative procedures will not cure the problem.

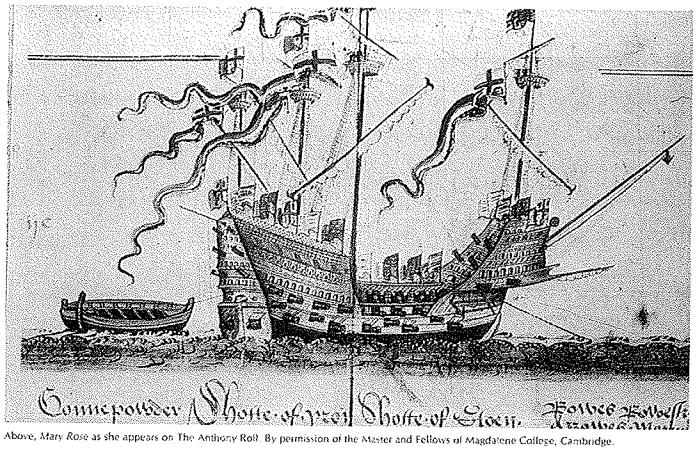
Above, Mary Rose as she appears on The Anthony Roll. By permission of the Master and Fellows of Magdalene College, Cambridge.

Figure 11. Mary Rose

Conclusions

The use of analytical Raman spectroscopic techniques for the non-destructive characterisation of a range of archaeological artefacts has provided some novel information for art historians and suggested the use of ancient

technologies for the production and treatment of materials and skeletal remains. The advantages of the molecular spectroscopic identification of minerals, resins and additives proves to be a powerful addition to analysts working at the interfaces of art history, museum science, chemistry and biology. In particular, curators and archaeological conservators are alerted to the need for directed conservation of specimens and artworks at risk from environmental damage in the preservation of cultural heritage from the identification of key spectral biomarkers ascribed to hyphal penetration of wall paintings at risk from stressed environmental changes.

Acknowledgements

Manchester Museum, National Museum of Scotland, National Maritime Museum, Greenwich, The London Museum, Maritime Museums of Merseyside, Liverpool, Humberside Museum, Metropolitan Museum of Art, New York, Museum of Archaeology and Ethnography, Sao Paulo, Textile Conservation Centre, Winchester, National Museum of Denmark, Copenhagen, The Queensland Museum, Brisbane.

References

1. Edwards, H.G.M., and Chalmers, J.M., eds., Raman Spectroscopy in Art History and Archaeology, Royal Society of Chemistry, London in press (2005).

2. Davy, H, "Some experiments and observations on the colours used in paintings by the Ancients", Phil. Trans. Roy. Soc. London (1815) **105,** 97-114.

3. Eccles, H., and Rackham, B., Analysed Specimens of English Porcelain, V & A Museum, London (1922).

4. Edwards, H.G.M., "Artworks Studied using IR and Raman spectroscopy", in Encyclopaedia of Spectroscopy and Spectrometry, eds. Lindon, J.C., Tranter, G.E., and Holmes, J.L., Academic Press, London (1999), pp. 2-17.

5.Ciliberto, E., and Spoto, G., eds., Modern Analytical Methods in Art and Archaeology, Chemical Analysis Series, J. Wiley and Sons, Chichester (2000) **155.**

6. Edwards, H.G.M., "Forensic Applications of Raman Spectroscopy to the Nondestructive Analysis of Biomaterials and their Degradation", in Forensic Geoscience : Principles, Techniques and Applications, eds. K.Pye and D.J.Croft, Geological society Special publication No. 232, Geological Society, London, (2004) pp. 159-170.

7. Petersen, S, Faurskov Nielsen, O., Christensen, D. H., Edwards, H.G.M., Farwell, D.W., David, A.R., Lambert, P., Harth Hansen, J.P., and Wulf, H.C. J. Raman. Spectroscopy, **34**, (2003), 375-379 .

8. Edwards, H.G.M., Wilson, A.S., Farwell, D.W., Janaway, R.C. J. Raman. Spectroscopy, **30**, (1999), 378-383.

9. Edwards, H.G.M., Farwell, D.W., Heron, C.P., Croft, H., David, A.R., J. Raman. Spectroscopy, **30**, (1999), 139-146.

10. de Faria, D.L.A., Edwards, H.G.M., Afonso, M.C., Brody, R.H., Morais, J.L. Spectrochimica Acta, Part A, in Press (2004).

11. Edwards, H.G.M., Farwell, D.W., de Faria, D.L.A., Monteiro, A. M.F., Afonso, M.C., de Blasis, P., Eggers, S. J. Raman. Spectroscopy, **32**, (2001), 17-22.

The use of a Mobile Raman Spectrometer for in Situ Analysis of Objects of Art

Peter Vandenabeele and Luc Moens
Ghent University, Laboratory of Analytical Chemistry, Proeftuinstraat 86, B-9000 Ghent (Belgium)

Abstract

Raman spectroscopy is becoming increasingly important as an analytical tool for the investigation of objects of art. This is clearly illustrated by looking at the number of publications on this subject. Moreover, several important museums recently purchased a commercial Raman spectrometer for their investigations, hoping to solve a diversity of their problems.

Raman spectroscopy enables the non-destructive molecular analysis of objects of art, antique as well as modern. Mobile Raman instrumentation is a way to investigate artefacts without the need of sampling, nor expensive and risk full transportation of the artefact to the laboratory. Moreover, by using mobile equipment, one instrument can be shared by multiple museums.

However, a commercial mobile Raman spectrometer is often not fully adapted to the specific needs of people working in the field of art analysis and several alterations have to be made. When someone wants to be able to investigate *in situ* different types of artefacts (ancient as well as modern, wall paintings, easel paintings, manuscripts, polychrome sculptures, etc..) this idea of flexibility has to be incorporated in the design of the instrumentation and the software. Suitable (micro-) positioning equipment is required and should be adapted to the specific task that has to be undertaken.

Introduction

During the last decades, due to instrumental improvements Raman spectroscopy became accessible to research groups, performing molecular analysis in different domains, such as pharmaceutical analysis, semiconductor research, geological applications, biochemistry, etc. [1]. This evolution made that the instrumentation became available as well for other applications, such as art analysis. Recently, an increasing number of research groups are experiencing the advantages of applying Raman spectroscopy for the molecular investigation of art and antiquities [2]. Results have been presented in areas as, among others, pigment analysis of wall paintings, manuscripts, easel paintings, glass and porcelain analysis, biomaterials (such as resins and binding media), corrosion products, etc.

By using Raman spectroscopy for the investigation of antiquities and precious art objects, it is of high importance to minimise the (risk of) damage of the artefact. Different approaches have been proposed, including the use of a gentle microsampling method [3]. Another opportunity is performing direct Raman analysis on the artefacts. Small objects can easily be positioned on the microscope table of a Raman microscope. Results have been published on the Raman analysis of porcelain cards [4] and on the investigation of glazed medallions [5]. Another approach consists of the use of a tilted microscope, which allows positioning the artefact in front of the microscope [6, 7]. Examples have been published on the use of fibre optics instrumentation for Raman investigations [8]. Opposite to the use of commercial instruments, we present here a dedicated instrument that was constructed for art investigation.

Experimental

These investigations were performed with a mobile Raman instrument (Mobile Art Analyser – MArtA), which was developed and optimised for art analysis [9]. The core of the instrument is a modified Portable Raman imaging microscope (PRIM) spectrometer (Spectracode Inc., West Lafayette, IN, USA), which is based on a SpectraPro-150i 150 mm spectrometer and a charge-coupled device (CCD) detector (Roper Scientific/Princeton Instruments). The 785 nm diode laser (Process Instruments Inc., Salt Lake City, UT, USA) has an adjustable output power up to 300 mW. The probe head is equipped with an infinity corrected objective lens and a digital colour camera for focusing and is connected to the laser and spectrometer unit with optical fibres. The probe head can be mounted on different posts and stands in order to align it with the surface under study.

Results and discussion

MArtA (Mobile Art Analyser) is a mobile instrument that was developed for *in situ* analysis of museum objects [9]. The weight of the instrument is ca. 30 kg and it is packed in an aluminium suitcase, which protects it during transport. Depending on the situation and the artefact, the probe head may be mounted on different stages and posts. This allows the stable positioning and focussing of the laser beam on the artefact, although – by having different macro-positioning systems (a post, an articulating arm or a large translation stage) – there is sufficient flexibility in the instrumental set-up to allow the investigation of different types of artefacts. All macro-positioning systems have to be combined with a micro-positioning system (motorized or not) to allow fine- tuning and focussing. The system is equipped with a colour camera, which allows visualisation of the area under examination. A fibre optic ringlight is used as a white light source to illuminate the sample, avoiding local heating, which is not desirable for art objects. An overview of the instrumental set-up as used for direct analysis of manuscripts is given in figure 1. In this set-up a vertical post was selected to mount the manual micro positioners. By introducing a rotational stage, it is possible to tilt the probe head to stay perpendicular to the parchment. This way, the manuscript

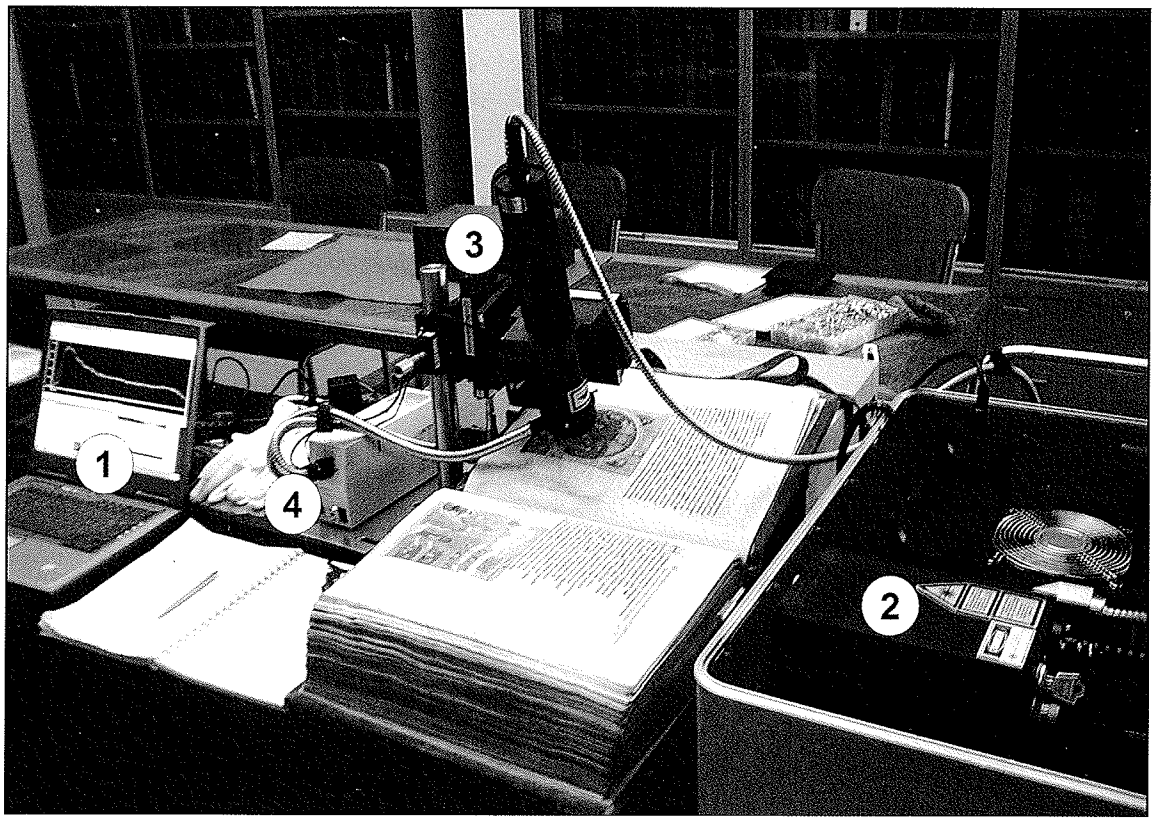

Figure 1. The Mobile Art Analyser (MArtA) set up in the library of Ghent University, during direct analysis of a mediaeval Mercatellis manuscript. 1: notebook computer that is connected to the spectrometer by USB coupling; 2: mobile spectrometer with the diode laser mounted on top; 3: probe head mounted on a vertical post and micro positioners to enable focussing on the manuscript; 4: fibre optics coupled white light source for visualisation of the area under examination.

is not damaged by flattening the pages.
Although the first experiments of this instrument are still being performed, some remarks mainly on the interaction between museum people and the scientific staff may be made yet. An important motive for this project is the existence of several small museums: opposite to the situation in a large museum, it is an advantage to have mobile equipment, which can be moved between the different museums. In these small museums, often the scientific staffs are minimal, pointing to the duty of the (external) scientist to explain the possibilities and limitations of the technique. This is of importance, as the conservation scientist should be aware what to expect from this research. Often they seem to expect to receive results from the experiments immediately. Moreover, recording a high quality spectrum from an artefact, may take some time, which is often limited when working directly on the artefacts; when working on samples, the time that the analyst can spend is less restrictive. Moreover, working conditions are often

far away from the optimal laboratory conditions: e.g. the presence of stray light is often hard to exclude and the stability of the floor (e.g. the parquet floor in a historical building) also determines the quality of the focussed laser beam.

Conclusion

In this work a mobile Raman instrument has been presented, along with an overview of some pitfalls when bringing the instrumentation in the museum environment. In the design of the instrument, rigidity and stability has been incorporated, but on the other hand flexibility in positioning systems is even so necessary. Although the advantage of being able to perform direct investigations of art objects is undoubted, there are some pitfalls that scientists as well as museum people should be aware off, when starting with this research.

Acknowledgements

The MArtA project was financially supported by the Flemish Government (Department of culture; 'museumdecreet'). P.V. is especially grateful to the Fund for scientific research – Flanders (F.W.O.-Vlaanderen) for his postdoctoral fellowship.

References

1. I.R. Lewis and H.G.M. Edwards (Eds.), Handbook of Raman Spectroscopy, from the research laboratory to he process line, Dekker, 2001.

2. P. Vandenabeele and L. Moens (Eds.), International conference on the application of Raman spectroscopy in art and archaeology, Book of abstracts, Story Scientia, Ghent, 2003.

3. Peter Vandenabeele, Bernhard Wehling, Luc Moens, Brigitte Dekeyzer, Bert Cardon, Alex von Bohlen, Reinhold Klockenkämper, Analyst, 1999, 124, 169-172.

4. P. Vandenabeele, L. Moens, Micro-Raman spectroscopy applied to the investigation of art objects, In: D.L. Andrews, T. Asakura, S. Jutamulia, W.P.Kirk, M.G. Lagally, R.B. Lal, J.D. Trolinger (Eds.), Proceedings of SPIE Vol.4098, Conference proceedings Raman spectroscopy and light scattering technologies in materials science/ the International symposium on Optical science and technology, San Diego (2000), 301-310.

5. A. Derbyshire and R. Withnall, J. Raman Spectrosc. 30, 185-188 (1999).

6. M. Bouchard, D.C. Smith, in: GeoRaman '99 – 4th International conference on Raman Spectroscopy applied to the earth sciences, June 9-11th 1999, Valladolid (Spain), GeoRaman '99 Abstracts. Special publication, Universidad de Valladolid press: Valladolid, 1999; 31.

7. D.C. Smith, Techne Sci. Serice Hist. Art Civil. 2000; 11, 69.

8. P. Vandenabeele, F. Verpoort and L. Moens, Journal of Raman Spectroscopy 2001, 32; 263-269.

9. P. Vandenabeele, T.L. Weis, E.R. Grant, L.J. Moens, Anal. Bioanal. Chem. 379 (1), 137-142 (2004).

Identifying and Localizing Proteinaceous Compounds in Paint Samples using Reflection Infrared Spectroscopic Techniques

Annelies van Loon and Jaap J. Boon
Molecular Painting Research Group, FOM Institute AMOLF, Kruislaan 407, 1098 SJ Amsterdam, The Netherlands.

Abstract

Several reflection infrared spectroscopic techniques were employed for spatial resolved and in-situ analysis of proteinaceous layers in paintings and polychrome sculpture. Layer separation for conventional analysis with GC-MS, DTMS, HPLC or normal transmission FTIR was not possible in these cases as the layers were too thin. We were capable of identifying thin, proteinaceous intermediate layers in paint cross-sections using Specular Reflection imaging. Reflection-Absorption and Attenuated Total Reflection were successfully applied for measuring thin proteinaceous surface layers. Usability and limitations of the three reflection techniques are being evaluated.

Introduction

Proteinaceous materials were widely used both as a binding medium and isolation layer in old master paintings and polychrome sculpture. Furthermore, they were and still are being used as restoration material, e.g. as consolidant, lining material or varnish. Several mass-spectrometric and chromatographic techniques, such as High Performance Liquid Chromatography (HPLC), Gas Chromatography - Mass Spectrometry (GC-MS), Direct Temperature resolved Mass Spectrometry (DTMS), are nowadays available to characterize proteins and amino acids in paint samples. [1] When analyzing very thin layers, however, these methods are limited due to the difficulty in separating or isolating the layer from the rest. Infrared Spectroscopy may offer more opportunities in these cases. First of all what makes FTIR a strong technique in characterizing proteins in aged materials is that one looks at the backbone structure of the peptide, the so-called peptide bond: R-(CO)-(NH)-R. This backbone structure is relatively stable in contrast to (some of) the individual amino acids that are analyzed with the chromatographic techniques where the sample is hydrolyzed to break up the peptide bonds and the amino acids are separated and detected by mass spectrometry or fluorescence. A second important advantage of Infrared Spectroscopy is that it can be used as a 2D-imaging technique and non-destructively, in contrast to mass-spectrometric and chromatographic methods where the sample material is sacrificed. Unfortunately, FTIR cannot make a distinction between the different proteins used in painting materials such as collagen (skin glue, fish glue, bone glue), egg (egg glair or whole egg) and casein.
This paper is about the analysis of thin proteinaceous layers using several FTIR techniques in order to get spatial or in-situ information: Specular Reflection (SR) imaging, Attenuated Total Reflection (ATR) and Reflection-Absorption (RA) infrared analysis. [2] The case studies described in this article comprise proteinaceous intermediate layers and varnish layers measured in paint cross-sections with SR imaging FTIR. A unique case of a thin protective coating on silver leaf gilding could be measured with RA FTIR, the silver acting as an internal reflecting substrate. Finally, the potential of ATR for surface measurement is being explored.

Material and Experimental

Samples and sample preparation
The samples are listed in the table below. The paint cross-sections (samples A to D) were embedded in Technovit 2000 LC, which is a 1-component methacrylate that polymerizes under visible blue light. After first grinding with silicone carbide (SiC) paper, the surface was dry polished with Micro-Mesh Sheets. This polishing step turned out to be crucial for successful Specular Reflection analysis of paint cross-sections. Attenuated Total Reflection and Reflection-Absorption measurements were done directly on the sample surface and did not require any further sample preparation (samples E to I).

FTIR instrumentation
FTIR analysis was performed on a Bio-Rad FTS-6000 FTIR spectrometer extended with a Bio-Rad UMA-500 IR Microscope (nowadays Digilab, Cambridge, MA, USA) and a single-point Mercury Cadmium Tellurium detector (4000-650 cm^{-1} range). The selected sample was applied onto a Graseby Specac P/N 2550 diamond cell (Graceby Specac, Orpington, Kent, UK) and analyzed in transmission mode. An empty diamond cell was used as background.

Specular Reflection

#	*Sample*	*Object*	*Artist + Date*	*Location*	*Additional*
A	*blue glaze on silver*	Altarpiece: Annunciation scene – polychrome wooden sculpture of the Virgin Mary (sample from the blue lining of her mantle)	Phillip Dirr 1617-1621	Freising, *Erzbischöfliche Kapelle des Kardinal-Döpfner-Hauses*	*SEM-EDX*
B	*carnation (flesh paint)*	Francis-Xavier Altarpiece: polychrome wooden sculpture of St. Isidor (sample from the head)	Ignaz Günther ±1765	Rott am Inn, former *Benediktiner-Abteikirche und Kath. Pfarrkirche St Marinus und Anianus*	*SEM-EDX*
C	*blue polychromy*	Wooden chandelier with painted porcelain surface imitation	J.Th. Sailler 1762	Pagodenburg in Nymphenburg Castle	
D	*varnish*	Painting: *Les Alyscamps* (Falling leaves), KM224	V. Van Gogh 1888	Kröller Müller Museum Otterloo	*Transmission FTIR; DTMS*

Reflection-Absorption

#	*Sample*	*Object*	*Artist + Date*	*Location*	*Additional*
E	*coating on silver*	Polychrome wooden sculpture of St. Stanislaus Kostka, belongs to a group of 4 sculptures (together with St. Aloysius Gonzaga and two Moorish Boys) (sample from the red costume)	18th Century	Landsberg am Lech, *Jesuitenkirche Hl. Kreuz*	
F	*egg glair coating on silver*	Reconstruction provided by Mark Richter 2002			

Attenuated Total Reflection

#	*Sample*	*Object*	*Artist + Date*	*Location*	*Additional*
G	*lining material*	Painting: Moses brought to Pharoah's Daughter Lined in 1832 in London	William Hogarth 1746	Tate Gallery London	*Transmission FTIR; DTMS*
H	*varnish*	Fragment of a painting of a Church Interior	J. Bosboom ±1850	Rijksmuseum Amsterdam	*Transmission FTIR*
I	*chalk/glue ground*	Testpanel			

Table 1 Description of the samples

Reflection-Absorption spectra of the silver glazes were recorded in reflection mode. A zinc selenide (ZnSe) window was used as a background for reflection-absorption. A Bio-Rad slide-on ATR accessory fitted with germanium single crystal was connected to the microscope objective for ATR measurements. The sensing surface is approximately 1 mm in diameter; beam penetration depth is in the order of 1 µm. The sample is brought in close contact with the crystal and than measured in reflection mode. Ethanol was used to clean the crystal after measurement. All single point spectra were recorded at 4 cm^{-1} spectral resolution, an undersampling ratio (UDR) of 2 and a mirror speed of 5 kHz. 100 spectra were accumulated to increase Signal to Noise ratio (S/N). Data were processed using Win-IR Pro 2.5 software of Bio-Rad.

Specular Reflection FTIR imaging data were acquired using a FTS Stingray 6000 system. It combines the above-mentioned spectrometer and microscope and a MCT detector (4000-1000 cm^{-1} range), which is a 64 x 64 pixels MCT Focal Plan Array system (Santa Barbara Focal Plane, California, USA). Images of the paint cross-section in a 400 x 400 µm area were recorded simultaneously at every mirror position of the step-scan interferometer with a spatial resolution of 6-7 µm. Imaging spectra were recorded at 16 cm^{-1} spectral resolution, an undersampling ratio (UDR) of 4 and a mirror step rate of 1 Hz. The step distance of the interferometer at UDR 4 was 1.266 µm. Approximately 500 interferosteps were needed to obtain the spectral resolution of 16 cm^{-1}. The low step rate (1 Hz) allows the frame grabber board in the camera to average 200 images during each step, leading to a high S/N. A zink selenide (ZnSe) window was used for calibration and background. The resulting data set contained 4096 interferograms, one for every pixel in the FPA. Further data processing was done using Bio-Rad Win-IR Pro software. The Kramers-Kronig transformation was applied to transform the specular reflectance spectra to absorbance-like spectra. Analytical results of the imaging FTIR technique are displayed as infrared spectra and false color images. Every spot or pixel in the cross-section image contains an infrared spectrum. A false color or gray-scale plot shows the intensity distribution of a specific absorption band on the cross-section surface.

Results

Thin intermediate layers

In the cross-sections A, B and C taken from polychrome sculptures and examined with specular reflection proteinaceous intermediate layers were discerned. The intermediate layer in cross-section A of the blue glaze on silver was 15-20 µm thick and was applied on top of a silver leaf gilding and below a thick blue smalt glaze. The function of this layer is to prevent the silver from tarnishing and it serves as an isolation or adhesive layer in order to increase the adhesion of the paint layer applied above it. [3] The imaging data of cross-section A are displayed in Fig. 1. An area of 400 x 400 µm of the cross-sectional surface was measured with specular reflection. A characteristic absorption peak of the embedding material is usually plotted to outline the position of the cross-section, see Fig. 1B. The IR spectrum that represents a spot (pixel) in the transparent intermediate layer contains peaks that are characteristic of proteinaceous material: a broad N-H stretch band at 3300 cm^{-1} and the combination of two strong, narrow bands at 1650 cm^{-1} and 1547 cm^{-1} of respectively the C=O stretch (amide I) and N-H bending (amide II) vibration, see Fig. 1D. The presence of nitrogen was confirmed by SEM-EDX. The amide I band at 1650 cm^{-1} is imaged in Fig. 1C: the white stroke is where the amide band is intense and corresponds with the intermediate layer. Another application of a thin intermediate proteinaceous layer was found in cross-section B of a carnation (flesh paint) sample (see Table 1). In this case the layer was just 8-10 µm thick and was in between the white preparatory layers and the flesh paint layer. Although the reason for this isolation layer is not entirely clear, it has been suggested that high gloss flesh paint was obtained in this way. [3] A transparent layer of about 100 µm was found between the original polychromy and the later additions in cross-section C of a chandelier (see Table 1). The image data gave evidence for proteins, so it can be stated that this layer is not an original lacquer as was suspected, but, instead, must be a restoration material, possibly animal glue used as consolidant.

Questions on the composition of the varnish (sample D) arose during cleaning tests on a painting by Van Gogh *Les Alyscamps*. The composition of the varnish layer was analyzed by FTIR transmission and DTMS on isolated sample

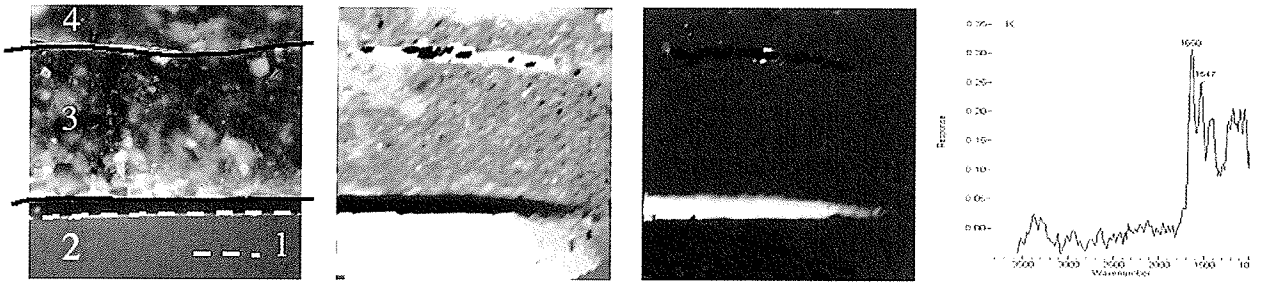

Fig. 1 Specular Reflection imaging data of cross-section A of a blue glaze on silver leaf from a polychrome sculpture:
A. Light microscopic image, layer build-up: 0 embedding resin, 1 silver gilding (= white dashed line), 2 proteinaceous intermediate layer, 3 thick blue smalt-containing glaze, 4 later overpaints
B. Map of 1727 cm^{-1} absorption band of Technovit (white= high intensity, black= low intensity; dimensions= 400 x 400 µm).
C. Map of 1650 cm^{-1} absorption band of Amide I.
D. Specular reflection FTIR spectrum that represents a spot in the proteinaceous intermediate layer.

material. The FTIR transmission spectrum, see Fig. 2G, shows a mixture of natural resin, proteins and carbohydrates. DTMS analysis under EI conditions gave evidence for mastic and under CI conditions for carbohydrates. Proteins were not detected by DTMS. Specular Reflection analysis of cross-section D, however, not only gave information on the composition of the varnish, but also on the location of the different components within the varnish (see Fig. 2A-F). Now it became clear that remnants of a protein and carbohydrate mixture were present on the paint surface, sitting in the interstices of the impasto paint and originating from an old restoration, probably a facing from the lining procedure. A mastic varnish was applied on top. A new cleaning strategy can now be sought that takes into account that the varnish layer consists of three components with different chemical behavior.

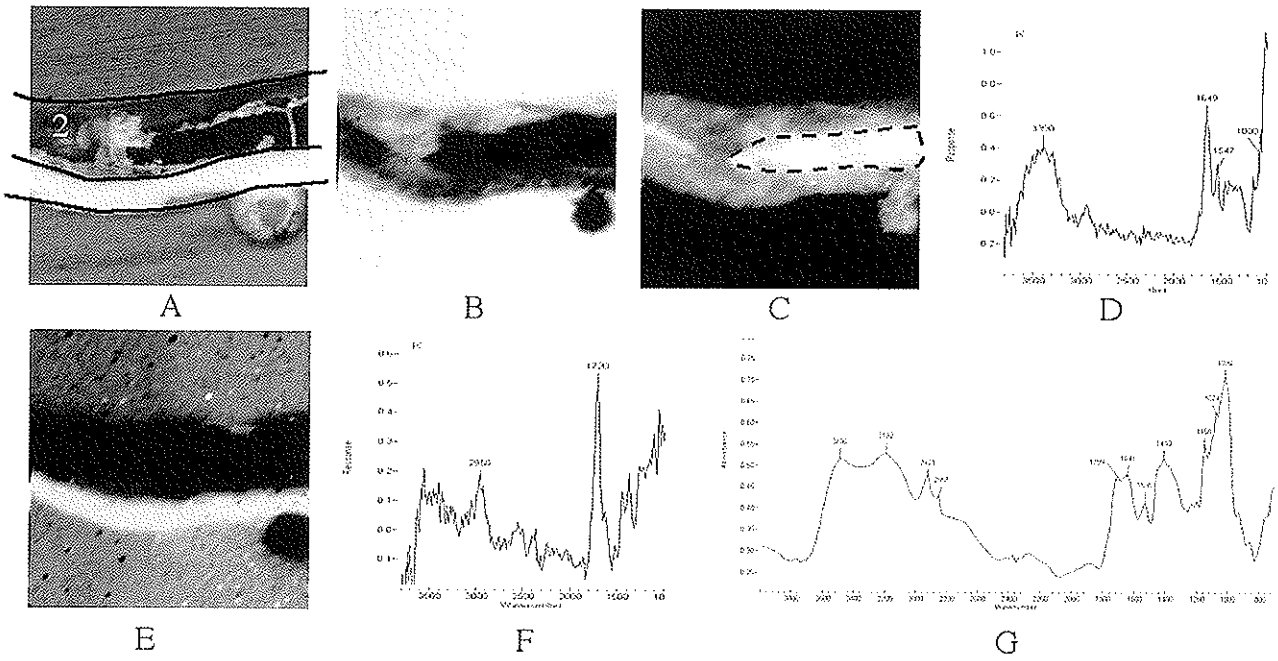

Fig. 2 Specular Reflection imaging data of cross-section D of Van Gogh's Les Alyscamps (1888):
A. Light microscopic image, layer build-up: 0 embedding resin, 1 yellow paint layer, 2 thick brown varnish layer, 0 embedding resin.
B. Map of 1727 cm^{-1} absorption band of Technovit (white= high intensity, black= low intensity; dimensions= 400 x 400 µm).
C. Map of 1649 cm^{-1} absorption band of Amide I, concentrated in area indicated by dashed line.
D. Specular reflection FTIR spectrum that represents a spot in the varnish layer that contains proteins and carbohydrates.
E. Map of 1020 cm^{-1} absorption band of sulfo/chromate in yellow paint layer.
F. Specular reflection FTIR spectrum that represents a spot in the varnish layer that contains natural resin (mastic).
G. Transmission spectrum of the varnish.

Thin protective coating on silver

The fact that silver can act as an internal mirror in samples of thin coatings on silver gilded polychrome sculpture offered the potential to analyze the coatings by reflection-absorption (samples E and F). A paint chip was positioned under the IR microscope and a silver area that was not covered by the red glaze and exposed the transparent protective coating was selected and recorded, see Fig. 3A. [3] A reference spectrum of a reconstruction of an egg glair coating on silver leaf is plotted in Fig. 3B. The thickness of the coatings is about. 5 µm. In both spectra the protein features are clearly recognizable. The IR beam is transmitted through the sample, reflected by the silver surface that acts as a mirror and transmitted through the sample again. This makes reflection-absorption comparable with normal transmission spectra. Theoretically one would also expect an interference of specular reflection, but the contribution of this in relation to absorption is apparently so low, that specular reflection peaks are not visible in the spectrum.

ATR surface measurements

The lining material was measured with ATR, directly on a piece of the lining (sample G). Transmission FTIR and DTMS (under EI and CI conditions, see table 1) were performed on isolated sample material. The ATR spectrum and transmission spectra are displayed in Fig. 4A and B. Both transmission and DTMS point to the use of a proteinaceous lining adhesive, DTMS being even more specific as amino acid markers for animal glue are present in

the mass spectra. No carbohydrates (from the paste/starch) were detected. ATR gives similar information as shown in Fig. 4A. The amide I and II bands are clearly present in the spectrum. The absorption bands characteristic for proteins at a higher wave number (shorter wavelengths) are less pronounced in the ATR spectrum. This applies to the N-H stretch band at around 3300 cm^{-1} and the shoulder at around 3080 cm^{-1}, the latter being attributed to an overtone of the N-H bend in the literature. [4] But this is inherent to the ATR technique, because longer

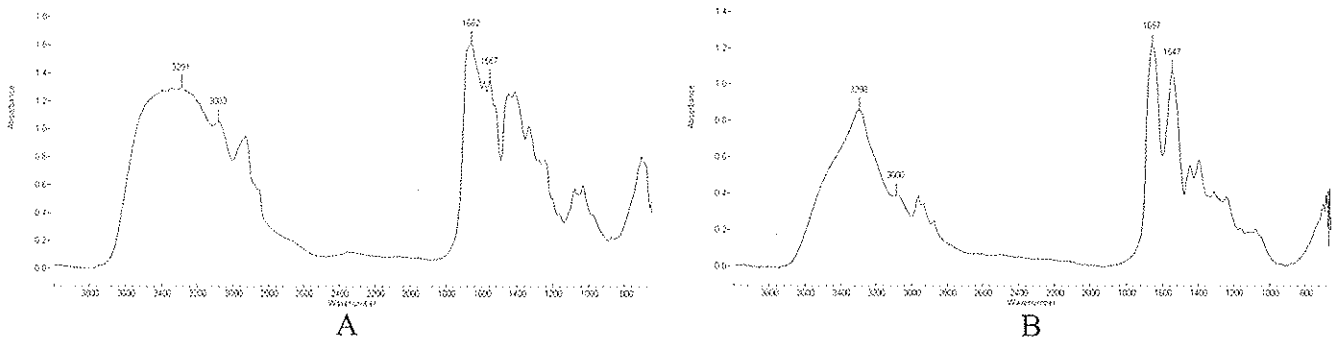

Fig. 3 Reflection-Absorption FTIR:
A. Reflection-Absorption FTIR spectrum of protective coating on silver (sample E).
B. Reflection-Absorption FTIR spectrum of egg glair coating on silver (sample F).

wavelengths penetrate deeper in the surface. The lining example shows that ATR can work quite well for protein analysis, especially in the case of a flexible substrate, which facilitates a good contact with the ATR element, and when there is no interference of inorganic pigments.
The ATR measurements on the rigid paint substrates were not so straightforward to interpret (sample H and I). The surface coating of a fragment of a painting, a Church Interior by J. Bosboom, that serves as a study object in our lab was measured with ATR in a few spots. It was difficult to make good contact and, with our instrumentation, where we cannot view through the ATR element, to estimate how deep the ATR crystal is pressed into the surface. Proteinaceous features are still recognizable in the spectra, but the intensity of the absorption peaks of the proteins is a factor of 10 less than with the lining sample, resulting in noisy spectra. Sample I, a test panel prepared with a typical chalk/glue ground, served as an example of a mixture of organic and inorganic materials. The question was whether the glue component could still be detected with ATR when present in a mixture. Several spots were measured but every time only peaks characteristic of chalk showed up in the spectrum, e.g. the intense broad 1404 cm^{-1} and sharp 872 cm^{-1} carbonate peaks. No trace of protein could be observed in the spectrum. Beyond the contact issue, there are a couple more factors to consider here that have contributed to the exaggerated presence of the carbonate bands in the spectrum and the evaporation of the peptide bands from the IR spectrum. It followed from

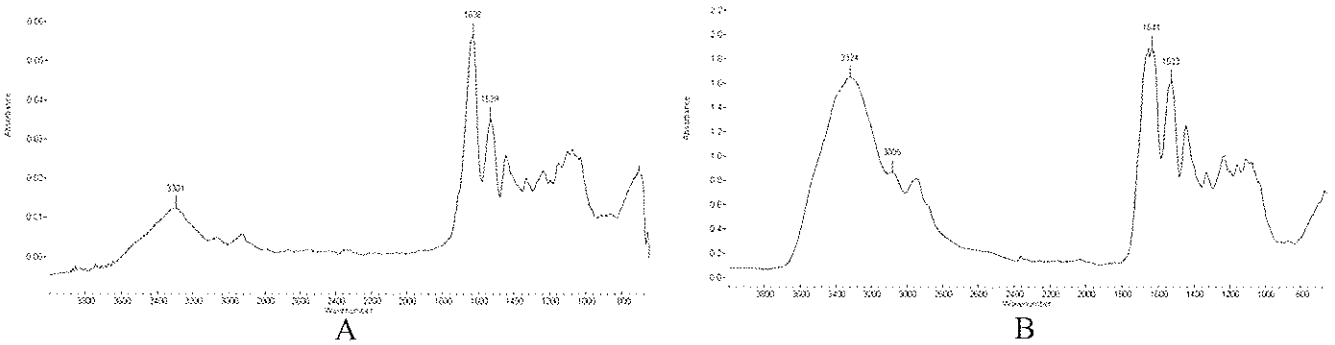

Fig. 4 Attenuated Total Reflection experiments:
A. ATR FTIR spectrum of lining material (sample G).
B .Transmission FTIR spectrum of the same lining material (sample G).

the spectra that the highest absorption signal of chalk in the mixture was already 10 times higher than that of pure glue. Add to this another factor of 20 due to the relative higher amount of chalk present in the ground mixture, a typical w/w chalk: glue ratio is about 20 : 1. Then it is not so surprising any more that the chalk peaks were overestimated in the ATR spectra.

Discussion and conclusions

The case studies that are described in this paper are showing that the nature of sample material available is the decisive factor for the analytical approach. We have seen that at least the overall spectral pattern of the amide backbone of proteins is similar for the different reflection methods compared to normal transmission FTIR. There are however slight differences in band position, intensity and peak resolution. Usability and limitations of the three reflection techniques for identifying and localizing thin proteinaceous layers will be evaluated in this section.

Specular Reflection imaging FTIR
Specular Reflection in combination with mapping has shown its capability for the analysis of paint cross-sections. The technique is often used in combination with other analytical mapping techniques that supplement each other. [5] In the given examples it was successfully applied for the identification and localization of thin proteinaceous intermediate layers in cross-section where other conventional techniques failed due to the difficulty of isolating these layers (sample A to D). IR spectra show the characteristic pattern of the amide backbone of the proteins. The prepared cross-sections required some extra polishing prior to analysis in order to obtain a plane surface. Wet polishing should not be used as the water (or other solvent) washes out the softer, organic materials from the paint cross-section due to erosion or causes swelling of the layers. Therefore the cross-sections were dry-polished to produce a good reflecting surface with all the layers in the same level. Our FTIR system allows for a spatial resolution of 6 to 7 µm. More advanced systems, at date, can go up to a resolution of 4 µm. This does not need to be a problem for thinner layers, because the sample can be polished under an angle to increase the exposed surface area. Comparison of the transmission and reflection FTIR data of the varnish on the Van Gogh painting clearly illustrates the additional spatial information obtained by SR imaging (sample D). So far, we have not been successful with identifying proteins when used as binding medium mixed with inorganic pigments. This is largely due to the lower reflectance of organic materials compared to inorganic pigments with higher refractive indices, the lower content of organic material present (at the surface) in those kind of mixtures and, probably most important, scattering within the sample complicating the reflection spectrum. [6]

Reflection-Absorption FTIR
Absorption-Reflection spectra are most useful for thin coatings on metal surfaces. The thin proteinaceous coating present on the silver gilding of the polychrome sculpture provided a nice illustration of the applicability of this technique, because the silver acts as a reflecting mirror (sample E). Attempts to separate the protective coating from the gilding (and underlying bole and ground layers) were not successful. The advantages of the reflection-absorption technique here were that in fact no sample separation was required and that the (proteinaceous) materials used in the bole and ground layer could not interfere in the spectrum. As the IR beam passes twice through the sample in a reflection-absorption experiment, thinner sample films (up to approx. 10 µm) are required than in normal transmission. The spectra generated in this manner resemble however those that would be obtained from normal transmission. Surface irregularities resulted in spectral distortions, so a smooth and level film spot should be positioned under the IR microscope. Reflection-absorption spectra may contain a specular reflection component if the surface of the sample is shiny, so that some of the radiation is reflected from the front surface of the sample rather than from the mirror. But in the examined cases of silver coatings no interference of specular reflection bands was observed in the spectra. This shows again (see the last paragraph) a highly polished surface is necessary for successful SR analysis.

Attenuated Total Reflection FTIR
ATR definitely shows potential as a surface sensitive analytical technique to measure directly on a paint surface or cross-section, so little to no preparation is required. Only the surface of the sample is analyzed since the beam penetrates just a few micrometers into the sample. The sampling depth depends on differences in the refractive indices between the sample and the ATR element and on the incidence angle. An ATR correction implanted in the processing software can be used to correct for the relative lower beam penetration (and consequently lower absorption signal) at higher wave numbers (∞ shorter wavelengths). We have seen that achieving intimate optical contact of the sample with the ATR crystal is extremely critical for successful ATR analysis. The flexible lining material produced much better quality spectra and higher absorption peaks than the hard and stiff surface coating of the painting fragment, as in the first case a better contact and more uniform pressure could be obtained. Also the positioning of the ATR element can be critical, but new technologies may solve this problem. Video systems are

nowadays available that allow the analyst to view through the ATR element of the ATR accessory in order to observe sample positioning and contact with the ATR element. More ATR experiments are planned in the near future in order to get a better understanding of its applicability to surface measurements directly on paintings.

Acknowledgements

The collaboration with Mark Richter and Michael Kühlenthal (Bayerisches Landesamt für Denkmalpflege, München) in the research project "Historical Polychromy" is highly appreciated. The samples of the polychrome sculptures were examined as part of this project. Inga Pelludat (Bayerische Verwaltung der staatlichen Schlösser, Gärten und Seen, Restaurierungszentrum München) provided the sample of the chandelier, Stephan Hackney (Tate Gallery London) the lining material and Luuk Struick van der Loeff (Kröller Müller Museum Otterloo) the sample of Van Gogh's *Les Alyscamps*. This work is part of the research in the De Mayerne Program project MOLMAP, which is supported by the Dutch Foundation for Scientific Research (NWO, The Hague), and is part of FOM Research program 49, supported by the Foundation for Fundamental Research on Matter (FOM), a subsidiary of NWO.

References

1. Schilling, M.R., and Khanjian, H.P., 'Gas Chromatographic Analysis of Amino Acids as Ethyl Chloroformate Derivatives. III. Identification of Proteinaceous Binding Media by Interpretation of Amino Acid Composition Data' in Bridgland *et al.* (eds), *ICOM Committee for Conservation Preprints Volume I, 11th Triennial Meeting Edinburgh, 1-6 September 1996*, James & James (Science Publishers) Ltd, London (1996) 211-219.
Wouters, J., 'Les liants au laboratoire: analyse des liants protéiniques = Laboratoriumanalysen van bindmiddelen: analyse van proteïnehoudende bindmiddelen', Bulletin de l'Institut Royal du Patrimoine Artistique = Bulletin van het Koninklijk Instituut voor het Kunstpatrimonium 28 (2002) 183-189.

2. See the introduction to different infrared spectroscopic techniques given by Derrick, M.R. et al., *Infrared Spectroscopy in Conservation Science*, The Getty Conservation Institute, Los Angeles (1999).

3. Kühlenthal M., and Miura S. (eds), *Historische Polychromie, Skulpturenfassung in Deutschland und Japan = Historical Polychromy, Polychrome Sculpture in Germany and Japan*, Hirmer Verlag, München (2004).

4. Meilunas, R.J., et al., 'Analysis of aged paint binders by FTIR spectroscopy', *Studies in Conservation* 35 (1990) 33-51.

5. Weerd, J. van der, et al., 'Chemical Changes in Old Master Paintings: Dissolution, Metal Soap Formation and Remineralisation Processes in Lead Pigmented Paint Layers of 17th Century Paintings', *Zeitschrift für Kunsttechnologie und Konservierung* 16 (Heft 1) (2002) 36-51.
Loon, A. van, and Boon, J.J., 'Characterization of the Deterioration of Bone Black in the 17th Century Oranjezaal Paintings using electron-microscopic and micro-spectroscopic imaging techniques', *Spectrochimica Acta Part B* 59 (2004) 1601-1609.

6. In the common case of radiation in air striking the surface of a medium with refractive index n at normal incidence the reflection is given by $(n-1)^2/(n+1)^2$: for an organic material with n=1.5 reflection at the surface is only 4%, whereas for an inorganic pigment such as lead white or chalk with n=2 the reflection is 25%.

Examination of Fresh and Aged Chinese Organic Binding Media Using FTIR Spectroscopy

Rocco Mazzeo[1], Edith Joseph[1], and He Ling[2]

[1] Chemistry Department "G.Ciamician", University of Bologna, Via Selmi, 2, 40126 Bologna (Italy)
[2] North Western University, Xi'an, Shaanxi, (P.R.of China)

Both Tung oil and Chinese lacquer have been extensively used in China as protective coatings, adhesives and paint media since ancient time. These applications are not mutually exclusive as it is not uncommon to find two or more used at the same time.
With the attempt to better understand the polymerisation and degradation mechanisms taking place during the curing of both tung oil and Chinese lacquer, fresh films have been spread directly on IR cards and left curing for one year under ambient exposure. The transmission IR spectra recorded at different aging times allowed a better characterisation of the chemical degradation mechanisms that took place. The results showed that when analysing with FTIR fresh or relatively new tung oil and Chinese lacquer films their characterisation is quite easy if compared with real samples dated back to archaeological times. To this purpose two case studies will illustrate the scientific results achieved.

Microscopic FT-IR Identification of Textile Fibers, Natural Dyestuff and Japanese Lacquers

Masanori SATO and Yoshiko SASAKI
Nara National Research Institute for Cultural Properties, Conservation Science Laboratory, Japan

Abstract

Excavated remains of organic objects fabricated in ancient Japan were analyzed by using micro-FT-IR (Fourier Transform Infrared Spectroscopy). Fragments of silk fabric found in a 6th century tomb were found to be variously degraded depending on the preservation conditions in the stone coffin.
The most notable changes in the infrared spectra of the degraded textiles occurred in the amide I (ca. 1650 cm^{-1}) and amide II (ca. 1550 cm^{-1}) bands due to the long-term underground exposure. The more degraded the silk fiber, the more the intensity of both peaks decreased. The two peaks finally merged in one peak in the heavily degraded sample. Colored silk fabric fragments excavated from a 3rd century tomb showed the same effect; the amide I and II peaks in the spectrum merged into each other as one broad band.
To elucidate the reason for the peak pattern change, peak deconvolution was performed by assuming that the experimental peak can be fitted as an assemblage of peaks, each having a Gaussian distribution shape. It was shown that the changes in the amide I and amide II peaks are primarily due to the break in the polypeptide bonding of the random coil molecular structure.
The non-destructive identification of natural dyestuffs used for ancient textile fabrics is rather difficult without a preliminary separation of dyestuff from the textile filament or fiber. To minimize sampling, the FT-IR microscope was used. But even when the dyed color at the surface of the fiber filaments is visible under the optical microscope, direct micro-FT-IR analysis is not sufficiently sensitive to detect such dyestuffs on very small samples of colored silk fiber. Micro-scale solvent extraction of dyestuff from a short filament of silk fiber was attempted on the surface of a metal disc normally used to prepare a thin layer film for FT-IR microanalysis. The choice of a suitable extracting solvent depended on its ability to extract the dye without co-extracting components of the silk fiber.
For several thousands years, Japanese lacquer (urushi) has been commonly painted on a variety of articles used in daily life. The infrared spectrum of ancient urushi is quite similar to those of modern urushi reference materials. Even in ancient articles, it has been found that urushi remains very stable without significant degradation. As urushi was usually applied in multiple layers, the use of two-dimensional spectral mapping was attempted for the elucidation of the molecular structure of the respective layers.

Introduction

Although many archaeological excavations have been conducted through the years in Japan, found organic materials are usually degraded, hence it is often difficult to identify the original substance. The establishment of a quick and versatile procedure for the identification of such materials is essential for the further conservation treatment of excavated articles.
As we know, FT-IR microscopy is one of the most suitable analytical techniques to fulfill this need for identification. Since the spectra of excavated materials usually differ from those of modern standard materials, a reference spectra database must be prepared which contains infrared spectra of organic materials commonly used in ancient times. Because we have acquired numerous infrared spectra of degraded ancient materials, we are able to identify many of the substances remaining after long-term burial by comparing the varied patterns in their infrared spectra to those of reference spectra.

Apparatus and experiment

A Horiba FT 520 microscope and Shimadzu IR Prestige 21 (FT-IR) + AIM 8800 microscope were used throughout the study. The latter instrument was equipped with an attachment for two-dimensional infrared spectral scanning of a selected microscopic area of sample.
No tedious sample preparation procedures are necessary to acquire infrared spectral data. A thin film of the sample is made by manually pressing a trace amount of samples (usually less than 1 mg) flat on the surface of flat metal disc. The metal disc with thin-layer sample is then transferred to the FT-IR microscope. Before the spectrum is obtained, the target area of the thin sample is determined under a visible light microscope. The IR beam perpendicularly penetrates the sample layer, is reflected at the metal surface and then returns in the same direction, reaching an IR

detector after passing through the sample layer a second time. The reflection-absorption infrared spectrum is acquired in transmission mode over the 4000-700 cm^{-1} range.

Results and discussion

3-1) Textile fibers

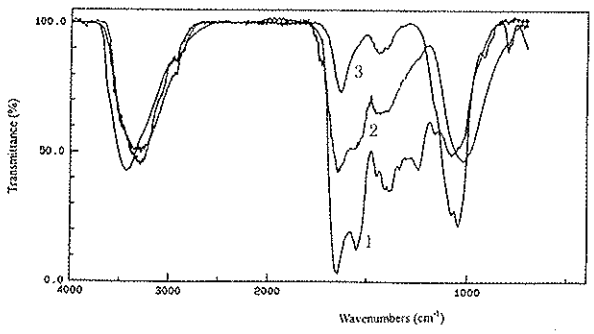

Fig.1 Infrared spectra of silk fibers found at Fujinoki tomb.
1. Sample found floating at the water surface in stone coffin;
2. Sample found at the bottom of stone coffin;
3. Sample found attached to an iron sword at the bottom of stone coffin.

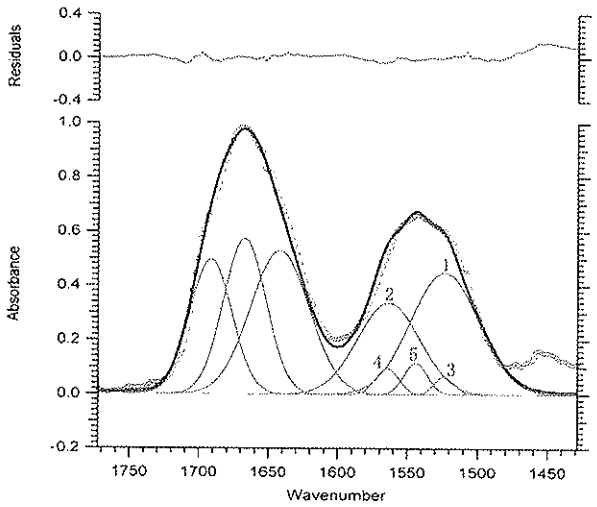

Fig.3 Curve fitting simulation of amide I and II peaks of reference Sample (modern silk fiber).
Secondary structure of protein molecule
1. α–helix (polarized parallel absorption);
2. α–helix (polarized perpendicular absorption);
3. β–sheet(polarized parallel absorption);
4. β–sheet(polarized perpendicular absorption);
5. Random coil.

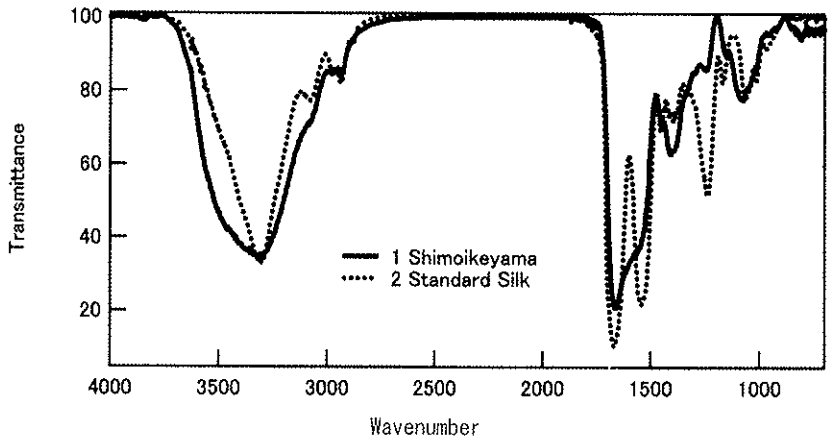

Fig.2 Infrared spectra of silk fiber found at Shimoikeyama tomb.
1. Sample silk fiber;
2. Reference sample (modern silk fiber).

The kinds of natural fibers used in Japan before ca. 8th century AD are exclusively silk, hemp or ramie. Flax and cotton were not used until later periods. In this paper, we will discuss some examples of silk fibers found at archaeological sites. One of the famous tombs is the 6th century Fujinoki tomb at Nara prefecture. When this tomb was excavated, many kinds of degraded fragments of silk fabrics made using several weaving techniques were found together with metallic articles. Since the stone coffin had been filled with water several times in the past, the degraded state of silk fibers depended on their position in the coffin as shown in the spectra of Fig.1. The figure shows that a distinct change in the spectrum is seen about the amide I and II peaks of silk fibers.
A second example is a fragment of silk fabric having a colored stripe-pattern found at the 3rd century Shimoikeyama tomb. These well-preserved silk fibers were identified by micro-FT-IR. The separation of the amide I and II bands were not distinct however, and the both peaks merged into one broad peak as shown in Fig. 2. To elucidate the reason for the change in the pattern of the two amide peaks over time, we assumed that the observed peaks can be simulated as the superposition of many single Gaussian shaped peaks. The same curve fitting simulation has been applied to the analysis of infrared spectra of ancient ambers [1]. The result of the curve fitting simulation for the amide I and II peaks of modern reference silk fiber is shown in Fig.3. The assignment of respective amide II

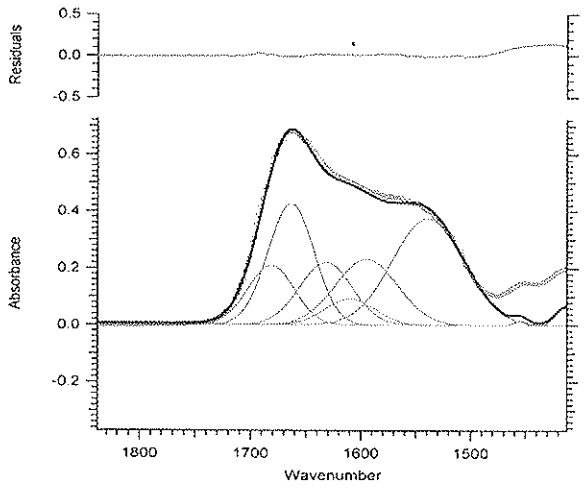

Fig.4 Curve fitting simulation of amide I and II peaks of sample silk fiber (Shimoikeyama).

component peaks was performed by considering the reported results for the model compound S-carboxymethylkeratin [2] which has similar polypeptide bonding.
A curve fitting simulation for the amide I and II peaks of ancient silk fiber found at the Shimoikeyama tomb was also undertaken as shown in Fig.4. Although the assignment for this composite curve is not finished, the fitted curve for the amide II band for ancient silk fiber shows distinct differences when compared to that of a reference silk fiber. The peak pattern change in both amide I and II peaks for composite curves of ancient silk fibers may be explained as the result of changes in the configuration of the protein molecule due to long-term burial.

Natural dyestuffs

In general, natural dyestuffs used in ancient times are aromatic compounds; hence, ultraviolet-visible absorption and fluorescence spectroscopies, both of which require sampling, are commonly used for their identification. As the solvent extraction of dyestuff from fiber filaments requires a sizable sample, this procedure is not generally suitable for the analysis of heavily degraded archaeological samples.
In this work, the FT-IR microscope was used for the identification of dyestuffs remaining in fragments of archaeological fibers. In a preliminary experiment, it was confirmed that a clear infrared spectrum could be obtained from a trace amount ($<50\mu^2$) of a modern solid dyestuff such as indigo. However, micro-FT-IR was not sufficiently sensitive to detect indigo on the surface of dyed silk fibers, even though the blue color was clearly visible under the optical microscope. In order to increase sensitivity, indigo was concentrated by a micro-scale solvent extraction (chloroform) from a single filament of silk fiber (a few mm long). After evaporating the solvent on the flat surface of a metal disc, a micro FT-IR measurement for residual dried dyestuff was performed and an increase in the sensitivity was achieved. However, solvent extraction resulted in the dissolution of trace amounts of silk fiber. The choice of a suitable solvent depends on its ability to extract the dye but still avoid the interaction with the silk fiber.

Japanese lacquer (urushi)

The Japanese lacquer (urushi) has been used for several thousands years for varnish the surface of articles used in daily life. As urushi is a rather stable material even over long period of time, FT-IR microscopy is suitable for the quick identification of excavated urushi. For example, a clear infrared spectrum was obtained for a small fragment of urushi (estimated to be several thousand years old) excavated at a Hokkaido district archaeological site. The spectrum has characteristics similar to that of modern reference urushi, though there are some spectral changes (ca. 1630-1000 cm^{-1}) presumably due to the elapse of time and burial conditions.
Since urushi is usually applied to an article in multiple layers, it is important to differentiate the characteristics of each layer. In this report, two-dimensional spectral mapping was undertaken to elucidate trace fragments of thin layers of the above-mentioned ancient urushi. The spectral contour map obtained by using the FT-IR microscope showed differences in the respective positions of urushi layers. It was found that some of the layers showed low concentration of urushi. Those layers may contain red iron oxide to produce a red color at the surface. The presence of red iron oxide was later separately confirmed by laser Raman spectroscopy and X-ray fluorescence spectroscopies.[3]

Conclusion

We have shown that the micro-FT-IR spectroscopy is a versatile procedure for the quick identification of excavated organic substance, such as textile fibers, dyestuffs and urushi. The FT-IR microscope is also useful instrument for investigating the degraded state of samples. Using this technique, we were able to clearly detect changes in the absorption peaks of ancient and degraded silk fibers. To investigate the reason for the change of spectral peaks, a further theoretical study was performed by the deconvolution of the main absorption peaks into several Gaussian-shaped component peaks. The degraded state of silk samples could be elucidated by a theoretical curve fitting

simulation of the experimentally observed combined absorption peak which corresponded to the usual proteinaceous amide I and amide II bands. As for the degradation of silk fibers recovered after long-term burial, the components of amide II peak were found to change mainly due to the break down of random coil molecular chains.
Natural dyestuffs are generally investigated by ultraviolet-visible absorption or fluorescence spectroscopy. However, only very small archaeological samples are often available, and the absolute amounts of dye present are below the limits of sensitivity for these methods. In this report, the application of micro-FT-IR was undertaken for the identification of trace amounts of archaeological samples. Although FT-IR microscopy is sufficiently sensitive to obtain a clear spectrum in the solid state of even trace amounts of modern reference dyestuffs such as indigo, it is rather difficult to get a distinct spectrum of indigo at the surface of silk fiber filament due to the superposition of strong silk absorptions. To avoid the influence of silk fiber component, the micro-scale solvent extraction of dyestuff was attempted from a single fiber filament laid on the surface of flat metal disc. After evaporation of the solvent, a reflection-absorption spectrum of the residual solid dyestuff showed the characteristic peaks of dyestuff. However, it is important to choose a solvent which will extract the dyestuff yet avoid the co-extraction of silk component.
Identification of urushi was performed by using micro-FT-IR. The trace sized fragments of samples taken from an archaeological site in the Hokkaido district in Japan showed a clear infrared spectrum of urushi. Since urushi was usually applied in several layers on articles even in the ancient period, it is important to clarify the structure of these multilayers. To distinguish the small differences in the respective layers of micro-scale samples, the two-dimensional infrared spectral mapping was achieved after multiple spectral scans of the whole sample area. A distinct difference in components of various layers of sample fragment was clarified.

References

1. Sato, M., Mimura, M. and Yamasaki, K., 'Studies on Archaeological Ambers in Japan' in *Scientific Research in the Field of Asian Art*, Proceedings of the First Forbes Symposium at the Freer Gallery of Art , Smithsonian Institution, Washington , D.C., Archetype Publications Ltd. (2003) 8-14.

2. Nishikida, K. and Nishio, E., 'Simulation by Curve Fitting Method (in Japanese)' in *FT-IR Spectrum (in Japanese),* Kodansha Scientific Ltd. (1990) 198-199.

3. In preparation. To be published elsewhere.

Stabilization and Protection of Cellulosic Supports with a Photosensitive Polymeric System

Narcisa Vrinceanu[1], Mihaela Avadanei[2], Sorin Ciovica[1], Virgil Barboiu[2], George Ervant Grigoriu[2]

[1] "Gh. Asachi" Technical University, Bd. D. Mangeron, nr. 71A, 700050, Iasi, ROMANIA
[2] The Romanian Academy - "Petru Poni"Institute of Macromolecular Chemistry, Aleea Grigore Ghica Voda, nr. 41 A, 700487, Iasi, ROMANIA

Abstract

The cellulosic supports, coated with films of 1,2-polybutadiene (with and without photoinitiators, namely benzoin derivatives) were treated with UV radiation, in order to enhance the aging properties.
The evaluation of structural changes in photocrosslinkable system was carried out by IR Spectroscopy technique (Transmission and ATR - Attenuated Total Reflectance).
The kinetics of photocrosslinking reactions within protective film has been underlined.

FTIR Analysis of Five Paintings by Pierre-Auguste Renoir

Suzan de Groot[1], Henk van Keulen[1], Aviva Burnstock[2] and Klaas Jan van den Berg[1]
[1] Netherlands Institute for Cultural Heritage (ICN) Gabriël Metsustraat 8, 1071 EA Amsterdam, The Netherlands
[2] Courtauld Institute of Art, Somerset House, Strand, London WC2R 0RN, UK

Abstract

The organic analysis of paint layers at ICN is part of a current technical study of four paintings by Pierre-Auguste Renoir in the Courtauld Institute Gallery, London and one large early work by the same artist from the Kröller-Müller Museum Otterlo, Netherlands.
The paintings painted between 1868 and 1919 span almost the length of Renoir's career, and therefore potentially exemplify the development in his style of painting and use of materials. The questions for ICN concern the identification of the binding media and organic additives to the paint and grounds.
The binding media of selected paint layers and the ground layers from the four paintings were analysed by FTIR and were identified as drying oil. These results were confirmed by GC-MS, the oils were identified mainly as linseed oil. FTIR analyses showed that the ground layers of the four paintings also contained lead white and a most likely lead carboxylate.
The calcium phosphate (bone black) containing paint from one of the paintings incorporated inclusions that were evident in cross section. Using FTIR it was possible to characterise the inclusions as starch. In two red paint layers from the Kröller-Müller Museum painting, starch was identified as inclusions in the paint layer.
In two other cases starch was also identified: firstly in a red lake containing paint layer of a van Gogh painting, and secondly in a paint tube from the 19th century containing a red lake.
The significance of the results in the historical and technical context will be discussed in a forthcoming article.

Introduction

ICN has undertaken the organic analysis of selected paint layers and ground samples of four paintings by Pierre-Auguste Renoir in the Courtauld Gallery, London. Two works by Renoir from the Kröller-Müller Museum in Otterlo, Netherlands have also been included in the present study.
The paintings: *'La Loge'* (1874); *'The Outskirts of Pont Aven'* (1888-90); *'Portrait of Ambrose Vollard'* (1908), and *'A Woman Tying her Shoe'* (1919) from the Courtauld Institute Gallery, and *'The Clown'* (1868) and *'Le Café'* (1887-8) from Kröller-Müller Museum span almost the length of Renoir's career, and therefore potentially exemplify the development in his style of painting and use of materials.
The paintings were examined at the Courtauld Institute of Art by Aviva Burnstock and samples were taken for organic analysis and for examination of the paint layers and inorganic pigments using light microscopy and scanning electron microscopy with energy dispersive X-ray spectroscopy (SEM-EDX). The organic analyses were carried out by FTIR microscopy using a Miniature Diamond Anvil Cell and by GC-MS using inline methylation and hydrolysis in combination with Curie-point pyrolysis. For each painting the ground and selected paint layers were analysed.
High Pressure Liquid Chromatography (HPLC) analyses for the identification of the lakes were performed by Jo Kirby at the National Gallery in London and FTIR analyses of a sample of red paint from 'La Loge' was undertaken by Catherine Higgitt, in the same department.
Comparable findings from the analyses of a red tube paint from the *'Corot painting box'* (Gemeente Museum Den Haag) and a red paint layer from a painting by Vincent van Gogh, *'Agostina Segatori in the café du tambourin'* (1887) (van Gogh Museum Amsterdam) are also discussed.

The Paintings

'La Loge' (Courtauld Institute Gallery) was painted in 1874. The artist's brother and a model, Nini from Montmatre, posed for this painting. This painting was one of Renoir's prime exhibits at the first group exhibition of the Impressionists in Paris in 1874. The subject of the theatre box was a favoured one among painters of modern Parisian life during the 1870s [1]. The painting has been relined with a wax/resin adhesive.
The *'Outskirts of Pont Aven'* (Courtauld Institute Gallery) was created between 1888 and 1890. The painting shows the surroundings of the town Pont Aven in Brittany, France.

The portrait of Ambrose Vollard (Courtauld Institute Gallery) was painted in 1908. Ambrose Vollard was an art dealer who became one of the principal dealers of Renoirs work. Later, Vollard wrote important books on both Renoir and Cezanne [1].
'Woman tying her shoe' (Courtauld Institute Gallery) was probably painted in 1918 at Cagnes, near Nice on the Mediterranean coast. In his last years, the female nude was one of his principal themes, but he also painted many images of women, dressed or half dressed, engaged in their toilette , playing music or just seated still. The colour is very rich, dominated by the reds and oranges which Renoir used to evoke the idea of the south of France [1].
The *'Clown'* (Kröller-Müller Museum) was painted in 1868, the earliest example of Renoir's painting in the present study.
The *'Corot painting box'* from the 19th century (Gemeente Museum Den Haag) is attributed to the French painter Jean-Baptiste Camille Corot. The box contains sketches inside the lid of the painting box, a number of paint tubes and other painting materials. The tube containing the red paint was probably bought late in the 19th century by the painter Matthijs Maris who owned the painting box [2].

Experimental

Fourier Transform Infrared Spectroscopy (FTIR) analyses were performed using a Perkin Elmer Spectrum 1000 FTIR spectrometer combined with a Perkin Elmer Autoimage FTIR microscope and a Miniature Diamond Anvil Cell. The sample was squeezed between the diamonds and spectra were taken from different parts of the sample to take account of its heterogeneous nature.
Gas Chromatography-Mass Spectrometry (GC-MS) analyses were performed using a ThermoFinnigan GC8000Top Voyager; modification: Solid Vapour Exit technique for fast removal of excess volatile reagent products, trapping of components on PTA5 pre-column (Supelco), in combination with on-line thermally assisted hydrolysis and methylation with tetramethylammonium hydroxide (TMAH) and pyrolysis at a temperature of 610°C. Separation was performed on a ZB5 colomn (Phenomex).

Results and discussion

La Loge
For the analyses of the ground layer of *'La Loge'*, a sample was taken from the tacking margin of the painting. Various FTIR spectra were recorded. Figure 1 shows a spectrum with the characteristics of lead white and an oil and an absorption band at 1528 cm^{-1}, which is typical for a metal carboxylate.
Figure 2 shows the spectrum of a more isolated metal carboxylate in the same sample which also shows the specific absorption bands at 1472 – 1417 – 730 – 719 – 706 cm^{-1}. The SEM-EDX results confirmed the presence of lead in the ground layer. Since lead carbonate is present in the ground layer, the metal carboxylate is likely to be a lead carboxylate.
A sample from the black paint layer from the man's jacket was analysed. The visual image of the diamond cell shows colourless inclusions (see figure 3). The FTIR spectrum of these inclusions shows the specific absorption bands of starch at 1153 – 1080 – 1033 – 926 – 855 and 759 cm^{-1} (see figure 4).

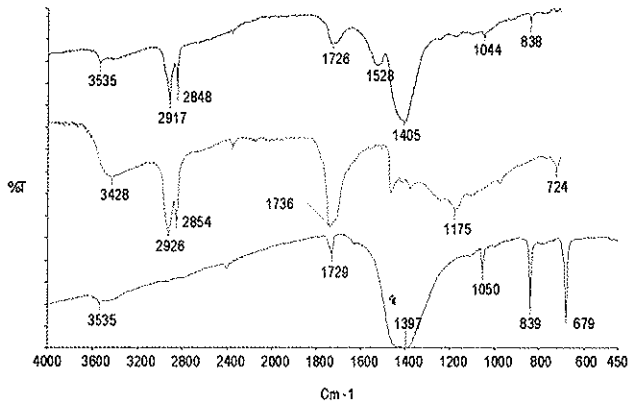

Fig. 1: Upper spectrum: ground layer La Loge
Middle spectrum: reference oil
Lower spectrum: reference lead white

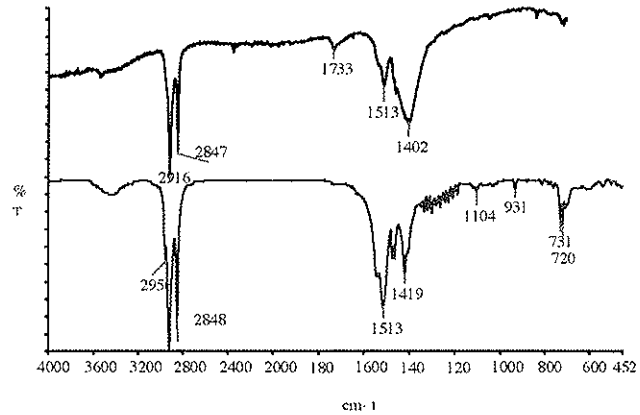

Fig. 2: Upper spectrum: ground layer La Loge
Lower spectrum: reference lead carboxylate

The spectrum from the area around the inclusions shows the absorption bands of beeswax, a natural resin and bone black (see figure 5). The beeswax and natural resin originate from the wax/resin adhesive that was used for relining the painting in the past. Due to the presence of the wax/resin adhesive in the sample, it was not possible to identify the binding medium of the black paint layer. The presence of calcium phosphate (boneblack) was confirmed by the presence of peaks for Ca and P using SEM-EDX.

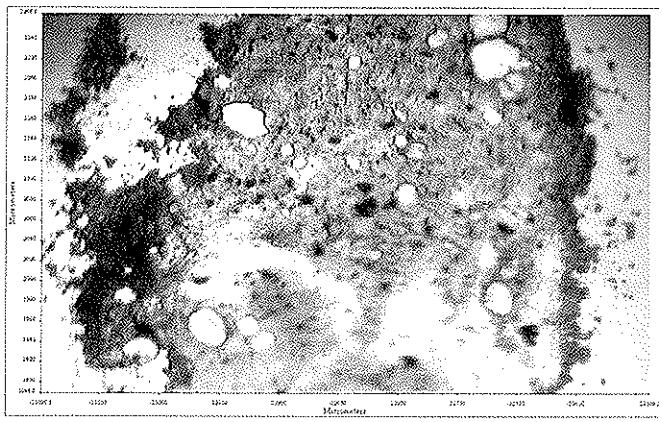

Fig. 3: visual image of diamond cell; black paint la Loge

Outskirts of Pont Aven

The FTIR spectrum of the ground layer of *'Outskirts of Pont Aven'* showed absorption bands that are specific for lead white, an oil and a metal carboxylate. These components were also identified in the ground of *'La Loge'*.

Portrait of Ambrose Vollard

A sample from the ground layer was taken from the lower edge of the painting. The FTIR spectrum shows the presence of lead white and gypsum and oil.

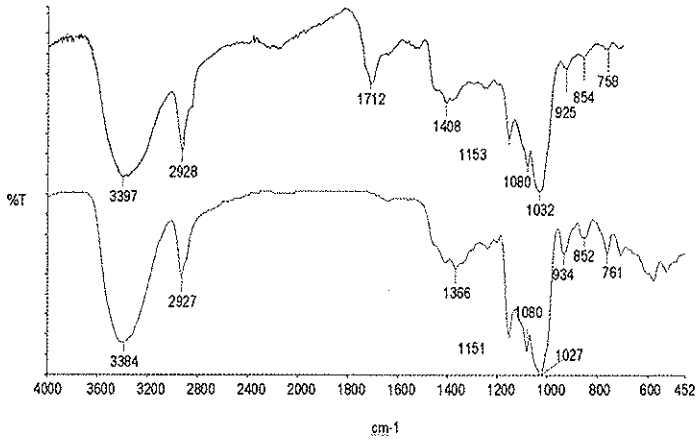

Fig. 4: Upper spectrum: white inclusions, black paint layer La Loge Lower spectrum: reference starch

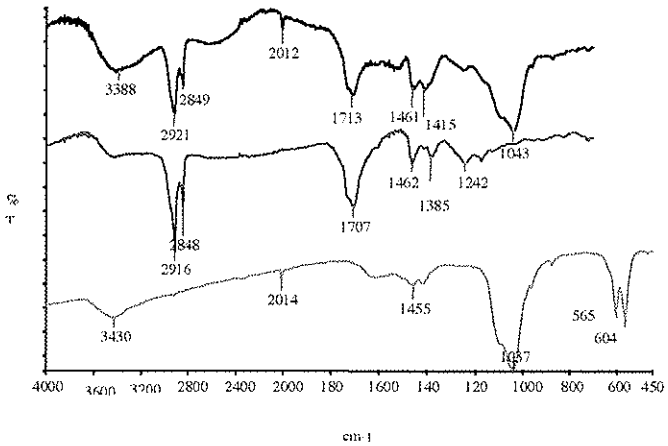

Fig. 5: Upper spectrum: black paint layer La Loge Middle spectrum: wax/resin adhesive La Loge Lower spectrum: reference bone black

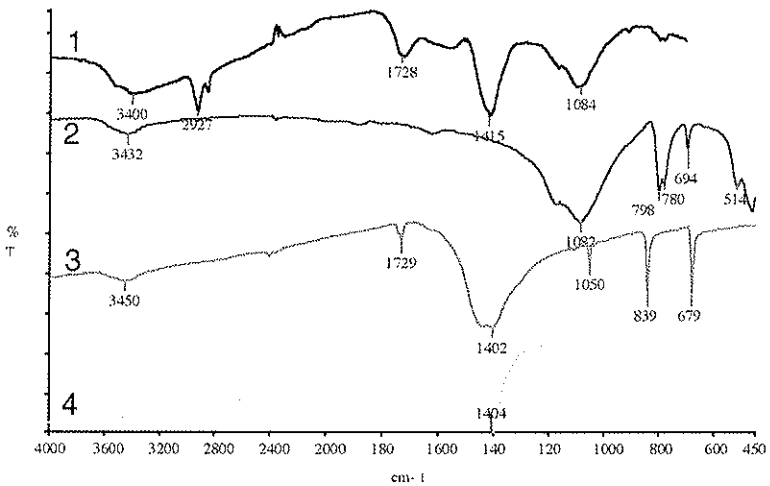

Fig. 6: Spectrum 1: pink paint layer Ambrose Vollard
Spectrum 2: reference silica compound
Spectrum 3: reference lead carbonate
Spectrum 4: reference lead oxide (PbO)

The spectrum also shows the absorption band at 1531 cm^{-1} which indicates a metal carboxylate, closely similar to that found in the grounds from *'La Loge'* and *'Outskirts of Pont Aven'*.
The FTIR spectrum of the pink paint layer from the table cloth shows absorption bands at 1167 – 1093 – 797 and 779 cm^{-1} that are also present in the reference spectrum of a silicate compound (see figure 6). The absorption band at 1416 cm^{-1} can be attributed to either lead oxide or lead carbonate. Since the small absorption bands at 840 and 679 cm^{-1} from lead carbonate are not present in the spectrum, a lead oxide is more likely. The carbonyl absorption band at 1728 cm^{-1} can be attributed to an oil.
The presence of silicon and lead was confirmed by SEM-EDX analyses.

A Woman tying her shoe
The FTIR spectrum of a sample of the ground of *'A Woman tying her shoe'* shows absorption bands that are specific for lead white, an oil and a metal carboxylate. These components were also identified in the ground layers of 'La Loge' and 'Outskirts of Pont Aven'
The FTIR spectrum of the pink paint from *'A Woman tying her shoe'* is closely similar to the spectrum of the pink paint from *'Portrait of Ambrose Vollard'*; the spectrum shows the absorption bands of a silicate compound, lead oxide and possibly an oil.

GC-MS analyses
The samples from the four paintings by Renoir from the Courtauld Institute Gallery were also analysed by GC-MS using inline methylation and hydrolysis in combination with Curie-point pyrolysis. The GC-MS analyses showed that the wax/resin adhesive from *'La Loge'* consists of beeswax and a mixture of colophony and Venice Turpentine. The binding media of the paint layers and the ground layers were identified as moderately preheated linseed oil.
The analysis of the sample of the ground layer from *'Portrait of Ambrose Vollard'* is presented in figure 7. The chromatogram shows the component peaks of the methylesters of the diacids with 7, 8, 9 and 10 C-atoms (2C7, 2C8, 2C9, 2C10) and those of palmitic (C16) and stearic acid (C18). For linseed oil the C16 and C18 peak heights are in the ratio of 1.4-1.7. Preheated oil shows a ratio of about 3 for the diacids 2C9 and 2C8, due to the prépolimerisation caused by the heating of the oil. The ratio of 2C9 and 2C8 in the ground layer is about 4.5 indicating a moderately preheated linseed oil.
A sample from the red paint layer from the banister of the balcony was analysed and the visual image of the diamond cell showed colourless inclusions in the red paint (see figure 8).

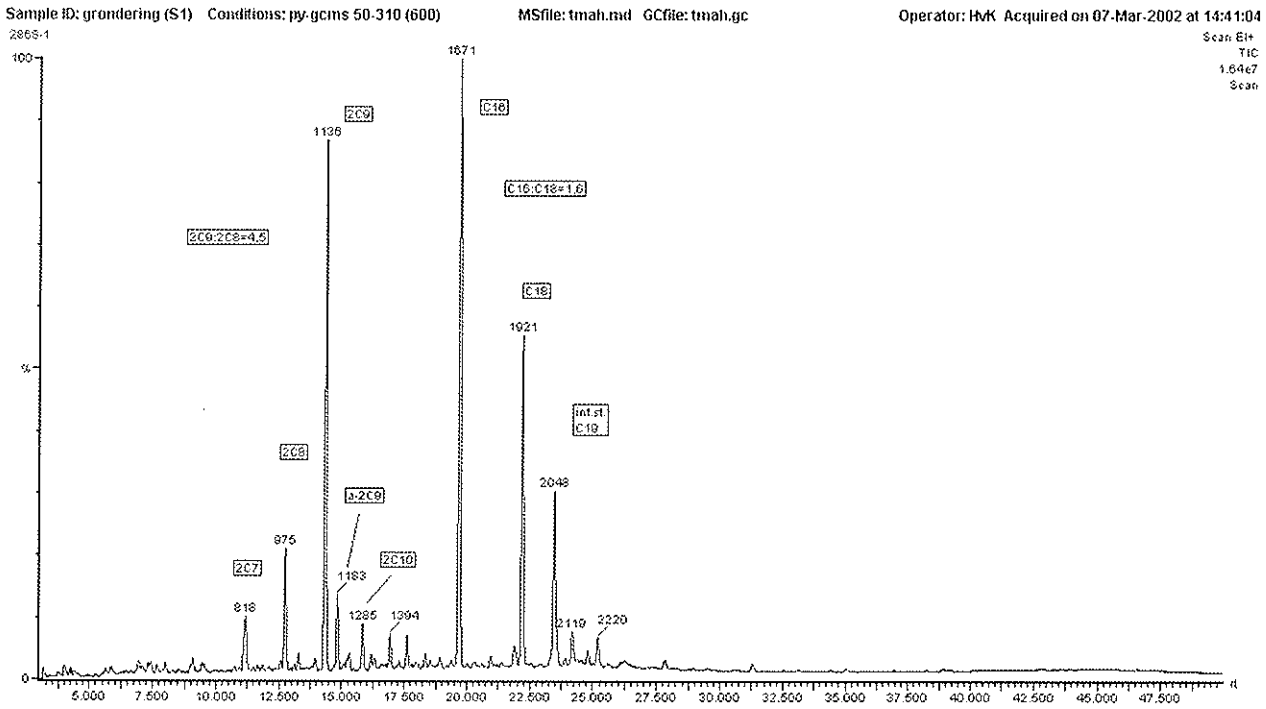

Fig. 7: GC-MS chromatogram: ground layer from Portrait of Ambrose Vollard

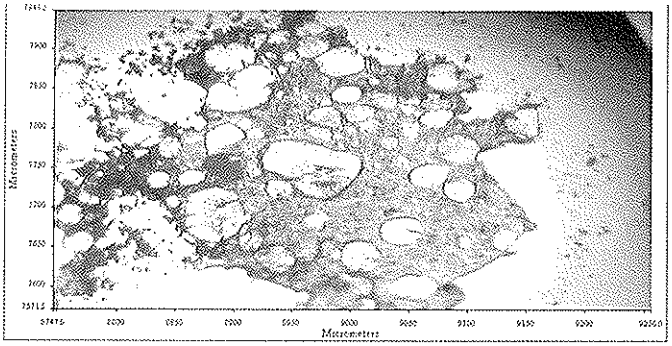

Fig. 8: visual image of diamond cell; red paint layer Clown

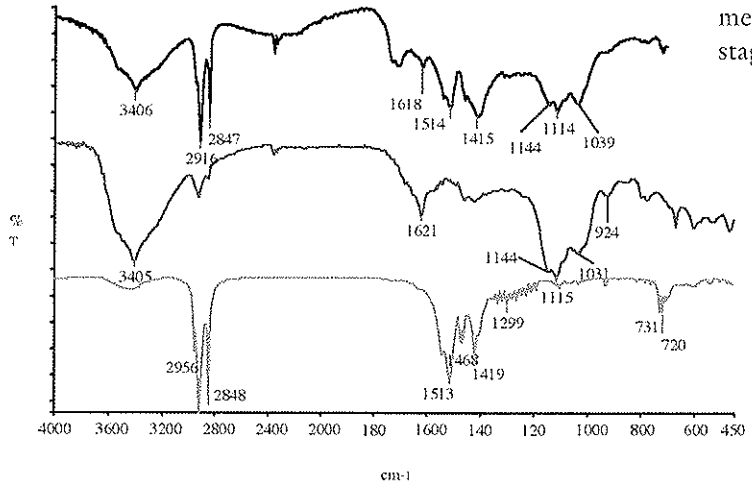

Fig. 9: Upper spectrum: red paint Clown
Middle spectrum: reference kugellack
Lower spectrum: reference of lead stearate

Fig. 10: Microscopic image, crossed polars, starch in red paint

The spectrum of the inclusions shows the absorption bands of starch. The spectrum of the red area (see figure 9) around the inclusions shows absorption bands at 1619, 1144, 1115 and 1040 cm^{-1}, these are also present in the reference spectrum of 'kugellack', which is a cochineal lake. The absorption bands at 1515 cm^{-1} and 1416 cm^{-1} are specific for a lead carboxylate.
A sample from a red paint layer from the stocking of the clown also showed the inclusions in the visual image on the diamond cell. The FTIR spectrum of the inclusions showed the absorption bands of starch.
The cross section of both red paint layers also shows the inclusions in the red layer.
For the samples of the Clown, GC-MS, SEM-EDX and HPLC analyses for identification of the binding medium and pigments will be performed at a later stage.

The Corot Painting box
Like in the black paint of *'La Loge'* and the red paints from 'The Clown', we have found starch inclusions in late 19th and early 20th century paints in several other projects at the ICN.
The red pigment in red paint from a tube from the 'Corot Painting box' was analysed by HPLC and appeared to be a natural lake. The visual image of the red paint on the diamond cell of the FTIR microscope shows colourless inclusions and the FTIR spectrum once again shows the presence of starch.
The presence of starch in the red paint was confirmed by polarised light microscopy. Figure 10 shows a sample of the red paint viewed with crossed polars where the characteristic cross for starch grains is clearly visible [3].

Van Gogh
The cross section of a red paint layer from a painting of Vincent van Gogh, *'Agostina Segatori in the café du tambourin'* (1887) showed inclusions in the red layer. HPLC analyses identified the red pigment as cochineal. Also in this case, the visual image of the diamond cell showed the colourless inclusions. The spectrum from the inclusions again shows the absorption bands of starch.

Conclusion

The analysed Renoir paintings from the Courtauld, *'La Loge'*, *'The Outskirts of Pont Aven'*, *'Portrait of Ambrose Vollard'* and *'A Woman tying her shoe'*, have a lead white ground with linseed oil as a binding medium. The FTIR spectrum of the ground layer of *'Portrait of Ambrose Vollard'* shows the presence of gypsum, this needs further investigation.
The four grounds contain a metal carboxylate. Presumably the metal carboxylates are lead carboxylates due to the presence of lead carbonate. The lead carboxylates are formed during the curing of the ground layer [4].
In the black paint layer from the painting *'La Loge'* and two red paint layers from *'The Clown'*, starch was identified as inclusions in the paint layer.
In two other cases starch was also identified: firstly in a red lake containing paint layer of a van Gogh painting, and secondly in a paint tube from the 19th century containing a red lake.
In conclusion, starch is present in 19th century oil paints, especially in red lake paints [5]. Its use was not limited to Renoir. It was probably used as an extender by colourmen, reflecting the paint technique of that time.
The analyses of the Renoir paintings are part of a broader study of the materials and techniques of these works. The significance of the results in the historical and technical context will be discussed in a forthcoming article.

Acknowledgements

The authors would like to thank Luuk van der Loeff and Piet de Jonge (Kröller-Müller Museum in Otterlo) for giving us the chance to sample the paintings the Clown and the Café, Ella Hendriks (van Gogh Museum Amsterdam) for the samples of the van Gogh painting and the Gemeente Museum Den Haag for the samples from the Corot painting box.
We thank Jo Kirby (National Gallery London) for the HPLC analyses of the Courtauld Renoir paintings, Catherine Higgitt (National Gallery London) for the FTIR analysis of a sample of red paint from *'La Loge'*, Muriel Geldof (ICN) for the microscopic analyses of the starch and Maarten van Bommel (ICN) for the HPLC analyses of the paint tube from the Corot painting box and the van Gogh painting.

References

1. Impressionist & Post-Impressionist Masterpieces: The Courtauld Collection, Yale University Press, New Haven and London (1987)

2. Hermens E., Kwakernaak A., van den Berg K.J., Geldof M., 'A travel experience: The Corot painting box, Matthijs Maris an 19th century tube paints'in *Art Matters, Netherlands Technical Studies in Art*, Waanders Publishers b.v., Zwolle (2002) 104-121

3. Wülfert S., *Der Blick ins Bild*, p.211: "Schliesslich finden sich pflänzliche Stärkekörnchen als Hilf- und Verschnittstof zum Beispiel in manchen Farblacken" and these particles have a "fast stehendes Kreuz" when viewed between crossed polars.(1999)

4. Boon J.J., van der Weerd J., Keune K., Noble P., Wadum J., *'Mechanical and chemical changes in Old Master paintings: dissolution, metal soap formation and remineralization processes in lead pigmented ground/intermediate paint layers of 17th century paintings'* in The 13th ICOM-CC Triennial Meeting Rio de Janeiro Preprints (2002)

5. Butler, M.H, 'Technical Note', in 'Paintings by Renoir' by Maxon, J, The Art Institute of Chicago, Illinois (1973) 208-214.

Discrimination of Contemporary Artistic Prints Based on the Analysis of Inks Using FTIR

A. Vila[1], N. Ferrer[2] and J.F. García[1]
[1] Departament de Pintura, Conservació-restauració. Facultat de Belles Arts, Universitat de Barcelona.
[2] Unitat d'espectroscòpia molecular. Serveis Científico-Tècnics. Universitat de Barcelona

Abstract

Prints are one of the most popular forms of artistic expression because they allow serial reproduction of original art pieces. Nevertheless, this characteristic has stimulated the introduction of fakes in the market, especially in the case of contemporary art.
Determination of chemical composition of the constituent materials could contribute to the identification and discrimination of original from not original artworks. In this work, the study is restricted to the characterization of pigments used in the formulation of modern black inks. The possibility to differentiate between these pigments could be considered the first and critical step to evaluate the potential success of the approach. Chemical composition have been determined by infrared spectroscopy and confirmed by scanning electron microscopy. The small amount of sample required has made these techniques suitable for this kind of determination. Results obtained allow establishing discriminative criteria between the different pigments and therefore the same consequence could be expected in the analysis of black and coloured inks.

Introduction

Artistic prints are composed of inks distributed onto paper, following artistic criteria.
The production process is based on the use of an original plate where the artist tries to reflect his/her design. This artistic composition, impregnated with black and coloured inks, is transferred to the paper support by pressure. This process allows us to obtain multiple original prints from a single original plate. The ease of the technique, together with their cheaper price, lead prints to be one of the most diffused artwork typologies, as well as the most forged objects (1).
Discrimination between original and fakes is generally based on stylistic criteria (2). However, in some cases, differences cannot be appreciated with the naked eye and it is necessary to obtain additional information about the physico-chemical composition and structural distribution of the constituent materials in order to identify the original characteristics.
An important question when analysing artworks is to reduce to a minimum the amount of sample necessary for analysis. FTIR supported by other techniques is a good option for a quasi-non-destructive chemical study (3).
The first step to establish the feasibility of this chemical approach is to determine whether the pigments used in the composition of the inks can be differentiated. The most difficult inks and pigments to distinguish are probably blacks due to their chemical similarity.
As many contemporary prints are made in black and white (Figure 1), the objective of this study is to characterize the chemical composition of the most used black pigments in printing ink formulations (4).
The tests established using KBr pellets in transmission mode will easily be applicable to IR microscopy bin the same mode.

Figure 1. Original Dalí Black and White print (private collection).

Experimental

Reagents
Pigments: Lamp black (reference 47250), French wine black (reference 47010), Genuine wine black (reference 47000), Ivory black (reference 47150), Bone black (reference 47100) all from Kremer Pigmente.

Instrumental
A Bomem MB-120 Fourier Transform Infrared Spectrometer equipped with a potassium bromide beamsplitter and DTGS detector was used for transmittance measurements on KBr pellets. FTIR spectra were measured with a resolution of 4 cm^{-1} and 30 scans were taken in order to obtain an appropriate signal-to-noise ratio. The spectral range used was between 4000 and 350 cm^{-1}.

A magnetic KBr pellet holder was used to hold 13 mm pellets in place.

Sampling.
KBr pellets were made for each sample of pigment analysed.

Measurement
Triplicates of every measure were made to evaluate the reproducibility of this step. All the results were processed using GRAMS 32 (Galactic) software. The spectra were treated with baseline and CO_2 corrections and a Y-Offset.

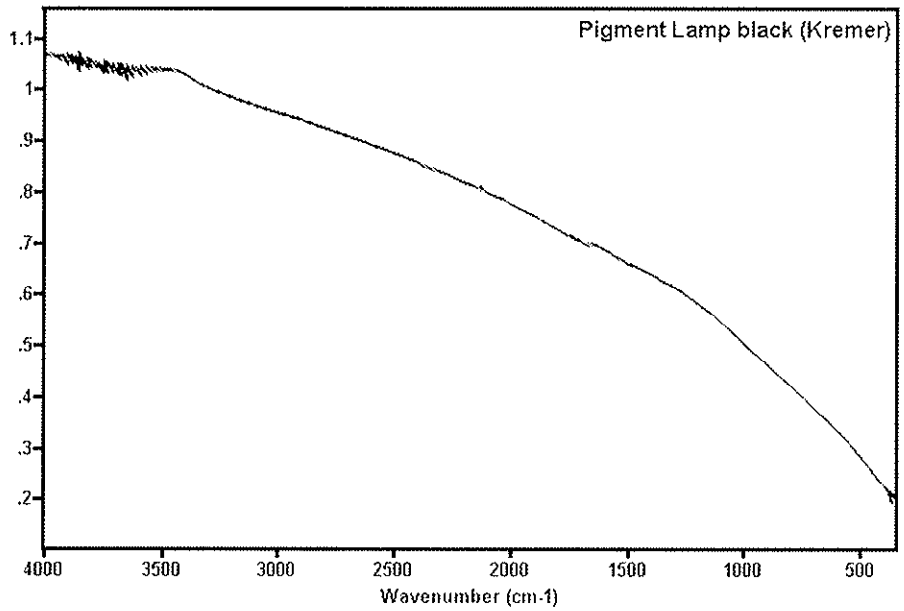

Figure 2. Infrared spectrum of Lamp Black pigment.

Results and discussion

The infrared spectra obtained for the pigments studied are shown in Figures 2-5. The spectrum for Lamp black (Figure 2) differs most from the others due to the absence of absorption bands. This result is confirmed by scanning electron microscopy (SEM) because just a small amount of sulphide is found for this pigment. The absence of bands in the infrared spectrum could be used to discriminate it from all the other pigments. The spectra obtained for Bone and Ivory black are shown in Figures 3-4.

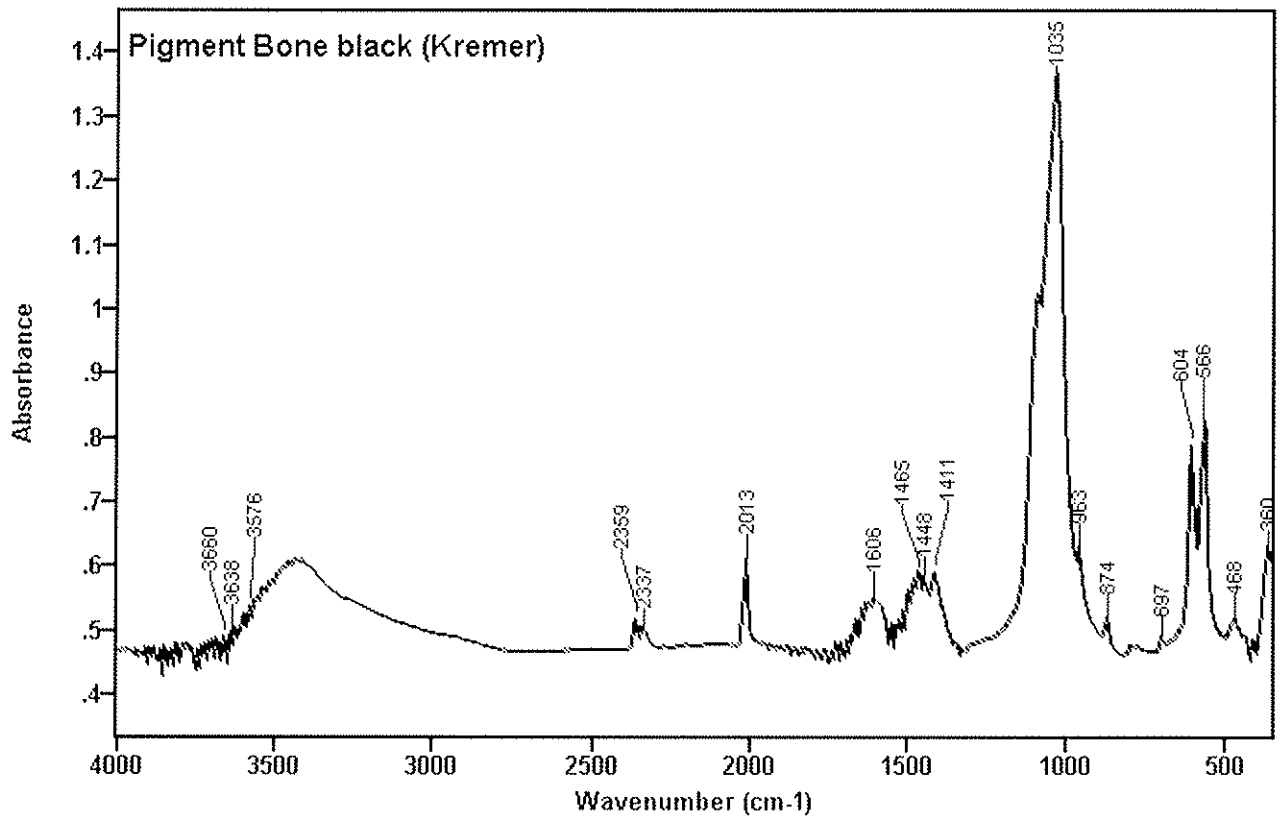

Figure 3. Infrared spectrum of Bone Black pigment.

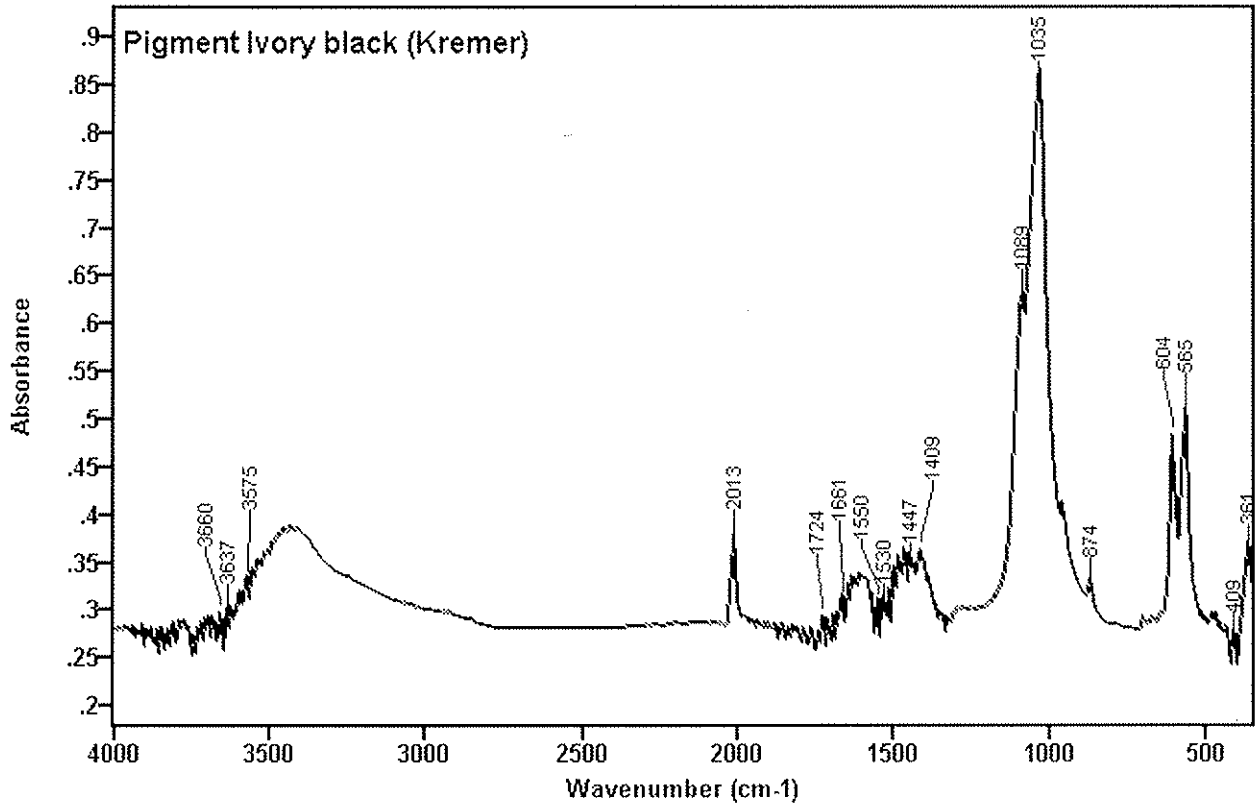

Figure 4. Infrared spectrum of Ivory Black pigment.

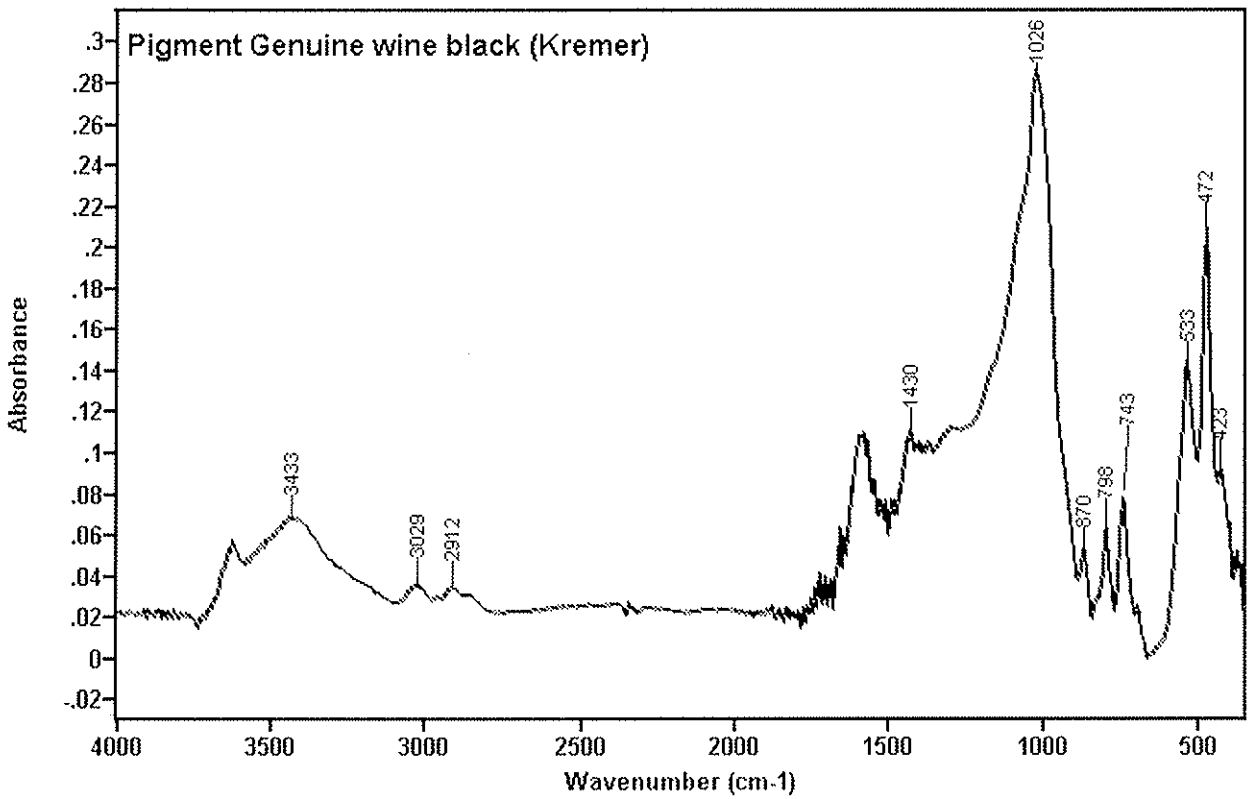

Figure 5. Infrared spectrum of Genuine Wine Black pigment.

These spectra are almost identical and they include bands at 1036, 604 and 567 cm^{-1}, which could be related to phosphate group of the hydroxyapatite, and at 2013 cm^{-1}. This last band is difficult to assign but, at this moment, we believe it to be due to the presence of diazocompounds in the pigment (5) (this is the subject of ongoing research). SEM results show the presence of calcium and phosphorous that agrees with the presence of hydroxyapatite. In this case, the presence of the 2013 cm^{-1} band can be used as the basis on which to differentiate these pigments from the other blacks. The spectrum of Genuine Wine black, Figure 5, shows some important peaks at 1026, 871, 798, 743, 533 and 473 cm^{-1}, indicating the presence of a silicate. This hypothesis is confirmed by the presence of silicon in the SEM spectrum. The presence of the band at 1026 cm^{-1} allows this pigment to be differentiated from the French Wine black, whose medium intensity bands are difficult to be assigned, but whose strong band at 578 cm^{-1} could be associated to the inclusion of an iron oxide in its composition(Fig. 6). This compound could be confirmed by the iron is present, using, for instance, SEM.

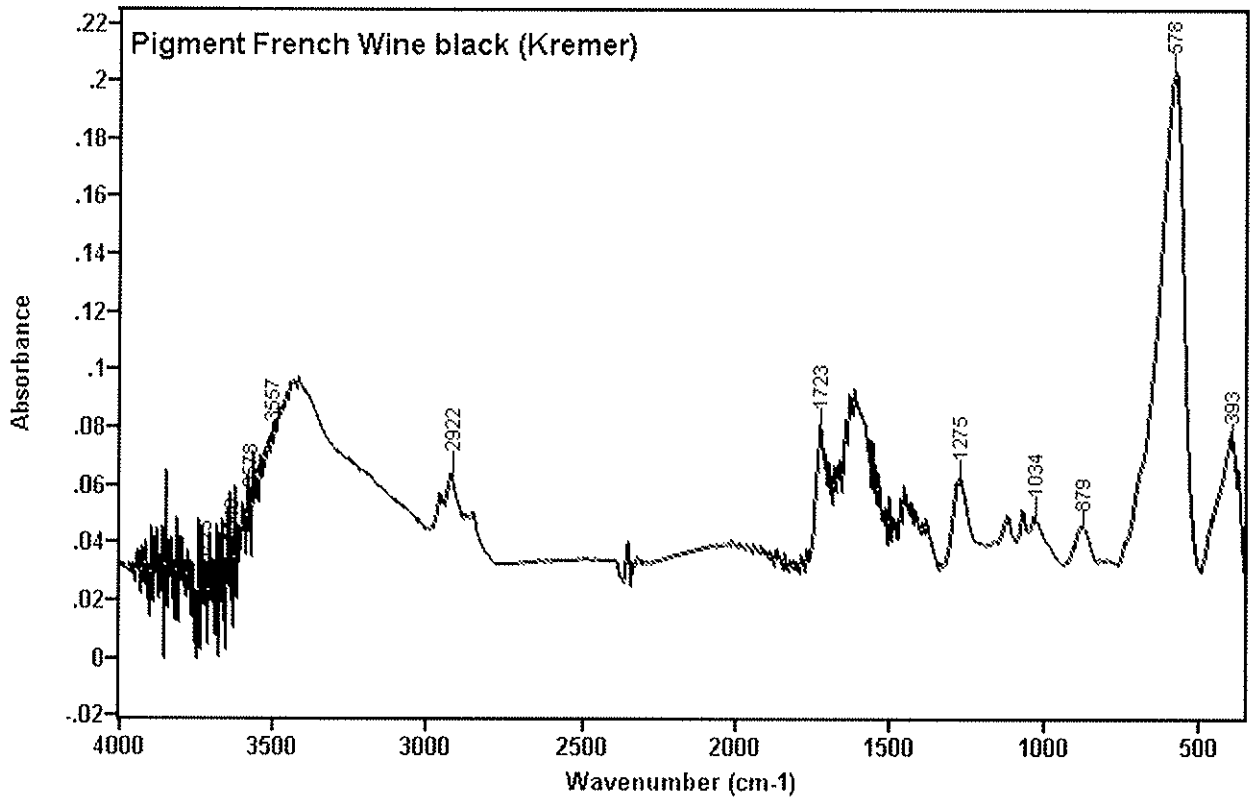

Figure 6. Infrared spectrum of French Wine Black pigment.

Conclusions

The information obtained in the chemical characterization of black pigments by infrared spectroscopy allows discriminating amongst various classes of black pigment, excluding bone based pigments. According to this result, it could be expected to differentiate among the inks formulated including these pigments and probably among the prints created by using these inks.

Acknowledgements

Authors thank the Ministerio de Ciencia y Tecnología by the Grant BHA-2002-02756. Authors also thank Àngels Miquel for her comments and to Ramón Fontarnau and the members of the Electronic Microscopy Unit (SCT) for their technical support.

References

1. Baer, B. 1998. *Picasso gravures 1900-1942*. Barcelona: Ajuntament de Barcelona-Museu Picasso.

2. Gascoigne, B. 1986. *How to Identify Prints*. Thames and Hudson. Spain.

3. Derrick, MR; Stulik, D; Landry, JM. 1999. *Infrared Spectroscopy in Conservation Science*. The Getty Conservation Institute. Los Angeles-USA.

4. Mayer, R. 1991. *The artist's handbook of materials & techniques.* Faber and Faber.

5. Socrates, G. 1980. *Infrared characteristic group frequencies.* John Willey & Sons (p. 43).

The Study of Photographic Coatings Using Angle Resolved ATR-FTIR Spectrometry

Herant Khanjian and Dusan Stulik
The Getty Conservation Institute, 1200 Getty Center Drive, Suite 700, Los Angeles, CA 90049, USA

The fading of photographic images was recognized in early stages of development and a number of trials were made to deal with the problem. Photographers attempted both chemical modification of silver particles in photographic images (toning) and application of various organic coatings to prevent moisture and oxygen from reaching the silver particles. The presence of a thin top coating on a number of 19th century photographs makes the identification of the photographic process difficult. In some cases the infrared spectrum of a photograph contains signal from both organic coating and the image layer, and in other cases even the analytical signal from the paper substrate. To identify individual layers of organic materials on photographic images and to resolve some problems of identification of photographic processes, the Angle Resolved ATR-FTIR spectrometric technique was used. By varying the depth of penetration of the infrared beam into the organic layer of photographic image, the sequence of organic layers in the photographic image and ways to distinguish between the use of multiple layer coatings and multi component varnishes was identified. Real application of developed methodology on 19th century photographs and problems of detection limits for very thin layers of organic material will be also discussed.

Research into the Influence of Impregnating Agents on the Ageing of Polturethane (PUR) Foams Using FTIR Spectroscopy

Thea B. van Oosten and Aleth Lorne
Netherlands Institute for Cultural Heritage (ICN), P.O. Box 76709, 1070 KA Amsterdam, the Netherlands

Abstract

In recent years, various impregnating agents have been tested for the conservation of flexible polyurethane (PUR) foams. In this study two of the most promising impregnating agents, *Plextol B-500* and *Impranil* and an *anti-oxidant,* vitamin E, were tested with an emphasis on their influence on visual, textural and chemical properties of treated PUR foams.
Test samples of several types of both PUR *ester* and *ether* foams were impregnated and artificially aged. It is known that PUR *ester* type foams predominantly undergo hydrolysis during ageing, while PUR *ether* type foams are especially sensitive to oxidation. Hence, the PUR *ester* samples were thermally aged in the dark at 90°C and exposed to large amplitude relative humidity cycles of 35-80% RH over 3 hours to enhance hydrolysis. The PUR *ether* samples were light aged by exposure to the radiation of a xenon arc lamp to induce oxidation.
Fourier Transform Infrared Spectroscopy (FTIR) is known to be a very useful and convenient technique for the detection of changes in active groups in polyurethane foam. Therefore in this study, FTIR was used to investigate changes due to the hydrolysis of PUR *ester* foams and photo-oxidation of PUR *ether* foams.
PUR *ester* foams
After thermal ageing, all of the impregnated PUR *ester* foams showed better handling properties than the non-impregnated samples. A total loss of flexibility for the non-impregnated test samples was noticed after 20 days of ageing, whereas the impregnated PUR ester test samples needed 27 days of ageing for total loss. FTIR analysis of PUR ester foams showed an increase in hydroxyl absorbance at 3450 cm^{-1} due to hydrolysis of *ester* components of the foams.
PUR *ether* foams
After 168 hours of artificial light ageing, the top layer of non-impregnated PUR *ether* foams had degraded and crumbled. Impregnated test samples showed a similar level of degradation of the top layer after 192 hours of exposure. FTIR analysis of non-impregnated PUR *ether* test samples showed an increase of carbonyl and hydroxyl groups due to photo-oxidation. The application of the anti-oxidant, vitamin E, inhibited the oxidation of PUR ether foam. *Plextol B-500* showed more yellowing after ageing than *Impranil;* overall the latter gave a better result.

Introduction

The production and the use of flexible polyurethane (PUR) foams in objects of cultural heritage have been described extensively in the literature [1-9]; as has the degradation of PUR foams under the influence of light, oxygen, moisture and heat [10–17]. Various conservation and restoration methods have also been performed and described, and various impregnating agents tested for the conservation of flexible PUR foams [18-23]. The two most promising impregnating agents, *Plextol B-500* and *Impranil*, were selected and further tested with an emphasis on their influence on the visual, textural and chemical properties of the treated PUR foams. Test samples of various types of both PUR *ester* and *ether* foams were impregnated and artificially aged. Some PUR *ether* foam test samples were also impregnated with the anti-oxidant, vitamin E and aged. After ageing, changes in photo-oxidation and hydrolysis of the PUR *ether* and *ester* foams were investigated using FTIR spectroscopy.

Polyurethane processes
The development of polyurethanes in the United States and Europe started after WWII following studies undertaken in Germany, particularly those by Dr. Otto Bayer in 1937. Although research on polyurethanes was begun in 1938 by DuPont in the US, it wasn't until just after the 1950s that polyurethanes became commercially available.
Polyurethanes are a group of polymers with various compositions and many applications including fibres, soft and hard elastomers, coatings and adhesives, flexible and rigid foams, thermoplastic and thermosetting plastics. Most polyurethane flexible foams are three dimensional block polymers in which flexible linear chains of poly*esters* or poly*ethers* are linked together with rigid di-isocyante segments. In the polyurethane flexible foam industry, mixtures of 2, 4- tolylene di-isocyanate and 2,6-tolylene di-isocyanate, two aromatic di-isocyanate types (T80 and T65) are used.

Polyester urethane
Hydroxyl-terminated polyesters were the first hydroxyl containing materials used in the manufacture of urethane flexible foams. The principal components are adipic acid, phthalic anhydride, dimerised linoleic acid, and monomeric glycols such as ethylene glycol, propylene glycol, 1,4 butylene glycol, and 1,6 hexylene glycol. Triols used are trimethylolpropane, glycerol and 1,2,6 hexanetriol. Most of the poly*ester* urethane flexible foams are based on diethylene glycol-adipic acid polyesters.

Polyether urethane
The commercial introduction of poly*ether* urethane foams by General Tyre started in 1956. The hydroxyl-terminated polyethers are prepared by the base catalysed reaction of propylene, ethylene- or butyleneoxide with di- or polyfunctional alcohols such as diols (propylene glycol, glycerol, trimethylolpropane), hexitols (sorbitol) and octols (sucrose). The earliest poly*ether* urethane foam was based on glycerol and propyleneoxide.

Degeradation of polyurethanes

The lifetime of a polyurethane object depends on internal factors (its product characteristics), and external factors such as light, heat, relative humidity, and chemicals.

Internal factors
Product characteristics depend on the type of polyurethane, e.g., its components and hence its structural composition (cross-linking); the presence of protective agents such as antioxidants and UV absorbers; built-in stress; and size and shape of object. The weak points in a polyurethane molecule are the urethane, ester, ether, and amide linkages. During degradation chain scission and cross-linking occur, but over a period of time cross-linking prevails resulting in the decrease of flexibility of the foam. Some physical properties are: molecular weight, degree of cross-linking, stiffness of chain segments, crystallinity and effective intermolecular forces. These properties will change during ageing of the polyurethane.

External factors
PUR foam, having a large internal surface because of its many open pores, is very prone to degradation. Open cellular, as well as, closed cell types of polyurethane foams contain about 3% of solid material and 97% air by volume. Polyurethanes are both (photo-) oxidised and hydrolysed by exposure to light, heat, relative humidity and chemicals. In general the esters are more sensitive to hydrolysis, whereas, the ethers are more sensitive to oxidation.

Light
The stability of polyurethane to light depends on the di-isocyanate and polyol used. Aromatic di-isocyanates are more sensitive to oxidation than aliphatic ones, resulting in the yellowing of the polyurethane. Poly*ether* urethanes are more sensitive to oxidation and photo-degradation than poly*ester* urethanes. Increased resistance to light can be achieved by incorporating antioxidants and UV absorbers. The best light resistant polyurethanes are those formed from polyester and an aliphatic diisocyanate.

Relative humidity and temperature
Resistance to hydrolysis depends on the polyester used. Polyester based on glycols and dicarbonic acids with at least five C-atoms improves the stability. The best results are based on 1, 6 hexandiol-adipic acid polyester. Poly*ester* urethanes based on adipic acid and ethyleneglycol/1, 4 butanediol are cheaper to produce but are less resistant to hydrolysis.
The best hydrolysis resistant polyurethanes are those formed from a poly*ether* and a di-isocyanate. Additionally, elevated temperatures affect ageing in its usual way, by increasing the rate of chemical reactions.

Chemicals
When polyurethanes are new and in a good condition, they show high resistance to organic solvents like aliphatic, aromatic and chlorinated hydrocarbons and mildly polar solvents such as acetone, methanol and di-ethyl ether. However, highly polar solvents like dimethylformamide will dissolve polyurethanes. The resistance to chemicals depends on the structure and composition of the polyurethane: the more cross-linked the less soluble. During ageing, resistance to the above mentioned solvents decreases. Resistance to acids and alkalies is dependent on the urethane group and is generally poor.

Methodos and materials

Impregnating agents
As a result of a literature survey, two of the most promising impregnating agents for the conservation of PUR foams, *Impranil DLV* (a polyurethane/PVAC emulsion) and *Plextol B 500*, (an acrylic emulsion) were selected for testing.

Polyurethanes
Large sheets of both poly*ester*- and poly*ether* urethane foam with thicknesses of 2.5 cm were acquired from a PUR factory. From those sheets, test pieces (5 x 5 cm) were cut with a pair of scissors. Test samples (PUR *ether* and *ester* types) were impregnated with 8 grams of either *Plextol B 500* or *Impranil DLV* by soaking them in the emulsions. After impregnation, the test pieces were dried on a tray.

Thermal ageing
Artificial ageing experiments were carried out on the impregnated and non-impregnated test samples. Ageing took place in the dark in a Vötsch Vc 0200; climate chamber at 90°C. Samples were exposed to large amplitude relative humidity of 35-80% RH in 3 hours cycles to enhance hydrolysis. Test samples were taken out the climate chamber for experiments at 1, 2, 3, 4, 5, 7, 10, 14, 20, and 27 days.

Light ageing
The PUR *ether* test samples were light aged: exposed to the radiation of a filtered xenon arc lamp for up to 192 hours to induce photo-oxidation in a Xenotest, Alpha High Energy from Atlas. Test samples were analysed at the following intervals: 0, 4, 8, 16, 24, 48, 72, 96, 120, and 216 hours.

Fourier Transform Infrared Spectroscopy (FTIR)
To verify the composition and study the molecular changes upon artificially ageing, FTIR spectra of the test samples before and after ageing were recorded. FTIR analyses were performed using a Perkin Elmer Spectrum 1000 FTIR spectrometer combined with a Golden Gate, Single Reflection Diamond ATR unit.
Polymers can be differentiated as urethanes by the presence of the absorption bands in IR spectra at approximately 1538 cm^{-1} for the amide II (NH deformation), 1724 cm^{-1} for the amide I (C=O stretch) and around 3300 cm^{-1} (NH stretch). The presence of polyester or polyether linkages in the polymer chain can be established by examining the relative intensity of the rather large bands around 1100 cm^{-1} due to the O=C-O-C (ester linkage) and C-O-C (ether linkage). In the case of poly*ester* urethanes, the ester linkage at 1124 cm^{-1} is more intense while the ether linkage at 1088 cm^{-1} is more dominant in poly*ether* urethane.
Chemical changes of PUR *ether* foam due to photo-oxidation can be seen in the FTIR spectrum as an increase of hydroxyl and carbonyl absorptions, whereas chemical changes of PUR *ester* foam can be investigated using the increase of hydroxyl absorption bands due to hydrolysis.

Anti-oxidants
PUR *ether* foam test samples were impregnated with a mixture of *Impranil* and vitamin E, an anti-oxidant, and artificially light aged up to 288 hours. Natural vitamin E (Tocopherol) that occurs in plants, especially wheat germ, was used.

Results

Flexibility
The non-impregnated PUR *ester* foam test samples began to degrade after 15 days and lost their flexibility completely after 20 days of thermal ageing (compression set test, DIN 53572). PUR *ether* foams test samples were thermally aged, as well, but no hydrolysis took place and their flexibility remained. Impranil and *Plextol* impregnated PUR *ester* foam test samples, showed a slightly different pattern. At 27 days of thermal ageing, these test samples were totally degraded (See fig.1).

Visual examination
Non-impregnated PUR *ether* foam test samples were thermally aged and a slight discoloration was seen. The impregnated PUR *ether* foams were discoloured after thermal ageing, the *Plextol B 500* more than the *Impranil DLV* (See fig.2).

The artificially light aged PUR *ether* samples, non-impregnated, as well as, impregnated yellowed. After 72 hours of light ageing, the surface of non-impregnated PUR ether foam began to crumble, while after 216 hours of ageing, a completely powdered surface layer was observed. The impregnating agents did not prevent degradation either and the crumbling started after 96 hours of light ageing (See fig.3).
Artificially light aged PUR*ester* foam test samples, non-impregnated, as well as, impregnated showed discoloration although this was not easily discerned due to the black colour of the test foam.

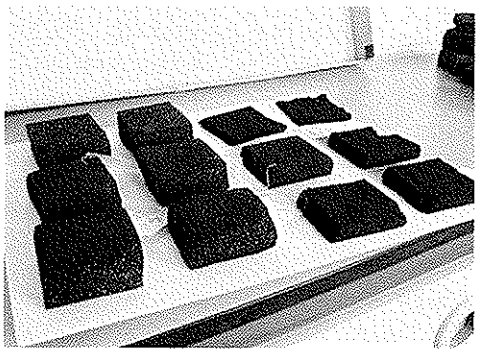

Fig.1. PUR ester foam test samples, thermally aged, left to right (10, 15, 21 and 27 days) after compression set test. Upper row: non-impregnated; Middle row: Plextol B 500 impregnated; Bottom row: Impranil DLV impregnated.

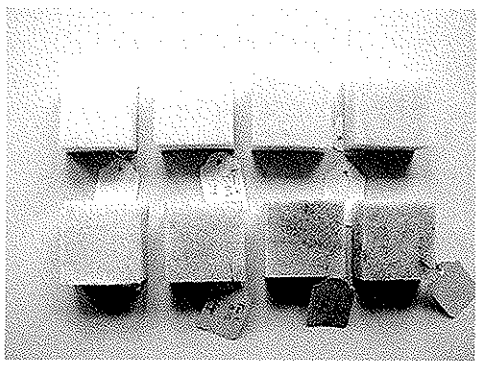

Fig.2. PUR ether foam test samples, thermally aged, left to right (10, 15, 21 and 27 days). Upper row: Impranil DLV impregnated; Bottom row: Plextol B 500 impregnated.

Chemical changes
FTIR spectra of ether and ester based polyurethane foams are shown in figure 4. The upper infrared spectrum shows the typical absorption bands of a poly*ether* urethane at 1088 cm^{-1} of C-O-C absorption and some small carbonyl absorption at 1717 cm^{-1}. Specific ester absorptions of poly*ester* urethane are the carbonyl at 1725 cm^{-1} and the O=C-C-O-C absorption at 1218, 1170, 1124 and 1078 cm^{-1}.

Thermal ageing
FTIR spectra of all thermally aged PUR *ester* foam test samples, both impregnated and non-impregnated, were recorded. In Figure 5 the infrared spectra of the non-impregnated PUR *ester* foam after 27 days of thermal ageing and non-aged PUR *ester* foam are shown. The increase of

Fig.3. Powdered surface layer of PUR ether foam test samples

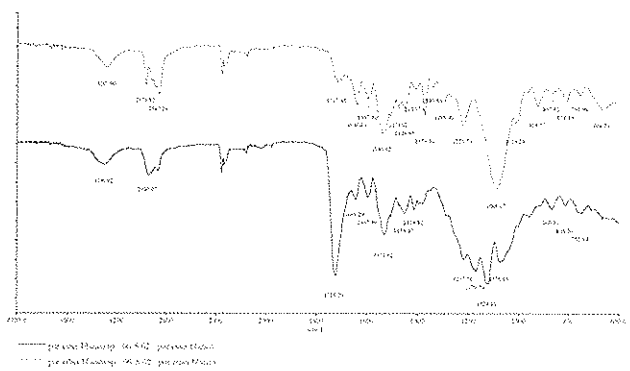

Fig.4. FTIR spectra of PUR ester (bottom) and PUR ether foam (top)

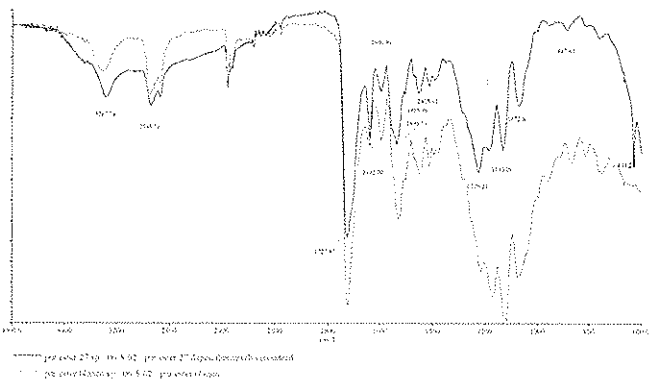

Fig.5. FTIR spectra of PUR ester foam, thermally aged (top) and non-aged (bottom)

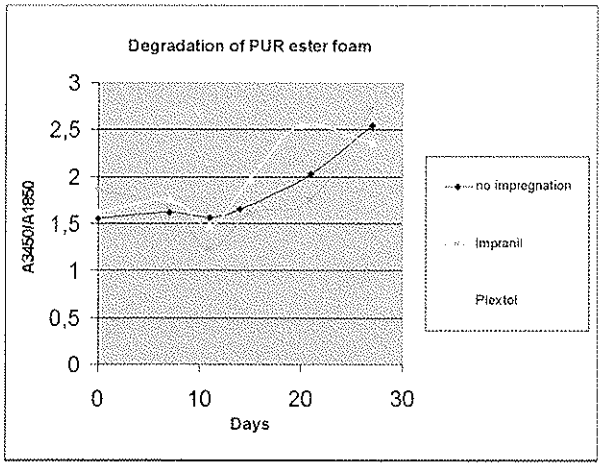

Fig.6. Degradation of PUR ester foam

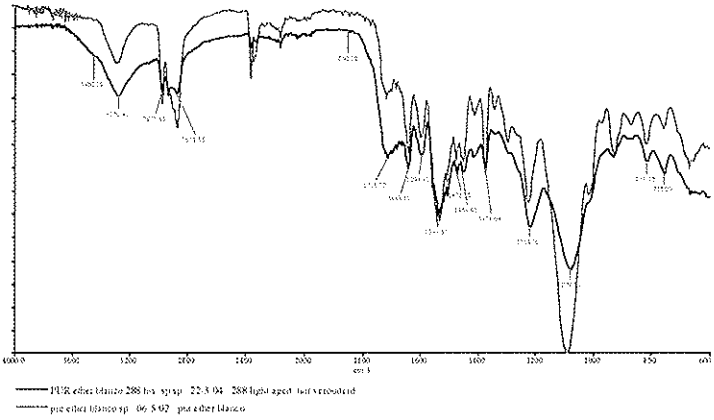

Fig.7. FTIR spectra of PUR ether foam, artificially light aged (top) and non-aged (bottom)

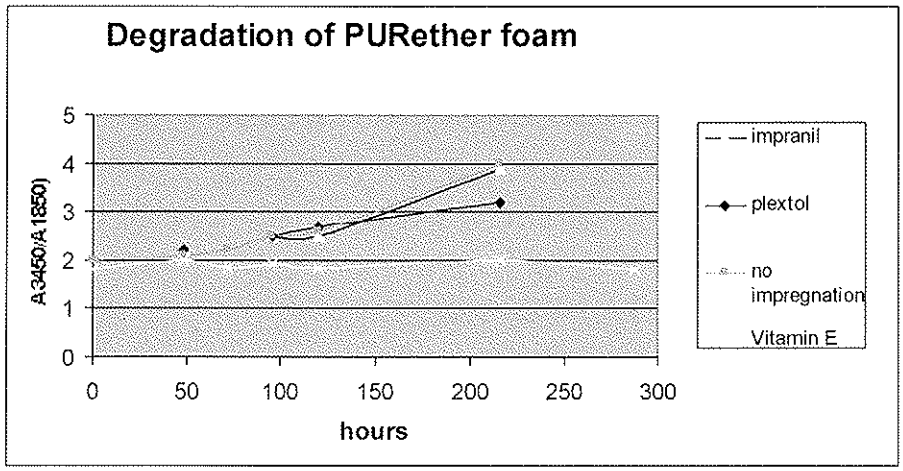

Fig.8. Degradation of PUR ether foam

hydroxyl absorption was determined by calculating the relative absorbance (A3450/A1850), which is the height of the absorption peak at 3450 cm^{-1} (A3450) divided by the height of the absorbance at 1850 cm^{-1} (A1850).
The degradation due to hydrolysis of all PUR *ester* foams, impregnated and non-impregnated, is expressed as the relative absorbance (A3450/A1850) and plotted against ageing in days in Figure 6.

Light ageing
FTIR spectra of all artificially light aged, impregnated and non-impregnated PUR *ether* foam test samples were recorded. In Figure 7, the FTIR spectra of PUR *ether* foam, non-aged and 288 hours of light ageing, are shown. The increase of photo-oxidation was determined by calculating the relative absorbance (A3450/A1850), which is the height of the absorption peak at 3450 cm^{-1} (A3450) divided by the height of the absorbance at 1850 cm^{-1} (A1850). The degradation due to photo-oxidation of all PUR *ether* foams, impregnated and non-impregnated, is expressed as the relative absorbance (A3450/A1850) and plotted against ageing in hours in Figure 8. The increase in carbonyl absorption could not be used as a marker due to the obscuring effect of the infrared absorptions of both impregnating agents.

Anti-oxidants
FTIR spectra of the artificially light aged PUR ether foams impregnated with Impranil DLV and anti-oxidant were recorded. No increase of hydroxyl absorption at 3450 cm^{-1} was observed (See also Fig. 8).

Discussion

The total loss of flexibility for non-impregnated PUR *ester* foams after 20 days, and the total loss of flexibility for impregnated PUR *ester* foams after 27 days, show that the impregnating agents, *Impranil DLV* and *Plextol B500*, do not prevent degradation, but prolong the "service-life" of PUR foam by "an adhering affect". Impranil DLV (polyurethane/PVAC) gave the best results: less discoloration, more flexibility and better "adhering" potential.
Adding an anti-oxidant (Vitamin E) inhibited the oxidation of PUR ether foam.
Future research will be focussed on the various application methods of impregnating agents and anti-oxidants. In addition, other types of anti-oxidant and UV absorbers will be investigated.

Acknowlegdements

We would like to thank Caligen Europe BV, Breda, the Netherlands (www.Caligen.com) in providing the PUR ester and PUR ether foams.

References

1. Bayer, *Kunststoffe*, Farbenfabriken Bayer "Aktiengesellschaft, Leverkusen (1963).

2. Bruins, Paul, F., *Polyurethane Technology*, Interscience Publishers, John Wiley & Sons, New York (1969).

3. *DIN-Taschenbuch, Schaumstoffe, Pruefung, Anforderung, Anwendung*, Beuth Verlag GmbH, Berlin, Koeln, December (1988).

4. Dombrow, Bernard, A., *Polyurethanes*, *Rheinhold Plastics Applications Series*, Reinhold Publishing Corporation, New York, Chapman & Hall, Ltd, London (1957).

5. Domininghaus, H., *Die Kunststoffe und ihre Eigenschaften*, VDI Verlag GmbH, Düsseldorf (1988).

6. Foerst, W. *Polyurethan-Schaumstoffe*, in: Ullmanns Enzyklopädie der technischen Chemie. Vol.14. 3rd ed. Munich and Berlin: Urban & Schwartberg (1963) 352-361.

7. Horie, C. V. *Materials for Conservation, Organic Consolidants, Adhesives and Coatings*, 4th ed. Oxford, London and Boston: Butterworth Heinemann (1995).

8. Schwarz, O., *Kunststoffkunde*, Vogel Buchverlag, Würzburg, Germany (1988).

9. Uhlig, K., *Polyurethan Taschenbuch,* Munich and Vienna: Carl Hanser (1998).

10. Dolezel, B., *Die Beständigkeit von Kunststoffen und Gummi*, Carl Hanser Verlag, München, Wien (1978).

11. Grassie, N., Zulfiquar, M., Guy, M. I., 'Thermal Degradation of a Series of Poly*ester* Polyurethanes', *Journal of Polymer Science*, Polymer Chemistry Edition, (1980) 18 265-274.

12. Kau, C., Huber, L., Hiltner, A., Baer, E., 'Damage Evolution in Flexible Polyurethane Foams', *Journal of Applied Polymer Science*, (1992) 44 2069-2079.

13. Keneghan, Brenda, 'Trouble in Toyland - Larry the Lamb Falls to Pieces', *From Marble to Chocolate, The Conservation of Modern Sculpture, Tate Gallery Conference,18-20 September 199,* Jackie Heumann, ed. London: Archetype Publications Ltd., appendix. (1995).

14. Kerr, Nancy, Batcheller, Jane, 'Degradation of Polyurethanes in 20th-Century Museum Textiles', Saving *the Twentieth Century: The Conservation of Modern Materials,* Proceedings of a Conference 15-20 September 1991, Ottawa, David Grattan ed. Ottawa: Canadian Conservation Institute, (1993) 189-206.

15. McGlinchey, C. W., 'The Physical Ageing of Polymeric Materials'. *In Saving the Twentieth Century. Proceedings of a Conference,* Ottawa (1991) 113-121.

16. Oosten, Th.,B., '59-18 by Henk Peeters', *Modern Art , Who Cares,* Hummelen et al ed. Amsterdam (1999).

17. Rabek, Jan, F., *Polymer Photodegradation, Mechanisms and Experimental Methods*, Chapman & Hall (1995).

18. Rek, V., Bravar, M., Govorcin, E., Suleska, M., 'Mechanical and Structural Studies of Photodegraded Polyurethane' *Polymer Degradation and Stability* (1989) 24 399-411.

19. Griffith, R. Storage: 'Not So Simple, Improved Storage. Specifications for Modern Furniture Collections' *MA Final Degree Project* (unpublished). London: Royal College of Art and V&A Joint Conservation Course (1997).

20. Lorne, A., 'Experiments in the Conservation of a Foam Object', *Modern Art, Who Cares,* Hummelen et al ed. Amsterdam (1999).

21. Winkelmeyer, I., 'Zeitgenössische Kunst aus Polyurethanschaum. Entstehung - Alterung - Restaurierung – Lagerung', *Diploma thesis (CD-ROM).* Stuttgart: Akademie der Bildenden Künste (2000).

22. Andorfer, R., 'Probleme der Erhaltung von bemaltem und durchgefärbtem Polyurethanweichschaum: Konservierung und Restaurierung von „Pietre di Fiume", *Diploma thesis.* Vienna: Akademie der Bildenden Künste (2001).

23. Bützer, J., Keßler, K., 'Kunststoff als Werkstoff, Celluloid und Polyurethan-Weichschaum, Material - Eigenschaften – Erhaltung', *Kölner Beiträge zur Restaurierung und Konservierung von Kunst- und Kulturgut,* Cologne (2001).

Consolidating agents

Impranil DLV (poly*ester*/poly*ether*-urethane dispersion of aliphatic isocyanate)
BAYER AG
Retailer: Chemie Jäkle
D-52650 Nürnberg

Plextol B 500
Retailer: Labshop, Enschede,
The Netherlands

Identification of Natural and Synthetic Dyes and Colorants in Tinted Photographs

Dusan C. Stulik, Herant Khanjian and Tram Vo
The Getty Conservation Institute, 1200 Getty Center Drive, Suite 700, Los Angeles, CA 90049, USA

Since the beginning of photography artists and photographers tried to deal with monochrome character of photographic images by local application of colors. The first tinted daguerreotypes produced as early as 1841 were tinted using mostly fine pigments. However, with the development of albumen and gelatin based photographs some natural and later synthetic dyes started to be used. To be able to identify dyes used on any given tinted photograph it is important to answer questions about the light stability of tinted photograph while in storage or during exhibition. The identification of dyes can also be used as supporting information for dating of photographic images due to the fact that the date of introduction of most synthetic dyes are well known. Using ATR-FTIR spectrometry a number of natural and synthetic dyes were analyzed in pure form, and applied to both albumen and gelatin surfaces to create a library of spectra that was later used to identify dyes and colorants found on real photographs. Because of relatively low concentration of dyes on photographic images, the spectral subtraction technique was used to identify organic dyes. The presentation will discus both the methodology of experiments and its application on 19th and early 20th century tinted photographs. The problem of detection limits and interference of decomposition products of aged dyes will also be covered.

Non-invasive Fiber Optic Reflectance mid-infrared spectroscopic analysis of white painted layers

L. Balcerzak[1], C. Cucci[1], M. Picollo[1], B. Radicati[1], S. Porcinai[2] and M. Bacci[1]
[1] Istituto di Fisica Applicata "Nello Carrara" – CNR, Firenze (I)
[2] Opificio delle Pietre Dure, Firenze (I)

Abstract

White pigments for painted materials (most notably lead white, zinc white, titanium white and calcium carbonate white) were analyzed using mid-infrared (MIR) Fiber-Optic Reflectiance Spectroscopy (FORS). This methodology was employed to measure reflection within the range 5500-900 cm^{-1} so as to simulate a non-invasive measurement of an art object. Prepared tiles served as samples. Tiles were constructed of a simple panel support material, with a gypsum and rabbit skin glue preparation layer followed by a final layer of pigment mixed with media. The media used were linseed oil and egg white tempera. Upon analysis of spectra obtained, it seems quite clear that in general protein media can be distinguished from ester media by MIR reflection spectroscopy, and in this specific work the linseed oil and egg white tempera can be characteristically identified by MIR reflection spectroscopy. Furthermore, lead white can be clearly differentiated from calcium carbonate white as each carbonate has a unique ($\nu_1 + \nu_3$) combination absorption band around 2500 cm^{-1}, in both position and shape. Although zinc and titanium white spectra do reveal peaks due to media, the pigments themselves do not show any characteristic peaks in this region. Finally, all spectra obtained were found to be easily reproducible.

Introduction

White pigments have had their role in artistic materials since antiquity. They are used to lighten colors, highlight and, especially in modern paintings, communicate artistic impression. Their presence has been found in Western textiles, pottery and oil paintings, as well as in Eastern paintings on paper.
Lead white has been used as an artistic pigment since Ptolemaic Egyptian times. It has also been synthesized since 300 B.C. in China and ancient Greece from vinegar and lead, making this one of the oldest synthetic pigments [1]. In Western Art, lead white had almost no rival white pigment until the modern era, when zinc white was introduced to the painting community in the mid to late 1800s, having only been used medicinally since antiquity. The health concerns associated with lead white made this white alternative appealing, despite its lower hiding power [2].
When titanium white (both rutile and anatase crystalline forms) became available to the artistic sphere around 1920, it was a good alternative to both lead and zinc white. Yet, with the major ore deposits in the US and Norway, production was limited initially making titanium expensive compared to the other whites available. However, by 1930, production plants had sprung up all over the world and the pigment had received a gradual acceptance into the artistic community, as its higher hiding power mimicked that of lead white (unlike zinc white) yet did not pose any risk to one's health [3].
The most common crystalline form of calcium carbonate white, calcite, has been used in frescoes since classical times, in preparation layers with animal glue since medieval times and in Japanese paintings, most commonly from the 17th century onward. This white pigment has served as both a supportive painting layer as well as a pigment in its own right, despite its low hiding power. This low hiding power, despite being disadvantageous in oil media, is a good characteristic for water based egg tempera media. Also of note is that when the Western world landed on Japan's shorelines in 1854, other whites such as zinc and subsequently titanium began to be used in Japanese art.
The current spectroscopic techniques for identifying these white pigments typically involve micro level destruction. The focus of the current paper is on non-invasive use of fiber-optic spectroscopy in the MIR (in this case, the range of the fibers is from 5500-900 cm^{-1}) to identify these important white pigments. Past work with this technique has focused on the reliability and reproducibility of using MIR fiber-optic reflectance spectroscopy for painted and powdered samples [4], as well as on using principal component analysis (PCA) for characterization of media and/or colorants [5]. Furthermore, using portable FT-IR spectrophotometers, this methodology made it possible to perform on-site non-invasive analysis on objects that cannot be moved from their current locations [6]. The MIR is well known as an important region of energy where fundamental vibrations and also overtones and combinations occur. That is, it is typically a good region for fingerprinting of materials. In this investigation, MIR FORS is able to reproducibly detect the samples' response to the IR light source. Although zinc and titanium white do not exhibit characteristic peaks with this technique, the two carbonates' spectra reveal the differences between lead and calcium carbonate whites.

Pigment	Manufacturer	Supply Code	Comments
Lead White	Carlo Erba	469155	RPE
Lead White	Alfa	33328	ACS reagent[§]
Lead White	Aldrich	24,358-2	-
Zinc White	Alfa	43141	99% pure
Zinc White	Alfa	87812	99.99% pure
Zinc White	Aldrich	25,160-7	ACS reagent[§]
Zinc White	Zecchi	785	-
Zinc White	Zecchi	S785	standard
$CaCO_3$ White	Carlo Erba	433185	RPE*
$CaCO_3$ White	Alfa	36399	ACS reagent[§]
$CaCO_3$ White	Aldrich	23,921-6	ACS reagent[§]
TiO_2 White	Carlo Erba	488257	RPE*
TiO_2 White	Alfa	42681	-
TiO_2 White	Aldrich	22,422-7	-
TiO_2 White	Zecchi	310	-
TiO_2 White	Zecchi	S310	standard

Table I. Technical information on the pigments investigated in this work.
*- Analytical grade reagent
§ - Chemicals meeting the specifications outlined by the American Chemical Society

Instrumentation

Reflectance spectra were acquired using a Nicolet Protégé 460 FT-IR spectrophotometer, connected to a Remspec fiber optic bundle equipped with a probe designed for reflectance measurements. The Y-shaped bundle is constituted of 19 fibers (500 mm diameter each), seven of which (99 cm long) carry the IR radiation from the interferometer to the sample, while the remaining twelve (74 cm long) collect the back-scattered radiation from the investigated surface. The fibers in the probe were arranged in concentric rings of 1, 6, and 12 fibers, respectively. The fibers are made of chalcogenide glass, allowing spectral coverage from 900 cm^{-1} to 5500 cm^{-1}, but showing a strong absorption due to the Se-H stretching, which results in a blind region in the 2050-2250 cm^{-1} range. Other spectral limitations may arise from environmental moisture at 3100-3500 cm^{-1} and 1500-1700 cm^{-1}, and from environmental CO_2 at 2250 cm^{-1}. The latter, if intense, is especially important as it could mask the $(\nu_1 + \nu_3)$ combination vibration from the carbonate ion around 2500 cm^{-1} found in calcium carbonate white. Likewise, the carbonate ion may combine with the hydroxide ion of lead white around 2410-2430 cm^{-1}, and could suffer interference from environmental CO_2 as well.

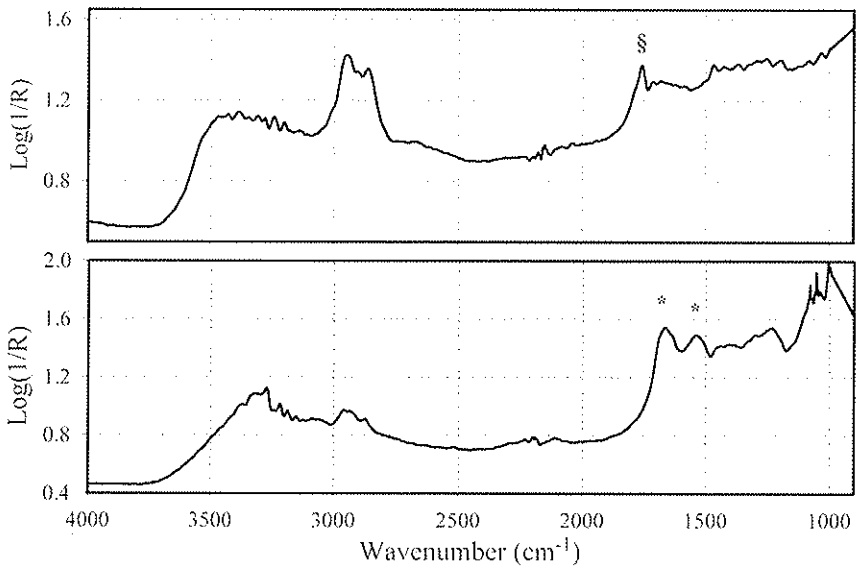

Fig. 1 spectra for linseed oil and egg white tempera mixed with titanium dioxide white. Top) Linseed oil is characterized by the peak at 1750 cm^{-1} (§), corresponding to the carbonyl vibration. Bottom) Egg white tempera has peaks at 1675 cm^{-1} and 1550 cm^{-1} (*), due to the carbonyl and the C-N-H vibrations, respectively.

The NIR range (5500-4000 cm^{-1}) of these spectra yields spectral information that needs more in-depth investigation.
The samples were kept on a base the height of which could be controlled by means of a micrometric screw, in order to have a precise and adjustable distance between the probe tip and the surface sample. The spectra

were collected with 4 cm^{-1} resolution and with 256 scans. A polished mirror was used as the reference material for the background spectrum. During the acquisition of the spectra, the FT-IR bench and the air-space between fiber probe and sample surface were purged with dry air.

Materials

Rectangular samples measure 2 cm by 3 cm and were made by a paintings conservator from Opificio delle Pietre Dure in Florence, Italy. Samples consist of a masonite panel support, a preparation layer of gypsum mixed with animal glue (from rabbit skin) followed by a final layer of pigment with either egg white media or linseed oil. Of the 44 tiles analyzed, 34 tiles were relevant to the current work. These included tiles with lead white, zinc white, titanium white or calcium carbonate white with each media, as well as tiles with only medium for the purposes of comparison. See table I for pigment manufacturer, supply code and other pigment details.

Results and Discussion

Figure 1 shows the spectra for linseed oil and egg white tempera mixed with titanium dioxide white. Egg white tempera can be differentiated from linseed oil by the absence of a peak around 1750 cm^{-1} due to the C=O vibrational mode in the oil [7]. Conversely, oil lacks a peak around 1675 cm^{-1} from the C=O in the amide group (Amide I), attributed to the egg white protein [7]. Also unobservable in oil is the peak around 1550cm^{-1} due to the C-N-H bending vibration in the egg white (Amide II) [7]. As will be discussed shortly, the spectra from the media are important as some white pigments do not have their own characteristic peaks and only show those of the medium they reside in, while other pigments may distort or hide certain elements of the media spectra. Moreover, it is important to note that the positions of the main peaks of these media (1750 cm^{-1} for linseed oil and 1675 cm^{-1} for protein) were shifted to longer wavenumbers compared to values typically quoted for transmission spectra (typically 1740 cm^{-1} for linseed oil and 1650 cm^{-1} for protein) due mainly to a contribution from specular reflection [8].
The spectra obtained for all tiles analyzed were reproducible, and is exemplified by the three spectra from three different spots on the same tile made with Alfa's calcium carbonate white in oil, (Figure 2). Furthermore, reproducibility was observed between pigments made by different manufacturers but in the same medium, save for the case of lead white in oil when Aldrich and Carlo Erba manufacturers yielded slightly different spectra (Figure 3). These differences found in the reflectance spectra were probably due to differences in particle size in the samples, which gave rise to different amounts of specular reflection in the total reflection spectrum. Indeed, Carlo Erba white pigment had larger particles, with sufficiently large facets on the particle surfaces that specularly reflect, whereas Aldrich lead white pigment had smaller particles and presented specular reflection component less intense.

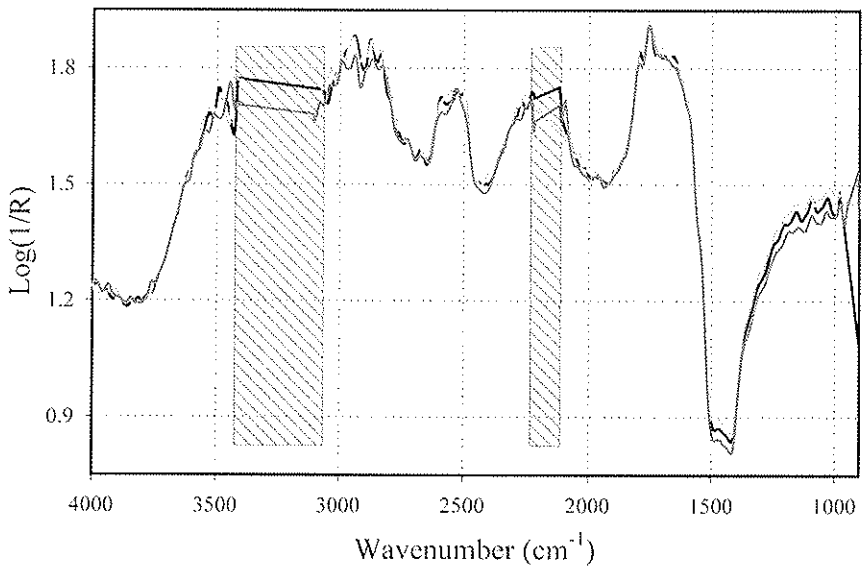

Fig. 2 Spectra from three different spots on one tile prepared with Alfa's calcium carbonate white in linseed oil (the blind portions of the spectra are highlighted with rectangular boxes).

By examining the spectra in Figure 4, it is clear that neither zinc nor titanium give characteristic peaks in the mid-IR region analyzed. That is, the peaks seen for each of these spectra reveal information on the medium only, and no peaks are seen from the pigment molecules themselves.
The spectra for calcium carbonate white and lead white show pigment specific peaks in each case. In fact, there are differences between these two carbonates in this region that allow for distinction between these two whites. Typically, the carbonate ion is characterized in the MIR region by the ν_3 vibration around 1400 cm^{-1}. However,

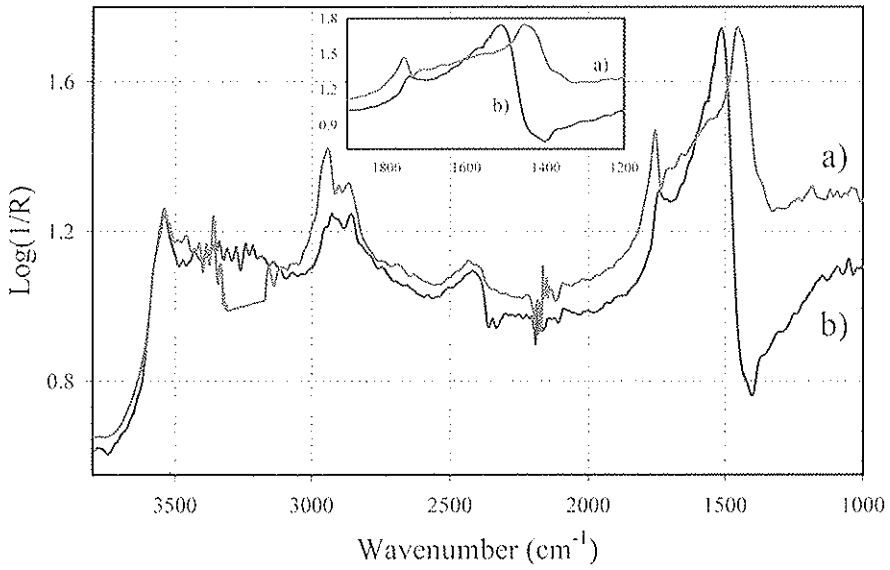

Fig. 3 Aldrich (a) and Carlo Erba (b) lead carbonates in linseed oil.

because samples analyzed were undiluted and acquisition of spectra was by total reflectance, this reflectance maximum is so intense that the so-called Reststrahlen band appears in and distorts the spectra. Therefore, other vibrations, significantly less intense than the ν_3 mode, become very important for the proper identification of the carbonate ion. Interestingly, these less intense vibrations manifest differently for the carbonate ion in the calcium carbonate environment versus the lead white environment. Furthermore, another possible reason for this is that the latter pigment's hydroxide ion manifests in the spectra and combines with the carbonate ion, thereby changing lead white's over all response in this region.

Figure 5 shows the two carbonate whites in both the egg white tempera and linseed oil media. Two sets of peaks due to the egg tempera medium are found in the spectra for each carbonate white. That is, the peak at 1640 cm^{-1} due to the amide I band (HN-C=O mode) and the peak at 1350 cm^{-1} due to C-H vibrations are both found in the calcium carbonate and lead white spectra, and are each attributed to the egg tempera. The amide II peak, usually found around 1550 cm^{-1}, is missing from these spectra because of the distortions caused by the Reststrahlen band at 1400 cm^{-1}, which distorts spectral information up to 1600 cm^{-1}. Besides these similarities, many contrasts are observed between these two pigments in egg white medium. At 1050 cm^{-1}, a medium sized peak is observed in the lead white spectra that is not seen in the calcium carbonate. This is attributed to the bending mode of the hydroxide ion [9]. In the region around 3540-3535 cm^{-1}, a sharp absorption band due to the OH stretching mode in the lead white can be found, and is therefore not observed in the calcium carbonate spectra. Also, around 1740 cm^{-1}, lead white exhibits another peak that the calcium carbonate does not. This absorption is likely due to the (ν_1 + ν_4) combination vibration of the carbonate ion [10], even if combination of vibrational modes of the 1795 cm^{-1} carbonate ion cannot be excluded. On the other hand, the (ν_1 + ν_4) absorption band of the carbonate ion is seen at around 1800 cm^{-1} for the calcium carbonate white. Meanwhile, the lead white does not exhibit a peak at this energy.

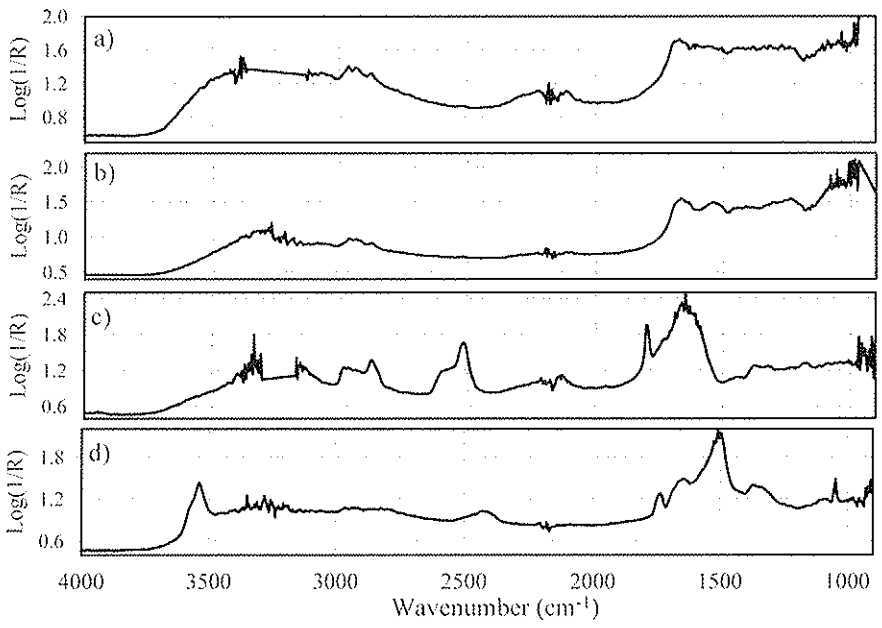

Fig. 4 a) zinc oxide b) titanium oxide c) calcium carbonate d) lead carbonate in egg white tempera

The final difference of note between these two white pigments in egg medium, and perhaps the easiest to observe, is their response to IR radiation around 2500 cm^{-1}. The calcium carbonate spectra show the characteristic features due

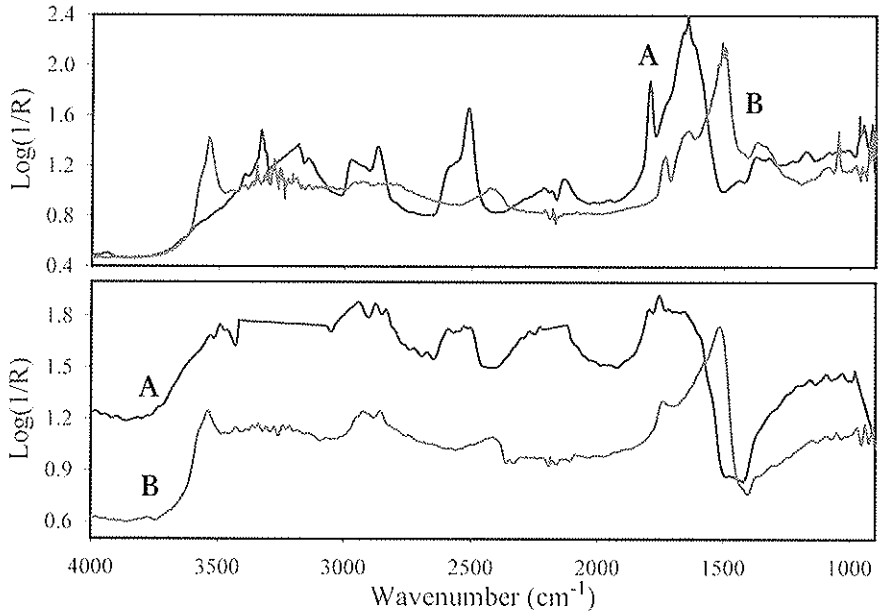

Fig. 5 Top: a) calcium carbonate and b) lead white with egg white tempera medium. Bottom: a) calcium carbonate and b) lead white with linseed oil medium.

to the $(\nu_1 + \nu_3)$ combination mode around 2515 cm^{-1} with a shoulder at 2590 cm^{-1}. This characteristic describes the simultaneous activity of the symmetric and asymmetric modes of the carbonate ion. Lead white on the other hand, exhibits the $(\nu_1 + \nu_3)$ carbonate ion combination mode around 2420 cm^{-1}. As stated earlier, this carbonate mode could be coupled with the pigment's own hydroxide ion deformation mode.
The linseed oil medium also shows the same differences between the two white carbonate pigments. However, there are a few points of interest that are specific to the oil medium. Both pigments show the peak around 1750 cm^{-1}, which, as noted earlier, is attributed to the linseed oil medium. In calcium carbonate white and lead white Aldrich, this oil peak is quite clear and unobstructed by other molecular vibrations. However, lead white Carlo Erba shows the oil peak broadened and shifted to slightly lower wavenumber, which might be explained by the distortion caused by the 1735 – 1740 cm^{-1} combination band of the pigment. This difference thereby sets lead white Carlo Erba apart from calcium carbonate and lead white Aldrich.

Conclusion

MIR Fiber-Optic Reflectance Spectroscopy has been used in this study to non-invasively identify egg white tempera, linseed oil, calcium carbonate white and lead white. Egg white, like other proteins including glue, collagen, blood, casein, etc, is characterized by a peak around 1675 cm^{-1} and linseed oil, along with other esters like PVAc and acrylic, by a peak near 1750 cm^{-1}. Calcium carbonate white is most easily identified by the $(\nu_1 + \nu_3)$ carbonate combination vibration around 2515 cm^{-1} (with a shoulder at 2590 cm^{-1}). Finally, lead white is characterized by the $(\nu_1 + \nu_3)$ carbonate vibration at about 2420 cm^{-1}, which might also include a combination with the bending mode of the hydroxide ion. Of further note is the means by which pigment identification was carried out in this study. Traditionally, carbonates are identified by their ν_3 vibrational mode at around 1400 cm^{-1}, however, that peak is a highly distorting Reststrahlen band in these spectra. Thus, carbonate combination modes and overtones, while traditionally only of minor note, become the primary means for differentiating between these two pigments in this study.

References

1. Gettens, R.J., Kuhn, H., Chase W.T., 'Lead White' in R. Ashok (ed.), *Artists Pigments: A Handbook of Their History and Characteristics (Volume 2)*, Oxford University Press, New York (1993) 67-81.

2. Kuhn, H., 'Zinc White' in R.L. Feller (ed.), *Artists Pigments: A Handbook of Their History and Characteristics (Volume 1)*, Oxford University Press, New York (1986) 169-186.

3. Laver, M., 'Titanium Dioxide Whites' in E. West Fitzhugh (ed.), *Artists Pigments: A Handbook of Their History and Characteristics (Volume 3)*, Oxford University Press, New York (1997) 295-355.

4. Fabbri, M., Picollo, M., Porcinai, S. and Bacci, M., 'Mid-Infrared Fiber-Optics Reflectance Spectroscopy: A Noninvasive Technique for Remote Analysis of Painted Layers. Part I: Technical Setup', *Applied Spectroscopy*

(2001) **55** (4) 420-427.

5. Fabbri, M., Picollo, M., Porcinai, S. and Bacci, M., 'Mid-Infrared Fiber-Optics Reflectance Spectroscopy: A Noninvasive Technique for Remote Analysis of Painted Layers. Part II: Statistical Analysis of Spectra', *Applied Spectroscopy* (2001) **55** (4) 427-433.

6. Williams, R.S., 'On-site non-destructive Mid-IR spectroscopy of plastics in museum objects using a portable FTIR spectrometer with fiber optic probe', *Mat. Res. Soc. Symp. Proc.* 462 (1997), 25-30.

7. Derrick, M., Stulik, D., and Landry, J.M., *Infrared Spectroscopy in Conservation Science*, Scientific tools for conservation, The Getty Conservation Institute, Los Angeles (1999), 183.

8. Salisbury, J.H., Hapke, B., Eastes, J.W. 'Usefulness of Weak Bands in Midinfrared Remote Sensing of Particulate Planetary Surfaces', *Journal of Geophysical Research* (1987) **92** B1 702-710.

9. Bessiére-Morandat, J., Lorenzelli, V. and Lecomte, J., 'Détermination Expérimentale et Essai D'Attribution des Vibrations Actives en Infrarouge de Quelques Carbonates Basiques Métalliques a L'Etat Cristallin', *Le Journal de Physique* (1970) 31 309-312.

10. Brooker, M.H.Sunder, S., Taylor, P. and Lopata, V.J., 'Infrared and Raman spectra and X-ray diffraction studies of solid lead(II) carbonates', *Can. J. Chem.* (1983) **61** 494-502.

Reflectance FTIR Study of Altered Calcium Carbonate Surface.

C. Miliani[1], C.Ricci[2], B. Brunetti[2], A. Sgamellotti[1]
[1] Istituto CNR-ISTM (Institute of Molecular Sciences and Technologies) Perugia Unit
[2] Centre of Excellence SMAArt " Scientific Methodologies applied to Archaeology and Art" c/o Department of Chemistry, University of Perugia, Via Elce di Sotto 8, 06123 Perugia.

The main difficulty in the study of inorganic and organic depositions on calcium carbonate surfaces (stones or frescos) by *in situ* reflectance FTIR spectroscopy arises from a strong matrix effect due to the asymmetric vibration of the $CO_3^{=}$ group inverted by the *reststrahlen* effect. The aim of the present study was to evaluate the capability of fiber optic mIR set-up to detect different organic patinas and inorganic incrustations on a carbonate substrate. Quarry Carrara marble samples were covered with thin layers of wax, protein, siccative oil, and with depositions of sulphates, oxalates, phosphates and nitrates. Measurements on these laboratory models allowed us to identify those diagnostic spectral features of both patinas and incrustations that are well-resolved from the carbonate matrix absorption. Only the identification of nitrate contamination was unsuccessful due to the large overlap of the relevant diagnostic peak ν(NO) of nitrate with the ν(CO) of calcium carbonate. Sulphate, phosphate and oxalate detection thresholds were determined. The portable FT-IR equipment was well suited to detect contamination of phosphates from a threshold of 1.2 μmole/cm², sulphates from 1.5 μmole/cm², and oxalates from 5.2 μmole/cm². Some examples of measurements collected *in situ* on both sculptures and mural paintings will be also discussed.

In-situ mid-IR Spectroscopic Analysis of Objects at Museums Using Portable IR Spectrometers

R. Scott Williams
Canadian Conservation Institute
1030 Innes Road
Ottawa, Canada
K1A 0M5

Abstract

Since 1996 the Canadian Conservation Institute has offered an on-site chemical analysis service using a portable IR spectrometer with a fiber optic probe (FOP) [1]. In 2001 this service was augmented by the addition of the Travel*IR*, a portable ATR based mid-IR spectrometer. In addition to many other advantages, this instrument allows analysis of rough and textured samples like paper and textiles that previously could not be analysed by FOP. The analysis of hundreds of plastic objects in museums, inks on parchment, and degradation of cellulose nitrate photographic film at the emulsion/film base interface, plus other examples, will be presented. The relative merits of the fiber optic probe instrument versus the ATR instrument will be discussed.

Fibre Optic Probe (FOP) IR Spectrometer (Midac/Remspec)

The CCI FOP spectrometer (Figure 1) was purchased in March 1996. This spectrometer was intended for on-site, *in situ* analysis of objects at museums, so portability and nondestructive (non-contact) analysis were of paramount importance. The instrument consists of a Midac Illuminator with IR source and interferometer [2], a bifurcated fiber optic probe and mercury cadmium telluride detector module from Remspec [3], and a laptop computer controller. Separation of the source/interferometer from the probe and detector results in small portable modules that can be easily handled and set up in different configurations on-site. The fiber optic probe contains a bundle of nineteen 500 µm diameter chalcogenide optical fibers, with seven in the input branch to direct radiation from the source to the object and twelve in the output branch to direct radiation reflected from the object to the detector. For operation, the FOP spectrometer must be located within about 2 feet of the sample due to the length of the fiber optic cable, the probe tip must be about 2-5 mm from the spot on the sample to be analysed, and the probe must be perpendicular to the sample surface (Figure 1 and 4). Sixty-four reflection spectra are collected, which takes about one minute. A polished steel mirror is used as reference. No sample is taken from the object and there is no contact with the object during analysis.
A spot about 5 mm diameter is illuminated. From my experiments, I estimate that the depth of penetration of the beam into the sample is less than 100 µm for a relatively transparent material like polyethylene, but may be only about 10 µm for an absorbant material like esters commonly found in polymers. The recorded spectrum is a

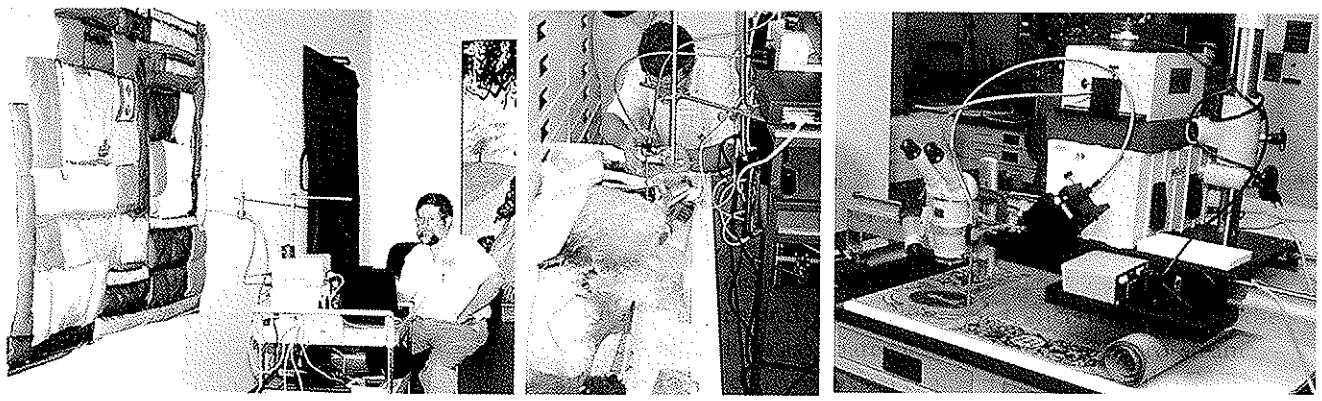

Figure 1. The Midac/Remspec fibre optic probe (FOP) IR spectrometer has been used to analyse objects that are on display in museum exhibit areas (left), in storage drawers (middle), and has been mounted on an XY-translating carriage to map locations of poly(vinyl acetate) on a large parchment (right). The Midac Illuminator is the lower box and supports the Remspec detector module on top. The Remspec fiber optic probe is clamped perpendicular to, and about 2-5 mm from, the object surface. The handles of fragile feather fans in the drawer shown above were determined to be protein (horn or tortoiseshell), bone or ivory, cellulose nitrate, cellulose acetate, and shell. The locations of poly(vinyl acetate) coincided with yellow discoloration of the parchment.

combination of the specular reflection spectra from the sample surface and other interfaces within the first 10 to 100 µm of the sample, plus the diffuse reflection spectrum from the top 10 to 100 µm of the sample. Any substance in that volume will contribute to the reflection spectrum is some way.
If the surface is sufficiently smooth, then the front surface specular reflection component is much stronger than the diffuse reflection component and the spectrum looks like, and can be treated as, a specular reflection spectrum. Smooth surfaced materials like plastics, beads, glass, etc. tend to produce specular reflection spectra. If the surface is rough or matte with roughness less than the wavelength of the probing radiation (about 3 to 11 µm), then the specular component is negligible and the spectrum is treated as a diffuse reflection spectrum. Surfaces with intermediate roughness somewhere between matte and specular produce very complicated spectra composed of specular and diffuse reflection components that cannot be resolved for interpretation. As a consequence, this instrument produces poor reflection spectra for materials with intermediate roughness like fibrous paper and textiles, and foams.
Production of reflection spectra that do not have the same shape as conventional absorbance spectra is a drawback, since these spectra in their raw form cannot be searched against commonly available absorbance spectrum libraries. Fortunately, absorbance-like spectra that are obtained by the Kramers-Kronig transformation of specular reflection spectra can be searched against absorbance spectrum libraries with some success. There are published libraries of reflection spectra of minerals [4], but I have found very little for organic and plastic materials. I usually search the raw spectra against my own libraries of raw untransformed reflection spectra that I have created.
Another drawback is the limited energy in the reflected spectrum. For an organic or polymeric material with a refractive index of about 1.5, the maximum reflected energy compared to a polished metal mirror is about 4%, as given by Fresnel's laws. Due to sample topography and geometry, reflected energy is usually in the range 1-2%. This produces noisy spectra, and this does not seem to be much improved by increasing the number of scans. These spectra are adequate to find the class of polymer, but usually not to find a component in the polymer. This is compounded by the fact that the complicated shape of the spectrum due to mixed contributions from specular and diffuse reflection is not amenable to data manipulation like spectral subtraction.
The main use for the fiber optic probe IR spectrometer has been to determine the chemical composition of many objects in collections so that storage and preservation strategies can be devised for the entire collection. The original intent was to analyse plastics, and this is by far the biggest group that has been analysed, but the technique is also suitable for minerals such as jewels, glass and shell.

Travel*IR* Spectrometer (Sensir Technologies)

In 2001 CCI purchased a Travel*IR* from Sensir Technologies [5], a self-contained portable IR spectrometer that uses the attenuated total reflection (ATR) principle of analysis (Figure 2). A small sample of less than 1 mm diameter is pressed against a 1.5 mm diameter internal reflection element (IRE) and an ATR IR spectrum of the surface of the sample in contact with the IRE is obtained. A video camera is focussed on the IRE surface to observe the sample position and to record the sample appearance. This technique requires placing the object in contact with the IRE or taking a sample from the object. Also, the configuration of the sample table and spectrometer body is such that the sample spot must be within 5 cm of the edge of the object to fit onto the IRE. The Travel*IR* allows analysis of paper and textiles, objects that could not be analysed by the FOP spectrometer.
Sixteen background scans are collected of the clean IRE immediately followed by sixteen scans of the sample pressed against the IRE. Sample preparation is trivial - press the sample against the IRE, collect spectrum. This takes about two minutes. It is a very fast technique for this sort of routine analysis. During on-site IR spectroscopic analysis surveys I can routinely run 100 spectra per day.
The primary advantage of the Travel*IR* is that it can be set up quickly at a museum, beside the objects, and samples taken from the object can be transferred directly to the Travel*IR* enabling collection of spectra within minutes, thus avoiding the taking, packing and transport of samples to remote labs. Although the IRE is 1.5 mm diameter, a spectrum can be obtained from a much smaller area. I have used this instrument to analyse particles and single fibers. The Travel*IR* requires a sample that is slightly larger than required for IR microspectroscopy using diamond cells in IR microscopes on conventional benchtop spectrometers. IR microspectroscopy provides greater spatial resolution and the ability to microscopically observe the specimen and select small fields of view for analysis, so, if analysis of very small samples with dimensions less than 50 µm is required, or if very small features in the range of 10-25 µm in a larger sample are being analysed, then the IR microscope is used, not the Travel*IR*. However, for larger samples, the Travel*IR* has proven to be very convenient for routine analysis.

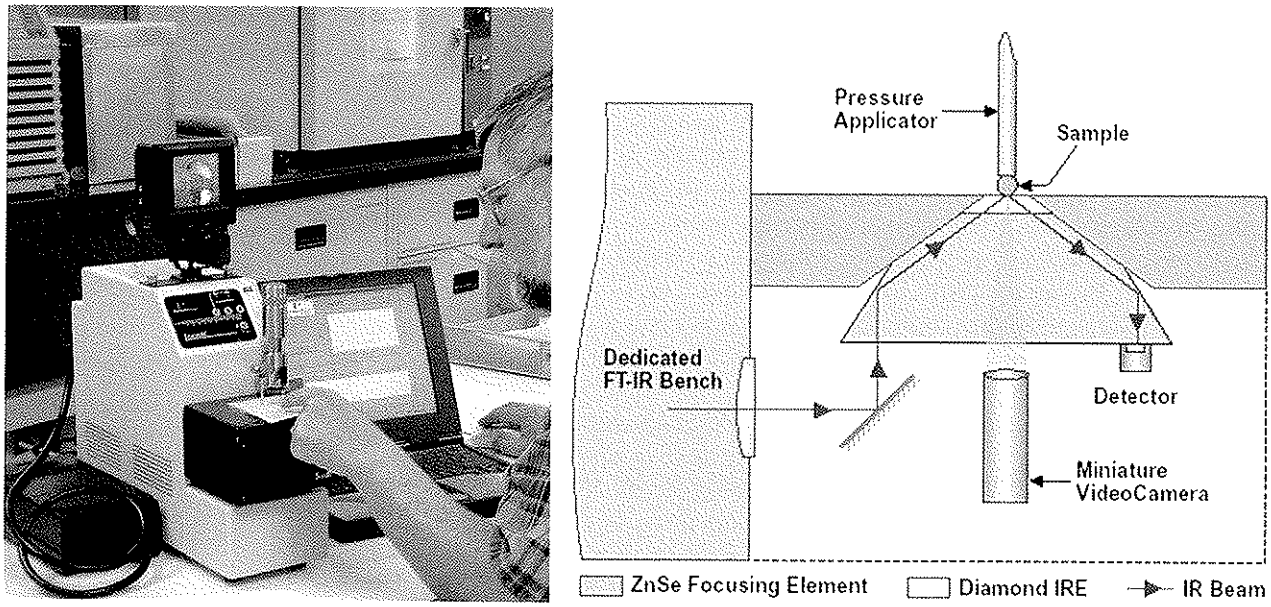

Figure 2. The Travel*IR* spectrometer can be set up on a cart to move to wherever the objects are located. The sample must be placed on the sample table, in contact with the internal reflection element (IRE) of the spectrometer, as indicated by the pointing finger. The schematic of the optical path shows the sample pressed against the 1.5 mm diameter IRE. Pressure required to produce spectra varies with sample, but plastics usually can be analysed by pressing them against the IRE with the sample held in the hand.

Case Studies

Analysis of objects on exhibit and in storage drawers

During site visits to museums, the spectrometers have been set up on lab carts and moved to objects throughout the museum. The FOP was used to analyse objects on display in exhibition galleries (Figure 1, left) and in storage drawers (Figure 1, middle). The handles of fragile feather fans stored in drawers were analysed by inserting the probe between the fans and feathers to collect reflection spectra without moving the fans. Typical specular

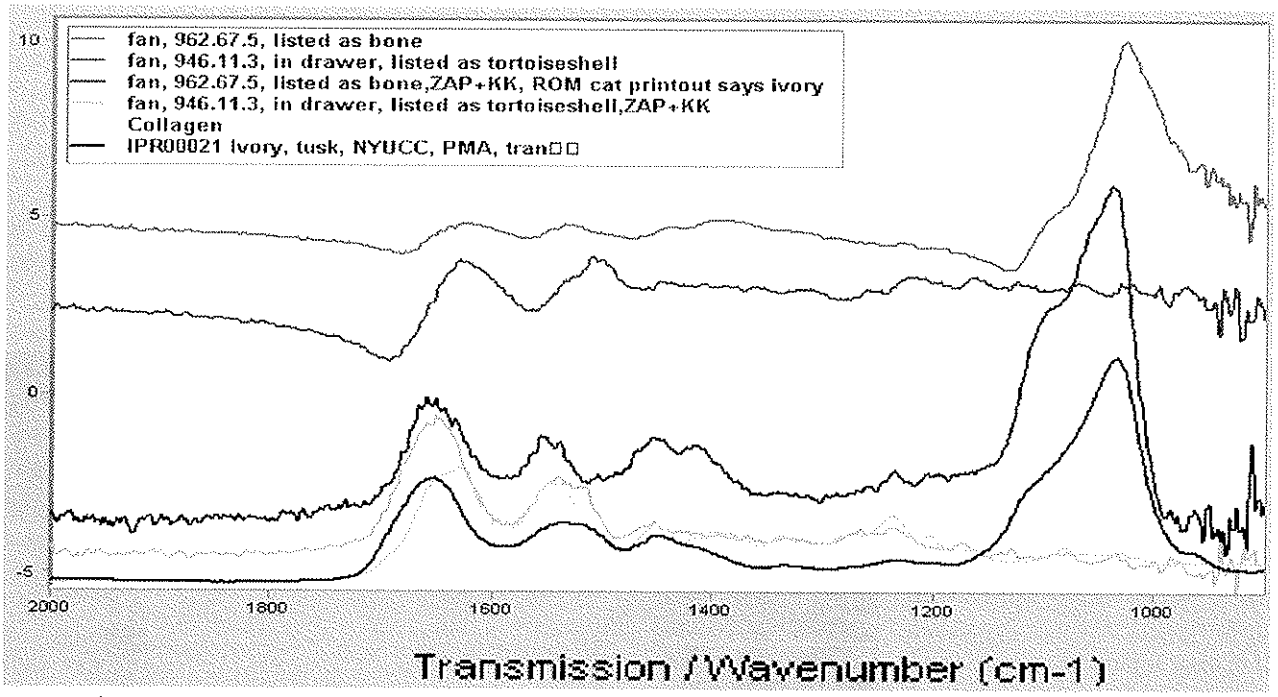

Figure 3. Fiber optic probe reflection spectra were collected from handles of fans in a storage drawer without moving fans. The top pair of raw specular reflection spectra are plotted against reflectance. The Kramers-Kronig transformation was applied to these spectra which were then replotted against absorbance in the bottom group of spectra, with absorbance spectra of collagen and ivory for comparison. The absorbance spectra of the handles closely match collagen (e.g., tortoiseshell or horn) and ivory (or bone).

reflection spectra obtained during these analyses are shown in Figure 3.
Figure 3 also shows the differences between raw specular reflection spectra and absorbance spectra, including changes in peak shapes and shifts in peak maxima. Searching the raw specular reflection spectrum against conventional absorbance spectrum libraries like the IRUG 2000 library, seldom returns meaningful hits, illustrating one disadvantage of the fiber optic probe. However, a search of absorbance spectra calculated by the Kramers-Kronig transformation, against the IRUG 2000 library and my libraries returned ivory, ivory black, and bone black as the top hits. The close match between the calculated absorbance spectra of the handles and collagen (e.g., tortoiseshell or horn) and ivory (or bone) is shown in the figure.

Mapping composition by non-destructive analysis

The *Hudson's Bay Charter* is a large parchment document, measuring 65 cm by 88 cm, dating from 1670. Irregular patches of yellow discoloration were observed. Microspectroscopic analysis of a few fibers showed that poly(vinyl acetate) (PVAc) was present in varying amounts across the surface, perhaps as a consolidant applied to prevent losses of ink. The capability of the FOP to do non-destructive analysis was exploited to map locations of PVAc consolidant to see if these matched the discoloration.
Figure 1, right, shows the FOP spectrometer mounted on an XY-translating carriage with the parchment under the carriage. The carriage was moved to predetermined spots at 10 cm intervals across the parchment and reflection spectra at 94 spots were collected. Typical spectra are shown in Figure 4. The ratio of peak intensities for ester from PVAc to protein from parchment was calculated to determine relative amounts of PVAc at each spot. This analysis confirmed that the PVAc/protein ratio was highest where the parchment was most discolored. The analysis was completed in one day, entirely without contacting the parchment or taking a sample. Such an analysis could not be accomplished by microspectroscopy of fibers removed from the parchment.

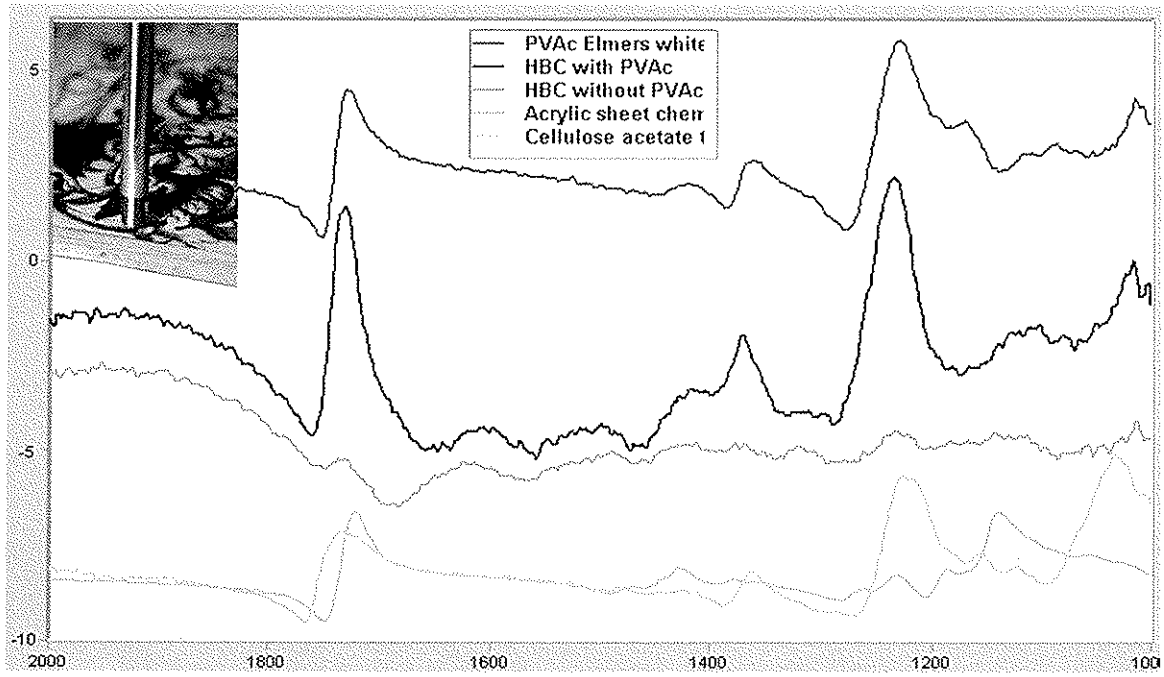

Figure 4. Reflection spectra obtained with the fiber optic probe from areas of parchment without poly(vinyl acetate) (3rd trace) and with poly(vinyl acetate) (2nd trace) are shown with reference spectra of possible consolidants, including poly(vinyl acetate) (1st trace), acrylic (4th trace) and cellulose acetate (5th trace). The closest match is to poly(vinyl acetate). The inset shows the position of the 6 mm diameter probe, about 2-5 mm above the surface of the parchment.

Analysis of parchment and inks on parchment with the Travel*IR*

Travel*IR* ATR spectra from front and back surfaces of four reference parchments dating from 1490 to 1814 show differences in calcium carbonate content (Figure 5). Parchments "1490" and "1814" are written on one surface only, and show much calcium carbonate on their front written surfaces but very little on the back unwritten surfaces. The writing surfaces seem to have been prepared by coating or rubbing with calcium carbonate, perhaps chalk. The

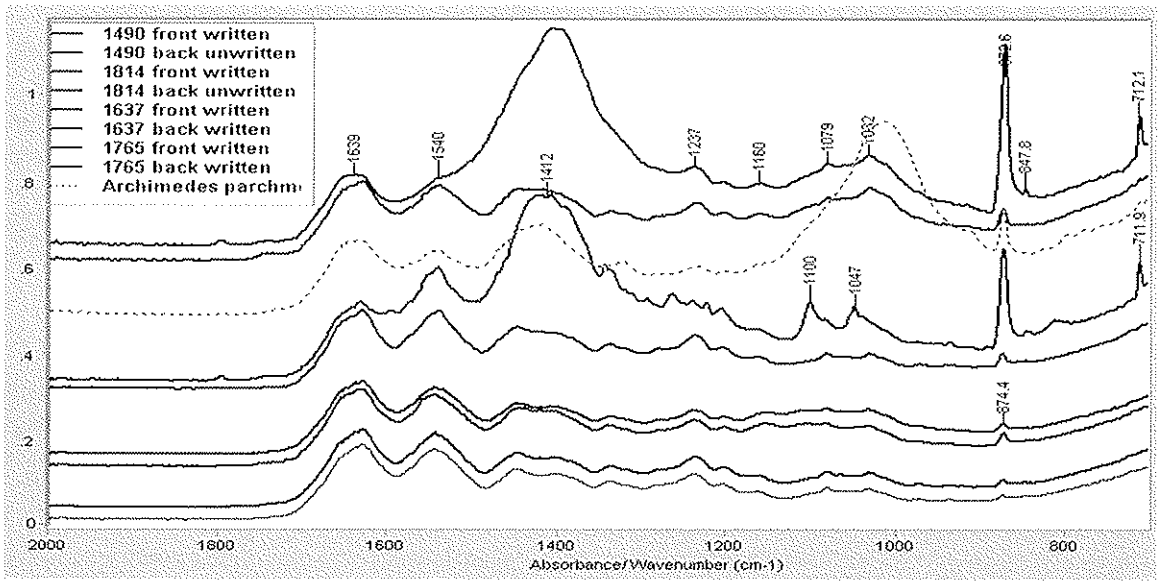

Figure 5. This figure shows Travel*IR* ATR spectra of reference parchment pages, normalized on the protein peak at 1632 cm^{-1}. Each pair of traces is from the front and back of the same parchment, ordered as indicated in the legend. Average spectrum of Archimedes Palimpsest parchment (dotted trace) is shown for comparison (see Figure 7).

spectra of both surfaces of parchments "1637" and "1765" are identical to each other, showing only protein with a negligible amount of calcium carbonate. These parchments are written on both sides, but their surfaces have not been "chalked" in preparation for writing. None of these four parchments shows significant silicate.

Travel*IR* ATR spectra of black inks on the reference parchments differ (Figure 6). Original ink has a band at 1112 cm^{-1} which is not in the parchment. Overwriting ink is a much darker, bluish black ink, and its spectrum shows a band at 1027 cm^{-1} that could be attributed to calcium phosphate in bone or ivory black, a bluish black pigment. The overwriting also has a band at 1322 cm^{-1}, which has been attributed to calcium oxalate from mold or ink medium. Since this band is not in the other parchment or ink spectra, calcium oxalate appears to be a component of the overwriting ink. Elevated

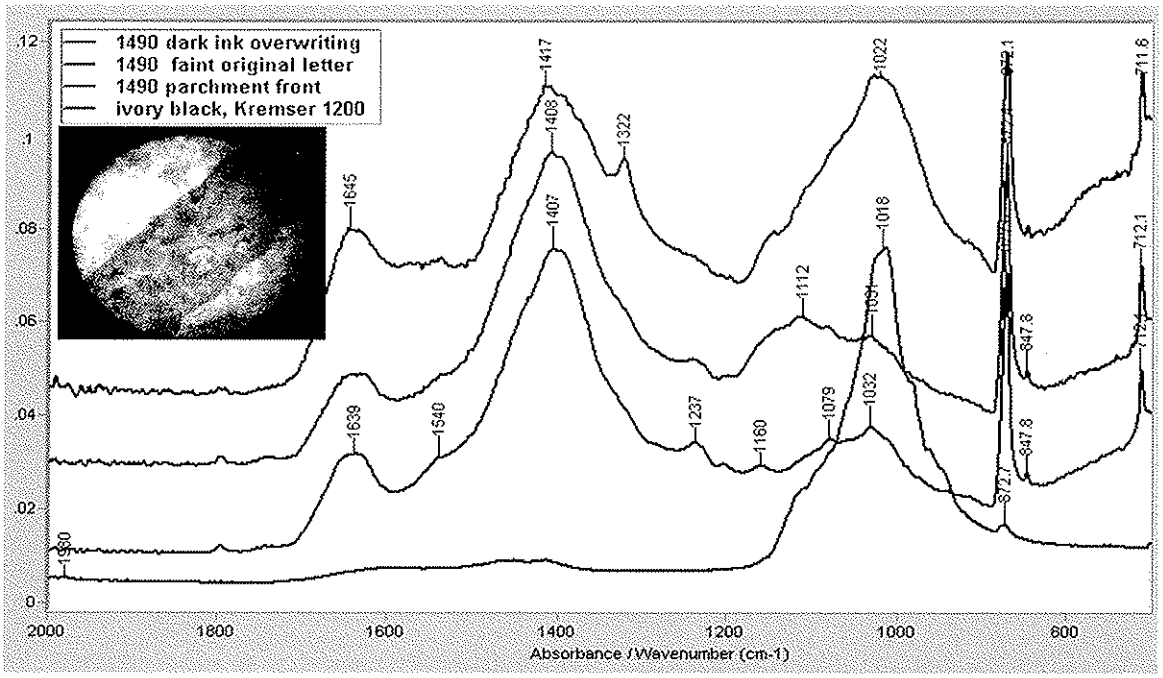

Figure 6. On parchment 1490, original ink (2nd trace) differs from parchment (3rd trace) by a band at 1112 cm^{-1} that is not in the parchment. Overwriting ink (1st trace), a much darker, bluish black ink, can be distinguished by an absorption at 1027 cm^{-1} attributed to calcium phosphate from bone or ivory black (4th trace). The overwriting has a 1322 cm^{-1} band, attributed to calcium oxalate, which is not present in the reference parchments or other inks, but has been observed in parchment and ink from the Archimedes Palimpsest (see Figure 7). The inset shows an image of an inked line as captured by the Travel*IR* video camera.

levels of calcium oxalate were detected in black Euchologion inks on the Archimedes Palimpsest (see below).
The Archimedes Palimpsest is a parchment manuscript containing the oldest existing copy of several of Archimedes' theorems, originally transcribed in the 10th century then subsequently erased and written over in the 12th century with a religious text called an Euchologion. Now the erased Archimedes text is only faintly visible in some areas so a program of image enhancement is underway. I used the Travel*IR* to analyse of the Archimedes Palimpsest at the Walters Art Museum in Baltimore to characterize the parchment, inks, and adhesives to assist in conservation of the parchment, and to gather information that might assist in the imaging efforts.
Over a period of three working days, 162 ATR spectra of parchment, ink, paint, adhesives, and accretions were collected. Seventeen spectra of parchment from four different pages were averaged to produce an Average Parchment spectrum. Similar average spectra were calculated for 10 red and 7 black Euchologion inks, and13 black Archimedes inks. These are shown in Figure 7.

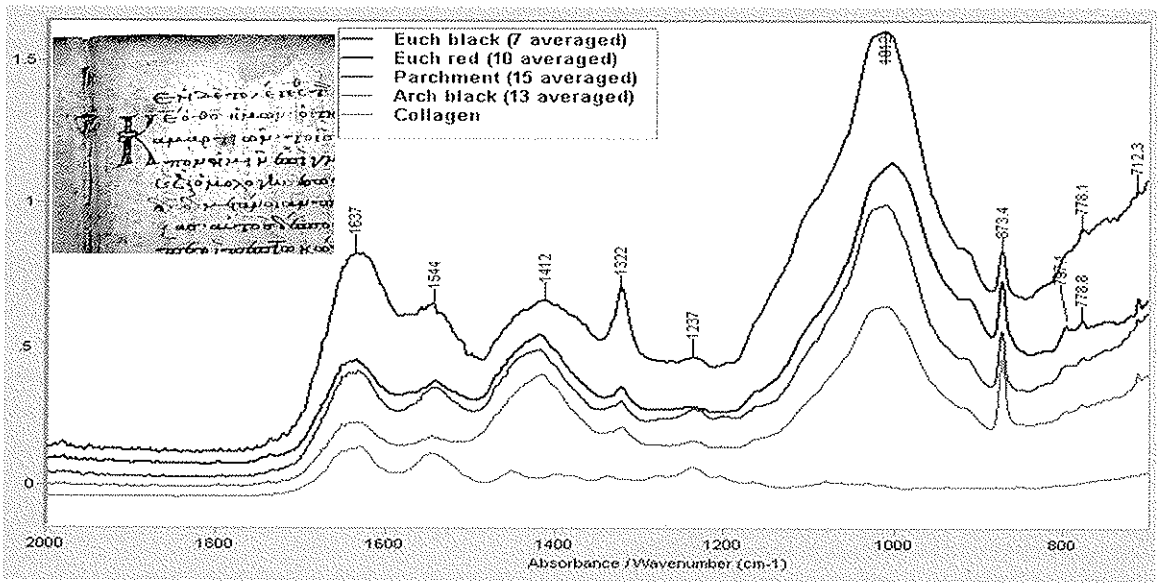

Figure 7. The Average Spectra for parchment and inks from the Archimedes Palimpsest, normalized on the carbonate peak at 1412 cm^{-1}, show calcium carbonate and silicate (1012 cm^{-1}) for all. Black Euchologion ink (1st trace) has a relatively large peak at 1322 cm^{-1} which is attributed to calcium oxalate, plus a relatively high protein content, indicating a protein medium. Inset shows part of the Archimedes Palimpsest with distinct Euchologion text running horizontally and faint Archimedes text running vertically.

All Palimpsest spectra show protein (1640, 1540 cm^{-1}), calcium carbonate (1420, 875 cm^{-1}), and silicate (1010 cm^{-1}) as major components plus calcium oxalate (1322 cm^{-1}) and sometimes quartz (797/777 cm^{-1}) as minor components. Calcium carbonate may originate from reaction of atmospheric carbon dioxide with residues of lime water used during parchment processing, or from chalk rubbed into the parchment surface to improve writing characteristics. The relatively low concentration and rather uniform dispersion of calcium carbonate observed in these spectra suggest that it originates from lime residue rather than chalk treatment. The palimpsest is very moldy, and oxalic acid which is a by-product of mold metabolism may have reacted with calcium carbonate to produce calcium oxalate. Calcium oxalate content is about the same in parchment, red Euchologion ink and Archimedes ink, but is much stronger in the black Euchologion ink, which suggests that the relatively high concentration of calcium oxalate in the black Euchologion ink is due to a component of the ink, and not just "background" from mold in the parchment. The ratio of protein to calcium carbonate is similar for all but the black Euchologion ink, which has much higher protein content, which suggests that the black Euchologion ink has a protein binder. This was corroborated by detection of protein by IR microspectroscopy of particles of red ink removed from the palimpsest. Some of the silicate on the Palimpsest may attributed to grime from the desert environment, or to talc or other mineral powder pounce sprinkled on the parchment by the 12th century scribe to dry their ink. Quartz could be a component of grime. However, red Euchologion ink, which has a weaker silicate peak (1010 cm^{-1}) than black Euchologion ink, has stronger quartz peaks, indicating quartz content greater than the "background" grime. This indicates that quartz is a component of the red ink and may originate from natural earth iron oxide pigments, like ochres and siennas which often contain quartz, clay and sometimes calcium carbonate.
The Archimedes Palimpsest has more or less equal amounts of calcium carbonate on both sides of the four pages

that were analysed, at a concentration intermediate between the two groups of reference parchments (Figure 5). Perhaps the levels of calcium carbonate in parchments 1637 and 1765 represent background calcium carbonate content from lime water residue. It has been reported that if solutions are used to erase writing, then the parchment may be softened by wetting so that it is necessary to treat the skin with dry lime to make it dry and white once again [7]. This could be the source of the extra calcium carbonate.
One purpose of this analysis was to see if there were spectral regions in the mid-IR region that could be used for image enhancement. Unfortunately the similarity of spectra of Archimedes ink and parchment, where the most contrast is required, probably precludes this.

Conversion of cellulose acetate film base to cellulose detected with Travel*IR*

CU-383, a degraded photographic negative, has a bluish colored anti-curl layer which is about 50% separated from film base, and small, sub-millimeter blisters between the film base and the anti-curl layer. The film base layer is slightly yellowish brown and slightly brittle. The emulsion layer is about 10% separated and there is no blistering. Because the negative is so degraded it is easy to separate millimeter sized pieces of the three layers so I could analyse each surface (six in total) by ATR IR spectroscopy with the Travel*IR*.
Spectra of the outer surfaces of both anti-curl and emulsion layers show gelatin/collagen, but spectra of the inside surfaces of these layers, adjacent to the film base, show tricresyl phosphate, which is a plasticizer commonly used in cellulose acetate film base.
Spectra of both sides of the film base show predominantly cellulose, with minor amounts of tricresyl phosphate and cellulose acetate (Figure 8). It appears that much of the original cellulose acetate in the film base has hydrolysed to cellulose (i.e., "regenerated cellulose").
ATR spectra are from material present in the first few micrometers of sample in contact with the ATR crystal. To determine if the cellulose is present just on the surface of the film base, transmission spectra of cross-sections of film base, mounted in a diamond cell, were obtained. These are spectra of the bulk or core of the film base, not just its surface. The transmission spectrum of the thick film base closely matches the ATR spectrum of the surface of the film base, indicating that hydrolysis of the cellulose acetate to cellulose has occurred throughout the entire thickness of the film base, not just the surface (Figure 8, inset).
The hydrolysis of cellulose acetate observed here seems to be a more general phenomenon, not just restricted to photographic negatives. I have previously observed hydrolysis of cellulose acetate to cellulose of spectacle frames, manifesting as creation of white fibrous spots of regenerated cellulose in the generally transparent plastic mass of

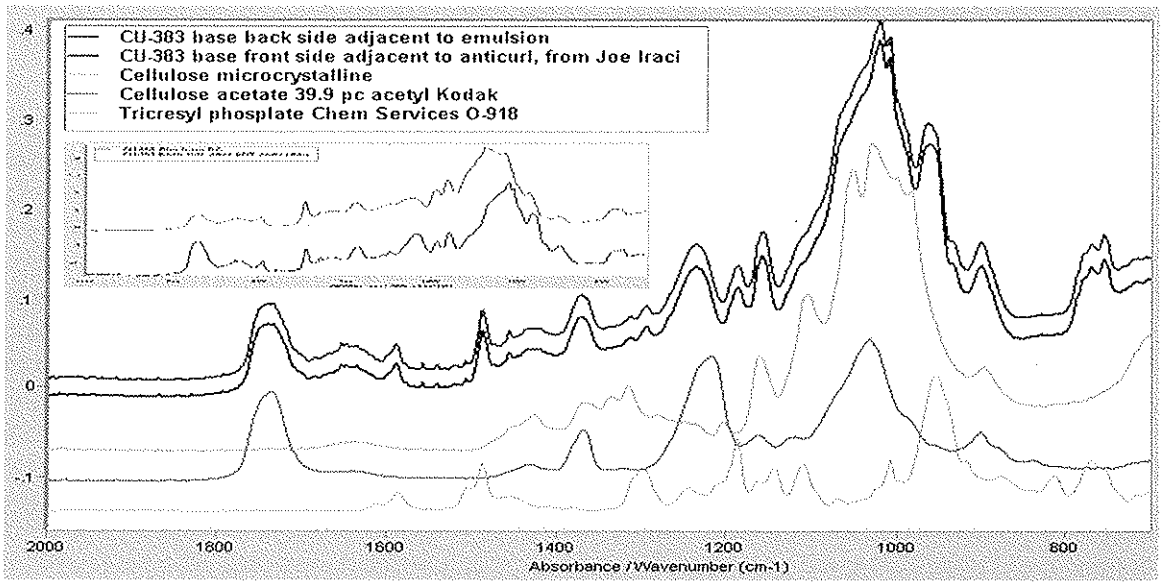

Figure 8. Travel*IR* ATR spectra of photographic negative CU383 film base surfaces adjacent to the gelatin anti-curl and emulsion layers (top pair of traces) show predominantly cellulose (3rd trace) with minor amounts of cellulose acetate (4th trace) and tricresyl phosphate (5th trace), indicating that the cellulose acetate film base has undergone considerable hydrolysis to cellulose. The absorption spectrum of a cross-section of the film base (inset, 1st trace) is similar to the ATR spectrum of the surface (inset, 2nd trace) indicating that hydrolysis has occurred throughout the bulk of the film base, not just at the interfaces with the gelatin layers.

cellulose acetate. I have also observed birefringent spherulites in degraded cellulose nitrate. Perhaps these are regenerated cellulose, indicating that the same type of hydrolysis reactions occur cellulose nitrate.
This could have significant implications for treatments. Cellulose has entirely different solubility and water sensitivity properties than cellulose acetate. Degraded cellulose acetate objects might respond entirely differently to liquid treatments than might be predicted based on the belief that the object is predominantly cellulose acetate. Attempts to soften brittle aged cellulose ester objects by reintroducing plasticizers, might be better planned if the possibility that the object is a mixture (or copolymer?) of cellulose and cellulose ester.

References

1. Williams, R.S. 'On-site non-destructive mid-IR spectroscopy of plastics in museum objects using a portable FTIR spectrometer with fiber optic probe' in *Materials Issues in Art and Archaeology V, Materials Research Society Symposium Proceeding Vol. 462*, Materials Research Society, Warrendale (1997), 25-30.

2. **Illuminator**, Midac Corporation, Costa Mesa, CA: www.midac.com/illumina.htm, accessed 22 March 2004.

3. **Reaction Probe**, Remspec Corporation, Charlton, Massachusetts: http://www.remspec.com/accessory.html, accessed 22 March 2004.

4. Salisbury, J.W., Walter, L.S., Vergo, N., and D'Aria, D.M., *Infrared (2.1 - 25 μm) Spectra of Minerals*, Johns Hopkins University Press, Baltimore and London (1991).

5. **Travel*IR***, SensIR Technologies, Danbury, CT: http://www.sensir.com/s_Products/Travel*IR*.asp, accessed 22 March 2004.(http://www.sensir.com/s_Products/Illuminatir.asp)

6. Down, J.L., Young, G.S., Williams, R.S., and MacDonald, M.S. 'Analysis of the Archimedes Palimpsest' in *Works of Art on Paper, Books, Documents and Photographs, Techniques and Conservation, Contributions to the Baltimore Congress'*, International Institute for Conservation of Historic and Artistic Works (2002) 52-58.

7. 'Palimpsest' in *Bookbinding and the Conservation of books - A Dictionary of Descriptive Terminology*, Matt T. Roberts and Don Etherington, http://palimpsest.stanford.edu/don/don.html, accessed 22 March 2004.

Decoration of Meissen Porcelain: Raman Microscopy As an Aid for Authentication and Dating

Francesca Casadio
Art. Institute of Chicago, 111 South Michigan Ave., Chicago, III. 60603-6110, USA

Abstract

Micro-Raman spectroscopy is a fast, non-destructive method, involving no sample preparation, that allowed testing of a number of Meissen porcelains in the collection of the Art Institute of Chicago, including teapots, plates, cups, vases and elaborate three-dimensional figurines. The study aimed at determining the feasibility of in-situ glaze analysis as a dating/authentication tool. Good results were obtained in the identification of green, yellow, brown, red, black and white enamels, allowing grouping of different pieces on the basis of manufacturing technology and offering insights into the time period in which the pieces were decorated.
When coupled to portable X-Ray Fluorescence (XRF) analysis, Raman microscopy proves to be a very powerful curatorial tool for discrimination of modern decoration.

1.Introduction

1.1 Historical overview

In the XVII and XVIII centuries European monarchs and their courts treasured exotic goods traded from the Far East: among them, hard paste porcelain imported from China had a prominent role. In Europe porcelain soon became desirable because it was better suited for food and hot beverages (the fashionable teas and coffees shipped from the Indies) than the silver and pewter dishware that was used until then, and was harder and of a more translucent white than maiolica. Porcelain was so highly prized to earn the appellation of "white gold". Repeated attempts at producing it were made in Europe: the first successful outcomes are represented by the production of Medici porcelain (1575-1587) and soft paste porcelain at St. Cloud, near Paris, in 1695. At the same time, Augustus the Strong, Elector of Saxony and King of Poland, an avid collector of Chinese porcelain, encouraged the experiments of an alchemist, J.F. Böttger, and a physicist, Count von Tschirnhaus, in their pursuits of uncovering the secret of hard paste porcelain. As a result of their combined efforts, in 1710 the first European porcelain manufactory was founded at Meissen.
During the first decade of its operation, Meissen-produced porcelain remained white or was decorated either with unfired colours or exploiting a restricted range of fired overglaze enamels where blue, gold, red and purple dominated. Due to the research into porcelain technology of another prominent scientist and painter, J.G. Höroldt, beginning in the 1720s the palette available to the painters at Meissen was greatly expanded, including new hues in the greens, blues, browns, purples and yellows, leading the way to the blossoming of pictorial themes and imagery [1]. Due to the high value and great reputation of Meissen ware many attempts have been made at imitation and forgery throughout the centuries. Even at the factory itself XVIII century pieces left undecorated in storage were painted in later epochs and offered on the market. In the XIX century replicas were made of popular figures using the original moulds: a practice still in use in present days. These observations emphasize the necessity of exercising great care when dating Meissen porcelain.

1.2 Raman microscopy

Curators, collectors and dealers are used to judging upon the authenticity of a piece based on meticulous visual examination and evaluation of factors such as hand, style and quality of the painted decoration. Nowadays, scientific analysis can provide invaluable aid to connoisseurship by determining a date *ante-* or *post-quem* the pieces were actually decorated. In particular, the detection of chemical markers in the composition of the glazes can easily differentiate porcelain decorated before or after the XVIII century. Copper oxide was used for the greens until 1802, then replaced by the oxide of chromium; cobalt oxide was used in the blues until 1760, when it was substituted by zinc oxide, Naples Yellow was replaced by uranium or vanadium oxides starting form the XIX century; platinum was first used in the last decade of the XVIII century, and bismuth oxide started to be employed as a flux for gold decoration only after the XVIII century [2]. While elemental analysis and XRD are well-established methods in the study of ceramic materials, only recently Raman microscopy has been applied to the analysis of ceramics, leading to a better understanding of the technology used in manufactory [3-5].
When colours are not "solution colours" (i.e. obtained by low concentrations of transition metals dissolved in the glaze, devoid of a characteristic Raman signature), but are applied in the glaze in the form of nanoparticles

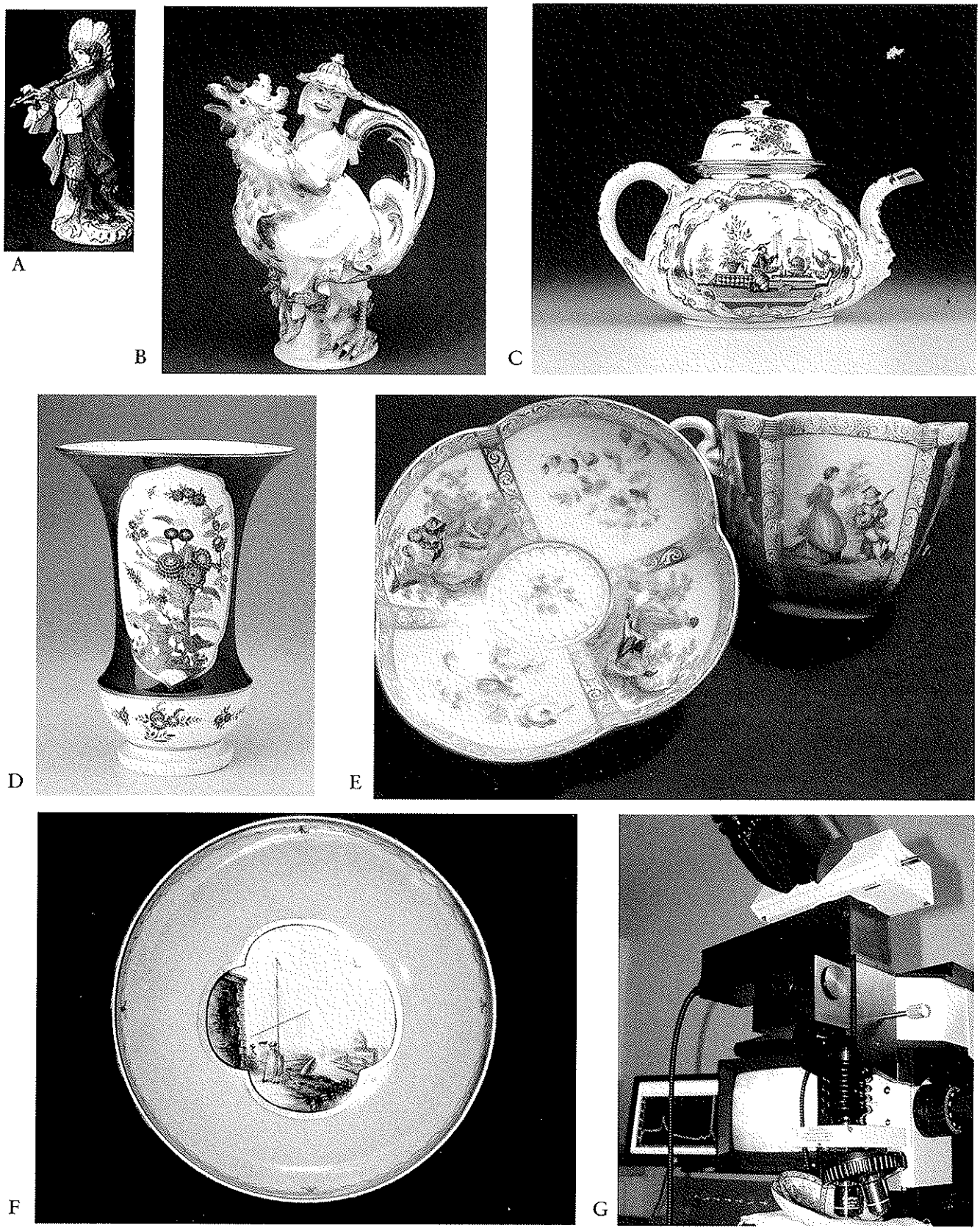

Fig. 1 – Meissen porcelains form the Collection of the Art Institute of Chicago: a) Flute Player from the Monkey Orchestra modeled by Johann Joachim Kändler (ca.1765, accession number 1946.488); b) oil and vinegar cruet modeled by Johann Joachim Kändler (ca. 1737; accession numbers 1998.504a-b); c) Teapot (ca. 1723/24, accession number 1991.I a-b); d) vase (ca. 1733, accession number 1984.820); e) tea-cup and saucer with turquoise ground and gold reserve (ca. 1780, accession number 1983.1041a-b); f) teacup and saucer with yellow background (dated ca. 19th century, accession number 1918.311); g) a detail of the experimental set-up for in-situ Raman analysis. © The Art Institute of Chicago

of pigments, Raman microspectroscopy is an invaluable tool for characterizing the palette of porcelain decoration [6,7].

Experimentals

Raman Microspectroscopy
A Jobin Yvon Horiba Labram 300 confocal Raman microscope was used, equipped with Andor multichannel air cooled open electrode charge-coupled device (CCD) detector (1024x256), BXFM open microscope frame (Olympus), offering high flexibility for analysis of large samples, holographic notch filter, and two dispersive gratings (950 and 1800 grooves/mm).
The excitation line of a Kr ion laser (λ_0= 514.5 nm), He-Ne laser (λ_0=632.8 nm), and a solid state diode laser (λ_0=785.7 nm), were focused through a 50x long working distance objective on to the samples and Raman scattering was back collected through the same microscope objective. Power at the samples was kept very low (never exceeding a few mW) by a series of neutral density filters in order to avoid any thermal damage.
XRF spectrometry - A Keymaster TRACeR III portable XRF spectrometer with X-ray tube with Re target was used. Acquisition times ranged between 60 and 120 seconds.

Samples
All measurements were performed non-destructively and in-situ on the analyzed objects (Fig. 1). The set of artifacts investigated included pieces modeled by the master Johann Joachim Kändler such as a Centerpiece and stand with pair of sugar casters and oil and vinegar cruet (ca. 1737) and a Flute Player from the Monkey Orchestra (ca.1765). Moreover, a Teapot (ca. 1723/24), a vase (ca. 1733), a teacup and saucer with turquoise ground and gold reserve (ca. 1780) and a teacup and saucer with yellow background (ca. 19th century) were also examined. It is important to know that the last three objects listed were indicated by the curator as possibly decorated in modern times.

Results and Discussion

Raman spectra were collected on several areas on the painted surface of the examined objects, as well as in-depth at the glaze-body interface, exploiting the confocality of the system. The Kr ion green laser was the most widely utilized excitation line, due to its highest efficiency in inducing Raman scattering and the larger spectral window obtained with multichannel spectrographs (a significant advantage when analyzing unknowns). The utilization of the red laser line was often impaired due to the occurrence of a significant fluorescence background, with few exceptions. In some cases, the effect of different excitation wavelengths on the obtained spectra, due to resonance effects, was also examined.
Based on the Raman spectra collected the analyzed objects could be grouped in different categories outlined in the following paragraphs.

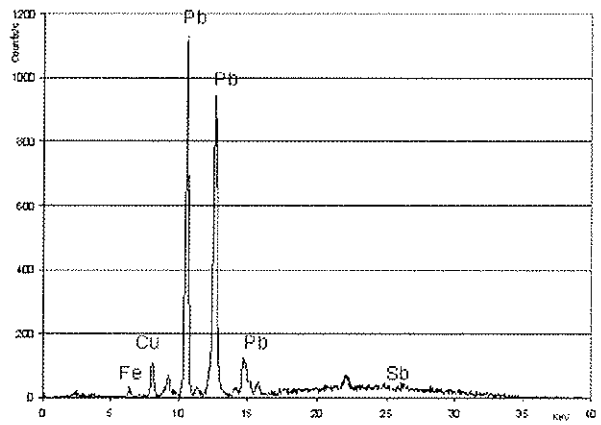

Fig. 2a – XRF spectrum recorded on a green area of the grass in the decoration of the teapot.

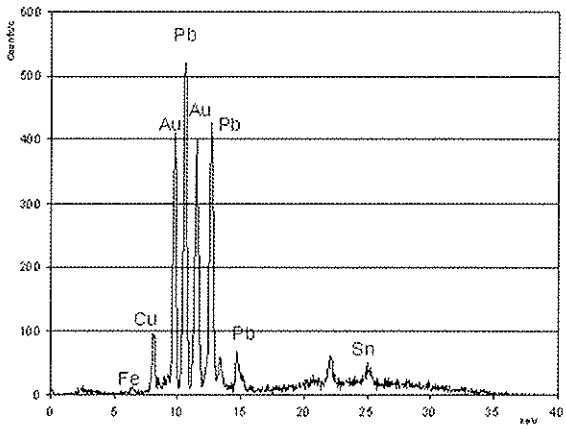

Fig. 2b – XRF spectrum recorded on the green cap (with gold rims) of the oil and vinegar cruet.

Teapot, Flute Player from the Monkey Orchestra and oil and vinegar cruet.
The base for the greens in this group of objects is similar, consisting in Cu ions dissolved in a lead based glaze, as evidenced by the XRF spectra (Fig. 2a, b).
However, Raman microscopy pointed out that two different techniques were used to arrive at a precise shade of green. In the case of the teapot, lead antimonate yellow particles (Naples Yellow, $Pb_2Sb_2O_7$) were detected in the glaze, with most intense, sharp peaks at 129 and 511 cm^{-1} and bands of medium intensity centered at 302, 336 and 458 cm^{-1} (Fig. 3). Addition of Naples yellow allowed the painter to achieve a luminous hue, high in chroma. On the other hand, cassiterite (SnO_2) was added to the glaze used for the suit of the Monkey flute player and the cap of the Vinegar cruet, in order to obtain a transparent, pastel-colored glaze. Focusing the green laser a few mm underneath the surface of the green glaze, the spectrum shown in Fig. 4 was obtained, where a strong peak at 634 cm^{-1} and weaker peak at 778 cm^{-1} are the Raman signature of cassiterite. Other interesting information about the glaze can be gleaned from this spectrum: the sharp peak at 513 cm^{-1} can be attributed to incompletely reacted feldspar grains, indicative of a medium temperature fired glaze; a low temperature of firing (< 1000°C) is required in order to prevent volatilization of antimony oxide. Indeed, it is known from the literature that at Meissen glazes were made with feldspars as a flux even before their introduction as body constituents [8]. As evidenced first by Colomban [9,10] the connectivity of the SiO_4 network in the glaze can be inferred by calculating the ratio of the areas of the two broad bands, approximately centered at 1000 and 500 cm^{-1}, that are envelopes of different constituents, attributed to Si-O

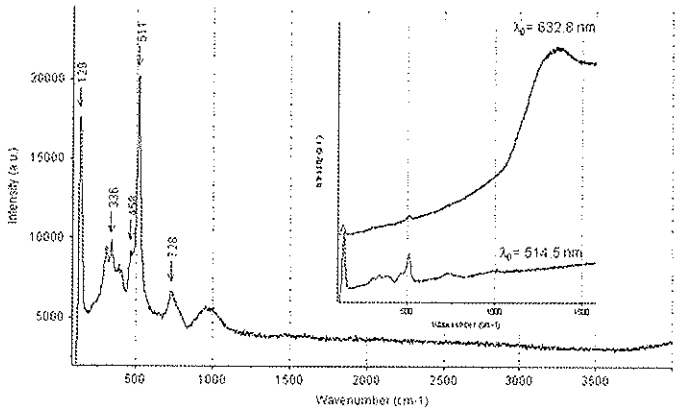

Fig. 3 – Micro-Raman spectrum recorded on a green leaf spectrum on the teapot (λ0= 514.5 nm), (in the insert, the effect of of the the different excitation laser lines is shown).

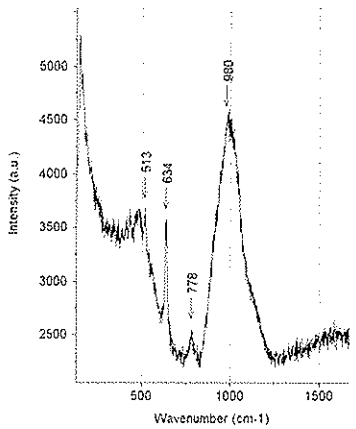

Fig. 4 – Micro-Raman obtained on the green glaze green suit of the flute player (λ0= 514.5 nm).

stretching and bending modes respectively. Although no spectral deconvolution was attempted, the observed highest intensity in the stretching mode envelope (800-1200 cm^{-1}, Fig. 4) can be related to structures made of tetrahedra with low connectivity. This was confirmed by detection with XRF of significant amounts of lead used as fluxing agent in all the glazes examined.
It is to be noted that while the Sn peak is well evident in the XRF spectra of the green glazes, the peak attributable to Sb exhibits a very low signal to noise, evidencing how, in this particular case, Raman microspectroscopy achieves less ambiguous results for the identification of the coloring agent. On the other hand, XRF is the only technique that can unambiguously identify Cu as the chromophore in the green base color. This underscores the advantage of using the two techniques in synergistic mode.
As regarding the yellow areas, Pure Naples yellow was used to decorate all the objects examined in this group. Similarly, for the red colors, haematite (α-Fe_2O_3) was identified in all the spectra recorded, with bands at 224 (m), 243 (w), 291 (s), 407 (s), 491 (w), 607 (m), 653 cm^{-1} (m) and a peak at 1317 cm^{-1} (attributed to a two-phonon mode [11]) that shows resonance effects depending on the excitation laser line used (very strong with λ_0= 514.5 nm; medium, on a high fluorescence background, with λ_0= 632.8, as evident in Fig. 5).
On the purple-colored decorations a high fluoresce was observed with 514.5 and 632.8 nm excitation laser lines, while when using the 785.7 nm excitation laser line no fluorescence was detected, but no primary Raman bands: these observation could lead to the hypothesis that such hue was obtained with Au nanoparticles.
As a result of the analysis, it can be said that all the pigmenting agents for the enamels of this group of objects are

consistent with an attribution to a decoration executed between 1700 and 1770, confirming the authenticity of these valuable artifacts.

Turquoise and yellow teacup and saucer

A variety of Cr-containing pigments were used for the decoration of green areas in this pair of teacups and saucers. In the green grass of the saucer with yellow quadrants, the spectrum of chromium (III) oxide, Cr_2O_3 was detected, with the most intense band centered at 549 cm^{-1}; in the same saucer, the green on the mantle of one of the painted figurines was identified as uvarovite garnet (or Victoria green, $Ca_3Cr_2(SiO_4)_3$) based on published literature [6] and confirmed by detection of Cr and Ca, along with Pb, Zn, Fe, and K in the XRF spectrum of the glaze. In the green grass of the turquoise saucer, the Raman signature of Naples yellow was detected, along with two sharp, strong peaks at 533 and 684 cm^{-1} assigned in the literature to Co and/or Cr-rich, spinel like phase [6,7]. It is important to note that the same spectral feature (a doublet at 534 and 686 cm-1) was recorded also when focusing the laser beam onto the monochrome turquoise glaze (Fig. 6).

Another interesting aspect of the manufacturing technology of these pieces comes to light when probing the black areas. The most prominent feature of the spectra is a broad band at ~640-660 cm^{-1}, attributable to magnetite: although the main peak for this iron oxide is reported by several authors at higher values of Raman shift (ca. 670 cm^{-1}) [12] in this case it might be possible that the crystal size, degree of crystallinity and temperature of firing, all contribute to causing a significant shift in peak position. The presence of a rather intense envelope centered at 490-

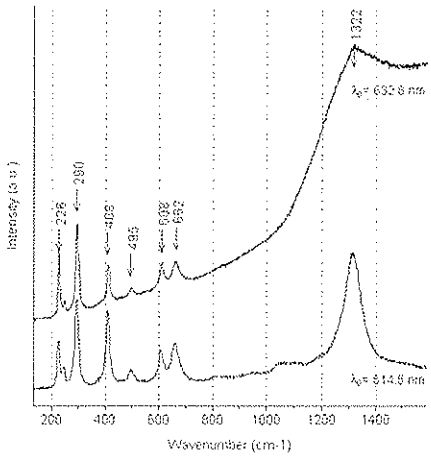

Fig. 5 – Micro-Raman spectra recorded on the red flower of the teapot, with red (λ_0= 632.8nm), and green (λ_0= 514.5 nm), exciting lines.

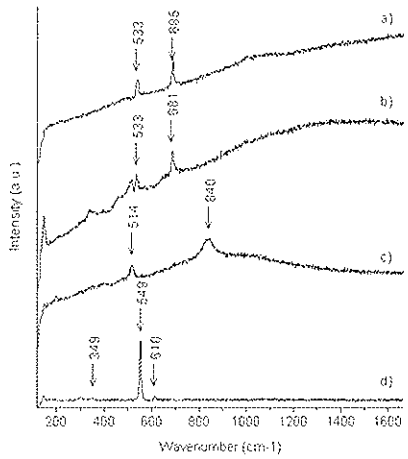

Fig. 6 – Micro-Raman spectra (λ_0= 514.5 nm), recorded on: 1) turquoise saucer - a) turquoise ground decoration; b) green grass; 2) saucer with yellow background: c) green mantle on a male figure ; d) green grass.

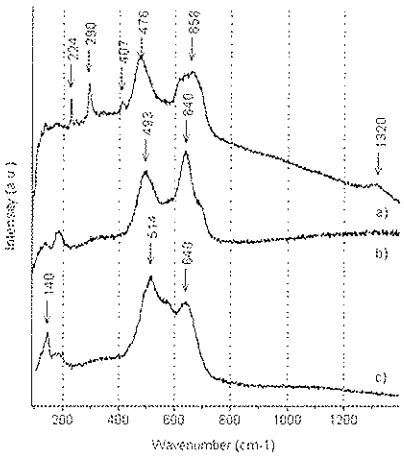

Fig. 7 – Micro-Raman spectra (λ_0= 632.8 nm) recorded on: 1) turquoise saucer - a) brown ship pole; b) black hat; 2) saucer with yellow background: c) black book.

515 cm^{-1}, coupled to the absence of a broad band centered at 1000 cm^{-1} could also be an indication of hard paste glazes, characterized by a Silica rich glass, with high connectivity of the Silica tetrahedra; however such an interpretation is still widely hypothetical and would benefit from supporting evidence obtained with other techniques of analysis. In fact, the broad band at 480-495 cm^{-1}, in conjunction with the other broad band at 640-660 cm^{-1} might as well be attributed to spinel-like phases. For the brown color, a mixture of magnetite and hematite was detected.
Based on the detection of Cr based pigments in the greens, the decoration of these objects can be assigned to a time period after 1800; it is interesting to note, however, that for the yellows Naples yellow was used in all cases and no substitution with more modern available alternatives was deemed necessary.

Blue vase
This vase was found to constitute an intermediary case between the above-mentioned two groups of objects. The curator raised doubts about this piece, based on the unusual finding of the same decorative motif on both sides of the vase. In authentic Meissen-wares in fact, the side exposed to view would normally carry the most elaborately decorated designs. In-situ XRF analysis of the piece confirmed the presence of Co in the blue monochrome areas (as well as Fe, Pb, and minor amounts of As, Ca, Sn), a finding consistent with period (ante-1800) decoration, but detected Cr on the floral motifs (together with Fe, Pb, Zn and minor amounts of Cu).
The analytical data can be interpreted with the fact that the object had been very likely decorated with underglaze monochrome blue color in the 18th century, then left in storage, and the white areas left in reserve successively decorated (post-1800) in order to increase the market value of the piece.

Conclusions

The analysis of several pieces of Meissen porcelains in the Art Institute of Chicago collection provided an opportunity to test the applicability and limitations of the Raman technique to the characterization of overglaze enamels. Raman microspectroscopy achieved good results in the characterization of green, yellow, brown, black and red colours, notwithstanding the scarcity of colouring particles (0.5-10% w/w in the glaze), their often poorly crystalline state and their small dimensions. The opportunity of performing in-situ, non-destructive analysis was a crucial factor for these artifacts, whose sampling is excluded due to their excellent quality and immaculate conservation conditions.
Compared with XRD and Elemental analysis (traditionally used to characterize porcelains), the Raman microprobe offered:

-high spatial resolution (higher than XRD and XRF, unless capillary optics are used with the latter).
-Characterization of both crystalline and glassy phases (the latter not identified by XRD, a technique that is also less efficient in characterizing phases of low crystallinity).
-Differentiation of various crystalline forms of compounds containing the same elements (an advantage over XRF).
-Confocality, allowing to study the glazes without interference from the underlying body (a phenomenon otherwise well evident in the XRF spectrum).

When coupled to portable XRF analysis for determining the nature of colours whose chromophores are ions dissolved in the glassy matrix of the glaze (therefore not showing primary Raman bands) the technique proves to be a very powerful curatorial tool for the discrimination of modern decoration, allowing determination of authenticity and dating of the decoration of Meissen porcelain.

Acknowledgements

The A.W. Mellon Foundation is gratefully acknowledged for its generous support of scientific research at the Art Institute of Chicago.
Special thanks are also given to Ghenete Zelleke, Samuel and M. Patricia Grober Curator of European Decorative Arts, for the enthusiasm, passion and expertise generously shared during the course of this project. Therese Howe of Keymaster technology is thanked for sharing of XRFdata.

References

1. Zelleke, G., 'An Embarassment of Riches: Fifteen Years of European Decorative Arts' *Museum Studies* (2002) **28**

(2) 22-89.

2. Page, J., and Chilton, M., 'APPENDIX: Scientific Analysis Of Meissen Commedia Dell'Arte Sculpture in the Gardiner Museum Collection' in M. Chilton (ed.) *Harlequin Unmasked*, The Gardiner Musuem of Ceramic Art, Toronto, Ontario, Canada (2001) 323-326.

3. Zoppi, A., Lofrumento, C., Castellucci, E.M., and Migliorini, M.G., 'Micro-Raman technique for phase analysis on archaeological ceramics', *Spectroscopy Europe* (2002) **14** (5) 16-21.

4. Colomban, P., 'Differentiation of Antique Porcelains, Celadons and Faiences from the Raman Spectra of their bodies, glazes and paintings', *Asian Chemistry Letters* (2001) **5** (3) 125-134

5. Sakellariou, K., Miliani, C., Morresi, A. and Ombelli, M., 'Spectroscopic investigation of yellow maiolica glazes', *J. of Raman Spectroscopy,* (2004) **35** (1) 61-67.

6. Colomban, P., Sagon, G., and Faurel, X., 'Differentiation of Antique Ceramics from the Raman Spectra of their coloured glazes and paintings', *J. of Raman Spectroscopy,* (2001) **32** 351-360

7. Colomban, P., Filande, V. and Lebihan, L., 'On-site Raman analysis of Iznik pottery glazes and pigments', *J. of Raman Spectroscopy,* (2004) **35** in press.

8. Kingery, W.D. and Vandiver, P.B., *Ceramic Masterpieces. Art, Structure and Technology*, The Free Press, New York,(1986), p. 173.

9. Colomban, P. and Treppoz, F., 'Identification and differentiation of ancient and modern Eurpean porcelains by Raman macro- and micro-spectroscopy", *J. of Raman Spectroscopy* (2001) **32** 93-102

10. Liem, N. Q., Thanhn, N.T., and Colomban, P., 'Reliability of Raman micro-spectroscopy in analyzing ancient ceramics: the case of ancient Vietnamese porcelain and celadon glazes', *J. of Raman Spectroscopy* (2002) **33** 287-294.

11. Massey, M.J., Baier, U., Merlin, R., and Weber, W.H., 'Effects of pressure and isotopic substitution on the Raman s pectrum of a-Fe_2O_3: Identification of two-magnon scattering', *Physical review B,* (1990) **41** (11) 7822-7827.

12. de Faria, D.L.A., Venancio Silva, S., and de Oliveira, M.T., 'Raman Microspectroscopy of some iron oxides and oxyhydroxides', *J. of Raman Spectroscopy* (1997) **28** 873-878

FT-RAMAN STUDIES OF THIN FILMS OF NATURAL VARNISHES

Andrea Cavicchioli and Dalva Lúcia Araujo de Faria
Instituto de Química – University of São Paulo Av. Prof. Lineu Prestes 748, 05508-900, São Paulo, Brazil

Abstract

The potentials of Raman spectroscopy as a non-destructive (or virtually non-destructive) characterization and diagnosis tool in conservation science are increasingly being recognized by a gradually wider public of perspective users. The Achilles' heel of this technique is the fluorescence exhibited by certain samples upon visible light excitation. This problem, which is particularly frequent in the case of old or aged materials which conservators, as a rule, deal with in their routine work, can be in most cases overcome using Fourier Transform (FT) Raman Spectroscopy with near-IR laser excitation.
In the present work, the characterization by FT-Raman of thin films of varnishes prepared from natural resins commonly used as artistic materials is proposed. Dammar and mastic were studied. FT-Raman spectra obtained from dried films of such varnishes, rather than from the pure solid or liquid preparations, are valuable because they form the basis for studies of layers of the same substances on the artistic artifacts themselves. Furthermore, such films can be used for degradation studies in real or simulated (i.e. accelerated) conditions, being possible to follow structural alterations through changes in the FT-Raman spectra.
Thin films were spin-coated on highly reflective metal disks to form films of approx. 30-50 μm, but also at a quite lower thickness (approx. between 1 and 4 μm) on one of the two polished Au electrodes of a commercial 10 MHz quartz crystal microbalance (QCM). In both cases, spectra displaying acceptable signal-to-noise ratios and highly reproducible bands were obtained, using a nominal excitation laser power of 500 mW (approx. 350 mW on the sample).

Introduction

Raman Spectroscopy has proved to be, in many ways, a rather effective analytical tool at the service of professionals concerned with the conservation of cultural heritage [1-2]. Typical applications encompass the identification of chemical substances in support to restoration works, the characterization of materials aiming at tracking the history (origins, commercial routes) of artifacts of historical value, the diagnosis of damage, recognition of degradation pathways and, finally, dating and authentication.
The features that make Raman Spectroscopy so attractive in conservation as well as other related areas (e.g. forensic sciences), can be summarized as follow [1]:

1)It is a non-destructive (or virtually non-destructive) technique inasmuch as it does not require chemical pre-treatment nor is it affected by the measurement process itself (provided suitable laser power and wavelength is employed);
2)Raman spectra can provide, at a time, a wealth of information on both the organic and inorganic components of a substance and their mutual interactions;
3)It is a highly reproducible technique;
4)It allows spatial specificity and bidimensional mapping;
5)Samples can be analyzed in their natural hydration state, since water molecules have very poor scattering properties;
6)The measurements are independent from the specimen's shape and surface texture and large objects can be examined using fiber optic probes, though in detriment to spatial resolution and sensitivity.

Furthermore, as a consequence of its non-destructive character, a single specimen can be analyzed many times, thus permitting, for instance, structural changes of materials to be followed with time. For this reason, provided that the target substances exhibit inelastic scattering properties, Raman spectroscopy can be a very useful technique to approach the study of natural and/or artificial ageing, as well as degradation processes. In this way, therefore, one would be able to establish the state of preservation of works of art, but also to monitor the dynamic development of the chemical composition of the materials of which they are made, especially aiming at detecting early signs of decay.
In recent years, alongside a broader interest in the microscopic implications (i.e. at molecular level) of the processes

of materials degeneration and a more systematic approach to the effect of environmental factors, either individually or in synergistic action, there has also been a stronger emphasis on preventive conservation strategies [3-4]. Clearly, the possibility of assessing the potential damage risk associated with conservation areas and, consequently, of predicting possible future macroscopic harm in the objects of the cultural heritage in order to adopt measures to prevent it, is highly desirable. To this respect, some researchers have proposed the use of dosimeters based on test panels for monitoring the environmental impact on painting materials [3]. The method consisted in the exposure of several stripes, covered with as many types of tempera-based paints, in selected display buildings, as well as in a chamber for controlled accelerated ageing. Subsequently, the chemical changes occurred in these substrates were assessed and related to the conditions of natural or artificial ageing upon removing samples of paint and submitting them to a range of analytical assays [5-8].

The principle of dosimeters has also been tested in a pilot study based on the use of quartz crystal resonators (known as quartz microbalances, QCM) modified with thin films of mastic varnish [9]. It was shown that the accelerated visible light ageing of the varnish can be correlated with negative shifts in the resonance frequency of the painted sensor. The effect is associated with mass increase of the varnish layer, in turn possibly caused by O_2 uptake during the autoxidation process promoted by light [10].

The present contribution, which focuses on NIR laser excitation FT-Raman spectroscopy of thin films of mastic and dammar varnishes, had a twofold goal. The first objective was to establish a procedure for obtaining FT-Raman spectra from films with minimum thickness, with the purpose of creating the condition of eventually extracting the analytical information from materials directly deposited on quartz crystal resonators (which need be extremely thin). In this way, it would be possible to obtain complementary microgravimetric and spectroscopic data in investigations targeting the study of natural and artificial ageing. Secondly, the definition of the operative conditions for Raman analysis of thin films of paint materials is in itself valuable since the layered form is the actual physical morphology of these materials in painted works of art, playing also a role in the effective extent and rate of material degradation.

The choice for FT-Raman, and therefore for NIR laser excitation, is justified – and perhaps also imposed – by the problem of fluorescence frequently exhibited by organic materials such as biomaterials, resins, varnishes, fibers etc., especially when they are already aged [2]. The necessity of this choice was confirmed by preliminary Raman assays carried out using the 514.5 nm and 632.8 nm excitation laser lines, showing that upon artificial photochemical ageing (by UV and visible light) films of both dammar and mastic varnishes displayed a considerable degree of fluorescence that utterly masked the fingerprint region, thus preventing the possibility of subsequent investigations focused on the most characteristic and significant portion of the Raman spectrum.

Experimental section

Materials

The liquid mastic and dammar varnish mixtures were prepared by grinding and dissolving the respective solid resins (from *Pistachia lentiscus* and *Agathis Dammara*, acquired by a local supplier, Casa do Restaurador, São Paulo, Brazil) in turpentine oil (Maimeri, Italy) in a ratio of 1:2, notably 5 g of resin in 10 g of oil. The resins were allowed to dissolve for 48 h in the dark and at a temperature of approx. 18 °C. At the end of this period, as some solid persisted, the thick liquid supernatant was isolated by careful aspiration by means of an automatic pipette and thereafter stored in a fridge at 4 °C. In some cases, in the preparation of the varnish layers and in order to obtain thicker films, it was necessary to thicken these mixtures. This step was carried out by evaporating part of the solvent under a flux of nitrogen in the dark and a room temperature.

Methodologies

The varnish films were prepared on: i) six 1.5-cm mirrored metal disks; ii) one 0.538" 10-MHz quartz resonators (ICM, USA); and iii) two KRS-5 disks. Both varnishes were spin coated onto the supports using a home-made spinner [11] which was adapted from a top bench centrifuge (Force 7, Denver Instrumentation, USA) by fitting to its central pivot a special plastic support carved to precisely secure support disks of the size used in the present experiments. The spin velocity was adjusted according to the desired film thickness and varnish viscosity between 3000 to 6000 rpm. With quartz resonators, the amount effectively deposited, which can be precisely checked by measuring the shift in resonance frequency, is limited by the geometry of the crystal and, typically, cannot cause a frequency shift larger than 2%. The thickness of the film deposited was estimated by microscope observation to be approximately 50 μm on the metal disks and on the KRS-5 disk. For a rough estimate of the film thickness on the 10-MHz quartz crystal, the Sauerbrey's equation (e.g., see [12]) was applied. From a calculated value of 0.3 mg mass

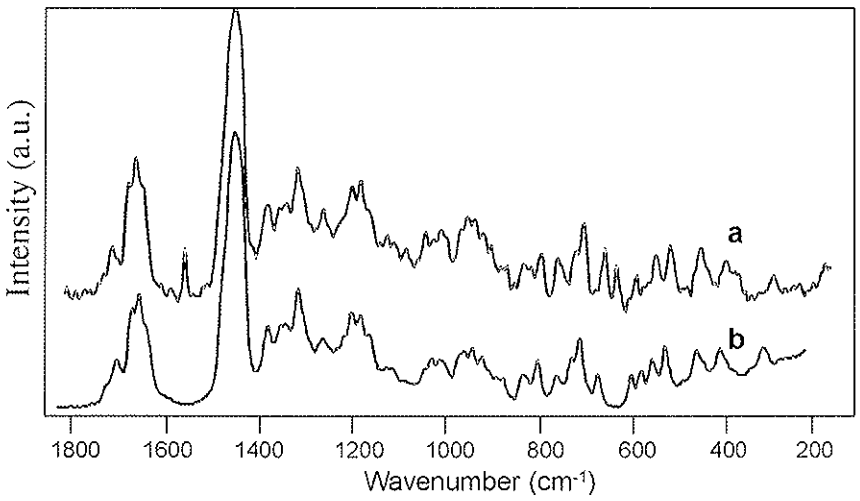

Figure 1. Superimposed FT-Raman spectra ("fingerprint" region) of: 50 µm-thin dammar varnish film spin coated on a highly reflective metal support (**a**) and solid ground dammar resin (**b**). Excitation laser: Nd^{3+}:YAG (1064 nm), nominal power: 500 mW (**a**) or 300 mW (**b**), number of scans: 4000 (**a**) or 512 (**b**)

load (assuming complete and uniform surface covering), a film thickness of $3.2<h<1.6$ µm is deduced, upon a likely density value of $2<d<1$ g cm^{-3}. Raman spectra were recorded approximately 200 h after coating. During this time, the varnishes were allowed to dry in a dark chamber kept at 18 °C and under weak vacuum.
FT-Raman spectra were obtained using a RFS 100/S Raman interferometer (Bruker), with Nd^{3+}:YAG near-infrared laser excitation at 1064 nm (laser spot of approximately 100 µm at the sample) and fitted with a liquid-N_2-cooled Ge detector. The optimum operational conditions for the thin varnish films were found to be: a nominal laser power of 500 mW (350 mW at the sample, approximately); 2000+2000 scans at different points of the film; a spectral resolution of 4 cm^{-1}; an aperture setting of 7.0 mm; a sample signal gain of 8. The spectra of the finely ground solid dammar and mastic resin (512 scans) were obtained using 300 mW nominal laser power (210 mW at the sample).
FTIR spectra were obtained using a Bomem MB100 interferometer (Bomen).

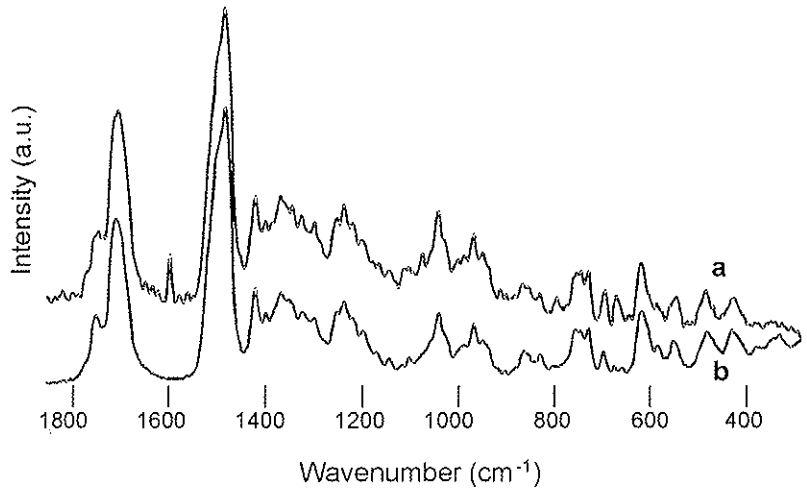

Figure 2 .Superimposed FT-Raman spectra ("fingerprint" region) of: 50 µm-thin mastic varnish film spin coated on a highly reflective metal support (**a**) and solid ground dammar resin (**b**). Excitation laser: Nd^{3+}:YAG (1064 nm), nominal power: 500 mW (**a**) or 300 mW (**b**), number of scans: 4000 (**a**) or 512 (**b**).

Results and data discussion
Under the experimental conditions described in the previous section, it was possible to obtain FT-Raman spectra of dammar (Figure 1, curve **a**) and mastic (Figure 2, curve **b**) varnish films that are very close to the spectra of the corresponding solid resins prior to dissolutions (same figures, curves **b**). Small differences, especially in the low-frequency range related to the weaker energy angular deformation modes of vibration, were expected. They can be mainly ascribed to the rearrangements of the tertiary macromolecular structure of the resin upon dissolution and film formation, also affected by the spin coating procedure adopted which might lead to a preferred chain orientation. A detailed discussion of the spectral features can be found in Brody *et alii* [13].
A spectrum exhibiting the same vibrational bands was obtained, under the same operative conditions, with the approx. 50-fold thinner film of dammar varnish deposited onto the QCM Au electrode (Figure 3). This outcome

confirms the possibility of collecting spectroscopic information from varnish films coated onto such quartz crystals and thus the viability of associate QCM Impedance Analysis to FT-Raman Spectroscopy into a powerful tool for studies on varnish films (the outcome of an ongoing comprehensive work of this kind is being elaborated into a publication soon to be published).

It is worthwhile stressing, at this point, the importance of the highly reflective base onto which the film is deposited. In fact, not only does this choice lead to the enhancement the Raman signal on account of the double transit of the excitation radiation through the transparent film, but it also minimizes the absorbance of the laser energy by the support and, therefore, problems of localized heating that would generate an undesired increase of the background. Also, the measurement of the spectrum from a portion of varnish film laying directly on the quartz disk is best avoided, since this material presents weak, though not negligible, Raman bands in the fingerprint region, beside a strong vibrational band at 466 cm^{-1}.

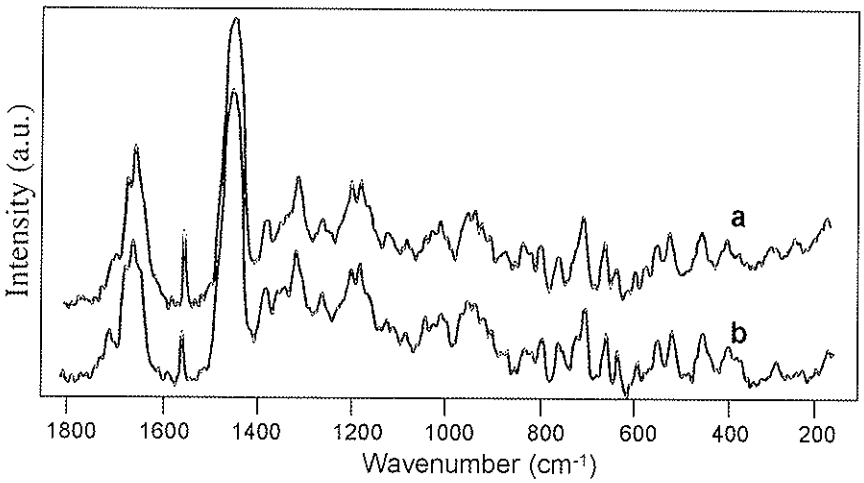

Figure 3. Superimposed FT-Raman spectra ("fingerprint" region) of: 1.6-3.2 µm-thin dammar varnish film spin coated on the Au polished surface of a QCM electrode (a) and 50 mm-thin dammar varnish film spin coated on a highly reflective metal support (b). Excitation laser: Nd^{3+}:YAG (1064 nm), nominal power: 500 mW, number of scans: 4000.

Furthermore, as shown in Figure 4 just for dammar, the overlapped spectra (n=6) of the varnishes are highly reproducible, a feature that is important if the FT-Raman spectrum is to be used to follow the extent of

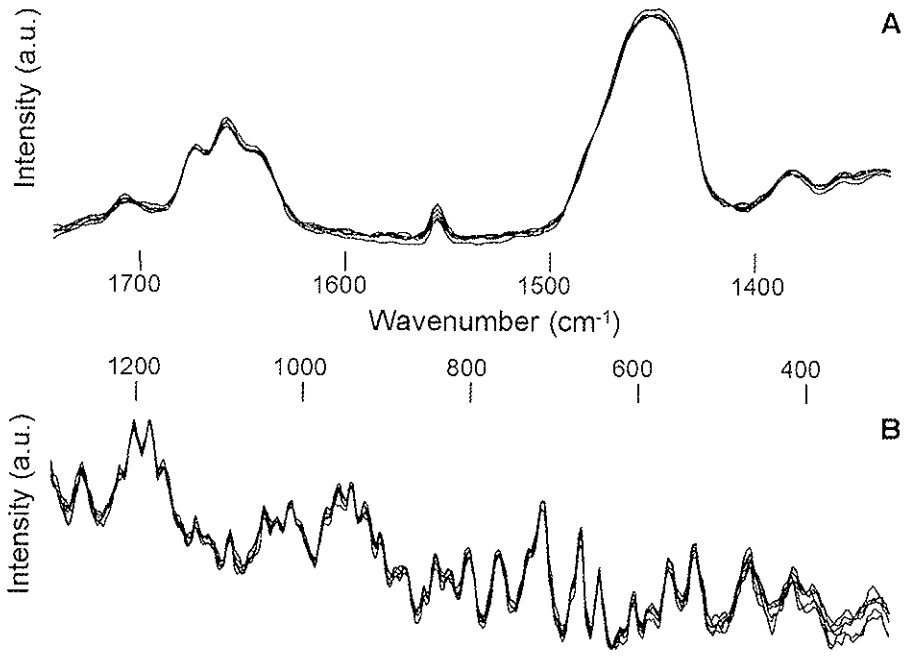

Figure 4. Superimposed FT-Raman spectra (1800-1500 (A) and 1300-500 (B) windows) and of six different films of 50 µm-thin dammar varnish films. Excitation laser: Nd^{3+}:YAG (1064 nm), nominal power: 500 mW, number of scans: 4000.

structural changes in the material over time and to assess the degree of degradation. To this respect, it is important to remark that, owing to the type of molecular changes expected with these kind of materials (i.e oxidation, formation of –OH, C=O and COOH) and to the usually poor scattering properties of O-containing functional groups, Raman is unlikely to respond to ageing processes with very strong spectral change. Therefore, on the one hand, a precise definition of true vibrational bands (as opposed to spectral artifacts) is vital in order to effectively use Raman

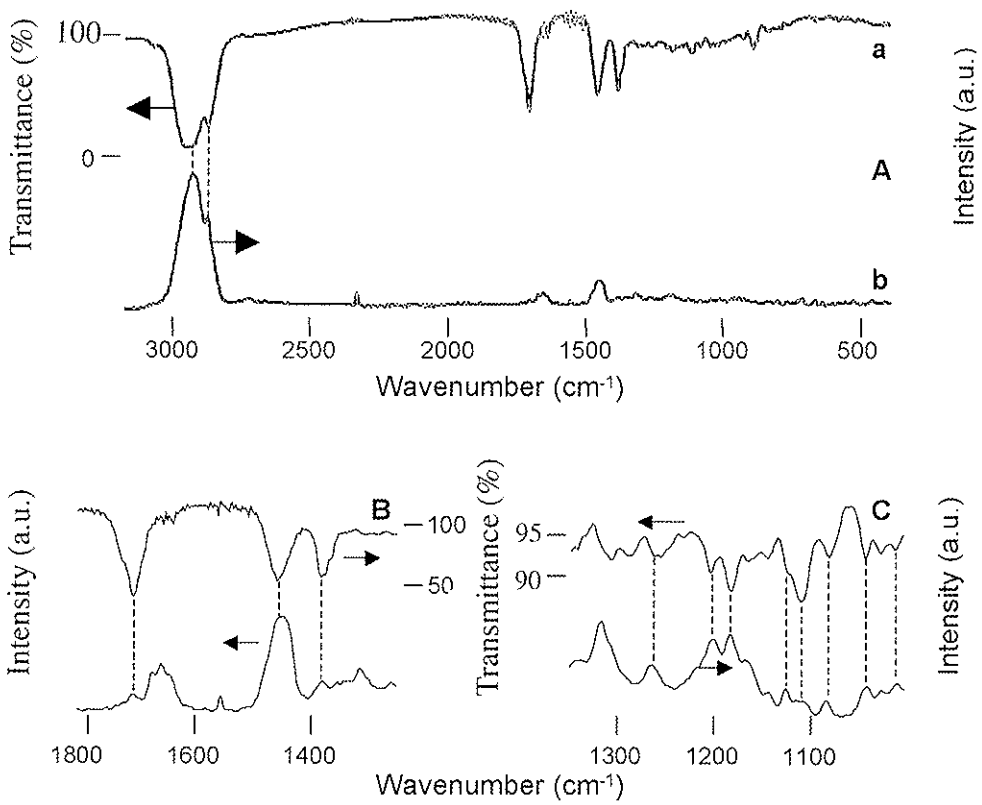

Figure 5. Superimposed FTIR (a) and FT-Raman (b) spectra (overall view (A) and spectral windows (B-C)) of dammar varnish films (approx. 50 μm thin) respectively spin coated on a KRS-5 disk and on a highly reflective metal support. Excitation laser: Nd^{3+}:YAG with nominal power: 500 mW (FT-Raman), number of scans: 256 (FTIR) or 4000 (FT-Raman).

spectroscopy in the kind of studies that are here devised; in fact, one might envisage that chemometrics would become an important aid in this kind of evaluations. On the other, the coupling with FTIR is also particularly valuable. As an example of the possibility of obtaining infrared information also from thin films of these varnishes, Figure 5 shows the FTIR spectrum of a 50-mm layer of dammar varnish coated on the surface of a KRS-5 disk. The complementary nature of the Raman and FTIR bands is evident from the comparison presented in the same figure.

Conclusions

The present work forms the basis for the use of FT-Raman as a non-destructive tool for studies involving thin films of varnishes of artistic interest, possibly in conjunction with FTIR (either in the transmission or grazing-angle reflectance mode), which, as was shown, represents a complementary characterization technique. FT-Raman spectra displaying satisfactory signal-to-noise ratios and very reproducible bands were collected from layers with a thickness of only a few mm. In this way, in particular, the results open the way to combined FT-Raman and Impedance Analysis studies of varnish films deposited onto conventional quartz resonators with gold electrodes. Although, admittedly, extremely slim films require particularly favorable conditions, such as the use of highly reflective supports that in turn allow employing a very intense excitation laser, thickness might not be a critical factor in many situations. An important research pathway that can now be pursued is the characterization of ageing and/or degradation and the following of the extent of these processes over time directly on the varnish films. This is a relevant point since films are likely to behave quite differently than bulk materials, which are sometimes used in simulated investigations of this nature (just consider, for example, problems of oxygen diffusion inside the material). Furthermore, it will be possible to perform FT-Raman analysis on real artifacts in which the resins are, in fact, found in the form of a varnish layer.

Acknowledgements

The authors wish to acknowledge financial support by the Brazilian Research Support Agencies, FAPESP and CNPq, and by Fundação VITAE (Brazil).

References

1. Edwards, H.G.M., 'Raman Microscopy in Art and Archaeology', *Spectroscopy*, **17** (2), 2002, 16-40.

2. Faria, D.L.A., Afonso, M.C., and Edwards, H.G.M., 'Espectroscopia Raman: una Nova Luz no Estudo de Bens Culturais', *Rev. Museu de Arqueologia e Etnologia*, **12**, 2002, 249-267.

3. Odlyha, M.; Boon, J.J., van den Brink, O., and Bacci, M., 'Environmental research for art conservation (ERA)' *J. Therm. Anal.*, **49** (3), 1997, 1571-1584.

4. Cassar, M., 'Preventive Conservation' in R. Vontobel (ed.) *Thirteenth Triennial Meeting of the ICOM Committee for Conservation, Rio de Janeiro, September 2002*, James and James Science Publishers, London (2002), 2-8.

5. van den Brink, O., Eijkel, G.B., and Boon, J.J., 'Dosimetry of paintings: determination of the degree of chemical change in museum-exposed paintings by mass spectrometry', *Thermochim. Acta*, **365**, 2000,1-24.

6. Bacci M., Picollo M., Porcinai S., and Radicati B., 'Evaluation of the museum environmental risk by means of tempera-painted dosimeters', *Thermochim. Acta*, **365**, 2000, 24-34.

7. Odlyha, M., Cohen, N.S., and Foster G.M., 'Dosimetry of paintings: determinatiion of the degree of chemical change in museum exposed test paintings (smalt tempera) by thermal analysis', *Thermochim. Acta*, **365**, 2000,35-44.

8. Cohen, N.S., Odlyha, M., Campana R., and Foster G.M. 'Dosimetry of paintings: determinatiion of the degree of chemical change in museum exposed test paintings (lead white tempera) by thermal analysis and infrared spectroscopy', *Thermochim. Acta*, **365**, 2000, 45-52.

9. Cavicchioli, A, 'Chemical Sensors for Indoor Environments', unpublished MSc dissertation, University of London (1996).

10. de la Rie, E. R., 'Old master paintings: a study of the varnish problem', *Anal. Chem.*, **61** (21), 1989, 1228-1240.

11. Jesus D.P, 'Cristáis Piezelétricos de Quatzo com Eletrodos Separados e Superfície Modificada como Sensores em Fase Líquida' unpublished MSc dissertation, University of São Paulo (1999).

12. O'Sullivan, C.K., and Guilbault, G.G, 'Commercial quartz crystal microbalances – theory and applications', *Biosensors and Bioelectronics* **14**, 1999, 663-670.

13. Brody, R.H., Edwards, H.G.M., and Pollard, A.M., 'Fourier-Transform Spectroscopic Study of Natural Resins of Archaeological Interest', *Biopolymer*, **67** (2), 2002, 129-141.

Raman and Gas Chromatography/Mass Spectrometry Investigation of Parmigianino's Wall Paintings in Santa Maria della Steccata Church in Parma, Italy

Danilo Bersani [1], Pier Paolo Lottici [1], Gianni Antonioli [1], Antonella Casoli [2], Elisa Campani [2], Carla Violante [2]
[1] Istituto Nazionale per la Fisica della Materia (INFM-CNR) and Dipartimento di Fisica, Università di Parma, Parco Area delle Scienze 7/a, 43100 PARMA Italy
[2] Dipartimento di Chimica Generale ed Inorganica, Chimica Analitica, Chimica Fisica, Università di Parma, Parco Area delle Scienze 17/a, 43100 PARMA Italy

Abstract

Parmigianino (Francesco Mazzola, 1503–1540) was one of the most important painters of Italian Mannerism. We investigated his last large wall painting, which is situated on the arch over the main altar in the church of *Santa Maria della Steccata* in Parma, Italy. The painting's pigments and binders were identified by micro-Raman spectroscopy and gas chromatography coupled with mass spectrometry (GC/MS). Polysaccharides were found in the plaster.

Introduction

Santa Maria della Steccata is a grandiose church in the form of a Greek cross, built in Parma between 1521 and 1539. In 1531, Parmigianino (Francesco Mazzola, 1503–1540) began to work on the Church's wall painting representing the parable of "The Wise and Foolish Virgins as found in St. Matthew's gospel". Eight years later, in 1539, the painting was still incomplete. The Steccata Confraternity then demanded repayment of the monies that had been advanced and Parmigianino was imprisoned. Upon his release in 1540, Parmigianino died.
In 2002-2003, a restoration of the *Santa Maria della Steccata Church* was undertaken and the scaffolding that was erected for conservation purposes facilitated a close examination of the wall painting. The painting's pigments and binding media were identified to obtain detailed information about the technique used by Parmigianino in his late work and to help the restorers to choose the best conservation treatments. The pigments were analyzed by micro-Raman spectroscopy and the organic material (binder) by GC/MS. The organic material studied came from the paint layers and plaster, which is unusually thin, compact, lucent, and "plastic-like".
This study also enables a comparison between the wall painting technique of the older Parmigianino and that of the young Parmigianino (1519-22) as found in the chapels in *San Giovanni Evangelista Church* in Parma; the latter wall paintings have been studied previously by our group [1]

Materials and Methodologies
Sampling was performed before the restoration work began; the restorers (Donatella Zari and Carlo Giantomassi) were consulted in order to minimize the number of samples removed from the painting while still identifying the entire palette of the artist. Using a scalpel blade, thirty-four millimetre size samples were taken from the surface of the wall paintings. Five additional samples were collected to investigate the presence of organic compounds in the plaster. For some samples, cross-sections were made by embedding the fragments with all of their layers intact, in a cold polymeric resin [2-4].
Micro-Raman measurements were performed with a Jobin–Yvon Labram apparatus, equipped with motorized xy stage, auto-focus, and 10x, 50x, and 100x microscope objectives. The spatial resolution was about 2 μm and the spectral resolution 3 cm^{-1}. The excitation wavelength was the 632.8 nm line of a HeNe laser (max. power 20 mW) and the 785 nm of a laser diode. Neutral density filters were employed to keep the laser power on the sample at low levels (0.05 -1 mW). The spectra were collected on fragments and their cross-sections. For each sample, a minimum of four spectra was recorded for every pigment.
For GC/MS analysis, the samples were subjected to a derivatization procedure consisting of two main steps: one for the lipidic components and the other for the proteinaceous material. [5-6]. Some of the samples were also investigated for the presence of polysaccharides [7]. A HP-5890 Series II gas chromatograph coupled to a HP-5971A mass selective detector was employed. Analysis was performed on a Mega SE52 fused-silica capillary column (25 m X 0.25 mm i.d.) coated with a 0.25 μm film of methylsilicone (5% phenyl), operated with temperature programming from 80°C (held for 2 min) with an increase of 20°C/min to 270°C (held for 6 min) for fatty acid derivatives; from 60°C (held for 3 min) with an increase of 25°C/min to 260°C (held for 6 min) for amino acid derivatives; and from 60°C with an increase of 9°C/min to 130°C, then 2°C/min to 190°C, and finally 20°C/min to 260°C (held for 2 min)

for monosaccharide derivatives. Mass spectrometer conditions were as follows: interface temperature 280°C, ion source temperature ca. 190°C, electron impact at 70 eV. The mass spectrometer was operated using the scan mode at 1.8 scan/s in the range of m/z 40-450, or in the selected ion monitoring (SIM) mode.
Micro X-ray fluorescence analysis at the synchrotron radiation facility of LURE (Paris) was performed on some cross-sections to help identify pigments and inorganic compounds that produced weak or no Raman signal.

Results and discussion

The Parminianino wall painting studied is shown in Fig. 1 The wall painting is divided into two sides, "foolish" and "wise" virgins. Table 1 summarizes the colours analysed, together with the results of the micro-Raman and GC/MS investigations. The Raman wavenumbers listed for the various pigments were measured on the best spectrum obtained for a given pigment. The pigments were identified by comparison with reference Raman spectra or literature databases [8-12].

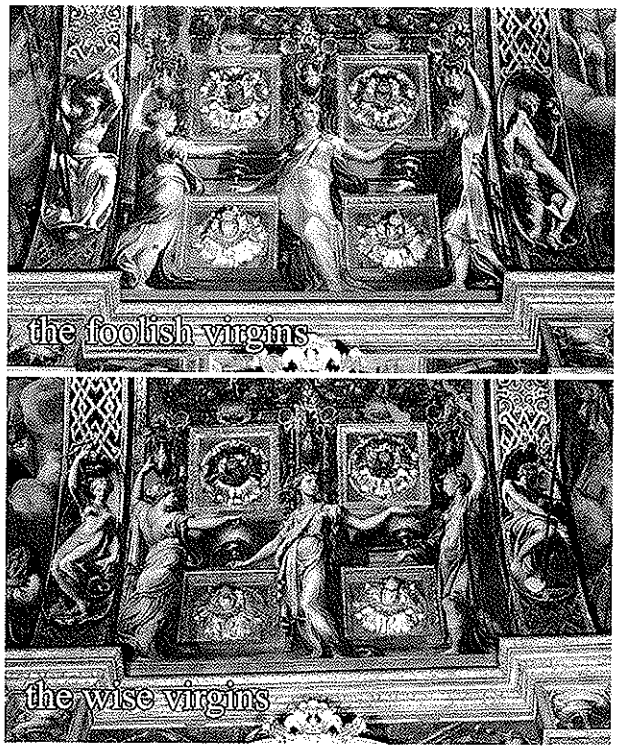

Fig.1 The Wise and Foolish Virgins wall painting in S. Maria della Steccata Church in Parma, painted by Parmigianino.

Blue Pigments

The blue palette is the most rich. An interesting result is the presence of indigo on the painting (Fig. 2). Indigo ($C_{16}H_{10}N_2O_2$, indigotin), is a blue pigment prepared from plants (*Indigofera tinctoria*, *Isatis tinctoria* - woad plant -, *Isatis indigotica, Polygonum tinctorum) and* was commonly used in textiles but rarely in wall paintings [13-16]. Parmigianino used indigo alone (sample #17) or in combination with other blue pigments such as smalt and lapis lazuli (lazurite). In sample # 1, indigo is found mixed with smalt over a red layer composed of hematite (Fig.3). This technique was used by Parmigianino to obtain the deep blue colours of the sky. Smalt (a potassium rich silica glass containing cobalt) was identified by means of micro-XRF measurements, which revealed the presence of cobalt. With the 632.8 nm excitation line, smalt produces only a broad fluorescence band without Raman features. In sample #8, indigo is mixed with lazurite, as revealed by Raman mapping of the sample cross-section (Fig.4). In sample #13, indigo and lazurite are present over a smalt background. Indigo is also found together with malachite in a green area of sample #34. In the wall painting of S. Giovanni Church, indigo was not detected; instead the young Parmigianino largely used the blue pigment azurite, which was not found in the Steccata wall paintings. Lazurite [$(Na,Ca)_{7-8}(Al,Si)_{12}(O,S)_{24}[(SO_4),Cl_2,(OH)_2]$, the main component of lapis lazuli, was found in sample #16 together with cobalt blue ($CoO.Al_2O_3$, cobalt (II) doped alumina glass). The cobalt blue pigment was probably used in a restoration as its first known use dates to the 19th century [17]. Cobalt blue and smalt are cobalt-doped glasses discernible upon microscopic

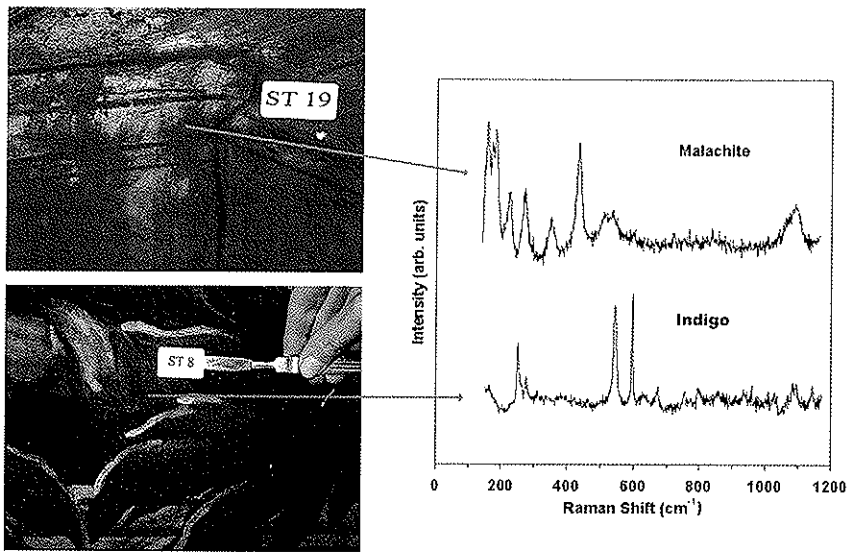

Fig.2 Raman spectra obtained on a blue (sample #8) and a green (sample #19) points.

inspection. Cobalt blue has a characteristic Raman spectrum with features at 203 and 514 cm^{-1}. Lazurite was also found together with malachite and a basic copper sulphate in green sample (#4).

Green Pigments

The green parts of the wall painting appear to be the most restored, as indicated by the large presence of chromium oxide (Cr_2O_3, chrome green) [18], a synthetic pigment produced after the discovery of chromium in 1797.

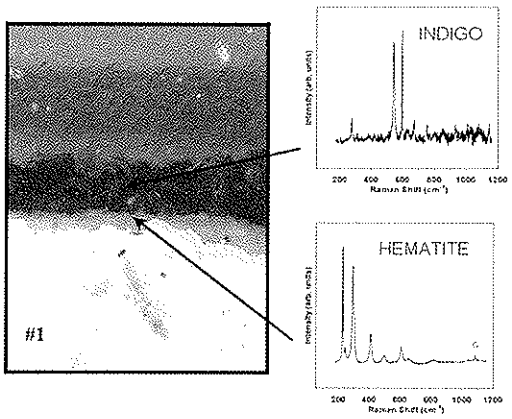

Fig.3 Raman spectra taken on a blue paint layer over a red paint layer (cross-section of the sample #1) showing the presence of indigo and hematite.

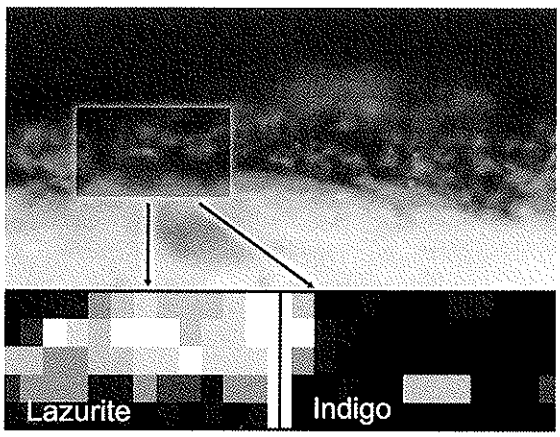

Fig.4 Raman maps obtained on the cross-section of the sample #8. The brightness is proportional to the intensity of the lazurite and indigo Raman bands.

Chromium oxide is found in samples #s 33 and 20. In the latter sample, it is mixed with an unidentified yellow pigment that displays characteristic Raman features at about 870 cm^{-1} and could be ascribed to some chromate salt. In sample #3, chrome green is found together with anatase (TiO_2), another restoration pigment that was introduced in 20th century, and at a greater depth chrome green was detected with calcite, goethite and carbon. Chromium oxide was also found with other pigments in grey sample #21 (see Table 1).

The other green pigment detected on the painting is malachite $CuCO_3 \cdot Cu(OH)_2$. It was used alone in sample #19 (Fig. 2) and mixed with indigo in dark green sample #34. In sample #4, the green layer (located under a layer of unidentified organic orange pigment and lazurite, and over a brown goethite layer), contains malachite and a basic copper sulphate. The Raman spectrum of the latter could not be used to distinguish between brochantite ($Cu_4(SO_4)(OH)_6$), posnjakite ($Cu_4(SO_4)(OH)_6 \cdot H_2O$) and langite ($Cu_4(SO_4)(OH)_6 \cdot 2H_2O$) [9,19,20]. The presence of basic copper sulphate may be unintentional, since it is often found in nature together with malachite.

Red-orange pigments

The red pigments used by Parmigianino in the Steccata wall painting are cinnabar (vermilion, HgS) and hematite (Fe_2O_3) (Fig. 5). Cinnabar was detected with calcite in sample #9 and over a hematite layer in sample #10. The combination of cinnabar and hematite was also detected in the red-gilding sample #5. To obtain the dark red in sample #11, carbon black was added to hematite. Hematite was also used to obtain purple (sample #14) and orange (sample #15). Goethite (FeOOH) mixed with hematite was used in the orange samples #22 and #23. Goethite was also detected in the background of the green samples #3 and #4.

Other pigments and inorganic compounds

Calcite ($CaCO_3$, San Giovanni's white) is the only white pigment found in this wall painting (sample #7). Calcite was detected in many paint layers and is often used to lighten the colours. It is also the main component of the plaster. Barite (barium sulphate) is found in two samples (#22, #23) together with goethite, but the small quantity of barite observed suggests that it may not have been added intentionally. Gold was detected by XRF measurements of the gilding in sample #2. Carbon black was used to darken the colours; its presence was revealed in samples #3, #11 and #23. In the greyish sample #21, which was taken from a heavily restored area of the painting, lead-tin yellow (I) (Pb_2SnO_4) and massicot (PbO, orthorhombic) were found along with many other compounds.

Organic binders: GC/MS results

Large amounts of amino acids, derived from proteinaceous material, were detected in samples #'s 1, 2, 4, 5, 8, 10, 12 and 17; while in sample #3, they are absent. Figure 6 shows the chromatogram obtained from sample #4. The pattern indicates the presence of alanine (Ala), glycine (Gly), leucine (Leu), proline (Pro), hydroxyproline (Hyp), aspartic acid (Asp), glutamic acid (Glu) and phenylalanine (Phe) derivatives. N-Val (norvaline) and N-Leu (norleucine) are

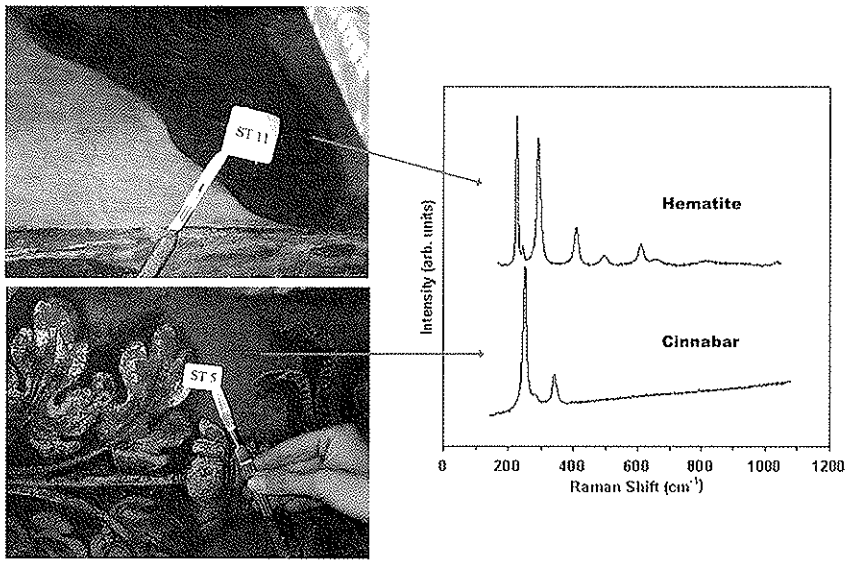

Fig.2 Raman spectra obtained on two red samples (#5,11).

internal standards. The data, obtained as area percentage values and corrected by using response factors, have been compared to reference proteinaceous materials analyzed with the same GC/MS methodology [21,22]. Casein was found in samples #'s 1, 8, 12, 17; while a significant proteinaceous content probably due to egg protein was detected in sample #10. In sample #5, a mixture of milk and animal glue was found, while in samples #2 and #4, a mixture of egg and animal glue is present.
The analyses of samples #'s 1, 4, 5, 8, 10, 12, 17 yielded very weak peaks due to fatty acids, without azelaic acid, which excludes the presence of drying oils in the samples. In sample #3, fatty acids are absent while in gilding sample #2, saturated fatty acids (palmitic and stearic) and dicarboxylic acids (mostly azelaic acid) are present, probably due to a siccative type oil, such as linseed. [5]. Some samples (1, 2, 5 and 17) were also analysed for simple sugars. Samples #1 and #17, in which indigo is present, show characteristic peaks for arabinose, rhamnose, xylose, mannose, galactose, glucose. The glucose-galactose mixture may be due to milk materials as indicated by the presence of casein. The use of plant gums (arabic, tragacanth, cherry gums) can be excluded as glucuronic acids are not present [7]. No polysaccharide material is observed in samples #2 and #5. Due to the characteristic plastic aspect of the plaster, GC/MS analyses were also carried out on five plaster samples taken from different zones of the painting (#'s 24, 26, 28, 29, 30) to detect organic components. Sugars and trace level proteinaceous materials were detected in the plaster samples, while no lipidic materials were detected. The peaks observed in the chromatograms of the plaster are similar to those of paint samples #1 and #17: arabinose, rhamnose, xylose, mannose, galactose, glucose. The polysaccharide material detected in indigo paint layers may be the same material added to lime plaster to improve its mechanical and chemical properties [23].

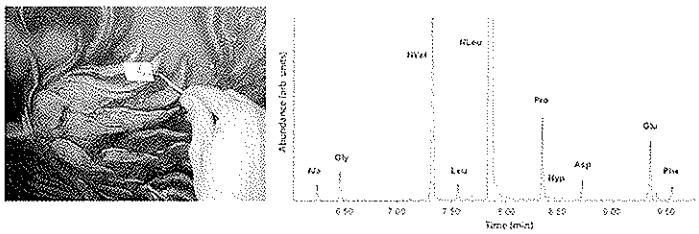

Fig.6 Chromatogram performed on the green sample #4, showing the presence of a mixture of egg and animal glue.

Conclusions

Parmigianino used a mixed technique to complete his last wall painting in *S. Maria della Steccata* Church. He used the fresco technique for some parts of the wall painting, but also made extended use of organic binders to apply on the dry plaster most pigments which are compatible with the fresco technique. The palette of Parmigianino is rich in colours, including expensive or unusual pigments such as lazurite, cinnabar and indigo. The pigments were used in different combinations, mixed together or applied in subsequent layers.
The detection of organic binders in the wall painting supports previous research [1] that Parmigianino used them to create different shades and visual. Also, the addition of polysaccharide material probably improved the mechanical and chemical properties of the plaster.
Extensive restoration is indicated by the presence of cobalt blue, anatase and Cr-based pigments that were not used in the 16th century.
Finally, GC/MS technique proved complementary to the micro-Raman analysis performed in this study because it could be used to detect small quantities of organic materials present in the wall painting.

Acknowledgements

The authors would like to thank Donatella Zari and Carlo Giantomassi (Restauratori Giantomassi e Zari s.n.c. – Roma – Italy) for their collaboration and the precious help in the sampling operations and in the interpretation of the results.

TABLE 1 – Pigments and Binders Identified by Micro-Raman, GC/MS, and XRF
[* = restoration materials; # = deduced from XRF]

Sample	Color	Pigments and Other Inorganic Compounds (Raman bands in wavenumbers (cm^{-1}) for selected samples -	Organic Binders (MS data not shown)
1	Blue	Indigo, smalt #, hematite, calcite	Milk, polysaccharide material
2	Gilding	Gold #	Egg+ animal glue, linseed oil No polysaccharide material
3	Green	Chromium oxide*, anatase*, calcite, goethite, carbon	No proteinaceous or lipidic material
4	Green-orange	Lazurite, malachite, **basic copper sulphate** (154 178 192 273 392 424 481 511 595 612 627 974), goethite	Egg+ animal glue
5	Red +gilding	Cinnabar, hematite	Milk + animal glue No polysaccharide material
7	White	**Calcite** (280 711 1086)	Not studied with GC/MS
8	Blue	**Indigo** (256 281 312 467 548 601 635 677 759 778 862 942 1100 1149 1227 1252 1312 1367 1582), lazurite, anatase	Milk
9	Red	Cinnabar, calcite	Not studied with GC/MS
10	Red	**Cinnabar** (254 285 345 353), hematite	Egg
11	Dark red	Hematite, carbon	Not studied with GC/MS
12	Blue	Smalt	Milk
13	Blue	**Lazurite** (266 547 584 814 1093) , indigo, **barite** (54 462 617 988), smalt	Not studied with GC/MS
14	Purple	**Hematite** (224 243 292 299 407 495 609 657 1313), calcite	Not studied with GC/MS
15	Orange	Hematite	Not studied with GC/MS
16	Blue	**Cobalt blue*** (203 514), lazurite, hematite.	Not studied with GC/MS
17	Blue	Indigo	Milk, polysaccharide material
19	Grey-green	Malachite	Not studied with GC/MS
20	Green	Chromium oxide*, "chromate" yellow	Not studied with GC/MS
21	Greyish	**Lead-tin yellow (I)*** (133 157 179 198 277 294 352 455 528 553 613), **massicot** (145 289 386), cinnabar, lazurite, **anatase** (148 198 399 511 636), calcite, chromium oxide*, hematite	Not studied with GC/MS
22	Orange	Goethite, hematite, barite	Not studied with GC/MS
23	Orange	Goethite, hematite, barite, calcite, carbon	Not studied with GC/MS
31	Blue	Smalt	Not studied with GC/MS
33	Green	**Chromium oxide*** (303 348 523 548 607)	Not studied with GC/MS
34	Dark green	**Malachite** (155 178 218 267, 429 509 531 1050-1090), indigo	Not studied with GC/MS

References

1. Bersani D., Antonioli G., Lottici P.P., Casoli A. *Spectrochimica Acta.* Part A, (2003) **59** 2409

2. Plester J., *Studies in Conservation*, (1956) **2** 110

3. Tsiang J. S., Cunningham R. H., *J. Am. Inst. Conserv.* (1991) **30** 163

4. Messinger J. M., *J. Am. Inst. Conserv.* (1992) **31** 267

5. Casoli A., Cauzzi D., Palla G.. *OPD Restauro* (1999) **11** 111

6. Casoli A., Musini P.C., Palla G. *J. Chromatogr. A* (1996) **731** 237

7. Casoli A., Cremonesi P., Palla G., Vizzari M., *Annali di Chimica* (2001) **91** 727

8. Bell I.M., Clark R.J.H., Gibbs P.J., *Spectrochim. Acta Part A* (1997) **53** 2159

9. Burgio L. and Clark R.J.H.., *Spectrochim. Acta Part A* (2001) **57** 1491

10. Bouchard M., Smith D.C., *Spectrochimica Acta. Part A*, (2003) **59** 2247

11. Database of minerals Raman spectra, Physics Department, University of Parma, http://www.fis.unipr.it/raman/index2.htm (accessed 15 march 2004)

12. Coloraman Project, University of Catania, http://www.ct.infn.it/~archeo/ (accessed 20 march 2004)

13. Tatsch E., Schrader B., *J. Raman Spectrosc.* (1995) **26** 467

14. Min E., Nam S.I., Lee M.S., *Bull. Chem. Soc. Japan* (2002) **75** 677

15. Coupry C., *Analusis* (2000) **28** 39

16. Vandenabeele P., Moens L., *Analyst* (2003) **128** 187

17. Rehren T., *Archaeometry* (2001) **43** 483

18. Farrow R.L., Mattern P.L., Nagelberg A.S., *Appl. Phys. Lett.* (1980) **36** 212

19. R.L. Frost, Spectrochimica Acta Part A **59** (2003) 1195

20. Martens W., Frost R.L., Kloprogge J.T., Williams P.A., *J. Raman Spectrosc.* (2003) **34** 145

21. Casoli A., Musini P. C., Palla G., *Chromatographia*, (1996) 42 421-430

22. Casoli A., Alberici L., Cauzzi D. , Palla G., *Proc. 2nd Int. Cong. on Science and Technology for the Safeguard of Cultural Heritage in the Mediterranean Basin*, Paris , *July 1999*, Elsevier, Amsterdam (2000)

23. Alberti B., *De re aedificatoria*

Raman Analysis of Native American Dyed Artifacts

Kenneth J. Smith[1*], Darlene Florence[1], Ruth Norton[2], David Graves[2]
[1] McCrone Associates, Westmont, IL, USA
[2] Field Museum, Chicago, IL USA
(*New address: Thermo Electron Corp, 217 S Wilmette Avenue, Westmont, IL 60559, USA.)

The Field Museum has a number of Native American artifacts in its collection. A group of these artifacts were collected ca.1900 by George Dorsey of the Field Museum's Anthropology Department from the Arapaho tribe in the central and western states. Many of these artifacts are decorated with dyed porcupine quills or dyed plant materials such as cornhusks. Using Raman microscopy, the dye materials were analyzed to determine the type of dyes used on the quillwork and husks. Dyes used on items from the Arapaho Wind River reservation in Wyoming were found to differ significantly from pigments used on artifacts collected from the southern Arapaho tribe reservation in Oklahoma. Using the Raman microscope we have found evidence of aniline dyes as well as natural dyes from items collected in Wyoming, and of inorganic pigments from the items collected in Oklahoma. This paper will present an overview of the samples analyzed, sampling methodology, reference materials analyzed including aniline dyes and vegetable dye extracts, and highlight significant results from the study.

Raman Spectroscopic Analysis of Romano-British Wall Paintings: Easton Maudit, Northants and Castor, Peterborough, UK

Paul S. Middleton[1], Howell G. M. Edwards[2], and N. F. Nik Hassan[2]
[1] Department of Humanities, Peterborough Regional College, Peterborough PE1 4DZ, UK;
[2] Department of Chemical and Forensic Sciences, University of Bradford, Bradford BD7 1DP, UK;

Abstract:

We report on the analysis of a collection of painted plaster fragments and fragmentary ceramic vessels, containing pigment, from the Romano-British villa at Easton Maudit, together with analysis of a complete ceramic vessel, also containing pigment, from a Romano-British workshop at Castor. A familiar palette of colours, common in Roman painted plaster, is described, but the identification of anatase, apparently used on both sites as a white pigment, calls for special comment.

Introduction

The growing number of Raman spectroscopic studies of wall painting in the provinces of the Roman empire and regions of Italy is steadily adding to our understanding of Roman wall artists' techniques and their preferred palettes. In particular, with the application of chemical analysis, a much clearer picture is emerging of the subtleties of artist choice in pigment preparation and application. With the identification of source materials for the pigments, wider questions such as the supply networks involved and the spread of specialised techniques can be more methodically addressed. Indeed, alongside the expected evidence for characteristics peculiar to an area, hinting at the existence of regional schools, it is increasingly clear that a number of artists had knowledge of pigments and finishing effects of a more specialised nature. This implies a detailed awareness of the commentaries of classical authors and widespread personal exchange networks [1]. A further exciting possibility is our ability to begin to address the question of taste exercised by villa owners in their choice of colour – something which has already been highlighted in studies focussed on villas at the heart of the Roman Empire [2] and now, significantly, in the provinces as well [3].
The aim of this study is to consider two rare finds of ceramic vessels, containing pigments, a group of which were found in the context of a villa building, itself displaying painted wall plaster. A number of issues are addressed:
- The characterisation of the colour palette employed at Easton Maudit.
- Comparison of the analyses of Easton Maudit wall paintings with studies on adjacent villa sites in the Nene Valley, Northamptonshire.
- Consideration of the unusual occurrence of anatase and its implications for our understanding of the ancient painting palette.

Experimental

Method
FT-Raman spectra were obtained with a Bruker IFS 66 system with FRA106 Raman module attachment. The spectral "footprint" in macroscopic and microscopic modes was 100 µm and 40 µm respectively, the latter achieved with a 40x microscopic objective lens. In order to obtain a satisfactory signal to noise ratio, 2000 spectral scans accumulated at 4 cm^{-1} were needed. Raman spectra of selected specimens were also obtained with a Renishaw In Via confocal microscope (CCD detector) operating at 785 nm (near infrared), 633 nm and 514 nm (visible) and with ten spectral scans accumulated to enhance the signal-to-noise ratio over individual scans.

Samples
The samples discussed in this paper were excavated from two sites, both situated in the Nene Valley, Northants. A complete, straight-sided chamfered bowl, measuring just 8 cm. in diameter at the mouth and standing 4.3 cm high, was found during excavations in 1969 on the site of a Romano-British workshop in Normangate Field, Castor. The context of the find indicates a mid-late 3rd century AD date [4]. The site of Normangate Field lies on the north bank of the River Nene, and was at the heart of a major industrial suburb of the Roman town of Durobrivae, some 8 km west of the modern city of Peterborough. The establishment from which the paint pot comes appears to have been engaged primarily in metalworking, and there is therefore no obvious connection with wall painting. Nevertheless,

there would have been ample opportunity for painters to use their skills on a number of wealthy villas within easy walking distance of the Normangate Field area [5].
Easton Maudit villa lies in the upper Nene valley, approximately 14 km east of the modern settlement of Northampton and 8 km south of the Roman small town of Irchester. The main residential building at Easton, excavated between 1987 and 1994, is one of a group of moderately wealthy villas clustered around the upper Nene. This group includes Piddington, where, uniquely in the region, cinnabar has been identified amongst the artists' palette [6].
The coins list from the excavations at Easton reveal the familiar Romano-British rural pattern of modest coin losses from first to early fourth centuries AD, with a significant increase in coin losses from the mid-fourth century onwards. Coupled with the pottery evidence, the villa can be regarded as having its origins in the first century AD, with the major villa building most likely being constructed during the early-mid second century. Towards the end of the second century, changes were underway.
Evidence for cutting of *tesserae* on site and a partially laid tessellated pavement in a main corridor of the villa, along with a lime slaking pit, still filled with lime mortar, adjacent to one of the villa entrances, demonstrate that a substantial refurbishment was in train. A deep cellar may have been part of this refurbishment, or may itself have been under construction, for on the floor of the cellar a heap of *opus signinum* was found unused. Smashed on the floor of the cellar was a group of fragmented paint pots, presumed to have fallen from a shelf and broken whilst still containing paint. These paint pots and samples of the extensive painted wall plaster from the main villa rooms form the bulk of the samples discussed below.
The abrupt end to building operations which is implied by the archaeological evidence may have been caused by a fire, debris from which had collapsed into the cellar and sealed the deposit including the paint pots. Nothing from this deposit can be dated later than the third quarter of the second century AD. The absence of stratified third and fourth century deposits in the main villa building indicates that habitation had moved nearby, but did not return to the main building.
The specimens available for study fall into three categories:

- Pigment powder – three samples from Easton Maudit and two from Castor.
- Ceramic vessels – four fragmentary vessels, each containing pigment, from Easton and one complete vessel, with pigment adhering to the inside and outside, from Castor.
- Fragmentary wall plaster, from the villa building at Easton Maudit.

Results

pigment powders
The two results for which background fluorescence was encountered are both thought to be the consequence of carbon/soot. In both cases, there is archaeological evidence for fire having been a factor in the formation of the deposits and it is entirely likely, therefore that these two samples are not pigments at all, rather a secondary deposit on the vessels.

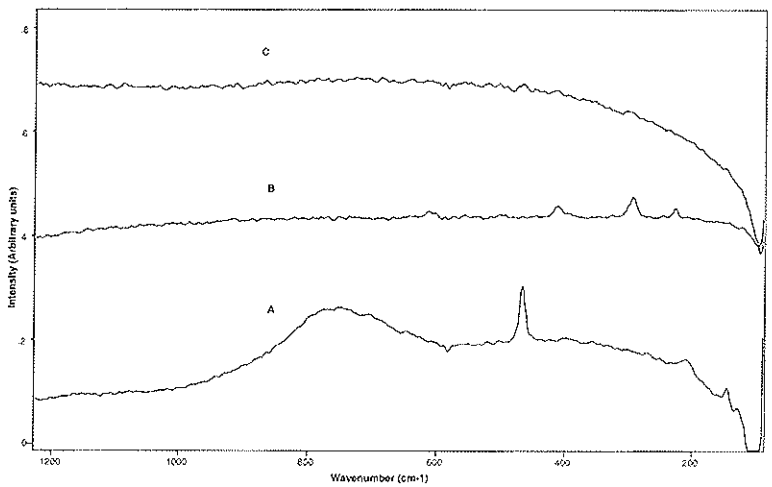

Figure 1
Raman spectra of pigment powders: A) white ash, Castor, CAS69.117; B) red pigment, Easton Maudit, DP887; C) red pigment, Easton Maudit, DP889.

Ceramic vessels
The pigments from the ceramic vessels are, on the whole, consistent with what is already known about commonly used pigments in Roman wall painting. The identification in Vessel 889 of limewash, the standard wall surface preparation, along with pigments associated with top-coats and finishing, illustrates the potential for multiple use of the paintpots.
The identification of litharge (PbO) is possible, but not certain. A separate, unpublished analysis of the Castor pot is reported as revealing lead [7]. Litharge, with

Site/Sample number	Description	Result	Band wavenumbers/cm^{-1}
Easton Maudit, DP887	Reddish brown	Red ochre – haematite	245, 291, 411, 611
Easton Maudit, DP888	Brown	Background fluorescent	
Easton Maudit, DP889	Red	Red ochre – haematite	As above
Castor, CAS69.117	White ash	Quartz,	465
		limewash	broad band, 780
Castor, CAS69.140	Brown	Background fluorescent	

Table 1: Pigment powders

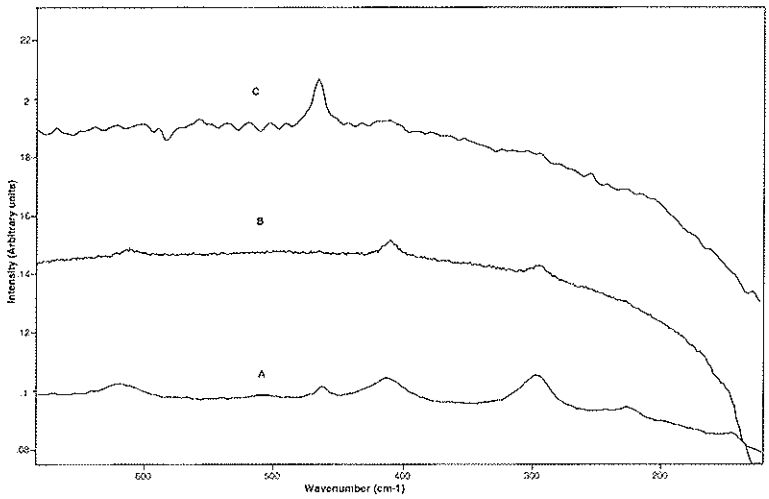

Figure 2 Raman spectra of pigments in ceramic vessel from Castor: A) haematite (standard); B) red pigment found adhering to inside of vessel, CAS69.136; C) red pigment found adhering to outside of vessel, CAS69.136.

distinctive Raman bands at 148 cm^{-1}, 291 cm^{-1}, 342 cm^{-1}, 387 cm^{-1} and 426 cm^{-1}, may, then, be suspected on the results obtained, although this is far from clear-cut. There is no doubt that haematite is present, and it may be that there is a mixture of the two pigments in this particular sample.

Fragmentary wall plaster

The samples of painted wall plaster, all of them from Easton Maudit villa, afforded many opportunities to analyse the white substrate to which pigments were adhering. In every case, this was revealed as a limewash (broad Raman band, centred on 780 cm^{-1}), with calcite (Raman band 1086 cm^{-1}) and traces of carbon (Raman bands 1320 cm^{-1}, 1590 cm^{-1}).

The choice of pigments revealed a limited palette of six colours – red, white, yellow, green, grey and black. The palette was heavily reliant on red ochre (haematite), with the addition of carbon to achieve darker hues of red, and calcite, white. Also present, but in smaller quantities, were yellow ochre (goethite: Raman bands 240 cm^{-1}, 246 cm^{-1}, 300 cm^{-1}, 387 cm^{-1}, 416 cm^{-1}, 482 cm^{-1}, 551 cm^{-1}) and green (malachite: Raman band 1491 cm^{-1}), the latter identified by the Renishaw microscope (see figure 3). Black and grey were obtained by mixing carbon and calcite.

On one of the ceramic vessel fragments (Sample number 889), whewellite, calcium oxalate monohydrate, was identified (Raman band 1480 cm^{-1}). This is probably a product of biodeterioration.

Discussion

Comparison of the palette employed by the painters at Easton Maudit with other villas in the Nene Valley shows a broad similarity with the group centred on the upper river valley. In these villas, the same extensive use of red ochre, haematite [iron(III)oxide], and white, calcium carbonate, is apparent. Although working with a small range of pigments, the artists also consistently made use of one or two more exotic ingredients, such as Egyptian blue (at Horestone Brook, Piddington and Whitehall Farm) and cinnabar (at Piddington). Although exhibiting neither of these pigments, Easton Maudit did boast the use of malachite, which Vitruvius considered expensive [8], and which has not otherwise been found within the group. [9]. Further similarities in technique are apparent in the universal use of a limewash putty as the substratum of plaster to which pigments were then applied and the common occurrence of quartz. The use of quartz could be as a lightener of hue, or, more likely, as an additive, in the form of pulverised river sand, intended to achieve a finer ground pigment during preparation.

In contrast to the similarities in technique and palette, Easton Maudit appears to be unusual in the Nene Valley villas, in the absence of purple, *caput mortuum* [10]. This absence seems particularly marked in the light of the

Site/Sample number	Description	Result	Band wavenumbers/cm^{-1}
Easton Maudit, 883	Greyish brown	Quartz	148, 357, 465
Easton Maudit, 887	Yellowish brown/red	Carbon, anatase, quartz, haematite, litharge(?)	1320, 1590 144, 396, 517, 639 148, 357, 465 225, shoulder 244, 291, 411 144 (?)
Easton Maudit, 888	Greyish, red	Background fluorescent	
Easton Maudit, 889	Yellowish brown/red	Anatase, quartz, haematite, limewash, calcite, litharge (?)	All as above + 780 (limewash) 154, 282, 712, 1086 (calcite)
Castor, CAS69, 136	Whitish brown (outside) Red (inside) White (inside)	Anatase, quartz Haematite, litharge (?) Quartz, anatase	144, 198, 396, 517, 639 148, 357, 465 224, 244, 292, 409, 610 145, 285, 336 as above

Table 2: Ceramic vessels

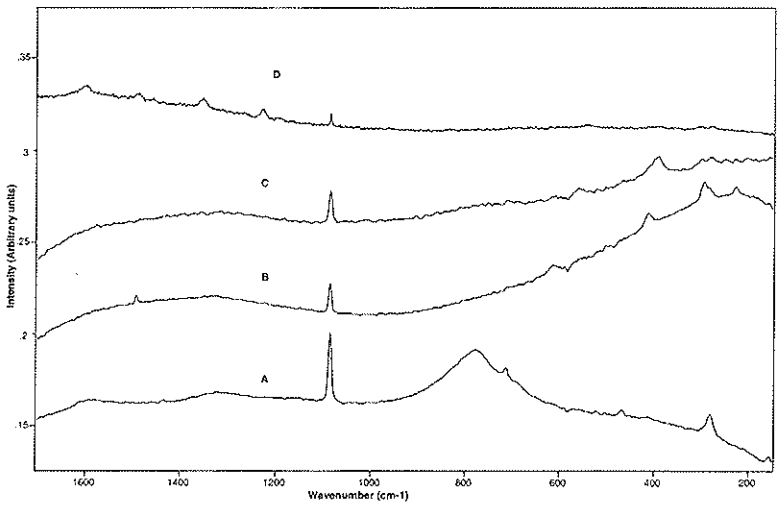

Figure 3 Raman spectra of fragmentary painted wall plaster from Easton Maudit: A) white, S1; B) red, R1; C) yellow, G03; D) pale green, E04.

extensive sampling of wall plaster made possible at Easton by the complete excavation of the main villa residence. In contrast, much smaller sampling opportunities have led to the identification of *caput mortuum* at both Rushton and Whitehall Farm. The fully excavated villa site at Piddington has also yielded evidence of the pigment. The earlier date to be assigned to the Easton Maudit samples (mid-late second century as compared to third/fourth century at the other sites) may be significant in this respect and hints at a change in taste for certain colours at the beginning of the third century AD. Perhaps a parallel can be found in the disappearance of cinnabar from the palette of wall painters working in the wealthy villa of the Domus Coiedii at Suasa, north Italy. Here, significant use of the highly prized and expensive mineral pigment cinnabar in the Republican house ceased with rebuilding in the Imperial Age, even though other factors indicate that the later villa owners were at least as rich, if not richer, than their Republican predecessors [11].

Turning to the ceramic vessels and their pigments, the group of pots from Easton mirrors the evidence of the wall plaster itself, in the emphasis on red and white pigments. Vessel 889, with traces of limewash as well as pigments more usually associated with wall painting, indicates that the vessel had been used on a number of occasions at different stages of wall preparation (figure 4).

Most significant is the identification of anatase, as a possible white pigment, in Vessel 889, where it appears to be mixed with a red pigment. It should be noted that there is no trace of anatase identified in any of the painted wall plaster as yet, but its identification, also as a possible white pigment, in the Castor vessel calls for special comment (figure 5).

Site/Sample number	Description	Results
All samples from Easton Maudit		
S1	White	Calcite
S2	White	Calcite
S3	Red	Haematite, calcite, limewash
S4	Dark red White	Haematite, carbon, calcite, limewash Calcite
S5	Green Red	Carbon, calcite Haematite, calcite, limewash
S6	White	Calcite, limewash
S9	Pale red	Calcite, haematite
S10	Red	Calcite, haematite, limewash
S12	White	Calcite, limewash
S13	Pale green	Calcite, limewash, malachite
R1	Red	Haematite, calcite, limewash, carbon
Y1	Yellow	Goethite, calcite, limewash
G03	Yellow	Goethite, calcite
E04	Pale green	Calcite, malachite
F1. O01	Red	Haematite, calcite, limewash, carbon
F1. O02	Greyish brown	Calcite, carbon
F1. O03	Green	Calcite, carbon
F1. 51	White Black	Calcite, limewash Carbon
F1. N03	White	Calcite, limewash, carbon, quartz
F2.50	Black	Background fluorescent
F9.B03	White	Calcite, limewash, carbon
F9 B04	Dark brown	Calcite
F11.I04	Red	Calcite, haematite
F9 B06	White substrate/plaster Walling material	Carbon, calcite, limewash Calcite, limewash, quartz

Table 3: Wall plaster fragments

Anatase (titanium dioxide) is the rarer of two natural forms of the mineral, its more common polymorph being rutile. Whilst titanium dioxide white pigments have become standard in recent times, following the discovery of synthetic manufacturing methods in the 1920s, the current view is that anatase, in its native form, was never used as a pigment in ancient times [12].

The archaeological context of both finds is secure – there can be no question of later contamination in either case. Any explanation must therefore deal with the presence of the mineral. Since the evidence is against the addition of anything other than pigments to either of the vessel contents, the circumstantial evidence is strongly in favour of the use of anatase as a pigment, rather than as a fortuitous addition as a trace element within another additive. At present, there is no convincing explanation for the presence of the anatase, other than its deliberate addition as a pigment.

The question then arises, for what purpose was such an unusual and presumably expensive, commodity added? Anatase would have had a particularly desirable effect in wall painting. Its high hiding power and reflective qualities would have undoubtedly enhanced the surface finish of any wall covering. Such effects are considered by Vitruvius to be highly desirable and, indeed, he spends some time in detailing how such effects may be achieved, in particular through the addition of fine grained substances, which he terms *politiones.* [13]. Mora, in an early discussion of this

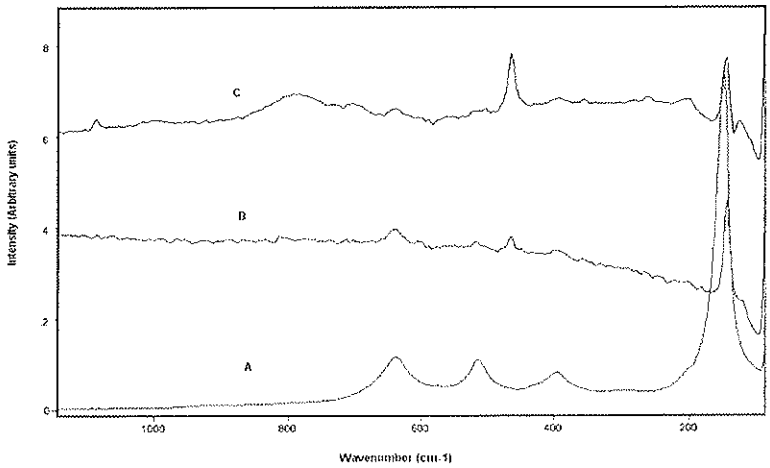

Figure 4 Raman spectra of pigment samples from ceramic vessels from Easton Maudit: A) anatase (standard); B) Easton Maudit, 887; C) Easton Maudit, 889 (note: limewash, centred at Raman band wavenumber 780 cm^{-1}).

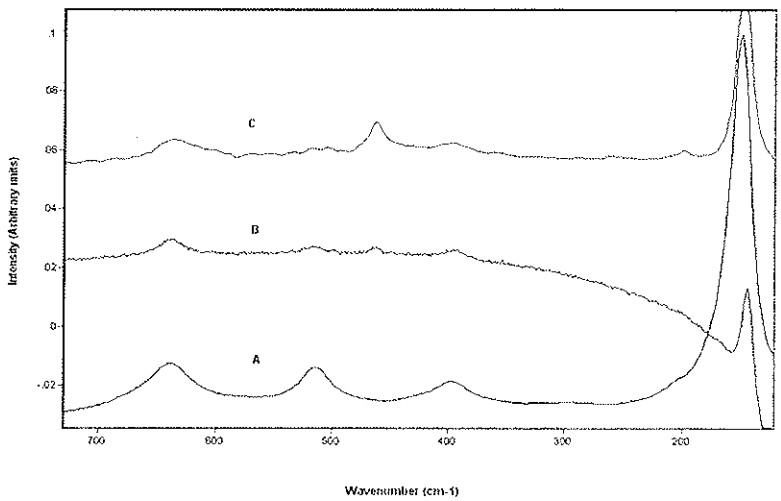

Figure 5 Raman spectra of pigment samples from ceramic vessel, Castor: A) anatase (standard); B) white crystal, inside vessel; C) white crystal, outside vessel.

passage, suggested that Vitruvius might be referring to fine clays, chosen to enhance the smoothness and brightness of the finished wall painting. Recent evidence from Italy and Roman Britain now supports Mora's theory [14]. It is possible, then, that anatase may have been seen as another additive, perhaps in clay, producing such desirable effects in the master artist's craft.

There remains the source of the mineral to consider. Although rare, there are a number of natural occurrences in Britain, which must be considered as possible sources for the mineral. South-western England is the most likely source, with recorded occurrences at Tavistock and Calstock, Devon and at Tintagel and Camelford, Cornwall. Other deposits are known in north Wales [15]. Access to such sources of raw materials is entirely plausible, based no doubt on empirical knowledge of the properties of the different products from the igneous rock formations of the south-west peninsula. In our own studies, we have drawn attention to the specialised use of Cornish kaolin at the villa of Rushton [16]. It is not difficult to imagine a mechanism whereby small quantities of specialist commodities could have been traded the several hundred kilometres required to reach the painters of wall painting workshops operating in Midland England.

Conclusions

Analysis of painted wall plaster from the Roman villa of Easton Maudit reveals a limited palette, similar in many respects to other comparable sites in the Nene Valley.

Selective use of more exotic mineral pigments characterises the group of villas in the upper Nene Valley and hints at the presence of skilled painters, who had a wide knowledge of techniques and materials which can only have derived from developed personal networks and/or widespread travel. The notable absence of the use of purple pigments at Easton Maudit seems to offer a glimpse of changing fashion in the decorative schemes commissioned by the wealthy landowners of the region.

The rare opportunity to study a group of paint pots from Easton, together with a single isolated example from Castor, is reported on. With their clear association with the decoration of the villa building at Easton, the results confirm the preferred red and white pigments, commonly found on painted wall plaster throughout the Nene Valley. The further, important identification of the rare natural white pigment, anatase, must lead to an adjustment in our understanding of the ancient artists' palette.

Much further work remains to be undertaken, but the ceramic vessels from Easton and Castor highlight the need to acknowledge the ingenuity and empirical awareness of artists in the ancient world, as well as the purchasing power and discernment of their wealthy villa owning patrons in all parts of the Roman Empire.

Acknowledgements

The authors acknowledge the Bozeat Historical and Archaeological Society for their generosity in allowing access to the samples of plaster and the ceramic vessels from their excavations at Easton Maudit, as well as for information

about the excavation prior to publication. Also, to John Peter Wild for permission to use results obtained from analysis of the Castor vessel prior to publication. NFNH recognises the support of the Malaysian Government through an Academic Staff Training Award.

References

1. See, for example, Bearat, H., Fuchs, M., Maggetti, M., and Paurier, D., *Proceedings of the International Workshop on Roman Wall Painting, Fribourg,* Institute of Mineralogy and Petrography, Fribourg (1996); Middleton, P.S., Ospitali, F., and di Lonardo, G., 'Painters and Decorators: Raman spectroscopic studies of five Romano-British villas and the domus Coiedii at Suasa, Italy' in H.G.M. Edwards and J. Chalmers, *Raman Spectroscopy in Archaeology and Art,* RSC, London, 2004, in press.

2. Allison, P., 'Colour and light in a Pompeian house: modern impressions and ancient perceptions' in A. Jones and G. MacGregor, *Colouring the Past*, Oxford, New York (2002) 195 – 207.

3. See, for example, on the use of purple, H.G.M. Edwards, L.F.C. de Oliveira, P.S. Middleton and R.L. Frost, 'Romano-British wall painting fragments: a spectroscopic analysis', *The Analyst* (2002) **127**, 277 – 281; also Middleton et. al. *op. cit.* (note 1).

4. H.G.M. Edwards, P.S. Middleton and J.P. Wild, 'A Roman paint pot from Castor, Normangate Field and its contents', in P. Irvine and G.B. Dannell, *Festschrift,* Oxbow, Oxford (2004, forthcoming).

5. J.P. Wild, 'Roman Settlement in the Lower Nene Valley', *Archaeological Journal* (1974) **131** 140 – 170; J.P. Wild, 'Normangate Field 1973', *Northamptonshire Archaeology* (1974) **9** 86 – 88.

6. Discussed in Middleton et al. *op. cit.*

7. Wild, J.P., University of Manchester, personal communication (10 December 2003).

8. Vitruvius, *de Architectura,* VII. 14. 2.

9. Middleton et al., *op. cit.,* Table 1 and Table 2.

10. For a discussion of the purple pigment, caput mortuum, see L.F.C. de Oliveira, H.G.M. Edwards, R.L. Frost, J.T. Kloprogge and P.S. Middleton, 'Caput Mortuum: spectroscopic and structural studies of an ancient pigment', *The Analyst* (2002) **127** 536 – 541.

11. Middleton et al. *op. cit.*

12. M. Laver, 'Titanium Dioxide Whites', in E.W. FitzHugh, *Artists' Pigments: a handbook of their history and characteristics Vol. 3,* National Gallery of Art, Washington, Oxford University Press, New York, Oxford (1997) 295 – 296; R.J. Gettens and G.L. Stout, *Painting Materials: a short encyclopaedia,* Dover Publications, New York (1966) 160 – 161.

13. Vitruvius *de Architectura* VII. 3. 7.

14. P. Mora, 'Proposte sulla tecnica della pittura murale Romana', *Bollettino dell'Instituto Centrale del Restauro* (1967) 63 – 84; Middleton et al. *op. cit.*

15. B. Potter, Department of Mineralogy, Natural History Museum, London, personal communication (13 February 2004).

16. Edwards et al. *op. cit. 2002* (note 3).

Comparative Study of the Pigments Found in Illuminated Manuscripts of the 16th Century in Belgium. A Particular Case: the Gérard Van Der Stappen Book of Hours

S. Denoël[1], G. Weber[2], B. Price[3] and B. Gilbert[4]
[1] European Center of Archaeometry, Bldg. B5 Sart-Tilman, B-4000 Liege
[2] Experimental Nuclear Physics, Bldg. B15 Sart Tilman, B-4000 Liege
[3] Philadelphia Museum of Art, Benjamin Franklin Parkway and 26th Street, Philadelphia, Pa 19130
[4] Analytical Chemistry and Electrochemistry, Bldg. B6C Sart Tilman, B-4000 Liege

Abstract

The Gérard van der Stappen Book of Hours is a small manuscript of private worship. It is the first known piece of Renaissance Art from the principality of Liège. Two main methods of analysis were applied to identify the pigments used by the illuminators: Raman microspectrometry and PIXE (Proton Induced X-ray Emission), two complimentary methods which have been used with success for other manuscripts in our laboratory. By combining these techniques with results obtained from infrared reflectography, we can propose a chronological estimation for the realisation of the manuscript: it was made in about 1520 for two patrons, both of them abbots of Saint Laurent's abbey, one of the most powerful ecclesiastical institutions of the former Liège diocese.
The analyses showed a great diversity in the choice of the pigments, even for pigments of similar colour. It turned out that the most interesting features were actually some details, which allowed us to propose a differentiation between the illuminators. Our results were compared with other analyses carried out on manuscripts originating from Flanders and of the same period.

Introduction

The Gérard van der Stappen Book of Hours (Liège, University of Liège - Ms. 3591) is the first known piece of Renaissance Art from the Principality of Liège, in the southern part of current Belgium. Very little is known about artistic production in Liège in the early 16th century. For this reason, this Book of Hours has been conferred such a choice ranking in Liège. The Gérard van der Stappen Book of Hours is a small manuscript of private worship (16 x 14 cm). It contains twelve illuminations illustrating the virgin hours, the penitential psalms and the office of the dead. Other types of decoration are present: borders and vignettes of either grotesques or illuminated letters. With regards to the initials, the responsible artist showed much creativity. For example, each sentence begins with a different pattern: Cesar heads, grotesques, vegetal elements or saints.
The manuscript was analyzed with various aims. The first was to determine the palette of the pigments employed for the illuminations. Secondly, technological studies were also made on other manuscripts in order to put the Gérard van der Stappen Book of Hours in perspective of a more general context. For this purpose, a corpus of illuminated manuscripts from the Principality of Liège and Flanders was analysed by Raman spectrometry and Infrared reflectography as well as by the PIXE method. Finally, we wished to see whether the technical analyses could confirm the conclusions made from a deep stylistic study by, for instance, assessing the possibility of distinguishing the various artists that participated in this project. During this research, the spectroscopic measurements eventually enabled us to clarify certain points such as the execution date of the manuscript.

Experimental

The Raman set-up is a "Labram" spectrometer made by Jobin-Yvon provided with a confocal microscope. With this microscope, the laser beam at the focal point has a spot size down to 1 micron, depending on the objective and laser in use. In addition, by adjusting the size of the confocal hole, the depth resolution can be reduced to about 2 microns.
Three lasers are available: an Argon, a Krypton and a Helium-Neon laser so providing many different excitation lines. The power of the laser is always adjusted to the minimum value needed to obtain a decent spectrum and is of the order of a few milliwatts maximum. The analyses were always made directly on the illuminations.
The PIXE measurements were carried out with a proton beam produced by a cyclotron. The precise position of the sample is achieved by using two small laser beams. A flow of He is blown towards the detector on the path of the X-ray emitted by the sample. This system reduces the X-rays absorption and permits detection of the light elements down to Na. Raman measurements are also made directly on the document and for this purpose the manuscript is

set on a movable stand in front of the proton beam.

An interesting case: the execution date of the manuscript

The verso of folio 2 (Fig.1) depicts the coat of arms of Gérard van der Stappen (1520-1558), an abbot of one of the most powerful ecclesiastical institutions of the former Liège diocese, Saint Laurent's abbey.

In the context of the stylistic study of the manuscript, it was important to try to specify the date of execution of the work among the 38 years of the career of the abbot. At first, an infrared reflectography study, by means of a Hamamatsu camera, revealed an under drawing

which represents another shield (Fig. 2 a and b). This last one belongs to Jean de Noville (1516-1520) an abbot which preceded Gérard van der Stappen.

The question which arises now is: at which stage of the execution was added the second blazon? When the manuscript was completed or during its execution? Raman spectrometry could provide some answer to us. A restricted zone, around the holly leaf at the top of the blazon, shows, after a careful examination, an inhomogeneous surface. By infrared reflectography, it is possible to distinguish a hidden drawing of a rose. An in-depth Raman analysis of the stratigraphic composition of the pictorial layers showed that vermilion was the only pigment used to paint the rose and that the rose is actually behind a coating layer of azurite which was used to mask it (Fig. 3). From Raman, it is possible to evaluate the thickness of the pictorial layers which is of the order of 5 to 10 µm. The shape of the rose indicates also that it belongs to the arms of Jean de Noville.

Since our analysis of other areas of the same illumination showed pigments found only in the coat of arms of Gerard van der Stappen and not that of Jean de Noville, we conclude that the brutal and unexpected death of the abbot Jean de Noville in 1520 doubtlessly left the manuscript in abeyance until it was resumed by his successor Gérard van der Stappen who gave his own name to the book.

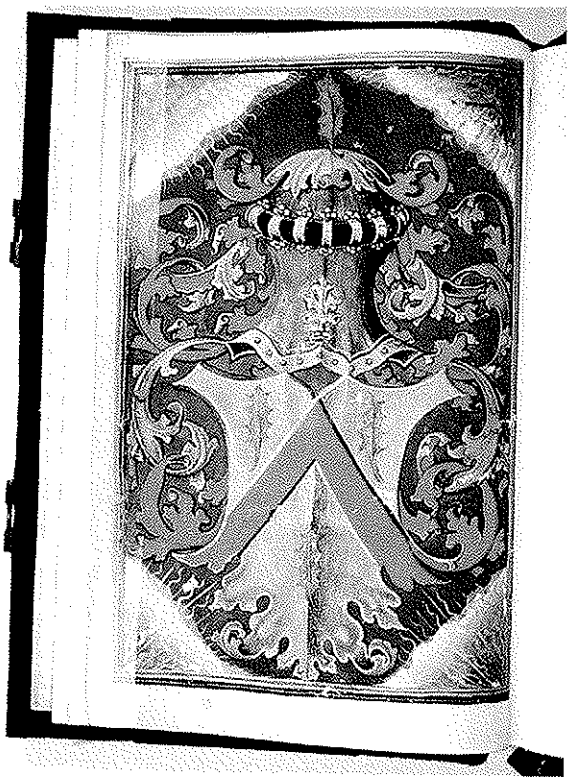

Fig. 1 Folio 2 verso, coat of arms of Gérard van der Stappen

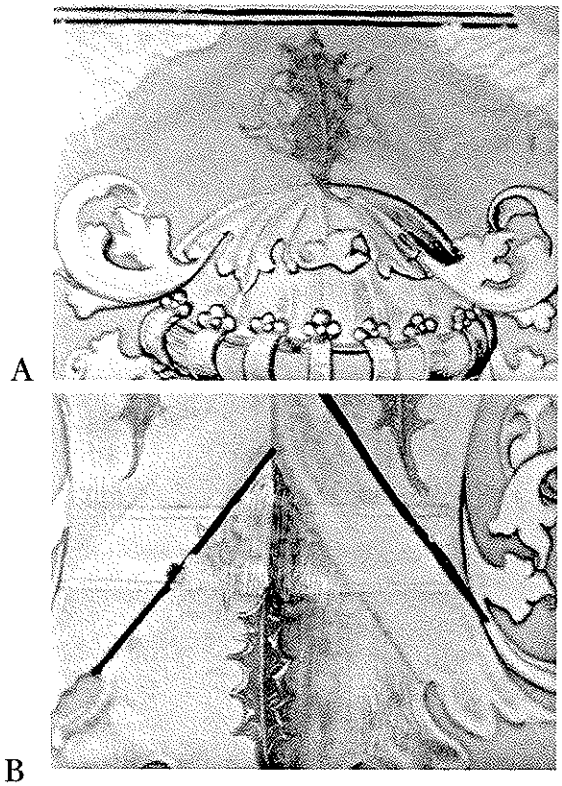

Fig. 2 Underdrawing of the coat of arms, (a) Rose behind the holly leaf, (b) Fesse from the shield of Jean de Noville

The palette of the illuminators of the Book of Hours of Gerard van der Stappen

In general, the range of pigments employed in this manuscript does not present large changes from page to page. Mainly very classical pigments were found such as vermilion, minium, azurite, ochre, etc. Most of the pigments found are summarized in Table I. However in certain parts or in certain colours of the illuminations, a closer analysis shows interesting peculiarities which are detailed below.

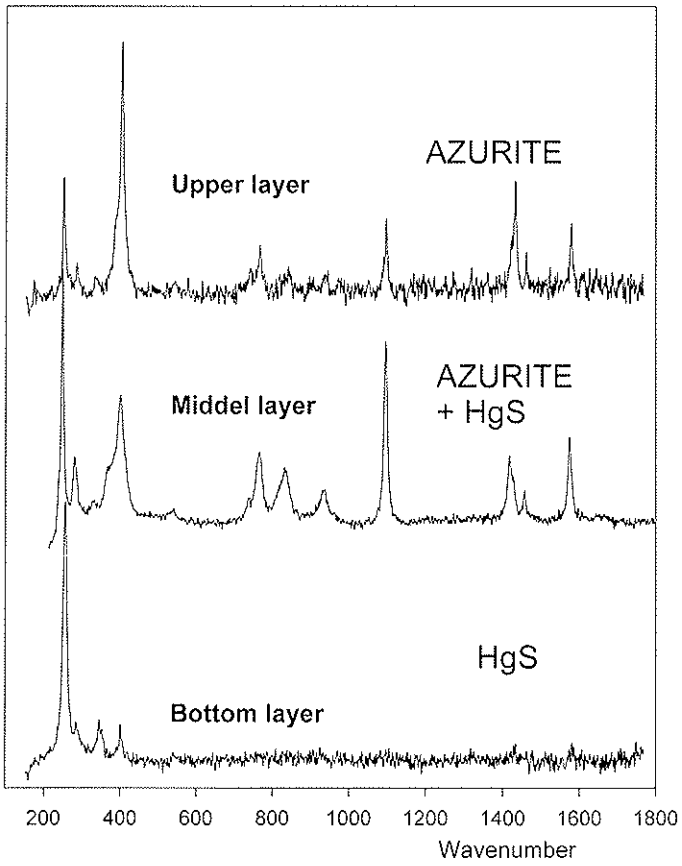

Fig. 3 In-depth analysis of the area around the holly leaf: vermilion under azurite.

The grey-blue colour

The discussion below concerns the painting used to represent the helmet on the top of the blazon. It is a good example of the complementarity of the two methods which we employ. The metallic grey colour of the helmet turned out more complex than initially thought. The PIXE method shows us that a large quantity of lead is present, together with traces of silver (Fig. 4). On the other hand, Raman spectrometry (Fig. 5) attests the presence of lead white as well as of a dark blue dye, indigo, which was impossible to detect by PIXE. One can then conclude that the grey-blue colour is obtained by a mixture of indigo and lead white, the metallic reflections being due to the application of a silver powder. This metallic layer is now oxidized and confers a dull aspect to the helmet.

The indigo has been used often in the manuscript since it was found in the great majority of the illuminations. Nevertheless, it is restricted to small and unimportant areas such as the roofs or some small metallic objects. The use of indigo is not common in the illuminations of the 16th century in Flanders although one finds it in the Hennessy Hours (Bruges, c. 1530 – Bruxelles, Bibliothèque

Colour	*Pigments*	*Colour*	*Pigments*
Yellow	Ochre + Gold Lead-tin yellow Type I	Pink	Lacquer
Orange	Minium	Mauve	Vermilion + Azurite
Red	Vermilion	Green	Posjnakite, Brochantite, Langite
Blue	Azurite Indigo	Brown	Earth
Grey	Lead white + carbon black	Black	Carbon Black

Table I Summary of the pigments found

Royale Albert Ier), but only in small amounts and mixed with other pigments such as lead white. Among all the illuminations we have investigated, only the French illuminations of the 15th century seem to be made with this dye on a large scale, as pure pigment or in a mixture. The study by B. Guineau and I. Villela-Petit [1] confirms the use of indigo by the famous Parisian artist, the Master of Boucicaut (15th century) in the realisation of different colours such as the mauves, the greens or the blues.

The yellow colour

Another pigment used in small quantity is the lead-tin yellow type I. We found it only in the margins mainly to illuminate, by its bright yellow colour, the heart of the flowers. The presence of this pigment is not an exceptional observation, but its use seems to have been limited to small zones or as mixtures with other pigments, for instance in the illuminations of the north of Belgium as the Breviary Mayer van den Bergh [2] or the Quadriptych Stein [3]. In

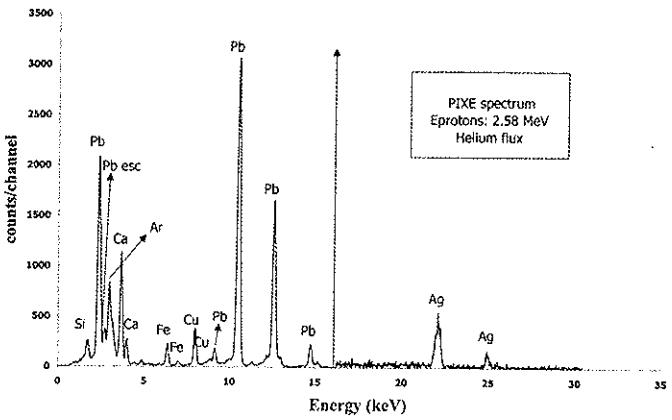

Fig. 4 PIXE spectrum of the grey paint used for the helmet. Components identified: lead and powdered silver

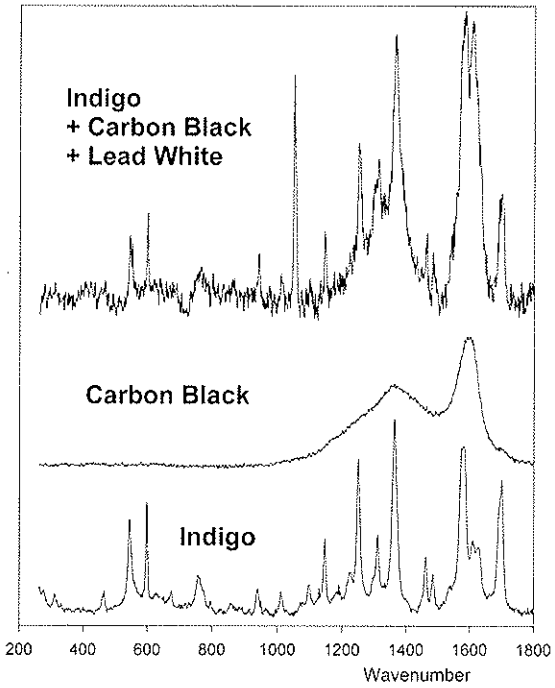

Fig. 5 Raman spectrum of the same area as in Fig. 4 Indigo, Carbon black and Lead white

all the other cases, as in the yellow background of the margins of this manuscript, the yellow colour is made from ochre. On the other hand, around 1530-40, the lead–tin yellow pigment has been used abundantly in a manuscript resulting from the same workshop that the Book of Hours of Gerard van der Stappen. The work in question, the Evangeliary of Jean de Falloize (Philadelphia, Free Library – Ms. Lewis E160), shows broad beaches of clear yellow colour made up of lead tin yellow. This new abundance is not explained, the question of the fashion for the lead stannate or of the supply possibilities can be evoked. A few years later, around 1565 in the Principality of Liege, this pigment became an essential component of the palette of Thomas van den Putte (Fig. 6 and 7), the illuminator of the Quercentius

Fig. 6 Gospel Book of Quercentius

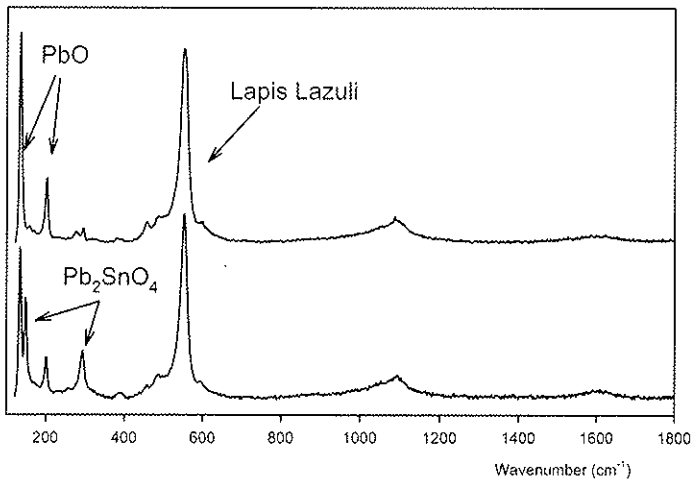

Fig. 7 Raman spectrum of the yellow area in Fig. 6: PbO + Lapis Lazuli + Pb_2SnO_4

Gospel Book (Liège, MARAM) [4] and there, it is also found in major areas, not only in representation of details.

The green colour

In the case of the green areas and in the twelve illuminations (clothing, foliages, grass, etc.) the pigment employed is exclusively a copper sulphate and no trace of malachite or verdigris was revealed by the analyses. In our results, posnjakite is the major green pigments even if in certain cases two other sulphates, brochantite and langite were discovered.

But in the Evangeliary of Jean de Falloize, the infrared spectrometry revealed the use of a mixture of malachite and brochantite (Fig. 8 and 9).
The nearly exclusive use of these copper sulphates as green pigments is an observation we made in many manuscripts of the end of 15th century and 16th century [5]. On the forty-five illuminations of this period coming from France, Germany and Belgium, the major pigment found is clearly posnjakite followed by malachite (Fig. 10).
For example, one of the most famous miniaturists of Belgium, Simon Bening, has largely employed this pigment in the green zones of the Hennessy Hours.
In certain cases we noted also that, to trace details such as the grass, the illuminator applied on the green uniform area thin yellowish lines, which under the microscope have a glassy surface. A Raman spectrum was obtained on these zones and found to belong to an organic pigment we have not been able to identify yet. Two hypotheses can be proposed concerning the composition of this pigment: it can be either a dye like the sap green or a resin. In the literature we found two cases [1,6] where a resinous glaze is employed for the realization of similar details.
Nevertheless during our research we were also confronted with the same spectrum in a German miniature of the 15th century which seems to confirm a frequent use of this kind of organic compound.

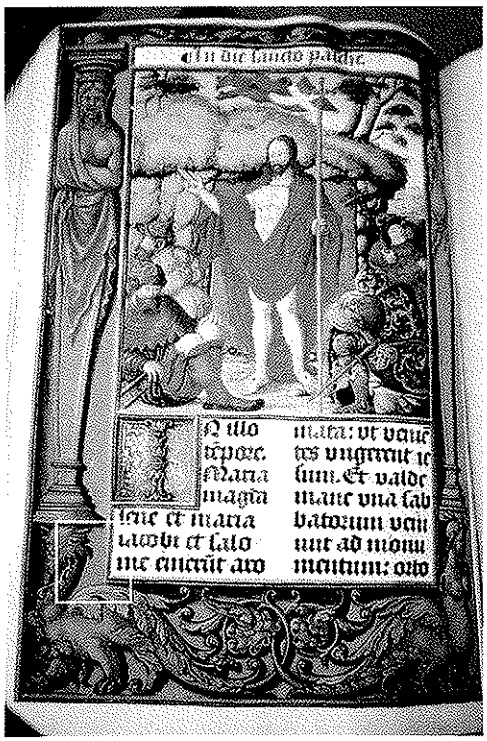

Fig. 8 Evangeliary of Jean de Falloize; the analysed green area is centered in the white square.

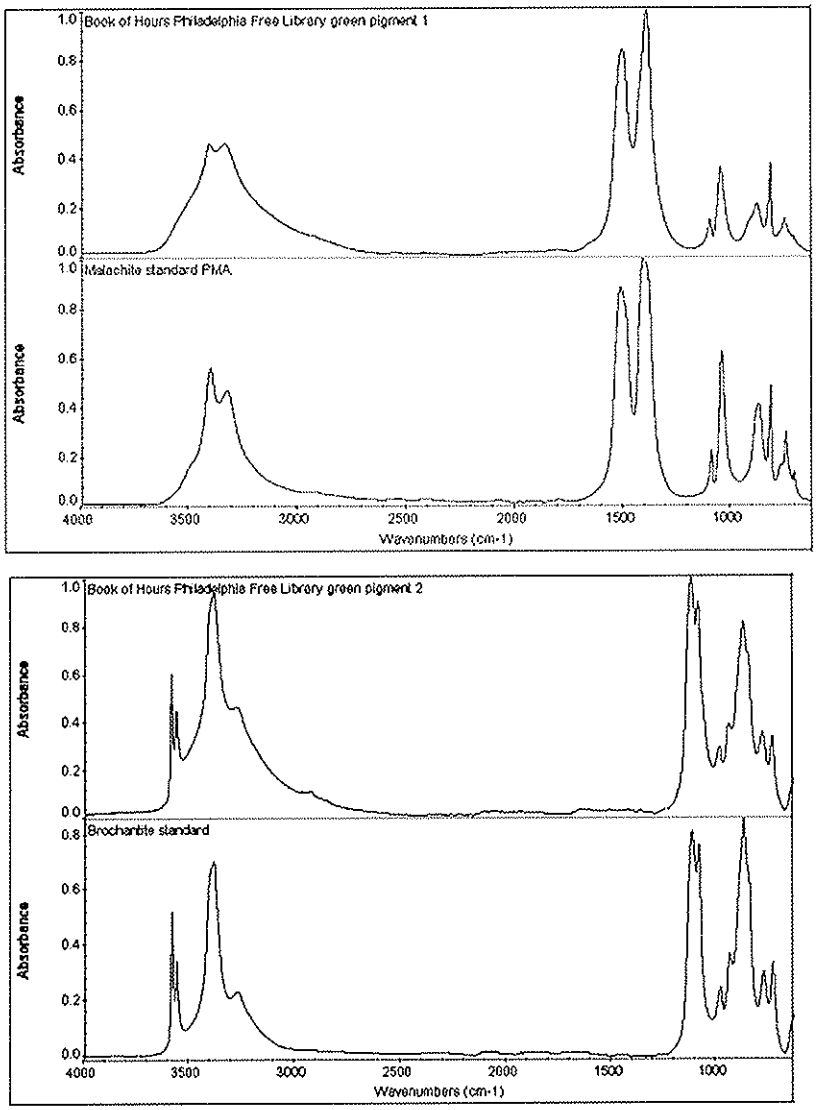

Fig. 9 Infrared spectra of the green area from Fig 8 malachite (top) and brochantite (bottom).

Tentative of differentiation of the illuminators

Finally in the context of the study of this manuscript we were interested to try to differentiate the painters having taken part in the realization of this work.
Indeed, in the 16th century, the realisation of a pictorial program results from collaboration between various illuminators and/or workshops, this with the aim of rationalizing the work and so increasing the speed of production. On the basis of a preliminary study of the characteristic stylistics on each illumination, for example considering differences and similarities in the execution of draperies, of faces but also in the choice of the chromatic palette, we came to the conclusion that at least four groups

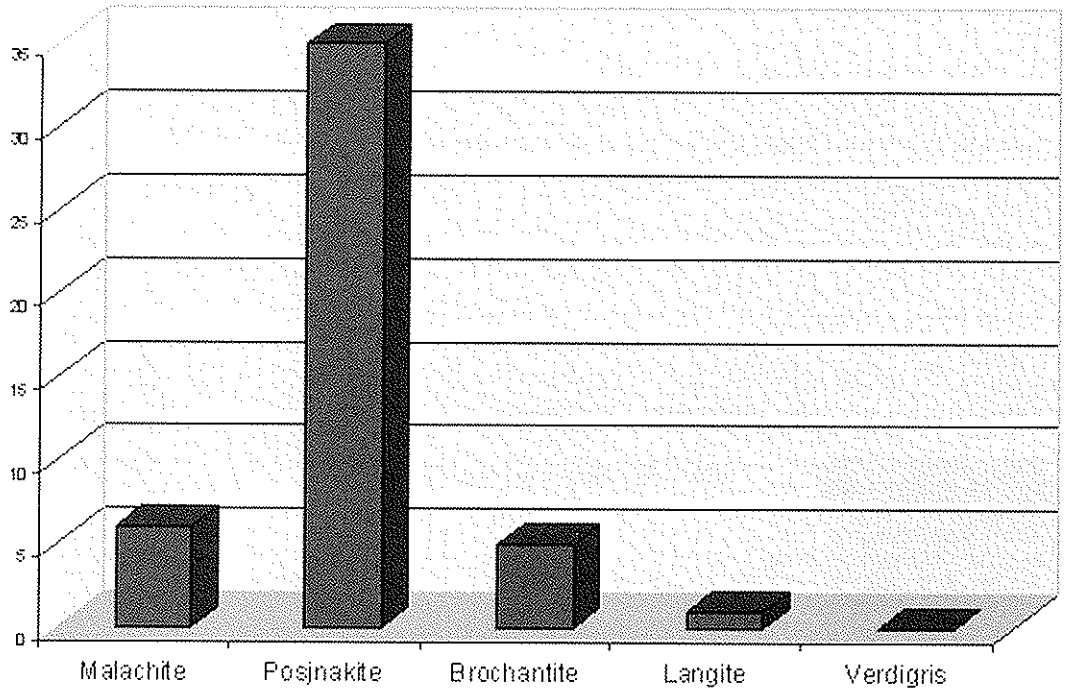

Fig. 10 Histogram of the occurrence of the various green pigments

could corroborate this classification or if we have to transfer an illumination to another group. At first, we were interested in the palette of the painters in order to deduce characteristics from the corpus, but as we already pointed out, the range of pigments employed is, at first sight, standard and does not vary much from one illumination to another.

However, we found that the mixtures of pigments and more particularly the grey zones of the walls could be used to discriminate the different hands. Indeed, the combination of certain pigments to reach an identical colour proved to be a true signature of the artist. The most obvious case is that of E since the walls, as in the miniature representing the *Massacre of the Innocents* (Fig. 11), consist of a complex mixture containing lead white, carbon black, lead yellow and another organic not yet identified (Fig. 12).

In contrast to these four pigments, the light grey area in the *Annunciation* is made up only of three pigments: azurite, lead white and indigo. When this colour is darkened, it is by means of addition of a small amount of carbon black. In the case of the *Visitation*, the colour of the grey walls is obtained by mixing lead white and carbon black but, this time, with posjnakite added. In that miniature the composition of the grey is then unique. All these observations are in agreement with the stylistic analysis results and allow attribution of this illumination to a single Master, different from the other ones since the mixture composition for the greys is unique and does not repeat itself in the manuscript.

Hand A	Annunciation
Hand B	Visitation, Flight to Egypt
Hand C	Nativity
Hand D	Adoration of the Shepherds, Adoration of the Magi
Hand E	Presentation of the Temple, Massacre of the Innocents, Bathsheba in her bath The three Dead and the three Livings, The man of sorrows.

Table II The five groups deduced from a stylistics analysis

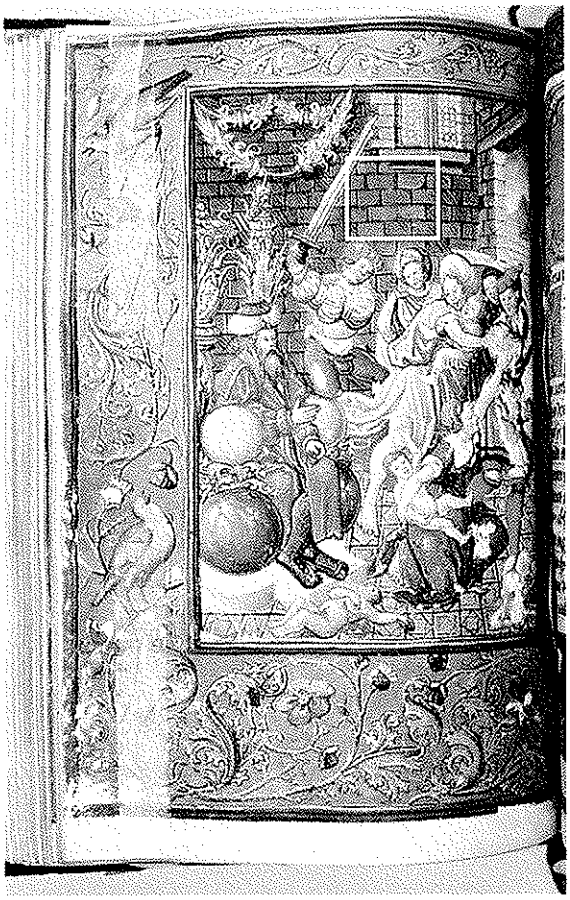

Fig. 11 *Massacre of the Innocents* Book of Hours of Gérard van der Stappen

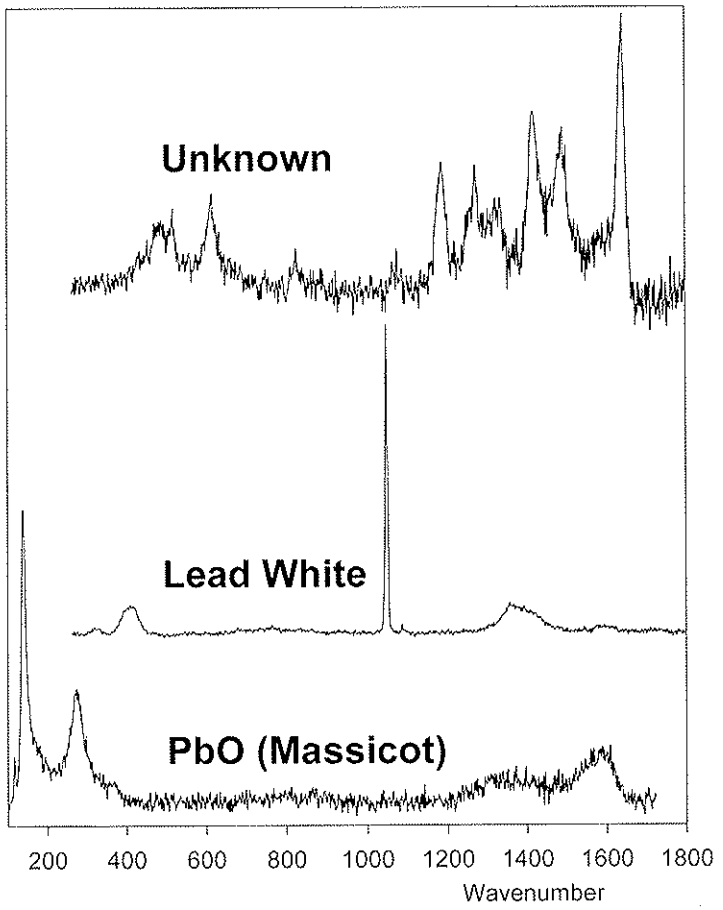

Fig. 12 Raman spectrum of the grey paint used for the wall: a mixture of lead white, carbon black, lead oxide and an organic pigment

Conclusion

The results obtained from the analysis of the Gérard van der Stappen Book of Hours are particularly interesting at various levels. First, a combined study of the blazon, by means of infra-red reflectography and Raman spectrometry, showed the presence of a hidden drawing which allowed a narrower chronological estimation for the execution of the manuscript. Secondly, the study of the range of colours used by the illuminators enabled us to confirm the prevalence of a copper sulphate, posjnakite, as green pigment.
Finally, in two cases, the scientific analyses of presumably unimportant areas confirmed the conclusions made from stylistic analyses and thus allowed a higher degree of certainty for the differentiation of the artists having taken part in the realization of this manuscript. This research emphasises the importance of investigating in depth not only major areas but also small details which are apparently of low significance.

Acknowledgements

The authors wish to thank the curators who agreed to loan their illuminations for analysis: Mrs. C. Opsomer keeper of the manuscripts of the University of Liège, Mr. J.-P. Duchene curator of the art collection of the University of Liège, Mr. A. Lemeunier curator of the Musée d'Art religieux et d'Art mosan at Liège and Mr. W. Lang curator of the Free Library Rare Book Department at Philadelphia.

References

1. Guineau B. and Villela-Petit I., 'Couleurs et technique picturale du Maître de Boucicaut', in *La Revue de l'Art* (2002) 23-42.

2. Vandenabeele P., Wehling B., Moens L., Dekeyzer B., Cardon B., von Bohlen A. and Klockenkämper R., 'Pigment investigation of a late-medieval manuscripts with total reflection X-ray fluorescence and micro-Raman spectroscopy', *The Analyst* (1999) **124** 169-172.

3. Quandt A. and Turner N., The Technical Analysis of the Stein Quadriptych: A premiminary Report, communication at the colloquium Illuminating the Renaissance, London, 21 February 2004.

4. Denoel S., Weber G., Allart D. and Gilbert B., 'Non-destructive analysis of a 16th century manuscript from the Gospel Book of Robert Quercentius', in Townsend J.H. *et al.* (eds.), *Conservation Science 2002, Edinburgh, May 2002*, Archetype Publication, London, 2003, 208-215.

5. Gilbert B., S. Denoël, Weber G. and Allart D., 'Analysis of green copper pigments in illuminated manuscripts by micro-raman spectroscopy', in *The Analyst* (2003) **128** 1213-1217.

6. Scott D.A., Khandekar N., Schilling M.R., Turner N., Taniguchi Y. and Khanjian H., 'Technical Examination of a fifteenth-century German Illuminated Manuscript on Paper: A case study in the identifications of materials', in *Studies in Conservation* (2001) **46**

Original and Fake Blue Pigments From the Church of S. Francesco in Montefalco Painted by Benozzo Gozzoli: a Spectroscopic Approach.

C. Miliani[1], C. Ricci[2], F. Rosi[2], I. Borgia[2], B. Brunetti[2], A. Sgamellotti[1-2]

[1] Istituto CNR-ISTM (Institute of Molecular Sciences and Technologies), c/o Department of Chemistry, University of Perugia, Via Elce di Sotto 8, 06123 Perugia.
[2]Centre of Excellence SMAArt " Scientific Methodologies applied to Archaeology and Art"c/o Department of Chemistry, University of Perugia, Via Elce di Sotto 8, 06123 Perugia.

Abstract

In order to establish the painting technique of Benozzo Gozzoli, a wide in situ non destructive XRF and FTIR characterization of the San Girolamo chapel, located inside the San Francesco church in Montefalco (Perugia-Italy), has been performed. After completing the famous cycle of San Francesco in the apse, Benozzo painted the first bay in the church's southern side aisle, known as the chapel of San Girolamo (1452). In the effort to better understand the nature of blue pigments some micro samplings have been carried out on zones selected using the XRF and mid-FTIR reflectance results. On these samples micro-Raman and micro-FTIR studies have been accomplished accompanied by stratigraphical investigations on cross sections at optical and scanning electron microscope.
In order to find out analogies and differences between the two frescoes of Benozzo Gozzoli, a comparison of these data with those acquired in the apse during a previous campaign of measurements has been carried out. In this way it has been possible to confirm the use by Benozzo Gozzoli of the same palette for both the mural paintings. Furthermore, the identification of two synthetic blue pigments, Prussian blue and ultramarine, dating back to two different nineteenth century restorations known by written documents, has made it possible to discriminate between original and retouched paintings.

Introduction

The church of San Francesco in Montefalco (Perugia-Italy) was built between 1335 and 1338. The internal of the church is given by a characteristic aisle, three choir stalls and an arched ceiling. Between the XIV and XV centuries, on the right side, six chapels were added, which were later put into communication between one another, so as to create the illusion of an apsidal church.
The central polygonal altar is completely covered with a collection of frescoes by Benozzo Gozzoli (1452) which contain episodes from the life of San Francesco considered the most famous after those of San Francesco of Assisi [1]. The first chapel of San Girolamo, was again painted by Benozzo Gozzoli [2].
Recent restorations of both frescoes offered the possibility to compare the painting technique used by the artist in the two cycles.
The cycle of San Francesco in Montefalco contains a total of 19 episodes from the life and work of the saint, arranged in a total of 12 pictures and a lost stained glass window. The cycle of pictures extends above the choir stalls along the five walls of the apsidal chapel, in three rows arranged one above the other. In the XIX century two important restorations occurred in the apsidal chapel: the former was carried out by Giuseppe Carattoli in 1832, the latter by Filippo Fiscali in 1889-91 after an earthquake [3].
The chapel of San Girolamo holds the date 1st november 1452. It retained its integrity for more than a century until when probably in 1610, it was drastically modified; in fact the building of an aisle lead to the demolition of all the lateral walls on the right side of the church, including that of the sacristy, and the opening of an entrance and a wide window. Hence the loss of the entire decoration from the left hand side walls as well as a great part from the chapel of San Girolamo. Nowadays the decoration is fragmentary, and the spatial relationships, proportions and lighting are completely different.
In the small chapel, not larger than 6x6 m, Benozzo painted some episodes from the life of San Girolamo, inspired by the Leggenda Aurea by Jacopo da Varazze. The walls on the left, demolished in XVII century, were probably episodes regarding the first part of the life of the saint, while the wall at the back depicts scenes accounting for two of the most important episodes of the cycle. In the first, the "*Partenza di San Girolamo da Roma*", the second "*San Girolamo toglie la spina dalla zampa del leone*". Beyond the stories of San Girolamo, on the altar walls, a large crucifixion completes the zone created by one of the most interesting and original decorative parties of the XV century. In front, leaning on a false altar ledge is the grand polittico, as false as the wooden capsa which contains it.

In the small vault, Benozzo painted the four evangelists, while the decoration of the chapel was completed by *"Cristo benedicente in gloria, tra serafini e gerarchie angeliche"*.
The paintings of the San Girolamo chapel too were subjected to different restorations in later centuries causing, in some cases, a masking of the original artwork. Due to the lack of comprehensive historical data for this cycle of frescoes, it is difficult to determine the exact chronology of the various restorations and in some cases also the identification of the original paint layers.
The scientific investigation here reported was carried out to identify the palette used by Benozzo Gozzoli in San Girolamo chapel. Furthermore, in order to discriminate between original and retouched painting, these data were compared with those acquired in the apse during a previous measurement campaign [1]. In particular, the identification of two synthetic blue pigments, Prussian blue and ultramarine, has allowed us to localize nineteenth century restoration retouches.
The first part of the study was carried out *in situ*, performing a wide non destructive X-ray fluorescence and fiber optic mid-FTIR characterization of San Girolamo chapel. In the effort to better understand the nature of blue pigments some microsampling have been carried out on selected zones using XRF and mid-FTIR reflectance results both in the San Francesco and San Girolamo frescoes. On these samples micro-Raman and micro-FTIR studies have been accomplished together with stratigraphical investigations on cross sections by optical and scanning electron microscopy.

Experimental Section

XRF is an analytical technique which permits elemental analyses. The characteristics of the portable instrument allow the detection of the elements with atomic number higher than silicon (Z>13).The X-ray generator is a EIS s.r.l. P/N 9910, with a tungsten filament and a silicon drift detector with a resolution of about 160 eV at 5.9 keV. The experimental parameters used during the investigations were: 35 kV and 0.05 mA. The acquisition time was 120 s. The distance sample-detector has been fixed at 4 cm. The beam diameter under these conditions is 4 mm.
The non destructive and *in situ* molecular investigation was carried out by a spectrophotometer FTIR JASCO VIR 9500 equipped with a Y probe of Remspec with 19 optic fibres. Seven of these bring the infrared radiation from the interferometer to the sample, while the other 12 acquired the scattered and reflected radiation from the analysed surface. The spatial resolution, determined by the probe diameter, is about 10 mm^2. The chalcogenide glass fibers allow for the collection of spectra from 4000 to 900 cm^{-1}, having an excellent signal-to-noise ratio throughout the range except in the 2200 - 2050 cm^{-1} region owing to the Se-H stretching absorption.
Micro-Raman spectra were obtained using a JASCO Ventuno double grating spectrophotometer equipped with an optical microscope, a CCD detector cooled at –50°C and 532 nm excitation from a Nd:YAG laser. In a typical experiment the laser was focused on to the sample through the 100x objective lens, the laser power at the sample was always kept between 0,6 and 3 mW. The resolution was 2 cm^{-1} and a polystyrene standard was used for the calibration.
Optical microscope (OM) images were taken by a Leica DM R microscope equipped with a digital camera Leica DC300. The stratigraphical study of the samples was performed on cross sections by scanning electron microscopy (SEM) provided with energy dispersive X-ray spectrometer (EDS) in order to determine the chemical composition of the different layers. The experimental equipment was a Philips XL30 equipped with an EDAX/DX4 detector. The work conditions were: accelerating voltage 15-20 kV, beam current 1.68 μA, work distance about 9 mm.
To assess a correlation between the Benozzo's polychromy and the pigment composition of his palette, first a wide investigation by non-destructive XRF technique was carried out on 80 points. XRF investigations allowed us to characterize the different pigmented areas. In particular, different types of blue hues were investigated. All the XRF collected spectra present the copper signal suggesting the use of azurite on all blue areas, except on the angels in the small vault, where the peak of copper was not always evident.
To understand better the blue zones molecular information coming from fiber optic mid-FTIR spectra were of particular interest.
Mid-infrared chalcogenide fiber optics coupled with a portable FTIR bench made it possible to perform *in situ* non invasive reflectance measurements.
It must be said that reflectance mid-FTIR measurements can present large distortions in the spectrum, both in band shape and absorption frequency [4], so that it is difficult to compare reflectance spectra with transmission spectra commonly collected in available databases. Responsible, in most cases, for the main distortions is the Fresnel reflection which, depending on the band strength, leads to different band shape. The most evident case is the so-called *reststrahlen* band, a reflectance maximum that occurs for bands characterized by a strong

absorption coefficient; these are thus inverted.
Due to the strong absorption of the lime plaster all spectra collected on fresco show similar principle features. In the 1400-1600 cm^{-1} region fresco spectra are characterized by the ν_3 band (asymmetric stretching of $[CO_3]$ group), which occurs as a distorted band due to the *reststrahlen* effect. Thus, the system fresco painting is extremely difficult to study because of the overlapping of a small spectroscopic signal from surface species (pigments and binder) with a very distorted signal from the substrate (lime plaster).
However, studying laboratory fresco models, it has been demonstrated [5] that it is possible to identify the presence of azurite, malachite and white San Giovanni by the shape of the combination band ($\nu_1 + \nu_3$) at about 2500 cm^{-1}. In fact, combination bands being forbidden show a small absorption coefficient and are not subject to distortions (Figure 1).

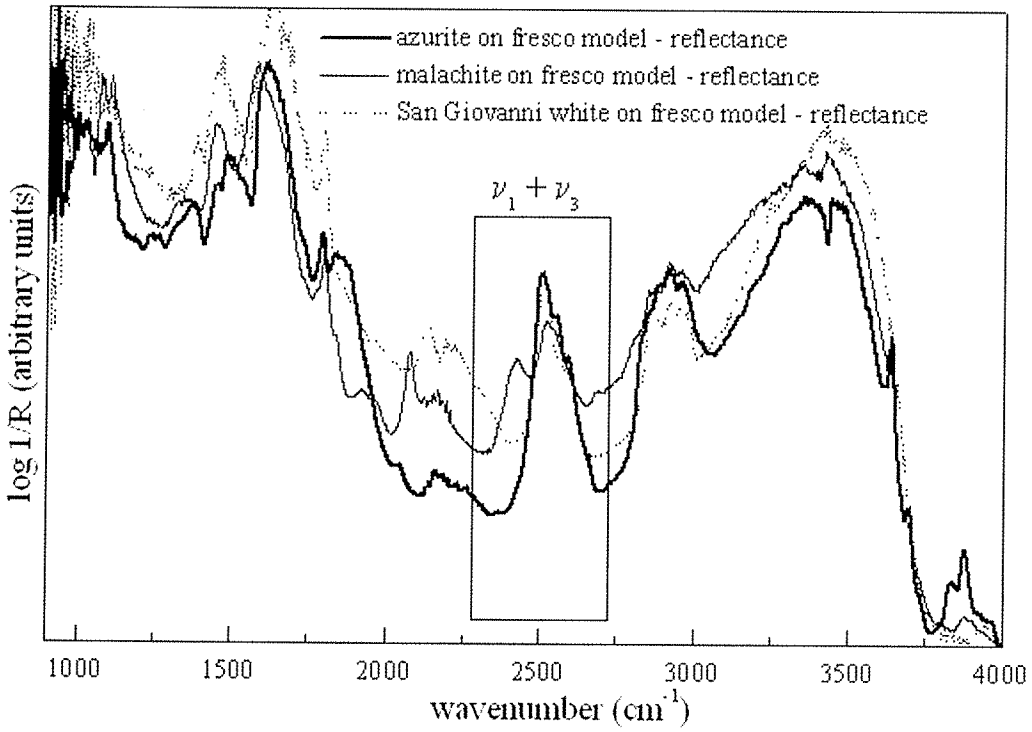

Figure 1: mid-FTIR reflectance spectra of azurite, malachite and San Giovanni white on fresco models. The spectral region of combination bands $\nu_1 + \nu_3$, useful for the carbonate identification, is put in evidence.

Moreover, it has been proved that also silicate pigments such as smalt, ultramarine blue and lapis lazuli are detectable by the presence of Si-O stretching occurring at about 1000 cm^{-1}, a spectral region quite free from the carbonate matrix distortion [5].
In most of the mid-FTIR spectra collected in blue areas the shape of $\nu_1 + \nu_3$ combination band at about 2500 cm^{-1} definitely proved the use of azurite as original pigment (Figure 2a).
The small vault, reported in Figure 3, showed lots of overpaintings and inpaintings. For instance, XRF measurements carried out on two original blues (points 21 and 22, Figure 3) and on a supposed blue inpainting (point 29, Figure 3) were compared. The original blues contained copper, while the inpainting showed a higher content of iron and a smaller contribution due to the copper. The fiber optic mid-FTIR spectra collected on different zones of small vault (points E52, E53, Figure 3) revealed the presence of a band at 2090 cm^{-1} due to the absorption of CN group, confirming, together with XRF data, the presence of Prussian blue. Furthermore, in certain points, a band at about 1000 cm^{-1} suggested, again together with XRF data, that ultramarine blue could be present.
Regarding the alteration products, the mid-FTIR technique put into evidence the presence of gypsum (see Figure 2), in some points, and of calcium oxalate in most of the analysed zone. The $[SO_4]$ stretching absorption at 1145 cm^{-1} resulted inverted owing to the *reststrahlen* effect. The gypsum was found in stuccoed zones while the presence of oxalate was due to the deterioration of organic matter used probably as binder for overpaintings and inpaintings.
The XRF and mid-FTIR results allowed us to better locate the areas to be investigated with stratigraphical and micro-spectroscopic analyses. This procedure minimized the number of samples needed.

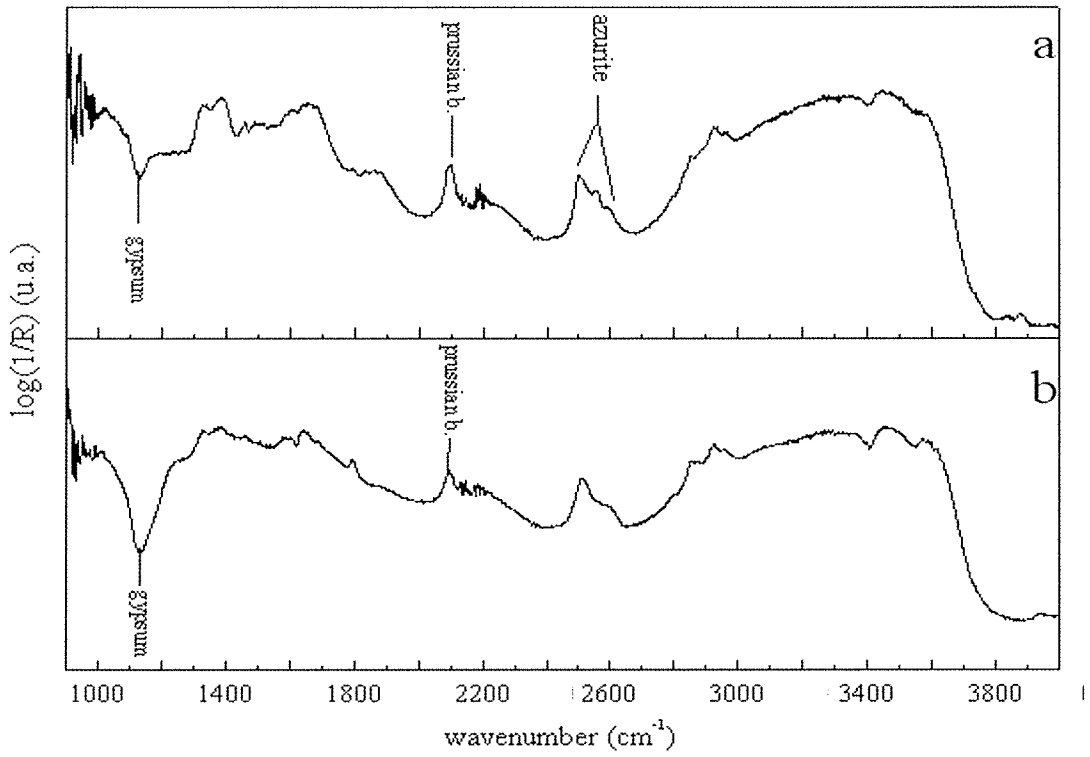

Figure 2: mid-FTIR reflectance spectra collected on blue areas of San Girolamo frescoes, a) azurite and gypsum; b) Prussian blue and gypsum. The [SO_4] stretching absorption of gypsum is inverted due to the *reststrahlen* effect.

To study thoroughly the blue pigments a micro sampling (MG2) was carried out by the restorers on the right arm of the first angel on the left under the entrance arch of the chapel. Under the optical microscope the paint layer of the sample seemed to be made up of blue crystals with two different hues: a lighter one and a darker one. Micro-Raman analyses carried out on the surface of the sample revealed that the paint layer was composed of a mixture of two blue pigments: azurite and ultramarine (see Figure 4). The Raman peaks of the spectrum collected on the white crystals present on the surface of the sample matched with those of calcium oxalate dihydrate (weddellite).

Figure 3: black and white photograph of San Girolamo chapel small vault. The labels indicate XRF (21-24, 27-29) measurement, mid-FTIR (E50-E53, E56, E57) measurement points and the micro sampling point (MG2).

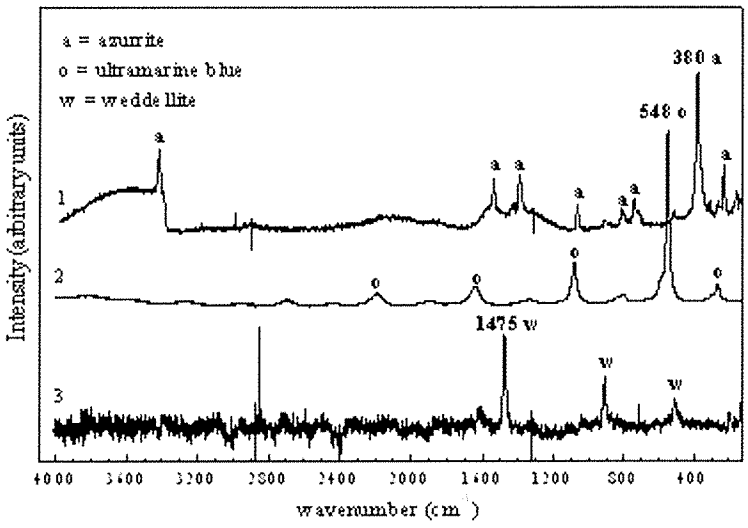

Figure 4: micro-Raman spectra collected on blue and white crystals of MG2 sample from San Girolamo chapel.

The cross section of MG2 shows a paint layer of about 100 μm with an evident discontinuity between lime plaster and paint layer. Cross section SEM-EDS investigations put in evidence the presence in the paint layer of copper rich crystals mixed together with smaller crystals made up essentially of Si and Al. On the bases of spectroscopic data, these crystals were identified as azurite and ultramarine respectively. Because of the morphology of ultramarine crystals it is plausible to think it is a synthetic ultramarine rather than natural ultramarine, lapislazuli. The analyses performed on the cross section revealed, also, the presence of crystals rich in Ba and S, probably $BaSO_4$ used as a filler of synthetic ultramarine.
Observations under the optical microscope of the surface of the sample MG4, belonging to the backwall, the first compartment on the right representing san Ludovico da Tolosa, revealed that on the metallic foil a blue layer was present. Micro-Raman spectra collected on the blue layer showed that the pigment used is azurite. FTIR analyses performed using a diamond cell revealed traces of an organic substance having both the proteinaceous and the lipid components. SEM-EDS investigations of the cross section pointed out, beyond the presence of copper rich crystals, two metallic layers: a tin foil applied over a gold foil.
Previous XRF investigations carried out *in situ* in the apsidal chapel revealed that the original blue, used by Benozzo, was a copper based pigment, azurite [1] as well as in the San Girolamo chapel.
For a better understanding of the materials used in the restorations carried out by Carattoli and Fiscali, a sampling operation has been performed by the restorers in some restored zones of the apsidal chapel. The samples are listed in Table 1 and their belonging to older or later restoration was established by restorers by visual observation.
Micro-Raman, FTIR and SEM-EDS investigations showed that, along with the San Girolamo chapel, the blue pigments present nowadays in the apsidal chapel are azurite (original), ultramarine and Prussian blue (both of restoration).
In particular, the cross section of the sample MB18 presented a paint layer made up of three different layers. Micro-Raman and cross section SEM-EDS investigations revealed that the inner most layer is of Prussian blue (*a* in Figure 5), while the outer most layer showed pigment grains with a composition and a morphology corresponding to those of synthetic ultramarine (*c* in Figure 5). The layer in the middle is lead white (*b* in Figure 5).

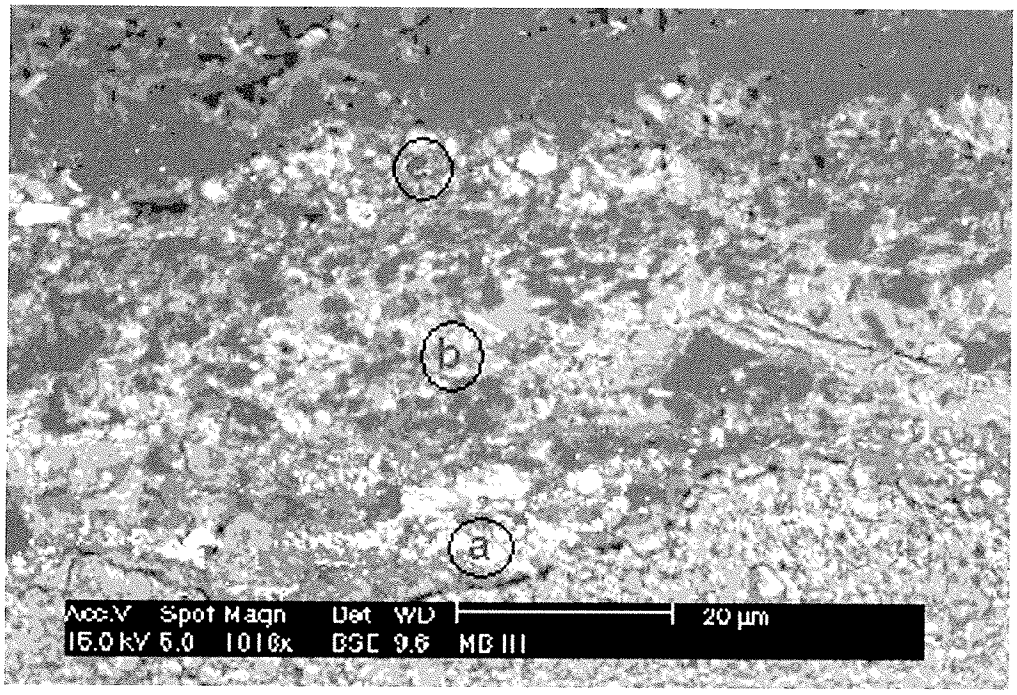

Figure 5: SEM-BSE image collected on the cross section of sample MB18 from San Francesco chapel.

Therefore, on the bases of sample MB18 it was possible to relate the older restoration carried out by Carattoli (1832) with the presence of Prussian blue, and the later restoration carried out by Fiscali (1889-91) with the presence of ultramarine blue.
For all the others samples the definition older or later reported by restorers matched quite well with our assignation based on molecular composition of sample MB18: the examples of Raman spectra collected on later and older stuccoed zones are presented in Figure 6; they have been identified as ultramarine and Prussian blue, respectively. Notably, as observed in San Girolamo, the synthetic ultramarine blue was mixed with barium sulphate as filler.

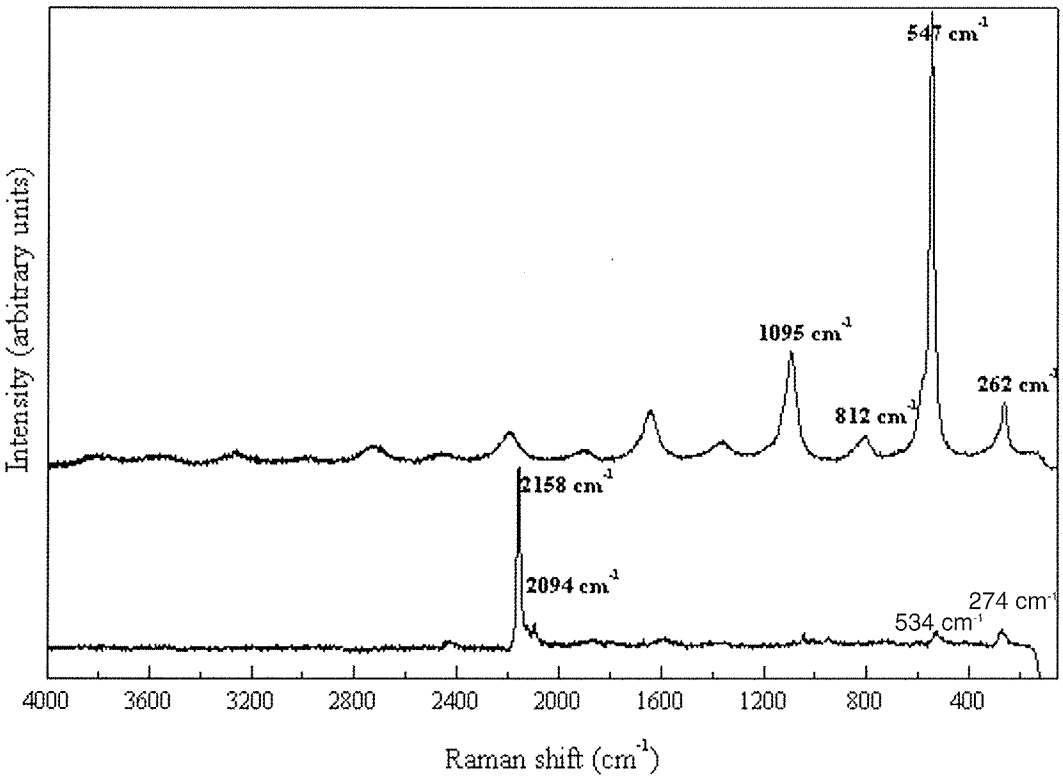

Figure 6: micro-Raman spectra of later (upper line, ultramarine) and older (lower line, Prussian blue) stuccoed zones of San Francesco chapel.

sample	*location*	*restoration*
MB18	zone 16	later
MBA1	zone 17	older
MBA2	zone 17	older
MBA3	zone 16	older
MBA4	zone 16	later
MBA5	zone 16	later
MBA6	zone 18	older
MBA7	zone 18	later
MBA8	zone 18	later
MBA9	zone 19	older
MBA10	zone 15	later
MBA11	zone 15	older

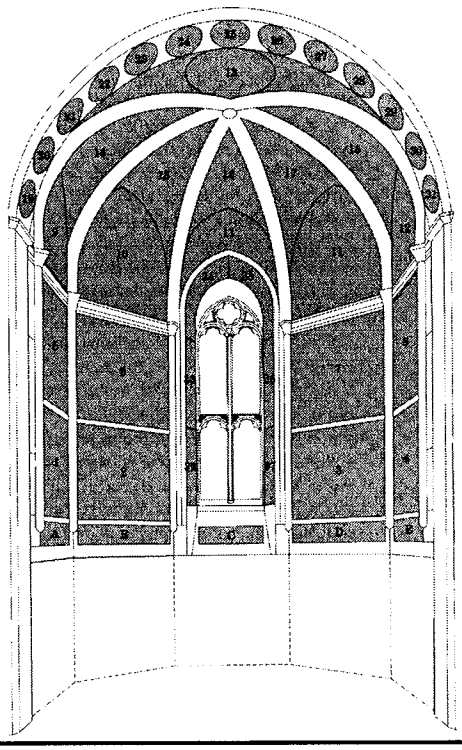

Table 1: Location and indication of the restoration period for the samplings performed on the apsidal chapel of Montefalco Church.

Conclusions

First, comparing the data acquired in the two chapels it was possible to establish that San Girolamo frescoes were restored by both Carattoli and Fiscali. Moreover, combining non destructive XRF and mid-FTIR data with micro destructive results it was possible to gain a compositional map of blue areas that revealed the original painting, the zones retouched by Carattoli in 1832 and the zones retouched by Fiscali in 1889-91.
Different from what was observed in San Francesco chapel, in San Girolamo the XIX century retouches were seen not only in the loss of paint but also directly on the original painting, as a mixture of azurite and Prussian blue or azurite and synthetic ultramarine blue.
The same kind of compositional map on restoration retouches was not acquired for red areas since both in San Francesco and in San Girolamo the retouches seemed to be made of red ochre.

References

1. A.A.V.V., *Benozzo Gozzoli allievo a Roma, maestro in Umbria*, Silvana Editoriale, Perugia, (2002).

2. A.A.V.V., *Benozzo Gozzoli La cappella di San Girolamo a Montefalco*, Quattroemme, Perugia (2003).

3. Archivio Storico soprintendenza Beni AA, Paesaggio, Patrimonio SAD dell'Umbria, cartella Montefalco 37, fascicolo 9, lettera dell'architetto direttore al Ministero dell'Istruzione Pubblica in data 14 aprile 1898.

4. Fabbri M., Picollo M., Porcinai S., Bacci M., *Appl. Spectrosc.*, **55**, 4 (2001).

5. Miliani C., Ricci C., Sgamellotti A., Brunetti B.G., to be published.

Synthesis and Weathering Process of Egyptian Green: Structural Characterisation by Raman Microspectrometry of a Synthetic Copper silicate Used as Pigment

Dr S. Pagès-Camagna
C2RMF-UMR 171 du CNRS Palais du Louvre, Porte des Lions, 14 quai François Mitterrand, F-75001 Paris

Abstract

Thanks to the combination of various analyses (SEM-EDS, μRaman, XRD and colorimetry) on undertaken archaeological and modern samples, the manufacturing process of the Egyptian green has been discovered. This synthetic pigment is often confused with the better-known and well-studied Egyptian blue. The green pigment was only used on the Egyptian territory and found on artefacts from 2100 BC to 1069 BC. The Egyptian green, a composite matter, has its own composition: the main phase is a copper-bearing glass, which is mixed with various crystalline species, such as quartz. Among them, parawollastonite (α-$CaSiO_3$) is characteristic of the pigment. The variation of flux amount or firing temperature acts on different phases: if higher temperature and higher amount of sodium modify structure of amorphous phase (polymerisation with high quantity of flux), wollastonite structure is indicator of firing temperature. Up to 1150°C appears another high-temperature polymorph, pseudowollastonite (β-$CaSiO_3$), never found in archaeological artefacts.
First step of weathering process in saline solution shows mechanical attack of the amorphous phase.

Introduction

During the Old Kingdom (2600 BC) Egyptian craftsmen created a blue pigment by firing a mixture of compounds containing silica, calcium and copper with a sodic flux: the Egyptian blue. Different origins of soda flux can be expected: natron [$Na_2CO_3 \bullet 10(H_2O)$], plant ashes or salt-rich soil near water; copper minerals or bronze scraps provided copper; silica came from Desert sand and calcium from chalky stones. This blue pigment, a lapis-lazuli substitute, was widely used during Antiquity, spreading all around the Mediterranean basin. A turquoise mineral substitute appeared shortly after the blue one: it has a similar elementary constitution, with a turquoise colour and is called Egyptian green because of its use on foliage decorations. This material is sometimes also called "green frit". They can be distinguished by their crystalline phases: cuprorivaite ($CuCaSi_4O_{10}$) in the blue and parawollastonite ($CaSiO_3$) in the green.

Materials and methods

Materials
A part of the samples came from the Egyptian Department of the Louvre Museum: they were raw materials found in Deir el Medineh, craftsmen village, and were used during the New Kingdom for the decoration of the wall painting in the Kings Valley. These green and blue pigment cakes were studied in order to obtain the real recipes for each colour [1].
A second part of samples consisted of modern Egyptian green, obtained by changing some firing conditions: temperature, quantity of flux. They were synthesised in laboratory by firing a mixture of silica sand, calcium carbonate, copper (metal or tenorite) and sodium carbonate in order to follow the sintering process, thanks to the structural characterisation of the material. The weathering process was studied by placing the modern sample in a saline water (pH=9) at 60°C, in order to explain the modification of this pigment on Egyptian stones, during various time (from two weeks till a few months).

Methods
The samples were studied by XRD on powder, SEM-EDS on cross-section, UV-visible spectrometry and μRaman spectrometry. These techniques aim at furnishing analytical and structural characteristics of each material. Cross-sections were polished with diamond paste and covered with carbon before SEM analyses.
The Jeol 8400 SEM was used for image processing and elemental analyses by electron beam of 20 keV, intensity of 3.10^{-9} A and distance between sample and Si-Li detector of 15 mm.
The Raman spectra were obtained with an Infinity Labram Jobin-Yvon equipped with air-cooled CCD, double Notchs filters and two lasers (Nd:Yag and He-Ne). Raman spectra of each phase were recorded with a long working

distance objective (x100). The irradiance was measured and found to be equal to 10^9 Wm^{-2} for a 1 mW laser power sample and spot diameter of *ca* 1.5 µm.

Results and discussion

The Egyptian blue pigment has already been studied [1, 2] and is not the subject of this paper.
Egyptian pigments are both composite materials, mixture of amorphous and crystalline phases (Figure 1) [3].
Egyptian green is characterised by parawollastonite (α-$CaSiO_3$) crystals smaller than 10 µm and residual silica (quartz and/or -tridymite or cristobalite-), embedded in a silica rich amorphous phase.
During the firing process, some phases appear and some of others disappear, depending on the firing temperature. But these results are able for the crystalline phases but no technique except Raman spectrometry can really give data on the modification of the amorphous phases.

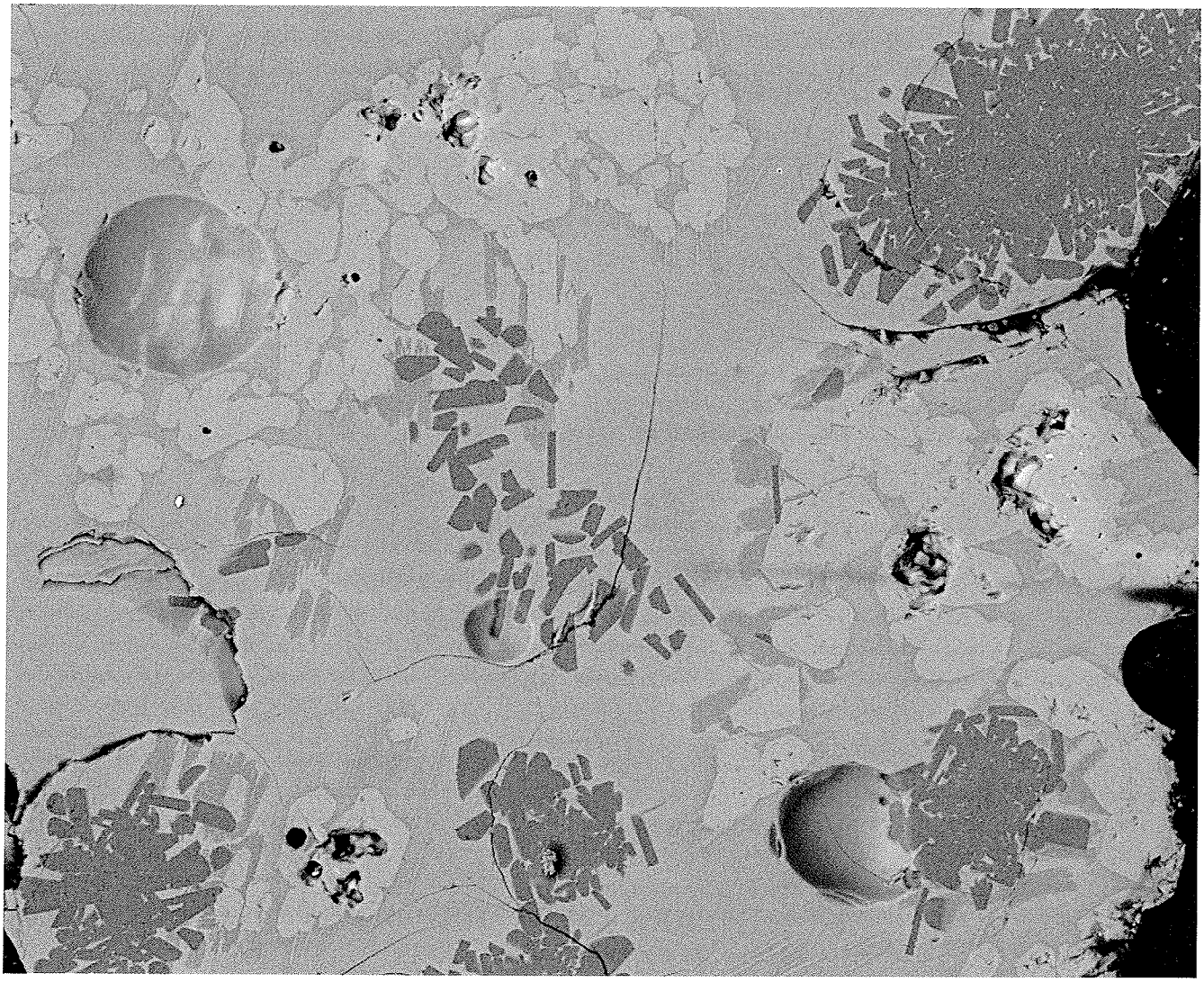

Figure 1: SEM image (BSE mode) of cross-section of Egyptian green: silica grains appear in dark grey. The amorphous phase is grey and contains 7-µm parawollastonite crystals, with quite white tone.

Crystalline phase: wollastonite ($CaSiO_3$)

Modification due to the temperature
The silicate crystals present vibration around 400, 600, 980 and 1080 cm^{-1}. Whatever the firing temperature, the fingerprint of the crystal is always the same, and no structural modification appears from 950°C, temperature of

wollastonite formation, to 1100°C. Between 1100 and 1150°C, a high-temperature polymorph of wollastonite is formed: pseudowollastonite (β-$CaSiO_3$) (Figure 2).

Pseudowollastonite totally replaces parawollastonite (α-$CaSiO_3$) and crystal shape is modified: parawollastonite is more or less cubic, but pseudowollastonite presents acicular formation. These crystals are never found in archaeological samples. This may set the high-temperature limit reached in the Egyptian furnaces to produce the turquoise pigment. At 1150°C, structural modification appears: 980 and 1080 cm^{-1} vibrations, stretching modes, are shifted to high frequencies. It means that crystal lattice is modified, expressing crystal concentration. The 380 and 620 cm^{-1} vibrations, bending modes, are shifted to low frequencies, between parawollastonite and

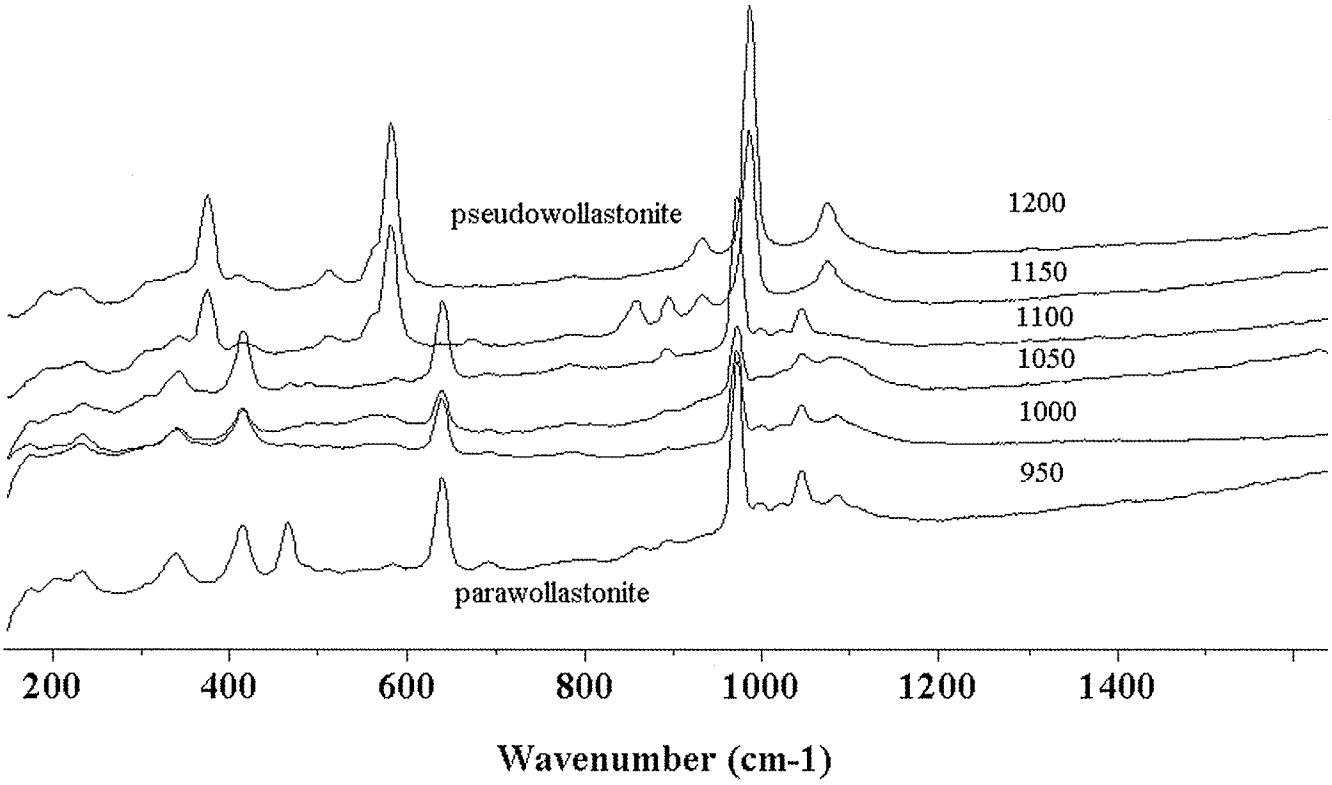

Figure 2: Raman spectra of wollastonite at various firing temperature. The transition between parawollastonite and pseudowollastonite, high-temperature polymorph, clearly appears between 1100 and 1150°C, with shifts of the bending and stretching vibrations.

pseudowollastonite transition. This can be explained by an increase of Si-O-Si angles from 105° to 120° [4]. This modification of crystal lattice, increase of Si-O-Si angles and reduction of crystal lattice, may be due to the fact that at higher temperature no more substitution of copper is observed in wollastonite.

Modification due to increasing flux quantity

Modern samples are fired by mixing silica sand, calcium carbonate, copper oxide (tenorite) with some sodium carbonate. This last compound serves as flux in order to obtain an eutectic with silica and minimise the firing temperature to create new compounds. Quantity of flux varies between 7 and 12%.

No shift is observed on Raman spectra obtained for parawollastonite for various flux proportion. The structure is not affected.

Amorphous phase containing copper and sodium

The vibrations in a silicate glass have three degrees of freedom, because of the degeneracy. One can distinguish stretching mode Si-O and bending mode Si-O-Si, for isolated SiO_4 tetrahedron: ν_1, a stretching symmetric mode around 825 cm^{-1}, ν_2 bending mode doubly degenerate around 200-300 cm^{-1} and finally ν_3 stretching mode triply degenerate between 880 and 1008 cm^{-1}. New bands appear around 550-750 cm^{-1}, depending on Si-O-Si angle, due to

the deformation of Si-O-Si bond. The deformation bands are located around 530-680 cm^{-1} [5].

Modification due to the temperature

Some vibrations are affected by the higher temperature and others are not modified (Figure 3).

The shape of the Si-O-Si contribution around 1085 cm^{-1} changes with firing conditions: clearly asymmetric, Raman shift becomes lower when temperature increases. The reason is the modification of quantity of bridging oxygen inside silicate matrix. Bending vibration around 200 cm^{-1} is modified in the same way as temperature: Raman shift becomes higher with higher temperature.

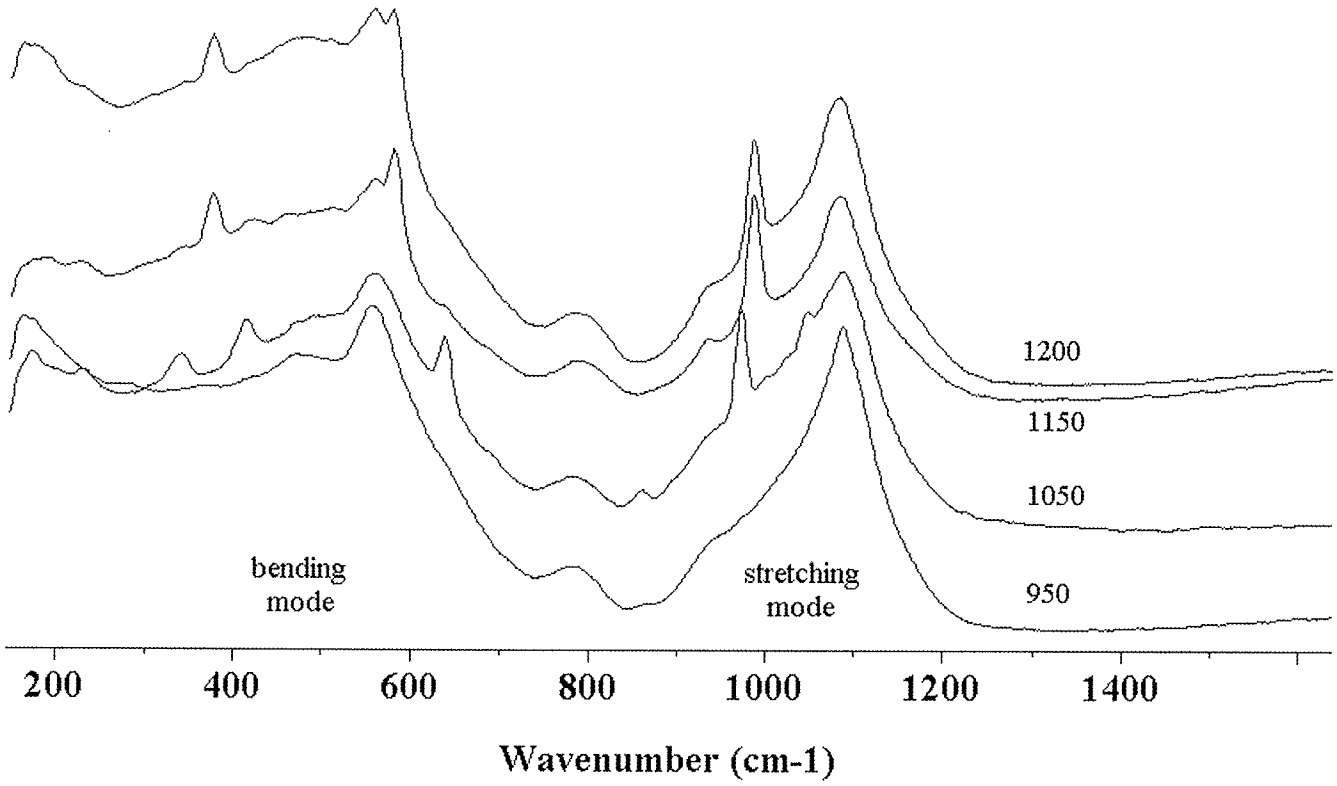

Figure 3: Raman spectra of amorphous phase at various firing temperature.

Firing conditions never modifies vibrations at 360, 560 and 780 cm^{-1}.

Modification due to increasing flux quantity

At constant temperature, no modification of Raman shift is observed on spectrum from 7 till 12% flux. Intensity of Raman vibration at 1085 cm^{-1} increases with higher content of flux: 24% for [Na] = 8% till 35% for [Na] = 12%. These results are in agreement with Farmer[5]. This can be explained by the number of non-bridging oxygen, and the degree of reticulation of the glass: in fact, the relative Q^3-Q^4 stretching components, Q^3 sheet-like region and Q^4 SiO_2 and tectosilicate, are increasing, expressing an higher polymerisation of the monomer SiO_4 [6] (Figure 4).

Vibration at 780 cm^{-1}, Si-O-Si stretching, moves to lower frequency with higher content of flux, because of the number of Si-O is decreasing.

The 470 cm^{-1} band always presents the same shift.

Effects of immersion in saline solution

These results could not explain all phenomena observed on Egyptian monuments, because it remains the first step of experimentation. After two weeks, surface of Egyptian green is modified, but no real structural modification is recorded. Week after week, holes inside matrix increase in number and in size. Finally, some parts of the material disappear because of lose of coherence. The first attack begins inside cracks in quartz crystal and on the amorphous phase. Matter is really consumed. At this step of alteration, wollastonite crystals are no more embedded inside glass

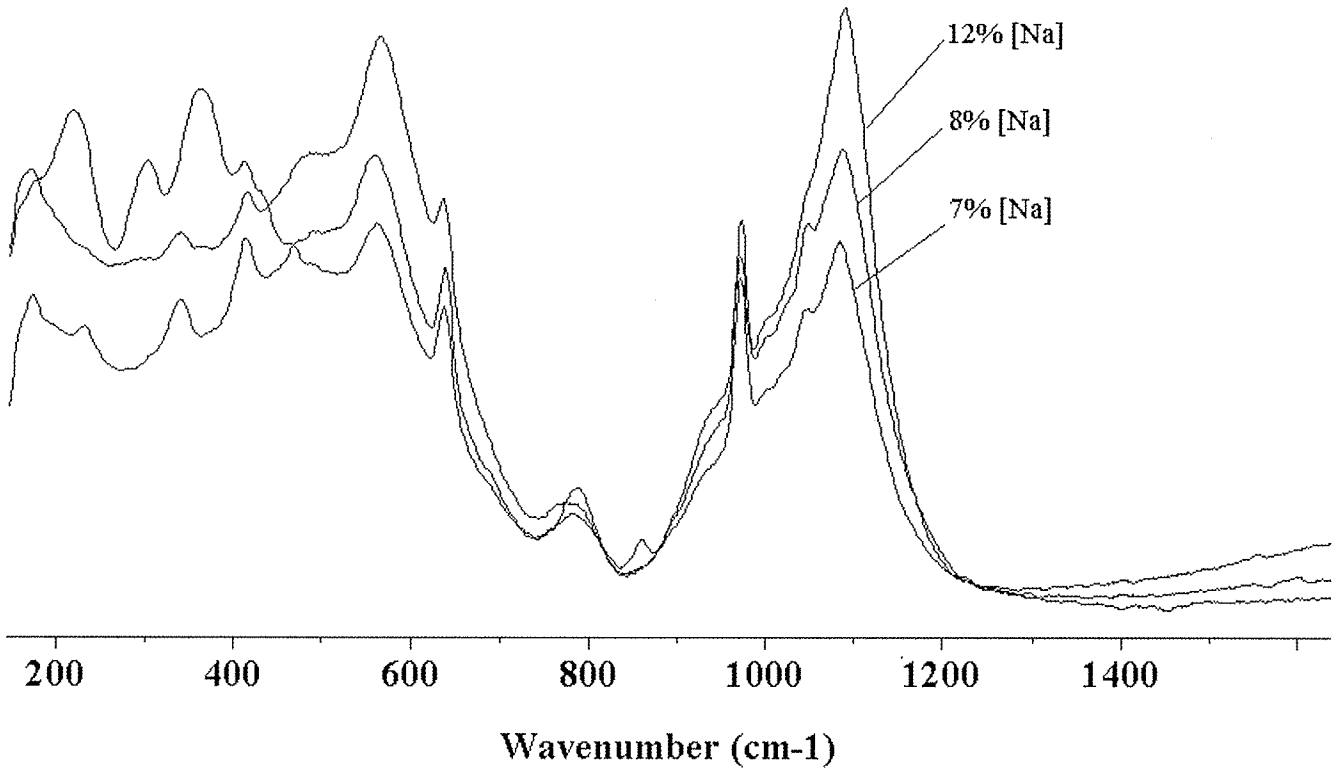

Figure 4: Raman spectra of amorphous phase at various flux amount: 7%, 8% and 12%.

and they can get out (Figure 5).
Parawollastonite seems not to be affected by the saline attack, as observed on the Raman spectra after 4 and 10 weeks of immersion.
The loss of amorphous phase yields difficulties to obtain a correct Raman spectrum; some modifications appear on those of the glass, but we are now not able to explain them.

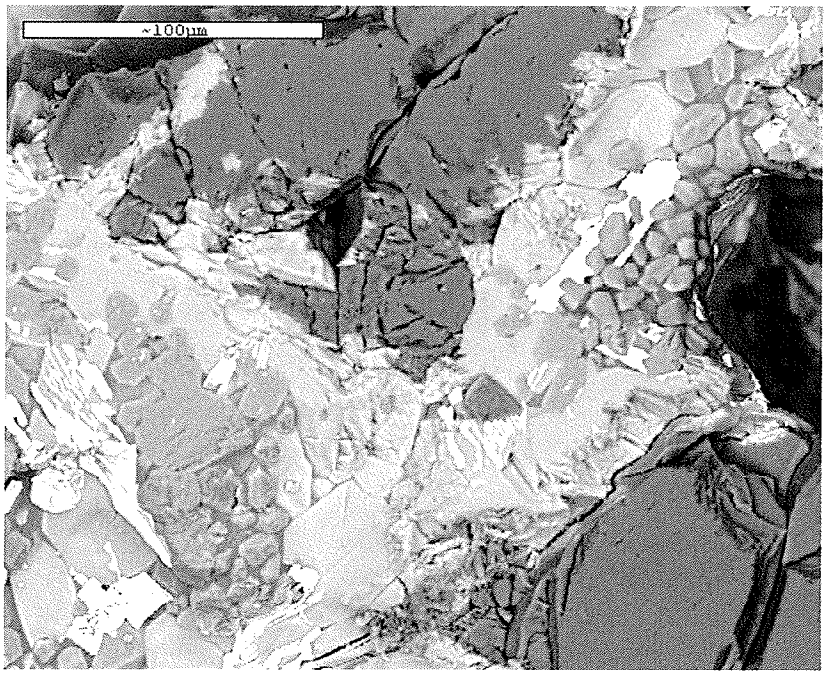

Figure 5: SEM image (SE mode) of cross-section of weathered Egyptian green: wollastonite crystals are no more totally embedded in amorphous phase.

Conclusion

Parameters of firing process such as temperature or quantity of flux may be approached by Raman spectra of Egyptian green. Composite material containing crystalline wollastonite and copper-bearing amorphous phase may be observed in two steps:
Wollastonite is a good thermal indicator because its polymorphs never exist together; they are stable during weathering or sintering process with various amounts of flux, but the structure changes above 1150°C, by concentration of the crystal lattice.
Firing conditions modifies amorphous phase: higher temperature modifies the structure and especially the number of bridging oxygen. The quantity of flux also plays a rule, by polymerisation effect.

References

1. Pagès-Camagna, S, "Propriétés physico-chimiques d'un pigment vert égyptien. Couleur, structure. Recherche des techniques d'élaboration", unpublished PhD thesis, University of Marne-la-Vallée (1999).

2. Pagès-Camagna, S., Colinart, S., Coupry, C. "Fabrication processes of archaeological Egyptian blue and green pigments enlightened by Raman microscopy and scanning electronic microscopy" *Journal of Raman Spectroscopy* (1999) **30** 313-317.

3. Pagès-Camagna, S., Colinart, S., "The Egyptian green pigment: its manufacturing process and links to Egyptian blue", *Archaeometry* (2003) **45** (4) 637-658.

4. Furukawa, T., Fox, K.E., White, W.B., "Raman spectroscopic investigation of the structure of silicate glass. III. Raman intensities and structural units in sodium silicate glasses", *J. Chem. Phys.* (1981) **75** (7) 3226-3237.

5. Farmer, V.C., *The Infrared spectra of minerals*, Mineralogical Society, London (1974).

6. Colomban, Ph., "Polymerization degree and Raman identification of ancient glasses used for jewelry, ceramic enamels and mosaics", *Journal of Non-Crystalline Solids* (2003) **323.**

POSTER SESSION

VIBRATIONAL SPECTROSCOPY REVEALS THE TECHNIQUES IMPLEMENTED FOR THE PRODUCTION OF HADRA HYDRIAI BY THE RHODIAN WORKSHOP (3RD - 2ND CENTURY B.C.)

K.S. Andrikopoulos[1], A. Giannikouri[2], S. Sotiropoulou[1], Sister Daniilia[1] and Y. Chryssoulakis[1,3]
[1] "ORMYLIA" Art Diagnosis Centre, Greece
[2] Historic and Archaeological Institute of Rhodes, Greece
[3] National Technical University Of Athens, Chemical Engineering Department, Greece

Abstract

Archaeological research in Rhodes' necropolis unearthed a great number of white ground Hadra hydriai. The archaeological claim that an independent and creative workshop existed in the island of Rhodos during the time period of 3rd – 2nd century B.C. is supported by scientific results mainly based on data provided by vibrational spectroscopy. The experimental data indicated the chemical composition and structure of the preparation and background layers as well as the paint layers, thus elucidating the techniques that were developed by the local craftsmen for the construction of Hadra hydriai. Spectroscopic data contributed in the identification of the pigments used for the painting of the decoration on the hydriai, many of which were artificial pigments proclaiming the high technological background that the particular craftsmen possessed. Furthermore the chemical composition of the white and yellow background layers was revealed, indicating the existence of a rare mineral, applied as a yellow grounding as well as yellow pigment in the decoration. The lustrous yellow colour of the specific pigment resembles gold and has been extensively used in order to imitate the luxurious golden coated hydriai that have been also found in the excavation area though in fewer numbers. Experimental evidence resolved that although among the different hydriai studied the style of drawing remains unchanged throughout the laboratory's lifetime, the techniques applied for their construction vary.

The Use of Infrared Photoacoustic Systems in Cultural Heritage Analysis

Lorenzo Appolonia, Andrea Bertone
Scientific Analysis Laboratory, Cultural Heritage and Activities Department - Autonomous Region of Aosta Valley, Piazza Narbonne 3 – Aosta – Italy

Abstract

Photoacoustic Spectroscopy (PAS) FTIR is a useful resource for the multifaceted problems that face a Scientific Laboratory of a Cultural Heritage Department. It needs little quantity of material (without pre-treatments which needed natural/artificial transformations), it is compatible with others techniques, it is not really affected by morphological problems, and it is not effected by diffusion or reflection phenomena. We present some possibilities for using this instrument: PAS analysis of wood shows congruence with our pellets-xilo-library; PAS analyses of the front and back of painted surfaces without damaging the sample; PAS monitoring a polymerization treatement on stones; the use of different materials mixed with ligands were tested to define the instrumental sensibility.

Introduction

These two gigantic statues of Amenhotep III (1390-1353 BC) stood at the entrance gate of his mortuary temple. But the statues are known as Colosses of Memnon. Why?

Fig. 1 – the northern statue of Memnon is on the right

In 27 BC during an earthquake, the upper part of the northern colossus collapsed and produced a strange musical sound, like snapped cittern strings. It was associated with the mythological Memnon, Ethiopia's king killed by Achilles, while appealing to his mother Aurora, the goddess of the dawn. After restoration under Septimius Severus, the statue never produced his voice again.
This sound phenomenon has been now explained as a microscopic movement of crystals due to the extreme temperature differences between night and day. The mechanical movement on the clean rock surface generated an air movement, like a sound wave. This is probably the first known example of a photoacoustic phenomenon.
The recent re-discovery of photoacoustic phenomena goes back to 1881, on the part of Graham Bell. He realised that materials struck by intermittent light could emit a sound. He also saw that the material struck could in some ways interfere with the sound phenomenon. Unfortunately, his research in this field was limited by the technology of the time. Other precursors tried to understand the interactions between radiation and material through sound, but the birth of the true photoacoustic spectroscope goes back to the early 1970s. At that time microphones were finally able to guarantee a high-level of sensitivity. In addition, a wide, even if incomplete, theory of photoacoustic effects was defined by Rosencwaig and Gersho [1].

Photoacoustic Spectroscopy (PAS)

This paper features some of the research activities, which can be carried out using photoacoustic technique in the field of cultural heritage. This technique can be applied in various spectral regions, which include mid-infrared. The Scientific Analysis Laboratory uses PAS in the study of various problems concerning the identification of materials for restoration and conservation.

When dealing with samples from cultural heritage artefacts several common considerations must be kept in mind: samples are usually small (a few milligrams or even micrograms); there is a small number of samples; there is a

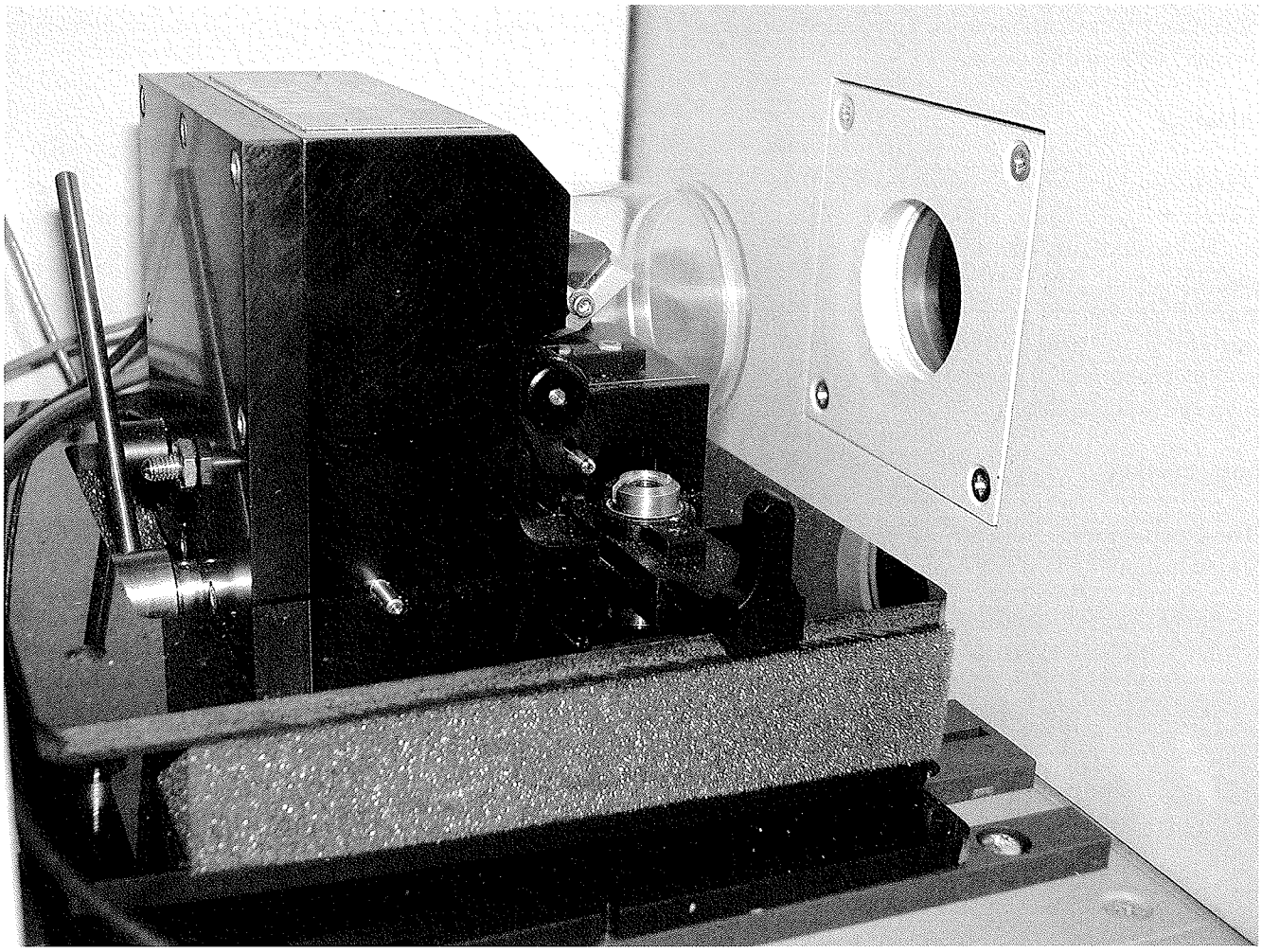

Fig. 2 - the photoacoustic detector, with the specimen holder awaiting insertion in the cell

preference for non-destructive analytical methodologies; a preference for methods compatible with other analysis techniques; samples change or are modified due to aging, deterioration, treatments, etc.
The principal characteristics of PAS [2] include:

- samples do not require pre-treatment;
- samples can be solid or liquid;

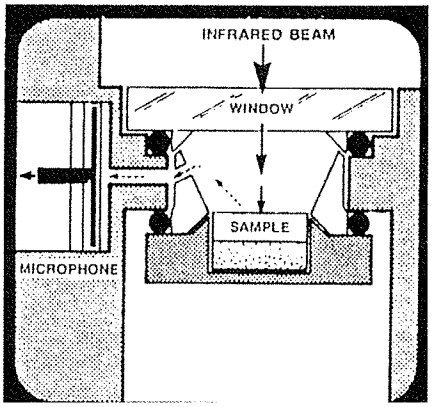

Fig. 3 – plan of the photoacoustic phenomenon in the section of the cell

- samples can also be highly radio-absorbent, in the chosen spectral region, e.g. mIR;
- samples can be studied during transformation processes, e.g. ageing;
- samples can have maximum dimensions, cylindrically-shaped with a maximum diameter of around 9 mm and a maximum height of around 6 mm;
- it does not destroy the samples (semi-destructive technique);
- it does not depend on the morphology of the samples;
- it is not affected by diffusion and reflection phenomena:
- it is compatible with other analysis techniques;
- it can analyse different layers of the same sample (in theory, at least).

In addition, PAS spectra can be acquired by just installing the photoacoustic detector in the correct position into the sample compartment of the spectrophotometer and linking it to a circuit of inert gas (e.g. He).
Infrared photoacoustics phenomenon is based essentially on the principle of absorption of radiation on the part of the normal vibration methods of the

different functional groups present in the sample. The vibrations lead to a transformation of radiant energy into thermal energy. This heat is transmitted to the gas above, causing an expansion that pushes and compresses it towards the walls, generating an impact "sound" in proportion to the vibration absorbed. The sound vibration is directly proportional to the energy absorbed by the functional groups. The more energy absorbed, the greater the sound reading, therefore the higher intensity of absorption peaks in the infrared spectrum. There is no danger of reading or reflection saturation.
The use of PAS required a series of procedural developments in order to obtain the best balance between quality of results and analysis times. The present procedure can be outlined as follows. If there are no temperature problems with the measuring instrument, you can heat the sample (e.g. up to 60°C in the oven) before inserting it in the photoacoustic cell, above all if you are dealing with porous systems. This operation permits the most efficacious removal of the air trapped in the pores, as the air present can cause a higher noise than the analytical signal. The sample is placed in a metallic container, placed in its turn in a special tub, which follows a track in order to be inserted in the cell. Once the sample is inside, the measuring cell is hermetically sealed. As far as possible, the gases inside, including those in the sample's pores, are substituted by inert gases (e.g. using a flux of He at 10-20 ml/second for 5-10 minutes). Once the purge has finished, you wait for the internal conditions of the cell to become balanced (e.g. about 5-10 minutes). You carry out a minimum number of spectrum scans (e.g. 64 scans). Some people increase the scan number (over 200) in order to improve the final spectrum. Analysis times are around 25 minutes per sample, however it can be increased if the sample is particularly porous and vice versa.
The detector used in this work is a MTEC Photoacoustic model 200. This detector was used, at first, inside a Bruker IFS25 Spectrophotometer, with a Cs-I window and a spectrum interval between 4000 and 250 cm^{-1}. At present it is inserted in a FTIR Spectrum 2000 Perkin-Elmer Spectrophotometer, with HeNe laser, with a spectrum interval between 4000 and 400 cm^{-1}. The suggested instrument setting is: OPD speed equivalent to 0.2 cm/sec., resolution of 8.00 cm^{-1}, J-stop resolution of 3.98 cm^{-1}, J-stop of 12.50 mm, B-stop of 21.20 mm.
An absorbent surface of black carbon is used for the background; it must be very thin in order to reduce the thermal mass.
Here are some examples of PAS analysis in the Scientific Analysis Laboratory of the Cultural Heritage and Activities Department of the Autonomous Region of Aosta Valley.

PAS Monitoring on Polymerization Process

The study aimed at the evaluation of behaviour with respect to the freezing of the stone of Roman monuments, before and after surface conservation treatments [3, 4], needed a non-invasive system, which guaranteed the possible polymerization. The rocks used by the Romans were pudding-stone, travertine and *bardiglio*. Travertine is a sedimentary chemical carbonatic stone, mainly consisted of calcite. The Dora Baltea pudding-stone is a sedimentary clastic stone of recent formation. *Bardiglio* is a marble quarried in Aymavilles (AO), a low porosity homogenous whitish stone [5].
In the study the most commonly-used materials in stone restoration were considered, such as ethylsilicate to

Fig.4 – PAS spectra of travertine (bottom) and travertine treated with ethylsilicate (top)

consolidate (Etil Silicate 70 Antares), a hydrophobic fluoride binding agent (Akeogard ME, 5% aqueous micro-emulsion of elastomeric copolymer vinilidene fluoride – esafluoropropene-tetrafluoroethylene), as well as two protective materials: silan-siloxane and acrylic composition. Presented here are the results of the first two treatments, the study of the protective treatments is still in progress.

All the treatments were carried out by immersion in the solutions for 30 minutes. The samples (6 mm high and 5 mm diameter) were preserved in a controlled atmosphere with a 80% relative humidity level. The polymerization process of the ethyl-silicate, $Si(OCH_2CH_3)_4$, took place in the presence of two equilibria (hydrolysis with elimination of alcohol and poly-condensation with elimination of water or alcohol). In the PAS spectra there were variations in the field of the ethyls and of the silicates. The relationship between the reduction of the ethyls and the increase of the

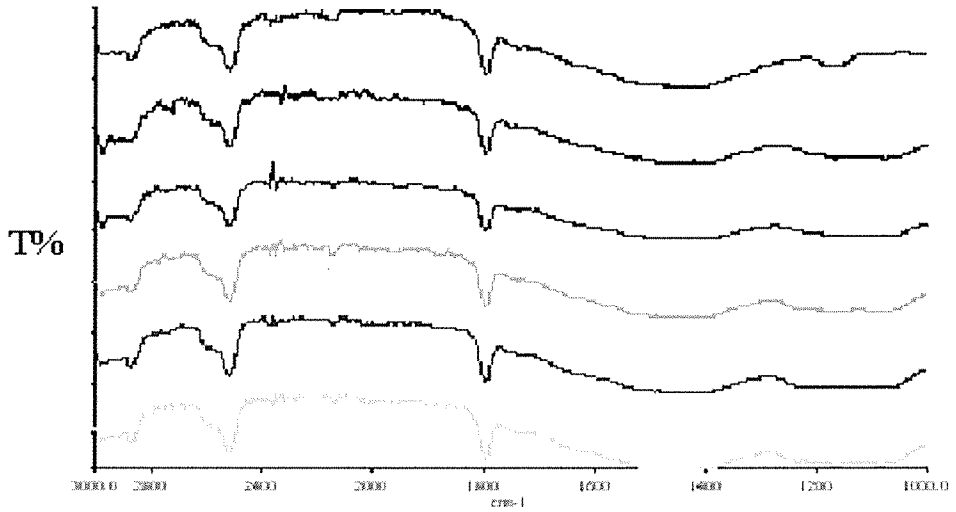

Fig.5 – sequence of PAS spectra in the interval 3000-1000 cm^{-1} of travertine (top) and travertine treated with ethylsilicate: after 1 day, 7 days, 14 days, 22 days, 3 months (last at the bottom).

silicates was monitored by integrating the peaks between the corresponding extremes: 3000-2858 cm^{-1} and 1242-1007 cm^{-1}. Figures 4 and 5 present the interaction between travertine and ethylsilicate.

Fig.6 – sequence of spectra of Akeogard ME: after 1 day (top), 4 days, 8 days, 11 days, 58 days (bottom)

The binding process of the fluoridated agent was monitored for about 60 days. During this time, the material revealed a reduction of the peak area involved in the process, between 1779 and 1661 cm^{-1}. This variation was

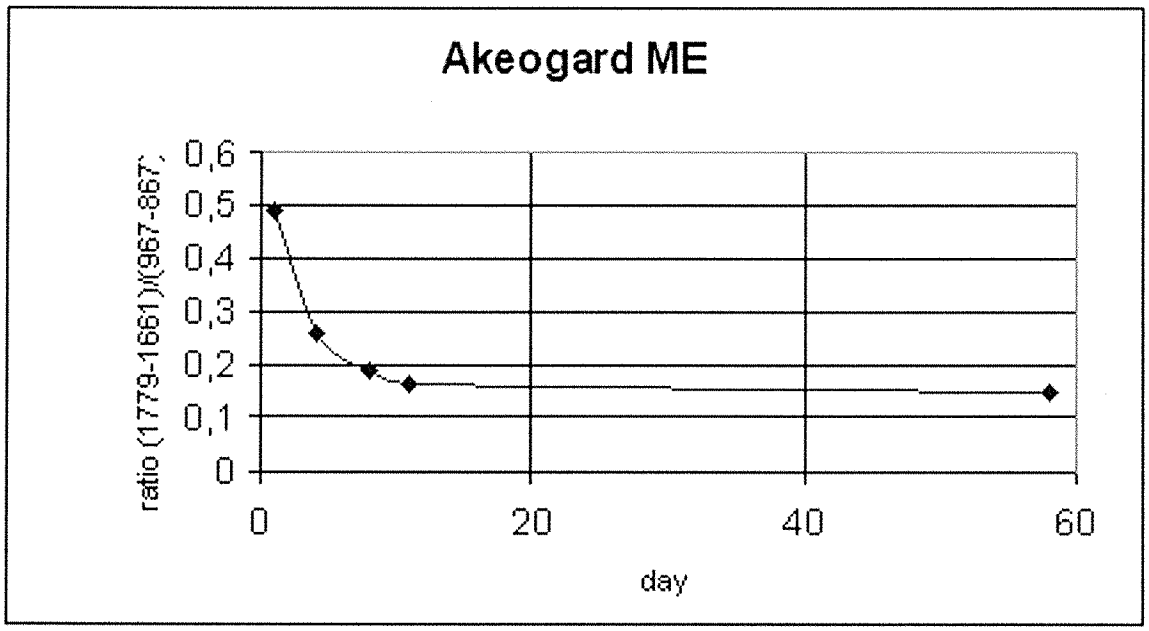

Fig.7 – graph of the transformation process of Akeogard ME

compared, following a relationship between areas, with a stable reading of the same spectrum, between 967 and 867 cm^{-1} (Fig. 6).
The binding process was monitored after 1, 4, 8, 11, 58 days, giving rise to the development seen in figure 7.

PAS-Pellets Congruence in Wood Analysis

Research on valdaostan woods was developed in order to create a catalogue of infrared spectra from our region woods. This information was compared with the analysis of the same material using PAS. The results show a good correlation between the PAS spectra and those obtained with pellets. The instrument used for pellets measurement is the same, a Perkin-Elmer SPECTRUM 2000 FT-IR, set between 4000 and 370 cm^{-1}, with 16 scan, resolution 4 cm^{-1}, OPD speed 0.2 cm/sec.
The composition of the woods is variable: almost 60% of the wood mass is cellulose and hemicellulose, the rest is

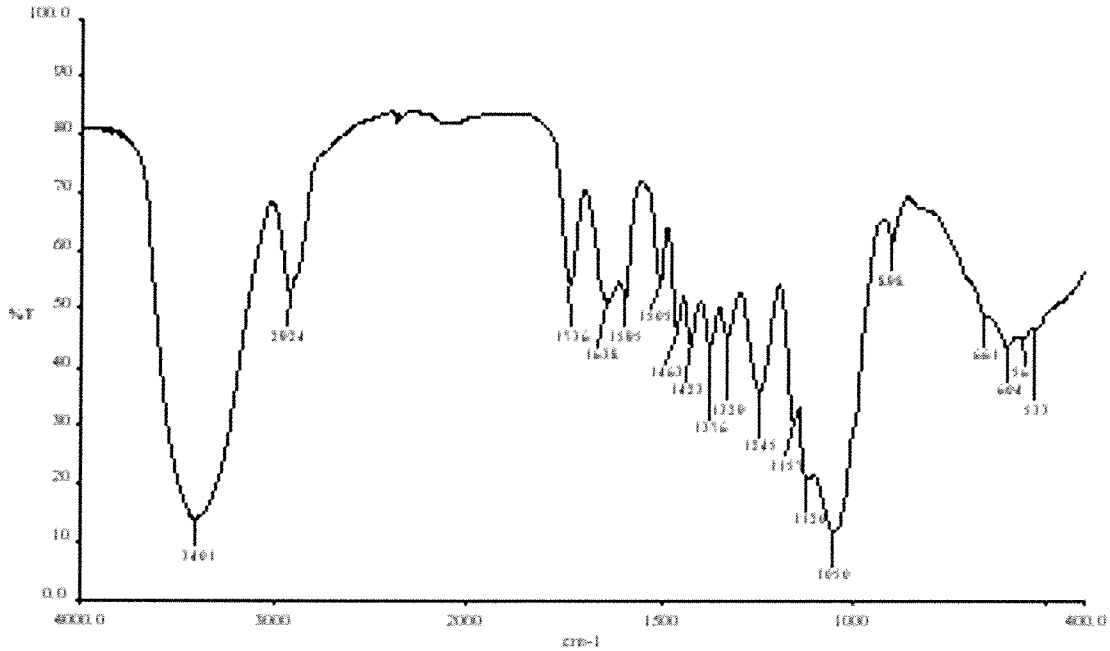

Fig.8 – KBr-FTIR spectrum of sycamore

lignin and other minor components. The infrared spectrum of any given wood is generally recognisable by the presence of characteristic peaks between 1800 and 800 cm^{-1} [6]. Between 1100 and 1000 cm^{-1} the cellulose and hemicellulose signals are superimposed. Features of the cellulose are still found around 1423, 898, 661 cm^{-1}, whilst the peaks around 1595, 1505, 1376, 1329 cm^{-1} are assigned to lignin. In figure 8 there are the readings of a hardwood KBr pellet spectrum.
The example in figure 9 presents the PAS spectrum of larch from a "rascard", typical valdaostan dwelling, and gives a similar result to that obtained with the larch samples analysed with the FTIR pellet technique. In this case we were able to have a wide comparison, that is the whole xylo-spectrum library. This is a further confirmation of the possibility of being able to use the spectrophotometer with the photoacoustic technique to study samples which could present characteristics inducing you to prefer this technique rather than the traditional KBr pellet one, for example, for samples which must be later analysed with other methods. Difference between the two peaks around 1639 cm^{-1} shows a greater humidity of valdaostan larch than the "rascard". Less perceptible is the variation around 1463 cm^{-1}, where the difference is due to a reduction of the cellulose/hemicellulose PAS peak in the "rascard" sample, possibly due to greater ageing.

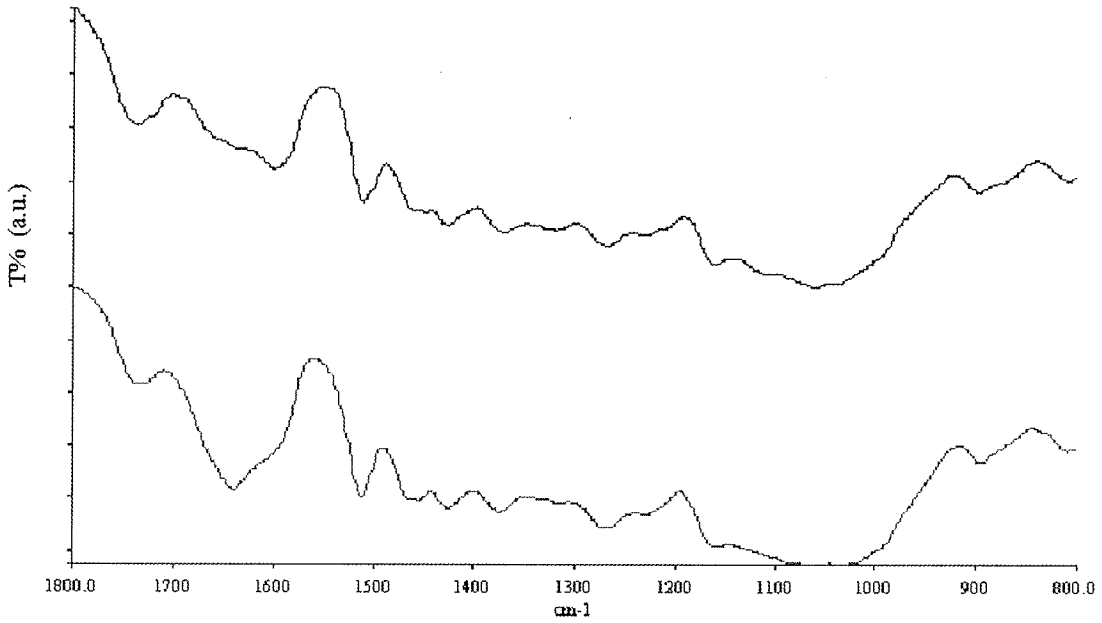

Fig.9 – PAS spectrum of valdaostan larch of "rascard" (above), KBr pellet spectrum of valdaostan larch (below)

PAS Sensibility on Material Mixtures

In the cultural heritage field you often have to face problems concerning mixtures of components and each component can be present in differing quantities. In order to obtain sufficient information for the aims of a laboratory, forced to carry out analyses in limited time, it is sometimes enough to give broad assessments of the materials present: carbonate material, protein material etc. On these bases a useful study was planned to establish whether the PAS technique could be used in the compositional study of complex mixtures, with some components present in low percentages.
An in-depth study was made in the field of pictorial bases, a constant presence in restoration work undertaken by the valdaostan Superintendence, as well as being constantly fraught with problems. The study was carried out using laboratory-made models. It was best to use two binding agents, an indicator of modification, mixed with two bases, because they are best suited to simulate a real situation. The two bases used, calcite and gypsum, are calcium carbonate and dehydrated calcium sulphate, respectively. The added materials were: whewellite, oil, protein, respectively monohydrate calcium oxalate, restorers' linseed oil, restorers' casein. Gypsum can be due to modification processes and, therefore, be present in low quantities. Moreover, the presence of calcium oxalate is important for attributing a modification process of the material.
Estimating the quantity of the various minor components is not necessary, and therefore a quality study, like PAS, can be sufficient.
In figures 10, 11, 12, there are some spectra showing the three materials potentially present in minimum quantities, differently mixed.

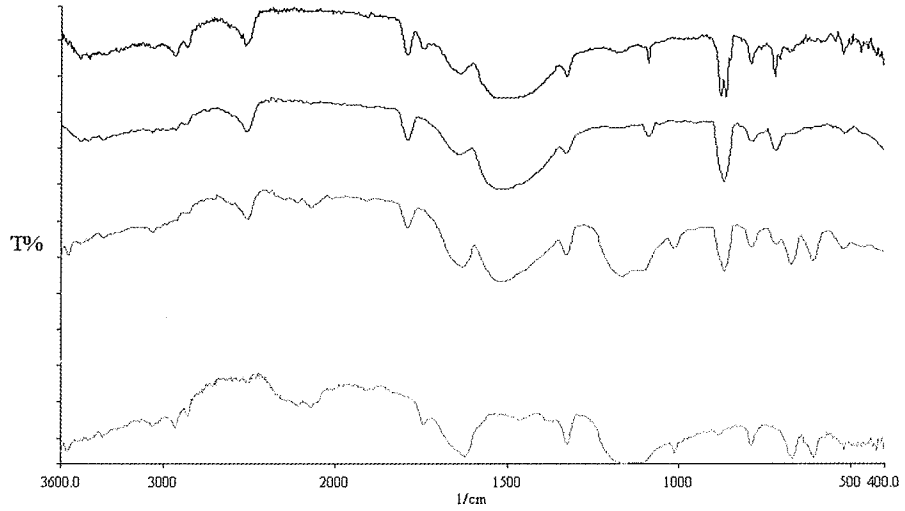

Fig.10 – PAS Spectra with oxalate					
Spectrum	components - fraction in grammes				
	calcite	gypsum	whewellite	oil	protein
Top	0.85		0.10	0.05	
Second	0.90		0.10		
Third	0.45	0.45	0.10		
Fourth		0.90	0.10		
Bottom		0.85	0.10	0.05	

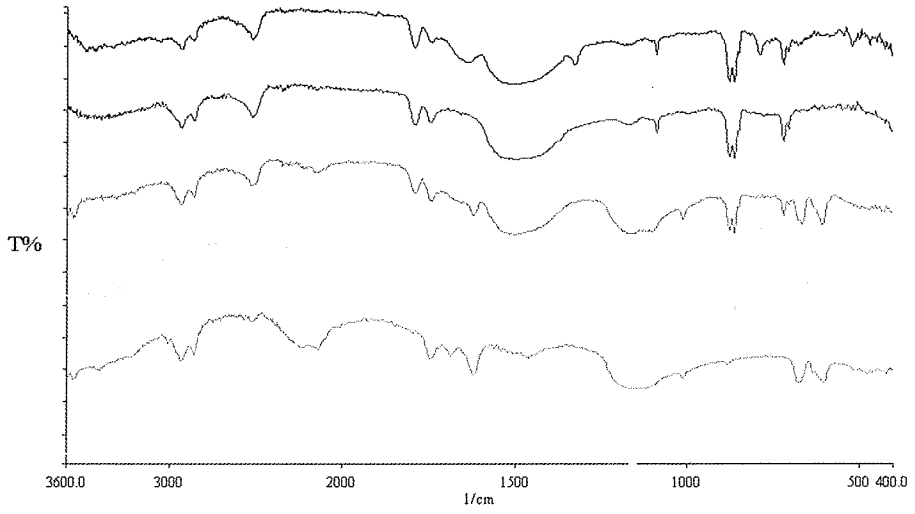

Figure 11 – PAS spectra with oil					
spectrum	components - fraction in grammes				
	calcite	gypsum		oil	protein
Top	0.85		0.10	0.05	
Second	0.95			0.05	
Third	0.45	0.45		0.05	0.05
Fourth	0.475	0.475		0.05	
Fifth		0.95		0.05	
Bottom		0.85	0.10	0.05	

For the spectroscopic analyses we used a Bruker IFS25 spectrophotometer, with Cs-I window and spectrum interval between 4000 and 250 cm^{-1}.

Whewellite

Calcium oxalate is recognised by peaks around 1634 and 1320 cm^{-1}. In all the spectra oxalate was detected.

Linseed oil

Linseed oil is seen in peaks around 2931, 2856, 1748, 1653, 1462 cm^{-1}. Peaks of CH groups around 3000 cm^{-1} are easily recognised, because they are clearly separated from the development of the base line. Peaks around 1748 and 1653 cm^{-1} can be seen in all spectra. In the spectrum with calcite and oil the signal around 1635 cm^{-1} is very weak. Calcite covers the reading around 1462 cm^{-1}, which in fact can be seen only in the gypsum and oil mixture.

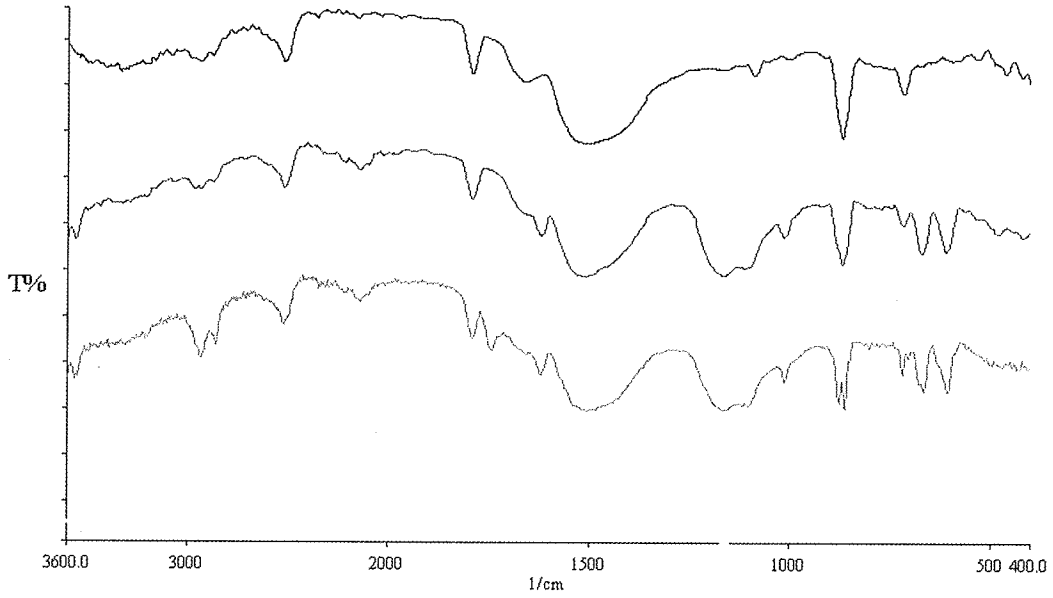

Figure 12 – PAS spectra with protein

spectrum	components - fraction in grammes				
	calcite	gypsum	whewellite	oil	protein
top	0.95				0.05
second	0.475	0.475			0.05
third	0.45	0.45		0.05	0.05
bottom		0.95			0.05

Casein

Casein has its peaks around 1632, 1514, 1444, 1392, 1237, 1079 cm^{-1}. Calcite absorption bands mask most of the casein spectroscopic features except the one at 1079 cm^{-1}. Gypsum, on the other hand, covers this last band but not the others between 1500 – 1400 cm^{-1}. Unfortunately, if the sample contains both calcite and gypsum, the absorption bands of casein are less evident.

PAS in Stratigraphic Analysis of Polychromies

PAS allows you to be able to examine a sample from different angles, by simply orientating it differently inside the measurement cell. The most common application concerns the study of surface structures, pictorial ones for example. An example is the study of the Annunciation of the Portal of Aosta Cathedral, needed to characterise the different structures and surfaces. The Portal is made up of a series of painted terracotta statues, stuccoes and painted backgrounds.

The study was carried out prior to restoration. The sample presented was from a yellow-coloured column. The colouring is due to ochre.

In fig.14 the two PAS spectra of the outer and inner parts have been superimposed. The outer part contains

Fig.13 – photos of the outer surface of the sample (10x), the section (35x), the inside (10x)

carbonates, gypsum and oxalates. The calcite features are around 1421, 875, 711 cm^{-1}. The gypsum is recognised in some peaks between 1140 and 1000 cm^{-1} and for a doublet at around 670 and 603 cm^{-1}. Weddellite (dihydrated calcium oxalate) is shown in the signals around 1634 cm^{-1} and 1320 cm^{-1} (similar to those of whewellite). In order to distinguish between the two types of oxalate a successive analysis was carried out with an X-ray micro-diffractometer. The quantity relationships varied according to the presence of original materials and their eventual modifications. In fact, the calcite becomes proportionally greater in the inner part, whilst the oxalates decrease, typical behaviour of a surface modification. In the same way, seeing that the gypsum is present in greater proportion in the outer layer, it would seem that the surface has undergone a sulphate modification. Another hypothesis is that the gypsum had been used as a base for the pictorial finishing of the layer of repainting found all over the monument. In order to solve these other questions it is possible, seeing that the sample has remained unchanged, to use other more specific analysis techniques.

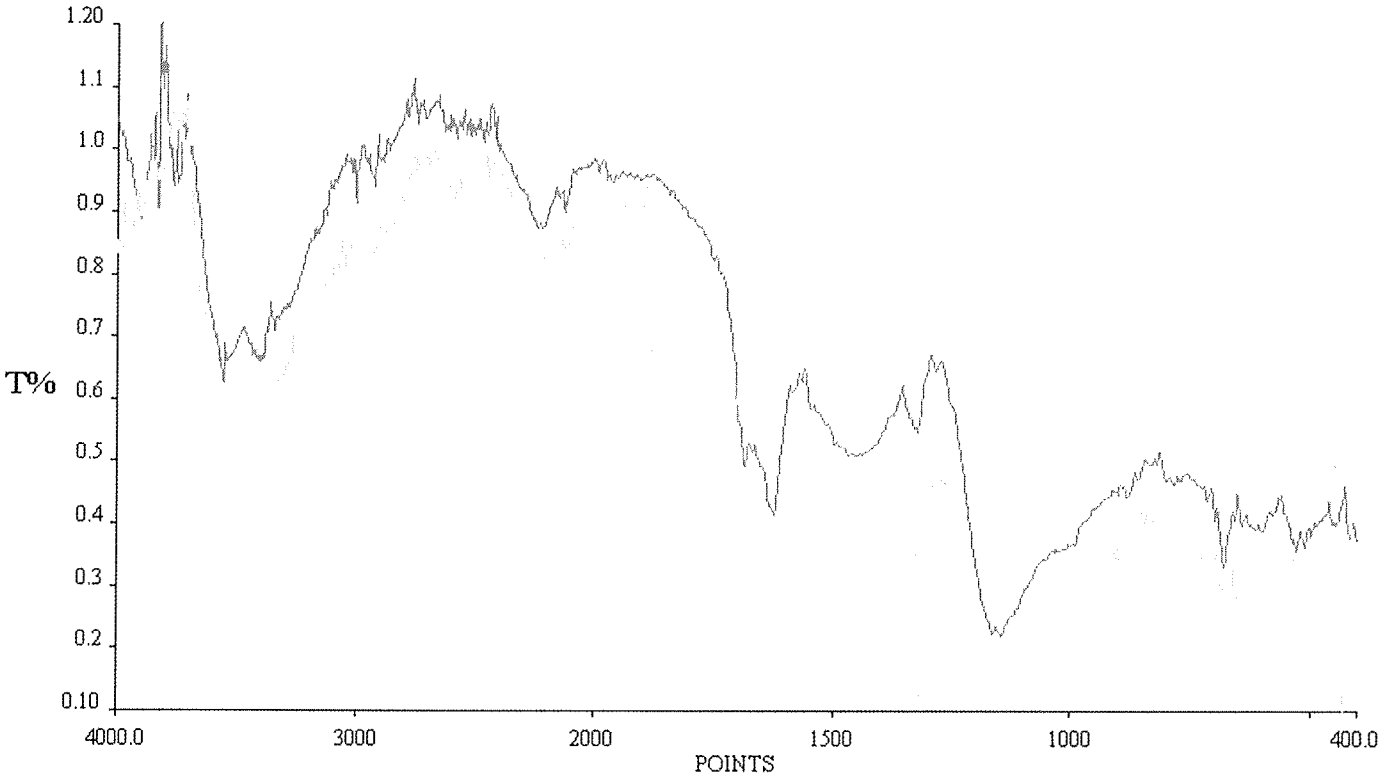

Fig.14 – spectrum of the outer surface (top), spectrum of the inner surface (bottom)

Conclusion

The photoacoustic instrument confirms its high potentials, above all if considered as application parallel or in succession to other analysis techniques. In assessing the method, it is important to note that samples are not modified by the PAS measuring, so they can be kept for further analyses. The chief analytical problem concerns the

noise of the spectra, and is mainly caused by the fact that dealing with porous materials reduces the possibility of having an environment with only inert gases. Further expedients, fine-tuned by the Laboratory, such as gentle heating of the sample, allow us to reduce this effect increasing the reading quality and the analytical abilities of the method.
The disadvantage can be assessed during analysis times, which can be rather long, particularly when purging operation is concerned. The method perfected by the Laboratory has permitted us to fix times for the more complex samples at around 25 minutes, which is sufficiently adequate in terms of signal to noise ratio.
The interpretation of the spectra, on the other hand, does not present difficulties differing from those of other infrared spectra.

Acknowledgements

We would like to thank the team of the Scientific Analysis Laboratory for all their help in all the research and PAS applications.

References

1. Rosencwaig A., Gersho A., *J. Appl. Phys.* (1976) **47**, 64-69 .

2. McClelland J. F., Jones R. W., Bajic S. J., 'FT-IR Photoacoustic Spectroscopy', in M. Chalmers, P. R. Griffiths, *Handbook of Vibrational Spectroscopy*, J. Wiley & Sons, New York (2002).

3. Appolonia L., Bertone A., Fambri L., Penati A., 'Valutazione delle variazioni di congelamento dell'acqua all'interno di materiali porosi a seguito di trattamenti di conservazione sulla pietra: il caso del Teatro Romano di Aosta', in *III Convegno "Restauro e conservazione dei beni culturali: materiali e tecniche"* dell'Associazione Italiana d'Ingegneria dei Materiali e del Consorzio Interuniversitario Nazionale per la Scienza e Tecnologia dei Materiali, Cassino, (FR), 3-4 October 2003.

4. Appolonia L., Bertone A., Penati A., Fambri L., 'The Water Freezing Process in Ethylsilicate Consolidated Stones of Roman Theatre in Aosta', in *XXIV National Meeting of Calorimetry, Thermal Analysis and Chemical Thermodynamics*, Catania, 15-18 December 2002.

5. Appolonia L., Vaudan D., De Leo S., 'Projet des travaux de conservation du Théâtre Romain d'Aoste: recherche et résultats', in J. Riederer (ed), *8th International Congress on Deterioration and Conservation of Stone*, September-October 1996, Möller Druck und Verlag gmbh, Berlin (1996) 1097-1107.

6. Bertone A., Appolonia L., 'Indagine spettroscopica FTIR dei legni del Museo Regionale di Scienze Naturali della Valle d'Aosta', *Rev. Valdôtaine Hist. Nat.* (2001) **55**, 175-192.

Illustrations

Image of the "Colosses of Memnon" taken from virtualtourist.com.
Images of the outline of the photoacoustic cell taken from the 'Photoacoustic' handbook, Graseby-Specac-Hellma Italia, srl., Milan.

FTIR Spectroscopy to Monitor Selcetive Cleaning on Wall Painting Surfaces

Emiliano Carretti, Luigi Dei, Azzurra Macherelli, Marcello Mauro, Costanza Miliani[1], Francesca Rosi[2], Barbara Salvadori
Department of Chemistry and Consortium CSGI, University of Florence, via della Lastruccia, 3 I-50019 Sesto Fiorentino (FI), Italy.
[1] Istituto CNR-ISTM (Institute of Molecular Sciences and Technologies) Perugia Unit.
[2] Department of Chemistry University of Perugia.

Abstract

One of the most important and crucial steps in the conservation of a work of art is the cleaning procedure, which should be carried out by choosing the most suitable products and by monitoring their selectivity with regard to the depth of layers removed. In this contribution, we show how FTIR spectroscopy can be a useful and powerful tool to monitor the selective cleaning procedure and to determine the effectiveness of conservation treatments. FTIR measurements allowed us to evaluate the efficacy of an innovative cleaning system in the removal of degraded acrylic and vinyl based copolymer layers from fresco surfaces, and to ascertain the effective desulphatization of a mural painting. Also, this study presents FTIR microreflectance spectroscopy as a reliable method to measure the efficacy of dispersed systems (oil-in-water microemulsions and micellar solutions) in removing hydrophobic materials (acrylic resins, grease and waxes) from the surfaces of real works of art (i.e. wall paintings).

Introduction

Due to their versatility and their favourable wetting properties, acrylic and vinyl polymers have been widely used as consolidants, surface coatings and adhesives [1-3] in the restoration of wall paintings [4], stone [5-6], etc.. Unfortunately, these polymers present many problems due to the low physicochemical stability associated with their natural aging [7-8]. Both thermal and photochemical reactivity lead to simultaneous depolymerization and cross-linking reactions [9], resulting in surface yellowing, mechanical stress on the adherent paint layers, and alteration of the chemical and physical properties of the interface between the work of art and the surrounding environment. Due to their yellowing and to the serious damage caused to the paint layer, it is often necessary to remove these aged polymers during a conservation treatment [8]. Solubilisation of the acrylic and vinyl polymers is partly obtained by using aggressive organic solvents with differing polarities [7]. The toxicity of these solvents and the spreading of the solubilised polymers into the porous structure of the work of art are the main limitations in their use. Two alternative cleaning systems, a 4-component microemulsion and a 6-part micellar solution were prepared and tested in the laboratory [10]. In order to detect the chemical nature of the patinas to be removed as well as the efficacy of the cleaning agents employed, FTIR spectroscopy was chosen. The micro-reflectance and transmittance FTIR analyses revealed the efficacy of these cleaning agents in the removal of acrylic and vinyl resins from the surface of aerial mortar samples simulating real frescoes [to obtain an "aerial" mortar the most common procedure is the

Composition System A [11]	Wt%	*Composition System B	Wt%
H_2O	86	H_2O	77
SDS	4	Surfactant	3.5
1-PeOH	8	Cosurfactant	7.5
p-xylene	2	Solvent 1	9
		Solvent 2	1.5
		Solvent 3	1.5

*CSGI patent in preparation.

Table 1. Composition in weight percent (Wt%) of the two dispersed systems for acrylic (oil-in-water microemulsion, System A) and vinyl (micellar solution, System B) solubilization.

following: washed sand, usually quartz, is mixed with slaked lime, mixture of $Ca(OH)_2$/water ca. 1:1 by weight called "grassello", in the 1:3 lime/sand ratio (by volume) until an homogeneous paste is obtained. The real binding medium, $CaCO_3$, is formed by the in situ carbonation of the $Ca(OH)_2$, due to the flow of the atmospheric CO_2 through this paste]. Further, the technique clearly showed that an innovative cleaning method based on aqueous nanocompartimentalised systems could be successfully applied to the removal of aged vinyl polymers in a real conservation treatment: the frescoes by Filippo Lippi (XV century, Cappella Maggiore of Prato Cathedral). FTIR measurements were also used to monitor and thus control the removal of gypsum and calcium oxalates from wall painting surfaces (frescoes by Pozzoserrato in the Dome of Conegliano Veneto (TV) [10]; XVII mural paintings in the Capponi Institute, Florence, *vide infra*).
The aim of the present work is to show that FTIR spectroscopy is the most efficient, least invasive and least expensive technique to monitor the effectiveness of certain cleaning treatments specifically, dispersed systems on deteriorated polymer films and ammonium carbonate method on gypsum.

Experimental

P-xylene (purity > 99.5%), 1-pentanol (1-PeOH, purity > 98.5%), Solvent 1, Solvent 3 and KBr for infrared pellets (purity > 99.5%) were purchased from Aldrich and used without further purification. Sodium dodecyl sulphate (SDS, purity > 99.5%) was purchased from Merck, Darmstadt, Germany. Wood poultice Arbocel BC1000®, pellets of Paraloid B72® (poly (EMA/MA, average molecular weight 80,000), and Solvent 2 were supplied by Zecchi, Florence, Italy. Water was purified with a Millipore MilliRO-6 and MilliQ (Organex System) apparatus: the resistance of the water was ≥ 18 MΩ cm.
Fourier transform infrared (FTIR) spectra in the transmission mode were obtained using a BioRad FTS-40 spectrometer (4 cm^{-1} resolution and 64 scans). Microreflectance spectra (8 cm^{-1} resolution and 128 scans) were obtained with the same apparatus equipped with a BioRad UMA500 microscope (MCT detector).
The two different dispersed systems (Table 1) were prepared by mixing the appropriate components according to the following procedure. The surfactant (SDS) was dissolved in water by heating for 15 min at 40 °C, and then cooled to room temperature. Cosurfactant (1-PeOH) was added dropwise to the surfactant solution at room temperature with stirring until a transparent solution was formed. The so-called oil phase (p-xylene in the system A and the solvent mixture in the system B) was then added at room temperature until a stable system was formed. These systems were stable (no observable phase separation) for more than a year.
To test their efficacy, the dispersed systems (microemulsion A (oil/water), and the micellar solution B) were applied to surfaces of outdoor mortar samples prepared to simulate real frescoes treated with a thin surface layer of Paraloid B72®. These mock-frescoes were prepared in the laboratory by putting the paste ("grassello" and quartz sand, as described above) on a 5x5x2 cm wood mould. The application of the copolymers was done 90 days after the preparation of the mortar in order to ensure good carbonatation of $Ca(OH)_2$ and consequent hardening of the

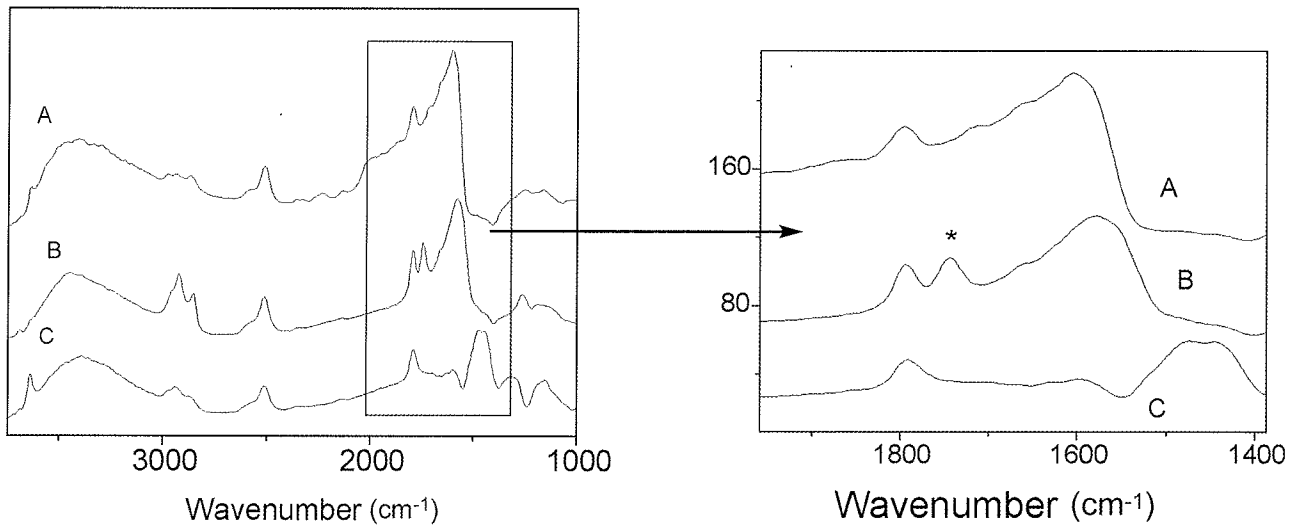

Figure 1. Microreflectance FTIR spectra of mortar samples simulating real frescoes. (A), untreated mortar sample (B), Paraloid B72® coated mortar sample; (C) Paraloid B72® coated mortar sample cleaned utilizing dispersed system A. The asterisk highlights the 1740 cm^{-1} carbonyl band.

samples. During this period all the samples were maintained at controlled environment conditions (T = 25°C ± 1 RH = 52% ± 1). Application of the cleaning systems was done by means of wood poultice compresses (contact time 2.5 hours); the painted surfaces were protected with Japanese paper sheets [12].

Results and Discussion

Microemulsion and micellar cleaning experiments

In order to evaluate the efficacy of the microemulsion and micellar cleaning solutions, micro reflectance infrared spectra were obtained in the laboratory from the surfaces of three samples. The spectra are reported in Figure 1. The main absorption at ~1740 cm^{-1} (*) has been assigned to the stretching of C=O ester group [10]. Since the region of this signal is free from carbonate absorption, it was chosen to follow the cleaning treatment. The microreflectance spectrum of the stratified system made of Paraloid B72 (poly (EMA/MA)) film on the carbonate matrix is shown in Figure 1B. The 1740 cm^{-1} (*) signal of the acrylic resin is easily differentiated from the substratum absorbance. The disappearance of the 1740 cm^{-1} peak is an indication of the cleaning efficiency, as shown in Figure 1C, the spectrum from the sample cleaned with the microemulsion.

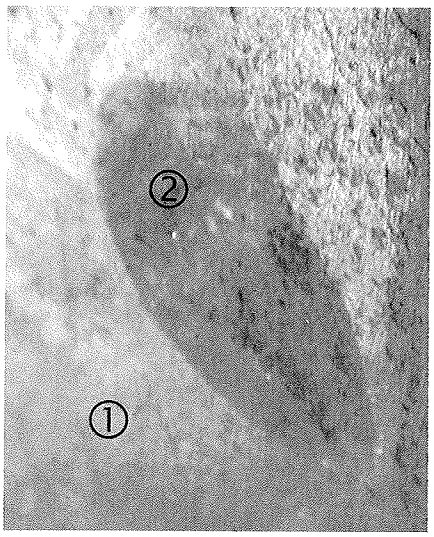

Figure 2. Prato Cathedral. Raking light image of area where the dispersed system B (zone ②) was tested. Zone ① is the uncleaned area.

The same experiment was repeated using a vinyl polymer coating. Micro reflectance FTIR monitoring of the cleaning action, performed with dispersed system B on the surface of mortar samples simulating real frescoes, successfully demonstrated the utility of the innovative method [13].

The same treatment was applied to some regions of a real fresco by Filippo Lippi (Cappella Maggiore, Prato Cathedral, XV century), where a compact shiny layer of organic substances covered the painted surface. Historical data [14] document that earlier restoration treatments had been carried out by applying a mixture of polymers, predominantly polyvinylacetate. In this case, due to the hardness of the polymeric layer, contact time for the wood poultice compress was increased up to 24 h. To minimize evaporation of the dispersed system components, the compresses were partially sealed to the painted surface using poly (ethylene) film. After removal of the compress, the surface of the fresco was washed several times with deionized water to eliminate any residual surfactant. Figure 2 shows the grazing light image of the region treated by the application of dispersed cleaning system B. In order to visualize the glossy area, the photograph was taken at a very low grazing angle after the mortar had completely dried. In these glossy areas (zone ①) the polyvinylacetate copolymer film was very thick, modifying the optical properties of the paint surface. After cleaning, the main macroscopic effect is the absence of glossy areas inside of the dotted line (treated region, zone ②).

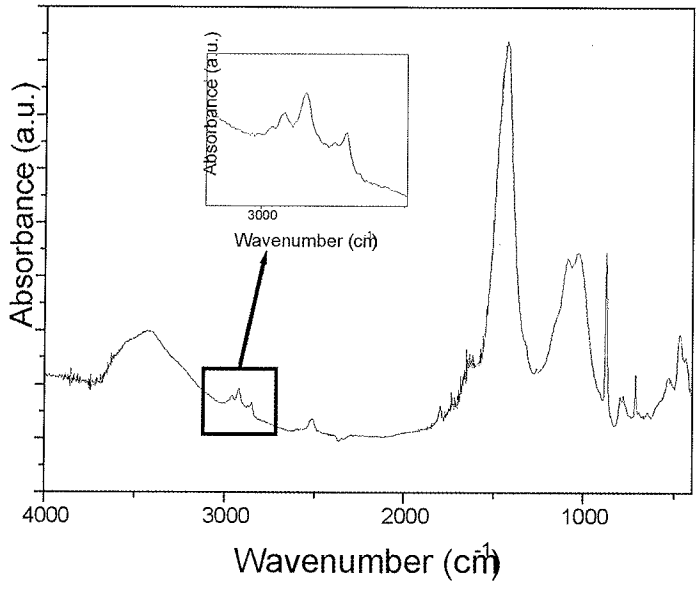

Figure 3. FTIR spectrum collected on a microsample taken from zone ② after cleaning with dispersed system B. The square highlights the typical peaks (C-H stretch) for aliphatic organic substances. The other peaks are characteristic of a lime plaster.

Absorbance FTIR spectra (KBr pellets) were collected from microsamples taken from the surface of the same work of art. After cleaning with the dispersed system B, the signal due to the presence of organic materials (2959-2850 cm^{-1}, Figure 3) decreases but does not disappear. This means that other layers of organic coatings are still present on the surface of the fresco and the removal of the polymer coating is not total. It is known that chemically different polymers had been applied in previous conservation treatments (1969-1972) [14] especially as consolidants and fixatives to avoid the detachment of the paint layer. So, to continue to maintain and preserve the integrity of the fresco, the present conservation treatment must simultaneously

remove the most external polymer layers but leave deeper invisible layers, which function to bind the fresco pigments.
It should be noted that the typical peaks for polluting salts (gypsum, oxalates, nitrates) commonly found in ancient painted surfaces are completely absent in this example. This indicates that the application of polymers had been carried out after desalination of the wall painting, which was then preserved from further environmental contamination by the polymer film.

Removal of gypsum
FTIR measurements were performed to ascertain the complete removal of gypsum (desulphatization) from the surface of a fresco (XVII century, Capponi Institute in Florence) after treatment with ammonium carbonate. The procedure adopted to evaluate the efficacy of cleaning allowed the quantitative determination of polluting salts in painted surfaces [15]. Microsamples of fresco taken before and after treatment were analysed, and the typical peak for gypsum at 668 cm^{-1}, the most reliable for quantitative purposes, was considered: the calculated amount of gypsum in the untreated sample was 4% by weight with respect to the mortar (Figure 4, dotted line). As a result of the cleaning procedure, the peak was no longer detectable showing that the removal of salt was complete (concentration below 0.5 % by weight, sensitivity limit for the method: Figure 4, full line).

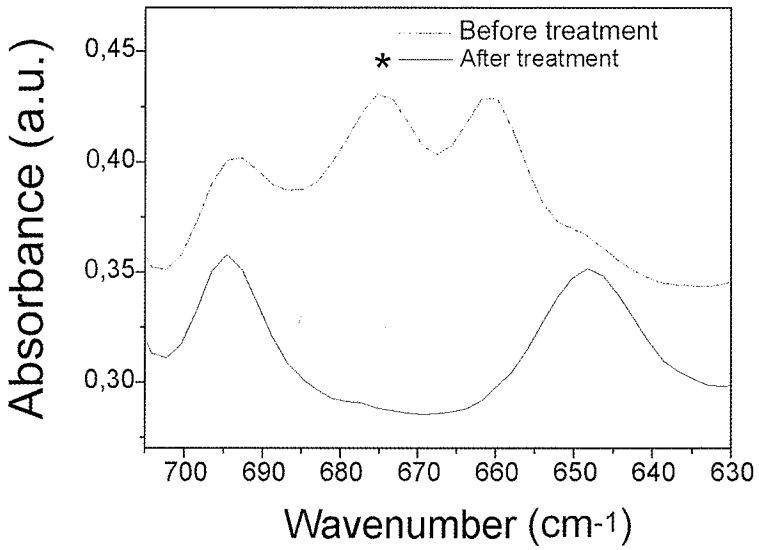

Figure 4. FTIR spectra of microsamples taken from the surface of the fresco in the Capponi Institute before and after treatment with ammonium carbonate. The asterisk (*) highlights the peak at 668 cm^{-1}; typical for gypsum and most reliable for quantitative purposes.

Conclusions

In this study we showed how FTIR spectroscopy is a suitable tool to monitor the efficacy of cleaning systems both on real painted surfaces and on test specimens. Two innovative cleaning systems for the removal of degraded acrylic and vinyl based copolymer layers from fresco surfaces were investigated, and positive results were obtained: micro-reflectance infrared spectra were run on untreated/treated mortar samples and the effective removal of contaminating substances was ascertained by following the disappearance of the typical FTIR peaks. The same system was applied to a real fresco treated many years ago using acrylic and vinyl resins: FTIR measurements showed that polymeric layers were reduced but not completely removed. Residual polymeric material was allowed to remain as it was needed to maintain the cohesion of the paint layer.
Absorbance FTIR spectra were performed to establish the extent of desulphatisation achieved by application of the inorganic ammonium carbonate method, , on the surface of a fresco. It was shown that the procedure was able to reduce the amount of gypsum below 0.5% by weight.

References

1. Ciabach, J., 'Investigation of the cross-linking of thermoplastic resins effected by ultraviolet radiation', *Symposium Resins in Conservation, 2000*, Scottish Society for Conservation and Restoration, Edinburgh, (1982) 5.1-5.8.

2. Horie, C. V., 'Acrylic resins', *Materials for Conservation - Organic Consolidants, Adhesives and Coatings*, Architectural Press (Butterworth-Heinemann), Oxford (1987) 103-112.

3. Luskin, L. S., 'Acrylic acid, methacrylic acid and the related esters', *Vinyl and Diene Monomers, part I*, Leonard, E. C., Wiley Interscience, New York (1970) 105-204.

4. Tintori, L., 'Studies for the preservation of the frescoes by Giotto in the Scrovegni Chapel at Padua. I. The state of conservation of the frescoes and the principal technical conservation problems', *Studies in Conservation*, (1963) **8**(2) 37-41.

5. Price, C.A. *Stone Conservation: an Overview of Current Research*. The Getty Conservation Institute, Marina del Rey (1996).

6. Lazzarini, L.; Laurenzi Tabasso, M. *Il Restauro della Pietra*. CEDAM, Padova (1986).

7. Feller, R. L. 'Influence of wavelength', in *Accelerated Aging - Photochemical and Thermal Aspects*, The Getty Conservation Institute, Los Angeles (1994) 63-90.

8. Feller, R. L., 'Speeding up photochemical deterioration', *Bulletin de l'Institut Royal du Patrimoine Artistique*, (1975) **15**(2), 135-150.

9. Morimoto, K., Suzuki, S., 'Ultra-violet irradiation of poly (alkyl acrylates) and poly (alkyl methacrylates)', *Journal of Applied Polymer Science*, (1972) **16**(11) 2947-2961.

10. Carretti, E., Dei, L., Baglioni, P., 'Solubilization of acrylic and vinyl polymers in nanocontainer solutions. Application of Microemulsions and Micelles to Cultural Heritage Conservation', Langmuir, (2003) **19**(19) 7867-7872.

11. Carretti, E., Dei, L., Baglioni, P. Italian Patent, FI / 99A000071.

12. Ferroni, E., Dini, D., 'Prospettive per la conservazione degli affreschi', *Scritti di storia dell'arte in onore di Ugo Procacci*, Electa Editrice, Florence, (1977) 17-22.

13. Grassi, S., Carretti, E., Dei, L., Unpublished results.

14. Tintori, L.'Conservazione, tecnica e restauro degli affreschi', *Mitteilungen* Kunsthist. Institutes in Florenz (1975), 149-180.

15. Salvadori, B.; Errico, V.; Mauro, M.; Melnik, E.; Dei, L. 'Evaluation of gypsum and oxalates in deteriorated mural paintings by Quantitative FTIR Spectroscopy'. *Spectroscopy Letters*, (2003) **36** (5 & 6), 501-513.

A NOVEL APPROACH TO AN OLD PROBLEM: APPLICATION OF TG/FTIR FOR EVALUATING MATERIALS FOR STORAGE AND DISPLAY CASES

Francesca Casadio[1] , Michael S. Bradley[2]
[1] The Art Institute of Chicago, 111 S. Michigan Ave., 60603 Chicago, Ill
[2] Thermo Electron Corporation, Spectroscopy division, 5225 Verona Rd., Madison, WI 53711

In order to be considered suitable for use with precious works of art, display and storage materials have to meet very demanding requirements; among these, an important aspect is to rule out emission of low molecular weight compounds, which can be damaging to the enclosed art. Wood has been found to emit significant quantities of acetic acid, methanol, formic acid and methyl acetate [1,2]; degradation of constituent proteins of wool and leather (comprising S-containing amino acids) can lead to evolution of sulphur-containing gases (responsible for tarnishing silver), the same volatile organic compounds emitted by many dyes; cellulose acetates fibres emit acetic acid, PVCs outgas hydrochloric acid and many paints, glues and plastics can release harmful solvents, additives and plasticizers. Lists of materials recommended for museum use have been compiled [3], founded on extensive testing or empirical observations during prolonged service. However, since new materials are continually appearing on the market, rigorous testing for potential atmospheric corrosiveness should be performed prior to use for display or storage of artifacts.
In general, the tests currently available can be divided into three main categories:
a) sampling of the atmosphere around the tested material (with passive sampling, adsorption tubes) and characterization of the outgassed compounds, generally with GC/MS [3-5];
b) microchemical-tests to be performed on the material under evaluation to check for the presence of specific chemicals [6,7];
c) accelerated aging tests, that aim at determining the long-term stability of the material under study.
Among the accelerated aging tests, one that has found widespread acceptance in Museums is the so called "Oddy test", introduced by British Museum's scientists in the early seventies, and, after a series of reproducibility tests and methodology revisions, is still in use nowadays [8-11]. The test requires that metal coupons (originally lead, copper and silver, but subsequently extended to other materials such as zinc, aluminum and magnesium [10]) be suspended in an air tight reaction vessel where the material to be tested is also present, along with a measured volume of distilled water, in order to guarantee 100% RH in the reaction container. The vessel is placed in an oven at 60°C for 28 days, then the metal coupons are checked for evidence of corrosion and, based on comparison with photographs of reference tokens, declared suitable, unsuitable or recommended for temporary usage only. The main drawbacks of this easily accessible, wide-spectrum method of testing is that it is very labour intensive (with lengthy preparation of the metallic tokens and a time-lapse of 28 days before the results of the tests are known) and highly dependent on the experience of the observers with the test (thus affecting reproducibility).
In order to address some of these issues (also involved with the other tests grouped under class a - needing long incubation times – and b – being specific, therefore requiring execution of many tests in order to rule out all possible harmful agents) a feasibility study was undertaken in order to determine if TG-FTIR methods would be helpful in determining materials' suitability for use in Museums.
The main advantages of TG-FTIR are:
• non specificity for a particular type of corrosive specie (the technique can detect all corrosive species present in a single run);
• FTIR provides qualitative information on the outgassed compounds (i.e. identification of pollutants) while thermogravimetry supplies quantitative data too;
• the method takes a few hours to complete, as opposed to 28 days for the Oddy test and several weeks of incubation for passive samplers;
• the technique guarantees high reproducibility (it doesn't depend on the purity of the metal tokens or their time of production, it is not affected by size of coupon, amount of distilled water, air-tightness of container, skills and judgement of analyst during comparison with references, as the Oddy test is).
A suitable method was devised (which would not lead to thermal degradation of samples) involving heating ramps with rates of 10°C/min up to 200°C in a flow of Nitrogen (60 ml/min), and a few tests were performed on samples of plywoods and velvet fabric previously subjected to the Oddy test in the Objects Conservation Laboratory of the Art Institute of Chicago.
Both plywoods were found to emit CO_2, isocyanic acid and ammonia, while the velvet sample outgassed CO_2, ammonia and acetic acid.

Although it is well known that lead will tarnish in the presence of amounts as low as 5 ppm of acetic acid, further research would be needed to correlate results of the traditional Oddy test with TG-FTIR testing, so as to constitute a database of materials that can be recommended for museum use and to establish threshold for emission of volatiles detected by TG-FTIR analysis that would classify a material as unsafe for storage or display.

Acknowledgements:

Thermo Electron Corporation is acknowledged for availability of the TG-FTIR instrumentation and of the application specialist's time. Barbara Hall, objects Conservator at the Art Institute of Chicago is thanked for providing test materials and sharing results of previous Oddy tests.

References

1. P.C.Arni, G.C. Cochrane and J.D. Gray "The emission of corrosive vapours by wood. I. Survey of the acid-release properties of certain freshly felled hardwoods and softwoods", J. Appl. Chem., 15, July, 1965, 305-313.

2. P.C.Arni, G.C. Cochrane and J.D. Gray "The emission of corrosive vapours by wood. II. The analysis of the vapours emitted by certain freshly felled hardwoods and softwoods by gas chromatography and spectrophotometry", J. Appl. Chem., 15, October , 1965, 463- 468.

3. Erhardt D. "Art in transit: material considerations" in Proceedings of : Art in Transit , Studies on the transport of paintings, M.F. Macklenburg (Ed.), 1991, pp. 25-36.

4. C. E. Miles, "Wood coatings for display and storage cases", Studies in Conservation, 31 (1986) 114-124

5. N. Larkin, N. Blades and E. Makridou, "Investigation of volatile organic compounds associated with polyethylene and polypropylene containers used for conservation and storage", The Conservator. 24 (2000), pp. 41-51.

6. J. Zhang, D. Thickett and L. Green, "Two tests for the detection of volatile organic acids and formaldehyde" JAIC 33 (1994) 47-53.

7. V. Daniels and S. Ward , "A rapid test for the detection of substances which will tarnish silver", Studies in Conservation 27 (1982) 58-60.

8. S. M . Blackshaw and V.D. Daniels " The testing of materials for usage in storage and display in museums", The conservator, 3 (1979) 16-19.

9. L.R. Green and D. Thickett, "Testing materials for use in the storage and display of antiquities – a revised methodology", Studies in Conservation 40 (1995) 145-152.

10. L.R.Green and D. Thickett "Modern Metals in Museum Collection" in : Proceedings of a conference Symposium '91 – saving the Twentieth Century: The conservation of Modern Materials, Ottawa, Canada (1993) , pp. 261-272.

11. J.A.Bamberger, E.G. Howe and G. Wheeler , "A variant Oddy test procedure for evaluating materials used in stage and display cases" Studies in Conservation 44 (1999) 86-90.

Evaluation of the Analytical Potential of Raman Microscopy Combined With Elemental Techniques

Angela Zoppi, Cristiana Lofrumento, Emilio M. Castellucci
European Laboratory for Non Linear Spectroscopy (LENS), Università di Firenze, Polo Scientifico, Via Nello Carrara 1, I-50019-Sesto F.no (Firenze)-Italy

Many instrumental analytical techniques which previously only provided bulk information have developed microscopic equivalents, as a result of the increasing degree of material complexity and the growing need to measure local properties of natural and man-made materials. Several well established methods exist (such Raman spectroscopy, electron probe micro analysis, Laser Induced Plasma Spectroscopy) which yield molecular or elemental data, and often only on the major constituents of the material being examined. In many cases, such as in the cultural heritage sector, there is a growing need for those techniques provided: they can furnish: (a) a combination of molecular and constituent elements information, (b) data on minor and trace-level constituents, in order to arrive at highly specific fingerprints of various materials. Preferably, such equipment also allows to extract this fingerprinting information from specific areas of large objects and/or from minute samples.
A useful answer is provided by combined micro-beam XRF/micro-Raman instrument that allows local characterization of sub-mm samples with minor/trace level sensitivity and combined micro LIBS/Raman instrumentation, a "all laser" diagnostic set up, also very useful in the cultural heritage domain. The purpose is to demonstrate the advantages of the combined application of these modern, complementary techniques in relation to the analysis and characterization of materials used in artworks.
The devices are to be used either as a table-top in a laboratory environment ('ex situ' measurements, e.g. on artistic materials taken away in a microdestructive manner) but are also readily transportable so that is can be employed for 'in situ' measurements (e.g., of artistic objects on display in a museum, exhibition, excavation site), providing routine compositional information with a lateral resolution of 2-5 μm.

ColoRaman Project: an On-line Resource for Raman and Fluorescence Spectroscopies of Pigments in Prepared paints.

Cosentino A.[1,2,3], Burrafato G.[1,2,3], Calabrese M.[1], Gueli A.M.[1,2,3], Troja S.O.[1,2,3], Zuccarello A.[1,2,3]
[1] Dept. of Physics & Astronomy, University of Catania, via Santa Sofia 64, 95123 Catania, Italy.
[2] CSFNSM, Sicilian Centre for Nuclear and Solid State Physics, via Santa Sofia 64, 95123 Catania, Italy.
[3] INFN, Italian National Institute of Nuclear Physics, via Santa Sofia 64, 95123 Catania, Italy.

Abstract

Raman spectroscopy allows the non-destructive in situ characterisation of materials of artistic-historical interest to archaeologists, art historians and restorers. At present, investigations on paint pigments seem to be by far the most promising. Unfortunately, it is not always possible to identify pigments when they are mixed with media in paintings. Fluorescence from the binding agents and the ground materials often masks the weak Raman signal. Nevertheless, identification is still possible by selecting an appropriate excitation wavelength. By examining the spectra obtained at different excitation wavelengths corresponding to each pigment and each painting technique, it is possible to determine the most suitable excitation wavelength for each context. In addition, some pigments may be identified by fluorescence spectroscopy. The ColoRaman project aims to make available on-line a database of Raman and fluorescence spectra, obtained at different excitation wavelengths, of pigments and paints on different grounds covering oil, egg and casein tempera, and fresco painting techniques. The results have been obtained using a combined system for Raman and fluorescence spectroscopies, operating with three different excitation wavelengths.

Introduction

Raman spectroscopy has been used successfully in the investigation of the chemical composition of materials employed in various types of artefacts of artistic-historical interest. In particular, good results have been obtained in the characterisation of some ceramics [1], resins and organic materials [2, 3, 4, 5], gemstones [6] and metal artefacts [7]. Similarly, there are many publications regarding investigations conducted on different types of coloured artefacts, such as manuscripts [8, 9], frescoes [10], prehistoric wall paintings [11] and pottery [12]. The ColoRaman project offers an on-line database of Raman and fluorescence spectra of pigments plus information regarding the suppliers of the pigments analysed. These data are of fundamental importance in that it has been observed that pigments, produced by different suppliers and marketed with the same name, can have different chemical compositions.
The ColoRaman project also offers an on-line database of Raman and fluorescence spectra of pigments in paints made by fresco, egg and casein tempera, and oil painting techniques. It is well known that the binding agents and ground material may produce fluorescence which masks the weak Raman signal emitted by the pigments. Nevertheless, the signal-to-noise ratio (noise here consisting of the emission of fluorescence) may be improved by selecting an appropriate excitation wavelength that produces less fluorescence while maintaining a measurable Raman signal, or stimulates a Raman emission so great that it can be distinguished from the fluorescence. This wavelength will depend on the pigment and on the painting technique used because the different binding agents and grounds can contribute in different ways to mask the Raman signal. From the above, it appears that it may be useful to provide the spectra corresponding to each pigment applied with each painting technique, to make it possible to evaluate, in each context, the most suitable excitation wavelength for the identification of the pigment.
Together with the database of Raman spectra, we also report the fluorescence spectra. Although these are easily acquired, practically with the same system used for dispersive Raman spectroscopy, to date few authors have investigated the characterisation of paint pigments also through their fluorescence spectra [13, 14]. This methodology can be particularly useful because, unlike the case of the weak Raman signal, in the emission of fluorescence there is generally such a high signal-noise ratio that pigments in paints on an artefact can be identified. Further, although only a small number of pigments can be characterised by their fluorescence, in the case where the Raman signal cannot be measured, it may be possible to identify the pigment through its fluorescence.

Experimental

Measurements were made using the microSPEC produced by Jobin Yvon, a combined system for Raman and fluorescence spectroscopies. This system uses a *TRIAX 190* spectrometer carrying three diffraction gratings, of

which one of 150 g/mm is used for fluorescence measurements and one of 1800 g/mm for Raman experiments. The signal is acquired by a *SpectrumONE* CCD which has a spectral resolution of 1-3 cm^{-1}, depending on the laser beam wavelength. The optical components for the excitation and collection of the signal consist of an OLYMPUS BX40 confocal microscope and a long working distance objective (50X). The system is equipped with three lasers; a NdYAG laser at 531.5 nm, a He-Ne laser at 632.8 nm and a Diode laser at 780 nm, of 40, 30 and 20 mW power, respectively. Neutral density filters were used to reduce the intensity of the laser radiation on the specimen. Raman and fluorescence measurements were obtained using the same system, changing only the diffraction grating.

Results and data discussion

The database of Raman and fluorescence spectra contains the spectra of 99 different pictorial pigments supplied by Kremer (Germany) and Zecchi (Italy).
Samples for Raman and fluorescence spectra of pigments in paintings were prepared according to documented recipes [15, 16, 17, 18]. Recipes and products for the four painting techniques were as follows:
Gesso: ground for oil and tempera, it was produced by mixing Bologna chalk (calcium carbonate sulphate), rabbit glue and rock alum.
Binding agent for egg tempera: one teaspoon of vinegar, one teaspoon of honey, one teaspoon of rock alum and one egg albumen (for cool colours) or one egg yolk (for warm colours).

Fresco:	quick lime, limestone sand.
Binding agent for casein tempera:	casein binding agent from Zecchi (Florence) art. 2050.
Binding agent for oil:	clarified linseed oil from Lefranc & Bourgeois (France).

Table 1, with all the spectra viewable, is published on-line at: http://www.ct.infn.it/~archeo/ .Table 1 reports the English name of the pigments, the supplier (K=Kremer, Germany; Z=Zecchi, Italy) and the item code for each of the 99 pigments analysed. For ease of identification, each pigment was assigned an identification number. In Table 1 the presence of a letter indicates whether it was possible to obtain a Raman or fluorescence spectrum. For each of the three-excitation wavelengths, the letters indicate in which painting techniques it was possible to identify the pigment. The following convention was adopted: P = Pigment, F = Fresco, C = Casein tempera, E = Egg tempera, O = Oil. Uppercase letters refer to Raman spectra, the corresponding lowercase letters refer to fluorescence spectra. From Table 1 it is easy to recognize that some pigments could be characterised by Raman spectroscopy only with one of the three lasers tested, confirming that operating with these three wavelengths allows the characterisation of more pigments than a system operating at only one or two excitation wavelengths. Even more importantly, some pigments which could be characterised using all three excitation wavelengths, could be identified with only one of the three laser once they have been painted. For example, although pigment 78, lead tin yellow, could be characterised with all three lasers, once applied in a fresco it was identified only with the laser at 531.5 nm. (Figure 1). Similarly, only excitation at 780 nm allowed the identification of pigment 81, cinnabar, when applied in oil painting (Figure 2).
Only excitation at 632.8 nm allowed the identification of pigment 92, zinc yellow, when applied with the egg tempera painting technique (Figure 3). Pigment 97, white lead, was

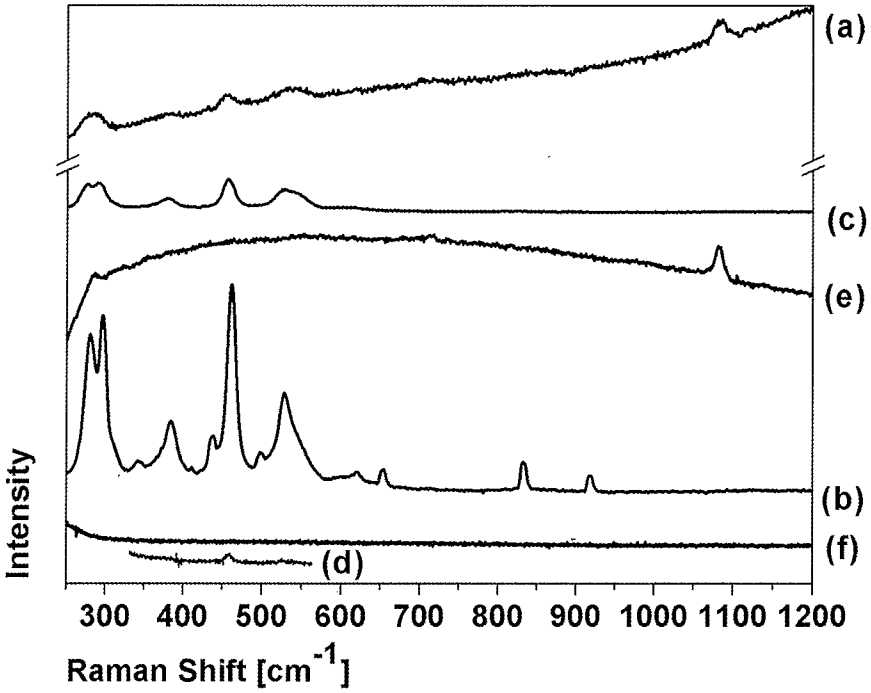

Figure 1. Raman spectra of pigment 78, lead tin yellow, acquired with excitation at 531.5 nm (c), 632.8 nm (b), 780 nm (d) and of the pigment in fresco painting with excitation at 531.5 nm (a), 632.8nm (e), 780 nm (f).

characterised with two lasers, but only excitation at 531.5 nm allowed its identification when applied with the casein tempera painting technique (Figure 4).
Some pigments gave characteristic Raman spectra only when analysed in paints. The spectra obtained from the painted pigments contribute to the completeness of the information contained in the databases, becoming particularly important in the case of pigments which otherwise cannot be characterised. Clearly, the spectra of paints include the

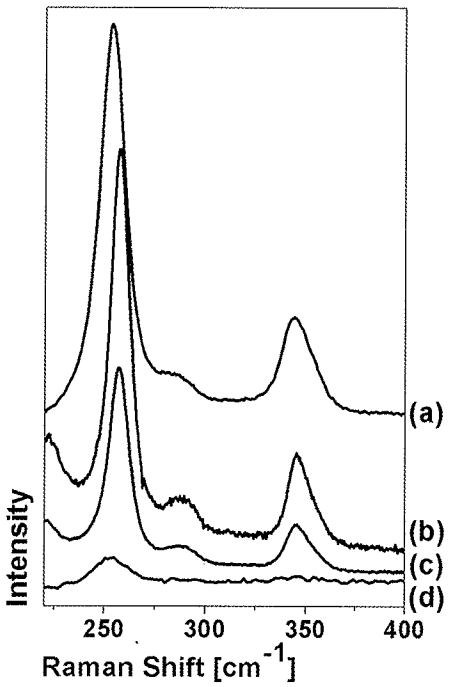

Figure 2. Raman spectra of pigment 81, cinnabar, acquired with excitation at 531.5 nm (d), 632.8 nm (a), 780 nm (c) and of the pigment in oil painting with excitation at 780 nm (b).

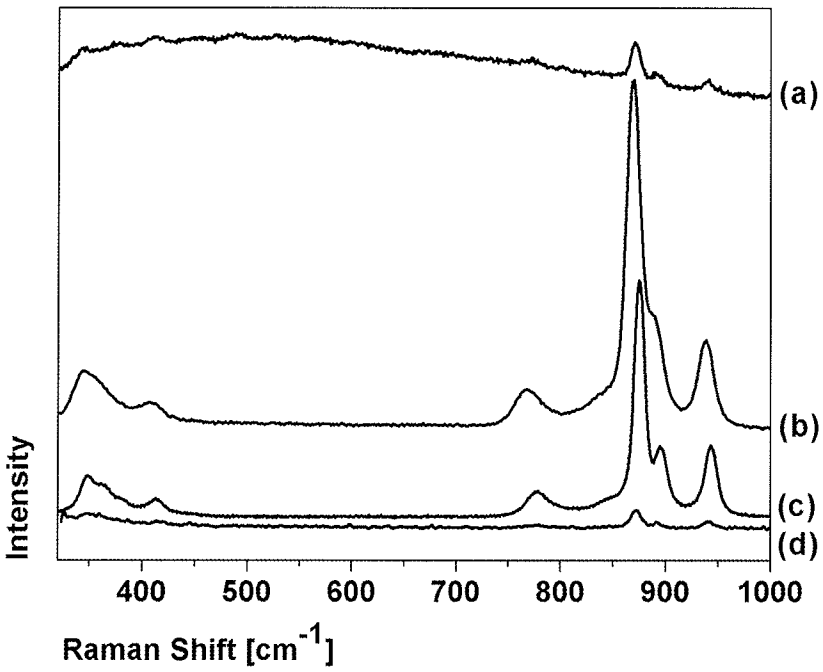

Figure 3. Raman spectra of pigment 92, zinc yellow, acquired with excitation at 531.5 nm (b), 632.8 nm (c), 780 nm (d) and of the pigment in egg tempera painting with excitation at 632.8 nm (a).

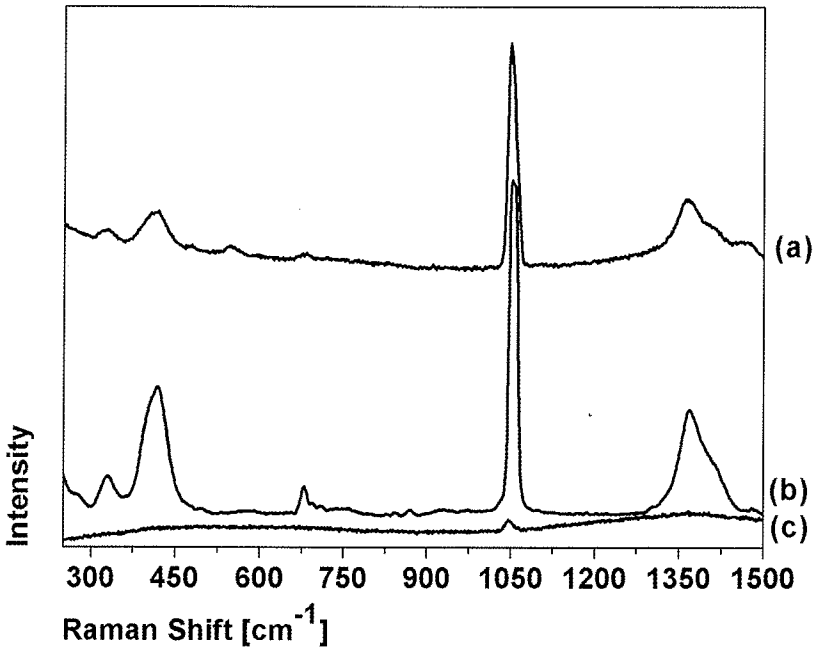

Figure 4. Raman spectra of pigment 97, white lead, acquired with excitation at 531.5 nm (a), 632.8 nm (b) and of the pigment in casein tempera painting obtained with excitation at 531.5 nm (c).

contribution from the binding agent. For example, pigment 55, indanthrone blue, could not be characterised with either of the three lasers, but only when applied in casein and egg tempera and fresco painting with laser excitation at 632.8 nm (Figure 5).

Fluorescence spectroscopy

Fluorescence spectroscopy allows the characterisation of a modest number of pigments. Table 2 (published on-line) shows the characteristic fluorescence peaks for these few pigments. Nevertheless its contribution can be decisive in cases where identification is not possible using Raman spectroscopy alone, and is a useful and complementary analysis method. For example, when applied in oil painting, pigment 13, cobalt cerulean blue, can only be characterised using its fluorescence obtained with excitation at 531.5 nm (Figure 6).

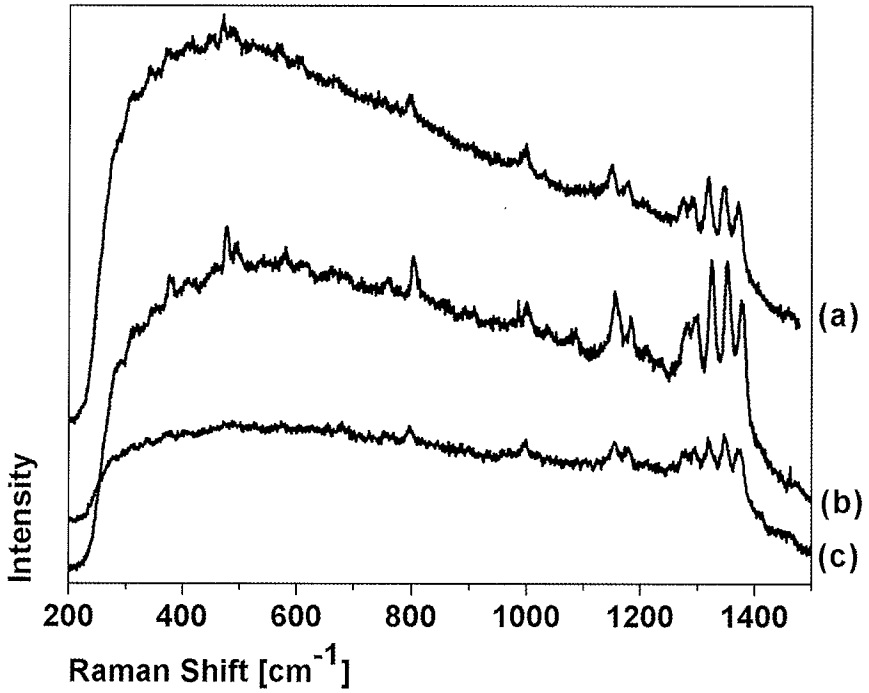

Figure 5. Raman spectra obtained with excitation at 632.8 nm of pigment 55, indanthrone blue, applied with the egg tempera (c), casein tempera (a) and fresco (b) painting techniques.

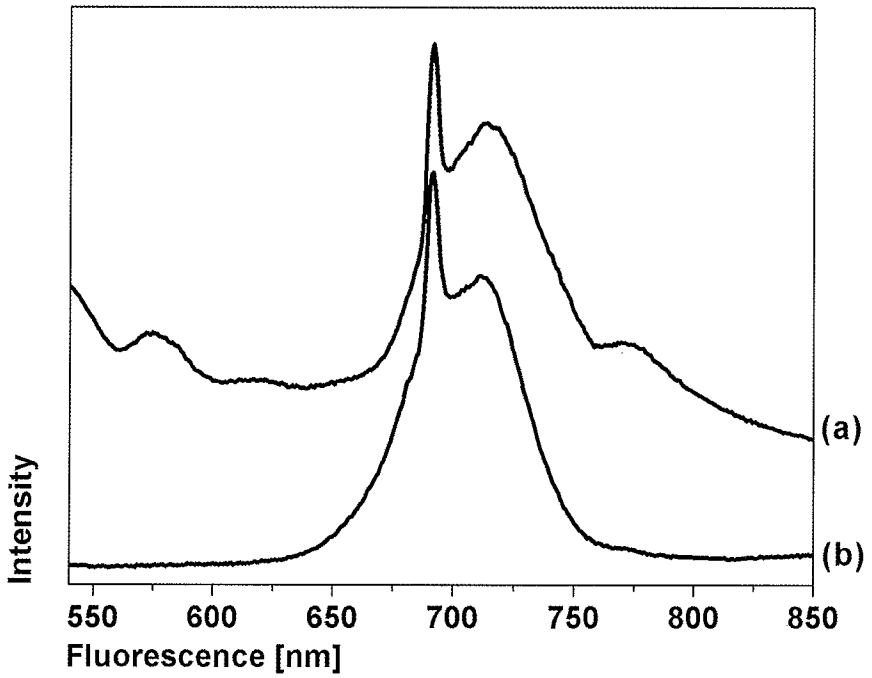

Figure 6. Fluorescence spectra of pigment 13, cobalt cerulean blue, (b) and of the pigment applied in oil painting (a), both obtained with excitation at 531.5 nm.

Conclusions

A combined system for Raman and fluorescence spectroscopies, equipped with three lasers (531.5, 632.8, 780 nm), allows the characterisation of a larger number of pigments than that possible with two, or worse, only one laser. However, given that even under these conditions it was not possible to characterise all 99 pigments examined, it would be advantageous to repeat the tests using other excitation wavelengths to obtain the characterisation of the remaining pigments through the elimination of fluorescence or the excitation of Raman resonance emission.

References

1. Zoppi A., Lofrumento C., Castellucci E. M., Migliorini M. G., 'Micro-Raman technique for phase analysis on archaeological ceramics', *Spectroscopy Europe*, **14**(5) (2002) 16-20.

2. Edwards H. G. M., Sibley M. G., Heron C., 'FT-Raman spectroscopic study of organic residues from 2300-year-old Vietnamese burial jars', *Spectrochimica Acta Part A.*, **53** (1997) 2373-2382.

3. Edwards H. G. M., Farwell D. W., Daffner L., 'Fourier-transform Raman spectroscopic study of natural waxes and resins', *Spectrochimica Acta Part A.*, **52** (1996) 1639-1648.

4. Vandenabeele P., Wehling B., Moens L., Edwards H., De Reu M., Van Hooydonk G., 'Analysis with micro-Raman spectroscopy of natural organic binding media and varnishes used in art', *Analitica Chimica Acta,* **407** (2000) 261-274.

5. Edwards H. G. M., Russel N. C., Seaward M. R. D., Slarke D., 'Lichen biodeterioration under different microclimates: an FT Raman spectroscopic study', *Spectrochimica Acta Part A.*, **51** (1995) 2091-2100.

6. Smith D. C., Robin S., 'Early Roman empire intaglios from "rescue excavations" in Paris: an application of the Raman microprobe to the non-destructive characterization of archaeological objects', *J. Raman Spectrosc., 28 (1997) 189-193.*

7. McCann L. I., Trentelmann K., Possley T., Golding B., 'Corrosion of ancient Chinese bronze money trees studied by Raman microscopy', *J. Raman Spectrosc.* **30** (1999) 121-132.

8. Clark R. J. H., Gibbs P. J., 'Raman microscopy of a 13th-century illuminated text', *Analytical Chemistry News and Features.* **70** (1998) 99 A-104 A.

9. Burgio L., Clark R. J. H., Gibbs P. J., 'Pigment identification studies in situ of Javanese, Thai, Korean, Chinese and Uighur manuscripts by Raman microscopy', *J. Raman Spectrosc.,* **30** (1999) 181-184.

10. Farwell D.W., Rozenberg S., Edwards H. G. M., 'Raman spectroscopic study of red pigment and fresco fragments from king Herod's palace at Gerico', *J. Raman Spectrosc.,* **30** (1999) 361-366.

11. Smith D. C., Bouchard M., Lorblanchet M., 'An initial Raman microscopy investigation of prehistoric rock art in caves of the Quercy district , S.W. France', *J. Raman Spectrosc.,* **30** (1999) 347-354.

12. Zuo J., Xu C., Wang C., 'Identification of the pigment in painted pottery from the Xishan site by Raman microscopy', *J. Raman Spectrosc.*, **30** (1999) 1053-1055.

13. Guineau B., 'Non-destructive analysis of organic pigments and dyes using Raman microprobe, microfluorometer or absortion microspectrophotometer', *Studies in Conservation.,* **34** (1989) 38-44.

14. Wallert A., 'Fluorescent assay of quinone, lichen and redwood dyestuffs', *Studies in Conservation.,* **31** (1986) 145-155.

15. Doerner, M., *The materials of the artist and their use in painting,* Harcourt Brace & Company, San Diego (1949).

16. Seymour P., *A short book about oil painting,* Lee Press, Yorkshire (1995).

17. Wehlte K., *The materials and techniques of painting,* Kremer Pigments Inc., New York (1975).

18. Thompson D.V., *The practice of tempera painting,* Dover Pubblications inc., New York, (1936).

Characterisation of Ink Components in Ancient Manuscript by FTIR Spectroscopy.

Núria Ferrer[1] and M. Carme Sistach[2]
[1] Scientific Technical Services. University of Barcelona
[2] Arxiu de la Corona d'Aragó

Degradation of paper and parchment has been an object of study because of the destructive effects it can produce in libraries and archives. Serious damages are caused by Iron-gall inks.
Different processes seem to be involved in the destructive mechanism of inks: characteristics of paper, ink composition and chemical reactions with other molecules.
Knowledge of mechanisms of reaction from original ink components is crucial to understand the damage caused to paper and parchment. Therefore, characterisation of final products over inks can help to both describe the above mentioned mechanisms and consequently try to avoid degradation.
One of the most important problems related to this kind of samples is the small amount of ink that is possible to remove from the manuscripts. That is why microscopic methodologies are required.
FTIR spectroscopy has been applied to the characterisation of ink components in ancient manuscripts.
Different methodologies have been used in order to obtain good infrared spectra. Reflection techniques, such as attenuated total reflectance (ATR) and transmission techniques have been compared. Both methodologies are coupled to an infrared microscope, due to the tiny amount of sample contained in ancient samples. Transmission techniques, using the diamond cell, need to remove some particles from the surface of the inks, trying to avoid paper or parchment. ATR techniques are not destructive at all.
A large number of inks have been analysed and different oxalate salts have been characterised. Good correlations between acidity of ink and oxalate cations have been observed. Iron (II) sulfate has also been detected in some samples.
Comparison with other techniques such as scanning microscopy and MS-HPLC give good results and agree with the infrared spectra.

Resin and Pitch of Pinaceae Wood in the Findings of the Ancient Harbour of Pisa

Gianna Giachi
Soprintendenza ai Beni Archeologici per la Toscana, Laboratorio di Analisi, L.go del Boschetto, 3- I50143 Firenze (Italy)

Abstract

An archaeological excavation in Pisa (Italy) near the S. Rossore railway station, which began in December 1998, has brought to light the remains of a harbour dating back to the Etruscan and Roman ages. During the excavation several shipwrecks and their cargo (amphorae, stones, glasses, and so on) were discovered. The amphorae, of different typologies, still show traces of an internal resinous coating that was applied to achieve impermeability for wine and oil storage. A significantly important discovery found in the ancient harbour of Pisa are the well preserved hulls of the shipwrecks which still exhibit waterproofing and caulking treatments and areas of painted surfaces. In order to identify the origin of the waterproofing materials used, a large number of samples was collected from the internal coatings of various amphorae typologies and from the Pisan ships' wood's finishing. Furthermore, samples of painted surfaces were collected in order to characterise the organic binder. The characterisation of the samples was performed by means of Fourier Transform Infrared Spectroscopy (FTIR). Analysis demonstrates that the waterproofing of the amphorae and the waterproofing and caulking materials of the hulls were performed with a tarry material obtained from the destructive distillation of *Pinaceae* wood, and that the painting binder was constituted of beeswax and *Pinaceae* resin.

Introduction

In December 1998, during the enlargement works of the Pisa S. Rossore railway station (Italy), the remains of a harbour dating back to the Etruscan and Roman ages were brought to light (Fig. 1) [1].

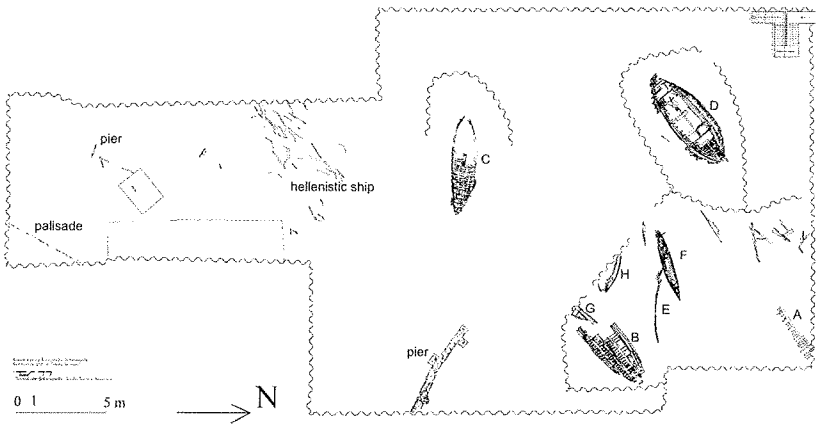

Figure1 - View of the actual excavation plan of the ancient harbour of Pisa

The discovery represented an outstanding event especially because the remarkable number of shipwrecks in the area, eighteen up until now, dating from 2nd cent. b.C. to 5th cent. A.D., and for the large quantity and variety of materials discovered at the site, such as amphorae and objects pertaining to the shipload and the ships' equipment.
All the discovered ships show a reasonably good state of preservation: the conservation of wood and other organic materials found is due to the wet and anaerobic environment which has lasted over the centuries and, for the shipwrecks, to the large amount of coating substances applied on the ships' surface.
All the ships still exhibit the waterproofing and caulking treatments and some of them still have parts of painted surfaces, especially on the external part of the hull. Also the several amphorae of different typologies still show traces of the internal resinous coating: it is well known, from ancient times, that amphorae were treated on their inside with natural products to make them adaptable for transport and storage of liquids, such as wine, oil and sauces with a fish base.
While excavation and archaeological research are still in course, studies have started regarding the technology and the materials employed in the ships' construction and in the production of the objects found in the excavation area. In order to identify the origin of the materials used as ships' finishing and amphorae coating, a large number of samples was collected from the internal surfaces of amphorae and from the Pisan ships. The characterisation of the samples was performed by means of Fourier Transform Infrared Spectroscopy (FTIR).

Materials and method

In order to characterise the substances used in the Pisan ships' wood's waterproofing, samples were collected from the external and internal surfaces of the planking of the ships named B (15), C (7, 9), and F (37, 38). Two samples of

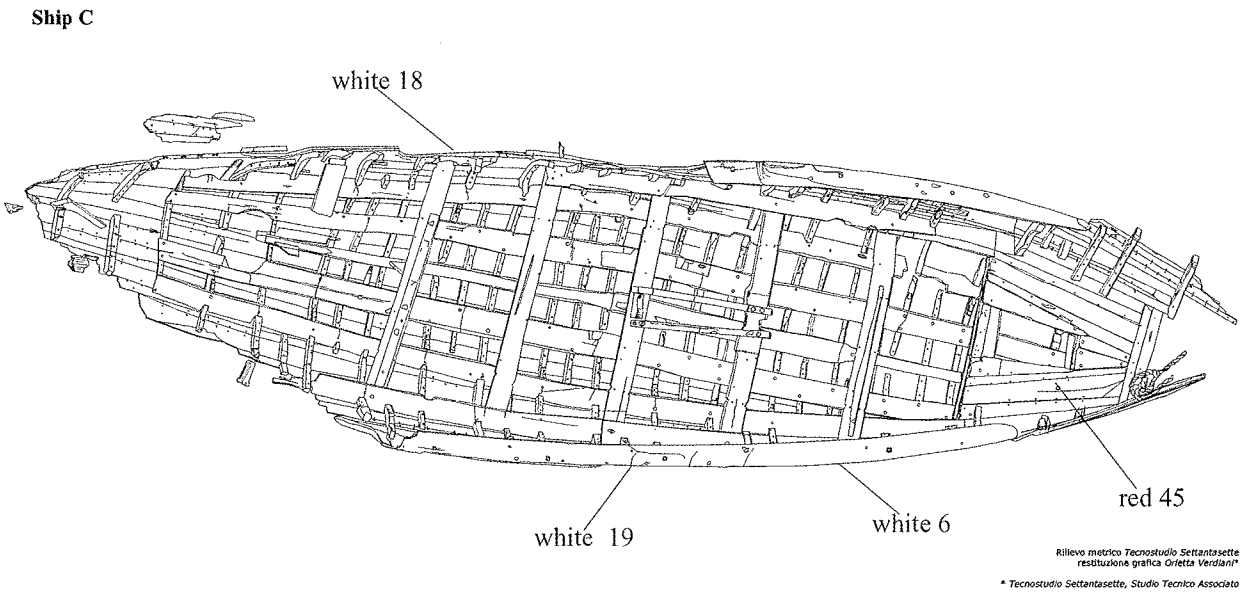

Figure 2 - Ship C: position of the painting samples collected

caulking material were collected between the planks of ship D and F, 13 and 43 respectively. Three samples of white painted areas (6, 18, 19) and one sample of a red painted area (45) were collected from the external part of ship C. Two samples of white paint (39, 41) were taken from ship E. One more sample (20) was collected from a white painted wood fragment not attributed to any particular ship.
The analysis of the internal coating of amphorae was performed starting from those found in the southern part of

Table I - Amphorae of the "Ampliamento Sud" sampled for the analysis

Type	*Production area*	*Known purposes*	*Sample code*
Dressel 1A	Italy: Tyrrhenian coast	wine	G9, G16, G18, G39, G44, G76, G108
Dressel 1B	Italy: Tyrrhenian coast (Etruria, Latium, Campania)	wine	G78, G80
Dressel 1C	Italy: southern Tyrrhenian coast	wine	G20, G100, G112
Dressel 9	Spain: southern coast (Baetica)	fish products	G117
Greco-Italic	Italy: Tyrrhenian coast	wine	G38, G43, G46, G48, G50, G55, G60, G67, G77, G89
Early Greco-Italic	Italy: southernTyrrhenian coast (Campania, Gulf of Sicily)	wine	G13, G17, G93
Transitional Greco-Italic	Italy: southern Tyrrhenian coast (likely Campania)	wine	G12, G27, G40, G62, G72, G88
Advanced Greco-Italic	Italy: southern Tyrrhenian coast (Campania)	wine	G21, G65, G95
Lamboglia 2	Italy: Adriatic coast	wine	G101, G83
Maňà C2b	Morocco: Tangeri area	fish products (?)	G66
Maňà C2c	Tunisia (?)	fish products (?)	G70, G71
Tripolitania	Libya (Tripolitania)	oil	G23
Unknown tipology			G22, G31, G36

the excavation area, the so-called "Ampliamento Sud", where different typologies were present (Table I). The majority of this coating has an ochre-yellow colour and is dusty, yet sometimes a compact, dark brown, shiny substrate with conchoidal fracture is present (Fig. 4).
All the samples were ground and homogenised.
Samples, of about 50 mg for waterproofing (of ships and amphorae) and caulking material and of about 10 mg for painting material, were extracted twice. First, extraction was done using 2 ml of acetone in order to dissolve the resinous fraction. After washing, the residue was extracted with the same volume of chloroform in order to dissolve wax and/or bituminous substances, which may be present. After drying them, the two fractions were analysed as KBr micropellets with a FT-IR spectrometer 16PC Perkin Elmer. Transmittance % was collected in the range of 4000-400 cm^{-1} with 4 cm^{-1} resolution.
Pinaceae resin (colophony), pitch and beeswax used as reference materials were obtained from the collection of natural materials of the Botanical Department of Florence University.

Results

The samples of waterproofing, both of ships and amphorae, and caulking materials gave very similar FTIR spectra. The spectra of the dried acetone extracts looked like that of a conifer resin submitted to thermal treatment, as performed during the preparation of tar or pitch. The main signals in the FTIR spectra collected for waterproofing and caulking materials can be assigned as reported in Table II. In Figure 3 the FTIR spectra of sample 43 (continuous line) is compared to a *Pinaceae* pitch (sketched line). The adsorption bands of the ester group are generally predominant with respect to acidic groups and at the same time the aromatic bands are more intense compared to the FTIR spectrum of a non-heated conifer resin. This finding can be related to the presence of a pitch, whose production from resin is known to lead to the aromatisation of terpenoids [2][3].

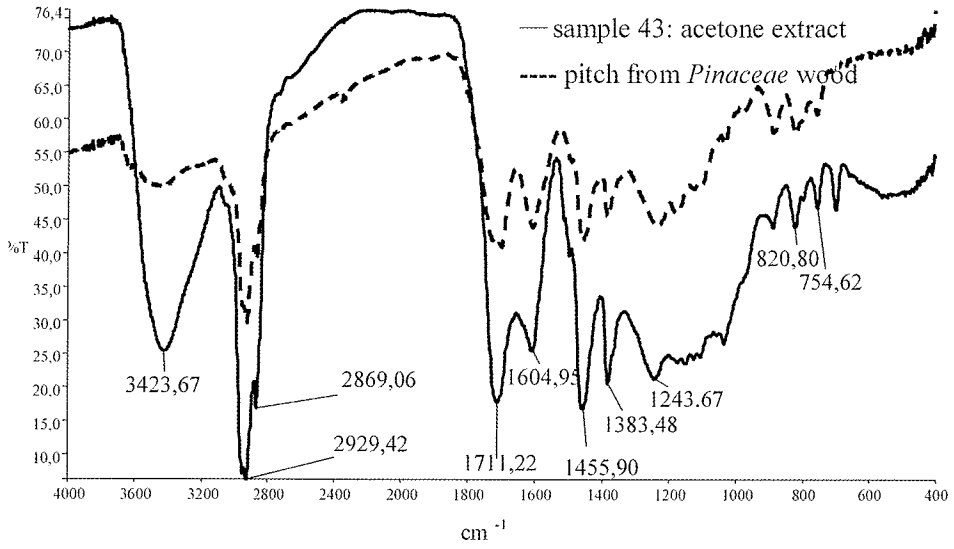

Figure 3 - Ship F: FT-IR spectum of dried acetone extract of caulking material and of reference pitch derived from *Pinaceae* wood

Table II - Vibrational group frequencies of acetone extracts of waterproofing and caulking samples (in this table the experimental range of the absorption bands for all the analysed samples are reported)

Assignment	*Range (cm^{-1})*	*Comment*
ν(O–H)	3433 – 3411	H bonded
ν(arC–H)	3054,	
ν(C–H)	2958 -2926, 2870 - 2855	CH_2 asymmetric, symmetric, CH_3
ν(C=O)	1726 -1700	
ν(arC=C)	1611 – 1593	
δ(arC–H)	1516 – 1515	
$\delta(CH_2)$, $\delta(CH_3)$	1460 – 1455	CH_2 scissoring, CH_3 asymmetric
$\delta(CH_3)$	1384 – 1381	CH_3 symmetric
δ(O–H)	1243	
ν(C–O)	1170 – 1178	Ester

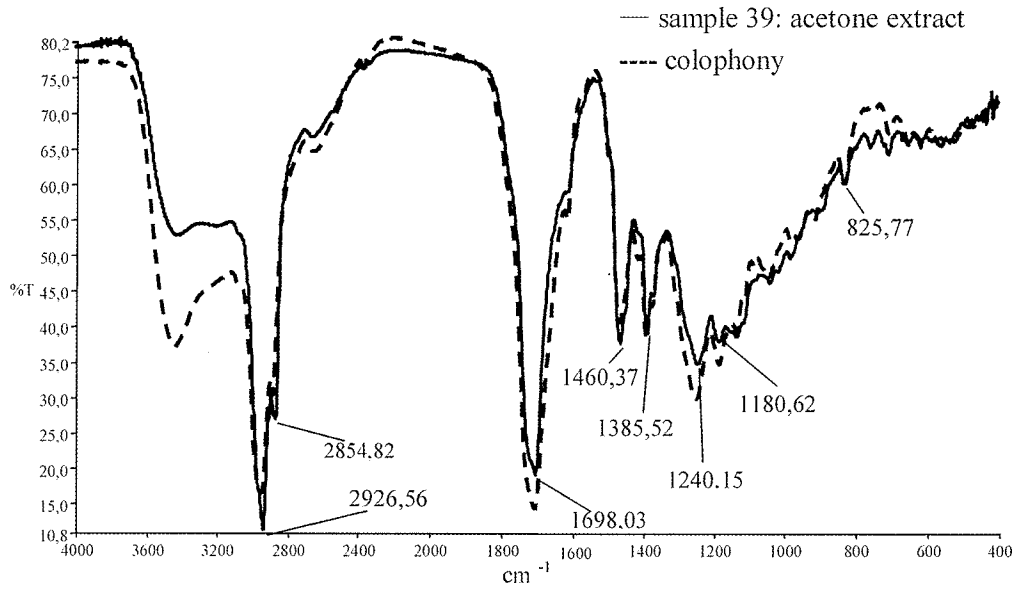

Figure 4 - Ship E: FT-IR spectrum of dried first extract with acetone of white painted surface and of reference *Pinaceae* resin (colophony)

Table III - Vibrational group frequencies of acetone extracts of paint samples 6, 20, 39

Assignment	*Range (cm^{-1})*	*Comment*
ν(O–H)	3436 – 3419	H bonded
ν(C–H)	2954 -2926, 2869 - 2851	CH_3, CH_2 asymmetric, symmetric
ν(O–H)	2649	Dimerized acid in solid phase
ν(C=O)	1713 -1698	Ester and acid
δ(CH_2), δ(CH_3)	1463 – 1460	CH_2 scissoring, CH_3 asymmetric
δ(CH_3)	1386	CH_3 symmetric
δ(O–H)	1244	
ν(C–O)	1181	

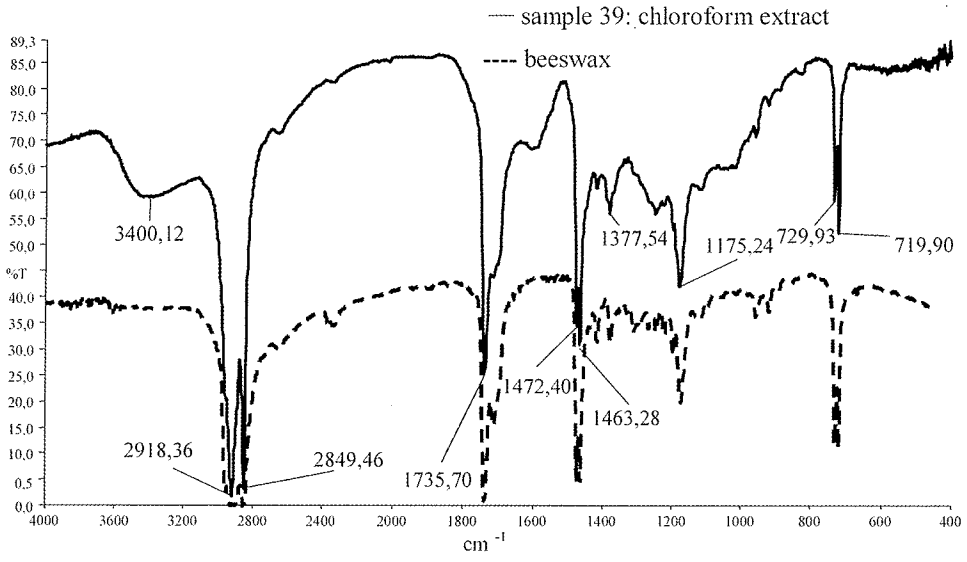

Figure 5 - Ship E: FT-IR spectum of dried second extract with chloroform of white painted surface and of reference beeswax. There is evidence of traces of resin

The chloroform extracts of waterproofing and caulking samples did not reveal the presence of any further substance. The FTIR spectra of acetone extracts of white paint samples 6, 20, 39 are very similar to that of colophony (dried residue from *Pinaceae* resin), as shown in Figure 4 where the spectra of sample 39 (continuous line) is compared to colophony (sketched line). The main signals of the FTIR spectra collected for binders of these samples can be assigned as reported in Table III. The acetone extracts of white and red paint samples 18, 19, 41 and 45 showed transmittance signals like those reported in Table II for pitch.
The FTIR spectra of the chloroform extracts of all paint samples (6, 18, 19, 20, 39, 41 and 45) highlighted the presence of long-chain aliphatic esters. A good similarity of the FTIR spectra of chloroform extracts of sample 39 (continuous line) and of beeswax (sketched line) is highly evident (Fig. 5). The main signals of the chloroform extracts of paint samples can be assigned as reported in Table IV.

Table IV - Vibrational group frequencies of chloroform extracts of paint samples 6, 18, 19, 20, 39, 41, 45 (in this table the experimental range of the absorption bands for all the analysed samples are reported)

Assignment	*Range (cm^{-1})*	*Comment*
ν(C–H)	2951 –2918, 2850	CH_3, CH_2 asymmetric, symmetric
ν(C=O)	1735	Ester
δ(CH_2)	1472	CH_2 scissoring
δ(CH_3)	1463	CH_3 asymmetric
δ(CH_3)	1380	CH_3 symmetric
ν(C–O)	1175	
δ(CH_2)$_n$	730 - 720	with n≥4

Table V - Summary of the results for ships samples

Ship	*Sample*	*N.*	*Organic materials*
B	waterproofing material	15	pitch from *Pinaceae* wood
C	white painted surface	6	beeswax, resin from *Pinaceae*
	waterproofing material	7	pitch from *Pinaceae* wood
	waterproofing material	9	pitch from *Pinaceae* wood
	white painted surface	18	beeswax, pitch from *Pinaceae* wood
	white painted surface	19	beeswax, pitch from *Pinaceae* wood
	red painted surface	45	beeswax, pitch from *Pinaceae* wood
D	caulking material	13	pitch from *Pinaceae* wood
E	white painted surface	39	beeswax, resin from *Pinaceae*
	white painted surface	41	beeswax, pitch from *Pinaceae* wood
F	waterproofing material	37	pitch from *Pinaceae* wood
	waterproofing material	38	pitch from *Pinaceae* wood
	caulking material	43	pitch from *Pinaceae* wood
X	white painted surface	20	beeswax, resin from *Pinaceae*

Discussion

The compositional results obtained from FT-IR analysis of ships samples, as reported in the Table V, show that all the samples collected from the waterproofing and caulking materials of the ships' hulls (7, 9, 13, 15, 37, 38, 43) are tarry materials obtained by distillation of wood containing diterpenoid resin.

The analysis of the forty-five samples of amphorae coating give the same result. These data agree with the literature relating to the use of conifer pitch as waterproofing materials in ancient ships and amphorae [2][4][5].
Samples of painted areas of the ships contain both beeswax and diterpenoid resin (*Pinaceae* resin) which were used as binders (6, 20, 39). Four of them (18, 19, 41, 45) also contain characteristic absorptions of resinous substance that underwent thermal treatments, indicating that these samples contained also traces of waterproofing materials.
The results are confirmed by GC-MS analysis performed by Dipartimento di Chimica e Chimica Industriale dell'Università di Pisa [6][7].

Conclusion

Analysis demonstrate that the waterproofing of the amphorae and the waterproofing and caulking materials of the hulls were performed with a tarry material obtained from the destructive distillation of *Pinaceae* wood using strong heating in absence of oxygen.
The results indicate that a diterpenoid resin from *Pinaceae* family and beeswax were the organic components of the paint present on the hulls of Pisan ships. In some paint samples the presence of pitch is due to the underlying waterproofing treatment.

References

1. Bruni, S., 'The urban harbour of *Pisae* and the wrecks discovered at the Pisa-San Rossore railway station', in S. Bruni (ed.), *Le Navi Antiche di Pisa*, Polistampa, Firenze, (2000) 21-79.

2. Robinson, N., Evershed, R.P., Higgs, W. J., Jerman, K., and Eglinton, G., 'Proof of a pine wood origin for pitch from Tudor (Mary Rose) and Etruscan shipwrecks: application of analytical organic chemistry in archaeology', *Analyst* (1987), **112** 637-643.

3. Pollard, A. M., and Heron, C., 'Archaeological Chemistry', *RCS Paperbacks*, Royal Society of Chemistry, Cambridge, (1996), 239-270.

4. Reunanen, M., Ekman, R., and Heinonen, M., 'Analysis of Finnish pine tar and tar from the wreck of frigate St. Nikolai', *Holzforschung* (1989), **43** 33-39.

5. Mello, E., and Pizzigoni, G., Resine, peci, bitumi, in F. Berti (ed.), *Fortuna maris. La nave romana di Comacchio*, Nuova Alfa, Bologna, (1990), 161-2.

6. Colombini, M. P., Giachi, G., Modugno, F., and Ribechini, E., 'Chemical characterisation of internal coatings of amphorae recovered in the ancient Pisa harbour', in P.A. Vigato (ed.), *Proceedings of the first Meeting "The Science of art", Bressanone (Italy) 25 Febbraio-1 Marzo 2001*, (2002) 303-308.

7. Colombini, M. P., Giachi, G., Modugno, F., Pallecchi, P., and Ribechini, E., 'Characterization of paints and waterproofing materials of the shipwrecks found in the archaeological site of Etruscan and Roman harbour of Pisa (Italy)', *Archaeometry* (2003), **45**(4) 649-664.

Micro Raman Spectroscopy Used for the Study of Corrosion Products on Copper Alloys: Study of the Chemical Composition of Aesthetic Artificial Patinas.

V.Hayez[1], J.Guillaume[2], T. Segato[3], A.Hubin[1], H.Terryn[1]
[1] Department of Metallurgy, Electrochemistry and Materials Science, Vrije Universiteit Brussel, Pleinlaan 2, B-1050 Brussels, Belgium
[2] Institut Supérieur Industriel de Bruxelles, Rue Royale 150, 1000 Brussels
[3] Université Libre de Bruxelles, Service Chimie Industrielle, CP165/63, 50, Av.Fr.Roosevelt, 1050 Brussels

Abstract

Studying the atmospheric corrosion of copper alloy artifacts is important to acquire a better knowledge about the condition of the object and its possible conservation and restoration. The nature of the formed product (e.g. sulfate, carbonate or chloride) depends on factors such as the amount of polluting elements and humidity, but may also depend on the nature of the aesthetic patina applied by the artist.
The composition of the patination solution and the method of patination will both influence the nature of this aesthetic patina, i.e. its chemical composition and morphology. However, although a lot of patination recipes exist, little is known about these patinas. Therefore different surface analysis methods, including X-Ray Diffraction Analysis and Raman spectroscopy, were used to study the characteristics of several patinas obtained on pure copper following several traditional recipes.

Introduction

The term of "patina" has had a lot of different interpretations over time. A patina is usually thought of as an attractive and desirable formation of copper compounds having various colors, most commonly translucent greens and browns.
Patinas have been prized since antiquity for their attractiveness, with an evolution of the color to be appreciated with time. The ancient Greeks, for example, took efforts to maintain their bronzes as a bright metal. Later, thin transparent oxides of brown became a desired patina. In the early part of the 20th century, the popular patina consisted of opaque, dark green surfaces due to exposition to modern atmospheres, especially those containing high amounts of sulfur. Later on, an opaque black patina, which also forms naturally on bronze in sulfur-polluted air, was valued. Currently, we accept both a variety of browns and greens, and even other unnatural colors, but prefer, as did those in the mid-19th century, a translucent effect.
Bronze will naturally and gradually attain these colors from reaction with the environment, making a patina therefore an authenticity guarantee. A way to produce artificial patinas, imitating the natural ones, has therefore been sought after recently.
Artificial patinas can quickly be formed through chemical applications and reactions [1] or through electrochemical processes [2]. These coloration techniques of copper alloys can be used to give objects an ancient aspect and also for restoration purposes, in decoration or architecture projects. For example, in the framework of the restoration of the Garnier Opera in Paris, it was necessary to replace some damaged plates from the copper roof. The plates have naturally corroded in time and present a beautiful green patina. To obtain similarly colored copper plates, various artificial patination methods were investigated. Patinas are usually preserved through application of clear waxes and sometimes a synthetic resin, which is only a temporal solution. If insufficient attention is paid to the maintenance of the object the artificial patina may evolve in time by changing color. This will alter not only the general aspect of the object, but even the composition, with the threat of formation of harmful products. It is thus necessary to investigate the chemical composition and structure of these artificial patinas.
Although a lot of different artificial patination recipes exist, little is known about the resulting patinas. Recent studies[3,4] try to improve this knowledge, more particularly on black patinas.
In this work, several green patinas were produced according to traditional recipes [1]. The composition and morphology of these patinas were investigated by the combined use of various surface analysis methods. To study the visual appearance of the patina, colorimetry, light microscopy and Secondary Electron Microscopy (SEM) analysis were used. Energy Dispersive X-Ray Analysis (EDX) provided elemental information about the composition of the surface components. Finally, molecular information was gathered by a combined use of X-Ray Diffraction Analysis (XRD) and micro-Raman spectroscopy (RS). In this paper however, only the results

concerning the molecular identification are given.
XRD has been used in the field of conservation to identify the composition of crystalline compounds that are present on an object. In order to avoid sampling, the method is confined to the study of small objects, which can be placed directly inside the diffraction chamber. As the whole surface is analyzed, an XRD measurement will provide an average composition.
RS has proved to be a valuable tool for the evaluation of different works of art[5,6]. The main advantages of the technique are its non-destructiveness and suitability for in situ measurements. Furthermore, it has an excellent lateral resolution, allowing measuring very selectively. In recent work this method was successfully used to study the corrosion of excavated metallic objects, identifying copper carbonates such as malachite and azurite and also two copper sulfates, i.e. antlerite and brochantite[7-9]. For example, we managed to apply RS to the study of the atmospheric corrosion of a bronze statuary[10].

Experimental Section

Material

Mr. A. Amarger collected a micro sample on the copper panels from the roof of the Opera Garnier, Paris, France. This sample was studied with RS and its composition identified in order to be able to compare it with the compositions obtained by artificial patination.
Pure copper was used in the artificial patination tests. This choice was made in order to reduce the complexity of the obtained patinas and thus be able to determine the influence of certain parameters of the patination recipes on the final composition and morphology of the patina.
Samples measuring 20mmx20mm were cut from a sheet of pure copper and used for the coloration tests. Before the tests, the samples were polished with abrasive SiC paper (up to 800 grade) and cleaned with acetone in an ultrasonic bath.
To determine the influence on the final patina of the different parameters like chemical compounds in the recipe, or method of patination, only simple patination recipes were experimented, containing little harmless compounds. In all recipes, only distilled water was used. The description of the ingredients and method used in the various recipes are given in Table 1. We refer to the recipes by their reference number in the book of recipes [1].
Three different methods of patination were experimented: immersion, brushing and torch technique. In the first case, the object is immersed for a certain time in a boiling solution. It is removed, washed in hot water and is then left to dry in air.
In the second case, the solution is applied with a soft brush or a soft cloth on the surface of the object and again left to dry in air. This process is repeated once or twice a day for several days, until the desired color is obtained.

patina	ingredients	quantity/100ml	method	hot/cold	time/applications
3.151	NH4Cl	15g	soft cloth	cold	2x a day, 5 days
	NH4CO3	10g			
1.138	CuSO4.5H2O	12.5g	immersion	boil	10 min
	NaClO4	5g			
1.130	CuSO4.5H2O	12.5g	immersion	boil	30 min
	NaClO4	5g			
	FeSO4.7H2O	2.5g			
3.129	Cu(NO3)2.3H2O	20g	soft cloth	cold	2x a day, 5 days
	NaCl	20g			
1.125	Cu(NO3)2.3H2O	20g	soft cloth	cold	2x a day, 5 days
1.123	Cu(NO3)2.3H2O	20g	torch	hot	several applications
1.131	CuCl2.2H2O	5g	immersion	hot	20 min
1.117	Cu(NO3)2.3H2O	2.5g	immersion	boil	2 hours
	NaClO4	10g			

Table 1: description of the various experimented recipes: ingredients and method.

In the torch technique, the desired color is obtained by application of a solution to a preheated metallic surface. This procedure is repeated until the desired color is achieved.
Copper nitrate is an ingredient recurrent in a lot of patination recipes and therefore special attention was paid to these recipes. Besides copper nitrate, recipes containing compounds like copper sulfate (1.138 and 1.130) or ammonia-based products (3.151) were selected.
Recipes 1.123 and 1.125 differ in method, but have the same ingredients. Recipes 1.138 and 1.130 have the same method, but one ingredient is supplementary in recipe 1.130, namely $FeSO_4.7H_2O$. Finally, the influence of the presence of chloride ions can be verified from, for example, the comparison between recipes 3.129 and 1.125.

Methodologies

Due to the small dimensions of the pieces studied, it was always possible to analyze the whole surface of a sample without sampling.
XRD analyses were taken on a Siemens D5000 powder diffractometer, with a Cu (1.5406Å) anti cathode, acquired at 40kV and 40mA. In this paper, no XRD spectra are illustrated. Only the identified compounds are given in Table 2.
The Raman spectrometer is a Dilor XY Raman spectroscope equipped with an Olympus BH2 microscope (50x and 100x objectives were used for simultaneous illumination and collection) and a liquid nitrogen cooled 1024x256 CCD detector. The excitation source is a Coherent Innova 70C Argon/Krypton mixed gas laser (excitation at 514.5 nm). Laser powers are held low at the sample surface to avoid burning of the sample. If necessary the power is slowly and carefully increased in order to improve the signal-to-noise ratio. Integration times range from a few seconds to a few minutes per spectral domain, depending on the sample. Spectra are recorded from 50 to 4000 cm^{-1}. No baseline is subtracted from the recorded spectra. Only a smoothing operation (Adjacent averaging) is performed to enhance readability.
To identify an unknown compound, both in RS and XRD, its measured spectrum is compared to the spectra of reference products, whose compositions are exactly known. In the case of XRD, a large database is available, while for RS it was necessary to use a database created specifically to study the atmospheric corrosion of copper alloys [10,11]. This database contains the Raman spectra of different minerals likely to be formed in this type of corrosion, such as sulfates, but also chlorides or carbonates. These products are not only copper based, but also based on alloying elements like tin, zinc or lead.
For the study of artificial patinas, the database was extended with the Raman spectra of the compounds used in the recipes: copper nitrate, ammonium carbonate, ammonium chloride, iron sulfate and sodium chlorate.

Results and data discussion

To illustrate the use of the database created to study the atmospheric corrosion of copper alloys, the Raman spectra of the copper sulfates are given, together with the Raman spectrum measured on the sample of the Opera roof. The Raman spectra of the ingredients used in the patination solution were added to the database and this extended version was used to study the composition of the artificial patinas. Finally, a comparison is made between the natural and the artificial patinas.

Database

As an illustration, the spectra of some copper sulfates - antlerite $Cu_3(OH)_4SO_4$, brochantite $Cu_4(OH)_6SO_4$, posnjakite $Cu_4(OH)_6SO_4.H_2O$, langite $Cu_4(OH)_6SO_4.2H_2O$ and chalcanthite $CuSO_4.5H_2O$- are given in Figure 1.
The different compounds can easily be differentiated by means of their low-frequency spectrum (<600 cm^{-1}), but most of all by the SO_4^{2-} vibrations (around 900-1000 cm^{-1}) as well as the region of water vibration, at higher frequencies (3100-3700 cm^{-1}). These two last regions will be used to differentiate between the various compounds. A more detailed description of these measurements as well as the exact band positions is given elsewhere [10].
The spectra of the ingredients used in the patination solutions are illustrated in Figure 2.
Table 2 reports the corresponding positions of the bands. Next to these positions the relative intensities of the bands are given, characterized as being very strong (vs), strong (s), medium (m), weak (w), very weak (vw), broad (br) and shoulder (sh).
From Table 2 and Figure 2, it is seen that the different compounds can be differentiated by means of their totally different spectrum. Copper sulfate and iron sulfate both present the typical SO_4^{2-} vibrations (around 900-1000 cm^{-1}).

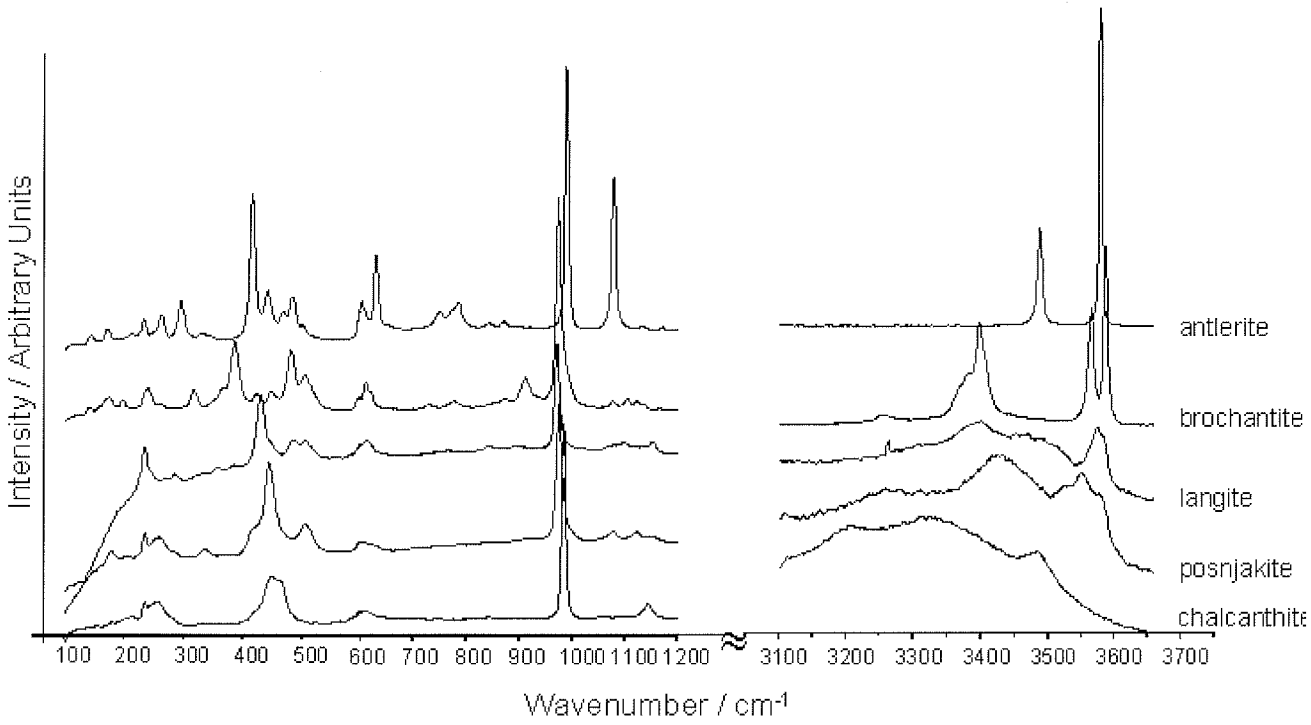

Figure 1: Raman spectra obtained on the reference copper sulfates included in the database.

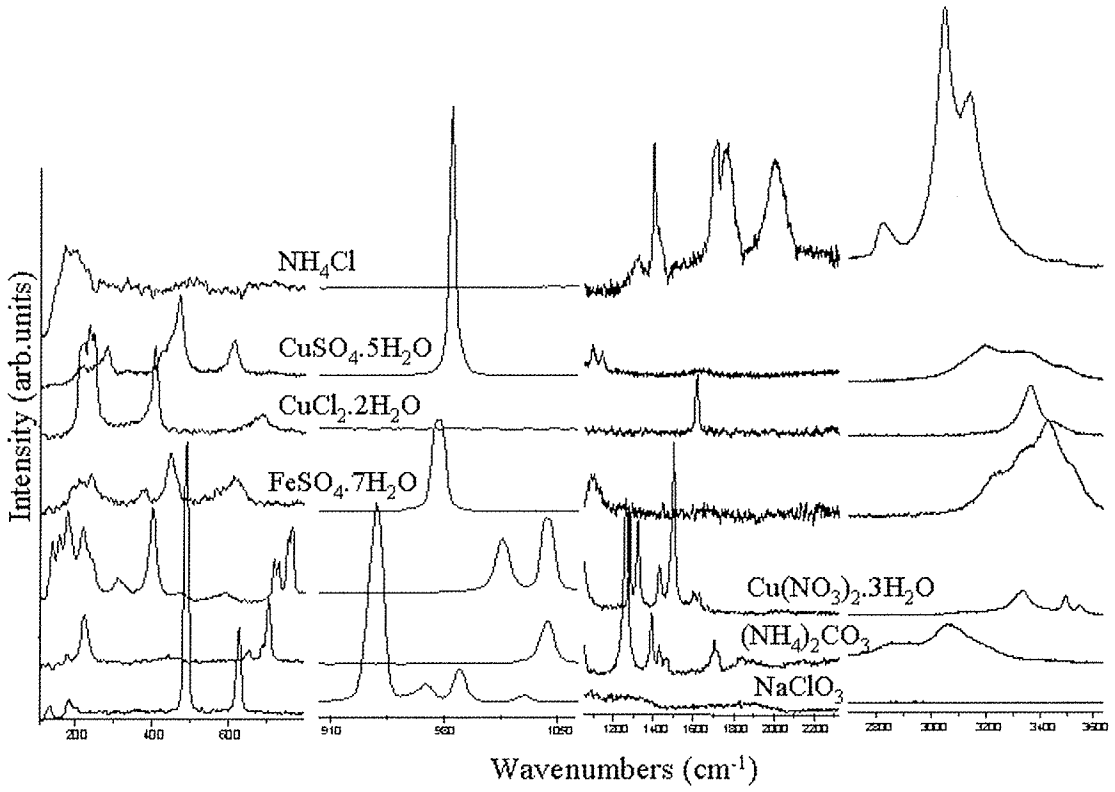

Figure 2: Raman spectra obtained on the various ingredients of the patina solutions: copper nitrate, ammonium carbonate, ammonium chloride, iron sulfate, copper sulfate and sodium chlorate.

Copper nitrate has an important band at 1044 cm^{-1}, corresponding to the NO stretch of the NO_3^- group. Copper chloride presents a strong band at 407cm^{-1}, typical for the Cu-Cl stretch. Ammonium carbonate has its most important band around 1000 cm^{-1}, corresponding to the CO stretch vibration. Ammonium chloride has a very strong signal in the high frequency region, like copper chloride.

Use of the Raman database to study the patina of the Garnier Opera

Cu sulf	Cu nitr	Cu chlor	NH4 carb	NH4 chlor	Na chlorate	Fe sulf.
130vw	114vw	222w	116vw	189m	135w	209w
155vw	141w	243s	132vw	511w	184w	244w
182vw	159w	407s	156vw	1315w	201w(sh)	378w
215vw	179s	687m	179vw	1404w	490vs	448w
236m	221br	1619m	224s	1717m	628s	613w
258m	240m(sh)	3360s	360vw	1767m	938vs	975vs
370vw	314w	3438s(sh)	381vw	2003m	969s	1094w
452m	402s		443w	2818m	990s	3244m(sh)
460m(sh)	477w		471vw	3046vs	1030m	3358m(sh)
524vw	590w		653vw	3139s(sh)		3433s
555vw	719m		689w			3513m(sh)
567vw	731m		703s			
610w	756m		1043vs			
844vw	765s		1264s			
918vw	791vw		1394m			
983s	802vw		1429w			
1058vw	820vw		1459w			
1097vw	1016vs		1472w			
1144m	1044vs		1705m			
3202s	1282m		1836w			
3326s(br)	1323m		2549m			
3483s	1431m		2855m			
	1502s		2920m			
	1606vw		3060s			
	1630vw					
	3117vw					
	3335s					
	3495m					
	3549w					

Table 2: Raman band positions for the various ingredients of the recipes: Cu sulf = copper sulfate CuSO4.5H2O, Cu nitr = $Cu(NO_3)_2.3H_2O$, Cu chlor = $CuCl_2.2H_2O$, NH_4 carb = $(NH_4)2CO_3$, NH_4 chlor = NH_4Cl, Na chlorate = $NaClO_3$, Fe sulf = $FeSO_4.7H_2O$.

The same spectrum was recorded all over the surface. This spectrum is given in Figure 3.
The measured spectrum presents the characteristics of hydrated copper sulfates, namely the typical vibrations of the SO_4^{2-} group around 980 cm^{-1}, as well as the vibrations of water around 3500 cm^{-1}. The quality of the spectrum in the low frequency region is worse than in the other regions so it cannot be used in identification. From the comparison between the spectra of the various copper sulfates on Figure 1 and this measured spectrum, it is possible to identify that the corrosion product present on the roof is antlerite.

Use of the extended Raman database to study the artificial patinas

The compounds identified with RS and XRD on the various patinas are summarized in Table 3.
On samples 1.138 and 1.130 antlerite alone was identified, although in 1.130 a supplementary ingredient, iron sulfate, was added to the recipe. Samples 1.123 and 1.125 have the same ingredients (copper nitrate and distilled water), but a different application method (torch, resp. soft cloth). Both present the same spectrum of a copper nitrate, however different from the copper nitrate used in the patination solution. To identify the composition of this copper nitrate,

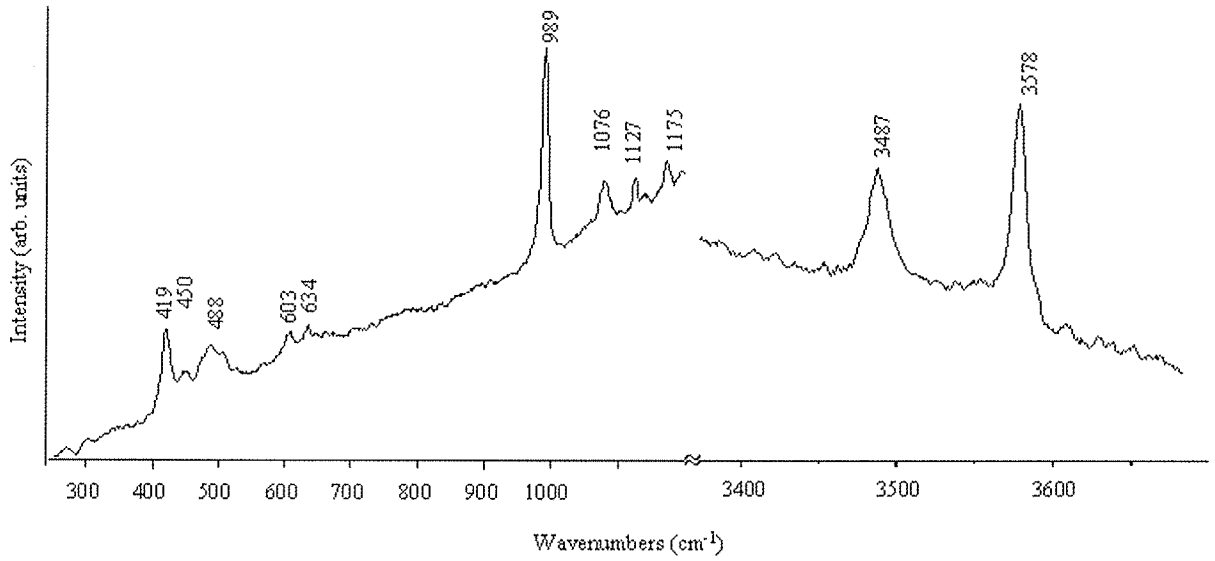

Figure 3: Raman spectrum measured on the green patina of the copper roof of the Garnier Opera in Paris, France.

it was necessary to perform an XRD analysis. As the same Raman spectrum was recorded on the whole sample and XRD analysis only identified one compound, namely gerhardtite, $Cu_2(NO_3)(OH)_3$, the Raman spectrum was linked to this compound. The same spectrum was also recorded on patina 1.117, produced with copper nitrate in combination with sodium chlorate.

As soon as chloride ions are present in the patination solution, copper chloride compounds are found in the artificial

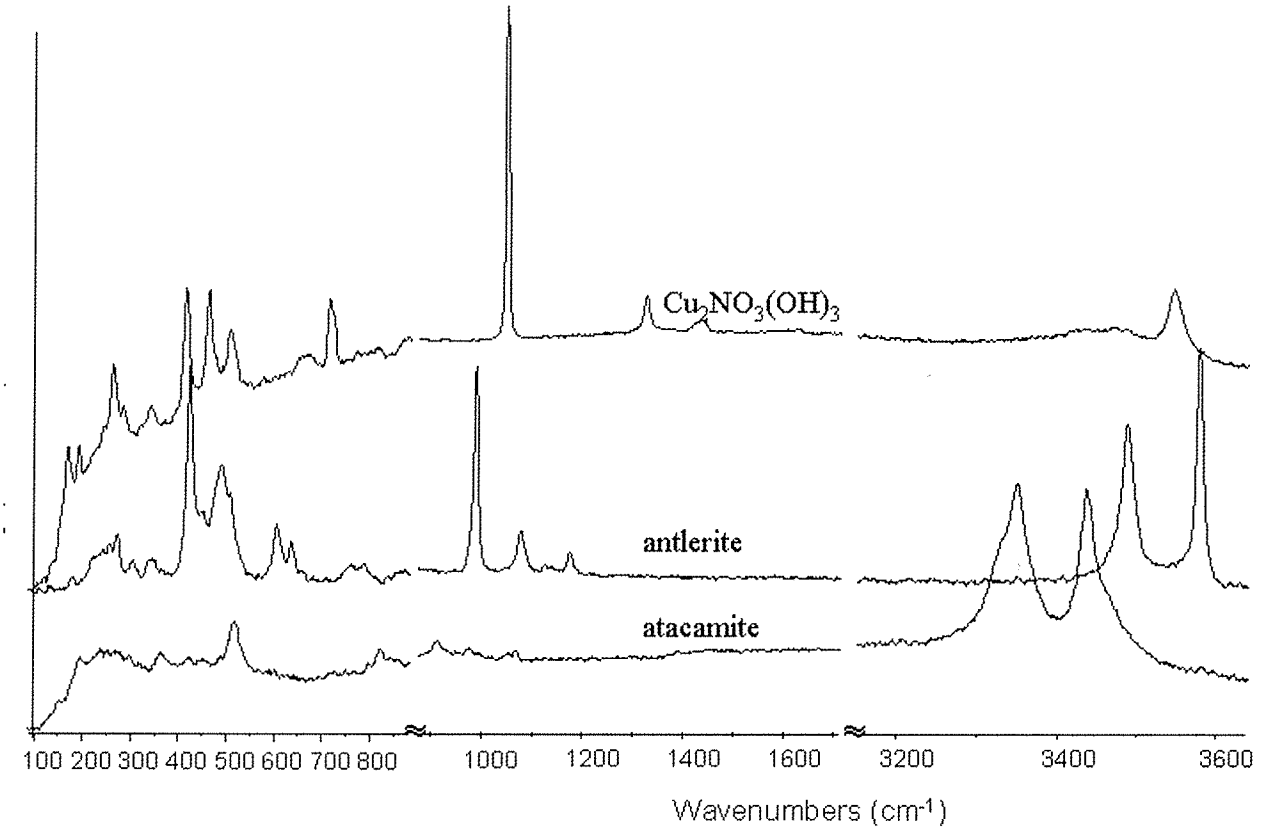

Figure 4: spectra of the various compounds recorded on the different patinas. From top to bottom: gerhardtite, $Cu_2(NO_3)(OH)_3$, present on patinas 1.123, 1.125 and 1.117; antlerite present on patinas 1.130 and 1.138; atacamite present on patinas 3.151, 3.129 and 1.131.

sample	Raman spectroscopy	XRD analysis
3.151	atacamite	atacamite
1.138	antlerite	antlerite
1.130	antlerite	antlerite
3.129	atacamite	atacamite, CuCl
1.125	Cu2(NO3)(OH)3	Cu2(NO3)(OH)3
1.123	Cu2(NO3)(OH)3	Cu2(NO3)(OH)3
1.131	atacamite, CuCl	CuCl
1.117	Cu2(NO3)(OH)3	Cu2(NO3)(OH)3, CuCl

Table 3: compounds identified on the various samples with RS and XRD.

gerhardtite	antlerite	atacamite
167m	84vw	197vw
189w	111vw	235vw
2261m	132vw	255vw
281w	177vw	272vw
343w	241m	287vw
414m	256m	315vw
461m	271w	363vw
508m	304w	389vw
714m	345w	420w
725w	366w	451w
1050vs	422vs	517m
1326s	448m	821m
1430w	488m	915m
3470m	506m	979m
3544s	605m	1060m
	634m	3350s
	758w	3436s
	788w	
	990vs	
	1078m	
	1126w	
	1174m	
	3488s	
	3580s	

Table 4: overview of the positions of the bands for the three different compounds identified with RS.

patinas. Atacamite was both identified with XRD and RS on samples 3.151 and 3.129. XRD identified CuCl on patinas 3.129, 1.131 and 1.117. This was only possible with Raman on 1.131, the quality of the recorded spectra being most of the time too low. Furthermore, on this sample, RS identified also atacamite, which was not seen by XRD. This can be due to a lack of sensitivity if the amount of atacamite present is too low.
The spectra of these 3 compounds, gerhardtite, antlerite and atacamite, are given on Figure 4.
The exact band positions of these products as measured on the patinas are given in Table 5.
Regarding the chemical composition only, artificial patinas consisting of pure antlerite (1.138 and 1.130) are the best suited to replace the original patinas from the roof of the Opera, as both have the same composition. However, the restorer in charge did not retain this option. Indeed, the results of supplementary color analyses, which are not given here, evidenced a difference in color between natural and artificial patina. Furthermore, it is not known how these artificial patinas will change when exposed to the atmosphere. Changes in color, but also in composition, are possible. Therefore, it was preferred to apply a better-known and stable paint layer.

Conclusion

In this work, Micro-Raman spectroscopy was successfully used in combination with X-Ray diffraction analysis to study the corrosion products of the natural patina formed on copper alloys after exposure to the atmosphere. To identify their chemical composition, a database containing the Raman spectra of various copper based compounds was set up and proved to be complete and efficient, as illustrated by the analysis of a micro-sample from the patina of the Garnier Opera roof.
However, a patina can also be artificially applied for aesthetic reasons or restoration purposes. Lots of different production modes exist, although little is known about the final result. Several green patinas were therefore realized on samples of pure copper, according to traditional recipes. Again, RS and XRD analysis successfully determined their chemical composition. Depending on the ingredients of the patination solution, 4 different compounds were identified on the artificial patinas: gerhardtite, $Cu_2(NO_3)(OH)_3$; atacamite

$Cu_2(OH)_3Cl$, nantokite CuCl and antlerite $Cu_3(OH)_4SO_4$.
No difference in composition was observed when using different methods. However, a discrepancy in morphology or a color distinction are still possible and have to be investigated. For this purpose, it is necessary to combine RS with other methods, like for example colorimetry or SEM/EDX. The combination of these various surface analysis methods provides a complete and efficient tool to gain a better knowledge of artificial patinas. Future work will use this tool to further investigate the chemical and structural characteristics of the artificial patinas and their suitability for restoration purposes.

Acknowledgements

Research is financed by the IWT: Institute for the Promotion of Innovation through Science and Technology in Flanders (IWT-Vlaanderen)
The authors wish to thank Mr. Antoine Amarger for his precious help and advice.

References

1. Hughes R., Rowes M., *The colouring, bronzing and patination of metals: a manual for fine metalworkers, sculptors and designers*, 2nd ed. (1991), Thames and Hudson, London, 1982

2. Constantinides, I., Adriaens, A. and Adams, F., 'Surface characterization of artificial corrosion layers on copper alloy reference materials', *Applied Surface Science*, (2002) **189** 90-101

3. Balta, I.Z., Robbiola, L., 'Study of black patinas on copper and bronze obtained by using 19th century Western traditional techniques of artificial patination', article to be published

4. Aucouturier, M., Keddam M., Robbiola, L., Takenouti, H., 'Les patines des alliages de cuivre: processus naturel ou oeuvre de l'homme?', *Techné*, (2003) **18** 86-84

5. Cariati, F., Bruni, S., 'Raman Spectroscopy' in Ciliberto, E., Spoto, G., '*Modern analytical methods in art and archaeology*' Chemical Analysis vol 155, Wiley Interscience (2000) 255-278

6. Smith, G.D., Clark, R.J.H., 'Raman microscopy in art history and conservation science', *Reviews in conservation* (2001) **2** 92-106

7. Bouchard-Abouchacra M., 'Evaluation des capacités de la microscopie Raman dans la caractérisation minéralogique et physico-chimique de matériaux archéologiques: métaux, vitraux & pigments', PhD thesis, Muséum National d'Histoire Naturelle, Laboratoire de Minéralogie, Paris (2001), unpublished.

8. McCann, L.I., Trentelman, K., Possley, T., Golding, B., 'Corrosion of ancient Chinese bronze money trees studied by Raman microscopy', *J. Raman Spectroscopy*, (1999) **30**(2) 121-132

9. Di Lonardo, G., Martini, C., Ospitali, F., Poli, G., Prandsraller, D., Tullini, F., 'Micro-Raman and Micro-IR Spectroscopy for the study of corrosion products on archaeological bronze objects', in Van Grieken R. *et al.*(eds), *Proceedings of the 7th international conference on non destructive testing and micro analysis for the diagnostics and conservation of the cultural and environmental heritage, Antwerpen, 2002*, University of Antwerp, Antwerp (2002)

10. Hayez, V., Guillaume, J., Hubin, A., Terryn, H., 'Micro-Raman spectroscopy for the study of corrosion products on copper alloys: setting up of a reference database and studying a few works of art', article, *J. Of Raman Spectroscopy*, to be published

11. Hayez, V., 'Database of Raman spectra', database, Vrije Universiteit Brussel, unpublished.

Infrared Spectroscopic Study of Some More metal Soaps

Christoph Herm
Dresden Academy of Fine Arts, D-01288 Dresden, Germany.

Abstract

Metal soaps occur as components of oil colours as well as other materials from artefacts. Infrared spectra of the stearates of aluminium, calcium, magnesium, cadmium, manganese, cobalt, and sodium are reported as a supplement to data published elsewhere. In addition, infrared spectra of the azelates of copper, cadmium, zinc and lead are given. The data is discussed with respect to the identification of metal soaps in oil paint. The investigation of Raffaelli solid oil colour is presented as a related case study.

Introduction

Metal soaps as components of oil colours or from other sources connected to art and archaeology recently have attracted increased attention. They are defined as salts of monobasic carboxylic acids combined with alkaline earth metals or heavy metals. Metal soaps are insoluble in water. They show various solubility in organic solvents and increased mobility as compared to an oil paint network.[1]
The sources for metal soaps in paint can be summarized as follows:
- reaction of free fatty acids with basic pigments (Pb-, Zn-, Cd-, Ca-compounds) or drying agents (salts of Pb, Zn, Mn, and Co); [2]
- drying agents themselves (e.g. lead carboxylates)
- reaction of "mature" (hydrolyzed) oil binder with pigments or drying agents; [3]
- soap (sodium or potassium salts of fatty acids) as emulsifier in tempera paint formulations and subsequent reaction with heavy metals. [4]
Particular interest has been laid on the formation of aggregates of lead or zinc carboxylates in paint layers, described as "protrusions". Furthermore, their typical infrared absorption bands could be used for FT-IR imaging. [1, 5]
A collection of FT-IR spectra of palmitic-, stearic-, oleic-, and linoleic acids and their salts with copper, zinc, and lead were published by Robinet and Corbeil [6]. The main diagnostic features of the infrared spectra are:
- carboxylate stretching bands: asymmetric ν_aCOO at around 1600 – 1500 cm^{-1} and symmetric ν_sCOO at around 1400 cm^{-1};
- a series of methylene wagging modes coupled to the carboxyl vibrations (δCH_2) at 1310 – 1185 cm^{-1}; the number of absorptions depending on the chain length.
It is one aim of this paper to present additional IR-spectroscopic data of metal carboxylates in order to support their identification in samples from artefacts, particularly in paint samples.
Azelaic acid (HOOC-$(CH_2)_7$-COOH) is formed during the drying process of drying oils by oxidative cleavage of unsaturated fatty acids. While first being attached with one end to the network, the azelate moiety is liberated by hydrolysis of the glycerol ester bond. [7] It is therefore likely that oxidized and hydrolyzed oil paint films form metal salts of azelaic acid analogously to the way described above for monocarboxylic acids. Although these azelates do not match exactly the definition for metal soaps, they have similar properties such as insolubility in water. The second aim of this paper is to present spectral data of some metal azelates and to compare it with the data of metal soaps.
Finally, a case study shows application of spectroscopic data of metal soaps. "Raffaelli solid oil colour" were solid sticks, introduced by Jean-Francois Raffaelli in 1902 and available until about 1920. [8] Three samples from original Raffaelli solid oil colours from about 1906, kindly provided by Winsor & Newton Ltd (Harrow, UK) were investigated by FT-IR spectroscopy and other appropriate analytical methods.

Experimental

Materials
The *stearates* of calcium, cadmium, cobalt, magnesium, manganese and lead were precipitated from a solution of sodium stearate (Fluka 58780) 1% in water / ethanol (95:5 v/v) by adding 1/2 equivalent of an aqueous solution of $CaCl_2$, $Cd(NO_3)_2$, $CoSO_4$, $MgCl_2$, $MnSO_4$, or $Pb(NO_3)_2$, respectively at 100 °C. After cooling the precipitates were

filtered and subsequently washed with water and methanol and dried on air at 60°C. Calcium and Manganese stearates were recrystallized from toluene. Aluminium monostearate ($Al(C_{18}H_{35}O_2)(OH)_2$, Fluka 6270), sodium stearate (Fluka 85780) and zinc stearate (Merck Darmstadt 108865) were commercial products. A lead soap was obtained by reaction of an aqueous solution of a solid household soap with a solution of $Pb(NO_3)_2$ and isolation as described above.
The *azelates* of cadmium, copper, lead, and zinc were prepared by dissolving azelaic acid with 2 equivalents NaOH in water at a concentration of c. 0.1 mol/l, and subsequently adding 1 equivalent of an aqueous solution of $Cd(NO_3)_2$, $CuSO_4$, $Pb(CH_3CO_2)_2$, or $ZnSO_4$, respectively at 100 °C. The precipitates were isolated as described above.

Method
All samples were prepared in a diamond anvil cell (High Pressure Diamond Optics). FT-IR spectra were recorded in transmission mode using a Perkin Elmer System 2000 spectrometer connected to a PE i-series microscope with MCT detector (4000 – 580 cm^{-1}, resolution 4 cm^{-1}, sum of 32 spectra). The given spectra are smoothed and base-line corrected.

Results

Stearates
Figure 1 shows the full infrared spectra of the stearates of calcium, cadmium, and cobalt representing typical, yet differing metal soap spectra. As seen in the spectrum of cobalt stearate, the carboxylate absorption can be broad, even though this sample has the same degree of purity as the others with sharp bands.
Table 1 gives the exact infrared absorption bands in the range 1600 – c. 1400 cm^{-1} of all investigated stearates. These values are also shown in Figure 2 for more convenient use. The absorption of the asymmetric carboxylate stretch ranges from 1588 cm^{-1} (for aluminium monostearate) to 1513 cm^{-1} (for lead stearate). The stearates of lead and calcium show doublets. The symmetric carboxylate band covers a narrower range of 1433 – 1397 cm^{-1}.
Like saturated fatty acids, the metal stearates show a series of almost equally-distanced weak absorptions in the range 1345 – 1180 cm^{-1} which are due to methylene wagging modes coupled to the carboxyl group (δCH_2). The intensity of these bands seems to depend on one hand, on the nature of the metal [6]. The most intense patterns were found for Na, Mn, and Pb (Figure 3), but the pattern is also present in spectra of Ca, Cd, and Co sterates (Figure 1). On the other hand it is clear that the purity of the carboxylate affects the differentiation of these absorptions. For comparison, the infrared spectra of a commercial solid sodium soap (with mixed carboxylates) and its lead derivative were measured. Here this pattern is not visible (Figure 4), in contrast to the pure stearates of the same metals.

Azelates
Figure 5 shows the full infrared spectra of the azelates of copper, cadmium, zinc, and lead. In general, the spectra show the same features as the stearate spectra. Due to the lower stoichiometric ratio of methylene/carboxyl groups of the azelates as compared to stearates the intensity of the alkyl bands (νCH) is lower than the intensity of the carboxyl absorption (ν_a / ν_s COO). Table 1 gives the carboxyl absorption absorption values of the azelates. The position of the asymmetric carboxylate absorption for azelates depends on the type of the metal following the same tendency as with the stearates: Copper azelate has the highest value, and lead has the lowest, whereas the other values do not match exactly. The ν_a COO absorption of zinc azelate shows a doublet. In most cases (except zinc) the symmetric carboxylate absorption coincides with a methylene deformation band in the range 1440 – c. 1400 cm^{-1}. The methylene wagging modes (1345 – 1180 cm^{-1}) show a complex pattern with higher intensity as compared to the stearates.

Case study
Figure 6 shows the infrared spectra of two "Raffaelli solid oil colour" sticks from c. 1906. Both spectra are dominated by strong alkyl bands (ca. 2920 / 2850 cm^{-1}) and an ester carbonyl absorption at c. 1740 cm^{-1}. The spectrum of stick "tint 28" additionally exhibits a strong carbonyl band at 1712 cm^{-1} which indicates free fatty acids. The binding medium of "Raffaelli solid oil colour" is composed of linseed oil and Japan wax, the latter consisting mainly of glycerol tripalmitate and higher homologues. [8] This can explain the strong ester bands in both spectra. The triglycerides can release fatty acids upon hydrolysis, which may account for the acids (ν_a at 1712 cm^{-1}) in the spectrum of sample "tint 028". Pigment analysis of this paint [8] revealed no basic pigment (only iron oxide, barytes,

gypsum, glass, and strontium carbonate), thus the free fatty acids were preserved.
In contrast, the spectrum of stick "tint 171" has strong absorptions at around 1586 cm^{-1} and 1540 cm^{-1} (shoulder). These bands can be attributed to carboxylates, the latter to zinc soaps. Pigment analysis [8] revealed a high amount of zinc white (ZnO) besides iron oxide red and yellow and synthetic ultramarine. Probably zinc oxide has reacted with the free fatty aids in this stick and the free carboxylic acid absorption is replaced by the carboxylate bands. The strong, broad infrared absorption at 1586 cm^{-1} could be an aluminium or copper soap. This extensive absorption up to 1540 cm^{-1} matches also to the doublet of calcium stearate (1577 / 1541 cm^{-1}). However, none of these metals were detected by X-ray fluorescence (ED-XRF).

Discussion

The infrared spectra of ten different stearates given in this paper confirm the dependence of the asymmetric carboxylate stretch absorption on the nature of the cation [6]. There seems to be a trend in the correlation of the asymmetric carboxylate stretch absorption frequency to the ionic radius of the metal (Table 1, Figure 2): The largest cation (Pb^{2+}) results in the lowest frequency and vice-versa (as for Al^{3+}). However, the relation is not as simple, because other factors like the coordination state of the metal in the carboxylate complex influence the vibration frequencies as well. For example, literature [6] reports an increased absorption wavenumber of copper soaps (around 1580-1590 cm^{-1}) which is explained by the covalent character of the copper-carboxylate bond. A lower value (1560 cm^{-1}) is reported for copper linolate as well [9].
The metal stearates show an equidistant pattern of methylene wagging absorptions (δCH_2) in the region 1345 – 1180 cm^{-1}. In comparison to literature [6] an expanded spectral region according to [10] is applied here. The number of these progression bands (m) for long chained carboxylic acids is related to the number of carbon atoms in the acid (n) by the rules:
m = n/2 (for even n) and
m = (n+1)/2 (for odd n). [10]
It can be seen that this rule also holds for Na, Mn, and Pb stearates (n = 18) spectra with nine absorption bands (Figure 3). Data from [6], when re-examined on the range 1345 - 1180 cm^{-1} also follow this rule for Zn and Pb stearates as well as stearic and palmitic acids. Furthermore, this rule holds for Cu, Pb, and Zn palmitates (n = 16) with eight absorption bands [11].
The investigated azelates generally show infrared spectra comparable to those of the stearates. Again, the frequency of the asymmetric carboxylate absorption is related to the type of metal. The methylene wagging modes of the azelates in the region 1345 – 1180 cm^{-1} do not follow a simple rule as given above for the longer-chained monocarboxylic compounds.
Absorption bands at relatively high values at around 1580 cm^{-1} frequently appear in oil paints. They show evidence for metal soaps, but can not be explained satisfactorily yet. A shift of the asymmetric carboxylate absorption to higher frequencies is attributed to oxidation, and a "featureless plateau" at 1550 – 1600 cm^{-1} was described for zinc soap containing paint. [1] For cured or aged oil paints containing lead white the formation of carboxylate absorptions at 1620 and c. 1540 cm^{-1} are reported in the literature [12], whereas absorptions at c. 1540 – 1510 cm^{-1} for lead soaps should be expected. Thus, the strong, broad absorption at c. 1586 cm^{-1} for the Raffaelli solid oil colour stick "tint 171" can be explained by some oxidized zinc carboxylates of unknown composition. Generally, this issue needs further investigation.
Determination of the metal cation in the carboxylate is not possible by the commonly used gas chromatography. Infrared spectroscopy has proved a powerful and complementary tool for the characterization of metal soaps, because the position of the asymmetric carboxylate infrared absorption is related to the type of metal cation. However, this is not sufficient for the identification of metal cation, as some metals lead to similar values (e.g. Na, Co, Mn, Cd, Mg in the range 1555 – 1575 cm^{-1}). A detailed examination of the methylene wagging absorption frequencies can give hints to the chain length of the carboxylate, though only applicable in the case of pure substances like in protrusions. [1, 5]

Acknowledgements

The author wishes to thank Laurianne Robinet for kindly making available spectral data. Special thanks to Marianne Taubert for making possible further measurements with the infrared spectrometer at the Swiss Institute for Art Research at Zurich.

References

1. van der Weerd, J., Geldof, M., van der Loeff, L. S., Heeren, R. M. A., Boon, J. J., 'Zinc Soap Aggregate Formation in 'Falling Leaves (Les Alyscamps)' by Vincent van Gogh', *Zeitschrift für Kunsttechnologie und Konservierung* (2003) **17**(2) 407-416.

2. Caldwell, M., 'Some developments in british paint manufacture over the last two hundred years, and the occurrence of white surface deposits on paintings' in *Deterioration of Artists' Paints: Effects and Analysis, joint meeting of ICOM-CC Working groups Paintings 1 & 2 and the Paintings Section, UKIC, London 10 – 11 September 2001,* 9-13.

3. van den Berg, J. D. J., van den Berg, K. J., Boon, J. J., 'Chemical changes in curing and ageing oil paints' in Bridgland, J. (ed.), *ICOM Committee for Conservation 12th Triennial Meeting, Lyon, 29 August – 3 September 1999,* James and James (Science Publishers), London (1999) 248-253.

4. Bosshard, E., Mühlethaler, B., 'Bindemittel in der Staffeleimalerei des 19. Jahrhunderts', *Zeitschrift für Kunsttechnologie und Konservierung* (1989) **3**(1) 41-99.

5. van der Weerd, J., Boon, J. J., Geldof, M., Heeren, R. M. A., Noble, P., 'Chemical Changes in Old Master Paintings', *Zeitschrift für Kunsttechnologie und Konservierung* (2002) **16**(1) 36-52.

6. Robinet, L., Corbeil, M.-C., 'The Characterization of Metal Soaps', *Studies in Conservation* (2003) **48**(1) 23-40.

7. Mills, J. S., White, R., *The Organic Chemistry of Museum Objects, 2nd ed.,* Butterworth Heinemann, Oxford (1994) 39-40.

8. Gros, D., Herm, C., 'Die Ölfarbenstifte des J.-F. Raffelli', *Zeitschrift für Kunsttechnologie und Konservierung* (2004) **18**(1), 1-28.

9. Gunn, M., Chottard, G., Rivière, E., Girerd, J.-J., Chottard, J.-C., 'Chemical reactions between copper pigments and oleoresinous media', *Studies in Conservation* (2002) **47**(1) 12-13.

10. Socrates, G., *Infrared Characteristic Group Frequencies, 2nd edition,* John Wiley & Sons, Chichester (1994) 90-91.

11. L. Robinet, unpublished data (by personal communication, Nov. 11, 2001).

12. Meilunas, R. J., Bentsen, J. G., Steinberg, A., 'Analysis of Aged Paint Binders by FTIR spectroscopy', *Studies in Conservation* (1990) **35**(1) 33-51.

metal	ionic radius [pm]	ν_a COO		ν_s COO	
		stearate	azelate	stearate	azelate
Al(m)	50	1588		1415	
Cu	72	1586*	1587	1422*	1434
Ca	99	1577, 1541		1433	
Mg	65	1572		1415	
Cd	97	1570, 1550sh	1547	1420	1425, 1397
Mn	80	1564		1432	
Co	74	1563		1413	
Na	95	1557		1420	
Zn	74	1539	1556, 1536	1397	1406, 1398
Pb	121	1541, 1513	1514	1419	1403

Table 1. Infrared absorption bands [cm^{-1}] in the region 1600 – c. 1400 cm^{-1} of metal stearates and azelates and ionic radii (Pauling) of the metal cations. *) data from [6] Al(m) = aluminium monostearate.

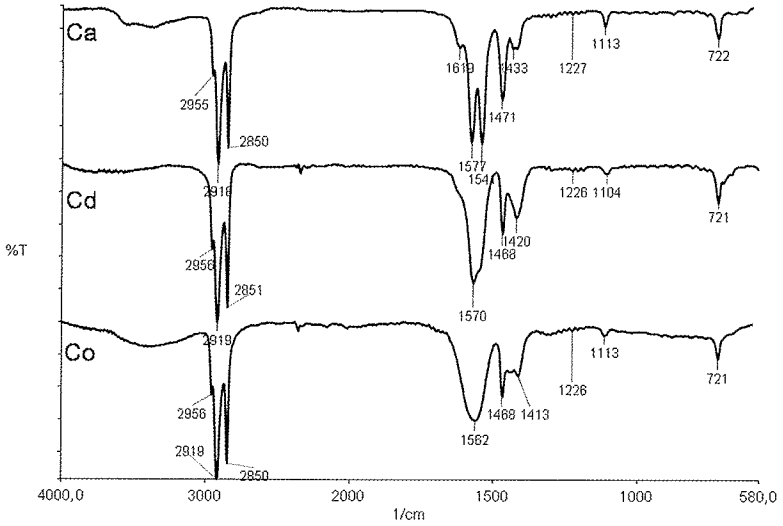

Figure 1. Infrared spectra of metal stearates as indicated in the diagram.

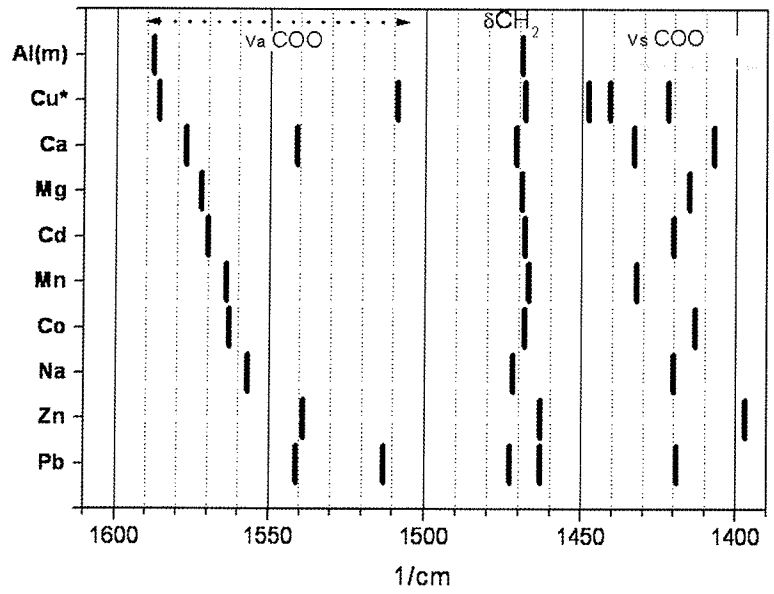

Figure 2. Infrared absorption bands [cm^{-1}] of metal stearates (values from Table 1).
*) data from [6] Al(m) = aluminium monostearate

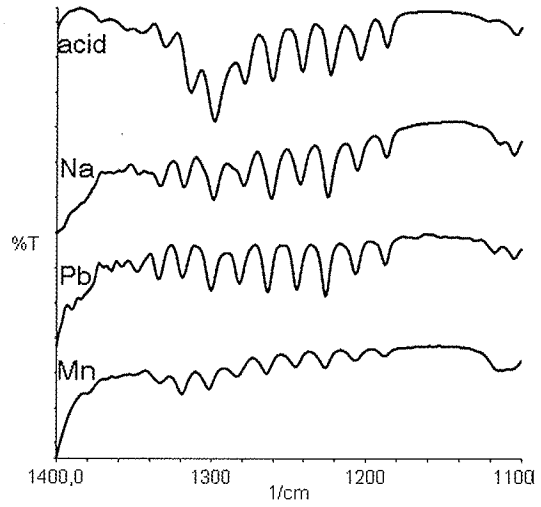

Figure 3: Infrared spectra of stearic acid and metal stearates as indicated in the diagram in the region 1400 – 1100 cm^{-1}.

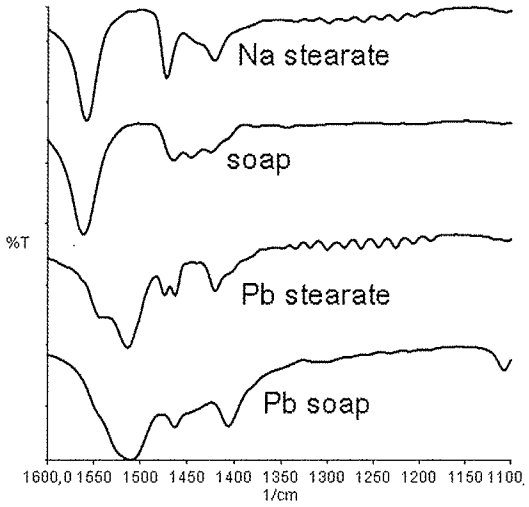

Figure 4: Infrared spectra of metal soaps as indicated in the diagram in the region 1600 – 1100 cm^{-1}.

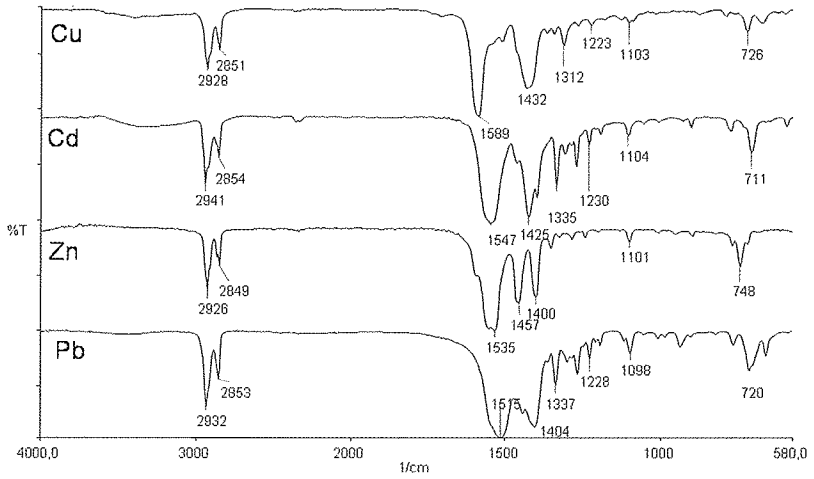

Figure 5. Infrared spectra of metal azelates as indicated in the diagram.

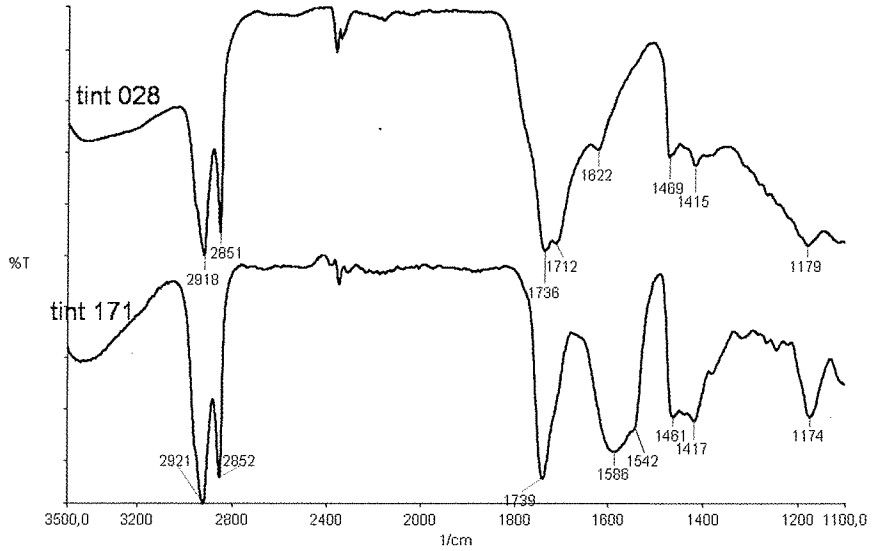

Figure 6. Infrared spectra of two "Raffaëlli solid oil colour" sticks: tint 28 = "Burnt sienna", tint 171 = "Caledonian Brown".

FTIR Spectra of Iridescent Art Nouveau Glass Artifacts

D. Jembrih-Simbuerger[1], M. Schreiner[1], M. Peev[2], P. Krejsa[2], Ch. Clausen[3]
[1]Science and Technology in Art, Academy of Fine Arts, Schillerplatz 3, A-1010 Vienna, Austria
[2]Austrian Research Centers Seibersdorf, A-2444 Seibersdorf, Austria
[3]Schinzlgasse 3, A-2500 Baden, Austria

Abstract

Measurements using Fourier transform infrared spectroscopy (FTIR) with subsequent multivariate statistical evaluation of the data enable the identification and classification of the iridescent Art Nouveau glass. Therefore, the spectra of about 600 glass fragments were collected on both the iridescent and non-iridescent sides of the fragments. Glass fragments of the New-York Historical Society/USA, the Passau Glass Museum/Germany, and private collectors were available. Additionally, half products and tiles manufactured by Loetz/Austria of the Museum of Applied Arts in Vienna/Austria were analysed. FTIR analysis was carried out in transmission and reflection modes.
In this work the FTIR-spectra of the Art Nouveau glass manufactured by Tiffany/USA and Loetz/Austria are presented and compared. It was found that the spectra collected in the transmission mode reflect mainly the information of the bulk glass, whereas the spectra taken in the reflection mode contain information of the surface and the bulk glass. Additionally, the results of the multivariate statistical evaluation of the FTIR spectra by using principal component analysis (PCA) algorithm are presented, where the essential information and a reduction of the original data sets could be achieved. Fisher projection (canonical variate analysis) was used to perform classification by a self written code package.

Introduction

The increasing interest in iridescent Art Nouveau glass [1] among public and private collections as well as the mounting number of imitations of this glass requires a clear classification and identification of the provenance of these objects. In the past, these determinations were made primarily by aesthetic and stylistic evaluations and by comprehensive archival studies. However, scientific analysis has become more important in distinguishing the originals from the copies which are created perfectly enough to deceive even experts. Therefore, scientific investigations of iridescent Art Nouveau glass made by Tiffany/USA, Loetz/Austria, Strini Art Glass/USA and Jack Ink/Austria have been carried out at various research institutions. One goal of these investigations was to determine the provenance and authenticity of the glass based on several non-destructive analytical techniques supplemented with efficient statistical evaluation procedures [2]. Thus, energy-dispersive X-ray fluorescence analysis (EDXRF) and Fourier transform infrared spectroscopy (FTIR) were applied for the characterization of the glass objects in a non-destructive way. This means that the analysis was carried out without sampling from the objects, which might have resulted in a significant reduction in their historical and pecuniary value. The analysis did not change or affect the chemical composition of the pieces investigated.

Experimental

FTIR spectroscopy
FTIR spectroscopy can provide information about the chemical compounds and the chemical bonds in glass. The spectra are like fingerprints for each manufacturer and can be used in subsequent statistical evaluations. The investigations were performed with a Perkin Elmer Spectrum 2000 instrument equipped with a DTGS detector, which enables measurements in the middle infrared range (between the wave numbers 7400 and 380 cm^{-1}). The spectra of the iridescent and non-iridescent surfaces of about 600 glass fragments were taken in transmission (4500-1500 cm^{-1}) and reflection mode (2500-370 cm^{-1}). The analysed fragments were made by the manufacturers Tiffany, Loetz, Jack Ink, Frederick Carder (Aurene), and some unidentified producers. In order to characterise the iridescent glass surface of the glasses showing inhomogeneous surface patterns, a selected subgroup of the samples was analysed using FTIR microscopy (Perkin Elmer, i-series, MCT detector) in reflection mode.

Results of the FTIR investigations

Fig. 1 shows the transmission spectra of the Loetz tile So Gl 12 and the Tiffany glass fragment T1. Due to the fact that there is no difference in transmission spectra between the non-iridescent and iridescent glass side, it could be found that the spectra collected in the transmission mode (4500-1500 cm^{-1}) contain mainly the information from the bulk glass. In Fig. 2 the spectra were taken in the reflection mode (2500-370 cm^{-1}) on the same glasses as mentioned in Fig. 1. As can be clearly seen in the spectra collected on the iridescent glass side a peak with the peak maximum at approximately 610-615 cm^{-1} could be observed, whereas this band is missing in the spectra taken from the non-iridescent glass side.

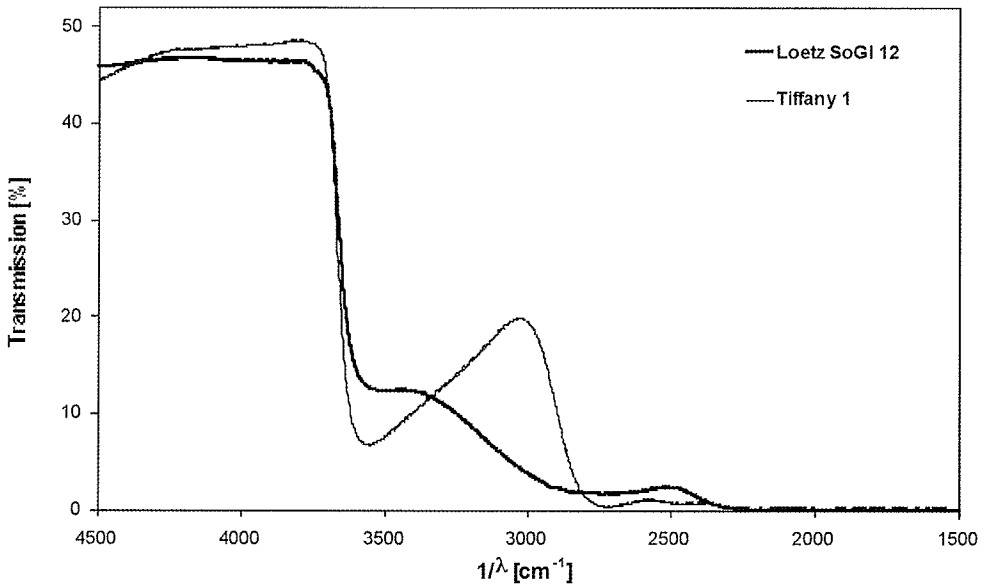

Fig. 1: Transmission spectra of the iridescent glass fragments of Loetz So Gl 12 and Tiffany T1 (30 scans, resolution 4 cm^{-1})

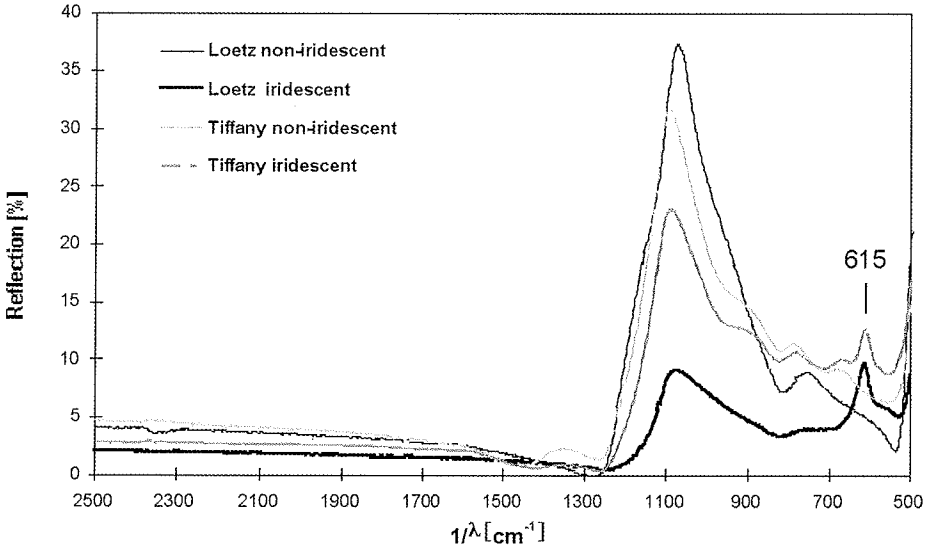

Fig. 2: Reflection spectra of the iridescent glass fragments of Loetz So Gl 12 and Tiffany T1 (30 scans, resolution 16 cm^{-1})

Multivariate statistical evaluation of the FTIR data

The multivariate statistical analysis (pattern recognition) of the FTIR spectra has two main advantages: (1) the degree of similarity between two spectra can be quantified, and (2) the comparison of hundreds of spectra including the

determination of their characteristic features and their greatest dissimilarities can be accelerated. Thus, the computerized pattern recognition techniques are better suited for the identification of provenance than the classical qualitative and quantitative analysis of the experimental data. The statistical evaluation was carried out by means of self-written code packages [3] based on the Principal Component Analysis (PCA) algorithm, with subsequently applied canonical variate analysis (Fischer Projection) [4].
For the evaluation, the FTIR spectra were saved as arrays which were directly used as an input in statistical pattern recognition algorithms. In order to eliminate the absolute values of the transmission and reflection coefficients, the spectra were normalized and the form of the spectra were compared. Using PCA algorithm the essential information and a reduction of the original data sets could be achieved. Subsequent canonical variate analysis was performed to obtain clustering characteristics for provenance and to establish fingerprints (provenance specific filter functions) for identification.
Both the results of the PCA evaluation of the FTIR data measured in transmission (Fig. 3) and reflectance mode (Fig. 4) demonstrate that Tiffany and Loetz glasses can be reliably differentiated, both from each other and from contemporary glasses. The differences are revealed in the chemical composition of the glass fragments, which is reflected in the FTIR spectra.

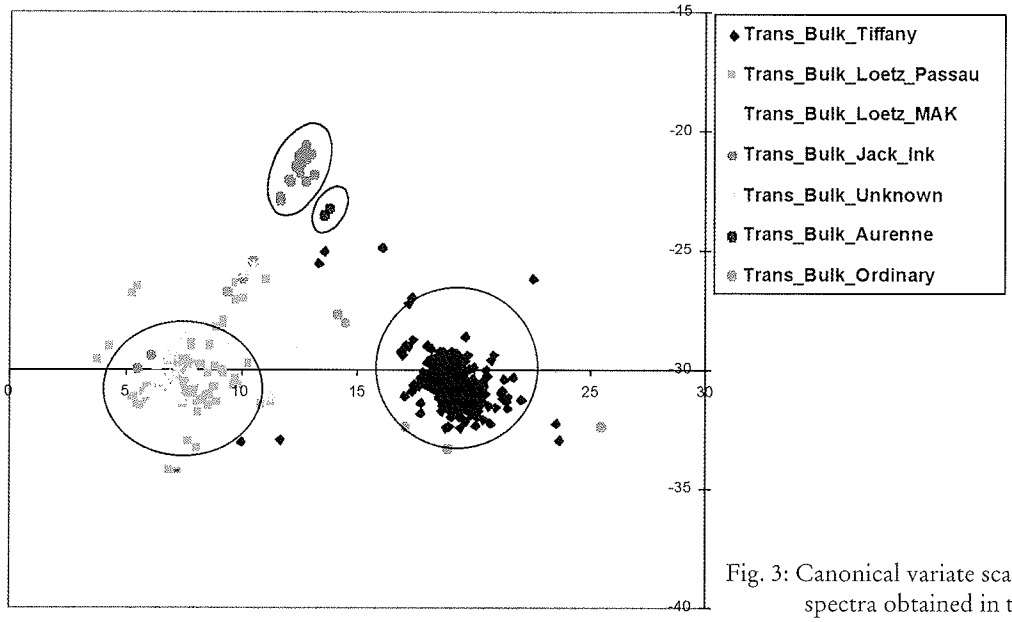

Fig. 3: Canonical variate scatter plot considering the FTIR spectra obtained in the transmission mode.

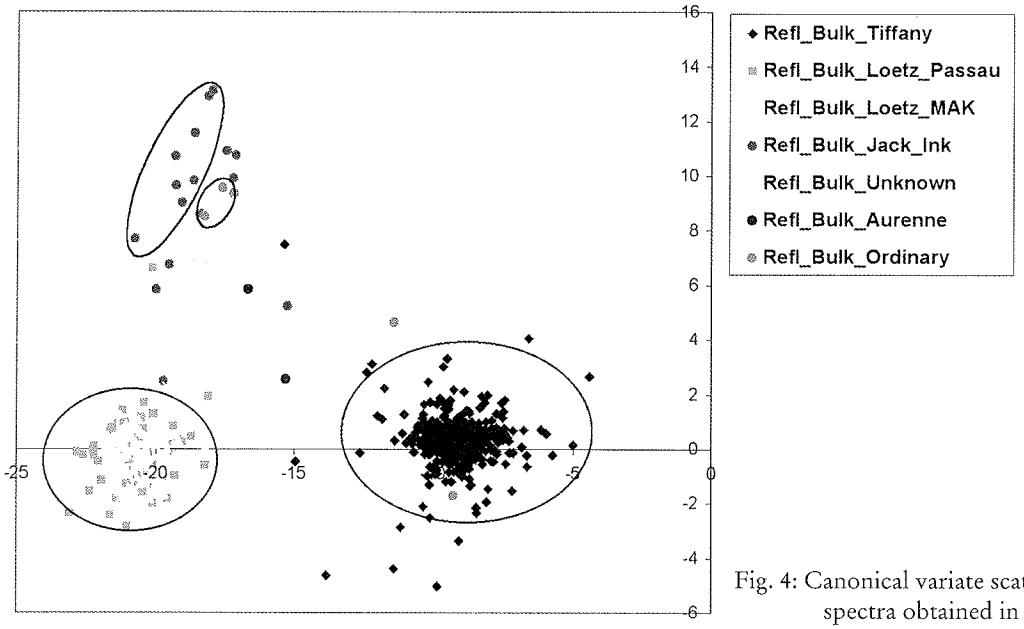

Fig. 4: Canonical variate scatter plot considering the FTIR spectra obtained in the reflectance mode.

Conclusion

FTIR as a non-destructive analytical method in combination with the multivariate statistical analysis is a suitable tool for differentiation between iridescent Art Nouveau glass artefacts (Tiffany, Loetz) and modern iridescent glass objects (Jack Ink).

Acknowledgement

We gratefully acknowledge the financial supports of Oesterreichische Nationalbank, Vienna and the New-York Historical Society, Passau Glass Museum, Museum of Applied Arts Vienna, and Jack Ink for providing us with original glass fragments of Tiffany and Loetz as well as modern glass samples.

References

1. Neuwirth, W., *Loetz Austria 1900,* Selbstverl., Wien (1986).

2. Jembrih, D., Peev, M., Schreiner, M., Krejsa, P., Clausen, Ch., ‚Tiffany oder Loetz? Identification and classification of Art Nouveau Iridescent Artifacts'. *18th International Congress on Glass, San Francisco/USA July 1998*, CD of the Conference proceedings (1998). B1, 90-95.

3. Peev, M., Jembrih, D., Schreiner, M., Krejsa, P., Clausen, Ch., Metzker, E., 'Identification and Classification of Art Nouveau Iridescent Glass Artifacts', unpublished final report, (Jubilaeumsfondsprojekt no. 6313, Oesterreichische Nationalbank), Austrian Research Centers Seibersdorf (1998).

4. Manly, B.F.J., *Multivariate Statistical Methods*, J. W. Arrowsmith Ltd, Bristol (1986).

Spectroscopic Analysis of a 4th-Century A.D. Roman Sarcophagus

Thomas Frey[1], Dane Jones[1], Zdravko Barov[2] and Constance Faber[2]
[1] Department of Chemistry and Biochemistry, California Polytechnic State University, San Luis Obispo, CA 93407 USA
[2] Ethos Conservators, Ethos, Cambria, CA 93428 USA

Abstract

We have performed detailed spectroscopic measurements on a 4th-Century A.D. Roman Sarcophagus ("The Nine Muses") located at Hearst San Simeon State Historical Monument in San Simeon, California. The sarcophagus is carved in high relief from Thassos marble. Remnants of what is thought to be the original paint are still present in small amounts on the surface. Various areas have been severely weathered and show evidence of oxidation and bacterial activity. A detailed Raman and infrared analysis has been made of the surface to identify oxidation products and components of the original paint. Comprehensive photographs of the sarcophagus illuminated with both visible and ultraviolet radiation sources also have been made.

Applications of Fourier-transform Infrared Spectroscopy (FT-IR) to the Study of Pastes from an Argentinian Seprentrional Patagonian Archaeological Site

Marta S. Maier[1], María T. Boschín[2], Sara D. Parera[1] and Ma. Florencia del Castillo Bernal[2]
[1] Departamento de Química Orgánica, Facultad de Ciencias Exactas y Naturales, Universidad de Buenos Aires, Pabellón 2, Ciudad Universitaria (1428) Buenos Aires, Argentina.
[2] Centro Nacional Patagónico, Consejo Nacional de Investigaciones Científicas y Técnicas, Boulevard Brown s/n (9120) Puerto Madryn, Chubut, Argentina.

Abstract

Two samples of residuals of red pastes (crayons) obtained from the archaeological site Cave Loncomán (Río Negro, Argentina) were analyzed by Fourier-transform infrared spectroscopy (FT-IR) and gas chromatography coupled to mass spectrometry (GC-MS) revealing the presence of hematite as the red pigment and lipids as binders. Analysis of organic extracts of both pastes showed the presence of sharp peaks due to carboxylic acids and carboxylate peaks, indicative of hydrolysis of triglycerides in the pastes.

Introduction

Previous chemical analysis of organic and inorganic components of rock art samples and painting residues (pastes) from archaeological excavations in Argentinian Septentrional Patagonia have shown that they were composed of inorganic pigments mixed with lipids of vegetable or animal origin [1]. This is consistent with the wide range of potential uses of lipids in the past as binders and waterproofing agents and with the fact that they are preserved under favorable conditions in association with various classes of archaeological artifacts [2].
Recently we have obtained two samples of residuals of red pastes (crayons) that were in stratigraphic position in the archaeological site Cave Loncomán, in Río Negro province, Argentina. The walls and roof of the Cave are completely covered with engravings, some over painted with red colors and oranges that represent human footfalls and local fauna, including also simple and complex geometric designs. The two samples come from the top of the early occupations, dated by ^{14}C in 2000 A. P., and they belong to hunter-gatherers societies that established in the region 2800 years ago, at the beginning of the stage of exploration of new territories. The pastes might have been used in the preparation of the colors for painting over the engravings and leathers used as shelter, for facial and corporal paintings and to apply on other supports that could have intervened in social activities of ideological nature. Fourier-transform infrared spectroscopy (FT-IR) is useful for the identification of minerals and organic binders and can complement results obtained by X-ray diffraction (XRD) and gas chromatography coupled to mass spectrometry (GC-MS). The goal of the present study was to attempt to characterize both red pastes by FT-IR and compare their spectra to those of a local mineral containing hematite, an animal fat of an American ostrich (*Pterocnemia pennata*) typical of this region, and of thermally aged mixtures of the red mineral and the ostrich fat.

Experimental

Samples of red pastes **1** and **2** were hydrolyzed in HCl 2% in methanol at 60° C for 2 h. After cooling, water was added and each mixture was extracted with methylene chloride. Evaporation under N_2 provided mixtures of fatty acid methyl esters which were analyzed by gas chromatography-mass spectrometry using a TRIO-2 VG mass spectrometer coupled to a Hewlett Packard 5890A chromatograph. Pastes **1** and **2** were crushed to a powder and extracted (ultrasonication) with chloroform:methanol (2:1) v/v at room temperature. Both extracts were concentrated under reduced pressure to give two lipidic residues that were analyzed by FT-IR. X-ray diffraction (XRD) analysis using CuKa radiation was carried out on a Phillips diffractometer. SEM-EDX analysis was performed on a Philips XL30 ESEM. The infrared spectra were collected using a Magna-IR™ 550 spectrometer. The samples were dispersed in KBr disks. Spectra of 4 cm^{-1} resolution were acquired by coaddition of 32 scans. The spectra were collected from 4000 to 400 cm^{-1}.

Results and discussion

Analysis by gas chromatography coupled to mass spectrometry (GC-MS) of mixtures of fatty acid methyl esters obtained by acid transesterification of pastes **1** and **2** revealed the presence of saturated (C_{14}, C_{15}, C_{16}, C_{18}) and

unsaturated acids (C_{16} and C_{18}) due to the presence of lipids. The FT-IR spectra of both pastes showed absorptions due to low wavenumber vibrations of Fe-O in the red mineral hematite at 589 and 487 cm^{-1} [3] together with sharp bands at 3700-3200 cm^{-1} and in the range of 1100 and 900 cm^{-1} that might be assigned to accessory minerals as kaolin

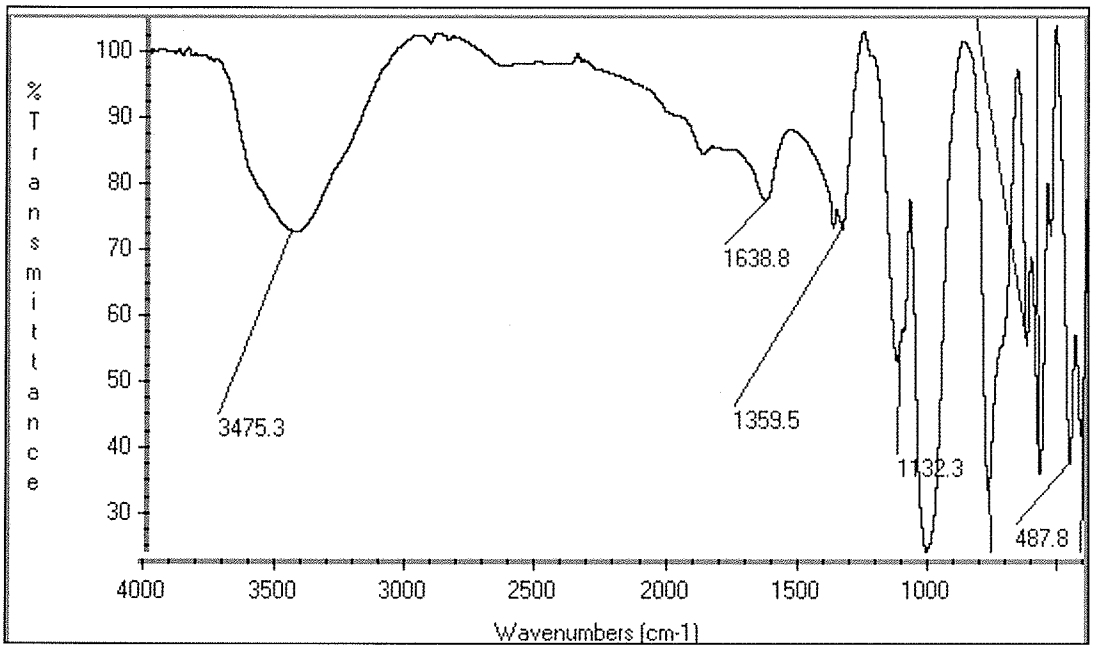

Figure 1: FT-IR spectrum of paste 1.

and quartz [4,5] (Figure 1).

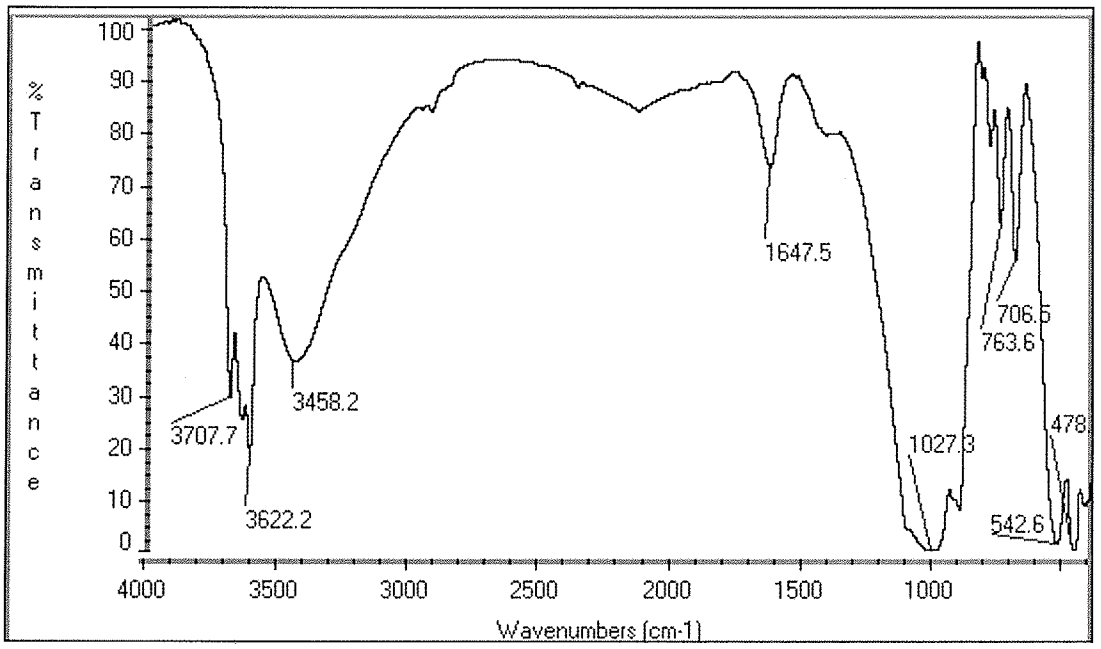

Figure 2: FT-IR spectrum of a local mineral.

Analysis by FT-IR of a reference local mineral containing kaolin, quartz and hematite, as determined by XRD and SEM-EDX gave the spectrum shown in Figure 2.

The spectrum showed strong hydroxyl bands at 3700 and 3622 cm^{-1} characteristic of the kaolin group clays. The broad O-H stretching band at 3458 cm^{-1} together with the water bending band at 1647 cm^{-1} and the Fe-O vibrations at 542 and 478 cm^{-1} are characteristic of hematite retaining hydroxyl units in its structure [6]. Strong bands in the

range 1100-1000 cm^{-1} are assigned to asymmetric Si-O-Si stretching bands in kaolin and quartz. Comparison of this FT-IR spectrum to the one shown in Figure 1 revealed that both were very similar and that peaks due to the lipid components in pastes **1** and **2** were very weak to be clearly assigned. In order to improve the detection of lipids in both pastes and to assess their state of preservation, we extracted pastes **1** and **2** with a mixture of chloroform:methanol (2:1). Analysis by FT-IR of both extracts (Figures 3 and 4) showed sharp peaks at 2940 and 2870 cm^{-1} due to C-H stretching vibrations in methyl and methylene groups and carbonyl bands at 1731 and 1658

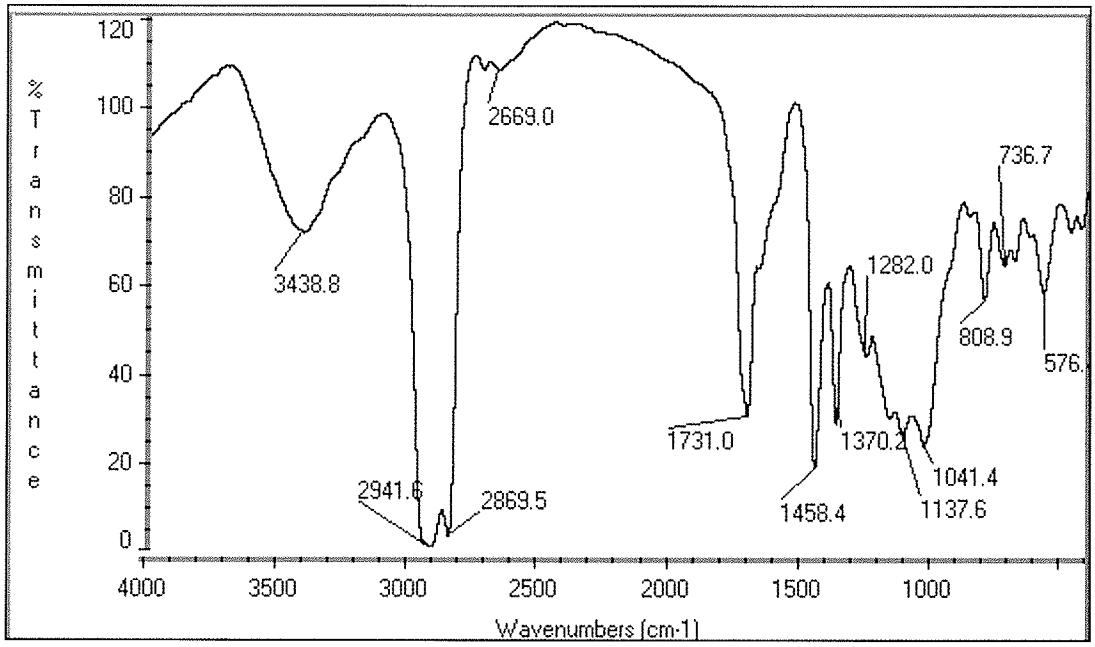

Figure 3: FT-IR spectrum of the $CHCl_3$:MeOH extract of paste 1.

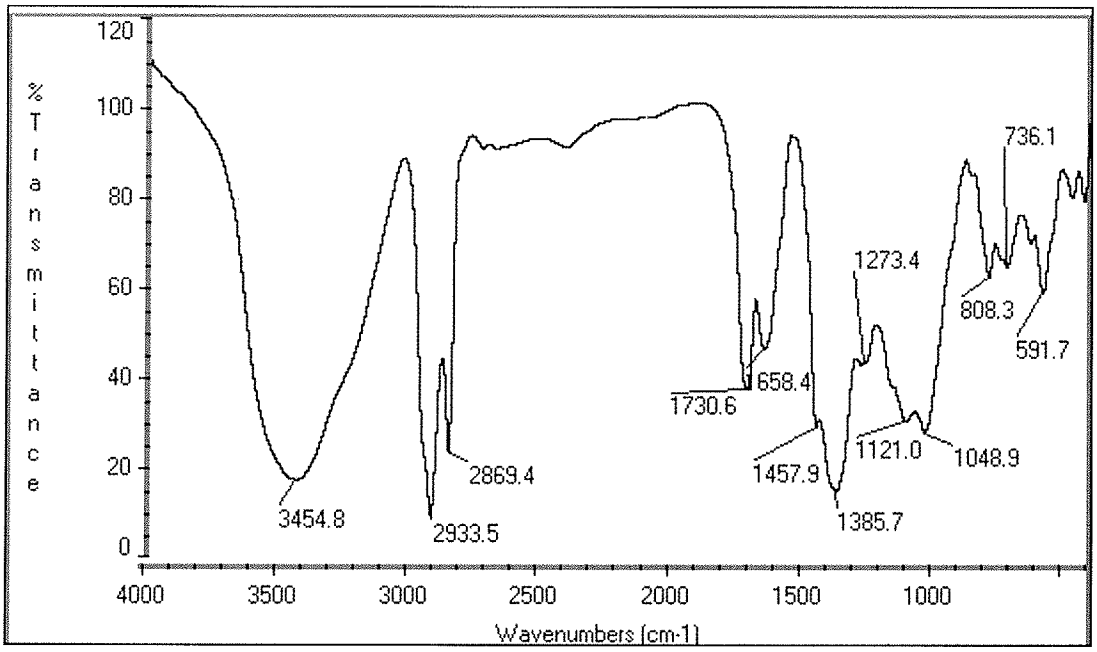

Figure 4: FT-IR spectrum of the $CHCl_3$:MeOH extract of paste 2.

cm^{-1}. These bands confirmed the GC-MS results regarding the presence of lipids in both pastes.
These spectra were compared to that of a mixture of an animal fat of an American ostrich (*Pterocnemia pennata*) and the local mineral containing hematite prepared according to an old recipe [7] (Figure 5). The FT-IR spectra of the mixture showed a characteristically sharp ester carbonyl group at 1763 cm^{-1} as well as intense absorptions in the range 3000-2850 cm^{-1} due to C-H stretching vibrations in methyl and methylene groups and a band at 3017 cm^{-1} due

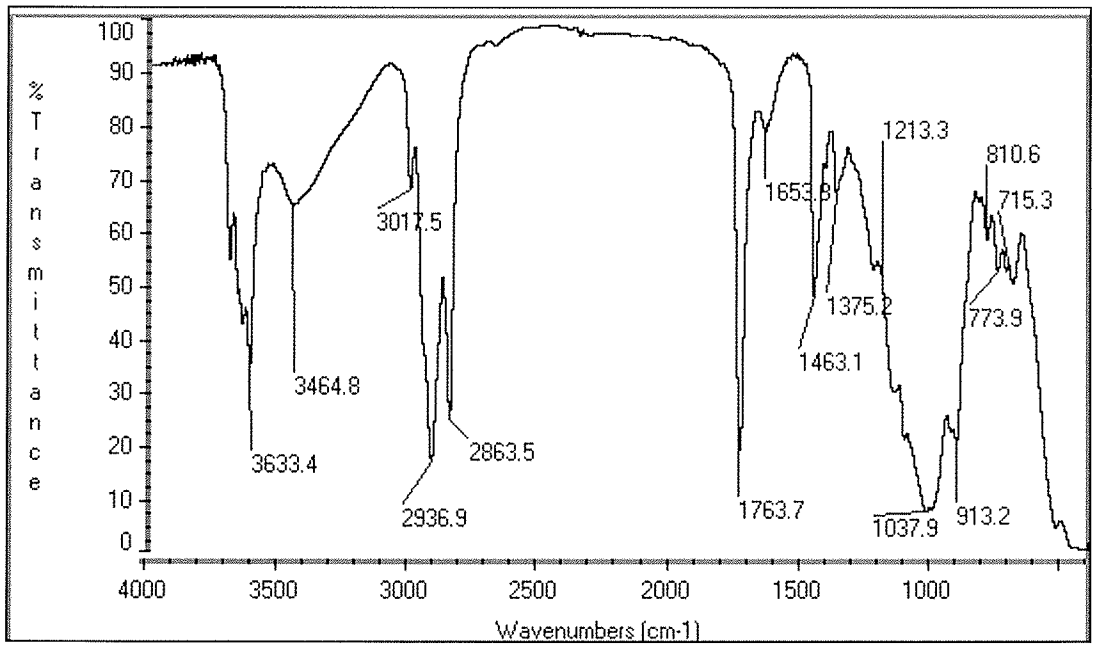

Figure 5: FT-IR spectrum of the mixture of a local mineral containing hematite and a reference fat of the ostrich *P. pennata*.

to alkene C-H stretching [8].

Evidence of hydrolysis of triglycerides can be seen in the spectra of both pastes. In Figure 3, the acid peak at 1731 cm^{-1} predominates with the ester carbonyl group forming just a slight shoulder on the acid peak. Carboxylate peaks due to further reaction of the free fatty acids with metal ions in the pigment to give salts form one broad split with the acid peak. In Figure 4, acid and carboxylate peaks at 1730 and 1658 cm^{-1} dominate the spectrum together with an intense O-H stretching absorption indicative of the presence of carboxylic acids in paste **2**.

In order to get insight into the process of hydrolysis of the fats used as binders in these pastes in the presence of the hematite pigment we performed a series of thermal accelerated aging tests of the reference mixture of the hematite mineral and the fat of *P. pennata*. Samples of the mixture were spread out as thin films and heated in two unhumidified dry ovens at 39-40 °C and at 50 °C and controlled periodically by FT-IR.

Figure 6 shows the FT-IR spectrum of the mixture heated at 50 °C for 40 days. Similar spectra were obtained for

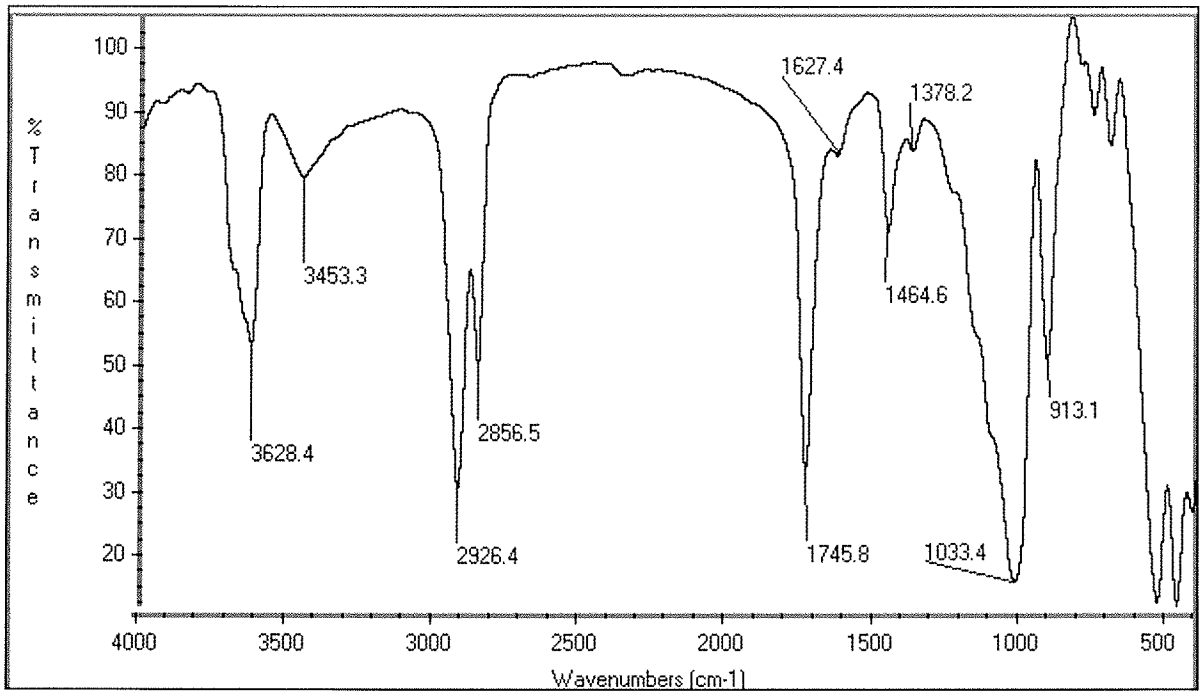

Figure 6: FT-IR spectrum of the mixture of the red mineral and the fat heated at 50 °C for 40 days.

samples of the mixture heated at 39-40°C.
The most important difference between this spectrum and that of the original mixture (Figure 5) is the absence of the band at 3017 cm^{-1} due to alkene C-H stretching. This has been already observed after seven days of thermal aging of the mixture at both temperatures. Films became more stiff and brittle with increasing times of heating. It is known that during the drying process of paint films the reactive unsaturated fatty acid components either polymerize to form crosslinks, or degrade to smaller compounds, such as diacids [9]. The carbonyl ester peak remains unaltered in the spectra of the accelerated thermally aged samples and there is no indication of carboxylic acids or carboxylate formation in presence of the mineral pigment.

Conclusions

Archaeological fats are degraded even when this process might be retarded due to burial in favorable environments. FT-IR spectroscopy provided useful information for the characterization of hematite as the mineral pigment and the state of preservation of the lipids in the pastes. This could be achieved by extraction of the lipid components with an organic solvent and further analysis by FT-IR of both extracts. Carboxylic acids and their salts were the main lipid components. The accelerated thermal aging experiments performed on a reference mixture of a local mineral containing hematite and a fat of an American ostrich were not comparable to natural aging of the samples with respect to hydrolysis of triglycerides but were indicative of the reactivity of double bonds in the fatty acids. It is possible that aging tests that combine heating at moderate relative humidity might simulate natural aging of these archaeological pastes.

References

1. Boschín, M.T., Seldes, A.M., Maier, M.S., Casamiquela, R.M., Ledesma, R., and Abad, G. 'Análisis de las fracciones inorgánica y orgánica de pinturas rupestres y pastas de sitios arqueológicos de la Patagonia septentrional Argentina'. *Zephyrus* (2002) **55**, 183-198.

2. Evershed, R.P., Dudd, S. N., Copley, M.S., Berstna, R., Stott, A.W., Mottram, H., Buckley, S. A., and Crossman, Z. 'Chemistry of Archaeological Animal Fats'. *Acc. Chem. Res.* (2002) **35**, 660-668.

3. Ruan, H.D., Frost, R.L., Kloprogge, J.T., and Duong, L. 'Infrared spectroscopy of goethite dehydroxylation: III. FT-IR microscopy of in situ study of the thermal transformation of goethite to hematite'. *Spectrochimica Acta Part A* (2002) **58**, 967-981.

4. Helwig, K. 'The characterization of iron earth pigments using infrared spectroscopy'. *IRUG2 Postprints* (1996), 83-91.

5. Derrick, M.D., Stulik, D., and Landry, J.M., Infrared Spectroscopy in Conservation Science, J. Paul Getty Trust, Los Angeles, USA (1999).

6. Ruan, H.D., Frost, R.L., and Kloprogge, J.T. 'The behavior of hydroxyl units of synthetic goethite and its dehydroxylated product hematite'. *Spectrochimica Acta Part A* (2001) **57**, 2575-2586.

7. Onelli, C., *Trepando los Andes*, El Elefante Blanco, Buenos Aires, Argentina (1998).

8. Silverstein, R.M., and Webster, F.X., *Spectrometric Identification of Organic Compounds*, John Wiley & Sons, Inc., New York (1998).

9. Erhardt, D., Tumosa, C. S., and Mecklenburg, M. F. 'Natural and accelerated thermal aging of oil paint films'. *Tradition and Innovation. Advances in Conservation* (2000) 65-69.

Reflectance FTIR and Raman Microspectroscopy Studies of 19th Century Chinese Export Pith Paintings

Jennifer Mass[1], Janice Carlson[1], Catherine Matsen[1], Betty Fiske[1], Jo-Fan Huang[1] and Gene Hall[2]
[1] Winterthur Museum, Garden, and Library, Winterthur/University of Delaware Program in Art Conservation
[2] Rutgers University Department of Chemistry

Small watercolors on pith paper (the sliced core of *Tetrapanax papyriferus*) were produced and exported from Canton in large quantities beginning in the second decade of the 19th century. These mass-produced images of birds, flowers, costumes, and scenes from daily life in China were produced in *hongs* or workshops for foreign traders and sailors in an attempt to portray a remote land in the years prior to photography. These paintings were not regarded as fine art because they were typically prepared in an assembly line style by artisans who each added a single color to an ink outline on the pith. Chinese export pith paintings are valued today, however, for their fine levels of detail, their jewel-bright tones, the softness of the image imparted by the pith substrate, and their unique role in documenting the complex relationship of China with the west in the 19th century. Since the paintings do not represent true scenes from Chinese life, but rather scenes that were thought to appeal to a western audience, these works have great historical and anthropological value outside of their artistic merit.
Perhaps because of the small scale of these paintings (typically they are no larger than 25 cm on a side) there has been little analysis of the pigments and binders used to prepare them. Nondestructive energy dispersive x-ray fluorescence was performed at the Victoria and Albert Museum (London) to characterize some of the pigments used in Chinese export pith paintings, and the results have indicated the presence of vermilion, yellow ochre, and lead white. Surprisingly, the blue and green pigments appeared to be organic lakes rather than the malachite and azurite that are typically observed on Chinese export watercolors on paper supports and Chinese painted silks. Raman spectroscopy, FTIR, reflectance FTIR, x-ray fluorescence, SEM-EDS, GC-MS, visible light microscopy, and infrared reflectography were carried out to more fully characterize the materials and methods used to produce pith paintings. One specific question that was addressed is the binding medium for these paintings, which has been alternately hypothesized to be an animal glue or a gum such as gamboge. The pith paintings studied were prepared with a proteinaceous binding medium, Prussian and ultramarine blues, emerald and Hooker's greens, red lead, vermilion, and cochineal lake reds. The absence of malachite and azurite indicates significant western influence in the materials of manufacture of these paintings.

The video Barellino

Milan Milosevic and Violet Milosevic
Harrick Scientific Corporation, Ossining, NY 10562

Abstract

The Video Barrelino (VB) is a diffuse reflectance sampling probe designed specifically for the Cary 50 UV-VIS-NIR spectrometer. Monochromatic light from the spectrometer is carried by a 1.5 m long fiber optics cable and focused onto a sample into a spot less than 1mm in diameter. Diffusely scattered light is collected and detected by a built-in detector. Remote diffuse reflection analysis of any sample within 1.5 m from the spectrometer is easily performed. The spatial resolution of the analysis is less than 1 mm. A video camera is integrated into the accessory allowing direct viewing of the illuminated spot. In this work we analyzed the color of a number of differently colored spots on a piece of drapery submitted to us for preliminary investigation by the Metropolitan Museum of Art, New York.

Introduction

Color changes can occur when artifacts undergo various conservation treatments or when they are exposed to bright light when exhibited. It is important to have an accurate measure of the color of the artifact before and after the event. This information can be used to assist in restoration. For artifacts whose color changes from point to point, local measurements of the color are essential. For this purpose a special diffuse reflection micro-sampling probe, the VB (Figure 1), was developed.

Figure 1. The Video Barrelino

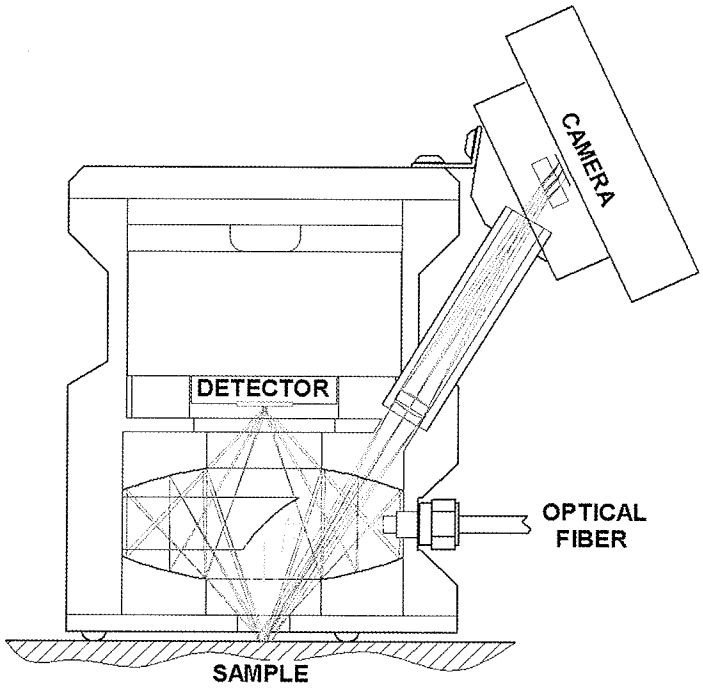

Figure 2. The Optical Diagram

Optical Design

The optical configuration of the VB is shown in Fig.2. Monochromatic light is carried from the Cary 50 spectrometer via an optical fiber. The exit aperture of the optical fiber is re-imaged onto the sample by a 1:1 imaging 90° off-axis ellipsoid mirror. Thus the illuminated spot on the sample is the same size as the end of the exit aperture of the optical fiber, typically less than 1 mm in diameter. The specularly reflected radiation reflects back into the illuminating ellipsoid and is not collected for detection. This feature of the VB is extremely important, since 'glossy'

reflection from the sample is not sample-specific and tends to obscure and dilute the sample specific information contained in the diffuse (non-glossy) component of the reflected light. The light reflected in all other directions is mostly the 'pure' diffuse component. This radiation is collected and reimaged onto the detector by two opposing coaxial parabolic mirrors. The focal point of the first mirror is on the sample; the focal point of the second mirror is on the detector.
The bottom plate of the VB housing has an opening in the center to enable the light to reach the sample and the reflected light to be collected. The sampling plane is 1.5 mm below the bottom plate. Three Teflon balls imbedded into the bottom plate project out 1.5 mm and define the sample plane. For analysis, the accessory is simply placed onto the sample.
In addition to the optics for spectroscopic analysis, there is also optics that enables viewing of the sample with the help of a built-in video camera. The 'zero order' mode of the Cary 50 spectrometer is used to illuminate the sampling spot with white light. This illumination delineates the exact area of the sample that is subsequently analyzed. Hence, *what you see is what you analyze!* The picture captured by the camera is displayed on the computer screen and can be stored for record keeping. Thus one can associate the visual image of the spot on the sample with a spectrum of the same spot.
In order to quickly locate the spot on the sample that is to be analyzed, a specially designed target is provided. The target is placed over the spot that is to be analyzed and the VB is placed into the target. The visual image displayed on the computer screen enables fine-tuning of the sample position. Since the sampling spot of the VB is small, the greatest challenge is picking the desired spot on the sample.

Color Measurement

The color of an object is a subjectively perceived quality. It is known that the eye can be deceived by the context in which the object is placed so that both the form and the color can be seen differently in differing contexts. Here we are concerned with the actual (objective) color of an object as measured by an instrument.
The color of an object is a property associated with the spectral composition of light involved in forming the image of the object on our retina (or film, camera sensor, etc.). That light may have been reflected off the object's surface, it may have been transmitted through the object or scattered by the object. The light scattered, reflected or transmitted by the object had to come from another source (such as the sun or a light bulb). The object's interaction with that illuminating light at any given wavelength can only reduce the illuminating light's intensity at that wavelength. Thus, the spectral composition of the light from the external source together with the object's interaction with that light determines the color of the object.
The majority of the light forming the picture of an object is usually due to the reflection off the object's surface. There are two types of reflection [1, 2, 3]: specular and diffuse. Specular reflection is a mirror-like reflection. A portion of the reflected light may be specular even though it may have been reflected by a rough surface [2]. Specularly reflected light is sometimes called *shine* or *gloss* [1]. Special coatings are put on paper to reduce gloss because the gloss dilutes or even obscures the information-rich reflection of the paper (text, pictures, etc.). The same is true with spectroscopic information [3]. The design of the VB discriminates against the collection of the specular component. The majority of light collected by the VB is diffusely scattered off the sample surface.
The areas of the sample surface that are in crevasses and thus hidden from the direct illumination appear darker than the illuminated areas. The distribution of the darker patches over the surface of the sample is what is referred to as texture. The amount of light reaching the detector from a 1 mm diameter circle on the surface of the sample may be greatly influenced by the exact position of the circle. If the sampling circle is moved on the surface of the sample, the detected total intensity of light may vary considerably, depending on the average size and density of the dark patches on the surface. Which areas appear dark to the detection process is greatly influenced by the direction of illuminating light. All these factors complicate color measurement. With materials such as carpets, the surface consists of tightly packed fibers that are not held in a fixed position. Combed fibers nicely aligned in a particular direction have a different texture from uncombed fibers arranged in random directions. The reflectance spectrum of combed fibers can differ significantly from the spectrum of uncombed fibers.
By ratioing the reflected light intensity to the incident intensity the reflectance spectrum is made independent of the spectral composition of the illuminating light. The spectra collected were baseline corrected using a stack of several sheets of white paper as a blank. The paper, although white, is not the best choice for the blank. The blank should be of the same texture as the sample. A small piece of the sample or a piece of fabric with a similar texture as the sample could be bleached to serve as the blank.

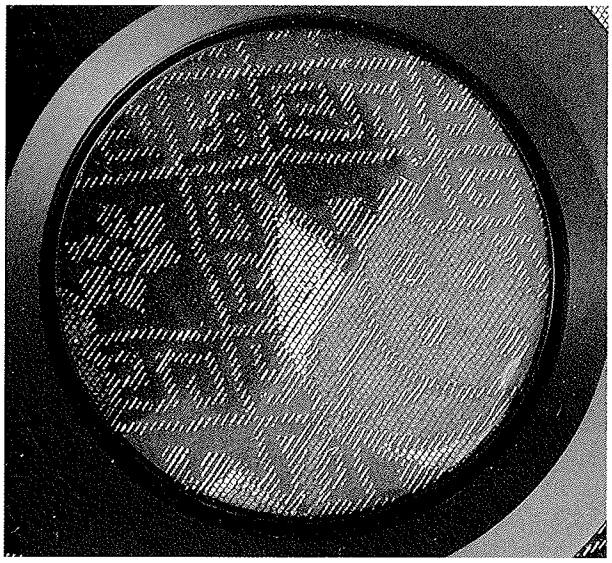

Figure 3. Selecting the spot

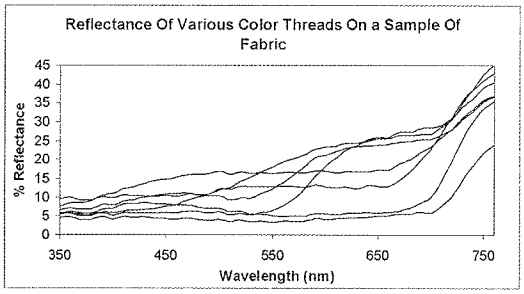

Figure 6. Spectra of seven differently colored spots on sample

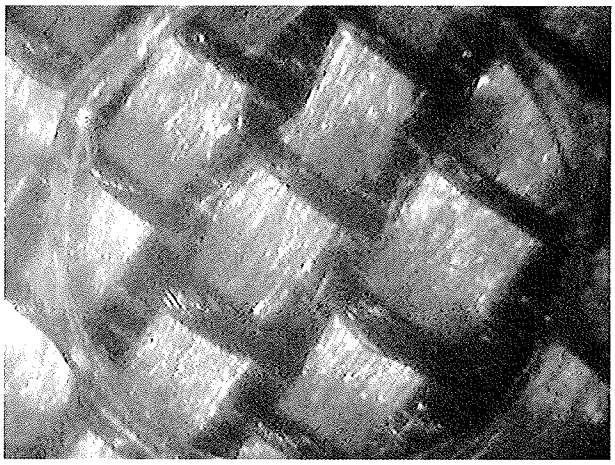

Figure 4. Sample seen by the Video Barrelino Camera

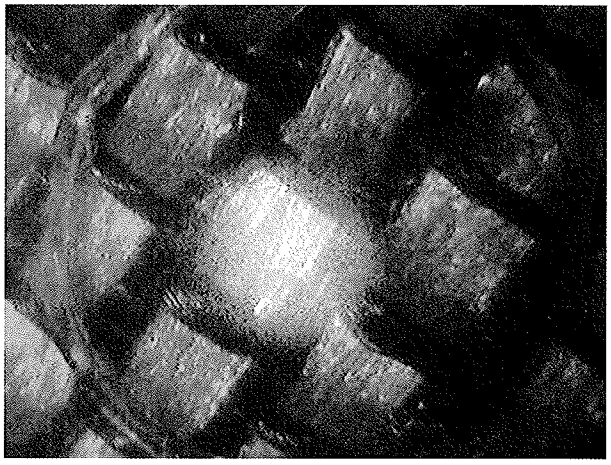

Figure 5. Highlighted is the area of the sample that is actually analyzed

Experiment

Figures 3 to 5 illustrate typical steps in collecting a spectrum at a particular point. The selection of the sample point is crucial in a repeated measurement. Unless exactly the same point is selected the second time, the differences measured could easily be due to a mismatch of the analyzed areas rather than to the change in the sample. The pre-selection of the area is made by centering the Target over the desired spot on the sample as shown in Fig. 3, which was recorded with a regular digital camera. The VB was then placed into the Target and Fig. 4 was recorded with the VB camera. Careful inspection reveals that the two pictures are showing the same area of the sample. In order to make that easily discernable the image in Fig. 3 was rotated to align the weave at the same angle as in Fig. 4. The image shown in Fig. 5 was produced by combining two images, the image in Fig. 4 and the image of the spot of illuminating light from the spectrometer in 'zero order' on white paper (not shown). The superposition delineates the area illuminated by the spectrometer and hence the area of the sample actually analyzed. Fig. 5 illustrates clearly the difficulty of being able to repeatedly select the same spot on the sample as well as the potential error in the measurement that selecting a slightly different spot on the sample could cause. One solution to that problem would be to employ a thinner optical fiber to make the analyzed spot size smaller than the individual stitch. The downside to using a finer fiber is the lower 'energy' level available to the measurement and consequently reduced S/N.

Results and discussion

The spectra shown in Fig. 6 are collected by repeating the above procedure on seven different spots on the fabric sample shown in Fig. 3. One sees that, in addition to sample color information, the spectra also contain information from the UV spectral region as well as NIR region. Changes detected in these non-visible regions may not be

important to the color of the object but could indicate a change in the sample that may be a precursor to color change (or another degradation) so that preservation measures can be taken to prevent damage to the artifact.

Colnclusion

Color measurement on small spots, while challenging, could be made using the VB and a Cary 50 spectrometer. However, much work remains to be done to characterize the strengths and weaknesses of the procedure described in this work

References

1. Kortum, G. *Reflectance Spectroscopy*; Springer: New York, 1969

2. Milosevic, M. and Berets, S.L. *Appl. Spectrosc. Revs.* **37**(4) (2002) 347-364

3. Milosevic, M. and Berets, S.L. 'Accessories And Sample Handling For Mid-infrared Diffuse Reflection Spectroscopy' in J. M. Chalmers and P. R. Griffits (eds.) *Handbook Of Vibrational Spectroscopy*, Wiley, Chichester, West Sussex, UK, 2002 (1154-1162)

A Systematic Study Of Red Paint Layers Degradation In Artworks Based On Spectrophotometric Information

A. Miquel[1], N. Ferrer[2], R. Tauler[3] and J.F. García[1]
[1] Departament de Pintura. Facultat de Belles Arts. Universitat de Barcelona. C/ Pau Gargallo 4, 08028 Barcelona.
[2] Serveis Científico-Tècnics – Universitat de Barcelona. C/ Solé i Sabaris s/n. 08028 Barcelona.
[3] Instituto de Investigación Química y Ambiental de Barcelona. CID- CSIC.

Abstract

Paint layers are important constituents of contemporary and classical artworks. Their degradation over time causes changes, not only to color, but also to their internal structure. Photo degradation processes are induced by the environmental conditions of the place in which artworks are located.
Among pigments, organic lakes are the most fugitive when exposed to light.
We have focused on the behavior of the three most widely-used traditional red lakes, agglutinated in raw linseed oil, and their evolution over time under different environmental conditions. Their ultraviolet, visible, near infrared and mid infrared spectra have been registered. Results show not only the changes in the pigments structure, but also the variations in the agglutinant composition. Information obtained regarding Madder Lake is limited, due to the relative low concentration of the pigment versus the precipitant agent.

Introduction

In the Renaissance, one important contribution in the field of color was the application of dyes to inorganic pictorial layers so as to make colors brighter and more "joyful" [1-3].
Inorganic reds, widely used pigments because of its color symbolism (fire, blood, earth, power) were enhanced and in some cases protected from the environment with organic lakes, such as Madder Lake, Crimson Lake and Lac-Dye [4-8]. However, unlike most of inorganic pigments, natural dyestuffs are very unstable to light [9-12].
Lake pigments are prepared from dyestuffs extracted from insect and plant species. To make them insoluble, they are precipitated or adsorbed onto inert inorganic substrates, such as calcium salts or hydrated alumina. Lake pigments based on the latter, which is the case in this study, are more light-fast than lake pigments containing calcium salts.
After the discovery of America, Crimson Lake replaced Tyrian Purple, the most expensive and exclusive lake, synonymous with wealth and power. Crimson Lake is manufactured with the extract of dry bodies of the female insect *Coccus cacti*, which lives on cactus plants. Its coloring principle, carminic acid, $C_{22}H_{20}O_{13}$, is soaked in dissolution of 5% alum and cream of tartar. Its natural deep red color is very sensitive to light, although it is more stable when agglutinated with oil (Figure 1).
Lac Dye is very similar in color and composition to Crimson Lake. It is a very ancient dye that was used originally and widely in the East. It is made of the resin-like secretion of the larvae of the female insect *Coccus lacca*, which lives in certain trees in India and the Far East. Its coloring principle is laccaic acid, $C_{20}H_{14}O_{11}$, or its salts. To use it as a pigment, the extract is precipitated with alum (Figure 1).
Among dyes, Madder Lake is the most important one of vegetable origin and, since the Middle Ages, is also the most commonly used as a pigment. It is a mixture of anthraquinone derivatives, as the proportion of these components is variable depending on the source of the plant and the extraction process of the dye. Its most significant coloring materials are alizarin (1,2-dihydroxyanthraquinone) purpurin (1,2,4-trihydroxyanthraquinone), and pseudopurputin (1,2,4-trihydroxyanthraquinone-3-carboxylic acid). It is prepared by adding alum to the extract of the root of the plant *Rubia Tinctorum*, and precipitating it with an alkali. In principle, it is one of the most stable to light (Figure 1).
The aim of this study is the characterisation of the mechanism of degradation by comparing the molecular change of the same sample in different periods of time through its natural ageing.

Experimental

Materials: Line canvas, calcium carbonate, rabbit glue, raw linseed oil, Madder Lake, Crimson Lake, Lac Dye. All materials have been supplied by Kremer Pigmente.
Instruments: Perkin Elmer UV-IR-NIR λ19, with Integration Sphere for reflexion measurements and Bomen MB-120 with spectra-tech microscope for Mid Infrared determinations.

Methodologies: a mock painting was prepared to be aged. Traditional materials such as line canvas, calcium carbonate and animal glue were used as a support and preparation layer. When the latter was dry to the touch, 5 x 5 cm squares were painted with the Lac Dye, Crimson and Madder pigment lakes agglutinated in raw linseed oil. The painting was exposed to high-intensity natural light for a period of approximately two years, with half of each painting square (5 cm x 5 cm) being protected from the light with a black band. We had therefore two different samples in each stage of the analytical process: one kept in dark storage, and a bleached one.
In the present work, the photo degradation of the paintings exposed to light has been followed by Visible and Infrared Spectroscopy. Analysis of the pure pigments was undertaken in order to characterize the compound before they were agglutinated.

Measurements
The first measurement of the paint samples was made seven days after their application on the canvas. Subsequent measurements followed at different established moments over the time-period of two years.
The Mid Infrared spectra were acquired with a Bomen MB-120 using a spectra-tech microscope. The micro samples were extracted from the pictorial layer with a tungsten needle, and placed on the diamond cell for study in transmission mode. Conditions: Frequency Range 4000 to 720 cm^{-1}, Resolution 4 cm^{-1}, 100 scans.
The Visible spectra were determined on a Perkin Elmer UV-IR-NIR _19, with an Integration Sphere for measurement reflection. In order to place the sample on the window of the integration sphere, a 1,3 cm x 2,5 cm piece of each sample was cut off and replaced once it had been analysed. For each sample, three spectra were acquired for UV-VIS-NIR at every different established moment, while only a single measurement performed in the Mid-IR on the same samples.

Results and discussion

As a consequence of the ageing process, physical changes in the structure of the paint layers were noted, especially for Madder Lake (Figure 2). In this pigment, an increase in the roughness of the surface could be observed by the naked eye. However, the most important change was the cohesion of the constituent materials of the layer, solid particles and agglutinant. During sampling, this phenomenon was clearly observed because the particles became detached and, in many cases, lost as soon as the tungsten needle contacted the surface.

In addition to this textural change, the most visible variations in time were related to fading in the paint layers. As can be observed in Figures 2-4, the most important change corresponded to Madder Lake. Some variations appeared in Crimson Lake, whereas there was hardly any alteration in the case of Lac Dye. These results were confirmed by the distribution obtained in the visible spectra. For Madder Lake, the intensity of the signal in the 300–650 nm range decreased from the first measurement to those obtained at different moments during the ageing process (Figure 5). Similar behaviour, but to a lesser extent in intensity and range (400-600 nm), could be observed for Crimson Lake (Figure 6). On the contrary, a very limited evolution in the spectra of Lac Dye in the range between 600 and 700 nm was registered visually (Figure 7).
The chemical changes in the molecules of the three pigments related to these observable variations could be tracked by the Mid-Infrared spectra obtained on the same date as the Visible spectra.
For Madder Lake, the spectra of the pure pigment and of the pigment agglutinated with linseed oil, at different stages of the degradation process, are shown in Figure 8. The main fact, in this case, is that no significant changes could be observed in the successive spectra. This could possibly be explained by the preparation procedure of this pigment, which included aluminium hydroxide as precipitant agent. The relative small amount of pure pigment in the final composition of the "coloured" mixture made it difficult to identify any anthraquinone compound. The spectrum obtained was that of the aluminium hydroxide, which barely changed over time in spite of the evident colour variations in the paint layer. Additional study of the small bands located in the fingerprint region is in progress.
The molecular changes for Crimson Lake could be better observed in this case. Figure 9 shows the Mid-Infrared spectrum obtained for this pigment and for the pigment agglutinated with linseed oil over time during the natural ageing process.
Evolution of linseed oil could be related to the decreasing intensity in bands at 3100 cm^{-1}, which could be associated with changes in the number of unsaturated bonds. The relationship between the intensity of the signals included in the 2960 and 2870 cm^{-1} bands could be related to the relative amount of CH_3 vs CH_2. The partially overlapped band at 1747 cm^{-1} was probably associated with the carbonyl group. Lastly , the shift in peaks located at 2930 cm^{-1} and

2850 cm^{-1} could be explained by a decrease in chain length [13]. All these changes could be considered part of the polymerization mechanism of the unsaturated oil.
On the other hand, the increase in the intensity of the bands at 1711-1645 cm^{-1} and 1430 cm^{-1}, which was probably related to changes in the carbonyl group, could be associated with the degradation process of the pigment. This would include the oxidation of alcohol functions with alteration in the chromophore properties of the carminic acid molecule.
In the case of Lac Dye, the changes in the Mid Infrared spectra that could be related to the evolution of the linseed oil structure were very similar to those described for Crimson Lake (Figure 10). Degradation in the pigment molecules would appear to be reflected in the decreasing intensity of bands located at 3405 and 1511 cm^{-1}, which is probably related to the disappearance of primary amines. Changes at peaks located at 1710, 1290 and 962 cm^{-1} could be related to the decrease of the number of the carboxylic acid functions. Furthermore, the increasing signal at 1576 cm^{-1} could also be associated with the formation of ester groups in the pigment molecules. By taking these results into account, the degradation in the laccaic acid would include the decrease in the carboxylic acid and primary amine functions and the increase in the ester functions. In this case, these changes would have a limited effect on the chromophore activity of the pigment.

Conclusions

The colour changes in the paint layers can be observed by the naked eye and also from the variations in their visible spectra. The structural alteration in the chromophore molecules produced by natural ageing can be followed through the changes registered in their Mid Infrared spectra.

Acknoledgements

The authors thank the Ministerio de Ciencia y Tecnología for the Grant BHA-2002-02756. They also thank Anna Vila for her comments.

References.

1. West Fitzhugh, Elisabeth, *Artists' Pigments. A Handbook of Their History and Characteristics*, Volume 3, National Gallery of Art, Oxford University Press, New York (1993).

2. AAVV, *Colour: Art & Science*, Press Syndicate of the University of Cambridge, Cambridge (1995).

3. Bakkenist, T., Hoppenbrouwers, R., Dubois Hélène, *Early Italian Paintings Techniques and Analysis*, Symposium, Maastricht, 9-10 October 1996, Limburg Conservation Institute, Maastricht (1997).

4. Gettens, R., Stout, G., *Painting Materials. A Short Encyclopaedia*, Dover Publications, Inc., New York (1966).

5. Harley, R.D., *Artists' Pigments. c.1600-1835*, Institute of Advanced Architectural Studies, University of York, Butler & Tanner Ltd., United Kingdom (1982).

6. Musée des Beaux-Arts de Carcassonne; Centre de Documentació i Museu Tèxtil de Terrassa, *Teintures précieuses de la Méditerranée*, (1999-2000).

7. Schweppe, Helmut, *Handbuch der Naturfarbstoffe*, Nikol Verlagsgesellschaft mbH&Co.KG, Hamburg (1993).

8. Kirby, J., Saunders, D. Cupitt, J. *Colorants and colour change*. Early Italian painting techniques and analysis. Ed. T. Bakkenist, R. Hoppenbronwer, H. Dubois. Limburg Conservation Institute (1997) 65-71.

9. Morris, H.R., Whitmore, P.W., Colaluca, G., *Preventing Discoloration in Films of Acrylic Artists' Media by Exposure to Ambient Light*, Studies in Conservation 48, (2003) 95-102.

10. Mills, John. White Raymond., *The Organic Chemistry of Museum Objects*, Butterworths, London, (1987).

11. Masschelein-Kleiner, L., Heylen, J.B., *Analyse des Laques Rouges Anciennes*, Studies in Conservation, 13 (1968), 87-97.

12. Meilunas, R., Bentsen, J.G., Steinberg, A., *Analysis of Aged Paint Binders by FTIR Spectroscopy*, Studies in Conservation 35 (1990) 33-51.

13. Ferrer, N., Romero, M.T., *Determination of oil and grease by solid phase extraction and infrared spectroscopy*, Analytica Chimica Acta 395 (1999) 77-84.

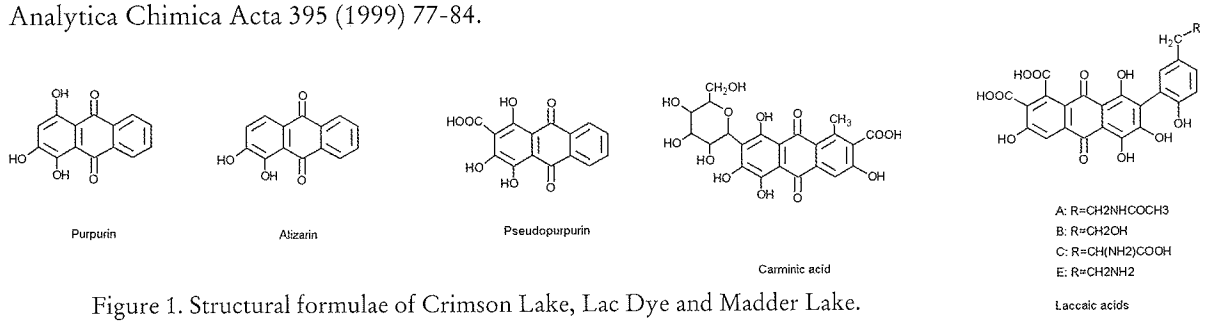

Figure 1. Structural formulae of Crimson Lake, Lac Dye and Madder Lake.

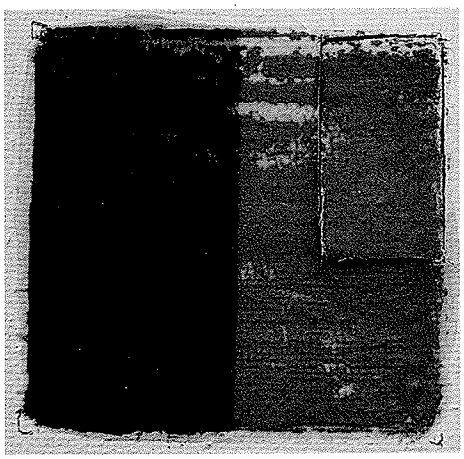

Figure 2. Square painted with Madder Lake. The discoloration on the right is very noticeable.

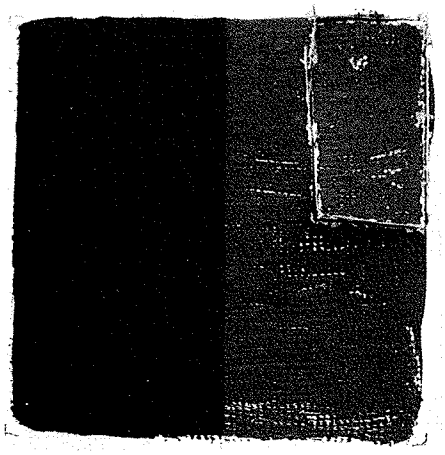

Figure 3. Square painted with Crimson Lake. Some discoloration can be observed.

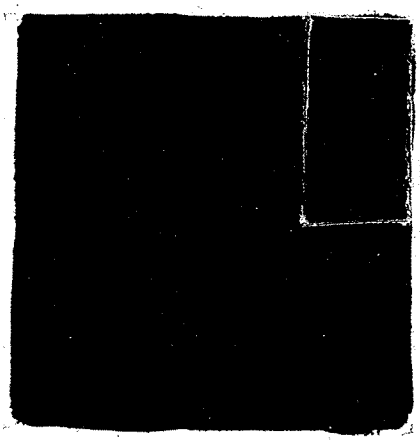

Figure 4. Square painted with Lac Dye. Difference in color is not very noticeable.

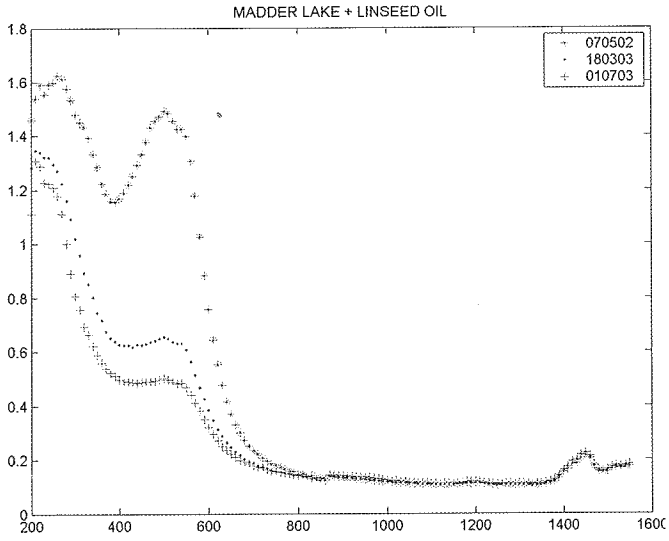

Figure 5. Visible spectra of Madder Lake at different moments during the natural ageing process.

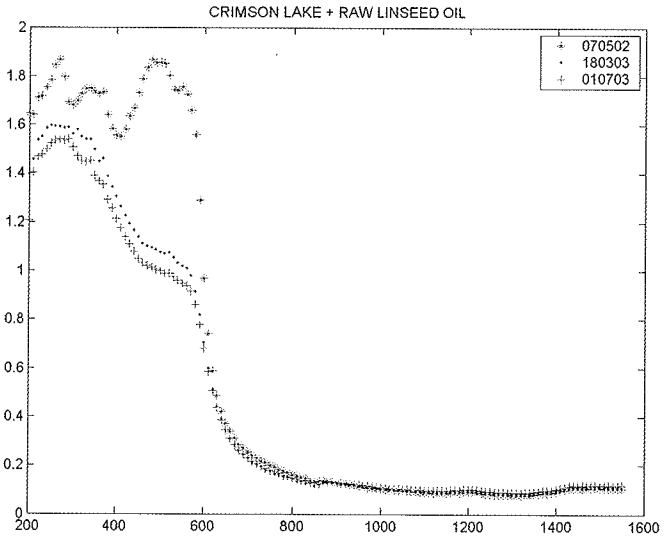

Figure 6. Visible spectra of Crimson Lake at different moments during the natural ageing process.

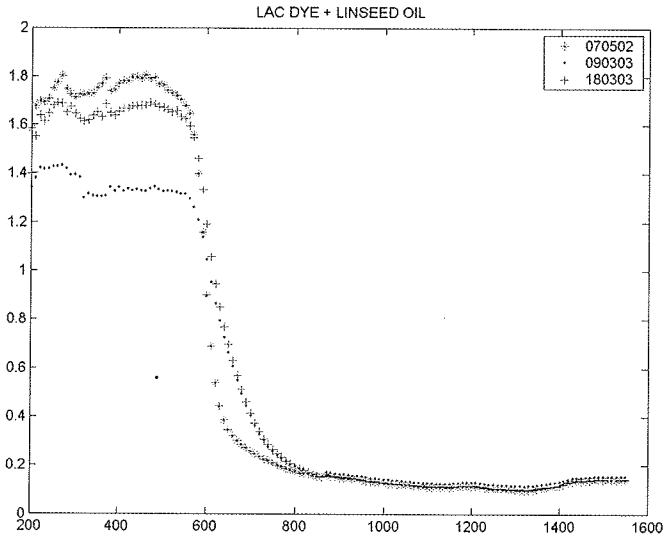

Figure 7. Visible spectra of Lac Dye at different moments during the natural ageing process.

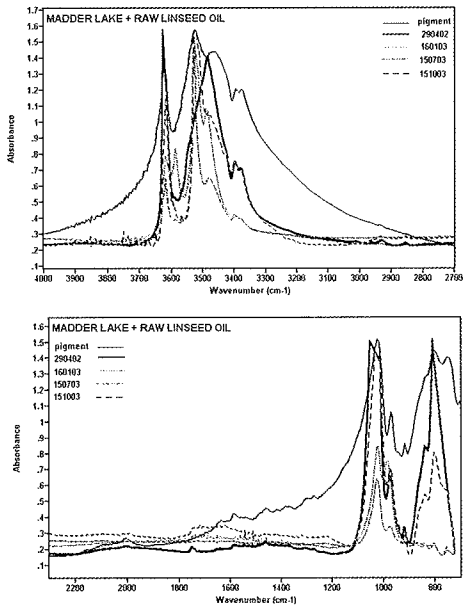

Figure 8. Mid Infrared spectra (4000 – 2700 cm^{-1}) - (2300 – 700 cm^{-1}) of Madder Lake at different moments during the natural ageing process.

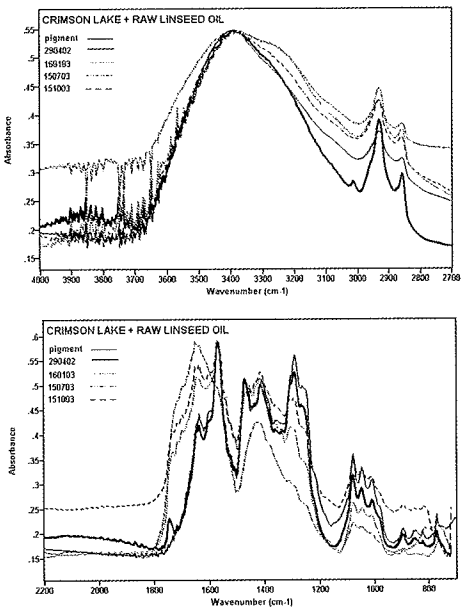

Figure 9. Mid Infrared spectra (4000 – 2700 cm^{-1}) - (2300 – 700 cm^{-1}) of Crimson Lake at different moments during the natural ageing process.

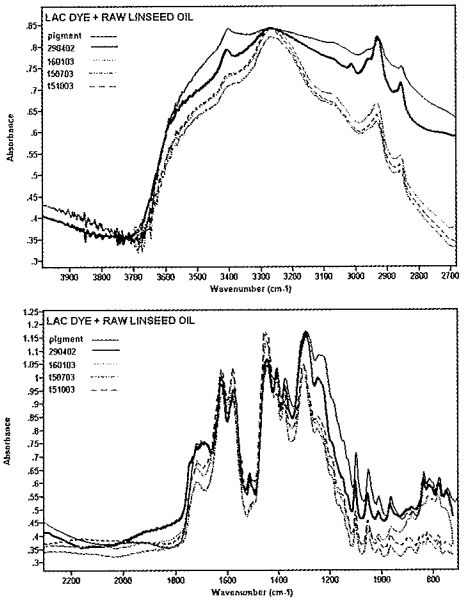

Figure 10. Mid Infrared spectra (4000 – 2700 cm^{-1}) - (2300 – 700 cm^{-1}) of Lac Dye at different moments during the natural ageing process.

The Infrared and Raman Users Group (*IRUG*) and the IRUG Database

Boris Pretzel[1], Beth Price[2] and Janice Carlson[2]
[1] Victoria & Albert Museum, GB-London SW7 2RL
[2] Philadelphia Museum of Art, Philadelphia, USA

The Infrared and Raman Users Group

IRUG is a collaborative effort to encourage the exchange of information, develop spectral standards, and distribute comparative high quality spectral data for the analysis of works of art, architecture, and archaeological materials.

Understanding and identifying materials, using techniques such as infrared spectroscopy, is fundamental to the process of conservation of cultural property. The technique is common in industry and scientific research establishments and many commercial infrared reference libraries exist. However, these do not cover most artists' materials and certainly do not include naturally aged organic substances. Furthermore, they are very expensive. Until now, there has not been an accurate and reliable spectral library for conservation. This has led to extensive duplication of effort in developing expertise and collecting reference data in many institutions all over the world specialising in the conservation / preservation of cultural heritage materials.

IRUG is a not for profit organisation set up collaboratively by conservation professionals using infrared and Raman spectroscopy for the analysis of cultural / preservation materials. It was first established in 1993, adopted a formalised structure in 1998 and incorporated in 2001.

IRUG meetings and early spectral libraries

From its initiation the group has held (and continues to hold) biennial meetings (alternately in Europe and the USA) to promote professional development and the exchange of expertise and spectral information amongst participants. Spectral information was collated by the group as received. Whilst these early library efforts were laudable, guidelines were not yet set for submissions to ensure quality of spectra and the spectra were not peer reviewed. Spectral quality issues included:

- *poor signal to noise, excessive noise and contamination*
- *oversaturated detector signals and unacceptable baselines*
- *incorrect material identification / classification, inadequate documentation*
- *absence of digitised files and lack of consistent formatting*

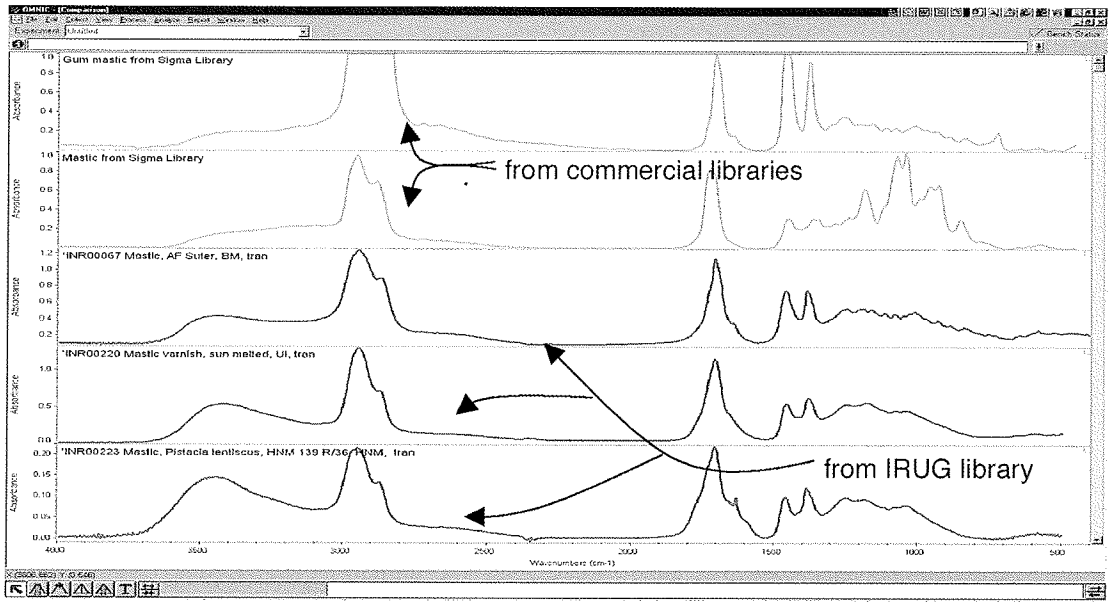

Comparison of spectra from Coatings Society and Sigma libraries with *IRUG* spectra and reference. Spectrum #1 contains totally absorbing bands in the C-H stretch region. Spectrum #2 has spurious bands centred at 1100 wavenumbers, probably due to a contaminant. *IRUG* spectra are f ree from such problems. These spectra were contributed by the Hungarian National Museum (HNM), the University of Iceland (UI), and the British Museum (BM).

The Editorial Committee

Following the 1998 *IRUG* meeting (*IRUG 3*), the group adopted a formalised structure and established an editorial team of 20 editors with experience in infrared and Raman spectroscopy. Fifteen of the editors met in Florence in 1999 to review all previous submissions to *IRUG* and reformat qualifying spectra to comply with the newly developed *IRUG* modified *JCAMP* file system. Only 25% of the 1200 submissions were kept for the new compilation following this exercise.

The *IRUG Edition 2000 Database*

The Edition 2000 database was:

- completed in March 2001
- over 1250 printed spectra and accompanying electronic records
- submitted by over 70 individuals in 50 institutions world wide
- contains materials encountered in the study of art, architecture, culture and history
- all files systematically named, classified and organised into 11 material groups

For the first time in this field

- all spectra are fully peer reviewed and quality assured
- for each spectrum, an electronic record contains all data pertinent to the spectrum, its acquisition and the material from which it is taken
- an extensive collection of high quality standard reference infrared spectra of materials found in the analysis of cultural, artistic and historic properties became available in a standardised and consistent format
- The collection has already become a valuable aid to conservation scientists, easy to share and providing a basis for continuing collaborative collection of reference data.

To find out more and contribute to *IRUG*

Logon to the IRUG web site **www.irug.org** for

- details of the biennial meetings program
- description of the *IRUG* modified JCAMP file format
- information on the new, on-line submission and distribution process contact details for the three regional chair persons
- information on other initiatives of the group

Future developments (currently in hand)

- new database releases
- discussion forum
- ... full database, online, ... searchable, ... downloadable

The Nature of Medieval Synthetic Pigments: the Capabilities of SR-Infrared Spectroscopy

Nati Salvadó[1*], Salvador Butí[1], Mark Tobin[2], Emmanuel Pantos[2] and Trinitat Pradell[3]
[1] Dpt. d'Enginyeria Química. EPSEVG. Universitat Politècnica de Catalunya, Av. Víctor Balaguer s/n 08800 Vilanova i la Geltrú. Barcelona
[2] Daresbury Laboratory, Kecwick Lane, Warrington WA4 4AD, UK
[3] Dpt. Física i Enginyeria Nuclear. ESAB. Universitat Politècnica de Catalunya, c/ Urgell 187, 08036 Barcelona.

Abstract

FTIR spectroscopy is a basic tool for the analysis of ancient painting materials because of its capability to identify most of the compounds present: inorganic compounds either natural or synthetic such as carbonates, sulphates or clays, and organic compounds such as bindings, glues or varnishes.
Samples smaller than one square millimetre in size were obtained from a medieval altarpiece from the 15th century AD, "El Conestable" (Capella de Santa Àgata, Barcelona) by Jaume Huguet. The samples were analysed by FTIR microspectroscopy. The use of the microscope is necessary because of the small quantity of material available from each of the micrometric sequences of layers forming the painting. Good spatial resolution in the FTIR spectra are needed to separate the heavily overlapping bands obtained from the complex mixture of compounds (pigments and binders) present and that show some natural degradation. The preparation of the samples must include cross sections and/or separation of the layers and particles forming the paintings, which are pressed into a diamond cell for analysis. With careful preparation, it is possible to focus on the different layers and particles allowing for the identification of the different compounds. Reference spectra must also be obtained and must include a broad set of aged materials, as degradation and ageing modify the intensity and positions of some of the bands.
Due to its brilliance and high collimation Synchrotron Radiation (SR) gives higher spatial resolution and signal/noise ratio than conventional spectrometers. Moreover, the high brilliance of SR-FTIR opens the possibility of making measurements in reflection mode.
In this paper we present the results obtained in the identification of the pigments and binding media and the link to the their technology of manufacture, and we analyse the potential of SR-FTIR compared with conventional spectrometers.

Introduction

Some pigments used in medieval times were synthetic and the technology used in their production is often related to other technologies such as glass and textiles.
Specific and well-focused analysis of painting materials can give several indicators on the origin of the technology linked to the pigment manufacture. These indicators may be related either to the composition of the pigments themselves or to the presence of residual compounds associated with the synthesis of the materials. In this work, the identification of different synthetic pigments is discussed on the basis of their manufacture. The paints analysed belong to Gothic paintings, more specifically to the altarpiece "El Conestable" a splendid artwork painted by the Catalan master Jaume Huguet in the 15th Century [1,2].
FTIR spectroscopy is a basic tool for the analysis of ancient painting materials [1-6] because of its capability in identifying most of the compounds present. FTIR microspectroscopy is a fundamental technique because it overcomes the main problems encountered: complex mixture of materials, micrometric layers and extremely small samples.
The use of FTIR microspectroscopy has represented an important step in the study of these complex materials because the different particles may be easily pinpointed and analysed. The use of Synchrotron Radiation represents a further advance in the technique as it gives higher spatial resolution and signal/noise ratio due to its brilliance and high collimation [7]. We demonstrate that this technique is the most advanced for the identification of ancient paintings.

Experimental

Analytical Techniques
In order to perform the non microscopic experiments a BOMEM MB-120 FTIR Spectrophotometer was used. The

apparatus is equipped with a N_2 removal compartment, DTGS detector allowing a measuring range between 4000-400 cm^{-1} and a beam condenser X^4 (Serveis Científico-Tècnics from Universitat de Barcelona). The use of a beam condenser and a diamond cell as sample holder allows the measurement of extremely small samples (about 100 microns spot size).
SR-FTIR has been developed on beamline 11.1 on the Synchrotron Radiation Source at Daresbury Laboratory, Warrington, UK. The NEXUS FTIR spectrophotometer is equipped with a Nicolet Continuum microscope, MCT detector, measuring range 4000-650 cm^{-1}. The collimated synchrotron beam is introduced directly into the spectrophotometer and towards the IR microscope. The infrared beam is very stable, with a high brilliance and allows to focus a 10 square micrometer spot.
In this paper we present the application of conventional micro infrared FTIR spectroscopy and SR-FTIR to the study of ancient pigments and paintings and we will also compare the capabilities of both techniques.

Samples, chemicals and reference materials
The painting samples consisted of a mixture of pigments, binding media and alteration products. The synthetic pigments identified were the green and the red pigments.
Reference materials of carminic acid, lead carbonate and lead basic carbonate were analytical reagent grade and were supplied by Sigma Aldrich Chemical. Copper acetate monohydrate and copper hydroxide carbonate were supplied by Probus. Verdigris was supplied by Zecchi.
The binding media such as egg yolk, egg white and drying oil were prepared in our laboratory from natural materials. In order to be able to compare them to the ancient materials, they were aged in the laboratory for at least five years.
Finally, several ancient recipes for the production of green pigments were also reproduced in the laboratory [8-10].

Methodologies, results and data discussion

A methodology for the identification of painting materials able to give information on the binding media, ageing products and on the pigments was fully developed [1]. The methodology included the use of different analytical techniques and specific sample preparation. Conventional techniques applied included Optical Microscopy, Scanning Electronic Microscopy with EDX, infrared spectroscopy (FTIR), Raman spectroscopy and x-ray diffraction. However, because of the complex nature of the samples, the information obtained using conventional techniques is often not definitive. Thus, Synchrotron Radiation micro-x-ray diffraction and Synchrotron Radiation FTIR were used to take advantage of properties such as the high intensity and brilliance of the beam, and small beam footprint.
As only microsamples were available, a meticulous study of the samples is fundamental in distinguishing the many compounds present. The sample preparation is very important to obtain accurate information on the sequence of the different micrometric painting layers. Small fragments are selected from each of the layers of the samples and placed in a diamond cell. An example is shown in Figure 1 where the IR spectra of the green chromatic layer show the presence of a yellow pigment, $2PbO{\cdot}SnO_2$, [11,12] and a white pigment $PbCO_3/2PbCO_3{\cdot}Pb(OH)_2$. The 3289, 3080, (2954), 2922, 2851, (1740), ~1650 and 1548 cm^{-1} absorption bands are related to egg yolk and correspond to the binding media. However, the green pigment is not clearly identified.
FTIR microspectroscopy is particularly important for this type of sample, due to the small dimensions required, of a few micrometer in size. The samples are first placed and pressed in the diamond cell, and then only one window of the cell (the one in which the sample is well distributed) is used for the measurement. The scattering of light in a conventional IR equipment often results in poor spectra. SR-FTIR, on the other hand, gives higher spatial resolution and signal/noise ratio due to its brilliance and small spot size (10x10 micrometer). Examples are shown in figures 2 and 3. SR-FTIR allows a single particle/compound to be pinpointed which may be crucial in the interpretation of the heterogeneous spectra obtained from the whole layer. One of the main problems is the selection of particles. In this case, microscopic contaminations may represent a significant fraction of the material resulting in a misleading identification of the painting layer. For this reason small fragments, which are carefully selected from each layer, are used.
Figure 2 shows the SR-FTIR spectra obtained from a surface alteration layer where major proportions of calcium oxalate and calcium sulphate were identified. The absorption band at 1321 cm^{-1} related to the oxalates is slightly shifted to an intermediate position between the characteristic band of $CaC_2O_4{\cdot}2H_2O$ (weddellite) and $CaC_2O_4{\cdot}H_2O$ (whewellite) [13-15]. This is probably related to a different hydration of the oxalates or most probably to compression of the sample applied by the diamond cell. The presence of calcium oxalates is associated to an

alteration of the organic media, the drying oil and egg protein. Figure 3 shows the SR-FTIR spectra of the green chromatic layer. The green pigment is found to contain: copper acetates, absorption bands at 3470, 3370, 3270, 1585, 1564, 1414 and 1353 cm^{-1}; $Cu_2Cl(OH)_3$ (structure of paratacamite), absorption bands 3446, 3354, 3338, 986, 947, 920, 895 and 847 cm^{-1}; $Cu_2CO_3(OH)_2$, absorption bands 820, and ~1400 cm^{-1} [16-24]. Moreover, the bands at 780, and 1318 cm^{-1} related to a calcium oxalate monohydrate and the bands corresponding to $PbCO_3/2PbCO_3 \cdot Pb(OH)_2$ were also identified. The binding media is found to be egg yolk, absorption bands ~3067, 2954, 2926, 2854, 1739, 1650 and 1542 cm^{-1}, that correspond to those found in a seven-year aged egg yolk. Finally, the presence of a drying oil is also determined.
Spectra were compared with the FTIR spectra of reference materials. The mixture of compounds found for the green pigment corresponds to a synthetic pigment obtained using the procedure given in the treatise of Theophilus, De Diversis Artibus [8,9]. The process described consists of smearing copper plates with honey and salt (sodium chloride) and exposing them to vinegar vapours in a sealed receptacle. A mixture of different copper-based compounds, such as acetates, basic chlorides and carbonates is obtained [25].
The green layer is a mixture of several synthetic pigments: white $PbCO_3/2PbCO_3Pb(OH)_2$, yellow $2PbOSnO_2$ and copper green. The binding medium is made of egg yolk and drying oil. The lead carbonates are also synthetic as is the yellow pigment which is associated to ancient glass technology.
The use of high brilliance SR infrared light and the high signal/noise ratio achieved, improves the detection and the quality of the spectra and thus opens the possibility for making measurements in reflection mode. For a reflection measurement, the preparation is made by embedding the painting samples in a polyester resin which is afterwards polished with a diamond paste. Figure 4 shows the IR spectra obtained in reflection mode after Kramers-Kronig transformation and Kubelka-Munk equation from a dark red sample.
FTIR of the red pigment shows the presence of a carminic acid (1078 and 1044 cm^{-1} absorption bands, figure 5) [26,27]. The presence of alum was determined by SR X-ray diffraction and SEM-EDX. This compound is used to precipitate the lake pigment, and this lake pigment is related to ancient textile activity. Also, in this dark red layer a proteinaceous material was determined. The proteinaceous materials found in the IR spectra belong in part to the binding medium but they are also related to the animal origin of the red pigment itself. Comparing the spectra obtained with our aged reference materials, the binding medium may be related to egg white.

Conlclusion

The use of Synchrotron radiation IR Spectroscopy has been demonstrated to be a superior technique for the study of ancient paintings. It gives well resolved spectra with a high signal to noise ratio on extremely small spots (about 10 microns size), and it improves the identification of complex mixtures even for compounds appearing in very low concentrations. It also opens the possibility of working in reflection mode on micrometric cross sections of painting layers.
The green and the red pigments were analysed and successfully identified. All the compounds identified for the green pigment are related to the recipe given by Theophilus for the synthesis of a green pigment. The yellow and the white pigments mixed with the green are also synthetic and the yellow is related to glass technology. The binding media used for the green pigments is egg yolk and drying oil. The red pigment is of natural origin (insects) but its extraction and precipitation followed the methods used in ancient textile industry. The binding medium used in the red has been identified as egg white.

Acknowledements

This work has been developed and funded by the Memorandum of Understanding Agreement between the Patrimoni UB-UPC (Universitat de Barcelona and Universitat Politècnica de Catalunya) and CCLRC-Daresbury Laboratory. Our acknowledgement is also given to Serveis Científico-Tècnics of the Universitat de Barcelona for allowing the use of the Infrared Spectroscopy utilities.

Reference

1. Salvadó, N., Ph.D Thesis. Universitat de Barcelona (2001).

2. Salvadó, N., Seco, M., Vendrell, M. 'Materials i tècnica en la pintura de Jaume Huguet (s. XV)', *Butlletí del Museu*

Nacional d'Art de Catalunya, Barcelona (2001) **5** 47-58.

3. MCCawley, J.C. 'Diamond cell infrared spectroscopy in the analysis of paints ad pigments'. *ICOM Committee for Conservation, 4th Triennial Meeting, Venice*, (1975) 75.

4. Laver, M. E.; Williams, R.S. 'The use of a Diamond cell Microsample Device for Infrared Spectrophotometric Analyses of Art and Archaeological Materials'. *Journal of the International Institute for Conservation- Canadian Group (JII-CG)*, (1978) 3, N2,.

5. Baker, M. *et al.*'FTIR microspectrometry: a powerful conservation analysis tool'. *Sixteenth annual meeting, New Orleans, Louisiana, 1988. The American Institute for Conservation of Historic and Artistic Works. Washington*, (1988).

6. Baker,M. *et al.* 'Non-destructive and micro-sample FTIR microspectrometric analysis of organic materials in art objects'. *2nd International conference on non-destructive, microanalytical methods and environment evaluations for study and conservation of works of art, Perugia*, (1988).

7. Dumas, P. & Tobin, M.J., 'A bright source for infrared microspectroscopy: synchrotron radiation', *Spectroscopy Europe* (2003) 15, 6 .

8. Escalopier, C., *Théophile prète et moine. Essai sur divers arts 1843*, París (1996).

9. Hawthorne J.G. & Smith, C.S. Theophilus on Divers Arts: the foremost Medieval Treatise on Painting Glassmaking and Metalwork. New York (1979).

10. Vitruvio: Los Diez Libros de Arquitectura. Alianza Forma ed. (2000), Madrid, Spain.

11. Vigoroux, J.P., *et al.*. 'Etude par spectroscopié vibrationnelle des oxydes Pb_3O_4, $SnPb_2O_4$ et $SnPb(Pb_2O_4)_2$'. *Spectrochimia Acta*, (1982) 38A.

12. Kühn, H. 'Lead-Tin Yellow'. *Artist's Pigments: A Handbook of their history and characteristics, volum 2. Ashok Roy, Editor, National Gallery of Art Washington*, Oxford University Press (1993).

13. Cariati, F. *et al.* 'Calcium oxalate films on stone surfaces: experimental assessment of the chemical formation'. *Studies in Conservation*, (2000) 45.

14. Petrov, I.; Soptrajanov, B. 'Infrared spectrum of whewellite', *Spectrochimia Acta* 31A, 1975.

15. Shippey, T.A. 'Vibrational studies of calcium monohydrate (whewellite) and an anhydrous phase of calcium oxalate', *Journal of Molecular Structure* (1980) 63.

16. Goldsmith, J.A. & Ross, S.D. 'the infra-red spectra of azurite and malachite' *Spectrochim. Acta*, (1968) A24, 2131-2137.

17. Dei. L. *et al.* 'Green degradation products of azurite in wall paintings', *Studies in Conservation* (1998) 43 80-88.

18. Gettens & Fitzhugh, 'Malachite and green verditer' *Studies in Conservation*, (1974) 19 2-23.

19. Farmer, V.C. *The infrared Spectra of Minerals*, Londres: Minerological Society, (1974).

20. Baraldi, P. & Fabbri, G., 'Study of the bands attributable to crystallization water in hydrated metal acetates', *Spectrochimia Acta*, (1981) 37A, 89-92.

21. Giangrande, C., 'Identification of bronze corrosion products by infrared absorption spectroscopy'. *Recent Advances in the Conservation and Analysis of Artifacts, Summer Schools Press, London* (1987).

22. Fuchs, R. & Oltragge, D., 'Utilisation d'un livre de modèles pour la reconstitution de la pienture de manuscrits. Aspectes historiques et fisico-chimiques' *Pigments et Colorant de l'Antiquité et du Moyen Age, Colloque Internationale du CNRS, Éditions du CNRS,* Paris, (1990).

23. Jones, G.C. & Jackson, B., 'Infrared transmission spectra of carbonate minerals', *Chapman&may ed.*, (1993).

24. Kühn, H., 'Verdigris and Copper Resinate', *Artist's Pigments. A Handbook of their History and Characteristics, v2, Ashok Roy (ed), National Gallery of Art Washington*, Oxford University Press, (1993).

25. Salvadó, N., Pradell, T., Pantos, E., Papiz, M.Z., Molera, J., Seco, M. and Vendrell-Saz, M, Journal Synchrotron. Radiation, (2002) 9 215.

26. Flieder F. 'Mise au point des techniques d'identification des pigments et des liants inclus dans la couche picturale des enluminures de manuscrits'. *Studies in Conservation*, (1968) 13.

27. Schepper, H.; Roosen-Runge, 'Carmine- Cochineal Carmine and Kermes Carmine'. *Artists' pigments. A handbook of their History and Characteristics, vol 1, R.L.Feller (ed.),* National Gallery of Art Washington, Oxford University Press, (1986).

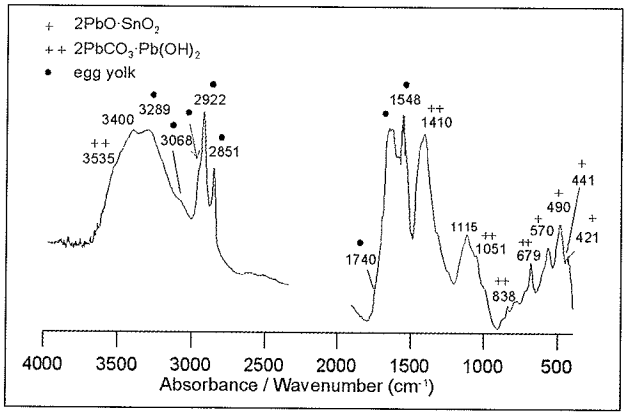

Figure 1. FTIR Spectra (diamond cell, beam condenser X^4, 125 scans, 4cm^{-1} resolution).

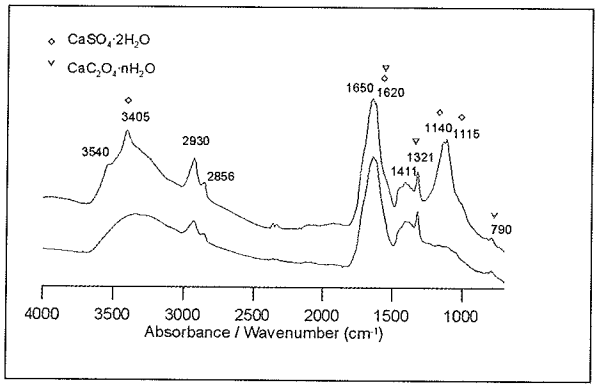

Figure 2. SR-FTIR microspectroscopy spectra (128 scans, 4cm^{-1} resolution, spot size 10x10) from superficial alteration layer.

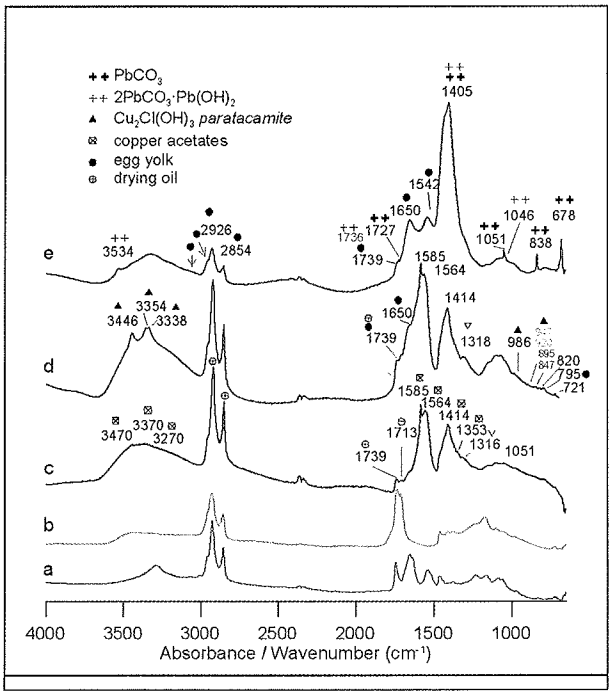

Figure 3. SR-FTIR microspectroscopy spectra (128 scans, 4cm^{-1} resolution, spot size 10x10) from green layer (c, d, e) and aged egg yolk (a) and aged drying oil (b).

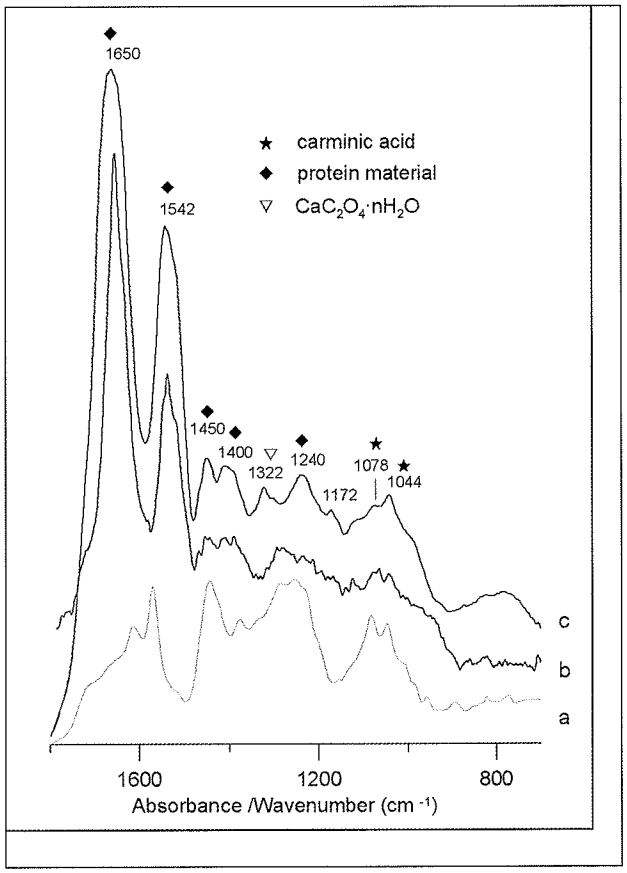

Figure 4. SR-FTIR microspectroscopy spectra (128 scans, 4cm^{-1} resolution, spot size 10x10) from dark red layer (c), reflectance spectra from polished dark red layer (b) and reference carminic acid Aldrich (a).

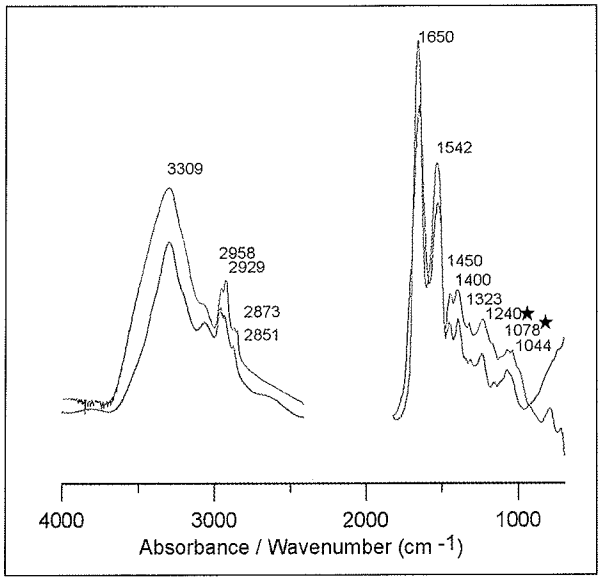

Figure 5. SR-FTIR microspectroscopy spectra (128 scans, 4cm^{-1} resolution, spot size 10x10) from dark red layer and aged egg white.

Identification and Classification Of Synthetic Organic Pigments Of A Collection Of The 19th And 20th Century By FTIR

A. Schaening, M. Schreiner, D. Jembrih-Simbuerger
Institute of Sciences and Technologies in Art, Academy of Fine Arts, Schillerplatz 3, A – 1010 Vienna, Austria

Abstract

This study presents an on-going project concerning the identification and classification of synthetic organic pigments, which were selected from the material collection of the Institute of Sciences and Technologies in Art at the Academy of Fine Arts in Vienna. The collection includes a large number of various pigments, dyes and binders. The results concerning the inorganic pigments are presented in an additional paper [1]. Data of more than 600 specimens of the early industrial period as well as the 2nd part of the 20th century were catalogued in a Microsoft ACCESS®- database. Extended research of source literature and the Colour Index [2] led to a preliminary classification of dyes and pigments. Selected samples were analyzed by means of energy dispersive x-ray fluorescence analysis (XRF), which detected the main elements with an atomic number higher than 11 (Na). Mainly, extenders, fillers or substrates present could be characterized, which was helpful for the interpretation of the results obtained by FTIR.

Introduction

Despite the increase in the use of modern pigments since their introduction in the early 20th century, a minority of those had been investigated on artifacts. Detailed data on the use of these modern materials and their FTIR spectra, which could be obtained by classifying and analyzing the synthetic organic pigments of the collection, might be helpful tools for future analytical challenges. As a first step in this direction the organic synthetic materials of the pigment collection of the Academy of Fine Arts in Vienna have been catalogued by using the Microsoft database software package ACCESS®. The commercial names of the samples and, where possible, also their color index names (CI) [2], chemical classification and manufacturer were taken into account along with the relevant literature. Additionally, small amounts of the specimens were analyzed by x-ray fluorescence analysis (XRF) in order to determine the main and trace elements from Na – Pb. The main goal was to build up a database with the FTIR spectra of all the samples in the material collection.

Experimental

The FTIR measurements were carried out with a Perkin Elmer instrument Spectrum 2000 with an attached microscope (Perkin Elmer, i-series). Small samples on a diamond cell were prepared and analyzed in the transmission mode. Due to the MCT-detector available a spectral range from 4000 - 580 cm^{-1} could be registered.

Results and Discussion

In the studies carried out so far, pure synthetic organic materials, as well as pigments with substrates, fillers or extenders have been investigated. Due to the great number of samples available only a few pigments are presented here as examples.

Synthetic organic pigments – pure materials
In Table 1 three pigments of our collection are summarized including their commercial names, chemical classification, colour index, institute-inventory-number and the elements which were detected by XRF:
FANALGELB (PY18, 49005) was introduced in 1924 and primarily used in printing colors of the Twenties and Thirties of the 20th century.
PARAROT (PR1, 12070) was the first organic red pigment, synthesized in 1885, and was manufactured for the first time in 1889 [4]. Formerly widely used, many manufacturers have stopped production [5] and nowadays PR1 is still in use only for industrial printings [7].
Although the reference spectra of both pigments were not available, FANALGELB and PARAROT could be classified as PY18 (Fanalgelb) and PR1 (Pararot) by using the Colour Index [2].
In contrast to the pigments mentioned above, ROTEXTRAKT/SIEGLE is not listed in the Colour Index [2] and

could be identified as Pigment Violet 1 (PV1, 45170) by comparing the data of the Tate Organic Pigment Archive [3]. Pigment Violet 1 is described as a basic dye-based pigment of the PTMA type (also named Triarylcarbonium PTMA), which is prepared by complexing a basic dye molecule with a complex inorganic acid such as phosphotungstomolybdic acid (PTMA) [6]. First introduced in 1924 by I.G. Farben (Germany), PV1 was employed for printing colors, paints etc. Recently PV1 was found in a catalogue for artists` paints formulations of Winsor & Newton/ Designers Gouache (W&N International Catalogue, 2003).
As can be seen in Figure 1, the pigment ROTEXTRAKT/SIEGLE (PV1), Inv. No. 938 of our collection, yields the same spectrum as the Fast Red Toner (PV1) of the Tate Organic Pigment Archive [3].

Institute Inv. No.	Commercial Name	Chemical Classification	Colour Index Name	Historical notes and aspects of use	XRF
951	Fanalgelb	Triarylcarbonium (PTMA/ phosphor-tungstomolybdic acid); lake of Thioflavine	Pigment Yellow 18 [PY 18, 49005]	Introduced 1924 (I.G. Farben, Germany); used in printing colours in 1920ies and 30ies, only minimal importance nowadays	W, Mo
759	Pararot	ß-naphtol	Pigment Red 1 [PR 1, 12070]	Introduced 1895; widely used for paints; still in use preliminary for industrial printing	-
938	Rotextrakt, Siegle	Triarylcarbonium (PTMA/ phosphor-tungstomolybdic acid); derived from Rhodamine B	Pigment Violet 1 [PV 1, 45170]	Introduced 1924, I.G. Farben (Germany); printing colours etc., recently: used in artists paints formulations as W&N/ Designers Gouache (W&N International Catalogue, 2003)	W, Mo
	Fast Red Toner, HY Pigments		Pigment Violet 1, Tate [3]		

Table 1: Synthetic organic pigments - pure materials

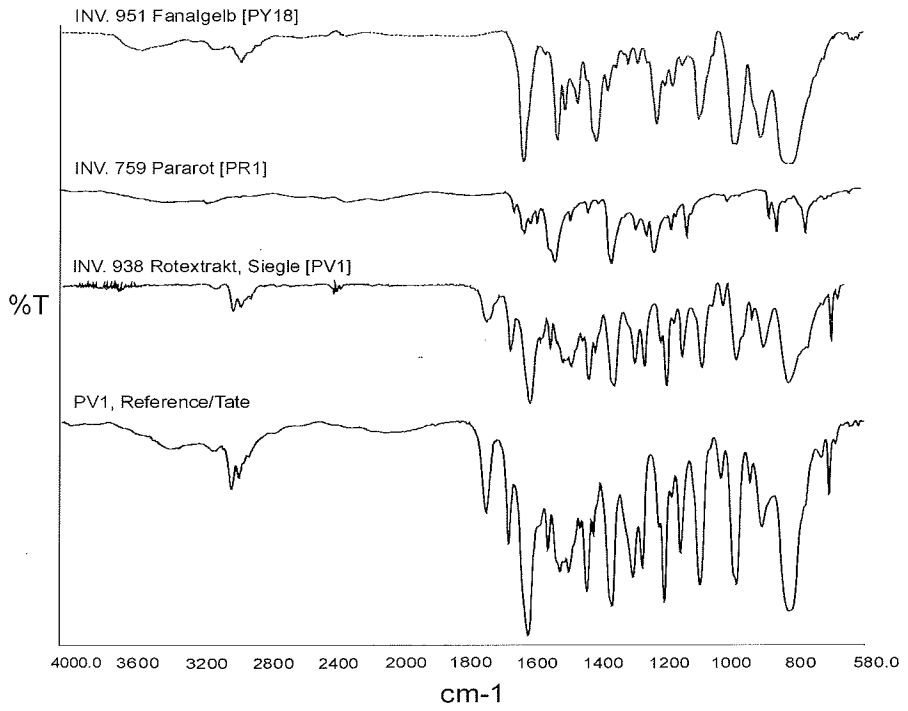

Figure 1: FTIR spectra (4000-580 cm^{-1}) of pure pigments

Synthetic organic pigments containing substrates/ fillers/ extenders

As can be seen in Table 2, the sample Inv. No. 896, ECHT SCHARLACHROT G of the company Siegle contains barium and sulphur. Siegle & Co. was a subsidiary company of BASF and sold pigments for artists and as decorative paints until they merged with BASF in 1970. As Siegle merely processed and marketed pure industrial products manufactured by other companies like BASF, their products were not listed in the Colour Index.

Figure 2 shows the results obtained by FTIR, where the spectra of the white pigment blanc fixe in our collection (Inv. No. 81) and of the Inv. No. 250 (ß-naphtol, PR3) were used as reference materials. For comparison, the spectrum of Hansa Scarlet RNC (PR3) of the Tate Organic Pigment Archive [3] is depicted. The spectrum of ECHT SCHARLACHROT G of Siegle can be identified as a mixture of $BaSO_4$ and a ß-naphtol pigment (PR3). As an example of this naphtol pigment LITHOLECHTSCHARLACH RN (Inv. No. 250) is also shown in Figure 2. Additionally, the spectrum of the red material is widely identical with the spectrum of Hansa Scarlet RNC [3], which was identified as ß-naphtol (PR3).

Institute Inv. No.	Commercial Name	Chemical Classification	Colour Index Name	Historical notes and aspects of use	XRF
81	Schwerspat	$BaSO_4$	**Reference:** blanc fixe (Schwerspat)	Known since ancient periods	Ba, S
896	**Echt Scharlachrot G, Siegle**	**ß-naphtol + $BaSO_4$**	**Pigment Red 3 [PR 3, 12120] + blanc fixe**	**Toluidine Red PR 3: introduced 1905, still used in printing colours, paints etc.**	**Ba, S**
250	Litholecht-scharlach RN	ß-naphtol	**Reference:** PR 3	PR 3, see above	-
-	Hansa Scarlet RNC, Clariant	ß-naphtol	**Reference:** PR 3, Tate [3]	PR 3, see above	

Table 2: Synthetic organic pigments – containing substrates/fillers/extenders

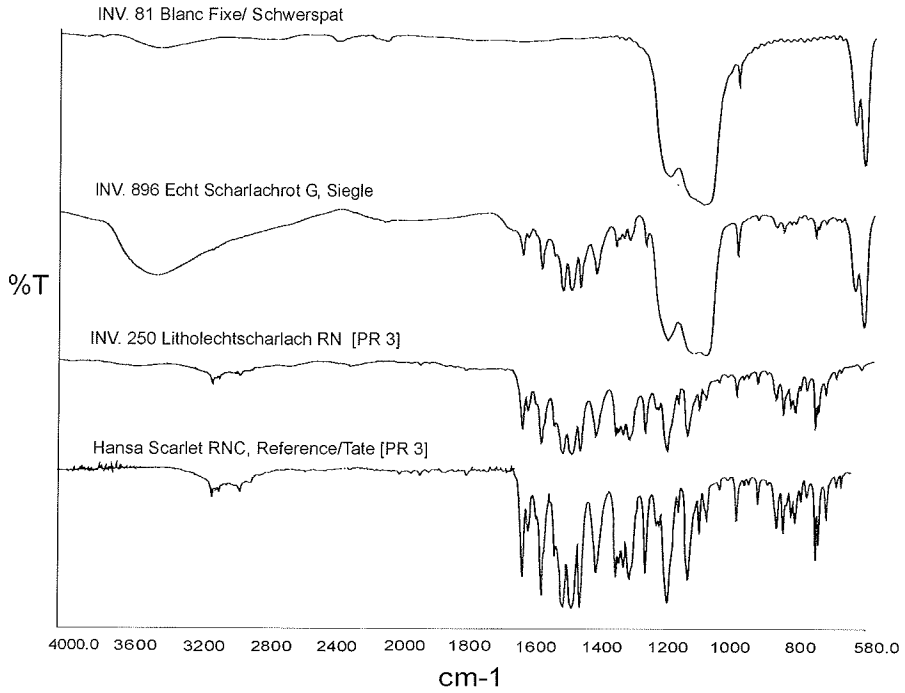

Figure 2: FTIR spectra (4000-580 cm^{-1}) of Echt Scharlachrot G/ Siegle (Inv. No. 896) as well as the reference of the materials blanc fixe (Inv. No. 81), Litholechtscharlach RN (PR3, Inv. No. 250) and Hansa Scarlet RNC (PR3, reference Tate [3]).

Conclusion/ Perspectives

A few FTIR spectra were obtained for the selected synthetic organic pigments of the collection. The spectra were compared with the data of the IRUG-database [8] and the Tate Organic Pigment Archive [3].
Future research will focus on further investigations of paint manufacturers` color charts (Siegle & Co., Winsor & Newton, Talens etc.) to obtain data with regards to the application of synthetic organic pigments to paintings from the first half of the 20th century.

References

1. Fruehmann, B., Schreiner, M., Mantler, M., *A database of inorganic historical pigments*, this conference

2. *Colour Index, Ed.*, Society of Dyers and Colourists and American Association of Textile Chemists and Colourists, 3rd Ed., Bd. 1-4, Bradford 1971, Bd. 5, 6, Bradford (1975)

3. Learner, T., 'Tate Organic Pigment Archive', unpublished FTIR spectra, Millbank, London SW1P 4 RG (2003)

4. Keijzer, M. de, 'A survey of red and yellow modern synthetic organic artists` pigments discoverd in the 20th century and used in oil colours' in J. Bridgland (ed.), *ICOM Comittee for Conservation 12th Triennial Meeting, Lyon 29. August – 3. September 1999, Preprints, vol. 1*, James & James (Science Publishers) Ltd, London, (1999) 369-374

5. Potdar, S., 'Toluidine, Para, and Chlornitroaniline Reds' in P. A. Lewis (ed.), *Pigment Handbook, Vol. 1, Properties and Economics*, 2nd Ed., Wiley Interscience, New York (1988) 441-452

6. Lewis, Peter A., 'Permanent Basic Dye-Based Pigments' in P. A. Lewis (ed.), *Pigment Handbook, Vol. 1, Properties and Economics*, 2nd Ed., Wiley Interscience, New York (1988) 579-586

7. Herbst, W., Hunger, K., *Industrielle Organische Pigmente*, VCH Verlagsgesellschaft, Weinheim (1995)

8. Price, B., Prezel, B., Carlson, J., *Infrared and Ramen Users Group Spectral Database*, Edition 2000, available at www.irug.org

A Database of Inorganic Historical Pigments

B. Frühmann [1,2], M. Schreiner [1,2], M. Mantler [3]
[1] Institute of Sciences and Technologies in Art, Academy of Fine Arts, Vienna/Austria
[2] Institute of Chemical Technologies and Analytics, Vienna University of Technology, Austria
[3] Institute of Solid State Physics, Vienna University of Technology, Austria

Abstract

Approximately 400 different inorganic pigments were analysed for this first study of its kind by combining three different methods. X-ray diffraction (XRD), x-ray fluorescence (XRF) and Fourier transform infrared (FTIR) spectroscopy proved to be suitable techniques to identify and characterize the various materials. The experimental work was focused on XRD analysis in order to detect the main components and to perform phase analysis for the identification of the crystallographic structure. XRF analysis was carried out and complemented by FTIR spectroscopy in order to facilitate the analysis of the diffractograms and investigate differences in the elemental composition. The data were used to build up a database of the experimental results. Additionally, two libraries for XRD and FTIR analysis were compiled containing the measured spectra of all pigments, which can be combined with conventional databases (ICDD, IRUG).

Introduction

The identification of pigments is an essential work for the analysis of art objects, where only small samples can be taken to identify the used materials. By knowing the chemical formula any pigment can often be characterised by one to three major constituents, which are then regarded as key elements [1-3]. In some cases, like ultramarine, the minor constituents or even traces are also typical and important for the characterisation of the provenance. Due to this fact it is obvious, that a database of pigments would be of great help. The Institute of Sciences and Technologies in Art of the Academy of Fine Arts, which has collected a great number of pigments over the last decades, made its collection available. This collection consists of historic (19th century) and modern (20th century) pigments, dyestuffs and adhesives with a wide variety of colours and materials. About 400 different inorganic pigments were used for this work, which range from different types of white over yellow, orange, red, brown, blue to green and black. Some of them are unique pigments, because they are not available on the market anymore. As many of the pigments are being manufactured by different companies, it was interesting to determine their composition, which can provide a better insight in the fabrication process [4].

In the present study x-ray diffraction (XRD) analysis and x-ray fluorescence (XRF) analysis have been used for the phase and elemental analysis of the pigments, respectively. These techniques are also widely used in the field of science in art and archaeology as well as during conservation and restoration of artefacts. An additional method applied to art objects is IR spectroscopy [5], which is also well established for the analysis of pigments. Therefore, Fourier transform infrared (FTIR) spectroscopy was applied to these samples too. The results of these measurements, together with the names and the collected literature information are summarized in a database (MS-Access). Additionally, two libraries were compiled, one with the diffractograms of the XRD measurements and one with the spectra of the FTIR measurements. They can be used like the commercial libraries from ICDD [6] or IRUG [7], whereas for handling the particular software of the used hardware is necessary.

Based on the big variety of pigments in this collection, only the inorganic have been analysed so far. In this case it was necessary to distinguish between the natural and the synthetic samples. Natural pigments deposit in mines and quarries [8]. In order to build up a system of the inorganic pigments in different aspects like colour, usability, production etc. can be used [9]. In our case the chemical composition and structure of the various pigments were utilized for their systematic ordering.

The nomenclature of these samples is rather arbitrary. The pigment names established by standards are only valid for a small amount of pigments. In most cases the samples are designated by trivial names, where no clear information about their chemical composition can be deduced. On the one side, pigments of the same chemical composition are characterized by several different names such as Prussian blue, which is also well-known as Antwerp blue, Chinese blue, Paris blue or Delft blue [10]. With the help of this database, a consistent method for this collection could be created.

Experimental Section

XRF Measurements
XRF analysis enables the identification of the chemical elements of the samples without loosing any material. Usually qualitative and quantitative analysis can be applied. Due to the lack of reference materials for the powdered pigments only a qualitative evaluation of the spectra could be carried out.
The XRF measurements were performed with a TRACOR X-ray SPECTRACE 5000 equipment with a Rh-tube as source and a liquid N_2 cooled Si(Li) detector. The excitation conditions were 8 kV (for measurements in vacuum), 30 and 50 kV (for measurements in air), which have been proved to be optimal for analyzing the various elements. The collecting time (time of acquisition) for each spectrum was 100 seconds.
In general, the knowledge of the chemical elements is sufficient for the identification of the pigments. The presence of Ca and S e.g. in a white layer or pigment is an indication for gypsum ($CaSO_4$). However, XRF is widely used as a supplementary method in powder diffractometry and phase analysis, where the information about the elemental composition helps to interpret the search-match pattern lists.
XRD Measurements
The main purpose of the XRD measurements was to achieve an identification of the pigments by crystallographic phase analysis [11]. The measurements were carried out using a SIEMENS D5000 diffractometer with a θ-θ - goniometer (diameter 401 mm), equipped with a Cu-tube with the excitation conditions of 40 mA and 40 kV and a scintillation counter. In order to obtain a sufficient number of datapoints for peak-fitting and an acceptable number of counts, especially from the small amount of sample material, a step size of 0.02° with a step time of 10 sec/step was used. The diffractograms were collected in the range of 5 - 80° (2θ) with an aperture slit of 2 mm, an anti-scatter slit of 6 mm and a receiving slit of 0.2 mm.
The diffractograms were analyzed by combining the measured diffractograms with the data of the commercial ICDD database [6] using the search/match algorithm. Because of the immense size of this database, it was necessary to constrain the search by using the results of the XRF measurements.
FTIR Measurements
The high advantage of the FTIR analysis is the fact that samples with a bad crystalline structure as well as amorphous samples can be analyzed. This technique supports the identification of organic components of the samples and ease phase analysis [12].
FTIR analysis was carried out with a Spectrum 2000 (Perkin-Elmer) in combination with a microscope (i-Series). The scan-region was in the range of 4000 - 580 cm^{-1}, where the measurements were accomplished in transmission mode with 200 scans. J-Stop resolution was 7.77 cm^{-1}, resolution 4 cm^{-1} and OPD-velocity 5 cm/sec. A MCT-semiconductor detector was available for detection.
The interpretation of the measurements can be done in two different ways, either by comparing the measured spectra with the entries in the IRUG database or by identifying the different bands. For samples with more phases, the identification is rather difficult. Due to the overlapping of bands it is often difficult or even impossible to characterize the analyzed material properly.

Results and Discussion

A number of blue pigments present in our collection is chosen in order to illustrate the experimental work. The results of all three analytical tools used (XRF, XRD and FTIR) are presented and discussed to demonstrate the difficulties of the experiments and the interpretation of the data. The numbers of the samples in this work correspond to the inventory numbers of the pigments in our collection.
Prussian Blue
In the collection of the Institute of Sciences and Technologies in Art at the Academy of Fine Arts three different samples of the pigment Prussian blue are present. The pigment name together with the number from the database and the manufacturer are listed in table 1. These samples (Prussian blue, Antwerp blue and Berlin blue) belong all to the darker kind of Prussian blue [13]. Some of them still carry the original label, which gives information about the manufacturer. Unfortunately, there is also one container, where no background information is available. The chemical structure of Prussian blue varies between $Fe_4[Fe(CN)_6]_3$ and $KFe[Fe(CN)_6]$, which causes the different colors of this pigment [14]. Antwerp blue, according to the literature, is often found as a blue pigment mixed with white pigments as carrier materials [15].
The major elements (Fe and K) could be detected by XRF measurements, except C and N, which are below the detection limit of the Si(Li)-detector used. Additionally, some impurities like Al, Si, S, Ca, Cr, Cu, Ba and sometimes

Pigment No.	Trivial name	Manufacturer/ trader	Verified elements
84	Prussian Blue	George Rowney & Co. Ltd.	**K**, Cr, **Fe**, Rb, Ba, Pb
131	Antwerp Blue	D.Sch., Düsseldorf	**Al**, Si, **S**, K, Ca, Cr, **Fe**, Cu, Sr, **Ba**, Pb
132	Berlin Blue	not reported	**K**, **Fe**, Cu, Rb

Table 1: List of the analyzed Prussian blue pigments, their trivial names and manufacturers (read from the tag) as well as the results of the XRF measurements (main components appear bold).

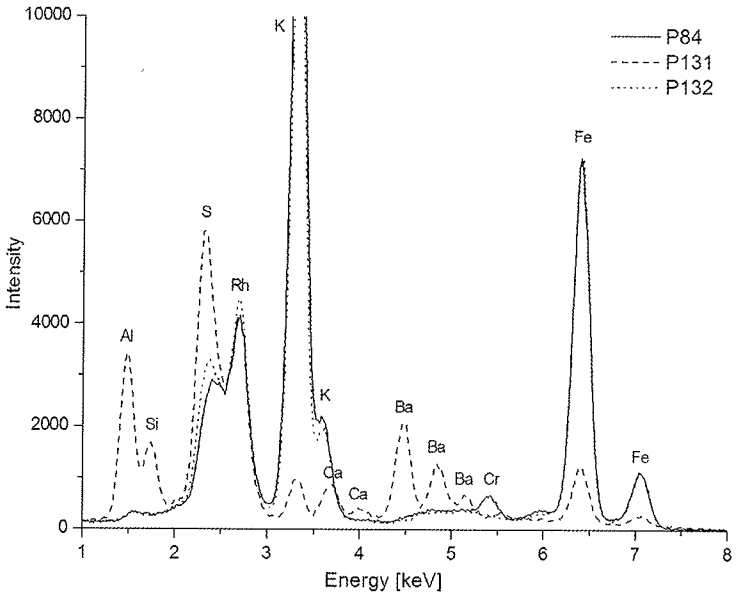

Figure 1: RFA spectra of the pigments no. 84, 131 and 132 measured at 8 kV under vacuum.

Pigment No.	PDF No.	Compound	Formula
84	01-0239	Iron Cyanide	$Fe_4(Fe(CN)_6)_3$
131	01-0239	Iron Cyanide	$Fe_4(Fe(CN)_6)_3$
	07-0324	Gibbsite	$Al(OH)_3$
	24-1035	Barium sulfate	$BaSO_4$
132	01-0239	Iron Cyanide	$Fe_4(Fe(CN)_6)_3$

Table 2: Results of the XRD measurements for the pigments no. 84, 131 and 132.

Pb could be found. The amount of these elements differs between the samples. Figure 1 shows the spectra of three samples measured with XRF at 8 kV in vacuum. As can be seen from the spectra the pigment no. 84 and 132 contain a lot of K and Fe, whereas in pigment no. 131 the intensity is rather low. In addition to the main elements the spectrum of pigment no. 131 shows intensities for Al, Si, S, Ca and Ba, indicating that this sample might contain different compounds compared to pigment no. 84 and 132. A summary of the XRF results are given in table 1.

With the use of XRD these questions could be clearly answered. Because of the cubic structure of Prussian blue, the diffractograms show a few single peaks [16]. Pigment no. 84 and 132 are identical (table 2) and show only the phase for $Fe_4[Fe(CN)_6]_3$. The diffractogram of pigment no. 131 reveals much more peaks. It contains not only the iron phase but also gibbsite and barium sulfate. These two compounds are well-known white pigments and have been used to modify slightly the color of Prussian blue.

By using FTIR spectroscopy the information gained by XRF and XRD could be confirmed. The spectra of these three pigments, shown in figure 2, appear very similar. The band for the CN ternary bond occurs at 2083 cm^{-1} [17]. Additionally, bands at 3377, 3256, 1686, 1611, 1414, 1047, 981, 835, 606 and 495 cm^{-1} can be identified. In the spectra for pigment no. 84 and 132 they can clearly be determined. For pigment no. 131 additional bands in the region around 3500 and 1100 cm^{-1} can be observed. These peaks are characteristic for sulfate compounds [18]. For barium sulfate, for instance, a strong band between 700 and 600 cm^{-1} is typical, which can be found in pigment no. 131 too.

The analysis of these blue pigments with the three different methods enabled the identification of the chemical compound of these samples. Prussian blue could be identified as a very pure pigment. Only one sample was mixed with white pigments in order to brighten the color. Although the pigments have different names the coloring compound is always the same.

Pigment database

In order to use the results in the daily routine, all collected information was summarized in a database. For every pigment the information about the sample, the results of the experiments and the information found in literature are stored in tables, e.g. the trivial and chemical name, formula, manufacturer and date, color, toxicity and photosensitivity as well as the results obtained by XRF, XRD and FTIR analysis. All these values are linked by the inventory number, are well defined and matched to one sample.

To facilitate the search, a query form was created (see figure 3). For an inquest within the database, it is possible to

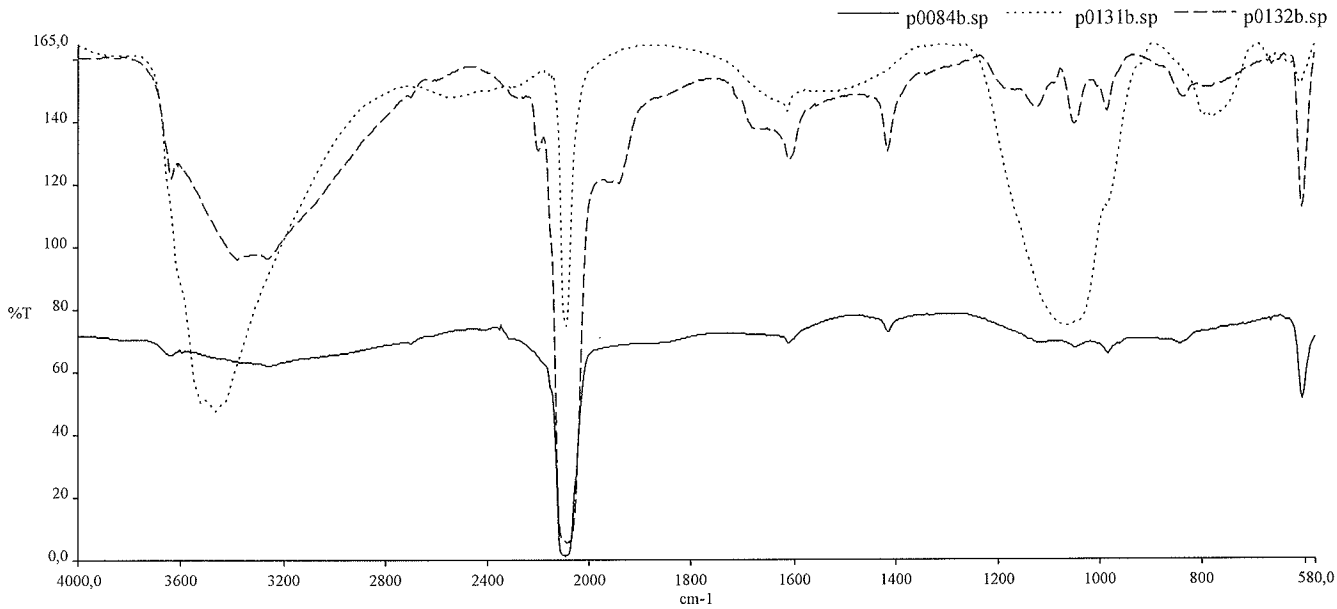

Figure 2: Comparison of the FTIR spectra of the Prussian blue pigments no. 84, 131 and 132.

run a search for every entry in this database which allows extended and direct access to the original information and eases the identification of unknown samples.

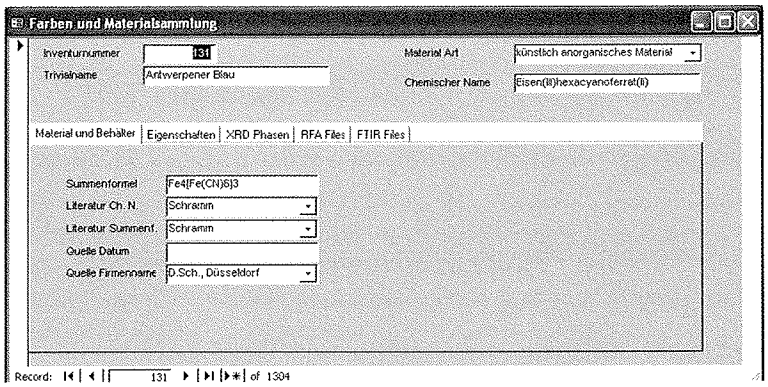

Figure 3: Query form of the pigment database.

In addition to this database two libraries were created, one for the XRD measurements and one for the FTIR spectra. The library with the FTIR spectra was compiled with the Perkin Elmer software (see figure 4). For this reason it is – at the moment – only usable by Perkin Elmer software. However each of the spectra is converted into the new JCAMP-DX format, which is readable by every commercial FTIR software. In this file the measurement parameters are saved as well as the trivial name of the pigment.

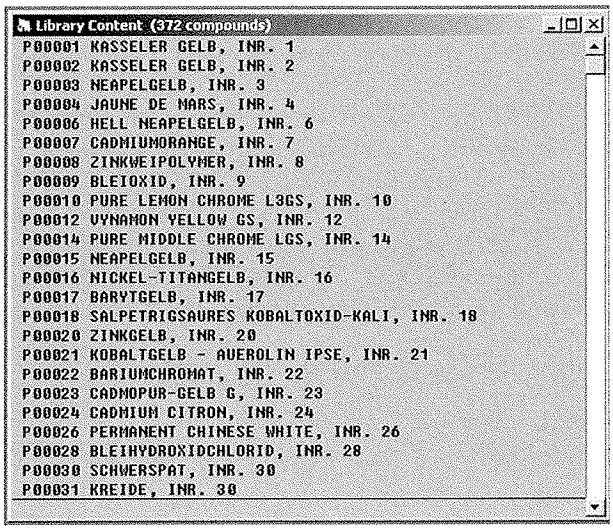

Figure 4: Excerpt of the compiled FTIR library.

Conclusion

The gained results showed in some cases remarkable differences in composition of pigments with the same trade name. Those differences consisted either with respect to the identified elements or to the added compounds such as pure white pigments. By combining these three experimental techniques it was possible to identify completely almost every pigment in our collection.
From the XRF measurements it could be shown that most of the historic pigments include impurities above the trace element level. By XRF analysis some but by far not all pigments could be identified by their containing elements. With XRD most of the phases in a sample could be related to a known pigment. At a closer look it was found that not all pigments carrying the same name consist of the same compounds and phases.
The FTIR spectra of a pure sample could be identified either by their bands or by comparing the measured spectra with data-set entries in the IRUG-database. Without the

knowledge of XRD and XRF measurements it was not always possible to characterize these pigments alone by FTIR spectroscopy, but it was a helpful tool by analyzing the organic component of the sample.
With all these experimental results a database for inorganic pigments was obtained. It is supplemented by additional information about the pigments as found in literature. Additional to that the diffractograms and the FTIR spectra are stored in two computer-aided catalogues (compatible with ICDD, IRUG) to ease further identification of unknown samples.
Further information is available at our website: http://www.fch.akbild.ac.at/.

References

1. Roy, A. *Artists' Pigments – A Handbook of their History and Characteristics*, Volume 2, Cambridge University Press, New York (1993) 37-66.

2. Schramm, H.-P., *Historische Malmaterialien und ihre Identifizierung*, Deutscher Verlag der Wissenschaften, Berlin (1989).

3. Mantler, M., Schreiner, M., Schweizer, F., 'Museum: Art and Archaeology', *Industrial Applications of X-Ray Diffraction*, Marcel Dekker Inc., New York (2000) 621-658.

4. Ullmann, F., *Encyclopaedia of Industrial Chemistry*, Volume 18: Pigments, 4th Edition Verlag Chemie GmbH, Weinheim (1979) 545-646.

5. Günzler, H., Heise, H. M., *IR-Spektroskopie - Eine Einführung*, VCH Verlagsgesellschaft, Weinheim (1996).

6. International Center for Diffraction Data (ICDD), 12 Campus Boulevard, Newton Square, PA (2002).

7. Price, B., Pretzel, B., Infrared and Raman Users Group Spectral Database, Edition 2000, Philadelphia (2002).

8. Kirk-Othmer, Raymond, E., *Encyclopaedia of Chemical Technology*, 3rd Edition, John Wiley & Sons Ltd., New York (1978) 251.

9. Kittel, H. , *Pigmente - Herstellung, Eigenschaften, Anwendung*, Wissenschaftliche Verlagsgesellschaft mbH, Stuttgart (1960).

10. Gardner, W., Ash, M., *Handbook of Chemical Synonyms and Trade Names*, 10th Edition, Gower, Aldershot (1994).

11. Jenkins, R., Snyder, R. L., *Introduction to X-Ray Powder Diffractometry*, John Wiley & Sons Inc., New York (1996).

12. Newmann, R., 'Some Applications of Infrared Spectroscopy in the Examination of Painting Materials', *Journal of the American Institute for Conservation* (JAIC) (1979) **19**(1).

13. West FithHugh, E., *Artist' Pigments – A Handbook of their History and Characteristics*, Volume 3, Cambridge University Press (1997) 191-219.

14. Patton, T.C., *Pigment Handbook*, John Wiley & Sons Ltd., New York (1973).

15. Bersch, J., *The Manufacture of Mineral and Lake Pigments*, 2nd Edition, A.C. Wright, London (1901) 194-203.

16. Wilde, R.E., Ghosh, S.N., Marshall, B.J., 'The Prussian Blue', *Inorganic Chemistry*, Columbus OH (1970) 9(11) 2512-2516.

17. Nakamoto, K., *Infrared and Raman Spectra of Inorganic and Coordination Compounds*, 5th Edition, Part B, John Wiley & Sons Inc., New York (1997).

18. Nyqist, R.A, Putzig, C.L., Leugers, M.A., *The Handbook of Infrared and Raman Spectra of Inorganic Compounds and Organic Salts*, Academia Press, San Diego (1997).

Effect of Formalin on Animal Glue – A preliminary study on the materials and techniques used in the paintings of "Panreal Art Group" in Japan

Masahiko TSUKADA
National Museum of Western Art, 7-7 Ueno-Koen, Taito-ku, Tokyo, 110-0007, JAPAN

Abstract

A group of Japanese artists, called "Panreal Art Group", applied formalin to animal glue paint in order to achieve their original expression. Nowadays their early works suffer severe flaking and loss of paint. These damages are suspected to be a result of the application of formalin. As a preliminary study for the investigation of materials and techniques of "Panreal Art Group", the effect of formalin on animal glue was studied with FTIR spectroscopy. It was observed that the absorbance of the peaks from animal glue around 1080 cm^{-1} and 1030 cm^{-1} was slightly increased by the application of formalin, and the absorbance around 1030 cm^{-1} became greater than that around 1080 cm^{-1} when formalin of concentration greater than 10% was applied. These changes could be due to the formation of hydroxymethyl group as a result of the reaction of formaldehyde with protein molecules. Here, the possibility and the limitations to detect these changes in analyzing paint samples are also discussed.

Introduction

This communication presents a part of an on-going cooperative research project among Kariya City Art Museum, Department of Art History and Conservation of Tohoku University of Art & Design, and the author about the materials and techniques used in the paintings of "Panreal Art Group" in Japan.
Immediately after Second World War, a group of young Japanese artists launched "Panreal Art Group" in Kyoto. Although they had received their training in the traditional Japanese painting (Nihonga) style, their works were created in quite an avant-garde style. In the traditional Japanese painting, the materials used are principally earth pigments mixed with aqueous binding medium of animal proteinaceous glue, and the techniques are somewhat restricted. The artists of "Panreal" tried to develop their techniques to seek for new ways of expression, which was difficult to achieve with traditional Japanese painting techniques. One of their distinguishing features in their early works was the application of formalin onto ground and paint layer. It was intended to overcome the restriction caused by the sensitivity of paint with animal glue to water. To give an example, with traditional Japanese paints, it is difficult to build up many layers and to recompose the painting in the working process. The artists of "Panreal" enabled these abilities by using formalin.
Nowadays, the early works of "Panreal" group have suffered severe damage such as flaking and loss of paint. We suspected that these damages were caused by the application of formalin. Therefore, a preliminary study was carried out with Fourier Transform Infrared (FTIR) spectroscopy applied over model samples in order to investigate the effects of formalin on Japanese painting materials, especially on animal glue, and to develop a method for the detection of these effects while investigating paint samples from "Panreal" paintings.

Information from literature about formalin and its reaction with protein [1, 2]

Formalin is the aqueous solution of formaldehyde (methanal) at the concentration of 37-40% by weight. It is used as preservative, fixing reagent for biological specimens, and tanning reagent of hide to produce leather, etc.
When reacting with protein, formaldehyde makes protein hard and resistant to swelling in contact with water. "Panreal" artists took advantage of these characteristics in their technique. The mechanism of the reaction between protein and formaldehyde is very complicated, and it seems various reaction paths are involved. The predominant one is considered as an addition reaction of a formaldehyde molecule to form a hydroxymethyl compound (Equation (1)), and a subsequent condensation reaction with the formation of a methylene bridge (Equation (2)).

$$R\text{-}H + CH_2O \Leftrightarrow R\text{-}CH_2OH \quad (1)$$

$$R\text{-}CH_2OH + H\text{-}R' \Leftrightarrow R\text{-}CH_2\text{-}R' + H_2O \quad (2)$$

When the other molecules of formaldehyde reacts with hydroxymethyl group it forms polyoxymethylene group (Equation (3)) and this can result in polyoxymethylene bridge ($-(CH_2O)_x-CH_2-$).

$$R\text{-}CH_2OH + xCH_2O \Leftrightarrow R\text{-}(CH_2O)_x\text{-}CH_2OH \quad (3)$$

In the reaction with protein molecules, both the addition and the condensation can take place with various functional groups of protein molecules such as amides and terminal amino groups. As mentioned above, the addition results in the formation of hydroxymethyl group, and the subsequent condensation results in the formation of methylene or polyoxymethylene bridge. When the condensation occurs intramolecularly, cyclic structures would be formed, and when it occurs intermolecularly, molecular aggregates would be formed. As a result of these reactions, the properties of protein molecules against water may change.

Experiment

The FTIR spectra of animal glue are complicated and it is difficult to attribute all peaks to certain structures due to various functional groups existing in protein molecules and also due to the fact that it could contain impurities. However, we applied FTIR analysis to model samples to observe possible changes in spectra. If the above-mentioned reactions occur in protein molecules, there might be some changes in spectra reflecting the above-mentioned changes in the molecular structure.

Preparation of samples

The samples were made of varied concentration of animal glue and formalin as follows;
Aqueous solutions of animal glue (*Sanzenbon*) at the concentration of 11, 20, 28, and 34% by weight were prepared with distilled water. Formalin, which contains approximately 37% of formaldehyde, was diluted with distilled water to make the concentrations of 1, 5, 10, 25 and 50% by volume. The samples were prepared in two ways: 1) animal glue solution and diluted formalin of each concentration were mixed in equal volumes and applied on a glass plate respectively; 2) 11% animal glue solution was applied on a glass plate and dried, then the equal volume of diluted formalin of each concentration were applied on it respectively. Experiment procedures such as mixing and applying of formalin, and drying of the samples applied on glass plates were carried out in the fume cupboard to observe health and safety cautions.

FTIR measurement

The surface of above samples were scraped with a scalpel and applied for FTIR analysis. The measurements were carried out by KBr pellet method using Perkin Elmer 1600 Series FTIR spectrometer or Bio-Rad FTIR spectrometer FTS-6000. Samples were scanned 64 times over 4000 cm^{-1} to 400 cm^{-1}, at a resolution of 4 cm^{-1}.

Results and Discussion

In spectra of the samples, no remarkable change was observed in its entirety, however, the absorbance of adjacent peaks around 1080 cm^{-1} and 1030 cm^{-1} slightly increased in the samples treated with formalin. In addition to that, as the concentration of applied formalin increased, the absorbance around 1030 cm^{-1} became greater than that around 1080 cm^{-1}, while the spectrum of animal glue which was not treated with formalin showed the absorbance around 1080cm^{-1} greater than that around 1030 cm^{-1} (Fig.1 and 2). These increments of the absorbance in the peaks around 1030 cm^{-1} and 1080 cm^{-1} could be respectively attributed to the CO stretch of the hydroxymethyl group (primary alcohol) and the asymmetrical COC stretch of the polyoxymethylene bridge [3]. This attribution of the peak around 1030 cm^{-1} could be supported by the increment of the absorbance in the region around 3600 - 3200 cm^{-1}, which is attributable to the hydroxymethyl group [4]. However, the attribution of the peak around 1080 cm^{-1} to the polyoxymethylene bridge would be less certain because the obvious increase of the absorbance in the region around 2790 - 2770 cm^{-1}, which would be attributable to the polyoxymethylene group [4], was not observed.

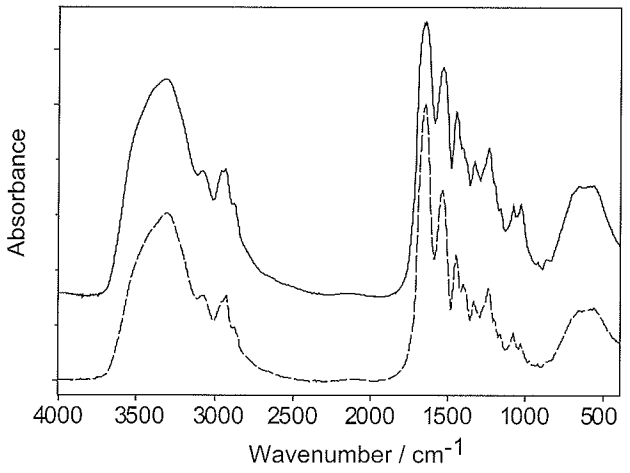

Fig.1 Infrared spectra of 11% animal glue solution dried on a glass plate (dashed line), and subsequent application of 20% formalin (solid line).

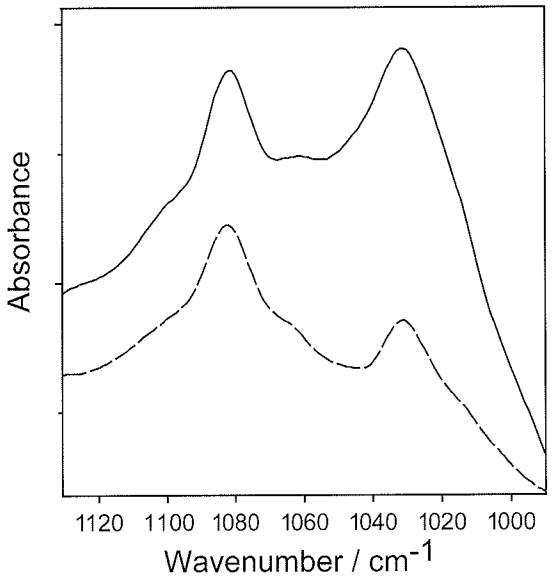

Fig.2 Detail of Fig.1

Concerning the formation of the methylene bridge, it is ambiguous since the increments of its characteristic absorption bands around 2960 - 2850 cm^{-1} and 1470 - 1430 cm^{-1} [4] were not observed in FTIR spectra. The formation of a polyoxymethylene or methylene bridge should be studied further with other analytical techniques. In the samples treated with formalin of extremely high concentration, the surface of the samples became clouded. Fig.3 shows the spectrum of this turbid area. As can be seen, it could be assumed that paraformaldehyde was formed in these samples [5]. To study this minute change of spectra in detail, the spectra were normalized at the peak around 1650cm^{-1} (amide I band), and then the ratio of the absorbance of the peak around 1030cm^{-1} to that around 1080cm^{-1} (A_{1030}/A_{1080}) was calculated and plotted against the concentration of applied formalin. Fig.4 shows the plot of the average of A_{1030}/A_{1080} from five spectra in each condition. It can be indicated that A_{1030}/A_{1080} increased along with the increment of concentration of applied formalin. Also it can be seen that in all conditions A_{1030}/A_{1080} surpassed 1.0 with the treatment with formalin concentrations between 5% and 10%, except the samples of 11% animal glue solution mixed with formalin.

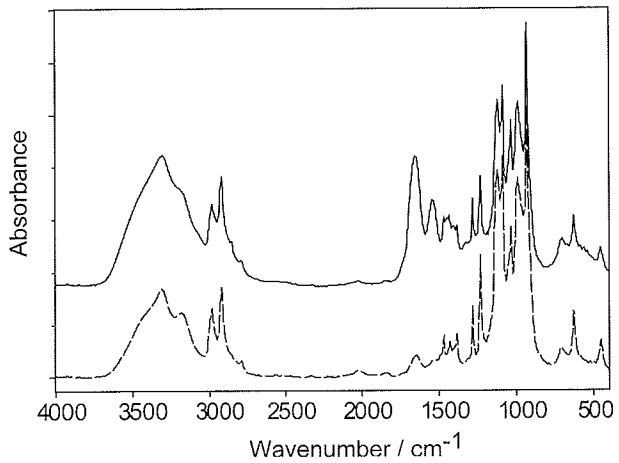

Fig.3 Infrared spectra of 11% animal glue solution dried on a glass plate followed by the application of 100% formalin (solid line), and residue after drying of 100% formalin (dashed line).

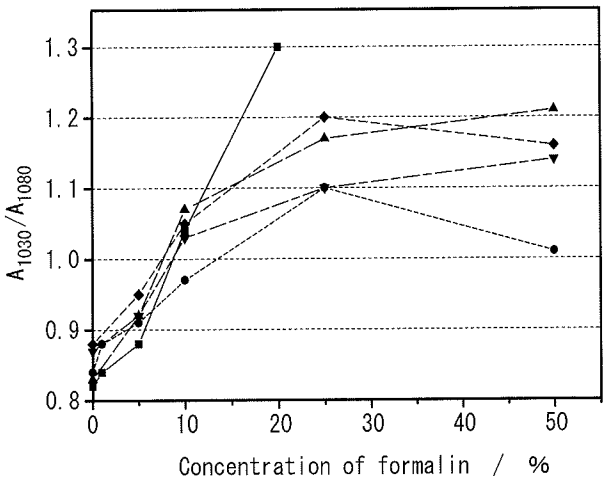

Fig.4 Plots of the ratio of the absorbance of the peak around 1030 cm^{-1} to that around 1080 cm^{-1} (A_{1030}/A_{1080}) against the concentration of applied formalin - solid line: 11% animal glue solution dried on a glass plate with applied formalin (■), dashed lines: animal glue solution at the concentration of 11% (●), 20% (▲), 28% (▼), and 34% (◆), mixed with formalin and then dried on a glass plate.

This means that with the treatment by formalin of the concentration greater than 10%, the absorbance of the peak around 1030cm^{-1} became greater than that around 1080cm^{-1} so that the difference between the treated and untreated samples became detectable in sight of the spectra. As for the samples of 11% animal glue solution mixed with formalin, the greater concentration required the absorbance of the peak around 1030cm^{-1} to surpass that around 1080cm^{-1}. This could be explained by reasons as follows; the amount of protein molecules in 11% animal glue solution was smaller and more dispersed than other conditions, hence the degree of the reaction with formaldehyde was lower than other conditions of higher concentration. In the samples of dried 11% animal glue on which

formalin were applied, greater amount of protein molecules could be in contact with formaldehyde at the surface, so the reaction could occur at the same level as the samples with animal glue of higher concentration. The treatment with formalin of the concentration of 25% and 50% did not differ much in A_{1030}/A_{1080}, save that the samples treated with 50% formalin had A_{1030}/A_{1080} rather smaller than 25%. This could be due to the formation of paraformaldehyde in the samples, which would decrease the amount of molecules of formaldehyde to react with protein.

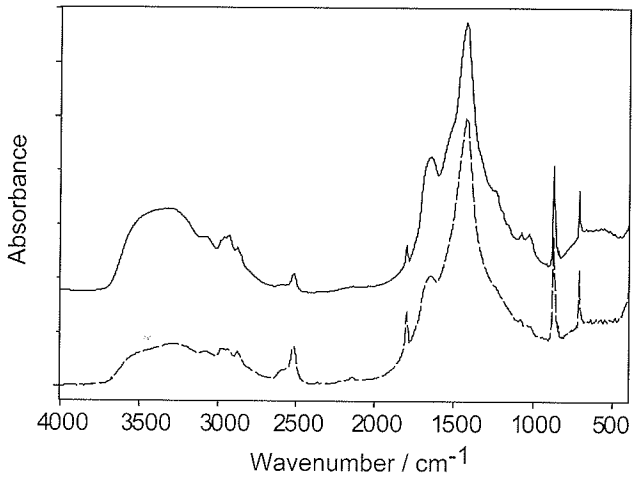

Fig.5 Infrared spectra of the mixture of calcium carbonate (calcite) and 11% animal glue solution dried on a glass plate which were followed by a 20% formalin application (solid line), and the pigment rich area of this sample (dashed line).

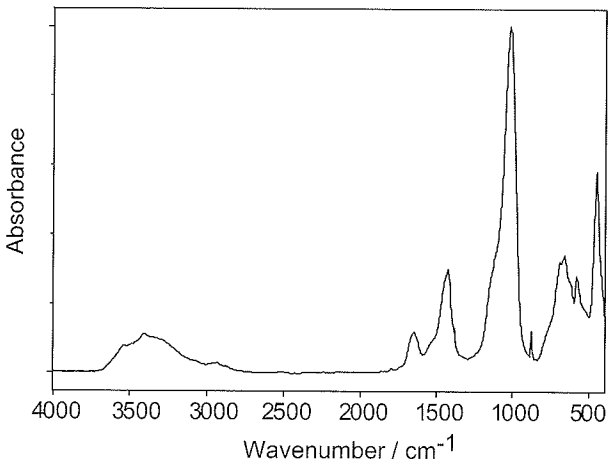

Fig.6 Infrared spectrum of the mixture of Japanese blue pigment for distemper and 11% animal glue solution dried on a glass plate and followed with a 20% formalin application.

Discussion about the detection of the above changes in paint samples

From the results described above, it was suggested that the changes in animal glue caused by the application of formalin could be detected using FTIR by comparing the absorbance of the peaks around 1030 cm^{-1} to that around 1080 cm^{-1}. However, in analyzing the samples from paintings, two limitations could be assumed: 1) the proportion of animal glue in paint could be too low to detect the peaks around 1080 cm^{-1} and 1030 cm^{-1}; 2) the absorption of the pigments could overlap with the peaks around 1080 cm^{-1} and 1030 cm^{-1}.

As the example for 1), Fig.5 shows the FTIR spectra of the model paint sample, which was made as follows: the mixture of 3.0 g of calcium carbonate (calcite) and 3.0 ml of 11% animal glue solution was applied and dried on a glass plate, then 20% formalin was applied on it in abundance. In this paint sample, the amount of animal glue would be approximately one and a half times as much as the paint of traditional Japanese painting. Besides that, calcium carbonate and animal glue solution were not mixed sufficiently. As a result, this sample turned out to be a non-homogeneous paint layer. The solid line of Fig.5 shows a typical spectrum of this sample. It was observed that the absorbance of the peak around 1030 cm^{-1} was greater than that around 1080 cm^{-1}. The dashed line in Fig.5 also shows a spectrum of the same paint sample, but the piece applied for FTIR measurement was taken from the pigment rich area. The peaks around 1080 cm^{-1} and 1030 cm^{-1} were still detectable, but they were very small and overlapped with the peak of calcite. From such a spectrum, it is difficult to recognize at a glance which peak was larger. In this case, it was verified with a peak fitting application that A_{1030}/A_{1080} was greater than 1.0. However, this spectrum implied that when the proportion of animal glue in paint is low, the peaks around 1080cm^{-1} and 1030cm^{-1} possibly become too small to be detected.

As for the second limitation mentioned above, Fig.6 shows a good example. The spectrum in Fig.6 is of the paint sample made of animal glue and a blue pigment for distemper, which is in use in Japanese painting as an alternative to the traditional pigment (its composition was not identified). This pigment showed a strong peak around 1020 cm^{-1}. In the spectrum, the presence of animal glue could be observed by amide I band, but the peaks of animal glue around 1080 cm^{-1} and 1030 cm^{-1} were completely overlapped with the peak of the pigment and not detectable. In this case, the calculation of A_{1030}/A_{1080} with peak fitting would become unreliable.

Conclusion

The effect of formalin on animal glue could be recognized with FTIR spectra by comparing the ratio of the absorbance at the peaks around 1080 cm^{-1} and 1030 cm^{-1}. The change of this ratio would occur by the formation of hydroxymethyl group as a result of the addition reaction of formaldehyde to protein molecules. However, in analyzing the samples from paintings, two limitations could be assumed: 1) the proportion of animal glue in paint could be too low to detect these peaks; 2) the absorption of the pigments could interfere the detection of these peaks. In the case of 2), if these peaks are still detectable, the peak fitting application could be useful for the comparison of the ratio A_{1030}/A_{1080}.

Acknowledgements

The author is grateful to the colleagues who are involved in this cooperative research project, especially Ms. Rie Ito, a graduated student at the Department of Art History and Conservation of Tohoku University of Art & Design, for her assistance in the measurement of FTIR spectra.

Reference

1. Budavari, S., O'Neil, M.J., Smith, A.,Heckelman, P.E., and Kinneary, J.F., *The Merck Index*, twelfth edition, Merck Research Laboratories, Whitehouse Station (1996) 717-718.

2. French, D., and Edsall, J.T., 'The Reaction of Formaldehyde with Amino Acids and Proteins', *Advances in Protein Chemistry*, **2** (1945) 277-335

3. Bockhoff, F.J., Guo, K-M., Richards, G.E., and Bockhoff, E., 'Infrared Studies of the Kinetics of Insolubilization of Soluble Nylon' in N.S. Brommelle et al. (eds), *Adhesives and Consolidants , Preprints of the Contributions to the Paris Congress, 2-8 September 1984*, The International Institute for Conservation of Historic and Artistic Works, London(1984) 81-86

4. Hesse, M., Meier, H., and Zeeh, B., *Spektroskopische Methoden in der organischen Chemie*, Georg Thieme Verlag, translated from English edition into Japanese by M. Nomura et al, Kagakudojin, Kyoto (2000) 41-42

5. Keller, R.J., The Sigma Library of FT-IR Spectra, Volume 2, Sigma Chemical Company, St. Louis (1986) 819

Participant list IRUG6 Conference (Florence 29/03/2004 - 1/04/2004)

Konstantinos Andrikopoulos
Art Diagnosis Centre
Ormylia-Chalkidiki
EL-63071 Ormylia - Greece
candrik@iceht.forth.gr
(+30) 371 0 98400

Lorenzo Appolonia
Soprintendenza Beni e Attività Culturali Val d'Aosta
Piazza Narbonne 3
Aosta - Italy
l.appolonia@regione.vda.it
(+39) 0165 272279

Mauro Bacci
Istituto di Fisica Applicata "Nello Carrara" - CNR
Via Panciatichi 64
50127 Firenze - Italy
m.bacci@ifac.cnr.it
(+39) 055 4235217

Laura Balcerzak
Istituto di Fisica Applicata "Nello Carrara" - CNR
Via Panciatichi 64
50127 Firenze - Italy
(+39) 055 4235273

Danilo Bersani
Physics Department - University of Parma
Parco Area delle Scienze 7/a
43100 Parma - Italy
danilo.bersani@fis.unipr.it
(+39) 0521 905278

Romina Bonaldo
Opificio delle Pietre Dure
Via degli Alfani 78
50100 Firenze - Italy
r_bonaldo@hotmail.com
(+ 39) 055 4625428

Giorgio Bonsanti
University of Florence
Via Santa Marta 17
50139 Firenze – Italy
gbonsanti@dada.it
(+39) 055400403

Jaap Boon
FOM Institute AMOLF
Kruislaan 407
1098 SJ Amsterdam - The Netherlands
boon@amolf.nl

Susanna Bracci
Istituto per la Conservazione e la Valorizzazione
dei Beni Culturali
via Madonna del Piano, Edificio C
50019 Sesto Fno. (Firenze) - Italy
s.bracci@icvbc.cnr.it
(+ 39) 055 5225413

Salvador Buti
Universitat Politecnica de Catalunya, Departament
d'Enginyeria Quimica
Av. Victor Balaguer s/n
08800 Vilanova i la Geltru, Barcelona - Spain
salvador.buti@upc.es
(+34) 938967717

Janice Carlson
Philadelphia Museum of Art
Box 7646
Philadelphia, PA, 19101-7646 - USA
jncarlson1@comcast.net

Emiliano Carretti
Consortium CSGI, Department of Chemistry,
University of Florence
Polo Scientifico, via Lastruccia 3
50019 Sesto F.no (Firenze) - Italy
carretti@csgi.unifi.it
(+39) 055 457 3031

Francesca Casadio
Art Institute of Chicago
111 South Michigan Avenue
60603 Chicago, Illinois - USA
fcasad@artic.edu
(+1) 312 857 764

Umberto Casellato
C.N.R.- I.C.I.S
Corso Stati Uniti, 4
35100 PADOVA - Italy
u.casellato@icis.cnr.it
(+39) 049 8295959

Emilio Mario Castellucci
European Laboratory for Non Linear Spectroscopy (LENS), Università di Firenze
Polo Scientifico, Via Nello Carrara 1
50019-Sesto F.no (Firenze) - Italy
castel@unifi.it
(+39)-0554572491/4573074

Andrea Cavicchioli
Laboratório de Espectroscopia Molecular-Instituto de Química-University of São Paulo
Av. Prof. Lineu Prestes 748/0419
São Paulo 05508-900 - Brazil
andrecav@iq.usp.br
(+55) 11 30913853 or 99048558

Oscar Chiantore
Department of Chemistry IPM, University of Torino
Via P. Giuria 7
10125 Torino - Italy
oscar.chiantore@unito.it
(+39) 011 6707558

Giacomo Chiari
The Getty Conservation Institute
1200 Getty Center Drive, Suite 700
Los Angeles, CA 90049 - USA
gchiari@getty.edu

Maria Perla Colombini
Chemistry Dept. - University of Pisa
Via Risorgimento 35
56126 Pisa . Italy
perla@dcci.unipi.it
(+39) 050 2219305

Antonino Cosentino
University of Catania
64 via S.Sofia
I-95123 Catania - Italy
antonino.cosentino@ct.infn.it
(+39) 095-378-5262

Marine Cotte
Centre de Recherche et de Restauration des Musées de France
6 rue des pyramides
75041 PARIS Cedex - France
marine.cotte@culture.gouv.fr
(+33) 1 46835951

Paola Croveri
Dipartimento di Chimica IPM Gruppo Materiali Polimerici
Via P. Giuria 7
10125 Torino - Italy
paola.croveri@unito.it
(+39) 011 6707554

Costanza Cucci
Istituto di Fisica Applicata "Nello Carrara" - CNR
Via Panciatichi 64
50127 Firenze – Italy
c.cucci@ifac.cnr.it

Dalva de Faria
Laboratório de Espectroscopia Molecular
C.P. 26077
5513-970, São Paulo - Brazil
dlafaria@iq.usp.br
(+55) 11 3091 3853

Suzan De groot
Netherlands Institute for Cultural Heritage (ICN)
Gabriel Metsustraat 8
1071 EA, Amsterdam - The Netherlands
suzan.de.groot@icn.nl
(+31) 20-3054740

Sophie Denoël
European Center of Archaeometry, University of Liége
Bldg. B5 Sart-Tilman
Liege, B-4000 - Belgium
sophie.denoel@ulg.ac.be
(+32) 43665853

Gianfranco Di Lonardo
Dipartimento di Chimica Fisica e Inorganica, Università di Bologna
Viale Risorgimento 4
40136 Bologna - Italy
dilo@ms.fci.unibo.it
(+39) 051 2093990

Howell G.M. Edwards
Department of Chemical and Forensic Sciences, University of Bradford
Bradford BD7 1DP - UK
H.g.M.edwards@bradford.ac.uk
(+44) 1274-233787

Ken Ehrman
Digital Bridgeway Inc.
4529 Wilde Street
Philadelphia, PA 19127 - USA
kehrman@digitalbridgeway.com
(+1) 215 487 1285

Monica Favaro
C.N.R.- I.C.I.S
Corso Stati Uniti, 4
35100 Padova - Italy
favaro@icis.cnr.it
(+39) 049 8295966

Jose F. García-Martínez
Departament de Pintura, Conservació-Restauració.
Facultat de Belles Arts. Universitat de Barcelona
C/ Pau Gargallo 4
08028 Barcelona - Spain
jfgarcia@apolo.qui.ub.es
(+34) 934021281

Gianna Giachi
Soprintendenza per i Beni Archeologici della Toscana
Laboratorio di Analisi - Centro di Restauro
Largo del Boschetto, 3
50124 Firenze - Italy
gianna.giachi@tin.it
(+39) 055 7131879

Rodorigo Giorgi
Department of Chemistry and Consortium CSGI,
University of Florence
via della Lastruccia, 3
I-50019 Sesto F.no (FI) - Italy
giorgi@apple.csgi.unifi.it

Valérie Hayez
Vrije Universiteit Brussel, TW/META
Pleinlaan 2
1050 Brussel – Belgium
valerie.hayez@vub.ac.be
(+32) 26292296

Sigurdur Jakobsson
Science Institute, Univ. of Iceland
Dunhaga 3
IS-107 Reykjavík, Iceland
sigjak@raunvis.hi.is
(+354) 525 4482

Pier Luigi Emiliani
Istituto di Fisica Applicata "Nello Carrara" - CNR
Via Panciatichi 64
50127 Firenze - Italy
p.l.emiliani@ifac.cnr.it

Nuria Ferrer
Serveis Cientificotècnics.Universitat de Barcelona
Lluís Solé Sabarís, 1
08028 Barcelona - Spain
nuri@giga.sct.ub.es
(+34) 93 4021346

Glenn A. Gates
Andrew W. Mellon Post-doctoral Fellow in
Conservation Science Harvard University Art
Museums
32 Quincy Street
Cambridge, MA 02138 - USA
ggates@fas.harvard.edu
(+1) 617 384 8717

Bernard Gilbert
University of Liège - Center of Archaeometry
Bldg. B5 Sart-Tilman
Liege, B-4000 - Belgium
b.gilbert@ulg.ac.be
(+32) 43663567

Jan J. Hansen
School of Conservation
Esplanaden 34
DK-1263, Copenhagen - Denmark
jjh@kons.dk
(+45) 33 744762

Herm Christoph
Dresden Academy of Fine Arts
D-01288 Dresden - Germany
herm@serv1.hfbk-dresden.de
(+49) 351 4402 107

Dubravka Jembrih-Simburger
Sciences and technologies in Art, Academy of Fine
Arts
Schillerplatz 3
A-1010 Vienna - Austria
d.jembrih@akbild.ac.at
(+43) 1 58816 203

Dane Jones
Chemistry and Biochemistry Department, Cal Poly State University
San Luis Obispo, CA 93407 - USA
djones@calpoly.edu
(+1) 805 756 2528

Edith Joseph
Corso di laurea Tecnologie per il Restauro e la Conservazione dei beni culturali - Ex-Asili
via Tombesi dell'ova 55
48100 Ravenna - Italy
edith.joseph@unine.ch
(+39) 0544 484511

Herant Khanjian
Getty Conservation Institute
1200 Getty Center Drive, Suite 700
Los Angeles, CA 90049 - USA
hkhanjian@getty.edu
(+1) 310 440 6258

Giancarlo Lanterna
Opificio delle Pietre Dure
Via degli Alfani 78
50100 Firenze - Italy
giancarlo.lanterna@tiscali.it
(+ 39) 055 4625486

Tom Learner
Tate Gallery
Millbank
London SW1P 4RG - UK
tom.learner@tate.org.uk
(+44) (0)20 7887 8066

Suzanne Lomax
National Gallery of Art, Scientific Reseach Department
6th Street and Constitution Ave.
Washington, DC 20565 - USA
s-lomax@nga.gov
(+1) 202 842 6763

Jennifer Mass
Conservation Department, Winterthur Museum, Garden, and Library
Winterthur, DE 19735 - USA
jmass@winterthur.org
(+1) 302 888 4808

Julia Jonsson
Tate Gallery
Millbank
London SW1P 4RG - UK
Julia.Jonsson@tate.org.uk
(+44) (0)20 7887 3980

Narayan Khandekar
Straus Center for Conservation, Harvard University Art Museums
32 Quincy Street
Cambridge, MA 02138 - USA
narayan_khandekar@harvard.edu
(+1) 617 495 4591

Hartmut Kutzke
Fachhochschule Köln
Ubierring 40
D-50678 Köln - Germany
kutzke@re.fh-koeln.de
(+49) (0)221 8275 3481

Susan Lake
Hirshhorn Museum and Sculpture Garden, Smithsonian Institution
7th and Independence, S.W.
Washington, D.C. 20560 - USA
lakes@si.edu
(+1) 202 633 2731

Marco Leona
Metropolitan Museum of Art
1000 fifth Avenue
New York, NY 10028 - USA
marco.leona@metmuseum.org
(+1) 212 396 5476

Marta Maier
Departamento de Química Orgánica, Facultad de Ciencias Exactas y Naturales, Universidad de Buenos Aires
Pabellón 2, Ciudad Universitaria (1428)
Buenos Aires - Argentina
maier@qo.fcen.uba.ar
(+54) 11 4576-3385

Rocco Mazzeo
University of Bologna, Chemistry Department
Via Selmi 2
40126 Bologna - Italy
rocco.mazzeo@unibo.it
(+39) 0512099532

Christopher McGlinchey
The Museum of Modern Art
NY - USA
chris_mcglinchey@moma.org
(+1) 212 708 9821

Paul S. Middleton
Peterborough Regional College
Park Crescent
Peterborough PE1 4YP - UK
paul.middleton@peterborough.ac.uk
(+44) 1733 762224

Angels Miquel
Departament de Pintura-Facultat de Belles Arts-Universitat de Barcelona
C/ Pau Gargallo v&ορδμ; 4
08028 Barcelona - Spain
angie@miquel.es
(+34) 93 252 28 00

Francesca Ospitali
Dipartimento Di Chimica Fisica e Inorganica,
Universita' di Bologna
Viale Risorgimento 4
40136 Bologna - Italy
ospitali@ms.fci.unibo.it
(+39) 051 2093709

James Parker
Department of Conservation Documentation and Science, The British Museum
Great Russell Str.
London WC1B 3DG - UK
jparker@thebritishmuseum.ac.uk
(+44) 207 3238174

Marcello Picollo
Istituto di Fisica Applicata "Nello Carrara" - CNR
Via Panciatichi 64
50127 Firenze - Italy
m.picollo@ifac.cnr.it
(+39) 055 4235273

Francesca Piquè
Getty Conservation Institute
1200 Getty Center Drive, Suite 700
Los Angeles, CA 90049 - USA
fpique@getty.edu

Bruno Messiga
Dipartimento Scienza della Terra Università di Pavia
Pavia, Italy
messiga@crystal.unipv.it
(+39) 0382 505892

Milan Milosevic
Harrick Scientific Corporation
88 Broadway, POBox 1288
Ossining, NY 10562 - USA
mmilosevic@harrickscI.com
(+1) 914 762-0020

Francesca Modugno
Chemistry Dept. - University of Pisa
Via Risorgimento 35
56126 Pisa. Italy
frances@dcci.unipi.it
(+39) 050 2219305

Sandrine Pagès-Camagna
Centre de Recherche et de Restauration des Musées de France
6 rue des Pyramides
75041 Paris cedex 01 - France
sandrine.pages@culture.gouv.fr
(+33) 1 40208436

Daniela Pawel
Norwegian University of Science and Technology,
Department of Archaeology and Kultural History
Erling Skakkes gt. 47
N - 7491 Trondheim - Norway
daniela.pawel@vm.ntnu.no
(+47) 73 592179

Sarah Pierce
Department of Chemistry, Duke University
Durham, NC 27708 - USA
sarah.pierce@duke.edu
(+) 919 613 1542

Rebecca Ploeger
Queen's University, Chernoff Hall
90 Queen's Crescent
Kingston, Ontario K7L 3N6 - Canada
ploegerr@chem.queensu.ca
(+1) 613 5336000 (ext. 75366)

Simone Porcinai
Opificio delle Pietre Dure
Via degli Alfani 78
50100 Firenze - Italy
s.porcinai@ifac.cnr.it
(+ 39) 055 4625428

Beth Price
Philadelphia Museum of Art
Box 7646
Philadelphia, PA, 19101-7646 - USA
bprice@philamuseum.org
(+1) 215 684 7552

Camilla Ricci
Chemistry Department, University of Perugia
via Elce di sotto 8
06123 Perugia - Italy
camillaricci@tin.it
(+39) 075 5855526

Nati Salvadó
Dpt. d'Enginyeria Química. EPSEVG. Universitat Politècnica de Catalunya
Av. Victor Balaguer s/n
08800 Vilanova i la Geltrú, Barcelona - Spain
nativitat.salvado@upc.es
(+34) 93 8967717

Yoshiko Sasaki
Nara National Research Institute for Cultural Properties
2-9-1, Nijo-cho
Nara 630-8577 - Japan
ysasaki@nabunken.go.jp
(+81) 742306847 Ex.522

Dominique Scalarone
Department of Chemistry IPM, University of Torino
Via P. Giuria 7
10125 Torino - Italy
dominique.scalarone@unito.it
(+39) 011 6707546

Anke Schaening
Institute of Humanities, Sciences an Technologies in Art, Department of Conservation-Restauration, Academy of Fine Arts
A-1010 Vienna - Austria
a.schaening@akbild.ac.at
(+43) 1 58816 223/285

Boris Pretzel
Victoria & Albert Museum
South Kemsington
London SW7 2RL - UK
boris.pretzel@vam.ac.uk
(+44) 20 7942 2116

Maria Pia Riccardi
Dipartimento Scienza della Terra Università di Pavia
Pavia, Italy
riccardi@crystal.unipv.it
(+39) 0382 505892

Francesca Rosi
Dipartimento di Chimica Università di Perugia
via Elce di Sotto 8
06123 Perugia - Italy
franci@thch.unipg.it
(+39) 075 585556

Barbara Salvadori
Department of Chemistry and Consortium CSGI, University of Florence
via della Lastruccia, 3
I-50019 Sesto F.no (FI) - Italy
salvadori@csgi.unifi.it
(+39) 055 4573021

Masanori Sato
Nara National Research Institute for Cultural Properties
2-9-1, Nijo-cho
Nara 630-8577 - Japan
msato@nabunken.go.jp
(+81) 742-30-6847 Ex.522

Michelle Scalera
The John and Mable Ringling Museum of Art
5401 Bay Shore Rd
Sarasota, FL 34243, USA
mscalera@ringling.org
(+1) 941 359 5734

Anna Schoenemann
The Getty Conservation Institute
1200 Getty Center Drive, Suite 700
Los Angeles, CA 90049 - USA
ASchoenemann@getty.edu
(+1) 310 440 7251

Herbert F. Shurvell
Art Conservation Program, Department of Art,
Queen's University
Kingston ON K7L 3N6 - Canada
shurvell@chem.queensu.ca
(+1) 613 389 3212

Helen Spande
Villa La Pietra - New York University
Via Bolognese 120
50139 Firenze - Italy
helen.spande@nyu.florence.it
(+39) 055 5007 229

Dusan Stulik
Getty Conservation Institute
1200 Getty Center Drive, Suite 700
Los Angeles, CA 90049 - USA
dstulik@getty.edu
(+1) 310 440 6224

Karen Trentelman
Getty Conservation Institute
1200 Getty Center Drive, Suite 700
Los Angeles, CA 90049 - USA
ktrentelman@getty.edu
(+1) 310 440 6262

Annelies van Loon
FOM Institute AMOLF
Kruislaan 407
1098 SJ Amsterdam - The Netherlands
vanloon@amolf.nl
(+31) 20 6081234

Peter Vandenabeele
"Ghent University, Laboratory of Analytical
Chemistry"
Proeftuinstraat 86
B-9000 Ghent - Belgium
peter.vandenabeele@UGent.be
(+32) 9 264 66 23

Scott Williams
Canadian Conservation Institute
1030 Innes Road
Ottawa, Ontario K1A 0M5 - Canada
scott_williams@pch.gc.ca
(+1) 613 998-3721

Kenneth J. Smith
Thermo Electron Corp
217 S Wilmette Avenue
Westmont, IL 60559
ksmith865@sbcglobal.net
(+1) 630 430 3053

Renee Stein
Michael C. Carlos Museum
571 South Kilgo Circle
Atlanta, GA 30322 - USA
ras@shap.net
(+1) 404 727 1097

David Thickett
Birkbeck College, University of London
5 Woodmansterne rd, Streatham Vale
London SW16 5UU - UK
David.Thickett@English-heritage.org.uk

Masahiko Tsukada
National Museum of Western Art
7-7 Ueno-Koen, Taito-ku
Tokyo 110-0007 - Japan
tsukada@nmwa.go.jp
(+81)-3-3828-5131

Thea van Oosten
Netherlands Institute for Cultural Heritage (ICN)
P.O. Box 76709
1070 EA, Amsterdam - The Netherlands
thea.van.oosten@icn.nl
(+31) 20 3054773

Anna Vila
Departament de Pintura, Conservació-Restauració.
Facultat de Belles Arts. Universitat de Barcelona
C/ Pau Gargallo 4
08028 Barcelona - Spain
avila@giga.sct.ub.es
(+34) 93 333 3466 (ext. 3712)

Angela Zoppi
Dipartimento di Chimica, Università di Firenze
Via della Lastruccia 3
50019-Sesto F.no (Firenze) - Italy
ange@lens.unifi.it
(+39) 0554573078

NAME INDEX

Finito di stampare nel mese di marzo 2005
presso le Arti Grafiche Padovane
per conto della Casa Editrice il prato.

il prato

ISBN 88-89566-07-8